

Technical Report Documentation Page

1. REPORT No.

CA-DOT-DS-9925-1-75-6

2. GOVERNMENT ACCESSION No.**3. RECIPIENT'S CATALOG No.****4. TITLE AND SUBTITLE**

Variability Of Fracture Toughness In A514/517 Plate

5. REPORT DATE

October 1975

6. PERFORMING ORGANIZATION

14030 609925

7. AUTHOR(S)

Carl E. Hartbower, F.H.W.A. and Roger D. Sunbury

8. PERFORMING ORGANIZATION REPORT No.

CA-DOT-DS-9925-1-75-6

9. PERFORMING ORGANIZATION NAME AND ADDRESS

Office of Structures
California Department of Transportation
Sacramento, California 95807

10. WORK UNIT No.**11. CONTRACT OR GRANT No.**

DOT-FH-11-8250

12. SPONSORING AGENCY NAME AND ADDRESS

Federal Highway Administration
Washington, D.C. 20590

13. TYPE OF REPORT & PERIOD COVERED

Final Report

14. SPONSORING AGENCY CODE**15. SUPPLEMENTARY NOTES**

This study was conducted under direct contract with the Federal Highway Administration under Contract No. DOT-FH-11-8250 Case Order No. 7.

16. ABSTRACT

Fracture toughness of A514/517 steel (grades F&H) is reported for 76 plates tested during the Bryte Bend Bridge and Tuolumne River Bridge litigation. Data is compiled, plotted and evaluated to show the variations with respect to steel type, grade, heat, slab, position in thickness, rolling direction and tensile properties. The reproductibility of data from laboratory to laboratory is evaluated. Precracked Charpy impact data is presented and evaluated to show its usefulness in estimating NDT temperature. Data is plotted and evaluated to determine the effect of loading rate on transition temperature based on compact tension testing versus Charpy impact testing and also the effect of notch acuity on transition behavior in the Charpy V-notch and precrack Charpy impact testing.

17. KEYWORDS

Steel, heat slab, fracture roughness, Charpy impact test, drop weight (NDT), dynamic tear test, transition temperature, lateral expansion, subcritical crack growth.

18. No. OF PAGES:

288

19. DRI WEBSITE LINK

<http://www.dot.ca.gov/hq/research/researchreports/1974-1975/75-58.pdf>

20. FILE NAME

75-58.pdf

5537

1 GOVERNMENT ACCESSION NO		3 RECIPIENT'S CATALOG NO LIBRARY COPY	
4 TITLE AND SUBTITLE VARIABILITY OF FRACTURE TOUGHNESS IN A514/517 PLATE		5 PERFORMING ORGANIZATION NAME AND ADDRESS Transportation Laboratory October 1975	
7 AUTHOR(S) Carl E. Hartbower, F.H.W.A. and Roger D. Sunbury		6 PERFORMING ORGANIZATION CODE 14030 609925	
9 PERFORMING ORGANIZATION NAME AND ADDRESS Division of Structures California Department of Transportation Sacramento, California 95807		8 PERFORMING ORGANIZATION REPORT NO CA-DOT-DS-9925-1-75-6	
12 SPONSORING AGENCY NAME AND ADDRESS Federal Highway Administration Washington, D.C. 20590		10 WORK UNIT NO	
		11 CONTRACT OR GRANT NO DOT-FH-11-8250	
		13 TYPE OF REPORT & PERIOD COVERED Final Report	
		14 SPONSORING AGENCY CODE	

15 SUPPLEMENTARY NOTES
This study was conducted under direct contract with the Federal Highway Administration under Contract No. DOT-FH-11-8250 Case Order No. 7.

16 ABSTRACT
Fracture toughness of A514/517 steel (grades F&H) is reported for 76 plates tested during the Bryte Bend Bridge and Tuolumne River Bridge litigation. Data is compiled, plotted and evaluated to show the variations with respect to steel type, grade, heat, slab, position in thickness, rolling direction and tensile properties. The reproducibility of data from laboratory to laboratory is evaluated. Pre-cracked Charpy impact data is presented and evaluated to show its usefulness in estimating NDT temperature. Data is plotted and evaluated to determine the effect of loading rate on transition temperature based on compact tension testing versus Charpy impact testing and also the effect of notch acuity on transition behavior in the Charpy V-notch and precrack Charpy impact testing.

75-58 DND

17 KEY WORDS Steel, heat slab, fracture toughness, Charpy impact test, drop weight (NDT), dynamic tear test, transition temperature, lateral expansion, subcritical crack growth.		18 DISTRIBUTION STATEMENT Unlimited	
19 SECURITY CLASSIFICATION OF THIS REPORT Unclassified	20 SECURITY CLASSIFICATION OF THIS PAGE Unclassified	21 NO OF PAGES 288	22 PRICE

ACKNOWLEDGEMENTS

This report was prepared under the general direction of Guy D. Mancarti, Office of Research and Development, Division of Structures.

The authors are indebted to the engineers and technicians with Aerojet General Corporation, Effects Technology, Inc., Naval Research Laboratory, National Bureau of Standards, Caltrans Division of Structures and Caltrans Laboratory who have participated in the development of data used in this report. They are particularly indebted to those with Caltrans Laboratory who under the direction of Eric Nordlin have over the past five years developed, collected and evaluated much of the data used in this report.

The authors also wish to express their appreciation to the Caltrans Legal Division and in particular to attorneys Orrin Finch and Fred Graebe who were assigned to the Bryte Bend Bridge and Tuolumne River Bridge litigation.

The contents of this report reflect the views and opinions of the authors who are responsible for the facts and the accuracy of the data presented herein. The contents do not necessarily reflect the official views or policies of the State of California or the Federal Highway Administration. This report does not constitute a standard, specification or regulation.

SUMMARY AND CONCLUSIONS

Reported are the fracture-toughness data and related failure analysis of the A517 grade-H steel used in the Bryte Bend box-girder bridge. Also reported are the data from (1) the Tuolumne River bridge which contained A517 grades F and H steel from the same producer supplying the Bryte Bend bridge steel and (2) the A514/517 grades F and H steel used in repair of both bridges. A total of 76 plates (75 ingot/slabs) of A514/517 steel were tested from 30 heats involving two steel producers, two melting practices (open hearth and electric-furnace), and two grades (ASTM A514/517 H and F). The objective of the study was to provide bridge and materials engineers with (1) data on the fracture toughness of quenched-and-tempered, 100-ksi-yield, A514/517 steel and (2) information on the variability of the steel from type to type (A514 and 517), grade to grade (H and F), heat to heat, and slab to slab.

Previously, relatively few data were available to show the heat-to-heat and slab-to-slab variability in fracture toughness of A514/517 steel. This report includes data from the 76 plates of A514/517 steel tested. The data were compiled, plotted and evaluated to determine the following:

- (1) the variation in tensile properties,
- (2) the variation in Charpy properties among:

- heats
- ingots of given heat
- grades (H versus F) and
- types (A514 versus A517).

- (3) the variation in toughness with respect to position in the thickness direction in both Charpy impact and drop-weight NDT testing.
- (4) the variation in toughness as a function of rolling direction,
- (5) the variation in toughness as a function of tensile percent reduction of area and percent elongation,
- (6) the reproducibility of Charpy data from laboratory to laboratory (California Department of Transportation, National Bureau of Standards, Effects Technology Inc., Aerojet General Corporation),
- (7) the usefulness of the precrack Charpy impact test for estimating NDT temperature,
- (8) the effect of loading rate on transition temperature based on ASTM E399 compact tension versus Charpy impact testing, and
- (9) the effect of notch acuity on transition behavior in the standard Charpy V-notch (CVN) and precrack Charpy impact (PCI) testing.

Based on the findings of this investigation, the following conclusions have been drawn.

The practice of assuming inherent toughness in A514/517 "T-1" type steels is unsafe; fracture control demands testing to determine the toughness of each plate of steel.

A514/517 grade-H chemistry is marginal for plate thickness of 2 inches and greater irrespective of melting practice. Moreover, when the melting practice is such that the boron addition is unprotected, the resulting lack of hardenability is attended by undesirable microstructure and low toughness. Even with controlled sequential additions of aluminum, vanadium, titanium and boron, there were 2-inch-thick A514 grade-H heats seriously lacking in toughness (Figure 4.53).

The present Charpy V-notch (CVN) impact requirements of ASTM A517-70a and the 1974 AASHTO Interim Specification for Bridges are sufficiently stringent to disqualify brittle steel such as the heat which caused the Bryte Bend Bridge failure (Figure 4.31.2).

Steel samples from the two bridges were tested using the Charpy V-notch impact test. Of seventeen slabs (from six heats) of A517 grade-H steel tested at zero F, not a single slab met the current AASHTO requirement of 25 ft-lb for group-2 service, and only one slab met the current ASTM A517-70a CVN-impact requirement of 15-mils lateral expansion.

The heats of A514/517 grade-F steel which were supplied for repair of the Bryte Bend and Tuolumne River bridges, with very few exceptions, not only met the current CVN-impact requirements (A517-70a and AASHTO-74 but also exceeded these requirements by a wide margin (Figure 4.69).

A few heat/slabs were found where the precrack Charpy impact test showed the steel to be highly crack sensitive at the lowest anticipated service temperature; whereas, the standard CVN-impact test indicated the steel to be acceptable according to AASHTO-74 and/or A517-70a (Figure 4.43).

The precrack Charpy impact test result was demonstrated to be highly reproducible both within a given laboratory and from laboratory to laboratory using a specified precracking and testing procedure.

A correlation was established between the fatigue-precracked Charpy impact test and static fatigue-precracked ASTM E399 compact-tension test results; viz.,

$$K_{IC}^2 E = 18 \text{ (PCI)}$$

where PCI is the precrack Charpy impact value in ft-lb for a nominal fatigue precrack depth of 35 mils, E is Youngs modulus in psi and K_{IC} is the static plane-strain fracture toughness in psi-in.^{1/2}.

Bridges that were fabricated from A514/517 grade-F or grade-H steel melted by the practice followed in producing the steel used in the initial fabrication of the Bryte Bend and Tuolumne River bridges should be given extraordinary inspection on a scheduled basis.

These bridges should be given not only careful inspection but also a realistic design review. Such a design review should cover all aspects related to fatigue crack growth to determine maximum size of cracks that can be tolerated with toughness levels in the range of 50 to 100 ksi-in.^{1/2} K_{IC} . In particular, emphasis should be placed on bridge members that constitute, or are part of, a one or two load-path system.

A design review and inspection may indicate the desirability of fracture testing samples obtained from the plates in question to determine the degree of brittleness that exists at the lowest anticipated service temperature (the LAST).

Fracture control involves protecting against not only catastrophic crack propagation from a pop-in crack but also catastrophic propagation from a fatigue crack that has grown to critical size. The former source of brittle fracture involves sudden crack growth with inherently high strain rate irrespective of the service loading (crack pop-in from an embrittled weld or weld heat-affected zone, an arc strike, an improperly made tack weld, etc.). Protection against this source of brittle fracture requires that the NDT temperature of the steel be at least 30°F below the LAST or that the steel be capable of through-thickness yielding based on precrack Charpy impact testing at the LAST (Figure 4.88 and 4.53).

Fatigue crack growth as a source of brittle fracture involves two considerations in fracture testing (1) static plane-strain fracture toughness (K_{IC}) measurements to determine the critical crack size at the maximum stress and the lowest temperature anticipated in service, and (2) fatigue crack-growth-rate (da/dn) measurements to permit a determination of the number of cycles for a fatigue crack to reach critical size.

Numerical integration of the crack-growth-rate expression

$$da/dN = 0.0066 \times 10^{-6} (\Delta K)^{2.25}$$

and laboratory testing of the steel causing fracture in the Bryte Bend Bridge indicated that there may be a serious problem in getting 500,000 cycles of fracture-safe service in bridges with stresses similar to those of the Bryte Bend Bridge, which have less than 100 ksi-in.^{1/2} of plane-strain fracture toughness (Figures 4.79 and 4.79.1). This observation is in part based on generally inadequate welding quality control and, consequently, undetected weld cracks at the outset of bridge service.

From a user's point-of-view, there is no basis for setting the A514/517 grade-F Charpy-impact energy and lateral expansion values as low as they are in the AASHTO-74 and ASTM A517-70 specifications. Frequency tables and histograms showed a wide margin between what can be supplied by the steel industry and the acceptance levels of the specifications. Greater toughness can and should be required to avoid Region-III fatigue crack-growth-rate behavior. For example, thirty (30) ft-lb CVN-impact for AASHTO service groups 1, 2 and 3, and twenty-five (25) mils of lateral expansion for ASTM A514/517 steel can easily be met in A514/517 grade-F steel at temperatures down to -40°F for thickness at least to 1 1/2 inches (Figures 4.67, 4.68 and 4.69).

TABLE OF CONTENTS

	<u>Page</u>
1.0 Introduction	1
1.1 Purpose of Study	1
1.2 Background	1
1.3 Source of the Material Investigated	5
1.4 Scope of the Investigation	11
2.0 Materials Investigated	13
2.1 Identification of the 76 Plates	13
2.2 Tensile Properties	13
2.3 Chemistry of the Plates	14
3.0 Test Method	21
3.1 Standard Charpy V-Notch Impact Test	21
3.2 Precrack Charpy Impact Tests	21
3.2.1 Instrumented Precrack Charpy Impact	23
3.2.2 Temperature Measurement	25
3.2.3 Impact Machine Calibration	27
3.2.4 Raw Data Reduction	27
3.2.5 Calculation of Strength and Toughness	31
3.3 ASTM E399 Compact Tension Testing	35
3.3.1 Computer Program	39
3.4 ASTM E208 NDT Temperature Test	44
3.5 Military Standard Method for 5/8 in. Dynamic Tear Testing (MIL-STD-1601 SHIPS) 8 May 1973	45
4.0 Test Results	50
4.1 Charpy Impact Test Results	50
4.1.1 Transition-Temperature Concepts	50
4.1.2 Fatigue Precracked Charpy Testing	53
4.1.3 Current Developments in Precracked Charpy Testing	59
4.1.4 A514/517 Charpy Data Plotting	62
4.1.5 Effect of Notch Acuity	75
4.1.6 Lab to Lab Reproducibility of Charpy Data	79
4.1.7 Slab to Slab Variability	91
4.1.8 Variation in Toughness with Respect to Rolling Direction	114
4.1.9 Correlation of Toughness and Tensile Test Data	117
4.2 Charpy Impact Correlations	120
4.2.1 Background	120
4.2.2 Charpy Test Results	136
4.2.3 Upper Shelf K_{IC} - CVN Correlation	145
4.2.4 Lower Shelf K_{IC} - PCI Correlation	147
4.2.5 Through-Thickness Yielding Criteria	151
4.2.6 Inhomogeneity of Plate in the Thickness Direction	161

TABLE OF CONTENTS (Continued)

	<u>Page</u>
4.3 Summary of CVN - Impact Test Results	169
4.3.1 Procedure for Data Presentation	169
4.3.2 Frequency Tables	169
4.3.3 Frequency Distribution Histograms	170
4.3.4 Frequency Distribution in 29 Slabs from a Single Heat	180
4.4 ASTM E399 Compact Tension Test Results	194
4.4.1 Effect of "Invalid" K_{IC} Tests	204
4.4.1.1 Effect of Fatigue Precracking Discrepancies	204
4.4.1.2 Effect of Specimen Size Discrepancies	211
4.4.2 Plate to Plate Variability in K_{IC}	212
4.4.3 Discussion of the K_{IC} Test Results	214
4.4.4 Subcritical Crack Growth in Plate CK	219
4.4.5 Effect of Regions II and III on Fatigue Life	222
4.5 Drop-Weight NDT and Dynamic Test Test Results	230
4.5.1 A517 Grade-H Heat 1027/44CK	231
4.5.2 Heats 1008/76D, 1020/46AL, 1024/91Y and 1026/92A	235
4.5.3 ASTM E208-69 Drop Weight NDT Temperature	243
4.5.4 A517 Grade-H Heat 1027/44CK NDT Temperature	244
4.5.5 Heats 1008/76D, 1020/46AL, 1024/91Y and 1026/92A	246
4.6 Effect of Microstructure on Fatigue	257
5.0 References	260
6.0 Appendices	266
A. Tensile Properties of 76 Slabs from 30 Heats of A514/517 Steel as Recorded in the Mill Test Report and as Determined by Caltrans Lab.	A1 thru A11
B. Chemistry of 30 Heats of A514/517 Steel as Recorded in the Mill Test Reports and as Determined by Caltrans Lab.	B1 thru B6
C. Charpy V-Notch and Precrack Charpy Impact Test Results of 76 Slabs from 30 Heats of A514/517 Steel.	C1 thru C63
D. Effects Technology, Inc. Charpy Impact Test Results on Seven Heats of A514/517 Steel.	D1 thru D17
E. National Bureau of Standards Charpy Impact Test Results of Selected Heats of A514/517 Steel.	E1 thru E18

LIST OF TABLES

<u>Table</u>		<u>Page</u>
1.1	A514/517 Plates Investigated in Recent Researches	6
2.1.1	Identification of Steels by Type, Grade, Heat, Slab & Thickness Indexed by Plate Identification	15
2.1.2	Identification of Steels by Type, Grade, Heat, Slab & Thickness Indexed by Heat & Slab	18
4.1	Test Plan for NBS Charpy Impact Testing and Computer Evaluation of A517-H Heat 1027/44	80
4.2	Charpy V-Notch Impact Data from Seven Slabs of A517-F Heat 1006	92
4.3	Precracked Charpy Impact Data from Seven Slabs of A517-F Heat 1006	93
4.4	Precracked Charpy Impact Energy and Lateral Expansion Values from Twenty-Nine Slabs of A517-F Heat 1006 Tested at Plus 20°F	95
4.5	Standard CVN - Impact Tests Showing the Effect of Specimen Orientation	116
4.6	Increase in Transition Temperature as a Result of Impact Loading (Reference 3)	128
4.7	U. S. Steel Plane-Strain Fracture-Toughness Data for A517-F Heat 73A377	146
4.8	Plane-Strain Fracture Toughness Calculated from Charpy V-Notch Upper-Shelf Energy	146
4.9	Transition-Range Charpy- K_{IC} Correlation Data	149
4.10	Charpy Energy Requirements for Through-Thickness Yielding	154
4.11	Standard Charpy V-Notch Impact Properties from Twenty-Nine Slabs of A517-F Heat 1006 (Mill Test Data)	185

LIST OF TABLES (Continued)

<u>Table</u>		<u>Page</u>
4.12	Standard Charpy V-Notch Impact Properties from Sixteen Heats, Twenty-Four Slabs of A514/517 Grade-F Steel	186
4.13	Standard Charpy V-Notch Impact Properties from Twelve Heats, Twenty-Five Slabs of A514/517 Grade-H Steel	187
4.14	Frequency Distribution for CVN-Impact Energy and Lateral Expansion in 74 Slabs of A514/517 Grade-F and Grade-H Steel at Selected Test Temperatures	188
4.15	Arithmetic Mean Values of CVN-Impact Energy and Lateral Expansion in A514/517 Grade-H and Grade-F Steels Tested at Selected Temperatures	189
4.16	Summary of A514/517 Grade-F CVN-Impact Test Results	190
4.17	Summary of A514/517 Grade-H CVN-Impact Test Results	191
4.18	Slab-to-Slab Variability in Selected Heats A514/517 Grade-F	192
4.18a	Slab-to-Slab Variability in Selected Heats A514/517 Grade-H	193
4.19	Summary of One-Inch-Thick Compact Tension Test Results for Seven A514/517 Steels	195
4.20	Summary of two-Inch-Thick Compact-Tension Test Results for Seven A514/517 Steels	196
4.21	Transition-Temperature Shift Due to Rate of Loading (Static K_{Ic} vs PCI)	205
4.22	Fatigue Precracking Discrepancies in Compact-Tension Tests	206
4.23	Summary of Compact-Tension Test Results from A517 Grade-H Plate CK-2	213
4.24	Temperature at the onset of Elastic-Plastic Behavior Under Plane-Strain Static Loading and Calculated Critical Crack Sizes at the LAST for AASHTO-74 Group-1 Service	216

LIST OF TABLES (Continued)

<u>Table</u>		<u>Page</u>
4.25	Predicted Life in a 30-Inch-Wide Flange as a Function of Edge Crack Depth, Fracture Toughness and Stress Range	228
4.26	Dynamic Tear Test Results from A517 Grade-H Heat 1027/44 CK as a Function of Thickness Position	231
4.27	Dynamic Tear Test Results from Selected Heats of A514/517 Grade-F and Grade-H Steels	235
4.28	ASTM E208 Drop-Weight NDT Temperatures for A517 Grade-H Heat 1027/44 CK	245
4.29	ASTM E208 Drop-Weight NDT Temperatures for Selected Heats of A514/517 Grade-F and Grade-H Steels	247
4.30	Summary of E208 NDT Temperatures and Dynamic Tear Test and Precrack Charpy Impact NDT Estimates	250

LIST OF FIGURES

<u>Figure</u>		<u>Page</u>
1.1	Typical Section of the Bryte Bend Bridge	2
1.2	Fracture Surface of Casualty Flange in Bryte Bend Bridge	3
1.3	Location of Heats and Slabs in the Bryte Bend Bridge	8
1.4	Location of Heats and Slabs in the Tuolumne River Bridge	9
3.1	Physmet (ManLabs) Charpy Impact Testing Machine (Photograph)	22
3.2	Instrumented Charpy Impact Testing System(<u>13</u>)	24
3.3	Typical Raw-Data Record from Instrumented Charpy Impact Testing System(<u>13</u>)	26
3.4	Idealized Load-Deflection Record(<u>13</u>)	29
3.5	Typical Raw-Data Tabulation(<u>13</u>)	30
3.6	Relationship of Equivalent Energy Fracture Load P* to the Actual Fracture Load(<u>13</u>)	34
3.7	Typical Fracture Toughness Results Tabulation(<u>13</u>)	36
3.8	Two-Inch-Thick Compact-Tension Specimen Dimensions and Tolerances	38
3.9	Double-Cantilever Displacement Gage	42
3.10	Computer-Printed Tabulation of Compact-Tension-Test Results	43
3.11	Double-Pendulum Machine of 2000 ft-lb Capacity for Testing 5/8-DT Specimens (Reference 22)	47
3.12	DT Test Results from Two Laboratories, Testing 5/8 in. Thick A514/517 Grade D Plate	49

LIST OF FIGURES (Continued)

<u>Figure</u>		<u>Page</u>
4.1	Charpy-Test Transition Temperatures Including Fracture Mode Transition	53
4.2	Comparison of Static, Dynamic and Instrumented Precracked Charpy Impact Fracture Toughness as a Function of Temperature	57
4.2.1	Comparison of V-Notch and Precracked Charpy Data with 5/8 in. Dynamic Tear Data on A533-B Steel(27)	58
4.3	ASTM E24.03.03 Precracked Charpy Round-Robin Phase-I Test Matrix (<u>NBS</u>)	61
4.4	Precrack Charpy Impact Transition Curve for A517-F Plate B Based on Energy Absorption and Lateral Expansion	64
4.5	Relationship Between Energy Absorption and Lateral Expansion in Precrack Charpy Impact Tests of A514/517 Grade F Steels	66
4.6	Relationship Between Energy Absorption and Lateral Expansion in Precrack Charpy Impact Tests of A514/517 Grade H Steels	67
4.7	Relationship Between Energy Absorption and Lateral Expansion in Standard Charpy V-Notch Impact Tests of A514/517 Grade F Steels	68
4.8	Relationship Between Energy Absorption and Lateral Expansion in Standard Charpy V-Notch Impact Tests of A514/517 Grade H Steels	69
4.9	CVN-Impact Energy Absorption and Lateral Expansion Transition Curves for A517-F Plate B	70
4.10	CVN-Impact and PCI Transition Curves for A517-F Plate A	72
4.11	Effects Technology, Inc. PCI W/A - versus - Temperature Plot for A517-F Plate A	74
4.12	CVN-Impact and PCI Transition Curves for A514-H Plate L	76

LIST OF FIGURES (Continued)

<u>Figure</u>		<u>Page</u>
4.13	CVN-Impact and PCI Transition Curves for A514-F Plate J	77
4.14	CVN-Impact and PCI Transition Curves for A514-F Plate CB	78
4.15	Lab-to-Lab Variability in CVN-Impact and PCI Tests of A517-H Plate CK	84
4.16	Super Position of Effects Technology, Inc. Precrack Charpy Impact Data on Aerojet General Corp. Data for A517-F Plate A	85
4.17	Super Position of Effects Technology, Inc. Precrack Charpy Impact Data on Aerojet General Corp. Data for A517-H Plate AL	86
4.18	Super Position of Effects Technology, Inc. Precrack Charpy Impact Data on Aerojet General Corp. Data for A514-H Plate L	87
4.19	Super Position of Effects Technology, Inc. Precrack Charpy Impact Data on Aerojet General Corp. Data for A514-F Plate M	88
4.20	Super Position of Effects Technology, Inc. Precrack Charpy Impact Data on Aerojet General Corp. Data for A514-H Plate R	89
4.21	Super Position of Effects Technology, Inc. Precrack Charpy Impact Data on Aerojet General Corp. Data for A517-H Plate Z	90
4.22	Histogram of PCI Values at +20°F from 29 Slabs of A517-F Heat 1006	96
4.23	PCI Tests of Four Slabs from A517-H Heat 1020	98
4.24	PCI Tests of Three Slabs from A517-H Heat 1024	99
4.24.1	CVN-Impact Tests of Three Slabs from A517-H Heat 1024	100
4.25	PCI Tests of Three Slabs from A517-H Heat 1027	101
4.26	Lateral Expansion Data from CVN-Impact and PCI Tests of Seven Slabs from Heat 1006	103

LIST OF FIGURES (Continued)

<u>Figure</u>		<u>Page</u>
4.27	Lateral Expansion Transition Behavior from CVN-Impact Tests of Seven Slabs of A517-F Heat 1006	104
4.27.1	Lateral Expansion Transition Behavior from PCI Tests of Seven Slabs of A517-F Heat 1006	105
4.28	Lateral Expansion Transition Behavior from CVN-Impact Tests of Three Slabs of A517-F Heat 1001	106
4.28.1	Lateral Expansion Transition Behavior from PCI Tests of Three Slabs of A517-F Heat 1001	107
4.29	Lateral Expansion Transition Behavior from CVN-Impact Tests of Three Slabs of A517-F Heat 1004	108
4.29.1	Lateral Expansion Transition Behavior from PCI Tests of Three Slabs of A517-F Heat 1004	109
4.30	Lateral Expansion Transition Behavior from CVN-Impact Tests of Four Slabs of A517-H Heat 1020	110
4.30.1	Lateral Expansion Transition Behavior from PCI Tests of Four Slabs of A517-H Heat 1020	111
4.31	Lateral Expansion Transition Behavior from CVN-Impact Tests of Three Slabs of A517-H Heat 1022	112
4.31.1	Lateral Expansion Transition Behavior from PCI Tests of Three Slabs of A517-H Heat 1022	113
4.31.2	Longitudinal and Transverse CVN-Impact and PCI Transition Curves for A514-H Heat 1027-44 CK	115
4.31.3	Correlation of CVN Impact Energy and % Reduction of Area of A514/517 Grades F and H	118
4.31.4	Correlation of CVN Impact Energy and % Elongation of A514/517 Grade F and H.	119
4.32	Limiting Yielding Strength, Plate Thickness and Fracture Toughness for Valid K_{Ic} Determinations Per ASTM E399	121
4.33	K_{Ic} Temperature Transition for A517-F Steel (Reference 32)	123
4.34	Energy, Lateral-Expansion and Fracture-Appearance Transition Curves from Standard CVN-Impact Tests of A517-F Heat 73B320 (Reference 32)	124

LIST OF FIGURES (Continued)

<u>Figure</u>		<u>Page</u>
4.35	Energy, Lateral-Expansion and Fracture-Appearance Transition Curves from PCI Tests of A517-F Heat 73B320 (Reference 32)	125
4.36	K_{IC} and PCI Temperature Transition Based on Data from Reference 32	126
4.37	Prediction of Dynamic K_{IC} Based on Precrack Charpy PCI and PCSB Tests (Reference 4)	129
4.38	Static and Dynamic K_{IC} Predictions Based on PCSB and PCI Testing	130
4.39	Upper-Shelf CVN-Impact K_{IC} Correlation (Reference 31)	132
4.40	CVN-Impact and PCI Transition Curves for A517-F Heat-Slab 1026-92	137
4.41	CVN-Impact and PCI Transition Curves for A517-H Heat-Slab 1020-46	138
4.42	CVN-Impact and PCI Transition Curves for A517-H Heat-Slab 1027-44	139
4.43	CVN-Impact and PCI Transition Curves for A514-F Heat-Slab 1017-62	140
4.44	CVN-Impact and PCI Transition Curves for A514-F Heat-Slab 1014-02	141
4.45	CVN-Impact and PCI Transition Curves for A514-H Heat-Slab 1019-31	142
4.46	CVN-Impact and PCI Transition Curves for A517-H Heat-Slab 1024-94	143
4.47	Reinforcement of the Energy-Temperature Plot with Lateral Expansion in A517-F Plates A and B	144
4.48	Upper-Shelf CVN-Impact Estimate of K_{IC} Fracture Toughness (solid symbols are ASTM E399 valid K_{IC} values; open symbols are CVN- K_{IC} estimated values)	148

LIST OF FIGURES (Continued)

<u>Figure</u>		<u>Page</u>
4.49	Transition - Range CVN-Impact Correlation with Static Compact Tension K_{IC} Test Results (valid K_{IC} data from Table 4.9)	150
4.50	Transition - Range Precrack Charpy Impact Correlation with ASTM E399 Valid K_{IC} Data (valid K_{IC} data from Table 4.9)	152
4.51	CVN-Impact Requirement at 0°F for Through-Thickness Yielding Based on the U.S. Steel Transition Temperature CVN- K_{IC} Correlation (Equation 4.12)	156
4.52	CVN-Impact Requirements at 0°F for Through-Thickness Yielding Based on the Upper-Shelf Correlation (Equation 4.3) and the Transition-Range Correlation (Equation 4.12-dashed lines)	158
4.53	PCI Requirements at 0°F for Through-Thickness Yielding Based on the Precrack Charpy Impact PCI- K_{IC} Correlation (Equation 4.13)	160
4.54	PCI Transition Curve for the Quarter-Point Position in A517-F Plate A	162
4.55	PCI Transition Curve for the Quarter-Point Position in A517-F Plate B	163
4.56	PCI Transition Curve for the Quarter-Point Position in A517-H Plate AL	164
4.57	PCI Transition Curve for the Quarter-Point Position in A517-H Plate Y	165
4.58	PCI Transition Curve for the Quarter-Point Position in A517-H Plate Z	166
4.59	CVN-Impact and PCI Transition Curves for the Surface, Midthickness and 1/4 Point Positions in A517-H Plate AL	168
4.60	Histogram of CVN-Impact Energy Values from 74 Slabs Tested at +20°F	171
4.61	Histogram of CVN-Impact Energy Values from 20 A514/517 Grade-H Slabs and 53 A514/517 Grade-F Slabs Tested at +20°F	173

LIST OF FIGURES (Continued)

<u>Figure</u>		<u>Page</u>
4.62	Histogram of CVN-Impact Lateral Expansion Values from 20 A514/517 Grade-H Slabs and 53 A514/517 Grade-F Slabs Tested at +20°F	175
4.63	Histogram for CVN-Impact Energy Values from 25 A514/517 Grade-H Slabs and 32 A514/517 Grade-F Slabs Tested at 0°F	176
4.64	Histogram for CVN-Impact Lateral Expansion Values from 25 A514/517 Grade-H Slabs and 32 A514/517 Grade-F Slabs Tested at 0°F	177
4.65	Histogram for CVN-Impact Energy Values from 25 A514/517 Grade-H Slabs and 34 A514/517 Grade-F Slabs Tested at -40°F	178
4.66	Histogram for CVN-Impact Lateral Expansion Values from 25 A514/517 Grade-H Slabs and 34 A514/517 Grade-F Slabs Tested at -40°F	179
4.67	Histogram for CVN-Impact Energy Values from 29 A517 Grade-F Slabs of Heat 1006 Tested at +20°F	181
4.68	Histogram for CVN-Impact Lateral Expansion Values from 29 A517 Grade-F Slabs of Heat 1006 Tested at +20°F	182
4.69	Histogram for CVN-Impact Energy Values from 27 A517 Grade-F Slabs of Heat 1006 Tested by The Steel Producer at Minus 50°F	183
4.70	Static Compact-Tension and Precrack Charpy Impact Test Results for A517-F Plate A	197
4.71	Static Compact-Tension and Precrack Charpy Impact Test Results for A517-H Plate AL	198
4.72	Static Compact-Tension and Precrack Charpy Impact Test Results for A514-F Plate L	199
4.73	Static Compact-Tension and Precrack Charpy Impact Test Results for A514-F Plate M	200

LIST OF FIGURES (Continued)

<u>Figure</u>		<u>Page</u>
4.74	Static Compact-Tension and Precrack Charpy Impact Test Results for A517-H Plate CK-1	201
4.75	Static Compact-Tension and Precrack Charpy Impact Test Results for A514-H Plate R	202
4.76	Static Compact-Tension and Precrack Charpy Impact Test Results for A517-H Plate Z	203
4.76.1	Compact Tension Test Results Showing Scatter Produced by Deviating from ASTM E399 Test Requirement - Plates Z and L	209
4.76.2	Compact Tension Test Results Showing Scatter Produced by Deviating from ASTM E399 Test Requirement - Plates AL and R	210
4.77	Static Compact-Tension Test Results for A517 Grade-H Plates CK-1 and CK-2 from Heat/Slab 1027-44	215
4.78	Schematic Representation of Fatigue-Crack Growth in Steel (Reference 46)	218
4.79	Log-Log dA/dN vs ΔK Plots for Two 1-inch-WOL Fatigue Crack Growth Rate Tests of Each of Two Plates - A517-F Plate D and A517-H Plate CK Tested at 45 ksi Maximum Stress and a 0.73 Stress Ratio	220
4.79.1	Computer Plotted Curves Showing Fatigue Life of an Edge Cracked 30" Wide Flange with $R = 33 \text{ ksi}/45 \text{ ksi}$	224
4.79.2	Computer Plotted Curves Showing Fatigue Life of an Edge Cracked 30" Wide Flange with $R = 27 \text{ ksi}/39 \text{ ksi}$	225
4.79.3	Computer Plotted Curves Showing Fatigue Life of an Edge Cracked 30" Wide Flange with $R = 33 \text{ ksi}/39 \text{ ksi}$	226
4.80	Dynamic Tear Test Results from A517 Grade-H Heat 1027/44 CK for Surface and Midthickness Positions	232
4.81	Force-Time Traces Corresponding to Selected Temperatures in Figure 4.80 Midthickness Position	234

LIST OF FIGURES (Continued)

<u>Figure</u>		<u>Page</u>
4.82	Dynamic Tear and Precrack Charpy Impact Test Results from Two Heats of A517 Grade-F Steel By Different Melting Practices	237
4.83	Dynamic-Tear-Test Force-Time Traces of A517 Grade-F Plate A	238
4.84	Dynamic Tear and Precrack Charpy Impact Test Results from A517 Grade-H Heat 1024/44 CK	239
4.85	Dynamic Tear and Precrack Charpy Impact Test Results from A517 Grade-H Heat 1020/46 AL	240
4.86	Dynamic Tear and Precrack Charpy Impact Test Results from A517 Grade-H Heat 1024/91Y	241
4.87	Summary of Dynamic Tear Test Results on Selected Heats of A514/517 Steel with ASTM E208 NDT Temperatures Indicated	242
4.88	ASTM E208 Drop-Weight NDT Temperature Test Results for A517 Grade-F Plates of Two Melting Practices and Bryte Bend Bridge Casualty Plate A517 Grade-H Heat 1027/44 CK	248
4.89	ASTM E208 Drop-Weight NDT Temperature Test Results for A517 Grade-H Plates Y and AL	249
4.90	Specimen Positions Relative to Hardness and Microstructure in Plate-A Thickness	252
4.91	E208 NDT Specimens Heat Tinted and Broken Apart to Show the Extent of Fracture in the NDT Testing (The E208 NDT Temperature was 0°F)	255
4.92	Crack Arrest in the Weld Heat-Affected Zone of Plate A ASTM E208 NDT Test of Specimen A-5	256
4.93	Fracture Surface in 2 inch Compact Tension Specimen from Plate AL	258
4.94	Fracture Surfaces in 2 inch Compact Tension Specimens from Plates R, M, L, Z, AL and A	259

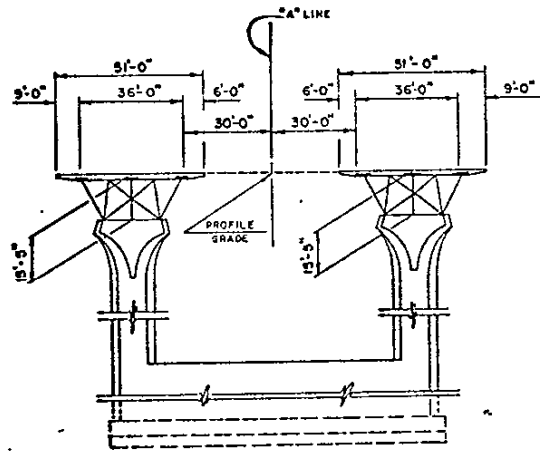
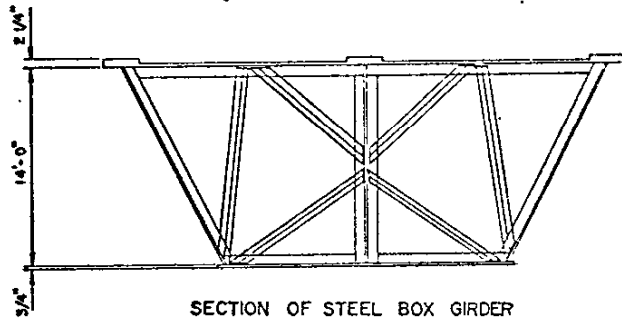
FRACTURE TOUGHNESS OF A514/517 STEEL1. Introduction1.1 Purpose of the Study

The objective of this report is to provide bridge engineers and material engineers with (1) data on the fracture toughness of quenched-and-tempered, 100-ksi yield-strength, A514/517 steel and (2) information on the variability of the steel from type to type (A514 and A517), grade to grade (H and F), heat to heat and slab to slab.

1.2 Background

On June 13, 1970, a large steel box-girder bridge under construction west of Sacramento, California developed a brittle fracture in one of three tension flanges over pier 12 as the concrete deck was being placed. The bridge consists of two parallel three-lane structures, each made up of a two cell trapezoidal box-girder section with three separate top flanges (Figure 1.1). The flanges over piers 12, 13 and 14 were 30-in. wide and 2-1/4-in. thick. The failure occurred catastrophically across the full width of a 30-in.-wide flange and was arrested about 4-in. down the web of the girder (Figure 1.2). The ambient temperature was +58°F. The steel was ASTM A517 grade H modified. By ASTM Specification, A514/517 grade H is limited to 2-in. thickness; for this bridge, grade H was allowed in thicknesses up to 2-1/4-in.

At the time that the bridge was designed and when the steel was purchased, toughness in A517 steel was taken for granted and was not a specification requirement. Of seventy-six bridges built in the United States prior to 1970 using A514/517 steel or comparable quenched and tempered proprietary steels, Charpy



TYPICAL SECTIONS OF THE BRYTE BEND BRIDGE

FIGURE I.1



2-1/4-IN.-THICK, 30-IN.-WIDE, FRACTURED FLANGE



FRACTURE ORIGIN AT WELD BETWEEN FLANGE AND
CROSS BRACING

FRACTURE SURFACE OF CASUALTY
FLANGE IN BRYTE BEND BRIDGE

FIGURE 1.2

V-notch impact testing was specified in the plans of only three bridges. In 1970, ASTM A517-70a provided a Charpy V-notch impact test requirement of 15-mils lateral expansion (at a temperature specified in the order but not higher than 32°F). In 1974, AASHTO adopted a Charpy V-notch impact test requirement for A514 steel of 25 ft-lb at 30°F for service involving ambient temperatures down to 0°F. Of the twelve 2-1/4-in.-thick plate samples cut from the casualty bridge, only two would have been found acceptable if the ASTM A517-70a or the AASHTO Charpy specifications had been in effect at the time the bridge steel was purchased.

Fracture-toughness studies performed subsequent to the bridge failure have demonstrated significant variations in this property for A514/517 steel. Results of these studies suggest that the very limited sampling employed in earlier fracture-mechanics research may have been inadequate to encompass variations observed, with the consequence that current specifications based on these earlier studies may be unconservative.

An assumption that the results of toughness tests on coupons from selected heats of steel in a structure of appreciable size are "representative" of all heats could endanger the structure or result in costly repairs.

Bridge engineers have been warned(1)* that

"The basic problem is not one of finding steel with adequate notch toughness to prevent brittle fracture, because steels that are extremely tough at all surface temperatures are available...however, it is possible for the inherent notch toughness of these steels to vary depending upon manufacturing variables, even though the material meets an existing materials specification such as ASTM. Thus, although a particular steel has had adequate notch toughness to perform satisfactorily in previous structural applications, the designer has no assurance that each and every new plate of the same grade of steel will have the same toughness level in future structural applications."

*Numbers in parenthesis refer to items in Section 5.0 References.

In four major studies involving bridge steels (FHWA-RD-74-59 DOT-FH-11-7836, NCHRP 12-14 and AISI Project 168), only eight heats of A514/517 steel were investigated. In the U.S. Steel researches providing back-up information for the present AASHTO Charpy V-notch (CVN) impact specifications, only two heats of A517 steel were used; furthermore, AISI Project 168, which was the principal basis for the new AASHTO toughness specifications, provided no A514/517 steel data. None of the studies included grade H.

Table 1.1 shows the A514/517 heats and plate sizes that have been investigated either directly in support of bridge construction, or indirectly as a basis for the AASHTO CVN impact specifications. In general, the materials listed in Table 1.1 were supplied from a single slab from the indicated heat. Only one heat had low toughness, with 25-ft-lb CVN-impact energy at +80°F; this heat would have been rejected by the current AASHTO specification. All other heats investigated easily passed the AASHTO specification. Plate thicknesses ranged up to three inches.

Plates used in the box girder flanges of the Sacramento River Bridge and Overhead, at Bryte Bend, were fabricated from fifteen slabs, comprising four heats, of A517-H steel. Plates used in the flanges of the Tuolumne River Bridge, on State Highway 49, constructed at nearly the same time, were fabricated from ten slabs comprising five heats, of A517-F and A517-H steel. In these plates, toughness varied from heat to heat and even from slab to slab in a given heat.

1.3 Source of the Material Investigated

When it was discovered that the heat of steel causing failure of the Bryte Bend Bridge had low toughness, samples were cut from the flanges elsewhere in the bridge to determine if the

TABLE 1.1

ASTM A514/517 PLATES INVESTIGATED IN RECENT RESEARCHES

<u>RESEARCH PROJECT</u>	<u>STEEL TYPE & GRADE</u>	<u>HEAT NO.</u>	<u>PLATE THICK</u>	<u>CVN-imp. 25FT-LB</u>	<u>REFERENCE REPORT</u>
FHWA-RD-74-599	A514-M	533Z0023	1/2	-110°F	"Fracture Toughness of Bridge Steels, Phase I" (Ref. 61)
	A514-P	521X0027	1	-20°F	
	A514-M	532Z0265	2	-100°F	
NCHRP 12-14	A514-E	50343	1	-100°F	"Subcritical Crack Growth in Steel Bridge Members" (Ref. 46)
	A514-F	70C125	1	-90°F	
DOT-FH-11-7836	A514-E	50478	3	+80°F	"Stress-Corrosion Susceptibility of Highway Bridge Construction Steels - Phase IIA" (Ref. 60)
	A514-F	71D653	3	-100°F	
	A514-J	516A0689	1	-160°F	
U.S. Steel Research	A517-F	73B320	1&2	-140°F	(ref 2)
	A517-F	73A377	1&2	-60°F	(ref 3-6)

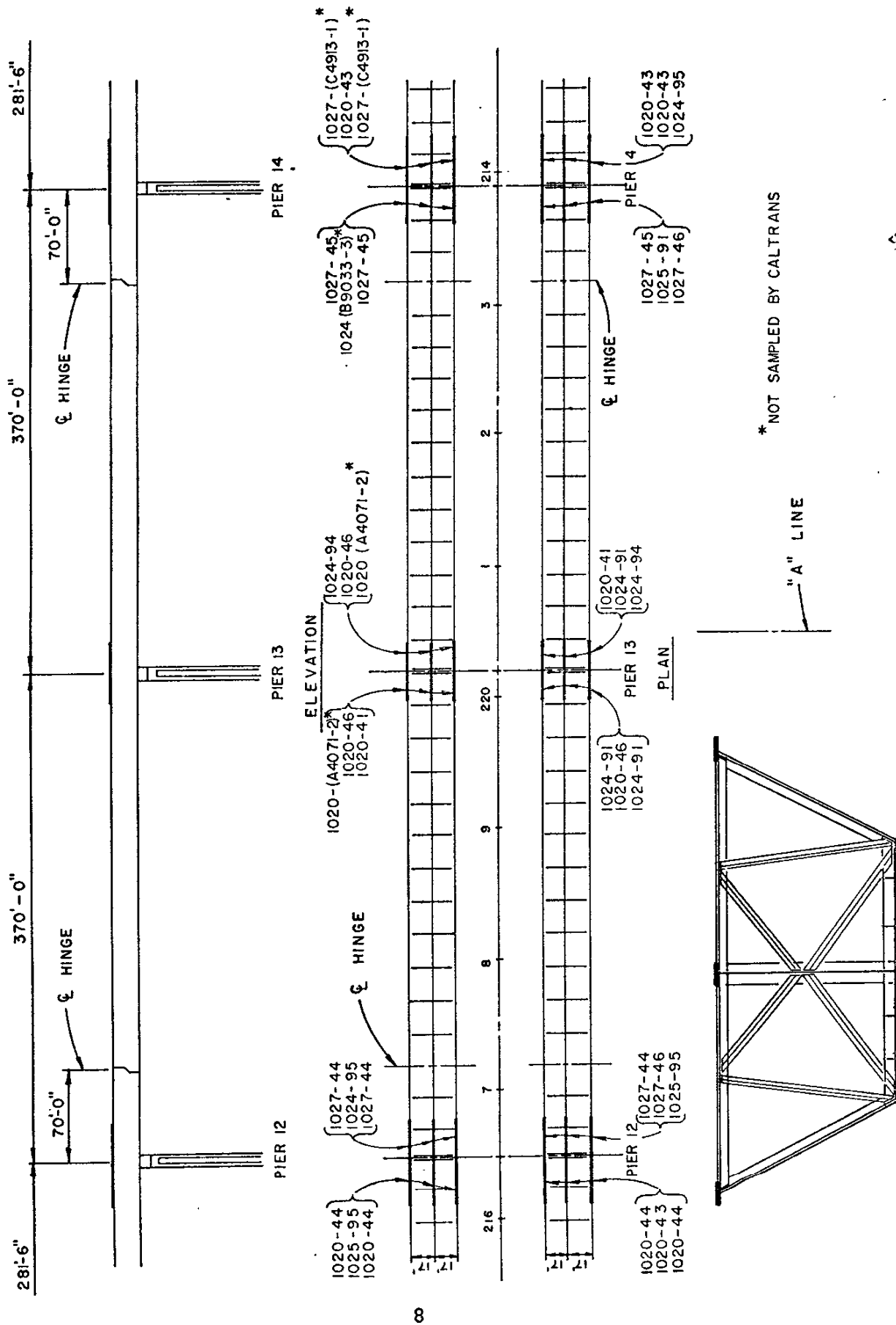
condition was confined to the one flange plate or a single slab (each heat provided several slabs; each slab, rolled to 2-1/4-in.-thick plate, provided up to three 30-in.-wide flange plates). The heat of steel in which the failure of the Bryte Bende bridge occurred was present in the bridge in ten different locations, involving four slabs. Twelve 2-1/4-in.-thick plate samples, involving four heats, including the heat in which the fracture occurred, were tested. All but two of the twelve plates were found to have low toughness. The position of the various heats and slabs in the Bryte Bende bridge is shown in Figure 1.3.

The Tuolumne River Bridge was being fabricated at the same time as the Bryte Bend Bridge which developed the brittle fracture, using A517 steel from the same supplier. Seven plate samples were taken from this bridge, involving four heats of steel in thicknesses ranging from 2 to 2-1/2 in. The position of the various heats and slabs in the Tuolumne River bridge is shown in Figure 1.4.

Inadvertently, two of the plates used in this bridge were A517-F rather than A517-H. Again the steel was found to have low toughness; none of the plates would have been found acceptable if the ASTM A517-70a or the AASHTO CVN-impact specifications had been in effect at the time the bridge steel was purchased.

Because of the low toughness of the A517-H and A517-F steel, both bridges were reinforced with bolted cover plates of A517-F steel. The steel used for the cover plates was subjected to both standard Charpy V-notch and precrack Charpy impact testing, with 15-mils lateral expansion in the CVN-impact test at the lowest anticipated service temperature a condition of purchase.

The above toughness requirement was not written into the purchase order, but a sample was requested by Caltrans for chemical analysis, and tensile and Charpy testing before each repair plate was purchased. Only three plates were rejected for not meeting 15-mils lateral

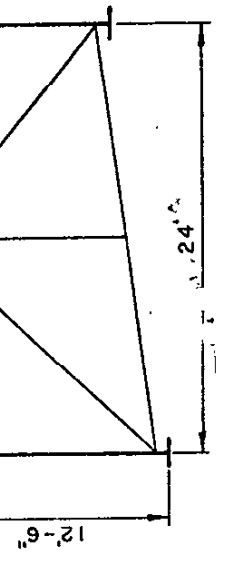
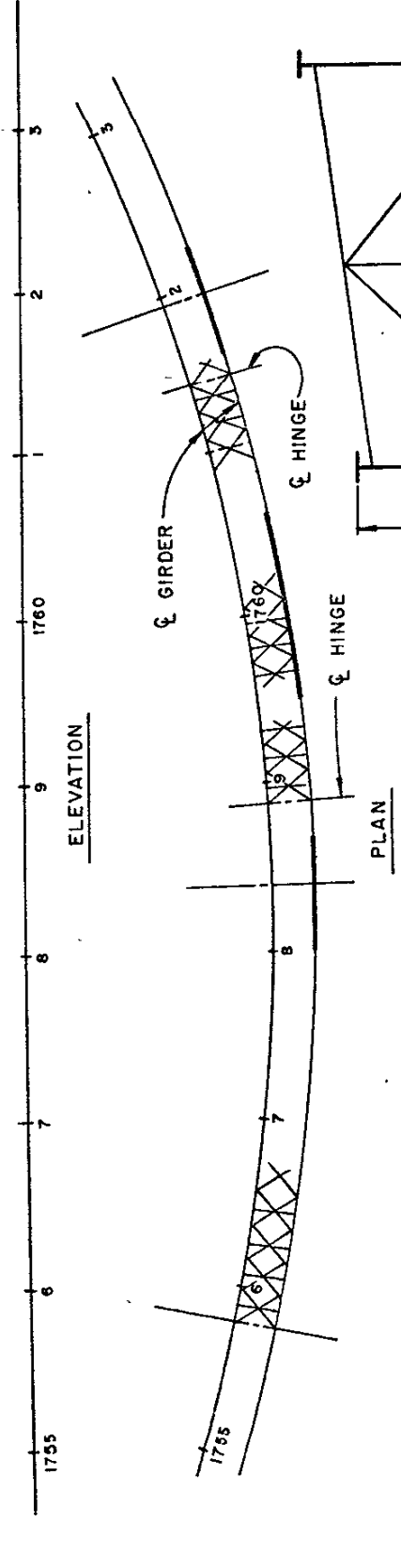
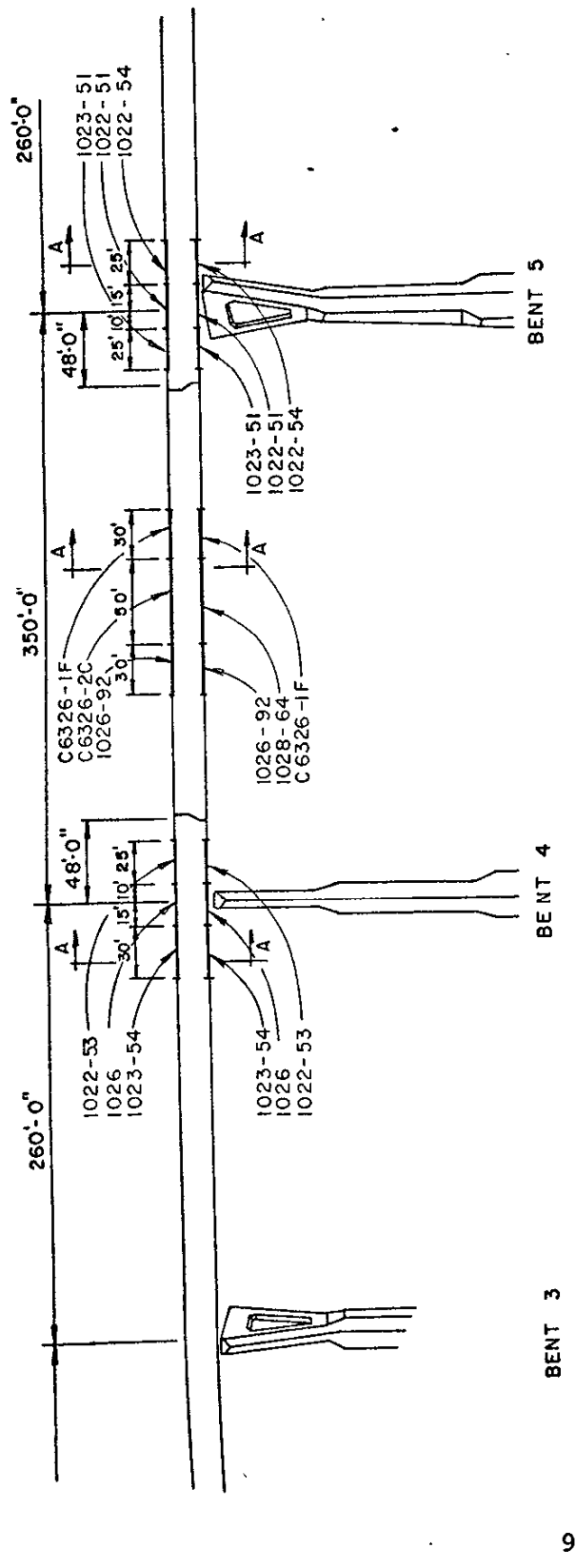


* NOT SAMPLED BY CALTRANS

"A" LINE

FIGURE 1.3 LOCATION OF HEATS AND SLABS IN THE BRYTE BEND BRIDGE

TYPICAL SECTION



LOCATION OF HEATS AND SLABS
IN THE TUOLUMNE RIVER BRIDGE

SECTION A-A

FIGURE 1.4

expansion at the lowest anticipated service temperature (LAST). All three of the rejected plates were 2-in.-thick A514 grade H; two of the plates were from the same heat. All three of the rejected plates also would have been rejected by AASHTO-74 (25 ft-lb at +30°F). The A517 grade-H plates in the bridges which necessitated the repair were 2-1/4-in. and 2-1/2-in. thick and, therefore, were not in compliance with ASTM A517 grade-H which is limited to 2-in.-thick plate. The fact that the 2-in.-thick A514 grade H plates also had low toughness suggested that the problem was not the allowed deviation from the ASTM thickness limitation.*

The rejected 2-in.-thick A517 grade-H plates with low toughness as well as the 1-3/8-in.-thick A517 grade-F plates used in the cover-plating repair of the bridges were open-hearth steel procured from warehouses or directly from the steel producers. A total of 45 plates were procured for cover plating; all of these plates were found to have acceptable toughness.

Files pertinent to the Bryte Bend and Tuolumne bridges contain fracture toughness information from seventy-six (76) plates of A514/517 steel. The fracture toughness data are for steels from two manufacturers producing two types and grades, with thirty heats ranging in thickness from 7/8 to 2-1/2 in. The testing confirmed Professor Rolfe's observation(1) that "...the designer has no assurance that each and every new plate of the same grade of steel will have the same toughness level...". Charpy values ranging from approximately 6 to 60 ft-lbs were measured in steels from a single type and grade at 0°F.

*Several heats of 1-1/2 to 1-3/4-in.-thick electric-furnace A517 grade-H steel produced for a third bridge (in another State) have been found to have low toughness, failing the AASHTO-74 group-2 service requirement (25 ft-lb at 0°F).

Selected heats were Charpy tested: (1) longitudinally and transversely with respect to principal rolling direction; and, (2) at the quarter-point and mid-thickness positions.

Selected heats also were Charpy tested in a number of laboratories including that of the National Bureau of Standards to determine the variability among various testing Laboratories, and selected heats were tested by Effects Technology Inc., using instrumented precrack Charpy impact to measure K_{Id} .

1.4 Scope of the Investigation

The following report provides (1) a compilation of all fracture test findings obtained in connection with the Bryte Bend and Tuolumne River bridges; and, (2) an evaluation of the findings in terms of product variability and fracture toughness specification requirements.

The compilation of tables and figures provide information pertinent to the variation in:

(a) tensile and Charpy properties among:

- (1) heats,
- (2) slabs of a given heat,
- (3) types (A514 vs A517), and
- (4) grades (H vs F)

(b) effect of notch acuity in the Charpy impact test as determined by comparing transition curves obtained from standard (10-mil-radius) V-notch Charpy impact specimens and fatigue-precracked Charpy impact specimens;

(c) reproducibility of Charpy data (National Bureau of Standards, Aerojet General Corporation and Caltrans Laboratory);

(d) variations in toughness with respect to position in the thickness direction in both Charpy impact testing and drop-weight NDT testing;

(e) variations in toughness as a function of rolling direction (cross-rolling ratio);

(f) usefulness of the precrack Charpy impact transition temperature for estimating the nil-ductility-transition (NDT) temperature; and

(g) the effect of loading rate on shift of transition temperature based on ASTM E399 compact-tension testing and Charpy impact testing.

Plates and heats for which data are now available from the Bryte Bend Bridge failure analysis and from the cover plate reinforcement steel procured for the Bryte Bend and Tuolumne river bridges include twenty-one (21) plates of A517 steel from one supplier and fifty-five (55) plates of A514/517 steel from a second supplier. The data included tensile, chemistry, Charpy V-notch (CVN), and precrack Charpy impact (PCI) tests over a range of test temperatures.

In addition to the tensile and Charpy testing of all heats, selected heats were tested, (1) under static (slow) loading using ASTM E399 compact-tension tests (K_{IC}); and, (2) dynamically (at the Naval Research Laboratory), using 5/8-in. dynamic tear tests, and drop-weight nil-ductility transition (NDT) temperature tests.

2.0

MATERIALS INVESTIGATED

2.1 Identification of the 76 Plates

Table 2.1 identifies the A514/517 steels according to type, grade, heat, slab and thickness. The 76 plates have been coded to provide a uniform system, permitting a distinction between types, grades, heats and slabs. Thus, the plate coded

A514 F 1013/32J

shows the steel to be ASTM type A514 grade F, heat 1013, slab 32. The final letter J provides a shortened code designation for this particular plate. However when only the alphabetical code is used, say K and P

A514 H 1016/11K

and

A514 H 1016/41P

the fact that these plates were from a single heat (1016) would be hidden.

For reader convenience, the steels are listed in two ways; Table 2.1.1 indexes the steels by an abbreviated plate code and Table 2.1.2 indexes the steels by heat and slab number.

2.2 Tensile Properties

The tensile properties (1) as obtained from the steel-producers' material certifications and (2) as determined by the California Department of Transportation Laboratory are presented in Appendix A. The test specimen was the 0.505-in.-dia tensile as specified by ASTM A370.

2.3 Chemistry of the Plates

The chemistry of the plates (1) as obtained from the steel producers' material certifications and (2) as determined by the California Department of Transportation Laboratory is presented in Appendix B.

TABLE 4.1.1

IDENTIFICATION OF STEELS BY TYPE, GRADE, HEAT, SLAB AND THICKNESS
INDEXED BY PLATE IDENTIFICATION

<u>ID</u>	<u>ASTM TYPE-GRADE</u>	<u>REPORT CODE HEAT/SLAB</u>	<u>STEEL COMPANY HEAT/SLAB</u>	<u>PLATE THICK</u>
A	A517-F	1026/92	B9863-2C	2-1/4
B	A517-F	1028/64	C6369-4	2-1/2
C	A517-H	1022/51	A5491-1B	2-1/2
D	A517-F	1008/76	74E002-001876	2-1/2
E	A517-H	1023/54	A5550-4A	2
F	A517-H	1022/53	A5491-3B	2
G	A517-H	1023/51	A5550-1A	2
H	A517-H	1022/54	A5491-4A	2
J	A514-F	1013/32	78L015-03W2	2-1/4
K	A514-H	1016/11	97L151-01W1	2
L	A514-F	1017/62	97L168-06W2	2-1/4
M	A514-F	1014/02	92L088-10W2	2-1/4
N	A514-H	1015/32	96L114-03W2	1-3/4
P	A514-H	1016/41	97L151-04W1	2
R	A514-H	1019/31	E07619-03W1	2
S	A514-H	1018/81	97L170-08W1	2
T	A514-H	1029/99	Unknown	1-3/8
Y	A517-H	1024/91	B9093-1	2-1/4
Z	A517-H	1024/94	B9093-4B	2-1/4
AA	A517-H	1020/41	A4071-1	2-1/4
AB	A517-F	1002/82	71D653-258582	1-1/2
AC	A517-F	1002/38	71D653-258638	1-1/2
AD	A517-F	1002/38	70E729-261282	1-1/2
AE	A517-F	1001/83	70E729-261283	1-1/2
AF	A517-F	1001/84	70E729-261284	1-1/2
AG	A517-F	1004/44	72A166-73144	1-1/2
AH	A517-F	1004/96	72A166-73196	1-1/2
AJ	A517-F	1004/98	72A166-73198	1-1/2
AK	A517-F	1012/99	75B082-30699	1-1/2
AL	A517-H	1020/46	A4071-6	2-1/4
AM	A514-H	1007/11	73A434-145011	1-1/2

<u>ID</u>	<u>ASTM TYPE-GRADE</u>	<u>REPORT CODE HEAT/SLAB</u>	<u>STEEL COMPANY HEAT/SLAB</u>	<u>PLATE THICK</u>
AN	A514-H	1007/12	73A434-145012	1-1/2
AP	A517-F	1010/47	75A179-63447	1-3/8
AR	A517-F	1006/47	72A625-212147	1-3/8
AS	A517-F	1006/48	72A625-212148	1-3/8
AT	A517-F	1006/50	72A625-212150	1-3/8
AU	A517-F	1006/51	72A625-212151	1-3/8
AV	A517-F	1006/52	72A625-212152	1-3/8
AW	A517-F	1006/57	72A625-212157	1-3/8
AX	A517-F	1006/58	72A625-212158	1-3/8
AY	A517-F	1006/61	72A625-212161	1-3/8
AZ	A517-F	1006/62	72A625-212162	1-3/8
BA	A517-F	1006/25	72A625-212225	1-3/8
BB	A517-F	1006/26	72A625-212226	1-3/8
BC	A517-F	1006/64	72A625-212564	1-3/8
BD	A517-F	1006/68	72A625-212568	1-3/8
BE	A517-F	1006/69	72A625-212569	1-3/8
BF	A517-F	1006/71	72A625-212571	1-3/8
BG	A517-F	1006/74	72A625-212574	1-3/8
BH	A517-F	1009/40	74E397-135040	1-3/4
BJ	A517-F	1006/49	72A625-212149	1-3/8
BK	A517-F	1006/53	72A625-212153	1-3/8
BL	A517-F	1006/54	72A625-212154	1-3/8
BM	A517-F	1006/56	72A625-212156	1-3/8
BN	A517-F	1006/59	72A625-212159	1-3/8
BP	A517-F	1006/60	72A625-212160	1-3/8
BR	A517-F	1006/65	72A625-212565	1-3/8
BS	A517-F	1006/66	72A625-212566	1-3/8
BT	A517-F	1006/67	72A625-212567	1-3/8
BU	A517-F	1006/70	72A625-212570	1-3/8
BV	A517-F	1006/72	72A625-212572	1-3/8
BW	A517-F	1006/75	72A625-212575B	1-3/8

<u>ID</u>	<u>ASTM TYPE-GRADE</u>	<u>REPORT CODE HEAT/SLAB</u>	<u>STEEL COMPANY HEAT/SLAB</u>	<u>PLATE THICK</u>
BX	A517-F	1005/22	72A618-209722	1-3/8
BY	A517-B	1000/39	69D478-198339A	7/8
BZ	A517-F	1006/73	72A625-212573	1-3/8
CA	A517-F	1011/92	75A703-217592	1-3/8
CB	A514-F	1003/29	72A033-033429	2-1/4
CC	A517-H	1025/91	B9131-1	2-1/4
CD	A517-H	1027/45	C4913-5	2-1/4
CE	A517-H	1024/95	B9093-5B	2-1/4
CF	A517-H	1020/43	A4071-3	2-1/4
CG	A517-H	1020/44	A4071-4	2-1/4
CH	A517-H	1027/46	C4913-6	2-1/4
CJ	A517-H	1025/95	B9131-5	2-1/4
CK	A517-H	1027/44	C4913-4	2-1/4
CM	A517-B	1021/42	A4099-2B	7/8

TABLE 2.1.2
IDENTIFICATION OF STEELS BY TYPE, GRADE, HEAT, SLAB AND THICKNESS
INDEXED BY HEAT/SLAB

<u>STEEL COMPANY HEAT/SLAB</u>	<u>REPORT CODE HEAT/SLAB</u>	<u>ID</u>	<u>ASTM TYPE-GRADE</u>	<u>PLATE THICK.</u>
69D478-198339A	1000/39	BY	A517-B	7/8
70E729-261282	1001/82	AD	A517-F	1-1/2
261283	1001/83	AE	A517-F	1-1/2
261284	1001/84	AF	A517-F	1-1/2
71D653-258582	1002/82	AB	A517-F	1-1/2
258638	1002/38	AC	A517-F	1-1/2
72A033-033429	1003/29	CB	A514-F	2-1/4
72A166-073144	1004/44	AG	A517-F	1-1/2
072196	1004/96	AH	A517-F	1-1/2
073198	1004/98	AJ	A517-F	1-1/2
72A618-209722	1005/22	BX	A517-F	1-3/8
72A625-212147	1006/47	AR	A517-F	1-3/8
212148	1006/48	AS	A517-F	1-3/8
212149	1006/49	BJ	A517-F	1-3/8
212150	1006/50	AT	A517-F	1-3/8
212151	1006/51	AU	A517-F	1-3/8
212152	1006/52	AV	A517-F	1-3/8
212153	1006/53	BK	A517-F	1-3/8
212154	1006/54	BL	A517-F	1-3/8
212156	1006/56	BM	A517-F	1-3/8
212157	1006/57	AW	A517-F	1-3/8
212158	1006/58	AX	A517-F	1-3/8
212159	1006/59	BN	A517-F	1-3/8
212160	1006/60	BP	A517-F	1-3/8
212161	1006/61	AY	A517-F	1-3/8
212162	1006/62	AZ	A517-F	1-3/8
212225	1006/25	BA	A517-F	1-3/8
212226	1006/26	BB	A517-F	1-3/8
212564	1006/64	BC	A517-F	1-3/8
212565	1006/65	BR	A517-F	1-3/8
212566	1006/66	BS	A517-F	1-3/8

Continued

<u>STEEL COMPANY HEAT/SLAB</u>	<u>REPORT CODE HEAT/SLAB</u>	<u>ID</u>	<u>ASTM TYPE-GRADE</u>	<u>PLATE THICK.</u>
72A625-212567	1006/67	BT	A517-F	1-3/8
212568	1006/68	BD	A517-F	1-3/8
212569	1006/69	BE	A517-F	1-3/8
212570	1006/70	BU	A517-F	1-3/8
212571	1006/71	BF	A517-F	1-3/8
212572	1006/72	BV	A517-F	1-3/8
212573	1006/73	BZ	A517-F	1-3/8
212574	1006/74	BG	A517-F	1-3/8
212575B	1006/75	BW	A517-F	1-3/8
73A434-145011	1007/11	AM	A514-H	1-1/2
145012	1007/12	AN	A514-H	1-1/2
74E002-001876	1008/76	D	A517-F	2-1/2
74E397-135040	1009/40	BH ₁	A517-F	1-3/4
75A179-063447	1010/47	AP	A517-F	1-3/8
75A703-217592	1011/92	CA	A517-F	1-3/8
75B082-030699	1012/99	AK	A517-F	1-1/2
78L-15-03W2	1013/32	J	A514-F	2-1/4
92L088-10W2	1014/02	M	A514-F	2-1/4
96L114-03W2	1015/32	N	A514-H	1-3/4
97L151-04W1	1016/41	P	A514-H	2
01W1	1016/11	K	A514-H	2
97L168-06W2	1017/62	L	A514-F	2-1/4
97L170-08W1	1018/81	S	A514-H	2
E07619-03W1	1019/31	R	A514-H	2
A4071-1	1020/41	AA	A517-H	2-1/4
3	1020/43	CF	A517-H	2-1/4
4	1020/44	CG	A517-H	2-1/4
6	1020/46	AL	A517-H	2-1/4
A4099-2B	1021/42	CM	A517-B	7/8
A5491-1B	1022/51	C	A517-H	2-1/2
3B	1022/53	F	A517-H	2
4A	1022/54	H	A517-H	2

<u>STEEL COMPANY HEAT/SLAB</u>	<u>REPORT CODE HEAT/SLAB</u>	<u>ID</u>	<u>ASTM TYPE-GRADE</u>	<u>PLATE THICK.</u>
A5550-1A	1023/51	G	A517-H	2
4A	1023/54	E	A517-H	2
B9093-1	1024/91	Y	A517-H	2-1/4
4B	1024/94	Z	A517-H	2-1/4
5B	1024/95	CE	A517-H	2-1/4
B9131-1	1025/91	CC	A517-H	2-1/4
5	1025/95	CJ	A517-H	2-1/4
B9863-2C	1026/92	A	A517-F	2-1/4
C4913-4	1027/44	CK	A517-H	2-1/4
5	1027/45	CD	A517-H	2-1/4
6	1027/46	CH	A517-H	2-1/4
C6369-4	1028/64	B	A517-H	2-1/2
Unknown-Unknown	1029/99	T	A514-H	1-3/8

3.0

TEST METHOD

3.1 Standard Charpy V-Notch Impact Test

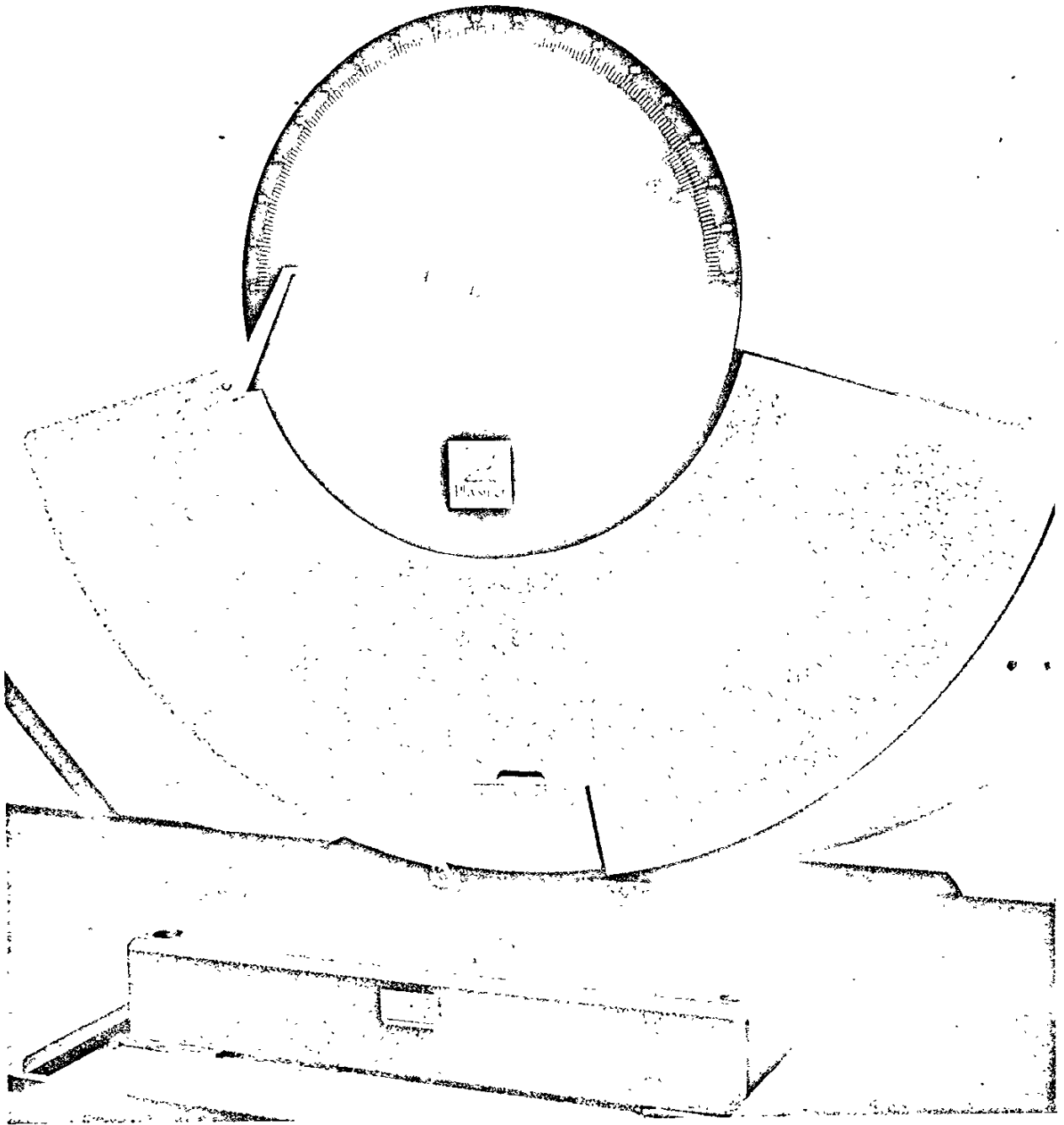
The standard Charpy V-notch (CVN) impact specimens were machined and tested in accordance with ASTM E23-66. The impact testing was done using a Physmet (ManLabs) machine at the Sacramento plant of the Aerojet Solid Propulsion Company (Figure 3.1). The measurement of lateral expansion in the broken test pieces was done in the Caltrans Laboratory in accord with par. 21.2.3 of ASTM Method A370-73.

In general, triplicate CVN-impact tests were made at the lowest anticipated service temperature (LAST) which was 0°F for the Tuolumne bridge steels and +20°F for the Bryte Bend bridge steels. For purposes of determining transition behavior, single specimens were tested at -40°F, 0°F, room temperature and +120°F, thus encompassing the anticipated service temperatures. Based on the trend established with these initial tests, at least four additional specimens were tested from each plate to develop the transition curve (the plot of energy versus temperature).

3.2 Pre-crack Charpy Impact Tests

The pre-crack Charpy impact (PCI) test is not an ASTM standard test; however, its development as a research test method dates back to the mid-1960's (7-12).

In the last decade the PCI test has been put into increasing use because it is consistent with the fracture-mechanics concept of testing with a natural crack and, like the standard CVN-impact test specimen, the PCI test is highly sensitive to metallurgical variables affecting fracture toughness, it is economical in terms of the amount of material required and the cost of machining, and it is easy to test over a wide range of temperature (compared to the ASTM E399 compact-tension specimen).



PHYSMET (MANLABS)
CHARPY IMPACT TESTING MACHINE

FIGURE 3.1

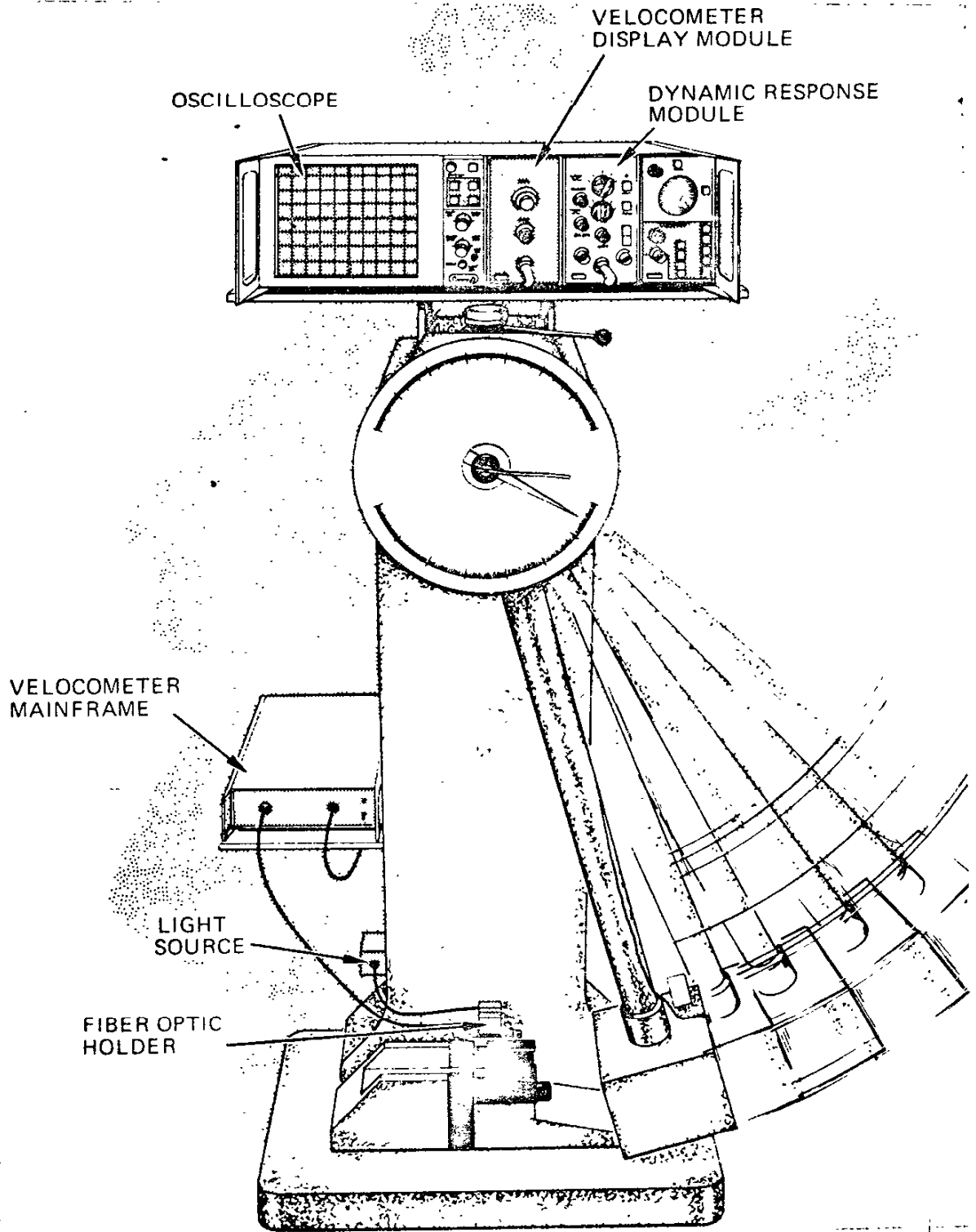
The initial precracking operation is basically the only difference between the CVN-impact test and PCI test. After machining standard ASTM E23-66 Type-A CVN-impact test specimens, each piece was precracked by cyclic loading the finish-machined test specimen in a specially designed (Physet) Charpy precracking machine. In most of the specimens, the fatigue-crack depth was held to 0.030 ± 0.010 in. and, therefore, it was deemed unnecessary to incur the added expense of measuring the net cross-section area for W/A determination. Thus, the measurements in the PCI testing were simply energy (ft-lb) to fracture and lateral expansion (mils) as in standard CVN-impact testing.

In general single PCI tests were made at -40°F , 0°F , $+20^{\circ}\text{F}$, room temperature and $+120^{\circ}\text{F}$, thus encompassing the anticipated service temperatures. Based on the trend established with these initial tests, at least four additional specimens were tested from each plate to develop the transition curve.

3.2.1 Instrumented Precrack Charpy Impact

Instrumentation System - The instrumented impact testing in this study was done by Effects Technology Inc., using the DYNATUP system. This is essentially a three-component system for use with conventional impact testing machines to monitor the dynamic behavior and supply a precision analog output signal of the load-time history of the impacted test piece. The major components of this system are the instrumented tup, Velocometer and Dynamic Response Module. A schematic of a typical DYNATUP System in operation with a standard Charpy impact machine is shown in Figure 3.2.

The instrumented tup is the load cell and, as the name implies, is securely fixed in the head of the striking portion of the pendulum. This device employs semiconductor strain gages to sense the compression loading of the tup while in contact with the specimen. These gages receive a constant d.c. power supply from the Dynamic Response Module.



INSTRUMENTED CHARPY IMPACT TESTING SYSTEM (13)
FIGURE 3.2

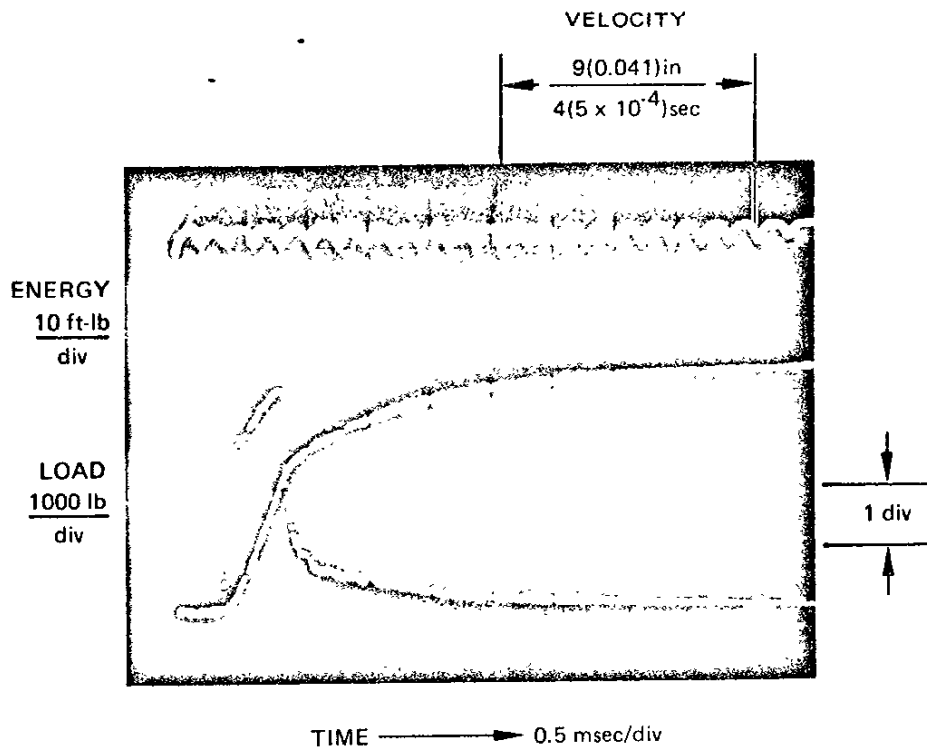
The Dynamic Response Module (DRM) is operated in the same manner as a conventional oscilloscope plug-in unit. The signal produced by the instrumented tup is passed through the DRM where it is amplified and integrated to produce a second signal. This integrated signal represents the area under the load-time curve and, therefore, is a measure of the energy absorbed at any time during the impact loading of the test piece. The direct load signal and the energy signal are displayed simultaneously on the cathode ray tube (CRT) of a Tektronix oscilloscope.

The other major component of the System is the Velocometer which supplies a controlled light beam and photosensor to insure accurate and reliable triggering of the oscilloscope. In addition, this component is a non-contacting velocity measuring device specifically designed to detect the head velocity of the pendulum. The Velocometer component is composed of the following subassemblies: mainframe, light source, fiber optic holder, and flag assembly. The latter, not clearly shown in Figure 3.2, is essentially a thin grid which is firmly attached to the head of the pendulum and passes through a light beam in the fiber optic holder before, during, and after the tup is in contact with the test piece.

An oscilloscope can be used to record all three data signals: load, energy and velocity. This CRT recording is photographed and the desired raw data is obtained by making measurements of signal positions on the film. A typical data record for a structural steel specimen is shown in Figure 3.3.

3.2.2 Temperature Measurement

Test temperatures were obtained by immersion of the specimen in liquid baths (isopentane, alcohol, oil, liquid nitrogen, etc.). The temperatures were measured with calibrated dial-type thermometers (when possible) and thermocouples. The time intervals



TYPICAL RAW-DATA FROM INSTRUMENTED
 CHARPY IMPACT TESTING SYSTEM (13)

FIGURE 3.3

between the transfer of the specimen and the impact test was kept to a minimum (never more than 4 seconds) so as not to allow any warming of the specimen. These procedures employed for the temperature baths and transfer time are in accordance with those of ASTM E23 for standard Charpy tests(13).

3.2.3 Impact Machine Calibration.

Army Materials and Mechanics Research Center calibration specimens were broken at the end of October 1972 to ensure the reliability of the dial energy values. The deviation from the nominal values for this set of specimens was within the allowable range of ± 1.0 ft-lbs or $\pm 5\%$ of the nominal value (whichever is greater) at all energy levels(13).

3.2.4 Raw Data Reduction

The initial step for data reduction was to obtain clear photographic records of the signals displayed on the CRT. The data obtained by measurements made on the photographs are defined on the idealized load-deflection record shown in Figure 3.4. The values measured from the load-time signal are P_{GY} , P_M and P_1 . The deflection is obtained by the product of the average tup velocity \bar{v} and the time as measured on the photograph. Deflection values measured are d_{GY} , d_{max} and d_1 . The subscripts are references to the load values defined in Figure 3.4. The values obtained from the energy-time record are referred to the load-deflection curve of Figure 3.4 and are defined in this figure. The values measured from the energy-time signal are W_T , W_I and W_F . The DRM is calibrated so that the integrated signal (energy) represents that for a constant initial impact velocity. However, substantial decreases in pendulum velocity can occur and, therefore, the energy measurements from the photograph were corrected as follows:

$$W \text{ (corrected)} = W \text{ (photograph)} \times \bar{v}.$$

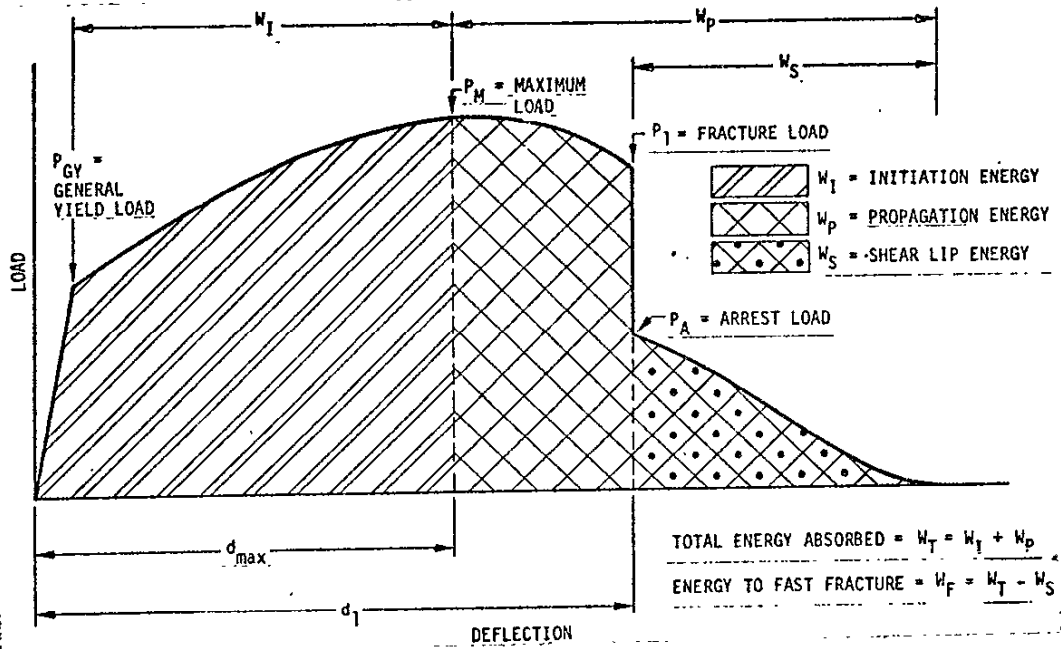
The \bar{v} values are clearly functions of the energy absorbed and the total available kinetic energy of the pendulum. The (1e latter value is obtained by the relationship $1/2 mv_0^2$, where m is the effective mass of the pendulum and v_0 is the velocity of the tup just prior to contacting the specimen.

The total energy absorbed by the specimen can also be obtained by dial measurements of pendulum swing retardation. The value obtained from the dial is defined as E_T and should clearly be equal to W_T , as defined in Figure 3.4.

The raw data were tabulated as shown in Figure 3.5. The table includes test temperature and the average static yield strength at that temperature. The table printed by computer techniques did not permit use of subscripts. Therefore, the following equivalence of terms between those discussed above and those listed in the table should be noted:

PF is P_M for the case $P_M < P_{GY}$,
PGY is P_{GY} ,
PM is P_M ,
Pl is P_1 ,
DGY is d_{GY} ,
DM is d_{max} ,
Dl is d_1 ,
WT is W_T ,
WI is W_I ,
WF is W_F .

Also included in Figure 3.5 is the parameter $ET/area$ which corresponds to the total energy to break the specimen divided by the cross-sectional area, i.e. $B(w-a)$ over which the process occurred. This is W/A .



IDEALIZED LOAD-DEFLECTION RECORD (13)

FIGURE 3.4

Specimen Code	Test Temperature F	Static Yield Stress KSI	Dial Impact Energy Ft-Lb	Load, Lb				Deflection, In			Integrator Energy Ft-Lb			Crack Depth In	ET/Area Lb/In
				PF	PCY	PM	PI	DCY	DM	DI	WT	WI	WF		
3812	-40	118.2	3.2	1980	0	1980	1980	0.000	.011	.011	3.7	.8	.8	.110	343
3814	0	115.1	4.0	1950	0	1950	1950	0.000	.012	.012	4.2	1.0	1.0	.137	474
3816	0	115.1	4.7	1860	0	1860	1860	0.000	.012	.012	5.0	.8	.8	.094	477
3811	40	113.0	5.5	2190	0	2190	2190	0.000	.013	.013	5.8	1.3	1.3	.116	603
3817	60	112.2	7.0	1935	0	1935	1935	0.000	.014	.014	0.0	1.1	1.1	.093	708
3815	72	111.8	6.0	2220	0	2220	2220	0.000	.013	.013	6.4	1.4	1.4	.122	672
3813	120	110.5	8.2	1920	0	1920	1920	0.000	.019	.019	8.4	1.6	1.6	.117	902
3818	120	110.5	8.0	1800	0	1800	1800	0.000	.022	.022	8.0	1.9	1.9	.120	889
3810	160	109.6	10.5	2730	0	2730	2730	0.000	.019	.019	11.7	1.9	1.9	.098	1080
389	200	108.8	12.1	3060	0	3060	3060	0.000	.021	.021	12.7	2.4	2.4	.098	1245

TYPICAL RAW-DATA TABULATION (13)

FIGURE 3.5

3.2.5 Calculation of Strength and Toughness

When general yielding occurs, the P_{GY} value can be used to calculate the dynamic yield strength, which is dependent on deflection rates.* The general equation for conversion is

$$\sigma_{yd} = P_{GY} \frac{L}{B (w-a)^2 C} \quad , \quad (3.1)$$

where the constant C is dependent on the notch flank angle (2β), notch root radius (ρ), and the type of loading (i.e., pure bending or three-point bending). For our purposes of three-point bending, $2\beta = 45^\circ$, and ρ varying between 0 and 0.010", Equation (3.1) is valid with $C \approx 1.21$. Therefore,

$$\sigma_{yd} = P_{GY} \frac{L}{B (w-a)^2 (1.21)} \quad (3.2)$$

The derivation and limitations of Equation (3.2) are discussed in Reference (14).

Fracture toughness is the major interest of most investigations. In these cases, fracture toughness refers to a critical stress intensity parameter, K_C or K_{IC} , that can be related to structural service performance by a relationship of the form

$$K_C \propto \sigma \sqrt{\pi c} \quad (3.3)$$

where σ is the nominal stress in the vicinity of a flaw having a size indicative of the linear dimension c . There is considerable

*The importance of clearly indentifying specimen strain rates or deflection rates is without question. In this report, the distinction between dynamic and static is assumed to be that of 10^1 to 10^2 and 10^{-4} sec⁻¹, respectively.

controversy regarding the calculation of a meaningful fracture toughness value based on data derived from a specimen which fractures after general yielding. For this reason, four different approaches to the calculation of fracture toughness are employed (13).

The first is based on linear elastic fracture mechanics (15).

$$K_{IC} = \frac{1.5Y_L (P_F)}{Bw^2} a^{1/2} \quad (3.4)$$

where (for $w = \frac{L}{4}$)

$$Y = 1.93 - 3.07 \frac{a}{w} + 14.53 \frac{a^2}{w^2} - 25.11 \frac{a^3}{w^3} + 25.8 \frac{a^4}{w^4}$$

and P_F is the applied load at fracture pop-in, when fracture occurs before general yielding, i.e. with fracture loads less than general yield loads ($P_F < P_{GY}$).

The second method employs the assumption of equivalence of critical strain energy release rates, G_c , to the ratio of impact energy to fracture surface area, W/A , where area (A) = $B \cdot (w-a)$. It has been found experimentally for static tests that using twice the area many times results in a better correlation (16). The relationships (used to calculate fracture toughness are:

$$K_C = \left(\frac{G_c \times E}{1 - \nu^2} \right)^{1/2} \quad (3.5)$$

or

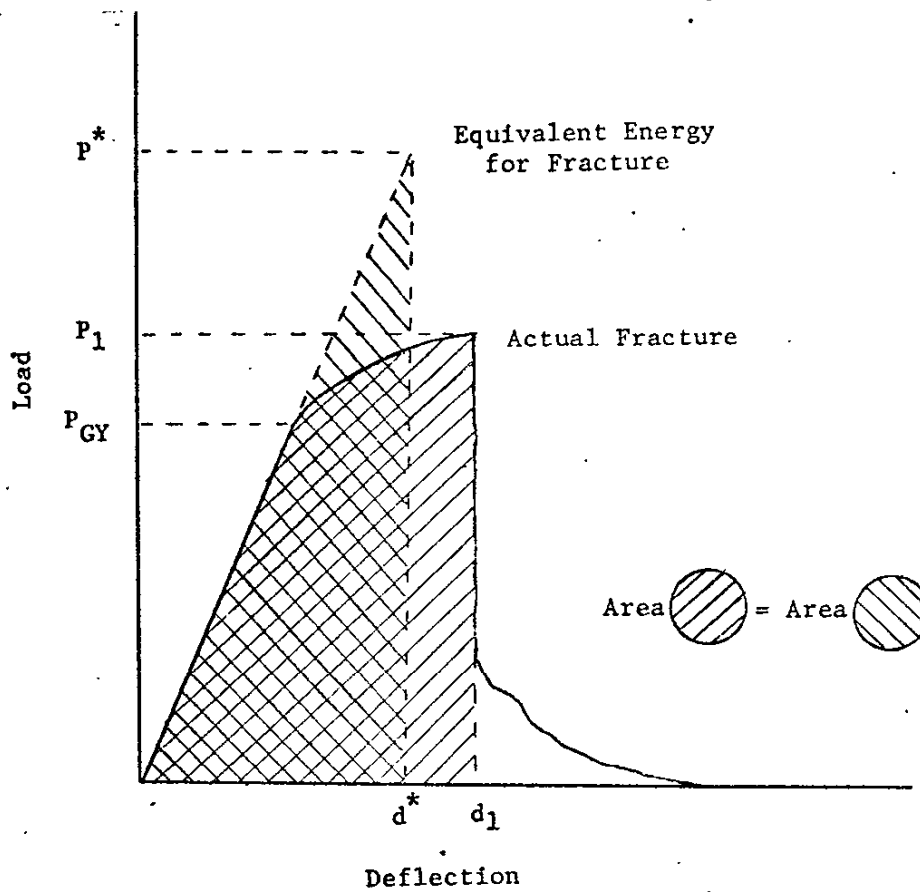
$$K_C = \frac{W \times E}{B(w-a) (1-\nu^2)} \quad (3.6)$$

where E is the elastic modulus and W is the impact energy (either W_T , W_I , or W_F). A value of 0.3 is assumed for Poisson's ratio ν .

The value most commonly used to calculate G_C or K_C is the total impact energy (W_T). Intuitively, these toughness values should be based either on the energy required to initiate fracture (W_I) or the energy consumed in creating the new surface (W_F). The K_C values determined by these energy values are presented for comparison of the relative contributions of the initiation and propagation processes to the total apparent toughness.

The third method employed for calculation of fracture toughness uses a lower-bound equivalent-energy approach(17). This method assumes that if a sufficiently large specimen had been employed, fracture would have occurred before general yielding and at an energy corresponding to that measured for the smaller specimen. From this method, values of P^* are estimated by extrapolating the linear slope of the elastic region of the load curve until the area (energy) under the linear curve corresponds to the energy measured (see Figure 3.6). These P^* values are then used to calculate K_{IC} from Equation (12). Both the initiation energy, W_I , and the energy to fast crack propagation, W_F , are used to calculate fracture toughness values (i.e., P^*_I and P^*_F , or in computer terminology, P^*I and P^*F).

The fourth method employed for calculation of fracture toughness uses a crack-opening-displacement (COD) approach. The COD approach essentially uses the deflection measurements to calculate the strain at the root of the notch(18). COD is intended to represent this strain and can be calculated from the following:



RELATIONSHIP OF EQUIVALENT ENERGY FRACTURE
LOAD P^* TO THE ACTUAL FRACTURE LOAD (13)

FIGURE 3.6

$$\text{COD} = 0.51 (w-a) d \quad , \quad (3.7)$$

where d is the appropriate deflection (d_1 or d_{max}). The generally accepted relation of COD to G_c is

$$G_c = \text{COD} \times \sigma_{yd} \quad , \quad (3.8)$$

and K_c is found from combining Equations (3.5), (3.7), and (3.8):

$$K_c = (\text{COD} \times \sigma_{yd} \times E)^{1/2} \quad . \quad (3.9)$$

For impact tests, σ_{yd} in Equation (3.9) is that determined by Equations (3.1) and (3.2). If the specimen breaks before general yielding occurs, either the static yield strength or a σ_{yd} calculated from the fracture load is used depending upon which is the largest. CODM is the computer code for this measurement.

Equation (3.7) is also used to evaluate COD at d_{max} and at d_1 . These values are shown in Figure 3.7 in the columns identified as D, and D1 under the COD heading.

The fifth method uses the maximum-load measurement (P_M) to calculate fracture toughness from Equation 3.4. For fractures occurring before general yielding, the toughness calculated from P_M is the same as that calculated from P_F . The computer designation for this calculation is PMAX.

3.3 ASTM E399 Compact Tension Testing

The standardized method for determining plane-strain fracture toughness of metallic materials was first covered in ASTM Standards (E399-70T) effective March 19, 1970. This test method was used

Specimen Code	Test Temperature F	Yield Stress KSI		Fracture Toughness Calculated From the Indicated Parameter, KSI-SQRT(In)								Critical Crack Length In	COD (0.001 In)	
		Static	Dynamic	PF	WT	WI	WF	P*1	P*F	CODM	P*MAX		D1	D1
3219	-40	118.2	0.0	64.6	119.0	74.5	74.5	53.9	53.9	99.9	64.6	.066	2.71	2.71
2817	0	115.1	0.0	70.8	139.1	96.9	96.9	69.1	69.1	109.0	70.8	.098	3.09	3.09
2816	40	113.0	0.0	74.8	151.6	97.3	97.3	71.7	71.7	111.3	74.8	.094	3.09	3.09
1813	72	111.8	0.0	87.2	191.4	123.5	123.5	88.6	88.6	133.6	87.2	.103	3.84	3.84
1812	100	111.0	0.0	73.6	198.3	111.7	111.7	73.9	73.9	122.2	73.6	.103	3.64	3.64
1816	120	110.5	0.0	81.0	203.1	128.5	128.5	78.5	78.5	145.6	81.0	.096	4.98	4.96
1814	140	110.0	134.7	0.0	213.9	144.5	144.5	93.5	93.5	146.3	82.1	.116	5.36	5.36
2813	160	109.6	135.7	0.0	238.4	152.0	152.0	116.3	116.3	151.4	86.7	.130	5.73	5.73
2815	200	108.8	126.7	0.0	244.4	161.2	161.2	120.0	120.0	154.7	83.8	.139	6.48	6.48
1815	240	108.0	129.7	0.0	264.7	165.5	165.5	109.6	109.6	150.7	85.0	.137	6.07	6.07

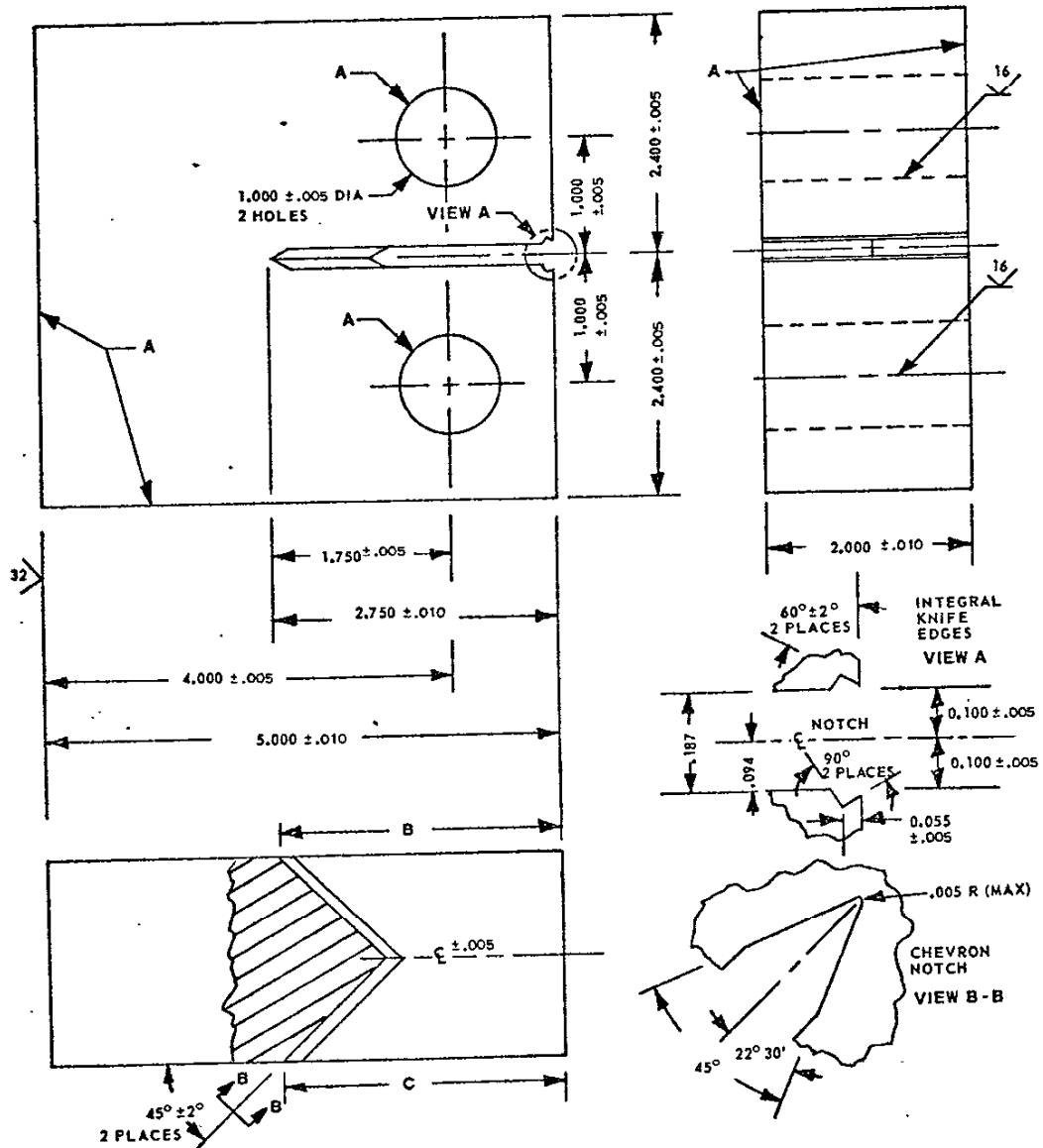
TYPICAL
 FRACTURE TOUGHNESS RESULTS TABULATION (13)
 FIGURE 3.7

in the one- and two-inch thickness for testing selected (seven) heats of A514/517 steel Plates A, AL, L, M, R, Z, and CK from the Bryte Bend and Tuolumne Bridges. Figure 3.8 shows the two-inch-thick compact tension specimens.

The specimens were fatigue precracked in a Wiedemann (Satec) Model SF 10U Fatigue Machine which is load controlled and operates at 1800 cpm. With this system, a static load of 10 percent of the maximum fatigue load was applied, and the fatigue cycling was done between the specified maximum and the static load. Specimens ZTD, ZUD, ZVD, ZWD, ZXD and ZZD (one 1-in.-thick specimen from each of the steels not previously tested) provided preliminary test data to determine the approximate critical stress intensity of each steel and to determine if the stress intensity used in fatigue cracking complied with the requirements of ASTM E399. These specimens were tested at the lowest temperature anticipated in the test program.

The stress intensity for fatigue cracking the six specimens conformed to ASTM E399 with the exception of ZTD. Based on the test results for the six specimens, adjustments were made in the loads for fatigue cracking the balance of the specimens.

For the low-temperature testing, the 1-inch thick specimens were submerged in a mixture of methyl alcohol and dry ice for test temperatures between minus 100 and plus 40°F; liquid nitrogen (LN₂) was used for testing at -320°F. A Checktronic Corporation temperature-controlled chamber was used for elevated-temperature testing both the 1-inch and 2-inch thick specimens, as well as for cryogenic testing the 2-inch-thick specimens at temperatures below minus 40° and the 1-inch-thick specimens at temperatures below minus 100°F. A thermometer was used to monitor the temperature of the methyl alcohol and



Note 1 - Dimensions are in inches.

Note 2 - A surfaces shall be perpendicular and parallel as applicable to within 0.008 TIR.

Note 3 - The points of intersection of the crack starter tips with the two specimen faces shall be equally distant from either pin hole center to within 0.020.

Note 4 - Each of the two parallel notch surfaces must lie in one plane to within 0.020 and must be perpendicular or parallel as applicable to the specimen faces to within 0.020.

Note 5 - B = C to within 0.020

TWO-INCH-THICK COMPACT-TENSION SPECIMEN DIMENSIONS AND TOLERANCES

FIGURE 3.8

a thermocouple was used for monitoring temperature in the chamber. The thermocouple was placed in the machined notch of each specimen, out of the direct path of the circulating air.

The specimens were tested in a Wiedemann Baldwin 60,000-lb machine using a manual-controlled load rate. The desired load rate was obtained by adjusting the load rate so the load-indicating pointer followed a moving circular dial, preset to the desired rate.

A crack-opening displacement gage (Figure 3.9 was used in determining the load (P_q) for calculating the plane-strain critical stress intensity. The gage was positioned so as to bridge the specimen preflaw by inserting the gage between knife edges machined into the face of the specimen at the end of the notch. The particular crack-opening-displacement gage employed has been developed specifically for pop-in and slow-crack-growth measurements where very small changes in compliance are anticipated. The gage consists of a full bridge of electric resistance strain gages mounted on a double cantilever beam with the amount of flexure in the cantilever arms controlled by the thickness of the spacer between the arms at the base of the cantilever.

3.3.1 Computer Program.

The compact-tension test results were evaluated by ASPC Univac 1108 computer program SA 017 dated 1/72. An example of the computer printout is shown in Figure 3.10; the following data were input to the computer:

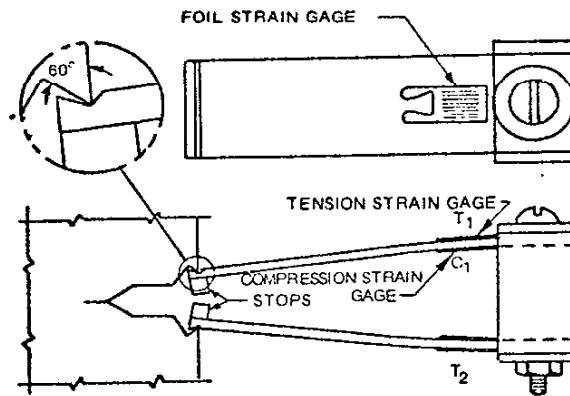
- a. specimen identification and test temperature
- b. specimen thickness, B
- c. yield strength, FTY
 - at room temperature, FTY
 - at test temperature, FTYTT
- d. specimen overall length, LENT

- e. hole diameter, DIA
- f. edge of hole to end of specimen, LENH
- g. crack measurements, A
 - (1) machined chevron notch, A1
 - (2) fatigue crack at free surface, A2
 - (3) fatigue crack at 1/4-point, A3
 - (4) fatigue crack at mid-thick, A4
 - (5) fatigue crack at 1/4-point, A5
 - (6) fatigue crack at free surface, A6
 - (7) machined chevron notch, A7
- h. load values, P
 - (1) secant load, PQ
 - (2) load at failure, PFAIL
 - (3) load for initial increment of fatigue, PIF
 - (4) load for final increment of fatigue, PFF
 - (5) loading rate, PLR
- i. fatigue crack increment, DELA
- j. Young's modulus, YMOD

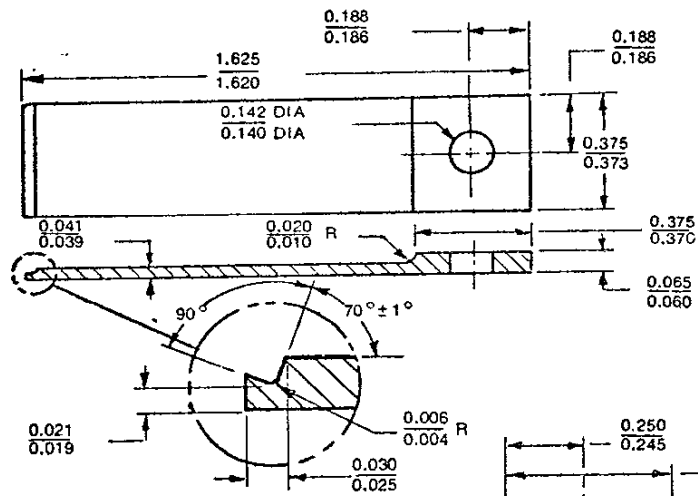
The computer printout includes, in addition to the critical stress-intensity value $K(Q)$, the following parameters specified by ASTM E399-72 to test the validity of the measured stress-intensity value:

A(AVG)/W	ratio of average crack length to specimen depth shall be 0.45 to 0.55 (ref ASTM E399 par. 7.3.3)
.05*A(AVG)	5 percent of the crack length (see par 7.2.3 and 8.2.3)
Max Absolute Difference	The difference between any of the crack length measurements shall not exceed 5% of the average (see par 8.2.3).

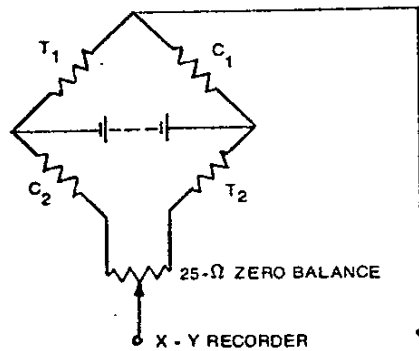
MINIMUM ABS. DIFF.	no part of the crack front shall be closer to the machined notch root than 5% (see par. 8.2.3).
A2/A(AVG) and/or A6/A(AVG)	the length of crack at the free surface shall not be less than 90% of the average crack length (ref par. 8.2.3)
1.2E-3*YMOD	the ratio of the maximum stress intensity used in the final stage of fatigue precracking to Young's modulus shall not exceed 0.002 in. ^{1/2} (ref par. 7.4.2).
.6*K(Q)	6 percent of the measured stress intensity.
K(FF)	the max. stress intensity in fatigue precracking shall not exceed 60 percent of the measured KQ value (ref par. 7.4.2).
K(LR)	specimens shall be loaded at a rate such that the stress intensity increases at a rate within the range of 30 to 150 ksi-in. ^{1/2} per minute (ref par. 8.4).
B(THEO)	2.5 (KQ/FTY) ² shall be less than the thickness (B) and less than the crack length (A) (ref par. 9.1.5).
PQ/P(FAIL)	the ratio of max. load to load at failure shall not exceed 1.10 (ref par. 9.1.2).



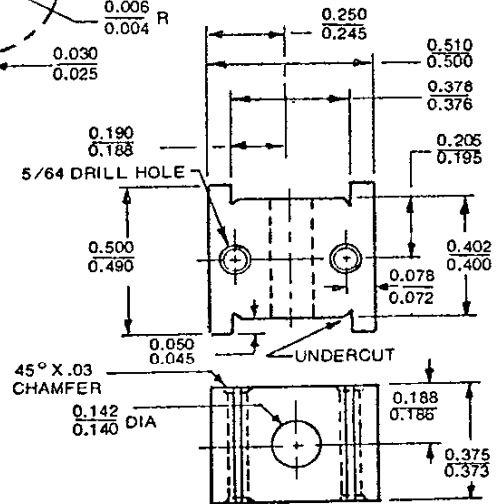
(a) GAGE MOUNTED ON SINGLE-EDGE-NOTCH TENSION SPECIMEN



(b) DIMENSIONS OF BEAMS



(c) BRIDGE MEASUREMENT CIRCUIT



(d) DIMENSIONS OF SPACER BLOCK

**DOUBLE-CANTILEVER DISPLACEMENT GAGE
(ALL DIMENSIONS ARE IN INCHES EXCEPT WHERE NOTED)**

FIGURE 3.9

SPECIMEN ZVC AT MINUS 100F

INPUT FOLLOWS...

\$OUT

```
A      =      .27510000E+01      .29080000E+01      .29900000E+01,
      .30170000E+01,      .30070000E+01,      .29450000E+01,      .27550000E+01,
B      =      .20030000E+01
DELA   =      .21000000E+00
DIA    =      .10000000E+01
LENH   =      .49900000E+00
LENT   +      .50010000E+01
FTY    =      .10980000E+03
FTYTT  =      .11700000E+03
PFAIL  =      .30950000E+02
PFF    =      .11000000E+02
PIF    =      .16000000E+02
PLR    =      .30000000E+02
PQ     =      .30950000E+02
YMOD   =      .30000000E+05
$END
```

```
A(AVG)                2.00567
A(AVG)/W              .50117
K(Q)                  74.43505
K(IF)                 33.17530
.6*K(Q)               41.91266
K(FF)                 26.45511
1.2E-3*YMOD           33.78461
K(LR)                 72.15029
B(THEO)               1.01187
MAX ABS A3-A4         .02700
.05*A(AVG)            .10028
MIN ABS A2-A1         .15700
A2/A(AVG)             .95180
A6/A(AVG)             .97025
PQ/P(FAIL)           1.00000
```

COMPUTER - PRINTED TABULATION
OF COMPACT - TENSION - TEST RESULTS

FIGURE 3.10

3.4 ASTM E208 NDT Temperature Test

ASTM E208-69 standard drop-weight tests were conducted at the U. S. Naval Research Laboratory (NRL) for the purpose of determining the nil-ductility transition (NDT) temperature in selected heats of A514/517 steel plate. The drop-weight test employs a simple-beam specimen specially prepared to create a material crack in the tensile surface of the beam in the first few degrees of bend. The test is conducted by subjecting each of a series of specimens (generally four to eight) of a given material to a single impact load at selected temperatures to determine the maximum temperature at which a specimen fractures in the presence of a deliberately brittle crack-starter weld. The impact load is provided by a guided, free-falling weight with an energy of 250 to 1200 ft-lb, depending on the yield strength of the steel tested. A stop prevents the specimens from deflecting more than a few tenths of an inch.

The test procedure was as follows: After preparation and temperature conditioning of the specimen, the initial drop-weight test was conducted at a test temperature estimated to be near the NDT temperature. Depending upon the results in the first test, the testing of the remaining specimens was conducted at suitable temperature intervals to establish the limits within 10°F for "break" and "no-break" performance. A duplicate test at the lowest no-break temperature of the series generally was conducted to confirm no-break performance at this temperature. Thus, the nil-ductility (NDT) temperature is the maximum temperature where a standard drop-weight specimen breaks when tested according to the provisions of the ASTM E208-69 standard method.

This method employs a small weld bead deposited on the specimen surface, whose sole purpose is to provide a brittle material for the initiation of a small cleavage crack flaw in the specimen base material during the test. The weld is produced

using a hard-surfacing electrode to assure easy crack initiation in the weld deposit. The final step in preparation of the specimen consists of notching the deposited weld at the center of the bead length.

In this study of selected heats of A514/517 steel, the drop-weight NDT testing was done using the NRL drop-weight machine. The weight (100 lb) and height (12 ft) were set to deliver an impact energy of 1200 ft-lb to each test specimen. The specimens were brought to the desired test temperature in agitated liquid baths, allowing a minimum of 20 minutes for each specimen to come to temperature. The measurement of both bath and specimen temperatures was accomplished with the equipment and procedures regularly used at the Naval Research Laboratory. For specific information concerning the equipment, the preparation of specimens and the general testing procedures at NRL, the reader is referred to the published literature(19-21).

3.5 Military Standard Method for 5/8-In. Dynamic Tear Testing (MIL-STD-1601 SHIPS) 8 May 1973.

The Dynamic Tear (DT) test was developed at the Naval Research Laboratory starting in 1960, and it has been used extensively for the characterization of fracture resistance of ferrous and nonferrous structural metals. The initial DT specimens were tested in a dropweight machine, and the test method was described as the "Drop-Weight Tear Test" (DWTT). Subsequently, pendulum machines with direct readout of the energy required to fracture the specimen were developed, and specimens of improved design with respect to crack-starter conditions were evolved. To reflect these evolutionary improvements, the name of the test method was changed to "Dynamic Tear" test in 1967. DT test facilities have been established at research laboratories and production plants of major metal-producing companies in this country and abroad.

The basic 5/8-DT test procedure consists of impacting a simple supported specimen having a notch on the tension side. There are two types of notches permitted in this method; one is a notch that is prepared by machining (type M), and the other is partially prepared by machining and uses a brittle crack-starter weld to provide a notch with a natural crack tip (type C). The brittle crack-starter welds are prepared by diffusing a small amount of embrittling material in an electron-beam (EB) weld to form a highly crack-sensitive region. The crack-starter-weld specimen is used when the specified sharp tip on the machined notch cannot readily be obtained; for example, in ultrahigh strength metals. The 5/8-DT specimens are fractured with pendulum or drop-weight machines, and the total energy for fracture is recorded.

In this study of selected heats of A514/517 steel, the DT testing was done using the U. S. Naval Research Laboratory 2000 ft-lb capacity double-pendulum instrumented-impact-testing machine as shown in Figure 3.11. A type-M notch was used, sharpened with a pressed tip produced using the procedures specified in par 7.3.2 of NRL Report 7159(22). The specimen dimensions were 7.125-in. long, 1.6-in. deep and 0.625 (5/8) in. thick. The net section after machining the notch and pressing the tip was 1.125 in.

The dynamic-tear-test procedure consisted of impacting the test specimens as a simple beam supported in the NRL double-pendulum machine. The specimens were brought to the desired test temperature in agitated liquid baths, allowing a minimum of 20 minutes for each specimen to come to temperature. The measurement of both bath and specimen temperature was accomplished with the equipment and procedures regularly used by NRL. By means of the impact-testing-machine instrumentation, force-time traces were obtained from each test as well as a recording of energy absorbed in fracturing each test specimen.

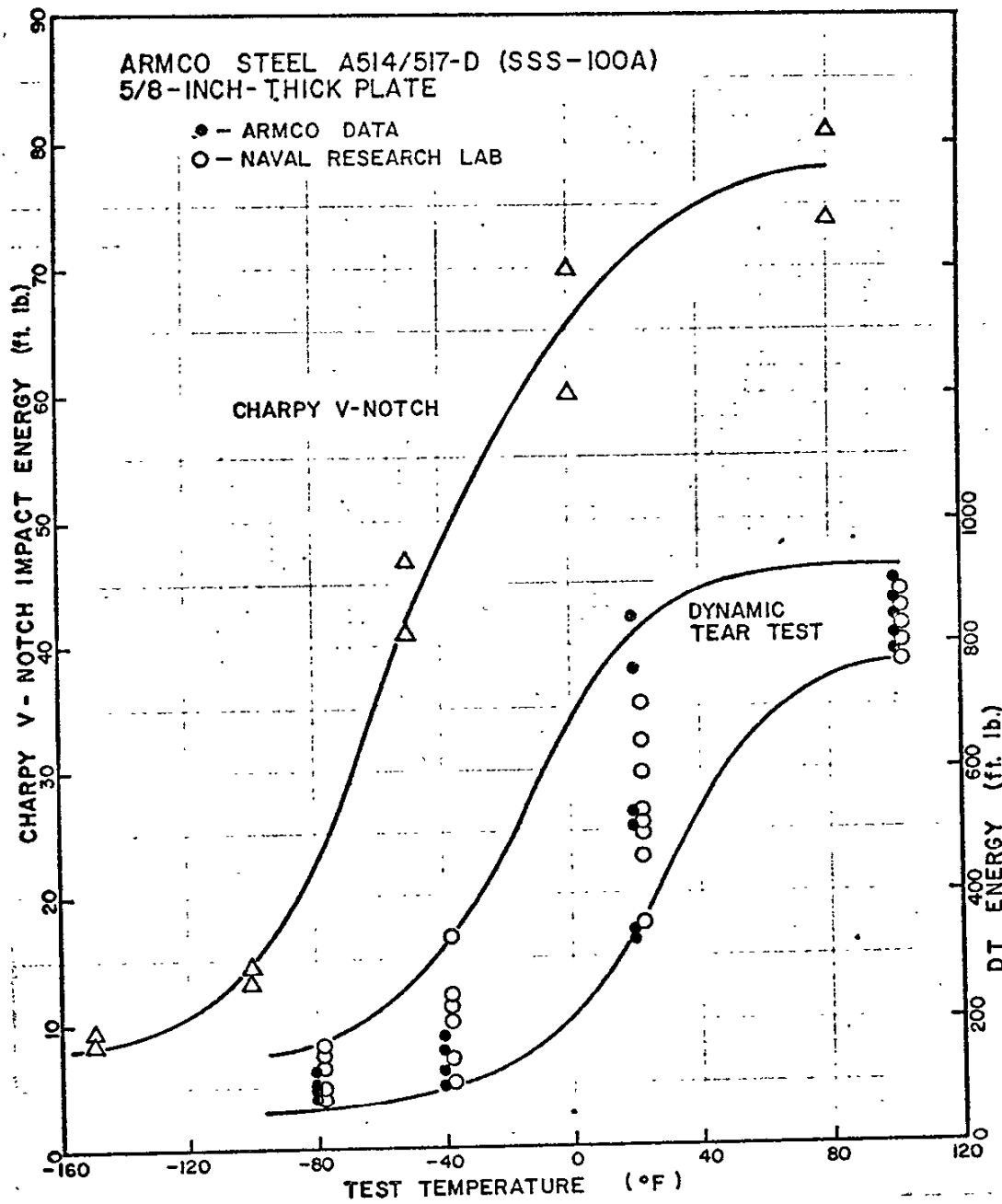


DOUBLE-PENDULUM MACHINE OF 2000 FT-LB
CAPACITY FOR TESTING 5/8-DT SPECIMENS(22)

FIGURE 3.11

An example of the test results that can be expected when two laboratories run DT tests on a single plate of A517 steel is shown in Figure 3.12. These data were obtained with 5/8-in. DT tests by NRL and Armco Steel Corporation in an ASTM Committee E24.03.01 round-robin test program. The testing done by NRL included both drop-weight and double-pendulum DT testing.

Note that there was a definite transition from brittle-to-ductile behavior starting at about -40°F , whereas the CVN-impact transition curve shows the transition starting at about -100°F . This is probably, at least in part, a notch-acuity effect. This will be discussed later in the report in connection with CVN-PCI comparisons.



DT TEST RESULTS FROM TWO LABORATORIES,
TESTING 5/8" THICK A514/517 GRADE D PLATE

FIGURE 3.12

TEST RESULTS

4.1 Charpy Impact Test Results4.1.1 Transition-Temperature Concepts

In the early 1960's the American Society of Mechanical Engineers Research Committee on Prevention of Fracture in Metals formed a Subcommittee on Brittle Fracture composed of the following experts:

Chairman,	J. E. Srawley, NASA Lewis Research Center
Secretary,	H. Corten, University of Illinois
Members,	W. F. Brown, NASA Lewis Research Center
	C. Carman, Frankford Arsenal
	D. K. Felbeck, University of Michigan
	G. R. Irwin, U.S. Naval Research Laboratory
	L. R. Jackson, Battelle Memorial Institute
	L. D. Jaffe, Jet Propulsion Laboratory
	F. M. Kloeblen, Linde Company
	J. D. Lubahn, Colorado School of Mines
	V. Weiss, Syracuse University Research Institute
	E. T. Wessel, Westinghouse Research Laboratory
	B. M. Wundt, General Electric Company (LSTG)
	S. Yukawa, General Electric Company (LSTG)

The committee described the transition-temperature approach(23).

"The transition-temperature approach as currently applied to structural steels below about 100,000 psi yield strength, consists of one of the following procedures:

- "1. Set the LOWEST PERMISSIBLE OPERATING TEMPERATURE at a value which is a certain amount HIGHER THAN THE LABORATORY-ASCERTAINED TRANSITION TEMPERATURE.
(Emphasis added.)

- "2. Select a material whose laboratory-ascertained transition temperature is at least a certain amount LOWER THAN THE LOWEST OPERATING TEMPERATURE ANTICIPATED. (Emphasis added.)

"The great advantage of the transition-temperature approach is its simplicity; no stress analysis, or even a knowledge of any stress or strain quantity, is needed for the application of this method, beyond the traditional procedures required to prevent gross yielding. The practical application of the transition temperature approach is limited, however, to temperature and steain-rate sensitive materials that exhibit abrupt behavior transitions, i.e., the low and medium-strength structural steels.

"Temperature and strain-rate sensitive materials do not differentiate between the high strain rate ... produced by rapid loading as compared with that produced by a rapidly propagating crack. Either phenomena, rapid loading or a rapidly propagating crack, cause a marked decrease in resistance to crack extension. Once crack extension is initiated, the reduced toughness due to the increased strain-rate causes very abrupt crack acceleration...

"For temperature and strain-rate-sensitive materials, the following design approaches are possible:

- "1. Limit the operating temperature to remain above the behavior transition-temperature range...
- "2. When the operating temperature is in or below the behavior transition-temperature range, two choices are available:
 - "a. Limit the stress and crack length to avoid initial crack extension.

"b. Limit the stress to a level that will not support fast fracture"

The above choices (a and b) are complicated by the fact that the stress must include the residual welding stresses if they act over a region that is large compared with the crack size and, furthermore, initial crack extension may occur as a result of local conditions such as yield-point-magnitude residual welding stresses, hydrogen, metallurgically embrittled regions produced by tack welding, arc strikes, etc. Thus, the 2nd of the design approaches involves fabrication uncertainties (indeterminants) that preclude a fracture-safe situation when service temperatures are below the behavior transition temperature.

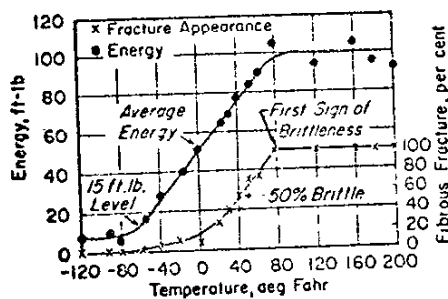
With the advent of linear elastic fracture mechanics, toughness of a material was related to nominal stress and flaw size in a quantitative manner. The standardized test method for measuring toughness (K_{Ic}) took into account the fact that minimum toughness is associated with a sharp crack, such as a fatigue crack. In spite of the quantitative advantage of the fracture-mechanics approach, the transition-temperature approach continues to be favored for material selection and quality control for structural-grade steels because of its relative simplicity, low cost and small specimen size. Specifically Charpy V-notch (CVN) impact specimens have been widely used for many years and the results found to be useful not only for material selection and quality control, but also to the metallurgist for comparing and controlling heat treatments and other production and fabrication processes.

Probably, the greatest single impetus to general acceptance of the CVN impact test in the United States was the statistical evaluation of casualty ship plate conducted at the National Bureau of Standards during and after World War II. Casualty plate was placed in categories according to whether it corresponded

to "fracture source, fracture through, or fracture end". V-notch Charpy impact tests showed that "fracture-source" plates were more notch sensitive than plates which did not contain a fracture source. The average energy absorptions were 7 ft-lb for source plates, 10 ft-lb for through plates, and 16 ft-lb for end plates. On the basis of these test results, a 15 ft-lb criterion is in general use for rimmed and semi-killed steels of the type used in ship-hull construction. It is important to note that the correlation between 15 ft-lb and service is reliable only for the particular type of steel used in ship construction.

4.1.2 Fatigue Precracked Charpy Testing

Since the transition from ductile-to-brittle behavior in the CVN-impact test is often not abrupt, the selection of a transition temperature must be somewhat arbitrary. Some of the common criteria used in CVN-impact testing are illustrated in Figure 4.1, taken from the work of Rinebolt and Harris(24). More recently (in the early 1960's) Orner and Hartbower(25) demonstrated that the CVN-impact test can be used semi-quantitatively to measure the fracture



Charpy Test Transition Temperatures,
Including Fracture Mode Transition
Figure 4.1

toughness of constructional metals in section thicknesses of .030 to .800-in. This is accomplished by introducing a crack at the root of the notch which simulates an actual defect. Another important

advantage in precracking over the relatively blunt machined V-notch used in the casualty-ship-plate investigations is the elimination of certain energy losses which tend to make measurements with uncracked V-notched specimens fictitiously high in brittle materials. Likewise, with the conventional (uncracked) V-notch Charpy test, the transition can be obscured by elastic energy losses in the low-temperature range. Additional evidence of elastic-energy loss is found in the fracture behavior of the specimens. Without precracking, the specimens tested in the low-temperature range tend to be ejected from the anvils with considerable velocity in a direction opposite to the movement of the pendulum. Thus, the elastic energy stored in the specimen and adjacent parts of the machine, over and above that required to propagate fracture, is converted into kinetic energy.

Currently the National Materials Advisory Board (NMAB) of the National Research Council has an ad hoc Committee on Rapid Inexpensive Tests for Determining Fracture Toughness. The committee is critically reviewing correlations which have been published between rapid, inexpensive test methods and valid ASTM E399 plane-strain fracture toughness (K_{IC}) measurements. In the course of their study, it became apparent that the committee would not be able to select a single fracture-toughness test method which would be useful for all materials, or applicable for a single material over the full range of possible strength levels (particularly in steel). It was therefore decided by the committee to single out the most promising test methods and recommend further experimental investigations to establish the precise quantitative correlation which might be used in a given application.

In evaluating the various rapid, inexpensive test methods which have been proposed to measure fracture toughness, the committee considered not only the degree of correlation which could be

demonstrated for a given test method but also the complexity of the measurements to be made or their analysis, the probable capability of quality-control personnel to make and analyze such measurements, and the relative cost of preparing specimens and carrying out the tests.

Of the rapid, inexpensive tests examined by the committee, the Charpy and the dynamic tear test specimens were concluded to be the most likely to yield useful results either in predicting K_{Ic} values or in predicting lower-limit values of K_{Ic} for specification or quality-control purposes. Charpy-size specimens were examined in a number of ways in an attempt to establish a reliable indication of the K_{Ic} value in a variety of materials and strength ranges. They concluded that this type specimen had the following advantages:

- a. small size,
- b. low cost,
- c. capability of measurement in several orientations, and
- d. capability of measurement over a range of temperatures.

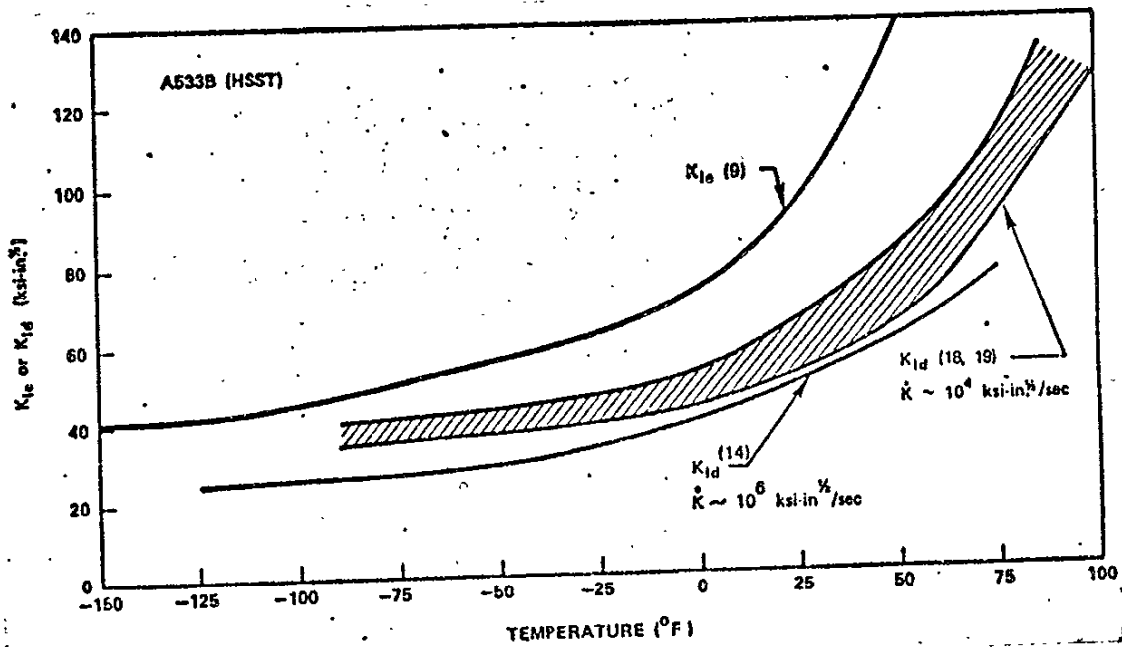
Therefore, the committee is recommending that the fatigue-precracked Charpy specimen tested in slow bending and used to measure the total specific energy to fracture (W/A) be adopted for establishing correlation with plane-strain fracture toughness (K_{Ic}) and minimum acceptance standards in quality-control programs.

Apparently the NMAB ad hoc Committee has tentatively concluded (the report has not yet been finalized) that precrack Charpy impact has no merit for correlation with static K_{Ic} . The committee has not drawn any conclusions with regard to possible correlation between precracked Charpy W/A and dynamic fracture toughness K_{Id} .

Studies sponsored by the nuclear power industry indicate that such a correlation exists(26); Figure 4.2 is a comparison of the results from several studies involving valid ASTM E399 compact-tension K_{IC} testing and dynamic-fracture-toughness testing of large specimens (two to eight inches thick). At the NDT temperature (+10°F), 6-in.-thick specimens were required for valid K_{IC} tests and 2-in.-thick specimens were required for "valid"* K_{Id} tests. Valid K_{IC} values could not be obtained above 50°F even with 12-in.-thick specimens and "valid" K_{Id} values could not be obtained above +125°F with 8-in.-thick specimens. Obviously the curves shown in Figure 4.2 were very costly to obtain (approximately 1.5 million dollars); the instrumented precracked Charpy data, on the other hand, which provided a lower bound to the K_{Id} test results(27) were obtained at relatively low cost (about \$500).

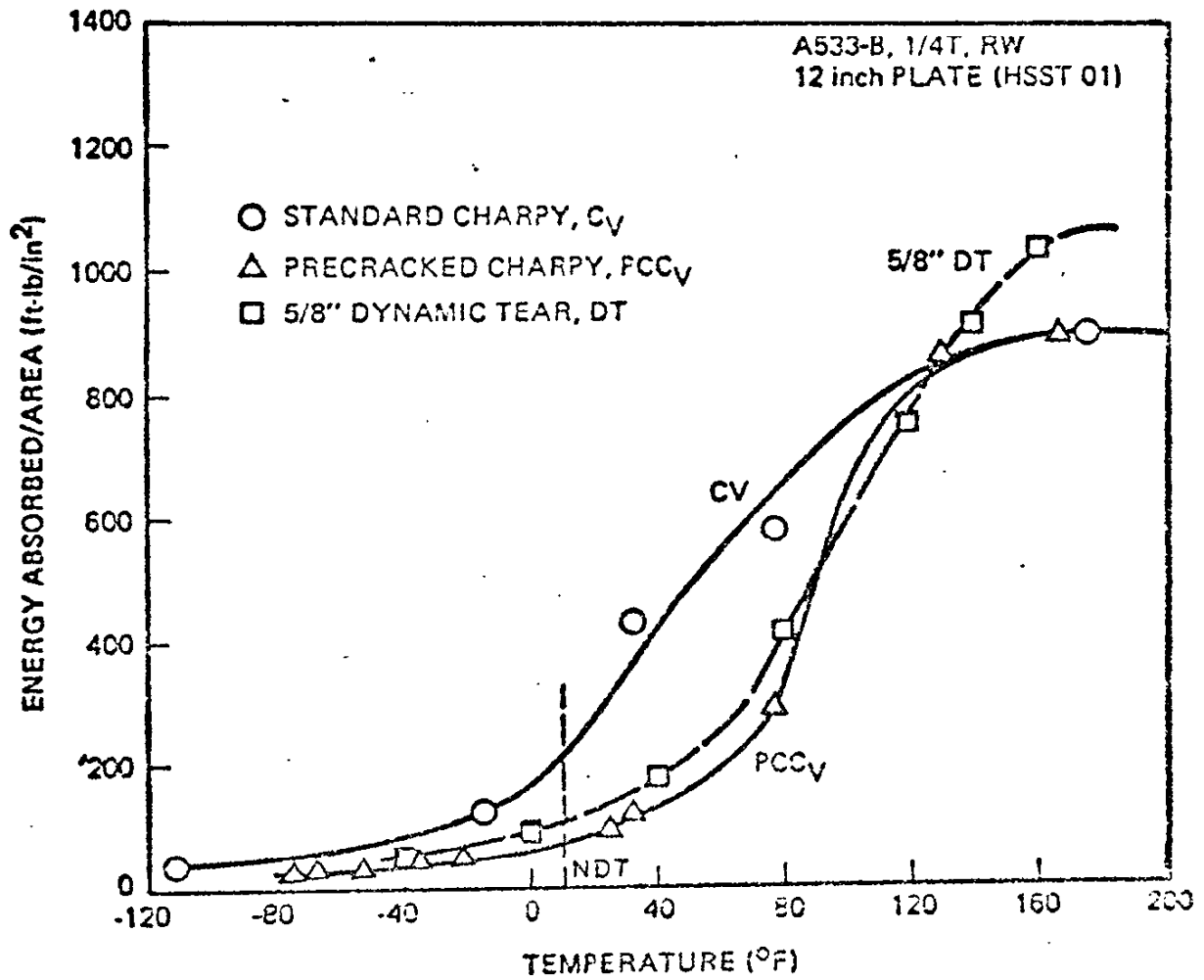
Much has been said about the deficiencies of the standard Charpy V-notch impact specimen(28), notably that on some occasions it has been found to give fictitiously high energy values. The problem is primarily the relatively blunt notch which results in high initiation energy for fracture. And in occasional heats where there is an extreme sensitivity to notch acuity (crack-sensitive steel), the precrack Charpy will give much lower values than the standard CVN-impact test; i.e., there is a marked displacement of the transition curves. To illustrate this point, Wullaert, Ireland, and Tetelman(27) tested CVN-impact and PCI specimens from identical material tested by Frank Loss of the Naval Research Laboratory using 5/8-in. dynamic tear specimens (Figure 4.2.1). Note that the energy transition for the PCI test was sharper than that of the CVN-impact test and corresponded

*There is no standard method for K_{Id} testing at the present time; "valid" implies use of the same criteria called out in ASTM E399 for static testing.



COMPARISON OF STATIC, DYNAMIC, AND INSTRUMENTED
 PRE-CRACKED IMPACT FRACTURE TOUGHNESS AS A
 FUNCTION OF TEMPERATURE
 (26)

FIGURE 4.2



COMPARISON OF V-NOTCH AND PRECRACKED CHARPY DATA WITH 5/8" DYNAMIC TEAR DATA ON A533-B STEEL (27)

FIGURE 4.2.1

closely to the DT test curve. Note also that the NDT temperature occurred below the "knee" of the precracked Charpy curve. "Thus, the small Charpy specimen, when precracked, can be used to obtain the type of data normally obtained from the dynamic tear test, at least for 5/8-in. and 1-in. DT specimens(27)."

4.1.3 Current Developments in Precracked Charpy Testing

It is clear that the precrack Charpy test will play an important role in future material evaluations and specifications. The Pressure Vessel Research Council/Metal Properties Council (PVRC/MPC) Joint Task Group on Fracture Toughness Properties for Nuclear Components has recently completed a study of Instrumented Precracked Charpy Testing under the chairmanship of C. Buchalet of Westinghouse Nuclear Energy Systems(29). The purpose of the study was to establish a limited testing program to obtain dynamic fracture toughness values on reactor pressure-vessel steels and to develop the corresponding test procedures to verify these values. The instrumented precracked Charpy test was one of the tests recommended by the Joint Task Group to obtain dynamic fracture toughness data.

The working group to study the instrumented precracked Charpy test was assigned the task of developing a recommended testing procedure capable of producing dynamic-fracture-toughness values for medium-strength steels used in the fabrication of nuclear pressure vessels. The values developed were to be marked by an acceptably narrow range of variability and were to be comparable to dynamic fracture toughness values obtained from other types of specimens.

The material tested was pressure-vessel-steel ASTM A533 Class 1 grade B which has a chemistry and strength not greatly different from some bridge steels; viz.,

A533 Class 1 grade B: yield 50 ksi
Carbon 0.25%
Manganese 1.15 to 1.50
Molybdenum 0.45 to 0.60
Nickel 0.40 to 0.70

The EPRI Round Robin Test Program - In 1974, Effects Technology, Inc. Santa Barbara, California was awarded the management of a program funded by the Electric Power Research Institute (EPRI) on fracture toughness data for ferritic nuclear-pressure-vessel materials. This program was to supplement the original program sponsored by the USAEC and carried out by the PVRC/MPC joint task group. In the EPRI study, seven heats of A533 B-1 steel are being used together with A302-B pressure vessel steel and weld heat-affected-zone in A533-B-1 steel. Several laboratories are participating in the round-robin test program. In addition to the instrumented precracked Charpy impact test, there are instrumented standard Charpy V-notch, drop-weight NDTT, static 1-in. compact-tension, dynamic 1-in. compact-tension, dynamic 1-in. 3-point-bend, and dynamic 3-in. compact-tension tests. The testing is presently underway.

In the EPRI study of instrumented impact tests procedures, emphasis is placed on assurance of conservative calculations of fracture toughness. The results of the program should provide ASTM with much valuable information for consideration in development of a recommended practice for dynamic fracture-toughness testing of ferritic materials.

The ASTM E24.03.03 Round Robin Test Program - In addition to the studies by the PVRC.MPC and EPRI working groups, ASTM Committee E24 on Fracture Testing has a working task group E24.03.03 which is to establish a standard procedure for precracked Charpy impact and slow-bend testing under the chairmanship of C. E. Hartbower. Two of the steels used in this study are of immediate interest to bridge engineers, viz., A36 and A514 steel.

ROUND ROBIN MATERIAL				
NOTCH DEPTH (mils)	NOTCH ACUITY	PRECRACKING LOAD		
		1/3 $K_f(m)$	2/3 $K_f(m)$	1 $K_f(m)$
110	SCR	2	2	2
	EDM	2	2	2
	005	2	2	2
150	SCR	2	2	2
	EDM	2	2	2
	005	2	2	2
200	SCR	2	2	2
	EDM	2	2	2
	005	2	2	2

Materials

Steels: A36, A533, A517

Aluminum: 2219T851

Titanium: 6 Al-4V

Specimens

54 per material

$K_f(m)$

Maximum allowable K_f

ASTM E24.03.03 PRECRACKED
CHARPY ROUND-ROBIN PHASE I TEST MATRIX (NBS)

FIGURE 4.3

The ASTM effort is broken down into two phases: - Phase I is to investigate the principal variables involved in the precracking operation and Phase II is to determine lab-to-lab variability using a proposed method for the precrack Charpy testing. A statistical test plan for assessing the effects of the precracking variables was designed by the National Bureau of Standards* as shown in Figure 4.3. Thus, the variables under investigation are (1) preparation of the Charpy V-notch: (a) as-machined to 5-mil radius, (b) electric-discharge machine (EDM) sharpened, and (c) 10-mil-radius notch scribed with a razor blade; (2) fatigue load level in precracking: (a) 1/3 maximum allowable stress intensity, (b) 2/3 maximum allowable stress intensity and (c) at maximum allowable stress intensity; and (3) machined-notch plus fatigue-crack depth: (a) 110, (b) 150 and (c) 200 mils. All fatigue precracking in Phase I was done by a single laboratory (Effects Technology, Inc.) to avoid possible lab-to-lab variability; likewise, all impact testing was done in one laboratory (Babcock and Wilcox Alliance Research Center) and all slow-bend testing will be done in one laboratory (U.S. Air Force Materials Laboratory, Dayton, Ohio) to avoid possible lab-to-lab variability in the test results. In Phase II a round-robin program will investigate lab-to-lab variability using the optimum fatigue precracking procedure evolving from Phase I.

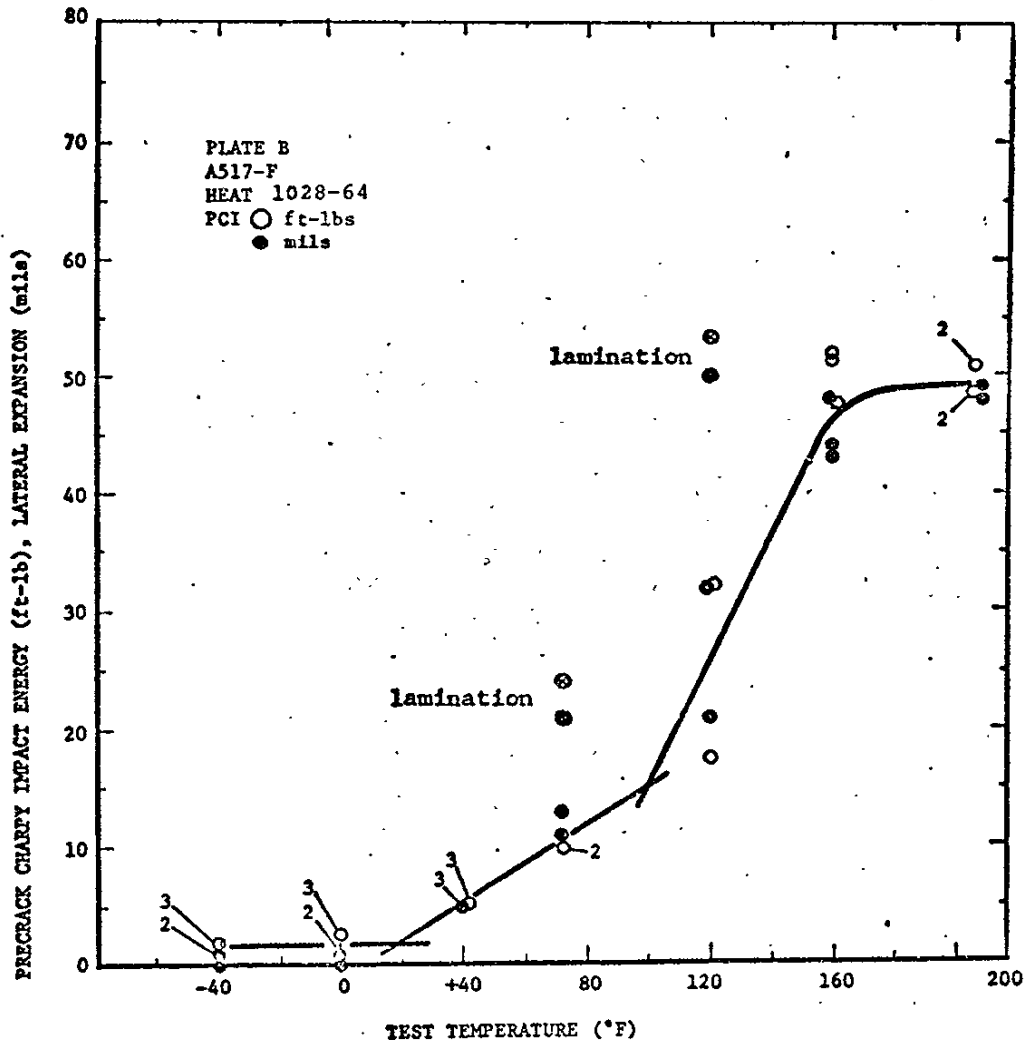
4.1.4 A514/517 Charpy Data Plotting

In this investigation of 76 slabs from 30 heats in the Bryte Bend and Tuolumne bridges, both standard Charpy V-notch (CVN) impact and precracked Charpy impact (PCI) tests were made. In most plates, tests were made over a range of temperature encompassing the lowest anticipated service temperature (LAST).

*Dr. J. Mandel, Dr. J. Filiben and Dr. C. Interrante of the National Bureau of Standards.

Plots of energy versus temperature are appended (Appendix C, Figure C1 thru C52). The plots are presented in the order of heat numbers. For convenience of cross reference and location of the respective plots, the Appendix C figures are preceded by a table of steel-producer's heat numbers, the report code for each heat/slab, the plate identification (alphabetical), the ASTM type-grade and the plate thickness. A second tabulation is also provided which places the heat/slabs in alphabetical order according to the plate-identification system used for brevity in the report.

A cursory review of the 54 plots shows little problem with scatter in the test data for either CVN-impact or PCI testing; however, in general, the precrack Charpy data were more reproducible than those of the standard CVN-impact test. Plate B was a notable exception, Figure C-51, where there were laminations evident in the fracture surfaces of two of the precracked Charpy specimens. As a result of the laminations, internal shear lips formed to produce fictitiously high energy values (at 72°F, 23.9 ft-lb and 21 mils, and at +120°F, 53.4 ft-lb and 50 mils). When the two laminated specimens were discounted and the lateral-expansion measurements were added to the energy-temperature plot (Figure 4.4), there was remarkably little scatter in the test data except in the transition region at +120°F and 160°F. There was no evidence of laminations in the standard CVN-impact test specimens to account for the extreme scatter in these data from plate B. Lateral expansion is a measurement that is independent of the energy determination (lateral expansion is measured in the broken test piece using a micrometer or dial indicator) and yet is directly proportional to the energy, as shown in Figures 4.5 thru 4.8.



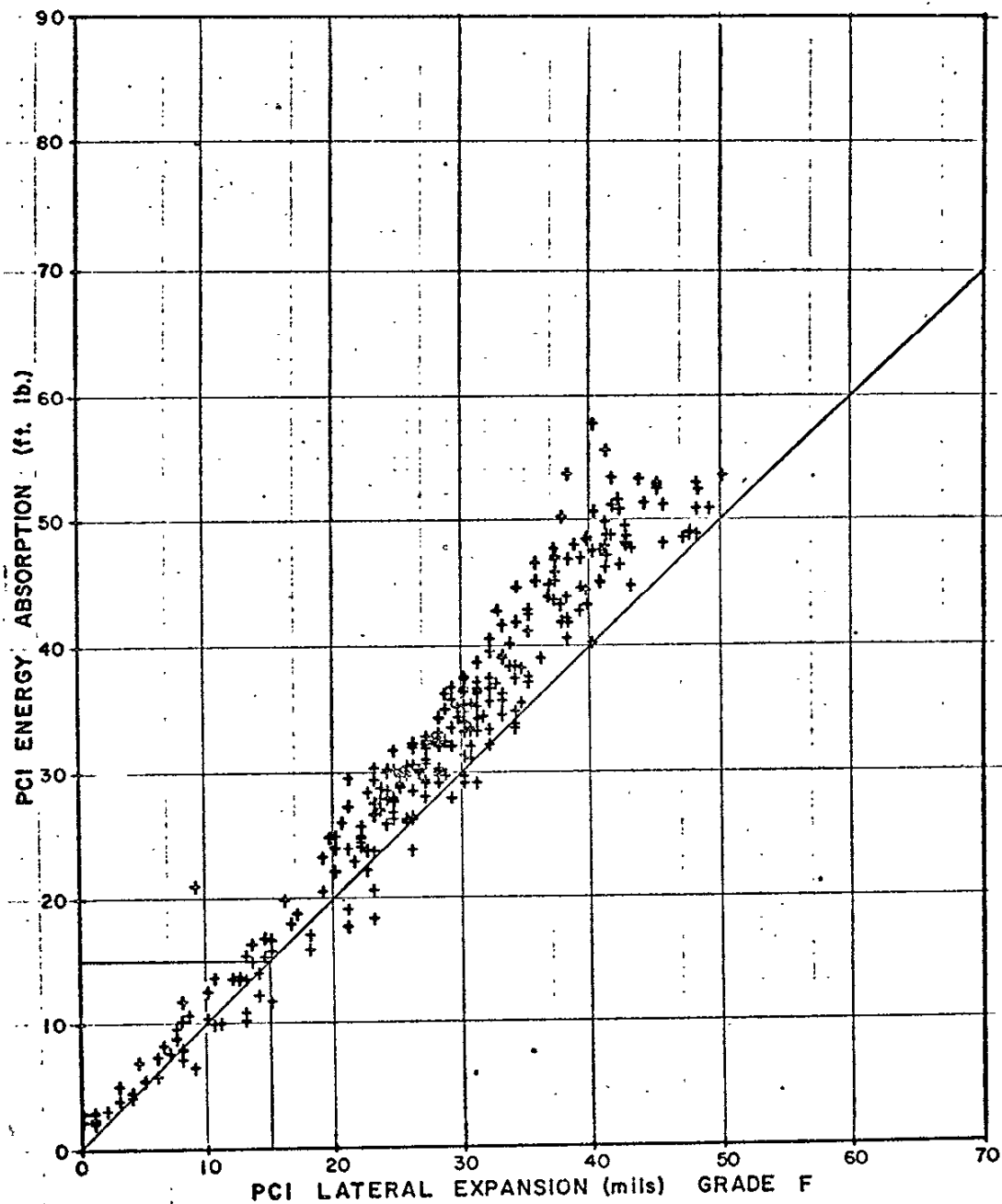
PRECRACK CHARPY IMPACT TRANSITION CURVE
FOR A517-F PLATE B BASED ON ENERGY ABSORPTION
AND LATERAL EXPANSION

FIGURE 4.4.

The plots presented in Figures 4.5 to 4.8 include all the data from the 30 heats of A514/517 steel tested. The data were plotted using a programmable calculator (HP9810A) and plotter (HP9862A). With this system, the programmable calculator was interfaced with the plotter; thus, given an X and Y coordinate value (an energy value and a corresponding lateral expansion value), the calculator scales the values, and then moves the pen to the coordinate location and marks the paper with the predetermined symbol (+, x, o, , etc.). Once the calculator is programmed one needs only to enter the X and Y coordinate values on a key board not unlike that of a typewriter and the desired plot is developed. The energy-temperature plots of Appendix C also were produced by this method.

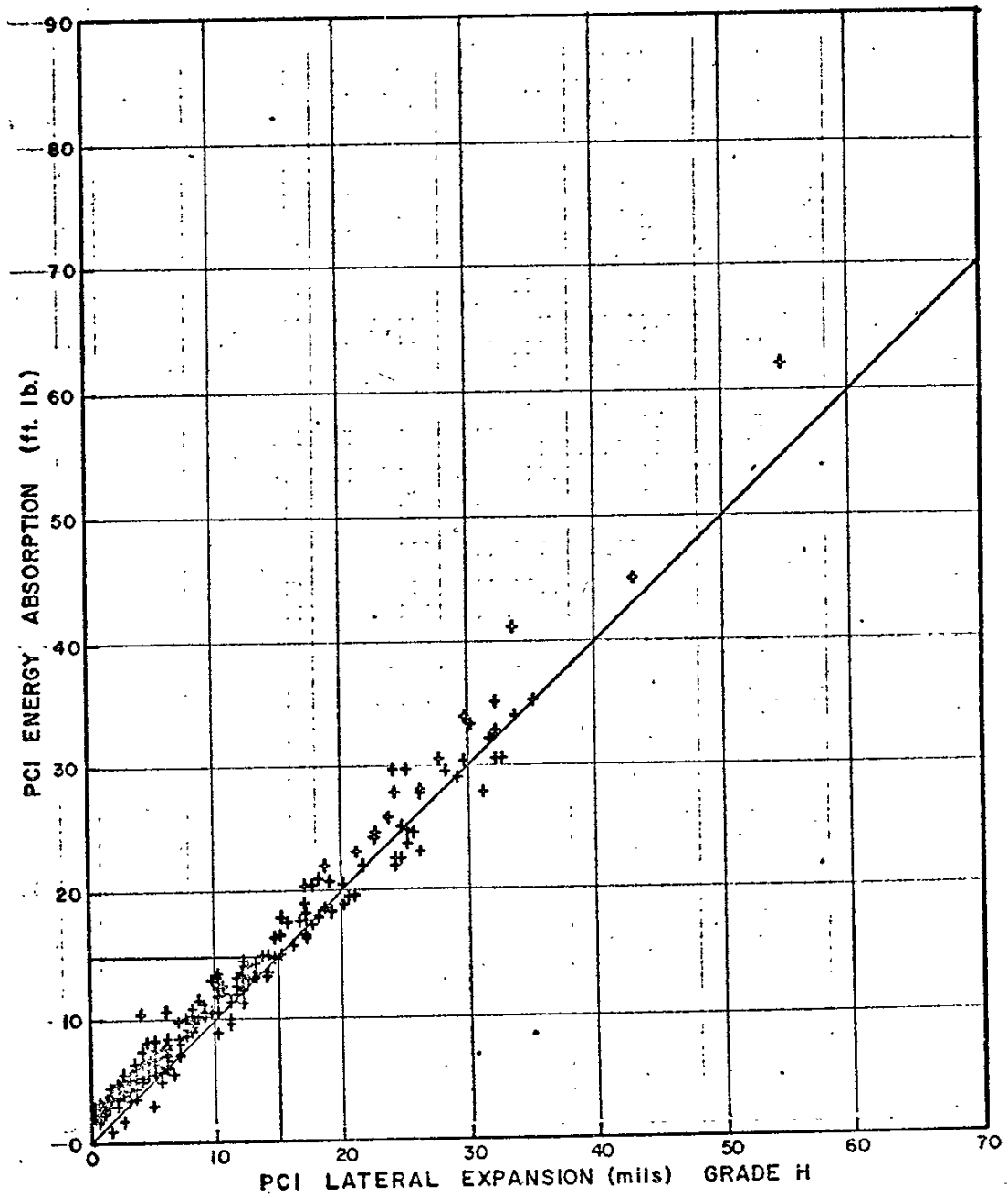
In Figures 4.7 and 4.8 note that in the CVN-impact test of A514/517 steel, 15 mils is equivalent to approximately 20 ft-lb of energy; whereas, in the PCI test of A514/517 steel, 15 mils is equivalent to 15 ft-lb. Thus, when lateral-expansion data and energy data from the PCI test are plotted together, the data for all practical purposes are superimposed; whereas, in the CVN-impact test there is a displacement of the energy and lateral expansion curves.

Figure 4.9 illustrates the displacement that occurs between the lateral expansion and energy transition curves with CVN-impact data; precrack Charpy lateral expansion and energy data, on the other hand, are superimposed (Figure 4.4). If the ordinate scale for lateral expansion were displaced upward in Figure 4.9 so that 15 mils of lateral expansion corresponded to 20 ft-lb of energy, the lateral expansion data would, for all practical purposes, be superimposed on the energy data. Note that much greater scatter occurred in the CVN-impact test results (Figure 4.9) as compared with the PCI test results (Figure 4.4).



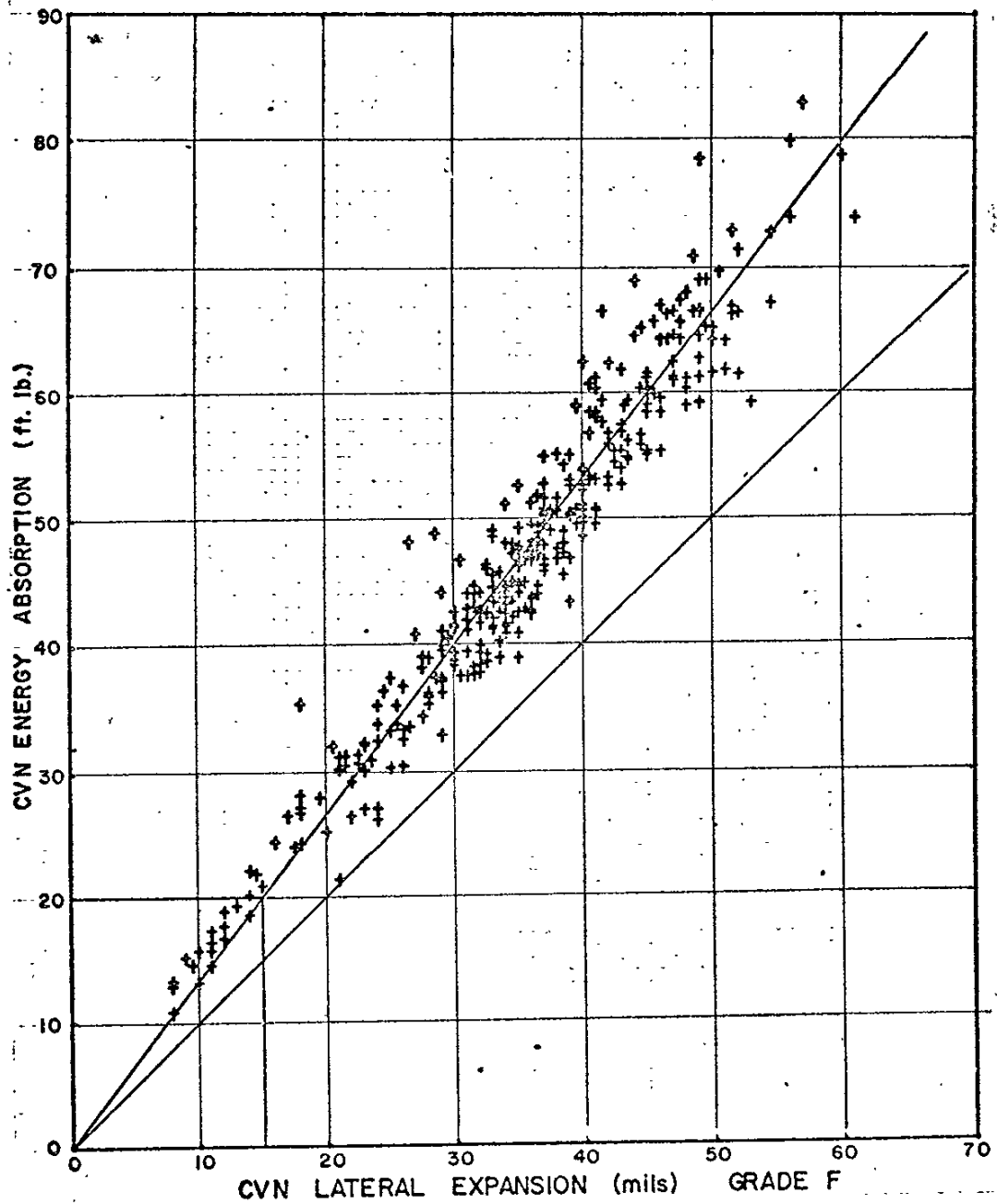
RELATIONSHIP BETWEEN ENERGY ABSORPTION AND LATERAL EXPANSION IN PRECRACK IMPACT TESTS OF A514/517 GRADE F STEELS

FIGURE 4.5



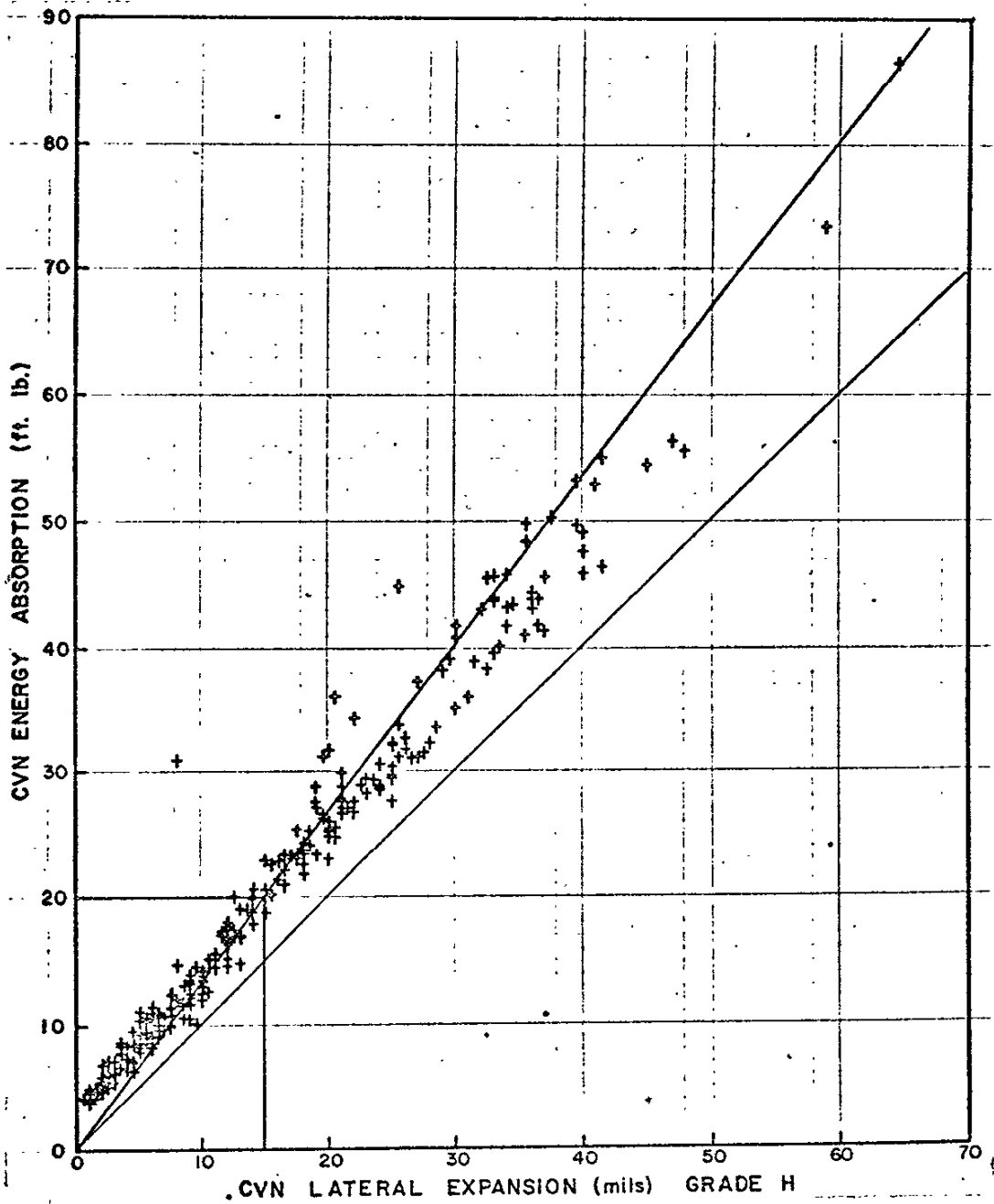
RELATIONSHIP BETWEEN ENERGY
 ABSORPTION AND LATERAL EXPANSION IN PRECRACK
 CHARPY IMPACT TESTS OF A514/517 GRADE H STEELS

FIGURE 4.6

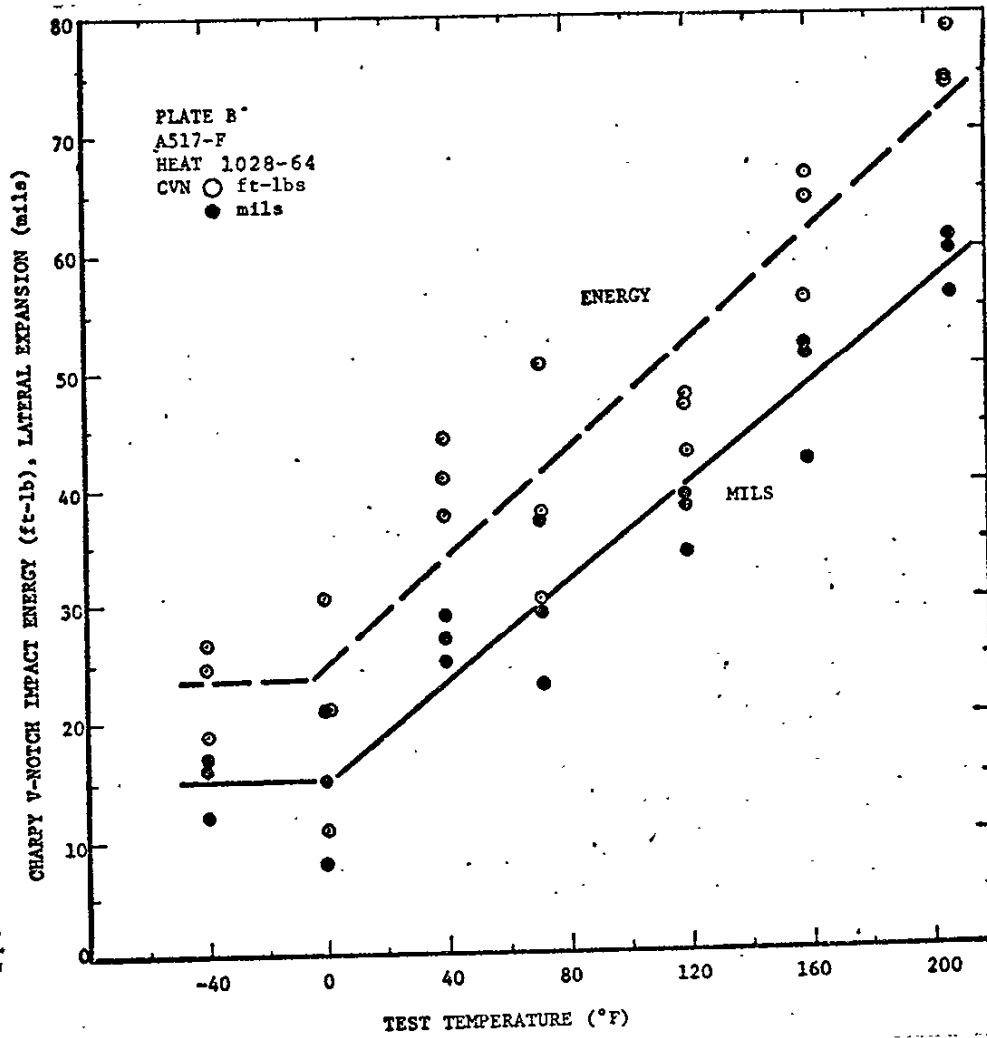


RELATIONSHIP BETWEEN ENERGY
 ABSORPTION AND LATERAL EXPANSION IN STANDARD
 CHARPY V-NOTCH IMPACT TESTS OF A514/517 GRADE F STEELS

FIGURE 4.7



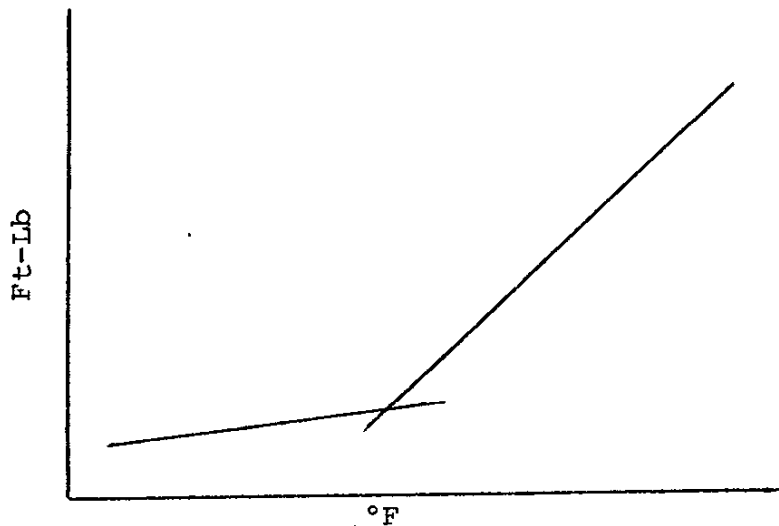
RELATIONSHIP BETWEEN ENERGY
 ABSORPTION AND LATERAL EXPANSION IN STANDARD
 CHARPY V-NOTCH IMPACT TESTS OF A514/517 GRADE H STEELS
 FIGURE 4.8



CVN-IMPACT ENERGY ABSORPTION AND LATERAL EXPANSION TRANSITION CURVES FOR A517-F PLATE B

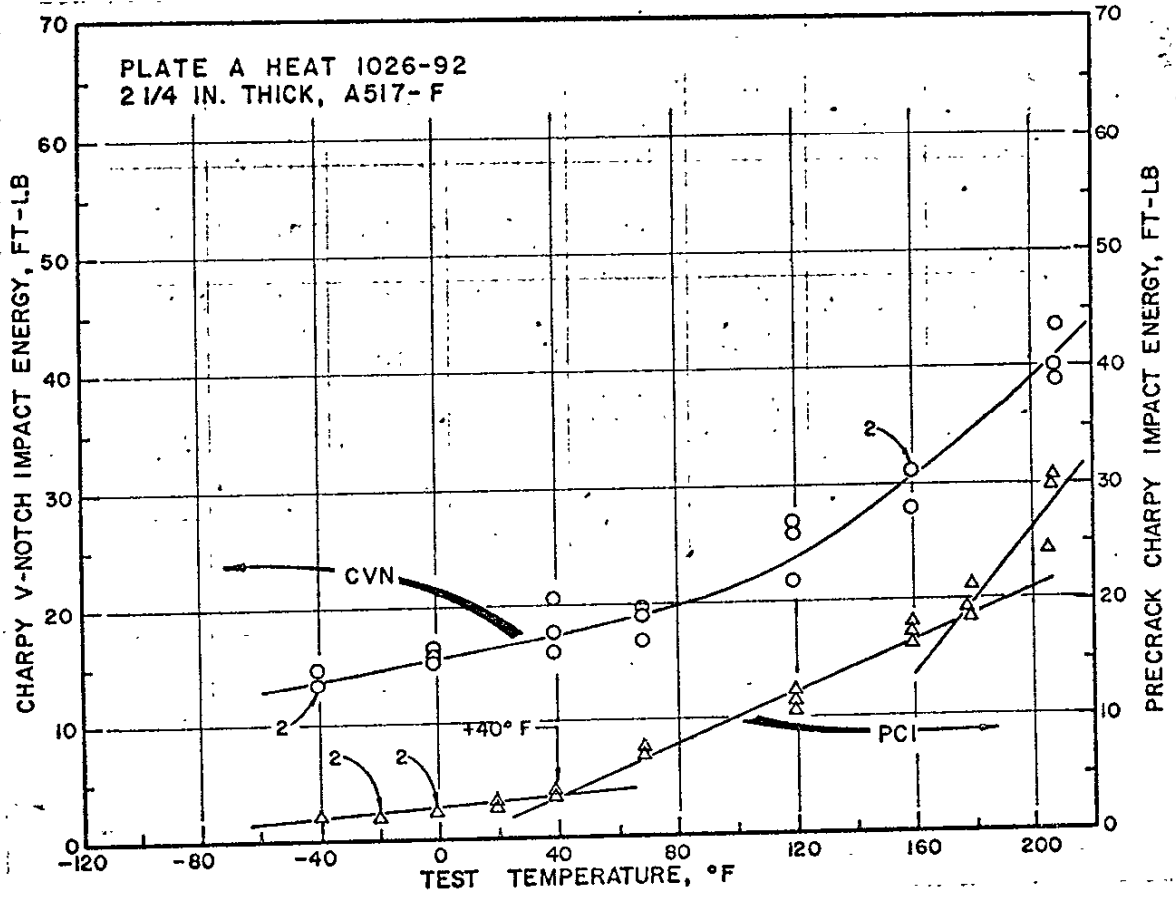
FIGURE 4.9

From an examination of the 52 plots of precracked Charpy impact data in Appendix C, it will be seen with very few exceptions, two intersecting straight lines nicely fit the data at the junction of the lower shelf and the transition region, as in the following schematic:



TYPICAL PRECRACKED CHARPY
IMPACT TRANSITION BEHAVIOR

Among the exceptions are cases where there were three intersecting straight lines in the transition region, as in plates A and B from the Tuolumne Bridge. The PCI transition curve for Plate B was shown previously in Figure 4.4. Figure 4.10 is the PCI transition curve for plate A. The ASTM E208 NDT temperature for plate A was found to be +120°F for the mid-thickness plate position. It should be noted, however, when the 3/4-in.-thick NDT test specimen was centered at mid-thickness, the material actually being tested approximately corresponded to the quarter-point position (see page 245 Figure 4.90). The Charpy specimen, because of its small size (0.394-in. as compared to 0.750-in. in the NDT test), provided a test of the mid-thickness microstructure, which was very poor because of a deficiency in hardenability in plate A. This problem is discussed in some detail in this

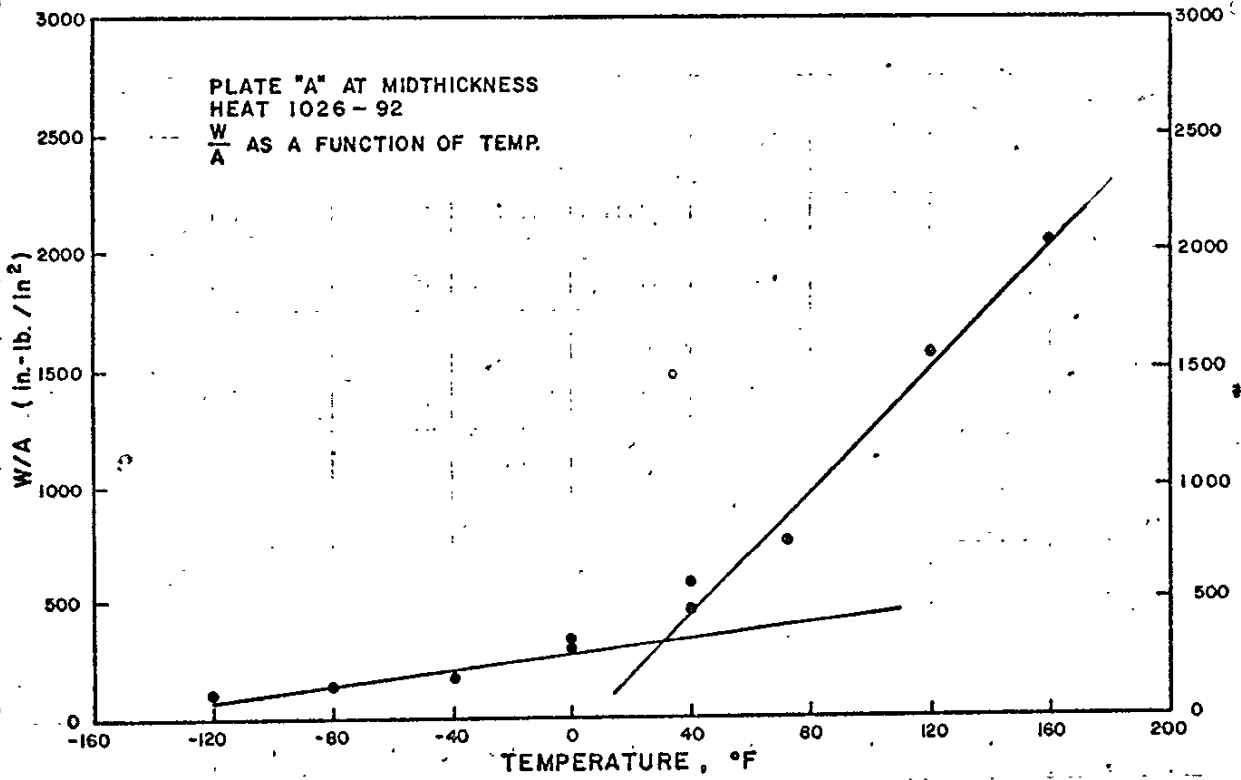


CVN-IMPACT AND PCI TRANSITION
CURVES FOR A517-F PLATE A

FIGURE 4.10

report in connection with the drop-weight NDT and dynamic-tear testing results. The subject is brought up here in connection with the double inflection point in plate A because it has been shown(25) that the point of intersection of the two straight lines (the inflection point) in the precracked Charpy energy and lateral-expansion plots provides an approximation of the NDT temperature. If the material at mid-thickness has a more brittle microstructure than that at the quarter point, the difference in NDT temperature shown by the precracked Charpy and the larger (thicker) E208 NDT test specimen could simply and correctly reflect the difference in microstructure in the two test positions. It is important to keep in mind that the microstructure at the tension surface of the NDT bend specimen controls the E208 test result.

Effects Technology, Inc. (ETI) also tested plate A using the instrumented precracked Charpy impact test(13). The ETI investigators measured the net-section in each test specimen after precracking and divided the total energy absorbed in fracturing the test piece by the net-section area to get W/A (in.-lb/in.²). This is generally the best procedure for recording the PCI test result because variations in the fatigue-precrack depth will introduce scatter in the test results when ft-lb energy values are plotted against test temperature. However, the scatter in the Caltrans and Aerojet PCI plots of ft-lb versus °F was minimal because there was little variation in the fatigue precrack depth (0.030 ± 0.010 in.). An example of the ETI precracked Charpy impact W/A-temperature plots is shown in Figure 4.11 for plate A. Note that there was very little scatter and the inflection point occurred at approximately the same temperature as in the Caltrans plot of ft-lb versus °F (+30°F as compared with +40°F). ETI did not test above +160°F and, therefore, did not find the 2nd inflection point.



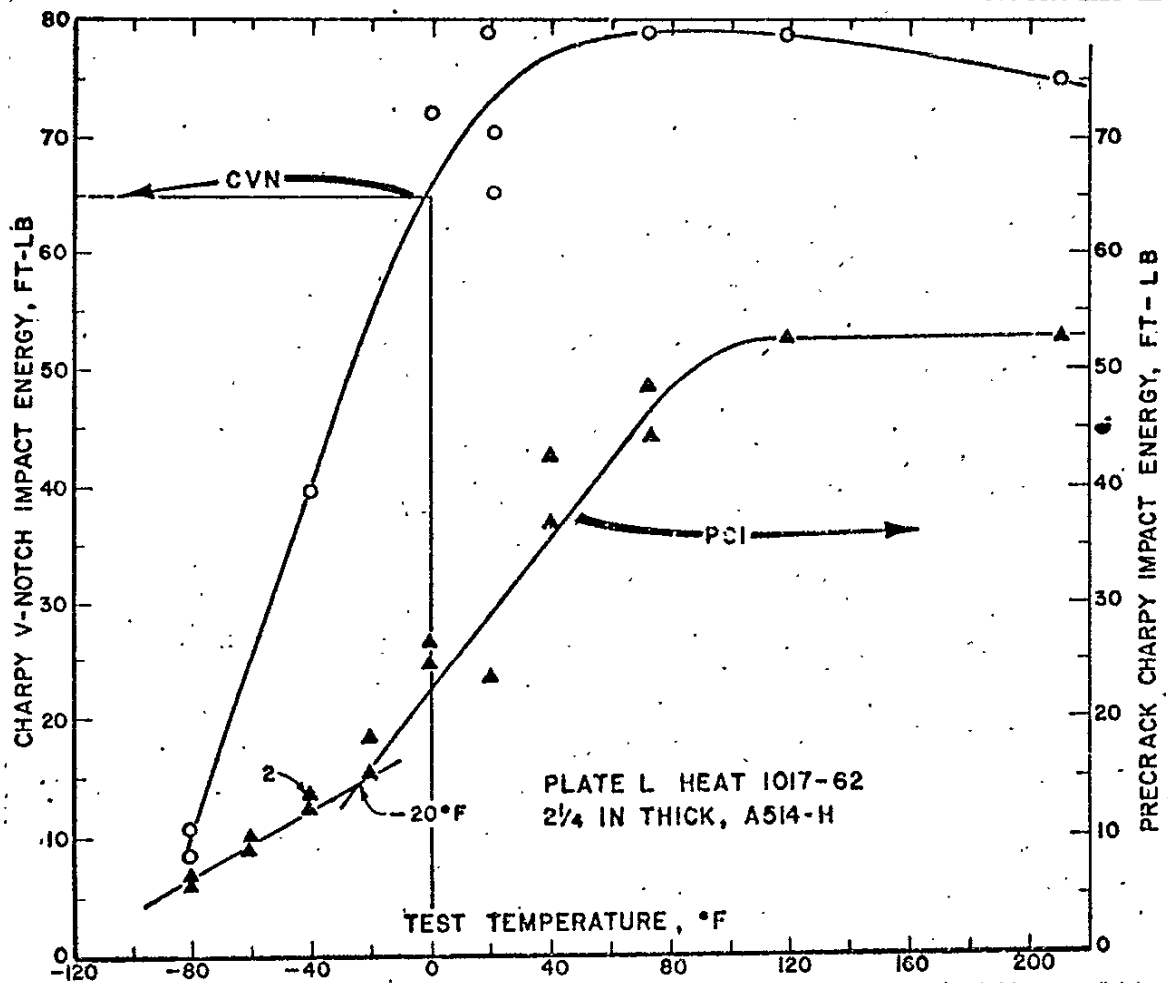
EFFECTS TECHNOLOGY, INC.
PCI W/A-VERSUS-TEMPERATURE PLOT FOR A517-F PLATE A
FIGURE 4.11

The ETI plots of W/A versus test temperature for plates A, AL, L, M, R, Z, and CK are reproduced in Appendix D, together with the instrumented precracked Charpy K_{Id} plots of $\text{ksi-in.}^{1/2}$ versus $^{\circ}\text{F}$ and plots of standard CVN-impact test data as obtained for plates L, M, and CK.

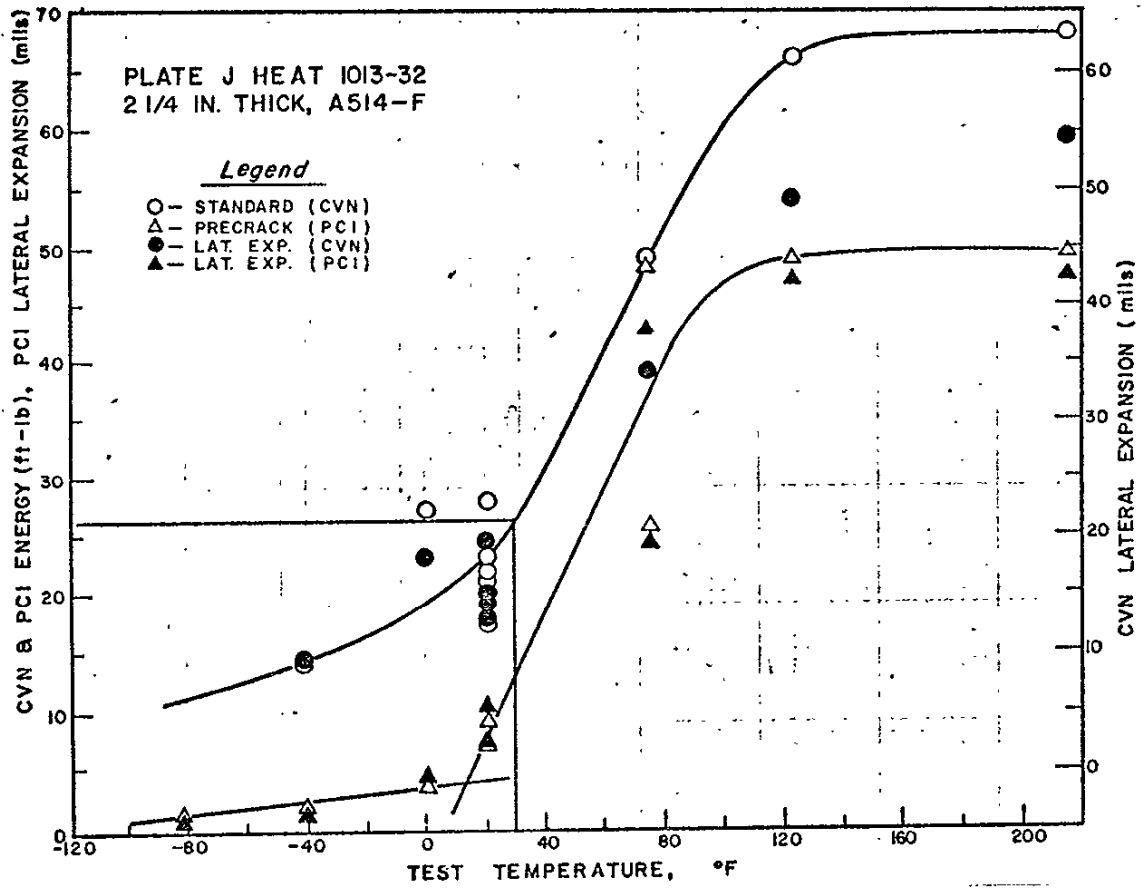
4.1.5 Effect of Notch Acuity

Occasionally there is a heat of steel that is extremely sensitive to notch acuity. In such a heat the transition curves for the standard Charpy 10-mil-radius V-notch and for the fatigue-precracked Charpy impact test specimens are considerably displaced from one another. Plate L provides an example of this phenomenon as shown in Figure 4.12. For group-2 AASHTO service at temperatures from -1° to -30°F , 25 ft-lb CVN-impact is required at 0°F ; in plate L the CVN-impact would average about 65 ft-lb at the test temperature (0°F) specified for group-2 service. However, in plate L the NDT temperature (-20°F) is above the lowest anticipated service temperature for Group-2 service (-30°F). For fracture-safe design, the NDT temperature should be at least 30°F below the lowest anticipated service temperature.

Plates J and CB provide additional examples of cases where standard CVN-impact testing at the temperature ($+30^{\circ}\text{F}$) specified for AASHTO Group-1 would have indicated acceptable steel; whereas, in the presence of a sharp crack (the fatigue precrack) the steel was indicated to have low toughness (see Figures 4.13 and 4.14). The NDT temperature was indicated to be at $+20^{\circ}\text{F}$ in plate CB and at $+10^{\circ}\text{F}$ in plate J; i.e., the NDT temperature was indicated to be above the lowest service temperature for AASHTO Group-1 service (0°F). In the event of a pop-in crack at service temperatures up to 30°F above the NDT temperature, crack arrest is unlikely. Thus, in plates J and CB there was only a nominal notch-acuity effect and yet the shift in the transition curve produced by fatigue precracking had an important effect with respect to the current AASHTO CVN-impact criterion.

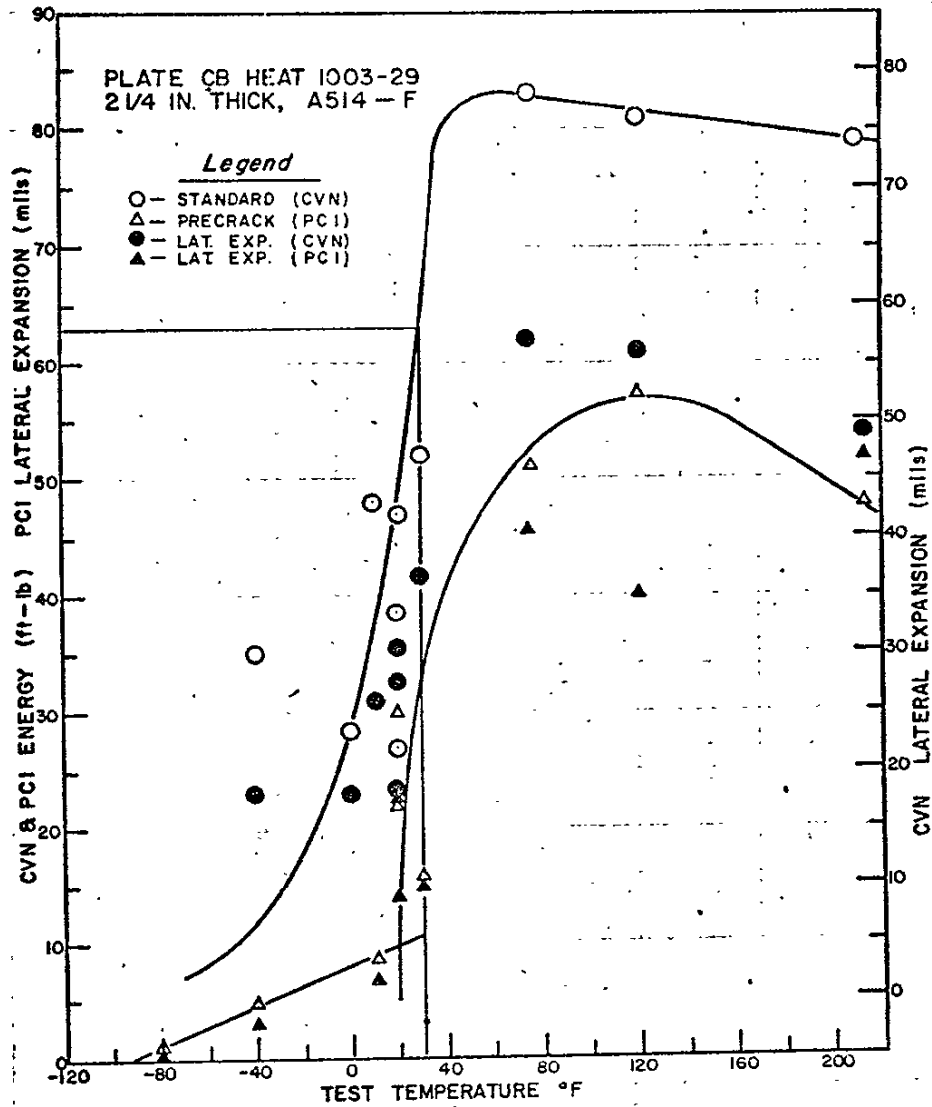


CVN-IMPACT AND PCI TRANSITION
CURVES FOR A514-H PLATE L
FIGURE 4.12



CVN-IMPACT AND PCI TRANSITION
CURVES FOR A514-F PLATE J

FIGURE 4.13



CVN-IMPACT AND PCI TRANSITION
CURVES FOR A514-F PLATE CB
FIGURE 4.14

4.1.6 Lab-to-Lab Reproducibility of Charpy Data

Four laboratories participated in standard and precracked Charpy impact testing of selected heats (from Bryte Bend Bridge and Tuolumne River Bridge) of A514/517 steel. One of the laboratories was the Mechanical Properties Section of the Metallurgy Division, National Bureau of Standards(30). Nine sets of Charpy specimens were forwarded to NBS either in the as-machined condition (CVN-impact specimens) or in the as-machined-and-precracked condition (PCI specimens). The specimens were inspected at NBS to assure that they were in compliance with the dimensional requirements of ASTM 23-72, Figure 4, Type A. The CVN-impact specimens were then tested in accordance with the requirements of ASTM E23-72, Section 8, and the PCI specimens were tested in accordance with the Tentative Proposed Method of ASTM E24.03.03. The testing was done using a Charpy impact testing machine that had been proof tested for the low, middle and high range values on July 21, 1971 and for the low and high-range values on August 1, 1973. The 1971 proof test was in conformance with all of the requirements of ASTM E23-72 Sections 6 and 11. However, for the 1973 proof test, middle-range specimens were not available.

Calculations, data tabulations and curve plotting was done using the computer program ITER, created at NBS. The test plan for the specimens submitted to NBS for testing and computer evaluation is shown in Table 4.1. The results of the impact tests are presented in Appendix E in computer-plotted Figures E-1a to 5c. Figures E-1 and E-2 are plots of longitudinal and transverse standard CVN-impact test results (energy and lateral expansion) for surface and mid-thickness of plate CK. Figure E-3 is a plot of longitudinal precracked Charpy impact test results (energy and lateral expansion) for surface and mid-thickness of plate CK.

TABLE 4.1

TEST PLAN FOR NBS, CHARPY IMPACT TESTING AND
COMPUTER EVALUATION OF A517-H HEAT 1027/44

Longitudinally Oriented (LT)

	Specimen Location	Test Temperature (F)				
		0	+80	+160	+240	+320
Charpy V-Notch (CVN)	Top	17CK1T	17CK2T	17CK3T	17CK4T	17CK5T
		18CK1T	18CK2T	18CK3T	18CK4T	18CK5T
	Center	17CK1C	17CK2C	17CK3C	17CK4C	17CK5C
		Bottom	17CK1B	17CK2B	17CK3B	17CK4B
			18CK1B	17CK2B	17CK3B	17CK4B
	Precracked Charpy (PCI)	Top	17CK6T	17CK7T	17CK8T	17CK9T
18CK6T			18CK7T	18CK8T	18CK9T	18CK10T
Center		17CK6C	17CK7C	17CK8C	17CK9C	17CK10C
		Bottom	17CK6B	17CK7B	17CK8B	17CK9B
			18CK6B	18CK7B	18CK8B	18CK9B

Transversely Oriented (TL)

Charpy V-notch (CVN)	Top	T17CK1T	T17CK2T	T17CK3T	T17CK4T	T17CK5T
		T18CK1T	T18CK2T	T18CK3T	T18CK4T	T18CK5T
	Center	T17CK1C	T17CK2C	T17CK3C	T17CK4C	T17CK5C
		T18CK1C	T18CK2C	T18CK3C	T18CK4C	T18CK5C
	Bottom	T17CK1B	T17CK2B	T17CK3B	T17CK4B	T17CK5B
		T18CK1B	T18CK2B	T18CK3B	T18CK4B	T18CK5B

Figures E-4 and E-5 provide a comparison of the Charpy test results obtained from heat 1027/44CK1 tested by Aerojet General Corporation and heat 1027/44CK2 tested by NBS. Thus, the same heat and slab was tested by the two laboratories; the designation CK1 and CK2 simply shows that two plates were involved (from a single slab). The NBS testing showed that the difference between impact test results of surface (top or bottom) and middle specimens from plates CK-1 and CK-2 were relatively small as compared to the differences found in other heats of steel analyzed in this report. Therefore, independent analyses were made for specimens of similar orientation (longitudinal or transverse) and type (PCI or CVN), but all data for the surface and mid-thickness locations were grouped for similar specimens from a given plate. The data from the two plates thus resulted in two longitudinal PCI sets, two longitudinal CVN sets, and one transverse CVN set.

In this way, the results from a multiplicity of specimens from each of the plates, CK-1 and CK-2, could be compared. For this comparison and with statistical methods, the 95 percent confidence limits for each of five data sets were determined(30).

Figures E-4 and E-5 show the results of this comparison for the 2 PCI data sets and for the 3 CVN data sets, respectively. Each data set is represented by (1) the combined observed data from surface and mid-thickness locations, and (2) a calculated curve of best fit for all of the data in the set. In addition, the best-fit curves for the longitudinal, CVN and PCI, tests of plate CK-2 are bound by a series of arrows that point toward the curve of best-fit. These arrows define the 95% confidence limits for the CK, LT data. The curve of best-fit is plotted as a dotted line for each curve that represents plate CK-1 data.

It is observed on these overlay plots that each of the dotted lines, representing data from plate CK-1 tested at another laboratory, falls close to the corresponding solid line for

longitudinal specimens of plate CK-2 tested at NBS. Some of the data for plate CK-1 falls outside the 95 percent confidence limits given for plate CK-2 but generally the data for CK-1 is within these limits and the differences between the two plates were small and within the limits expected for variations in impact characteristics from plate to plate within a heat. Furthermore, the data for transverse specimens from plate CK-2 are not substantially different from the data for longitudinal specimens, except at elevated temperatures. There, the transverse data are lower than the longitudinal data, indicating that at these temperatures the upper shelf is being approached. However, it appears that the upper shelf was not attained within the temperature range of these tests(30).

Effects Technology, Inc. also ran Charpy tests on plate CK-1. These data are superimposed on those from the National Bureau of Standards in Figure 4.15. This plot again involves two variables; viz., a possible plate-to-plate variation in heat 1027/44 and a lab-to-lab variation. Note that the scatter bands were nearly the same and superimposed for the two sets of data. Likewise, superposition of the scatter band for the Aerojet data from plates CK-1 and CK-2 show remarkably little variation from lab-to-lab. The PCI specimens tested at NBS and ETI were fatigue precracked at Aerojet.

In addition to the CK-1 plate, Effects Technology, Inc. made precrack Charpy impact tests of the following heats:

1026/92A
1020/46AL
1017/62L
1014/02M
1019/31R
1024/94Z

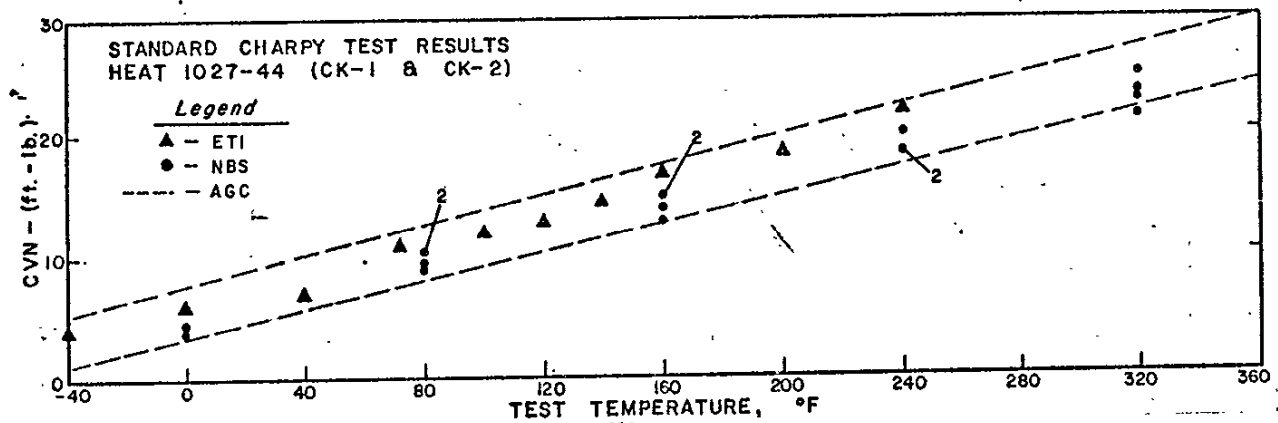
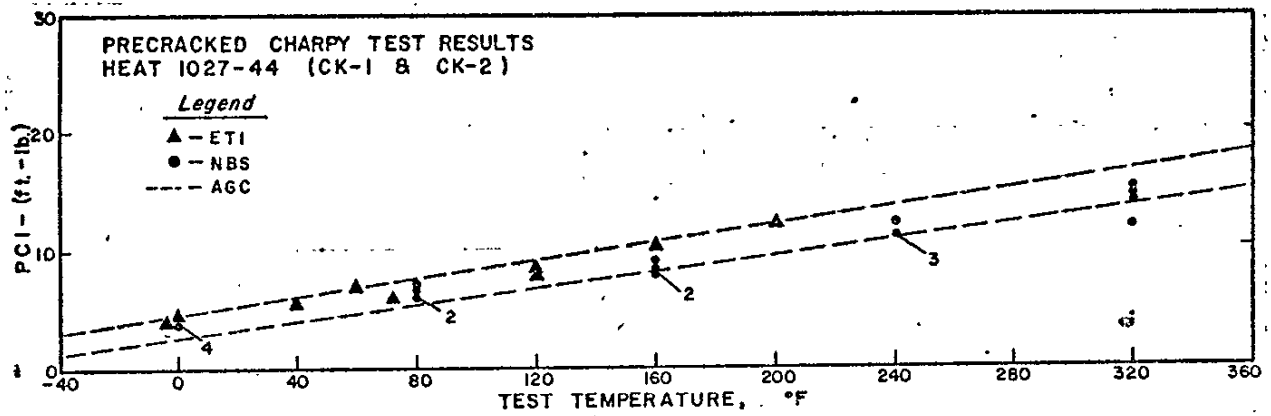
Figures 4.16 to 4.21 are a superposition of the ETI data on the Aerojet General Corporation plots as presented in Appendix C.

It will be noted that where the two laboratories were in disagreement, the ETI data tended to be lower than the AGC data. Discrepancies in the equipment and/or techniques rarely produce fictitiously low values and, therefore, it would appear that the AGC data are slightly higher than the true values. Before the Aerojet tests were made the ManLabs CIM-128 Charpy impact testing machine was proof tested for the low, middle and high-range and found to be in conformance with ASTM E23. However, as will be seen from the following tabulation of results, there was a trend toward higher values with increasing use.

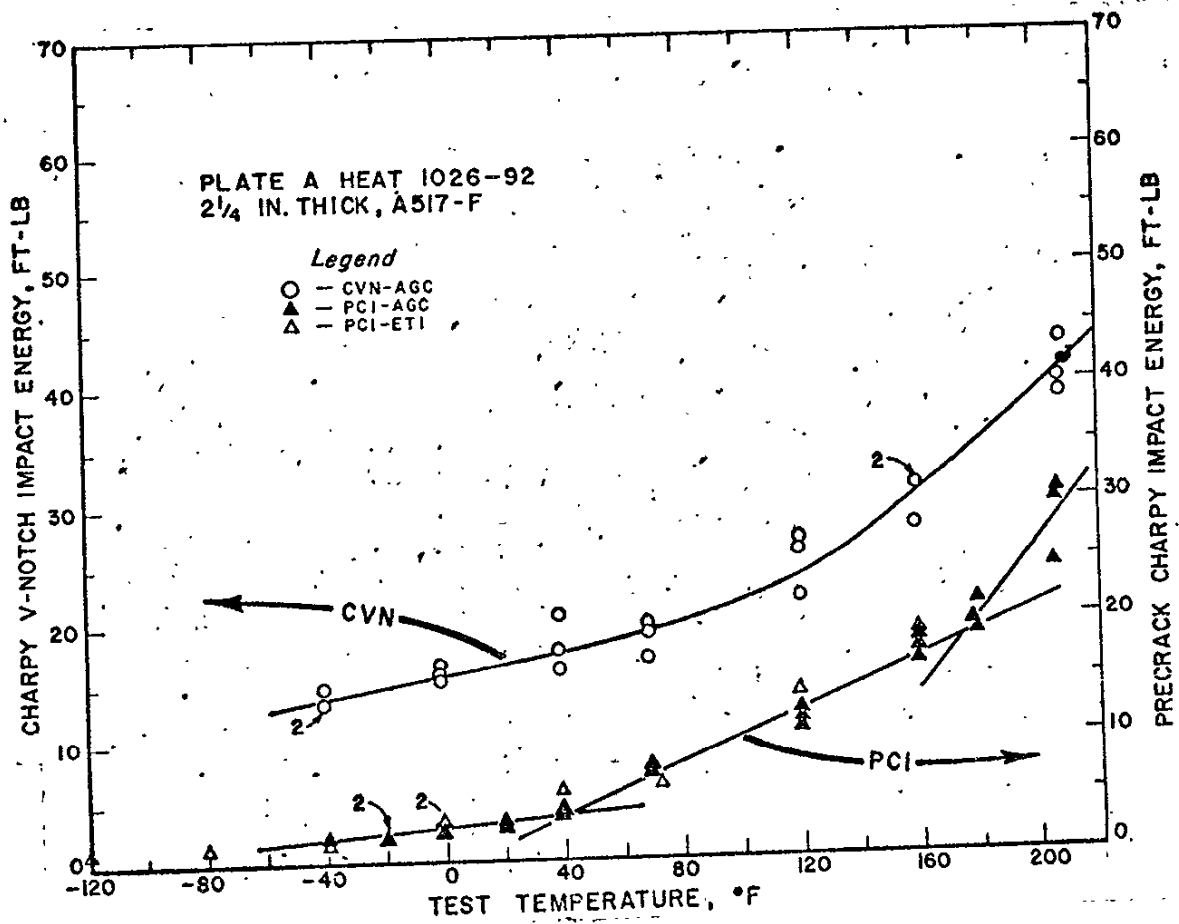
<u>Specimen</u>	<u>Nominal Values</u>	<u>Aerojet CIM-128 Values</u>
J7-608	12.6	14.15
625		13.25
655		12.85 Avg(3) <u>13.4</u>
674*		14.50
698*		<u>13.83</u> Avg(5) <u>13.7</u>
K7-119	44.2	42.45
138		44.30
151		47.10 Avg(3) <u>44.6</u>
182*		47.61
190*		<u>44.80</u> Avg(3) <u>45.2</u>
M7-643	69.3	68.70
630		71.40
655		64.60 Avg(3) <u>68.2</u>
664*		68.56
693*		<u>72.39</u> Avg(5) <u>69.1</u>

Plates A, AL, L, M, R, and Z were tested at Aerojet after the proof testing shown in the above table (excluding data with asterik).

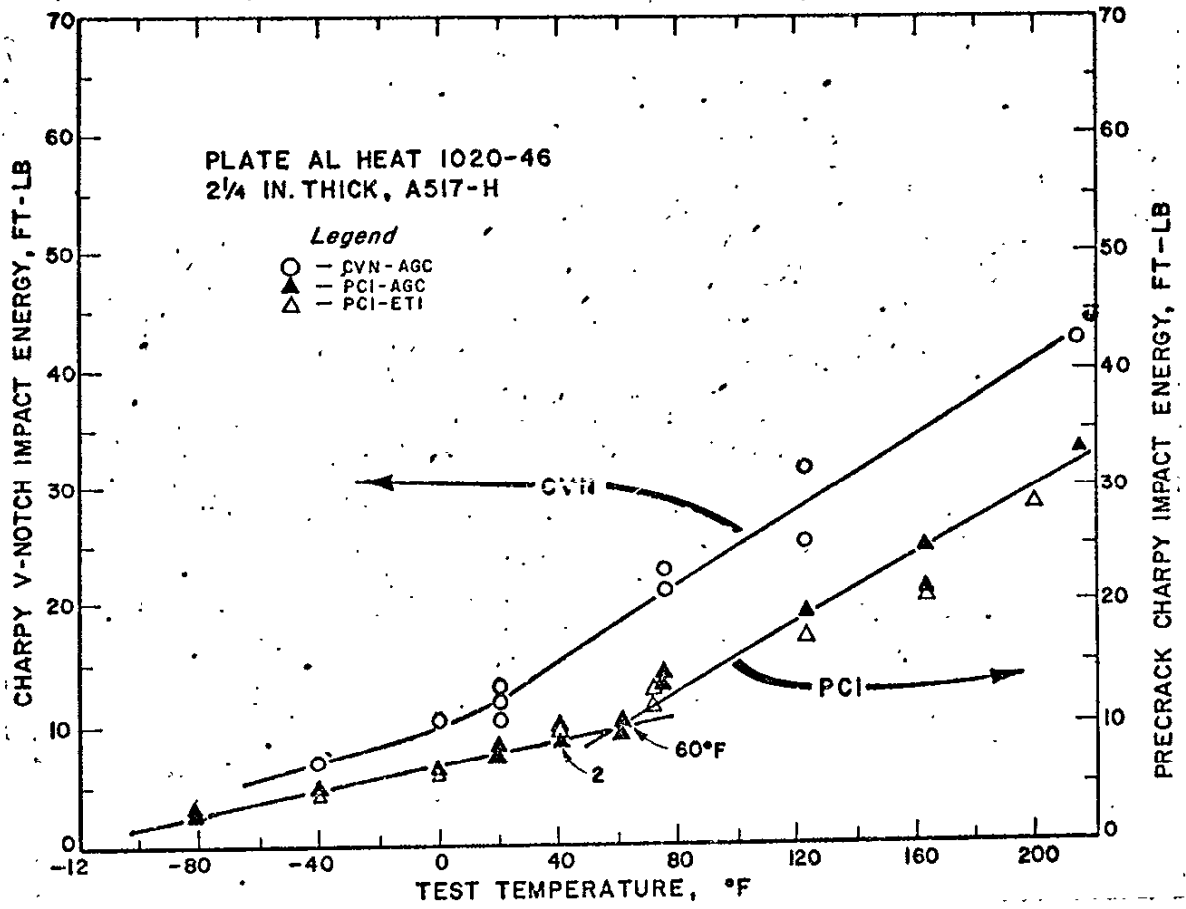
*Specimens tested after the CK-1 data collection. An accurate machine will produce average values within 1.0 ft-lb or 5.0 percent of the nominal values, whichever is the greater.



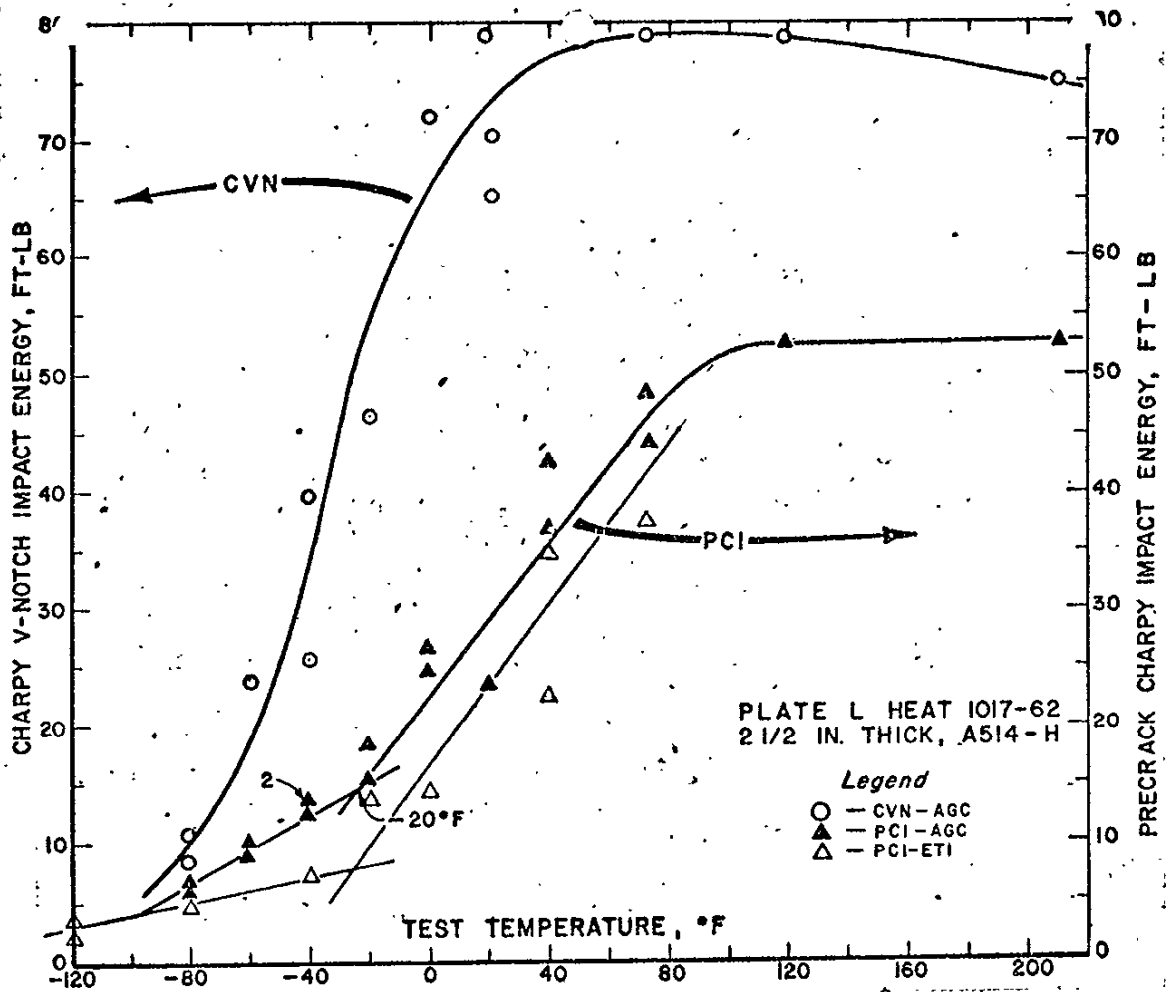
LAB - TO - LAB VARIABILITY
IN CVN-IMPACT AND PCI TESTS OF A517-H PLATE CK
FIGURE 4.15



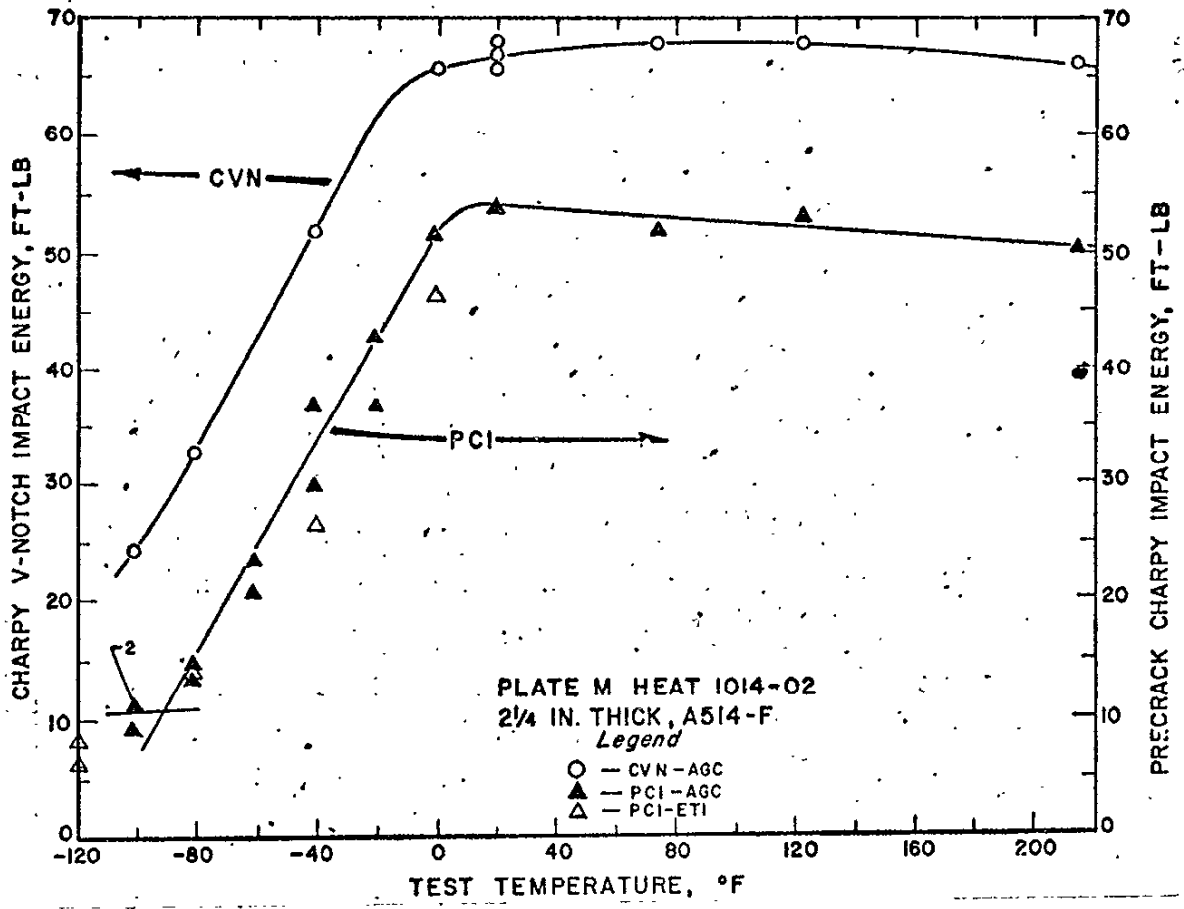
SUPER POSITION OF EFFECTS TECHNOLOGY, INC.
 PRECRACK CHARPY IMPACT DATA ON AEROJET GENERAL CORP.
 DATA FOR A517-F PLATE A
 FIGURE 4.16



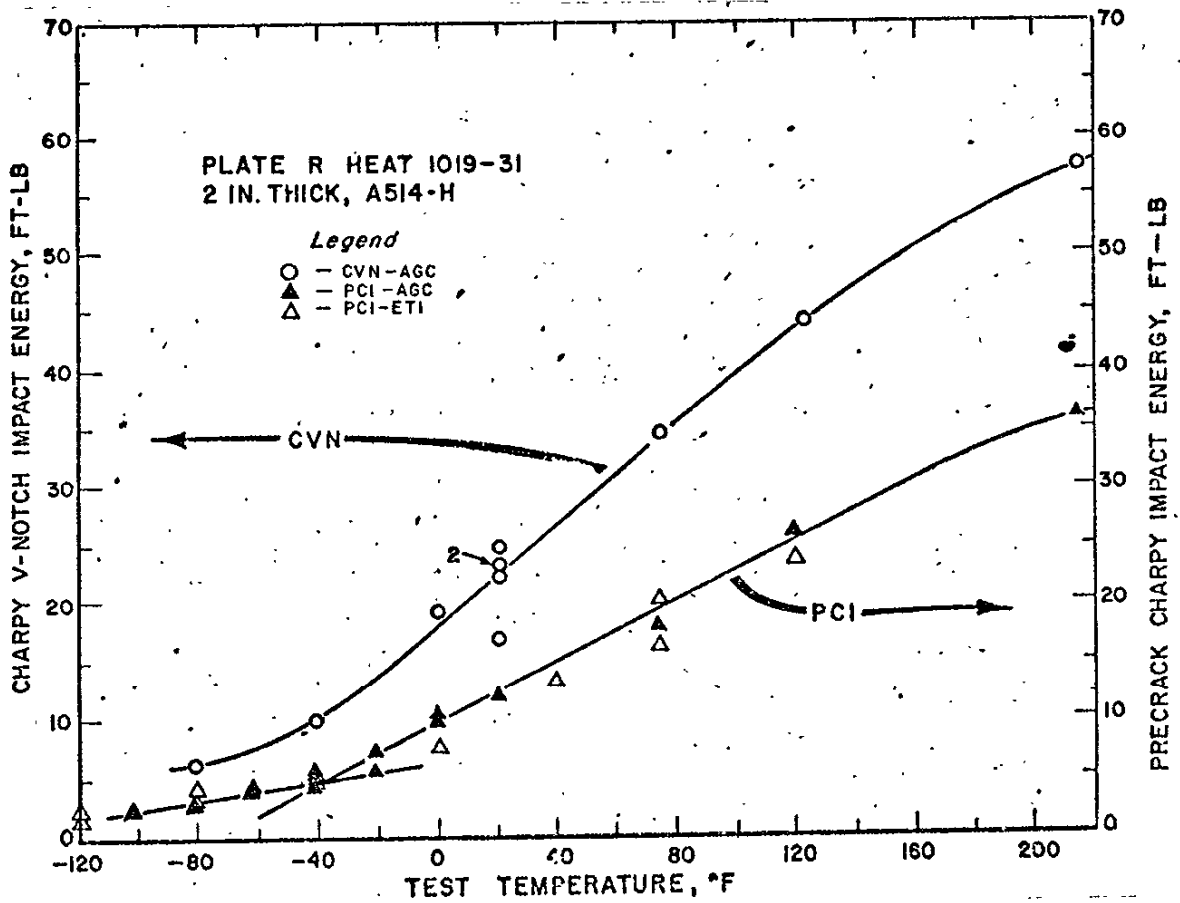
SUPER POSITION OF EFFECTS TECHNOLOGY, INC.
PRECRACK CHARPY IMPACT DATA ON AEROJET GENERAL CORP.
DATA FOR A517-H PLATE AL
FIGURE 4.17



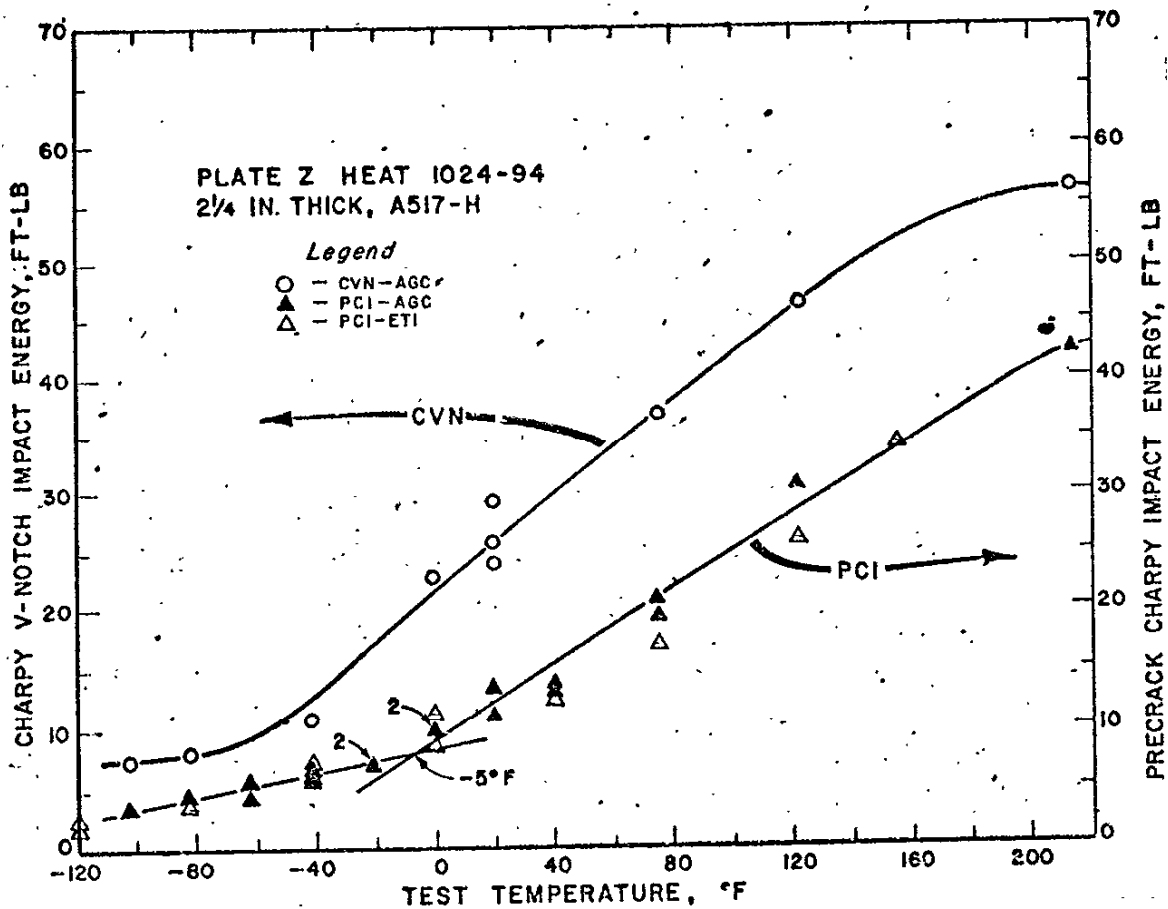
SUPER POSITION OF EFFECTS TECHNOLOGY, INC.
 PRECRACK CHARY IMPACT DATA ON AEROJET GENERAL CORP.
 DATA FOR A514-H PLATE L
 FIGURE 4.18



SUPER POSITION OF EFFECTS TECHNOLOGY, INC.
 PRECRACK CHARY IMPACT DATA ON AEROJET GENERAL CORP.
 DATA FOR A514-F PLATE M
 FIGURE 4.19



SUPER POSITION OF EFFECTS TECHNOLOGY, INC.
 PRECRACK CHARY IMPACT DATA ON AEROJET GENERAL CORP.
 DATA FOR A514-H PLATE R
 FIGURE 4.20



SUPER POSITION OF EFFECTS TECHNOLOGY, INC.
 PRECRACK CHARTY IMPACT DATA ON AEROJET GENERAL CORP.
 DATA FOR A517-H PLATE Z
 FIGURE 4.21

4.1.7 Slab-to-Slab Variability

The heat providing the most data for slab-to-slab comparisons is A517 grade-F heat 1006. This is an open-hearth heat from the Homestead Plant of the U. S. Steel Corporation; there were twenty-nine slabs from this one heat supplied as reinforcement steel for the Tuolumne Bridge. The plate was 1-3/8-in. thick. Of the eighty-seven standard CVN-impact tests made at +20 F, the test values ranged from 36 to 58 ft-lb with an average value of 45.5 ft-lb, and 28 to 44 mils lateral expansion with an average value of 34.8 mils. Table 4.2 lists the individual CVN-impact test data from each of seven slabs at each temperature tested. Table 4.3 lists the individual precrack Charpy impact data from each of the seven slabs at each temperature tested.

TABLE 4.2
 CHARPY V-NOTCH IMPACT DATA FROM SEVEN
 SLABS OF A517-F HEAT 1006

TEMPERATURE	CHARPY V-NOTCH IMPACT ENERGY (FT-LB)					CHARPY V-NOTCH IMPACT LATERAL EXPANSION (MILS)						
	A517 Grade F Heat 1006					A517 Grade F Heat 1006						
	-80°	-40°	0°	20°	210°		-80°	-40°	0°	20°	210°	
Plate AS	35.4 35.4	44.0	38.5	37.7 39.1 39.2	36.4	36.4	25.5 24.0	28.5	30.0	30.5 28.0 27.5	31.0 31.0	28.0
BB	44.7 44.3	44.2	44.4	44.7 42.8 42.0	42.5	42.5	33.0	31.0 29.0	34.0	33.0 30.0 31.0	32.0	34.0
BF	51.8 48.4	52.4	53.4	55.5 52.9 51.5	51.2	51.2	37.0 36.0	40.0	42.0	43.0 43.0 40.5	45.0	40.0
BK	-----	36.4	37.4	38.9 39.7 37.5	37.8	37.8	-----	29.0	29.0	30.0 29.0 28.5	30.0	31.5
BM	-----	42.3	43.9	40.4 43.7 38.6	39.1	39.1	-----	34.5	36.0	33.5 36.0 32.0	35.5	33.5
BV	-----	44.1	46.5	44.7 43.1 44.8	42.7	42.7	-----	31.5	32.5	34.0 31.5 31.5	36.0	32.5
BZ	40.1	41.4	-----	43.4 43.3 40.1	38.8	38.8	29.0	33.0	-----	33.5 34.0 32.0	34.0	32.5

TABLE 4.3
 PRECRACKED CHARPY IMPACT DATA FROM SEVEN
 SLABS OF A517-F HEAT 1006

		PRECRACKED CHARPY IMPACT ENERGY (FT. LBS)					PRECRACKED CHARPY IMPACT LATERAL EXPANSION (MILS)										
		A 517 Grade F Heat 1006					A517 Grade F Heat 1006										
TEMPERATURE		-80°	-40°	0°	20°	RT	120°	210°			-80°	-40°	0°	20°	RT	120°	210°
Plate AS		26.0 24.8	25.7	27.1	29.0 27.7 28.4	27.9	26.8	26.6			20.5 19.5	22.0	23.5	25.0 24.5 22.5	24.0	24.5	23.0
BB		30.0 30.2	28.6	31.1	32.8 32.2 32.5	32.7	32.2	30.6			24.0 24.0	24.0	28.0	27.0 31.0 27.0	28.0	27.0	26.0
BF		37.3 38.7	39.0	36.6	36.6 38.4 37.1	39.0	34.8	37.1			30.0 31.0	33.0	30.0	32.0 34.0 31.0	36.0	34.0	35.0
BK		27.5	27.2	-----	27.8 28.1 29.0	28.8	30.0	27.9			21.0	23.5	-----	23.0 23.5 23.5	26.0	28.0	24.5
BM		30.3	32.6	-----	32.3 30.5 32.3	29.4	28.2	29.4			28.0	28.0	-----	29.0 28.0 29.0	28.0	29.0	30.0
BV		30.7	32.5	-----	32.8 34.5 35.2	32.3	32.7	32.2			25.5	26.0	-----	27.5 28.0 28.5	28.0	28.5	27.0
BZ		-----	29.1	-----	30.2 29.9 30.0	29.4	26.3	28.0 26.5			-----	25.0	-----	26.5 25.0 25.5	27.0	25.5	24.5 26.0

Of the eighty-six precracked Charpy impact tests made at +20°F, the test values ranged from 22.5 to 39.7 ft-lb at +20°F. The data from each slab are given in Table 4.4. A cursory examination of this table shows that the variation from slab-to-slab was not great. The variation in the ft-lb values between individual tests of a given slab was appreciably less than the variation in average values between slabs; therefore, there was a significant difference from slab-to-slab in a given heat. The largest variation was in slab 1006/61AY where the average value was 24.1 ft-lb as compared with the overall average of 32.3 ft-lb. The tensile properties for this particular slab offered no explanation for the lower toughness, nor were the tensile properties informative for slab BA which had the highest precracked Charpy impact value of the 29 slabs.

Figure 4.22 is a histogram showing the number of times (the frequency) the precracked Charpy impact energy value occurred in each of six intervals when the 29 slabs of heat 1006 were tested at +20°F. The intervals selected were:

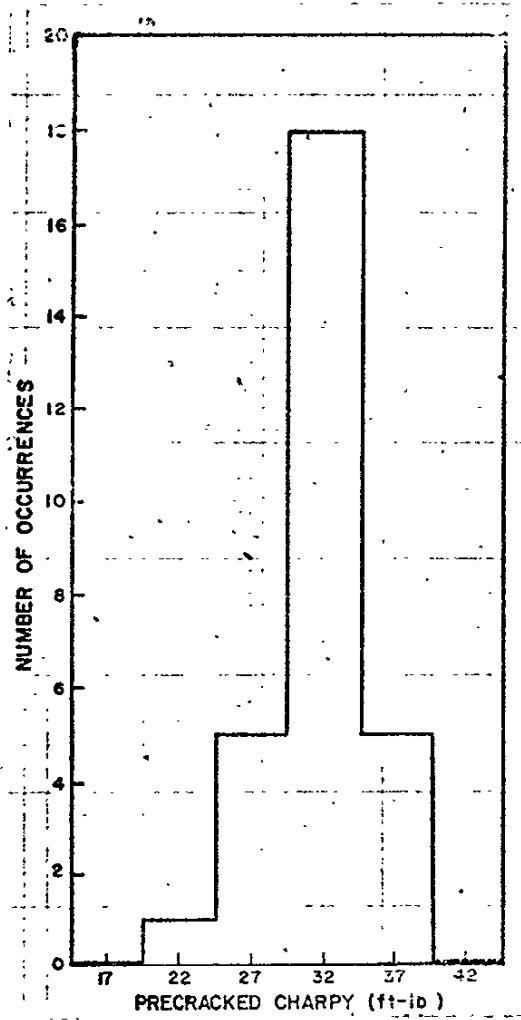
<u>ft-lb</u>
15 to 29
20 to 24
25 to 29
30 to 34
35 to 39
40 to 44

From Figure 4.22 note that the mode of the distribution occurred at 32 ft-lb (in the interval 30 to 34 ft-lb). Eighteen slabs had average PCI values in this interval.

TABLE 4.4

PRECRACKED CHARPY IMPACT ENERGY AND LATERAL EXPANSION
VALUES FROM TWENTY-NINE SLABS, A517 GRADE F HEAT 1006
TESTED AT PLUS 20°F

Plate ID	Impact Energy		Lateral Expansion	
	Ft-Lb Values	Avg.	Mils	Avg.
AR	35.5-34.2-36.3	(35.3)	32.5-33.0-33.5	(33.0)
AS	29.0-27.7-28.4	(28.4)	25.0-24.5-22.5	(24.0)
AT	34.3-33.4-35.5	(34.3)	31.5-32.0-34.5	(32.7)
AU	26.6-27.2-27.3	(27.0)	23.0-23.0-24.0	(23.3)
AV	32.3-32.2-33.0	(32.5)	28.0-28.0-28.5	(28.2)
AW	28.8-30.6-30.2	(29.9)	25.0-26.0-29.0	(26.7)
AX	30.2-27.9-29.8	(29.3)	24.5-25.5-24.5	(24.8)
AY	24.7-23.8-23.7	(24.1)	22.0-22.0-20.5	(21.5)
AZ	34.2-31.2-32.2	(32.5)	31.0-27.0-28.0	(28.7)
BA	35.4-39.7-39.3	(38.1)	30.5-34.5-34.0	(33.0)
BB	32.8-35.2-32.5	(33.5)	33.0-31.0-32.0	(32.0)
BC	37.4-38.9-37.2	(37.8)	32.0-36.0-31.5	(33.2)
BD	31.3-34.7-35.2	(33.7)	30.0-31.0-31.0	(30.7)
BE	33.2-32.1-30.2	(31.8)	30.0-29.0-26.0	(28.3)
BF	36.6-38.4-37.1	(37.4)	32.0-34.0-31.0	(32.3)
BG	32.1-32.9-33.1	(32.7)	30.5-31.0-33.0	(31.5)
BJ	33.5-32.2-32.3	(32.7)	29.0-29.0-29.5	(29.2)
BK	27.8-28.1-29.0	(28.3)	23.0-23.5-23.5	(23.3)
BL	33.3-33.9-31.9	(33.0)	30.5-29.5-30.0	(30.0)
BM	32.3-30.5-32.3	(31.7)	29.0-28.0-29.0	(28.7)
BN	28.6-31.5-31.9	(30.7)	26.0-25.0-25.0	(25.3)
BP	28.1-28.4-29.7	(28.8)	27.0-26.5-23.5	(25.6)
BR	35.6-33.3	(34.4)	32.0-31.0-30.5	(31.2)
BS	35.6-36.9-35.8	(36.1)	33.0-32.5-33.0	(32.8)
BT	34.3-33.6-33.5	(33.8)	29.5-30.0-28.5	(29.3)
BU	35.7-30.9-33.7	(33.4)	30.0-23.0-29.0	(27.3)
BV	32.8-34.5-35.2	(34.2)	27.5-28.0-28.5	(28.0)
BW	31.0-31.5-32.7	(31.8)	27.0-28.5-28.0	(27.8)
BZ	30.2-29.9-30.0	(30.0)	26.5-25.0-25.5	(25.6)
	Overall Average	(32.3)		(28.6)



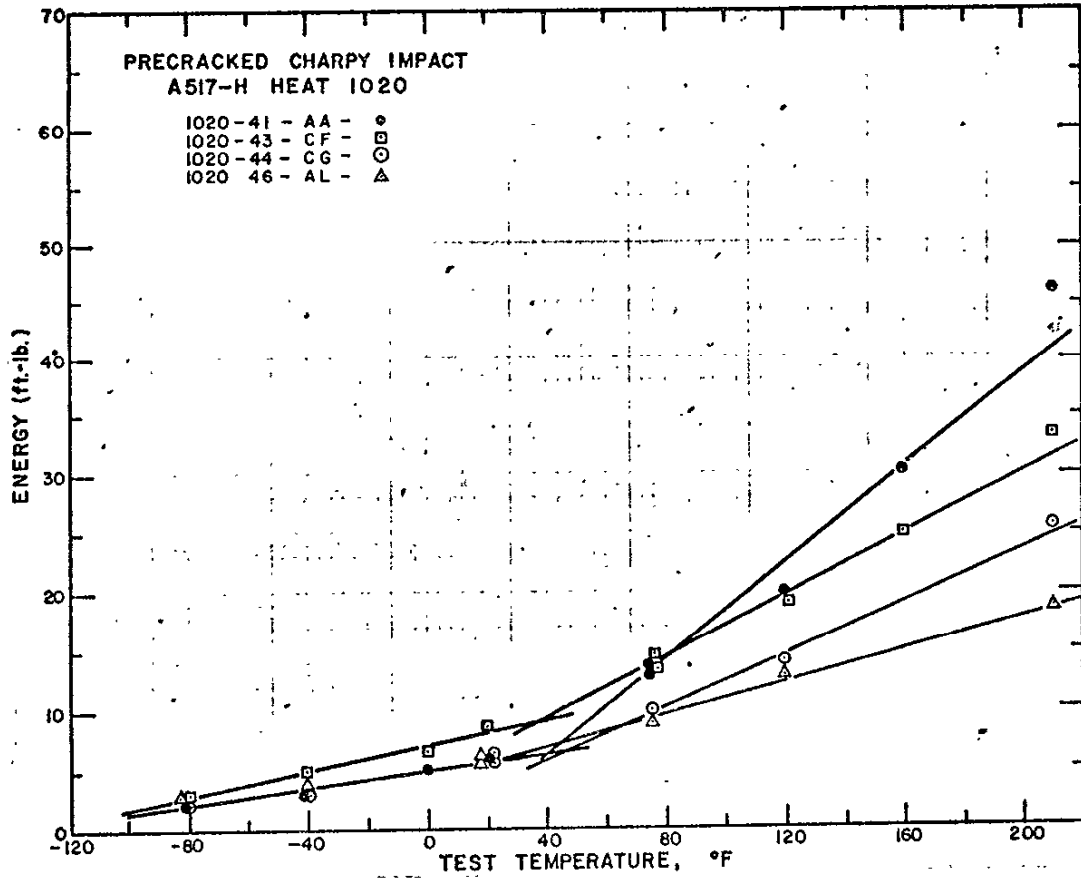
HISTOGRAM OF PCI VALUES
 AT +20°F FROM 29 SLABS OF A517-F HEAT 1006
 FIGURE 4.22

Among the other heats in the two bridges or in the reinforcement steel, there were many heats represented by only one slab; in a few cases there were three or four slabs from a single heat. There were three such heats among the A517 grade-H steels in the bridges: heat 1020 with slabs 41AA, 43CF, 44CG and 46AL; heat 1024 with slabs 91Y, 94Z and 95CE; and the heat which fractured in the Bryte Bend Bridge, 1027, with slabs 44CK, 45CD and 46CH. Figures 4.23 and 4.24 are plots of the PCI data for heats 1020 and 1024.

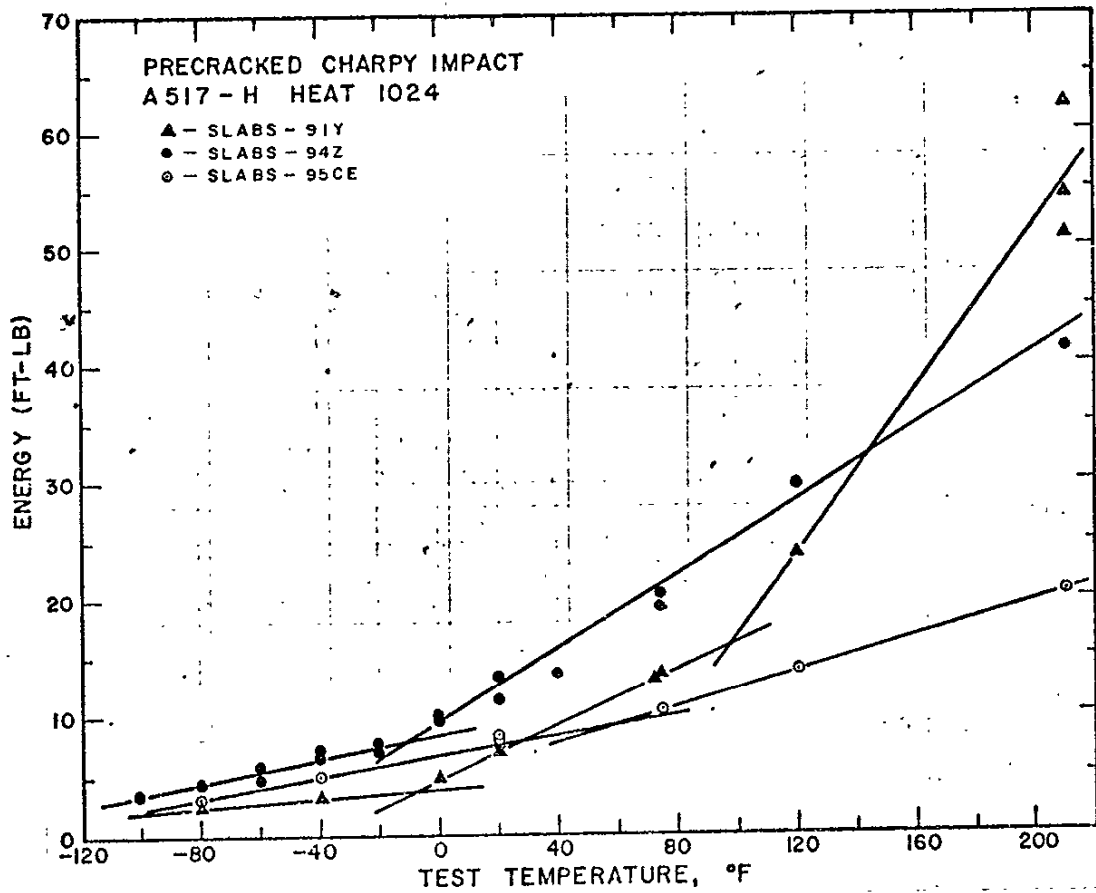
From the curves, note that below the transition-temperature inflection point, there was little difference between the slabs of a given heat, but in the transition region there were some marked differences from slab to slab. In heat 1020 there was little difference in the NDT (inflection-point) temperatures from slab to slab, but in heat 1024, marked differences were indicated. However, the double inflection that was found in the plate-Y data suggests that if additional tests were made of the other slabs there might be a double inflection similar to that in slab Y. Thus, in the case of heat 1024 more testing would be required to verify the indicated differences.

Figure 4.24.1 is a plot of the standard CVN-impact test results for heat 1024. Note that the scatter in the data from slab Y was among the worst of the entire study. Note that CVN-impact and precrack Charpy both showed plate CE to have the lowest toughness.

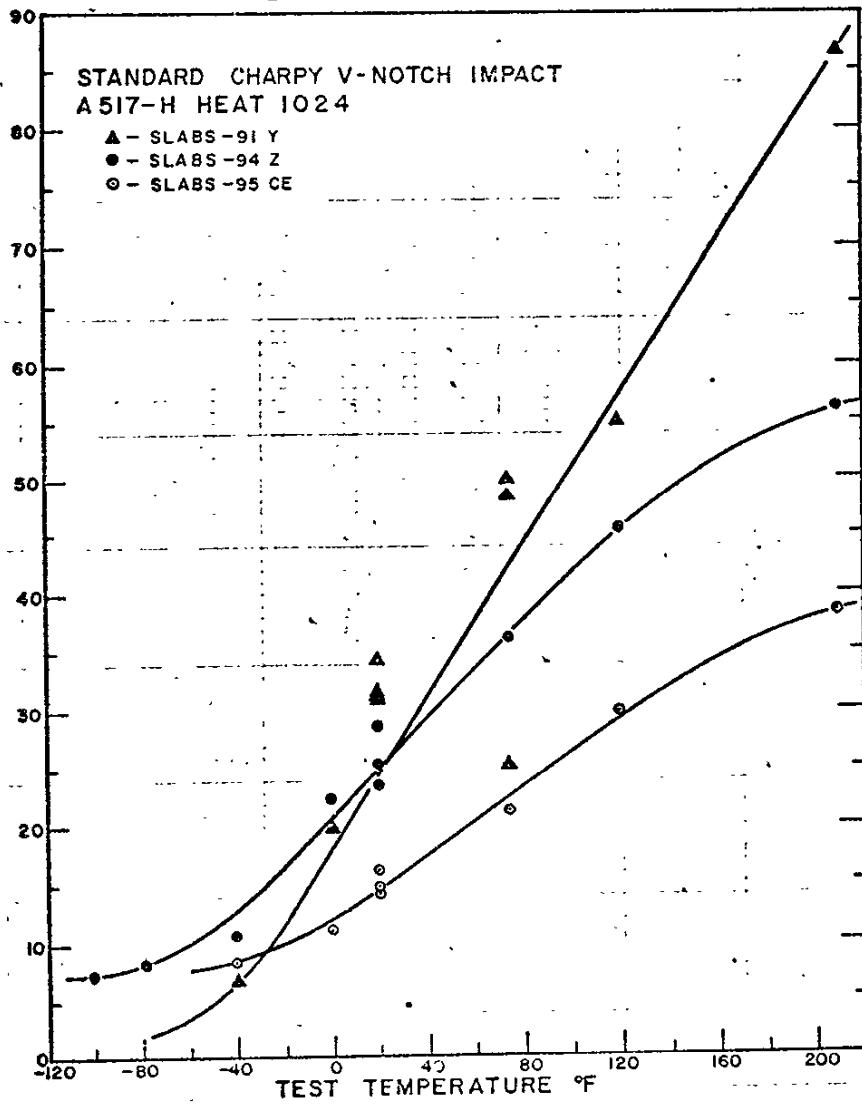
The transition curves (Figure 4.25) for the three slabs of heat 1027 are for all practical purposes superimposed. In other words, there was little or no difference between the slabs from heat 1027 at any temperature tested. This was the heat that fractured in the Bryte Bend Bridge; slabs from this heat were in ten locations in the bridge.



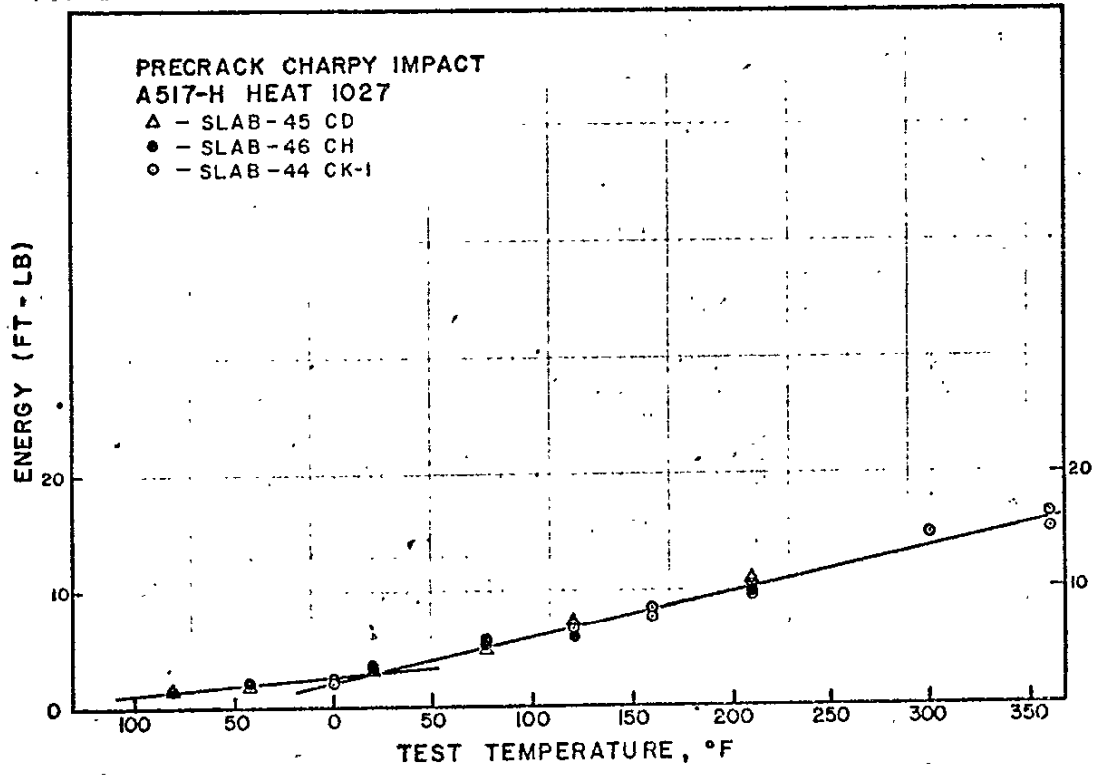
PCI TESTS OF FOUR SLABS FROM A517-H HEAT 1020
FIGURE 4.23



PCI TESTS OF THREE SLABS FROM A517-H HEAT 1024
FIGURE 4.24



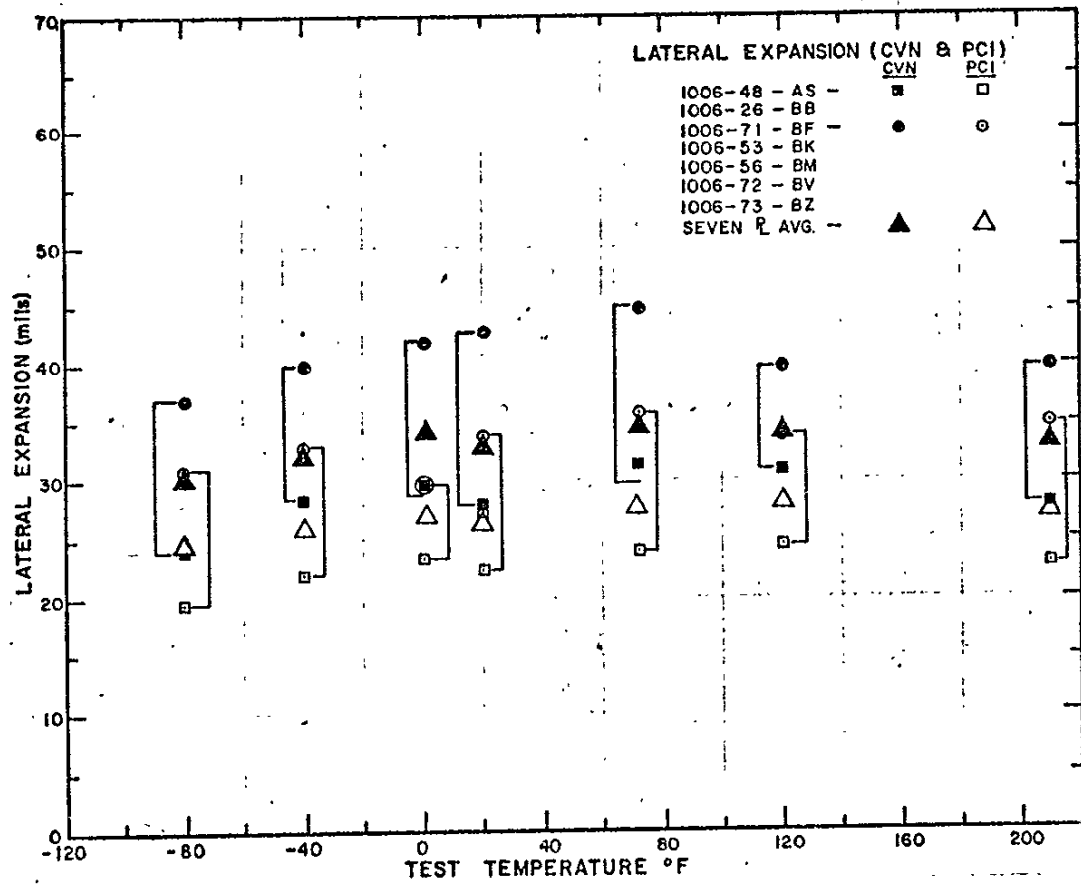
CVN - IMPACT TESTS OF THREE SLABS
FROM A517-H HEAT 1024
FIGURE 4.24.1



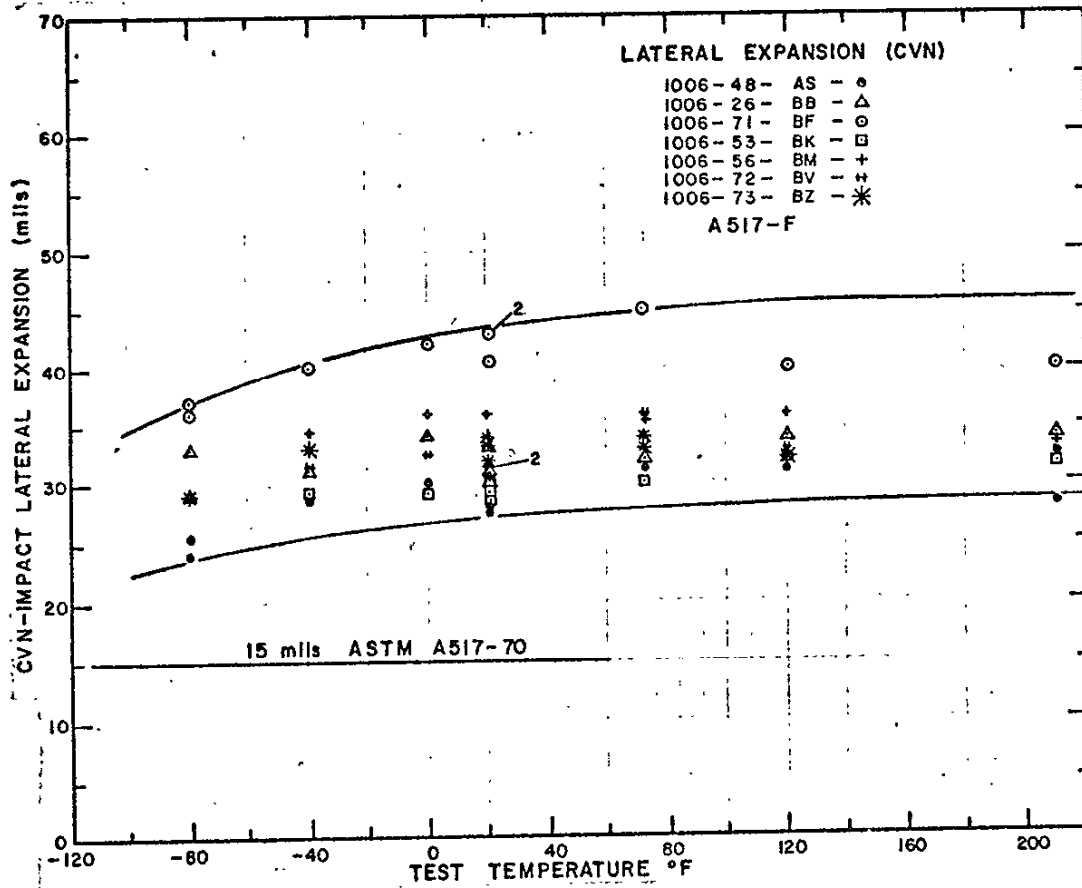
PCI TESTS OF THREE SLABS FROM A517-H HEAT 1027
FIGURE 4.25

Lateral expansion is an independent measurement that can be made in both standard CVN-impact and precrack Charpy impact specimens. It has been shown (Figures 4.5 to 4.8) that lateral expansion is directly proportional to the energy absorbed in fracturing the Charpy impact specimens. Figure 4.26 shows the range and average values of lateral expansion in seven slabs from A517 grade-F heat 1006 for both standard and precracked Charpy tests. Note that the top of the range was one slab (BF) and likewise, the bottom of the range was generally one slab (AS); this observation was generally true for the standard CVN-impact test and consistently true at all temperatures tested for the precracked Charpy impact test.

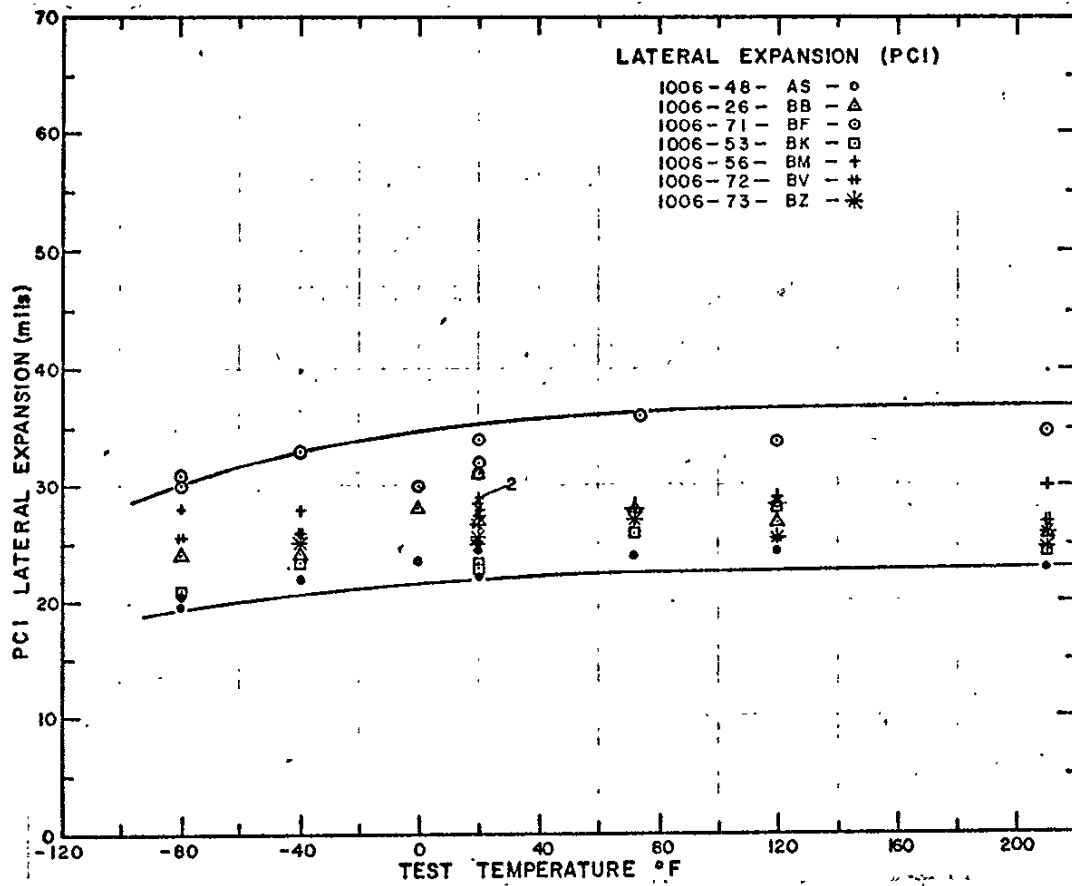
Figures 4.27 thru 4.31 show the variation in lateral expansion occurring from slab to slab in a given heat. Also shown is the transition behavior (a decrease in lateral expansion) as a function of test temperature. Note that the particular ASTM A517 grade-F plates tested involving multiple slabs from a given heat consistently showed lateral expansion values considerably in excess of the ASTM A517-70 15-mil requirement at all temperatures tested; whereas, the ASTM A517 grade-H plates tested involving multiple slabs from a given heat failed to meet the 15-mil requirement at temperatures commonly experienced in the United States. Note also that marked slab-to-slab differences were indicated by both standard CVN-impact and PCI. For example, in ASTM A517 grade-H heat 1022, the 15-mil CVN-impact transition temperature for slab H was about +20°F, whereas the transition temperature for slab C was about +90°F. (See Figure 4.31.)



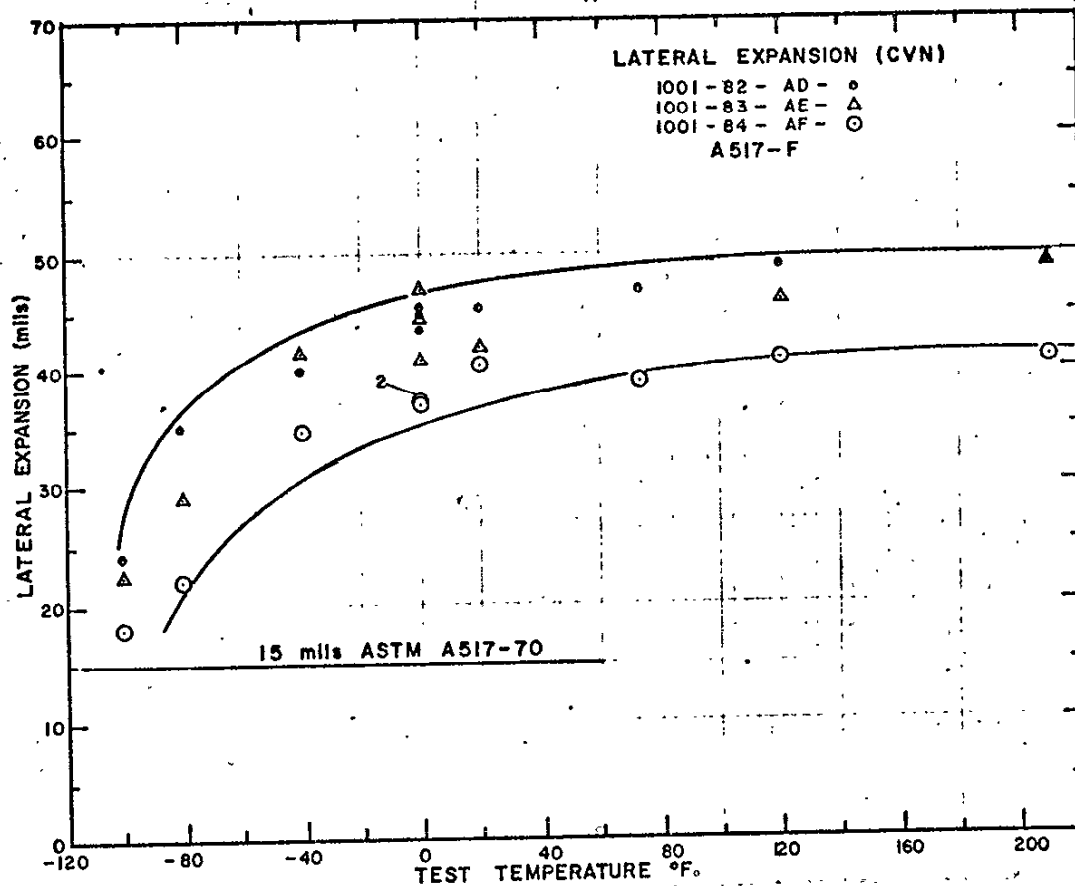
LATERAL EXPANSION DATA
 FROM CVN-IMPACT AND PCI TESTS
 OF SEVEN SLABS FROM HEAT 1006
 FIGURE 4.26



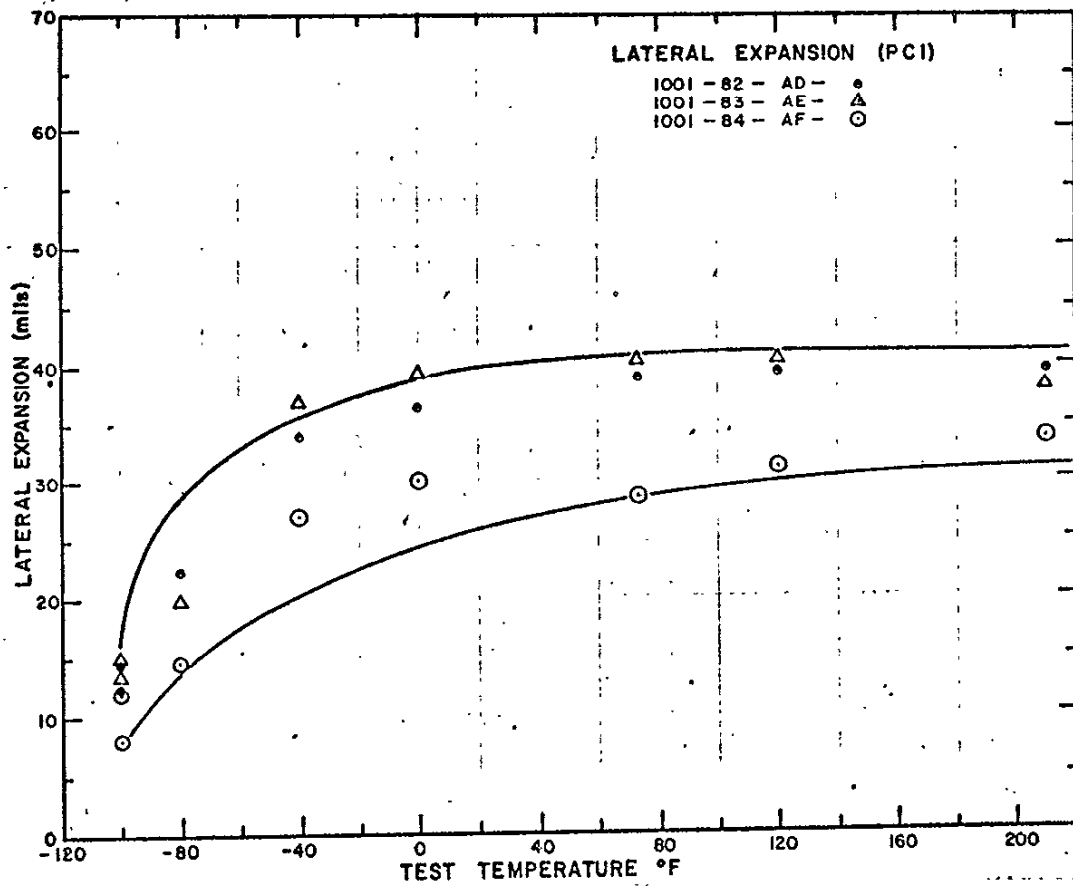
LATERAL EXPANSION TRANSITION BEHAVIOR
 FROM CVN IMPACT TESTS OF SEVEN SLABS
 OF A517-F HEAT 1006
 FIGURE 4.27



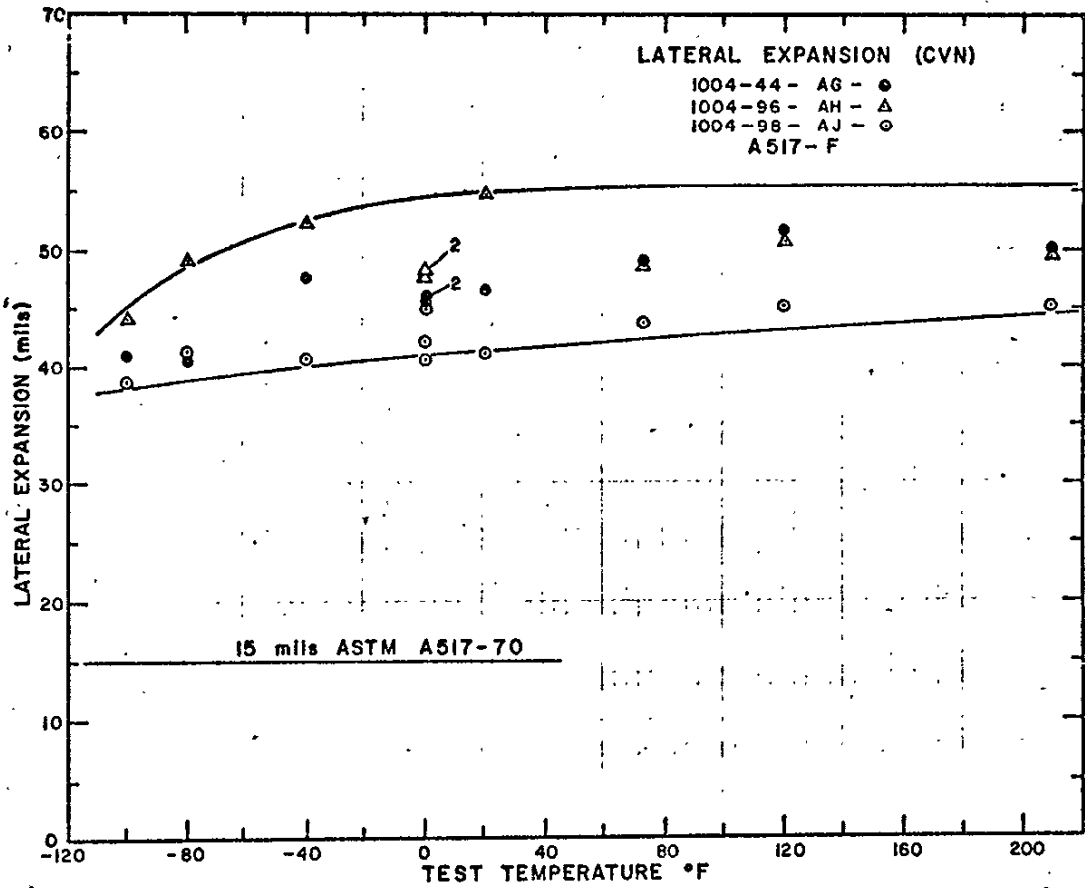
**LATERAL EXPANSION TRANSITION BEHAVIOR
 FROM PCI TESTS OF SEVEN SLABS
 OF A517-F HEAT 1006
 FIGURE 4.27.1**



LATERAL EXPANSION TRANSITION BEHAVIOR
 FROM CVN IMPACT TESTS OF THREE SLABS
 OF A517-F HEAT 1001
 FIGURE 4.28

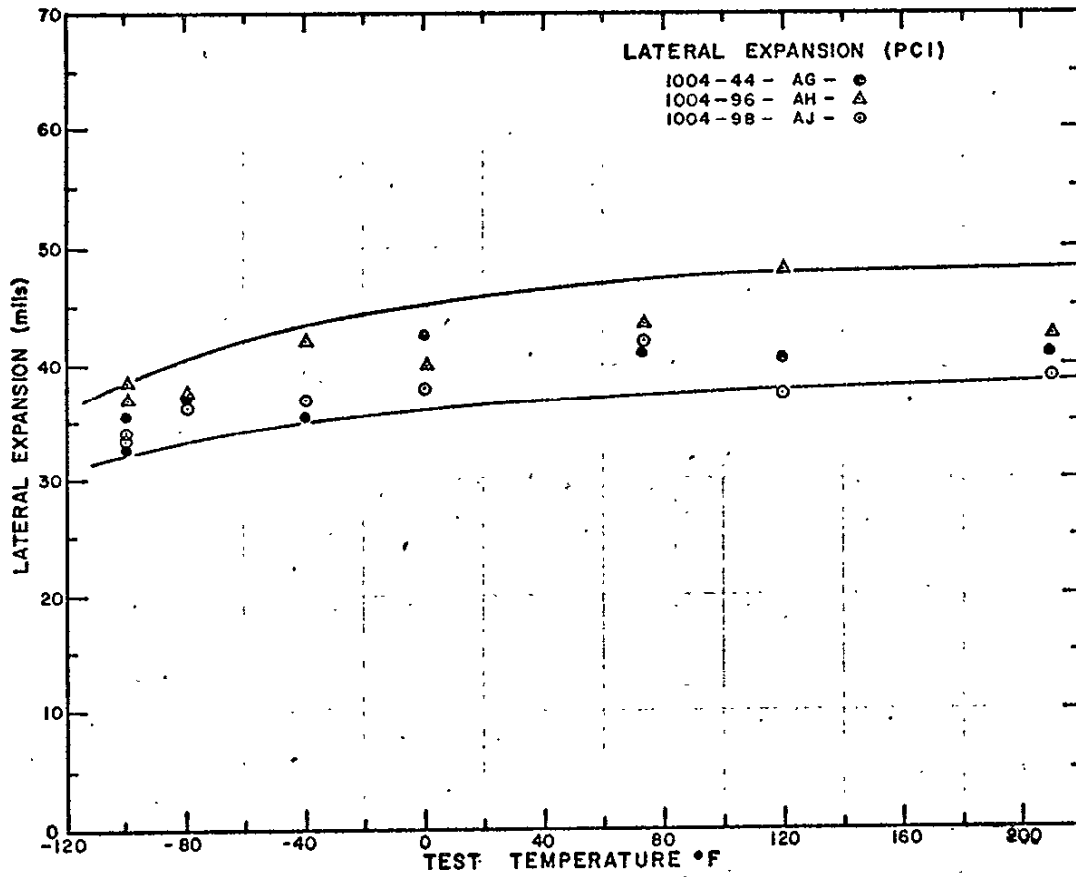


LATERAL EXPANSION TRANSITION BEHAVIOR
 FROM PCI TESTS OF THREE SLABS
 OF A517-F HEAT 1001
 FIGURE 4.28.1

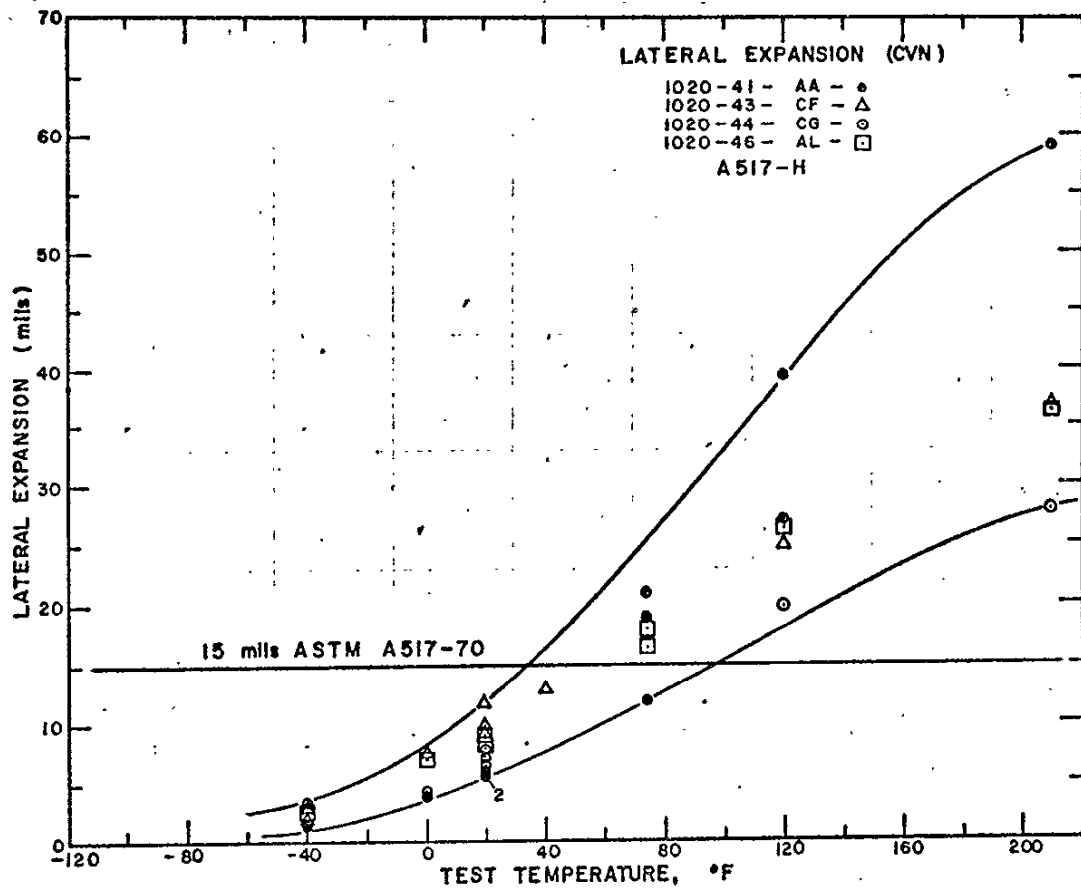


LATERAL EXPANSION TRANSITION BEHAVIOR
 FROM CVN IMPACT TESTS OF THREE SLABS
 OF A517-F HEAT 1004

FIGURE 4.29

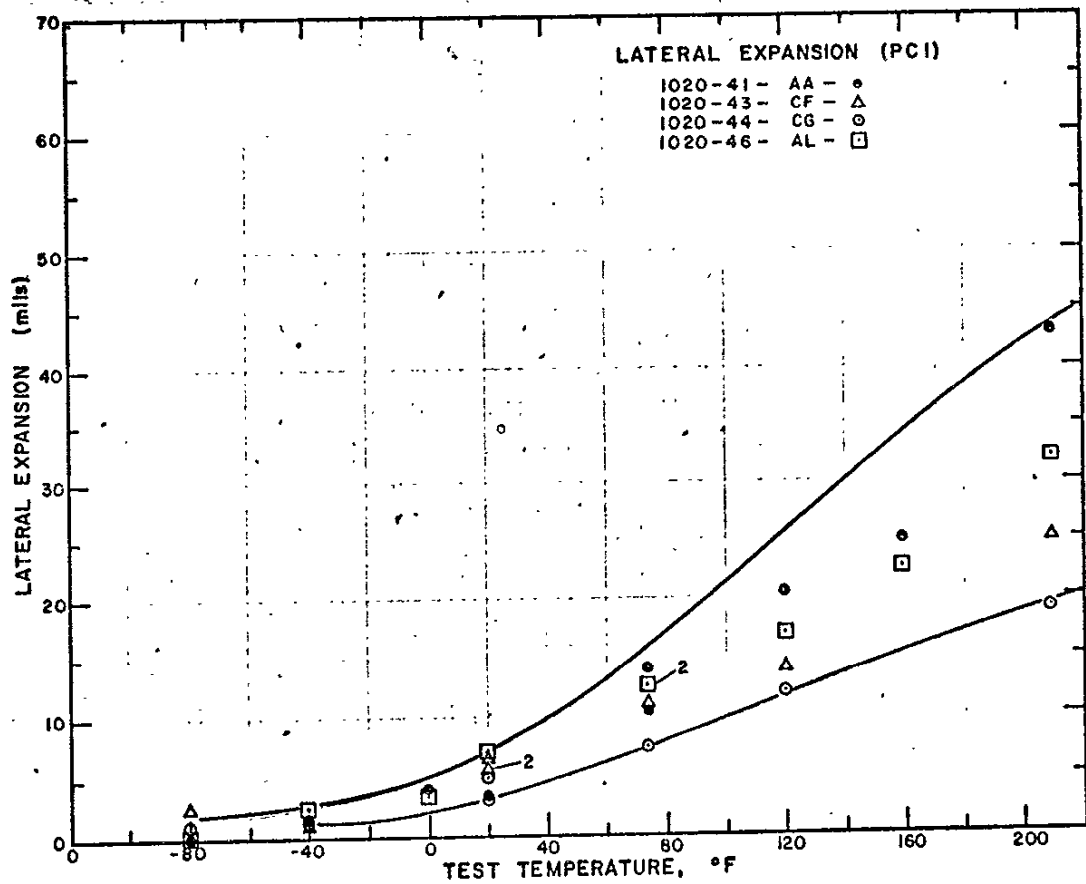


LATERAL EXPANSION TRANSITION BEHAVIOR
 FROM PCI TESTS OF THREE SLABS
 OF A517-F HEAT 1004
 FIGURE 4.29.1

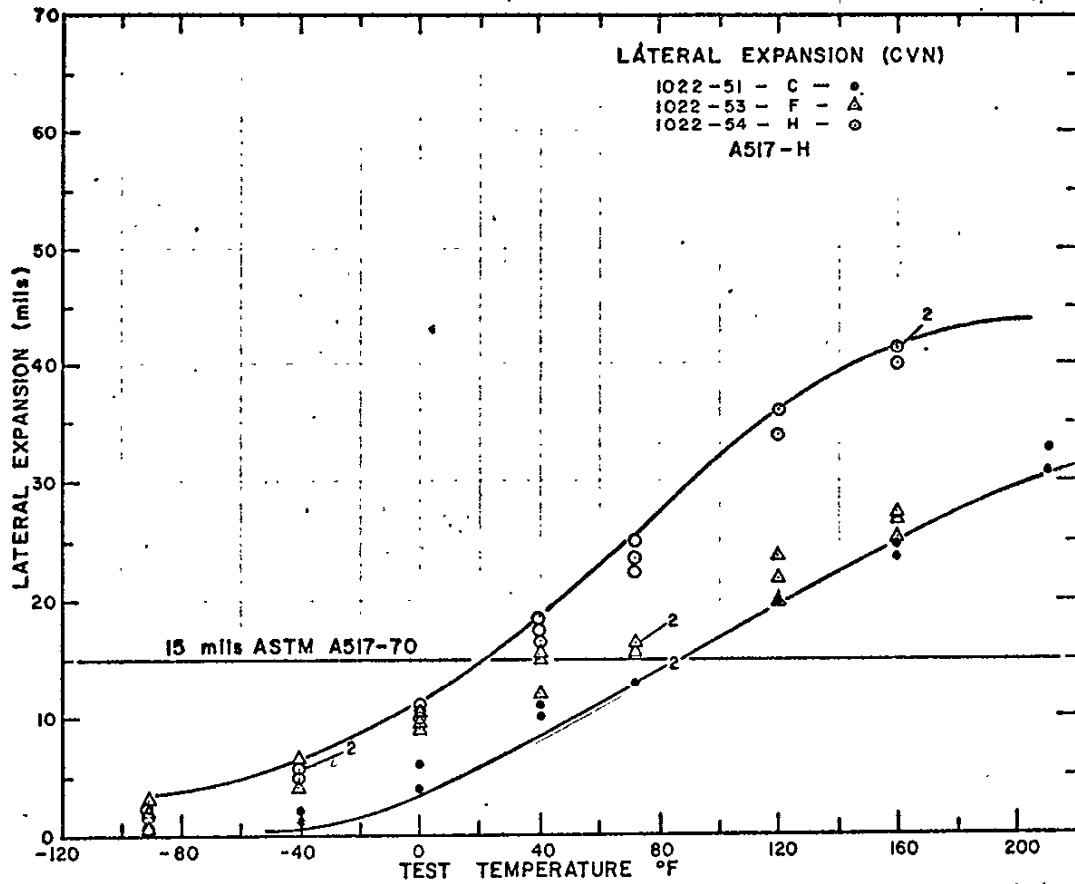


LATERAL EXPANSION TRANSITION BEHAVIOR
 FROM CVN IMPACT TESTS OF FOUR SLABS
 OF A517-H HEAT 1020

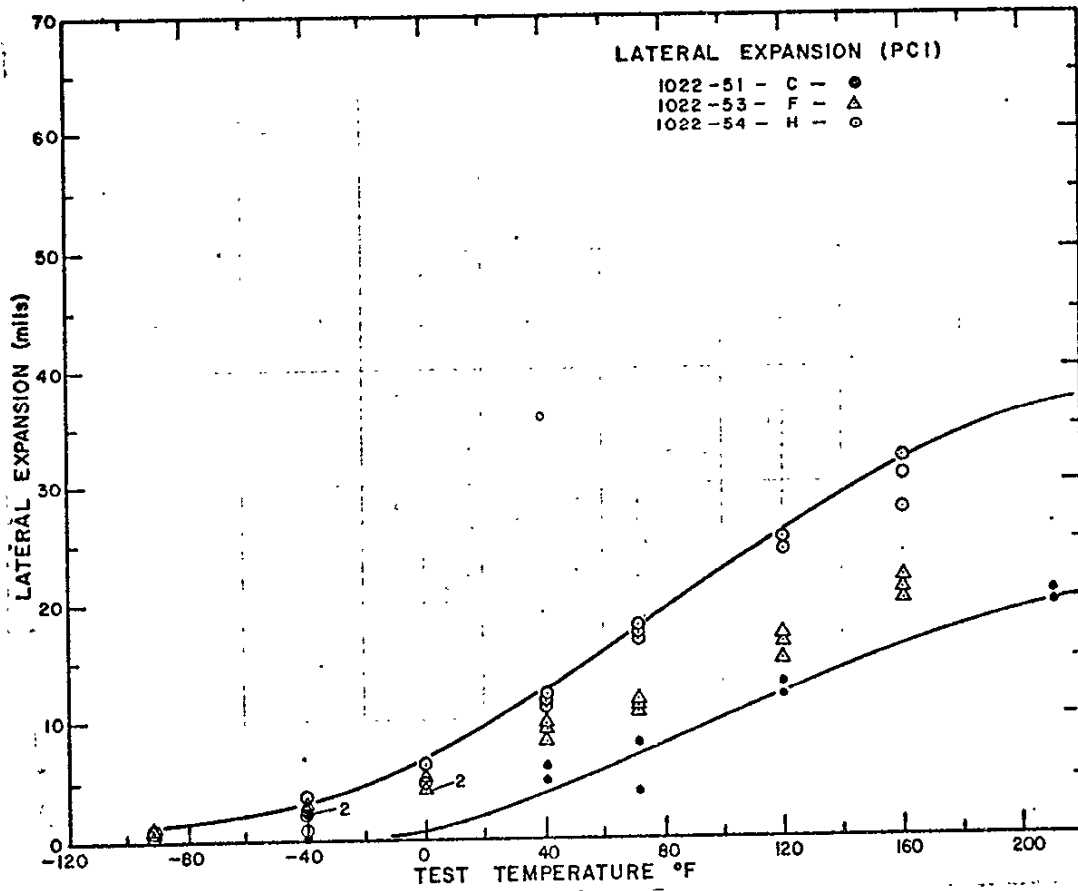
FIGURE 4.30



LATERAL EXPANSION TRANSITION BEHAVIOR
 FROM PCI TESTS OF FOUR SLABS
 OF A517-H HEAT 1020
 FIGURE 4.30.1



LATERAL EXPANSION TRANSITION BEHAVIOR
 FROM CVN IMPACT TESTS OF THREE SLABS
 OF A517-H HEAT 1022
 FIGURE 4.31



LATERAL EXPANSION TRANSITION BEHAVIOR
 FROM PCI TESTS OF THREE SLABS
 OF A517-H HEAT 1022

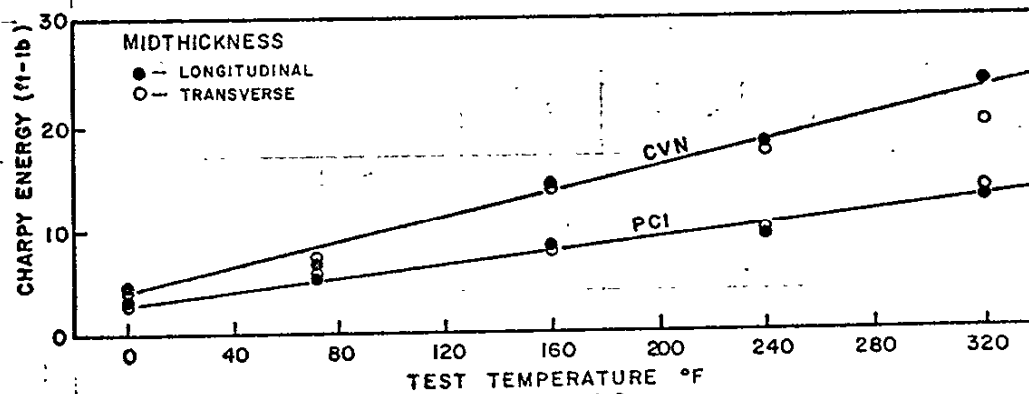
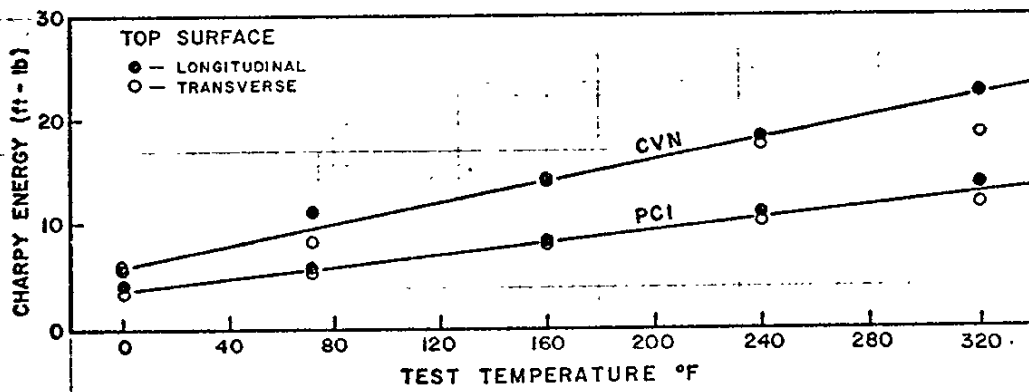
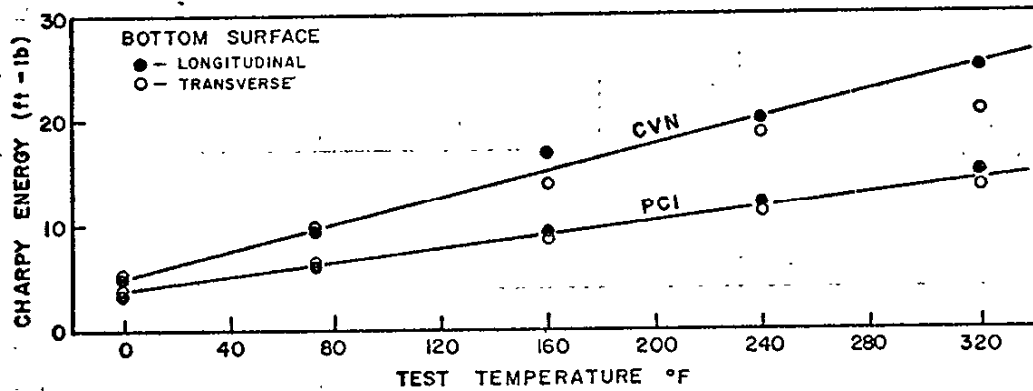
FIGURE 4.31.1

4.1.8 Variation in Toughness with Respect to Rolling Direction

Fracture in the Bryte Bend bridge flange occurred at 90 degrees to the principal rolling direction (the length of the flange). This is consistent with the fact that the principal stresses in a flange are parallel to the length of the flange and thus, force fracture, if it occurs, to run transverse to the principal rolling direction. This is favorable from the standpoint of toughness because most steel is more resistant to fracture when the crack is propagating at 90 degrees to the principal rolling direction. Anisotropy is minimized by cross rolling the steel. In applications where the stress state is significantly biaxial (as in a pressure vessel), cross-rolling ratio is specified; however ASTM A517 does not specify a ratio. "T-1" steel is supposed to have a cross-rolling ratio of 3:1; industrial practice varies greatly - A514 steel might have a cross-rolling ratio of 10:1 or smaller for flange plates.

The cross-rolling ratio for the Bryte Bend casualty heat is not known. Transverse CVN-impact and precrack Charpy impact tests were made of Plate CK at midthickness and at both the top and bottom surfaces. At +320°F the CVN-impact consistently showed a significantly lower value (approximately 4 ft-lb lower) for the "transverse" test specimen (fracture driven parallel to the principal direction of rolling). As seen in Figure 4.31.2, at lower temperatures the difference between the two orientations of test specimen was generally less than 1 ft-lb for both the CVN-impact and the precrack Charpy impact tests.

Standard CVN-impact tests were made in three other heats in the specimen-transverse orientation machined from the midthickness of the plate. These data together with the companion CK-1 test results are shown in Table 4.5. In the Bryte Bend casualty heat, note that there was little if any difference between the two specimen orientations; the steel was brittle in both orientations.



LONGITUDINAL AND TRANSVERSE
 CVN-IMPACT AND PCI TRANSITION CURVES
 FOR A517-H HEAT 1027-44CK

FIGURE 4.31.2

The Plate-A, and Plate AL test results were anomalous because they indicated the steel to be slightly tougher with the crack propagating longitudinally (specimen transverse) in the flange plate. Plate Z was consistent with the anticipated result, greater toughness with the crack propagating transversely (specimen longitudinal) in the flange plate.

TABLE 4.5

STANDARD CVN-IMPACT TESTS SHOWING THE EFFECT OF SPECIMEN ORIENTATION

Plate I.D.	Test Temp (°F)	Specimen Thickness Position	Specimen Transverse		Specimen Longitudinal	
			Energy (ft-lb)	Lat. Expans. (mils)	Energy (ft-lb)	Lat. Expans. (mils)
CK	RT	1/4-Point	9.3	7.0	9.9 ^(a)	6.9 ^(a)
		Midthick.	7.3	4.7	7.0	6.0
A	0	1/4-Point	19.4	13.1	---	---
		Midthick.	19.5	14.2	15.8	10.3
AL	20	1/4-Point	12.8	10.6	---	---
		Midthick.	13.5	12.2	11.8	7.7
Z	20	1/4-Point	22.0	17.2	---	---
		Midthick.	18.1	14.2	25.9	18.2

(a) machined from the surface of the plate.

4.1.9 Correlation of Toughness and Tensile Test Data

Figures 4.31.3 and 4.31.4 are plots of room temperature CVN impact test data, from A514/517 grades F & H, vs % reduction of area and % elongation respectively (avg. Caltrans data used).

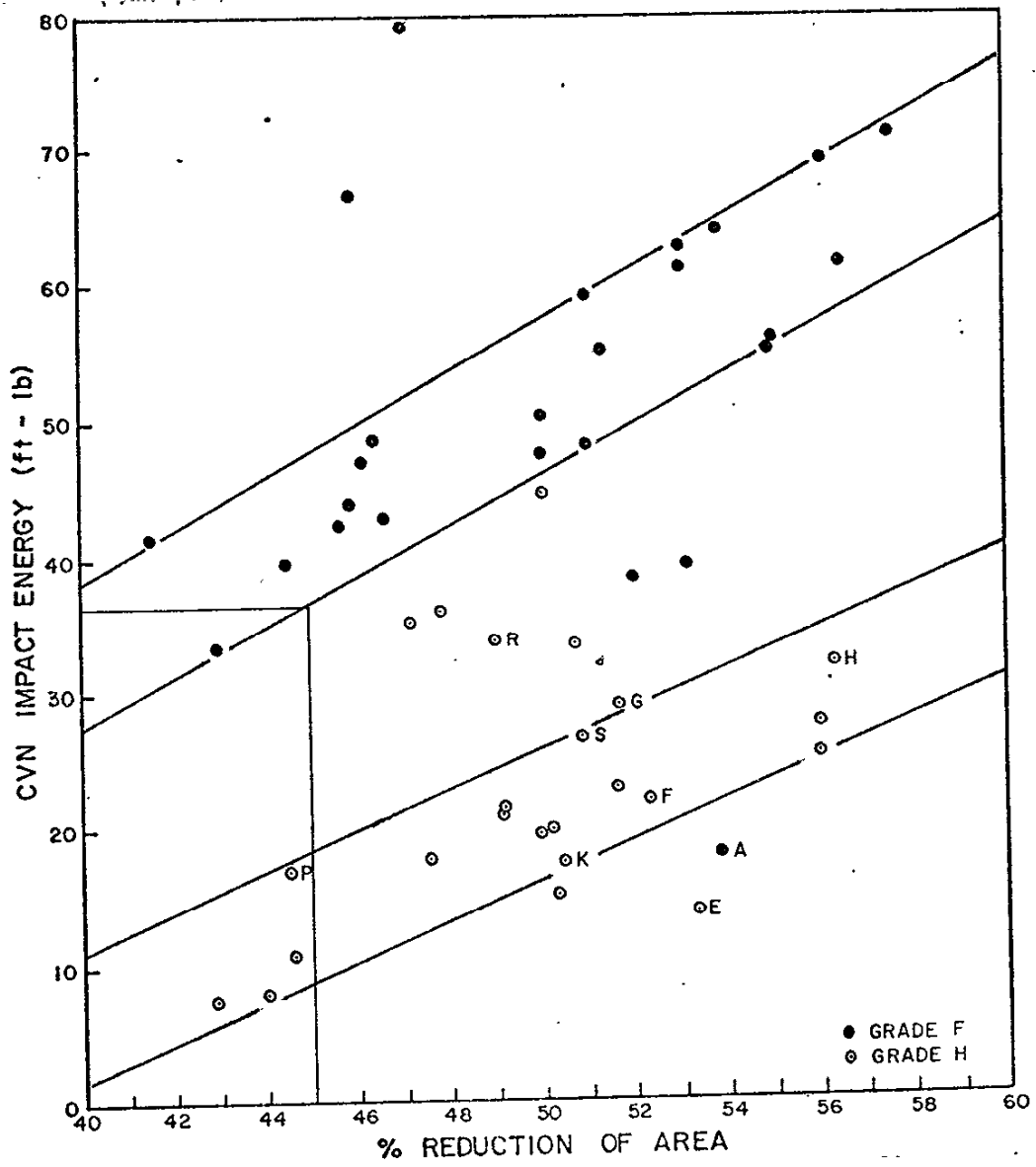
These plots show two correlations, one for grade H and one for grade F. Grade F is predominately from one producer and varies in thickness from 1 3/8" to 2 1/2". Grade H is from two producers and varies in thickness from 2" to 2 1/2", thus those plates supplied over 2" are a modified grade H. The grade-H tested included eight slabs from five heats coded E, F, G, H, K, P, R and S in the 2-in. thickness.

The correlations of Figures 4.31.3 and 4.31.4 indicate that with the ASTM A517 minimum requirement of 45 percent RA and 16 percent elongation, one can expect better than 35 ft-lb CVN-impact values at room temperature in A514/517 grade-F steel; whereas, in grade-H steel, one can have CVN impact values of less than 20 ft-lb with the same tensile ductility values. The 20 ft-lb level is below the AASHTO CVN-impact energy requirement and corresponds to a lateral expansion value slightly under the 15-mils required at ASTM A517-70a.

Note that 2-in. grade-H plates K (heat 1016), F (heat 1022) and E (heat 1023) developed over 45 percent RA but less than 25 ft-lb CVN-impact energy at room temperature (likewise for A517-F Plate A).

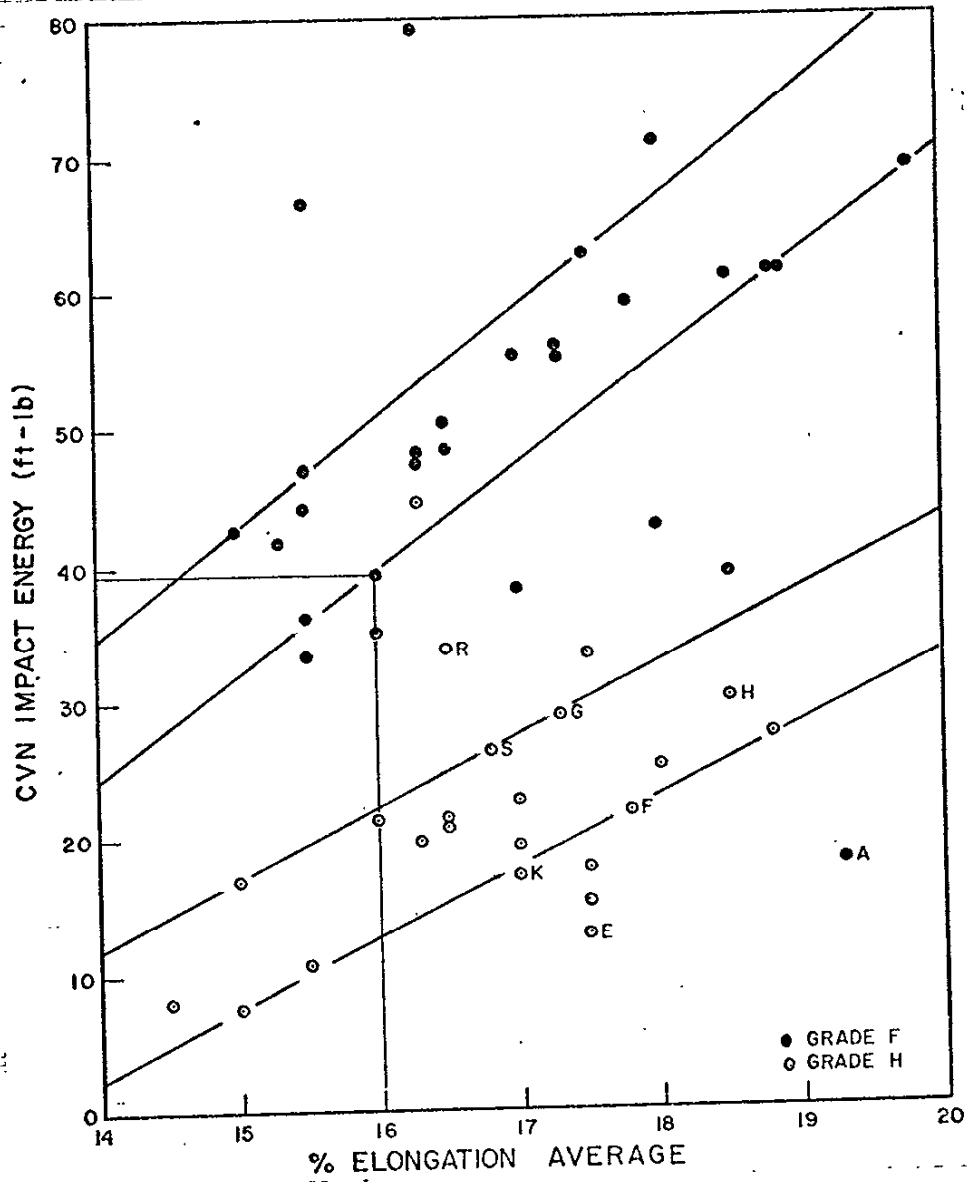
If credibility were given to the correlations indicated in Figures 4.31.3 and 4.31.4, it is apparent that grade F steel produced to meet the current ASTM Specification could be expected to easily meet the current AASHTO toughness specification, while grade H might not meet either of the specification toughness requirements.

The Charpy specimens tested were longitudinal while the tensile specimens were transverse. This raises a question as to whether better correlation would have been achieved if all specimens had been oriented the same.



CORRELATION OF CVN IMPACT ENERGY AND
% REDUCTION OF AREA OF A514/517 GRADES F AND H

FIGURE 4.31.3



CORRELATION OF CVN IMPACT ENERGY AND
% ELONGATION OF A514/517 GRADES F AND H

FIGURE 4.31.4

4.2 Charpy Impact Correlations

4.2.1 Background

The ASTM E399 K_{IC} plane-strain fracture-toughness test requires both the specimen thickness, B , and the crack length, a , exceed

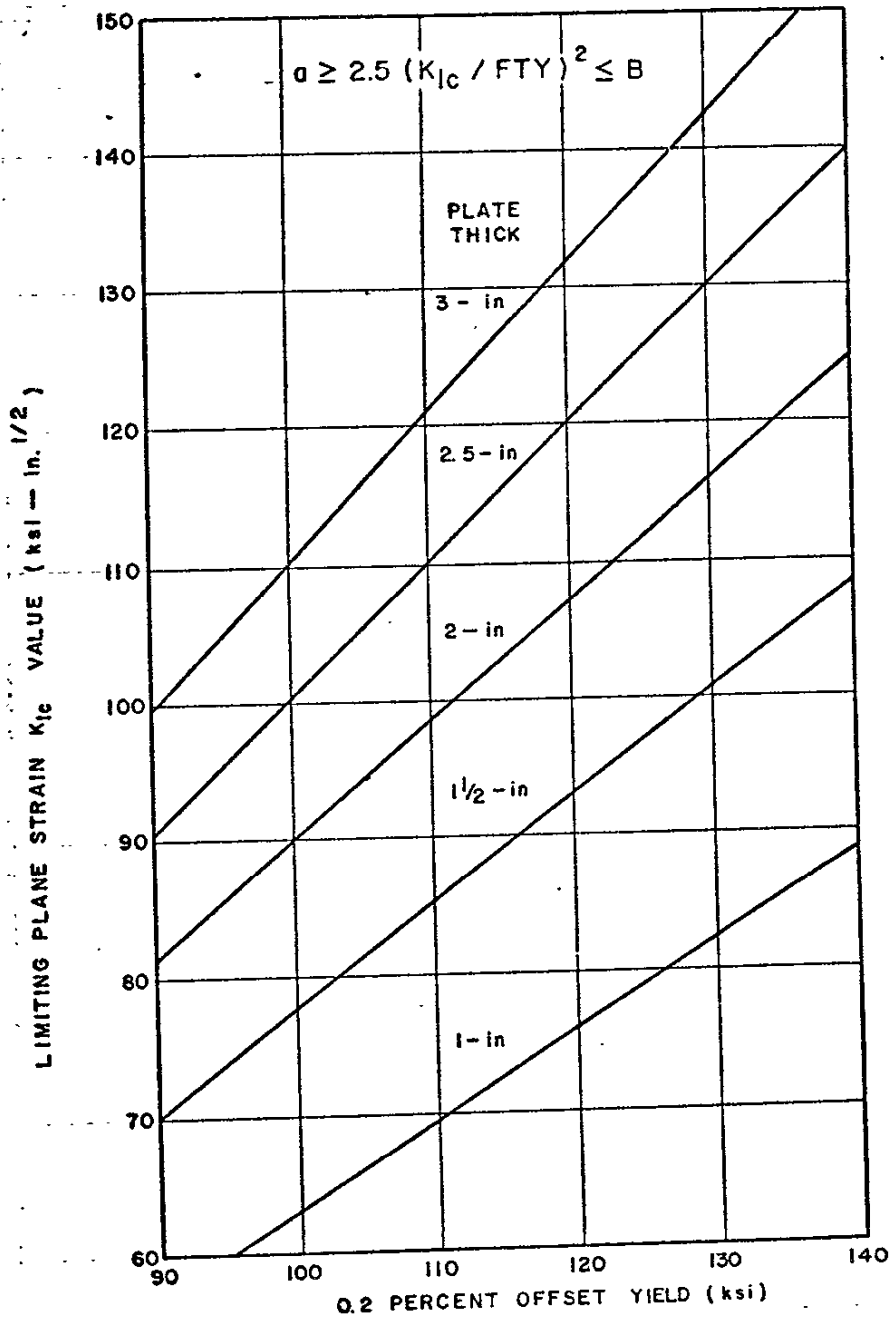
$$2.5 (K_{IC}/FTY)^2$$

where FTY is the 0.2% offset yield strength of the material for the temperature and loading rate of the test, there are many situations where the ASTM E399 Standard Method for K_{IC} testing cannot be used because the plate thickness to be tested is not great enough for a valid test. Figure 4.32 shows this limitation for A514/517 strength levels in thicknesses common to bridge construction. Note that for 110-ksi yield-strength steel, in 1-in.-thick plate the largest K_{IC} value that would be valid according to ASTM E399 is 70 ksi-in.^{1/2} and for 3-in.-thick plate, 120 ksi-in.^{1/2}. With such severe limitations and with K_{IC} testing as expensive as it is, it is easy to see why people are anxious to find a correlation between the Charpy test and K_{IC} .

Investigators at the U. S. Steel Applied Research Laboratory have reported that static plane-strain K_{IC} fracture toughness values correlate with:

1. precrack Charpy slow-bend (PCSB) data,
2. Charpy V-notch (CVN) impact data in the transition-temperature region,
3. CVN impact data in the upper-shelf region,

and that dynamic plane-strain K_{IC} fracture toughness values correlate with precrack Charpy impact (PCI) values.



LIMITING YIELD STRENGTH,
THICKNESS AND FRACTURE TOUGHNESS FOR VALID K_{Ic}
DETERMINATION PER ASTM E399

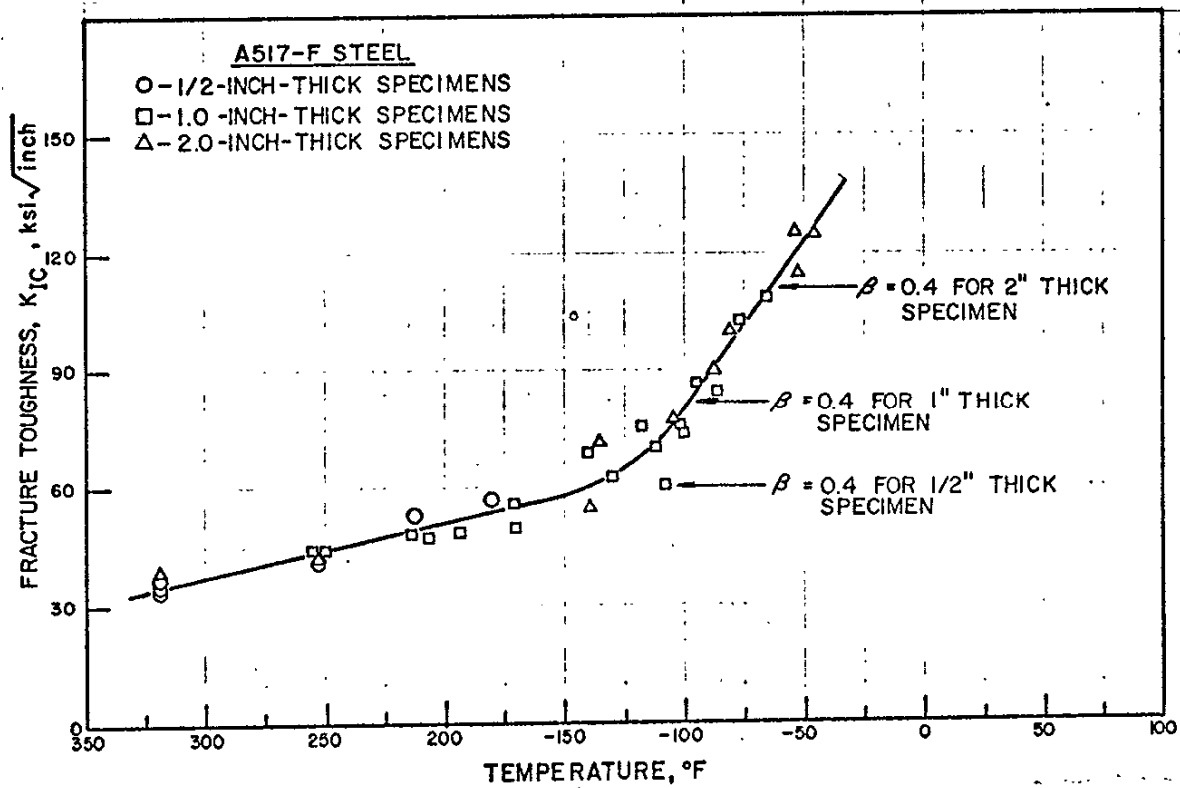
FIGURE 4.32

Rolfe and Gensamer(31) found that a K_{IC} -CVN correlation exists for steels having yield strengths greater than 110 ksi when tested at plus 80°F, a temperature which produced full-shear behavior in their steels.

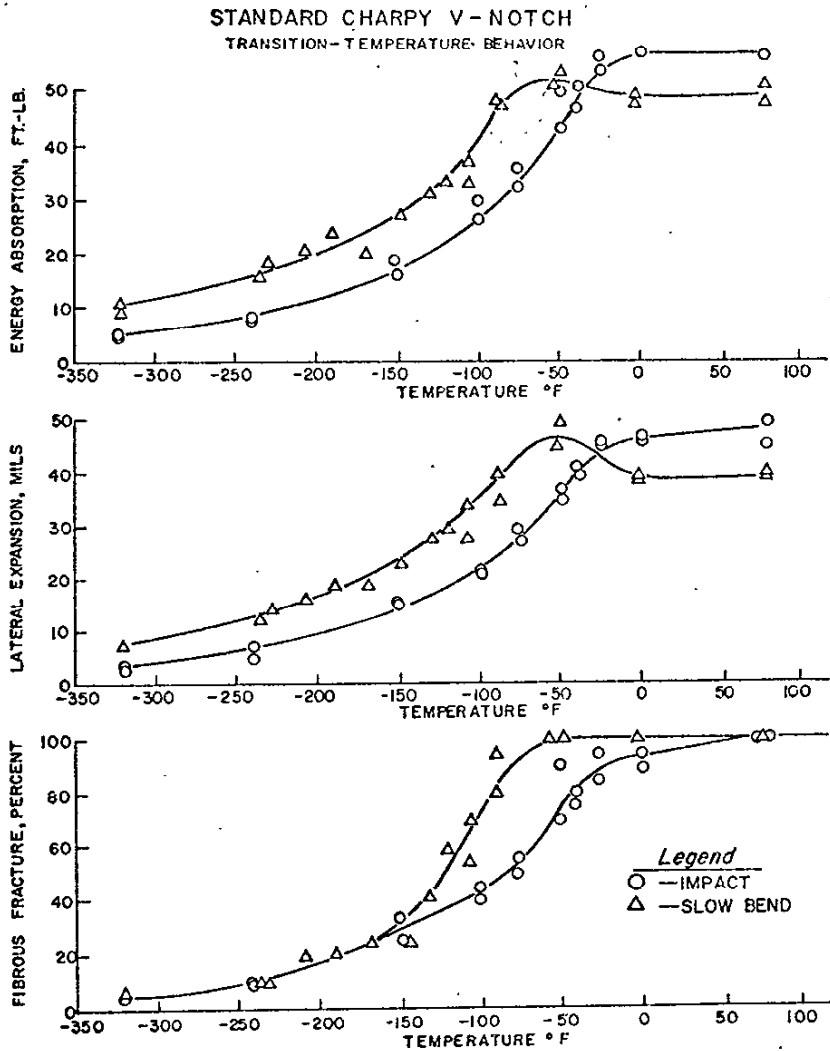
Barsom and Rolfe(32) showed that a K_{IC} temperature transition exists for A517-F steel that is independent of specimen thickness (Figure 4.33). In addition to K_{IC} bend testing, standard Charpy V-notch (CVN) and precrack Charpy slow-bend (PCSB) and impact (PCI) tests were made. From fractographic analysis, it was shown that in both the K_{IC} tests and Charpy tests, the transition was associated with a change in fracture mode from quasicleavage at cryogenic temperature to dimpled rupture at room temperature. The plots of energy absorption, percent shear, and lateral expansion are shown in Figures 4.34 and 4.35. In this particular heat of steel, a 50°F increase in transition temperature was indicated as a result of the higher strain rate associated with impact as compared with slow bend (0.025 in./minute). The investigators also made the observation that the static plane-strain K_{IC} transition-temperature range was the same as that defined by fatigue-cracked slow-bend Charpy tests*.

A procedure was proposed by the U. S. Steel investigators for predicting the dynamic K_{IC} behavior of a material by shifting static K_{IC} test data along the temperature axis by the same amount as the static Charpy (PCSB) energy values are shifted by impact testing (PCI). Shoemaker and Rolfe(3) studied the effect of loading rate on the K_{IC} of seven structural steels. The shift

*When Aerojet investigators compared the U.S. Steel data from static K_{IC} and Charpy tests, the temperature transition for the static K_{IC} and PCI tests appeared to nearly coincide (at approximately -120°F) inspite of the difference in rate of loading (Figure 4.36).

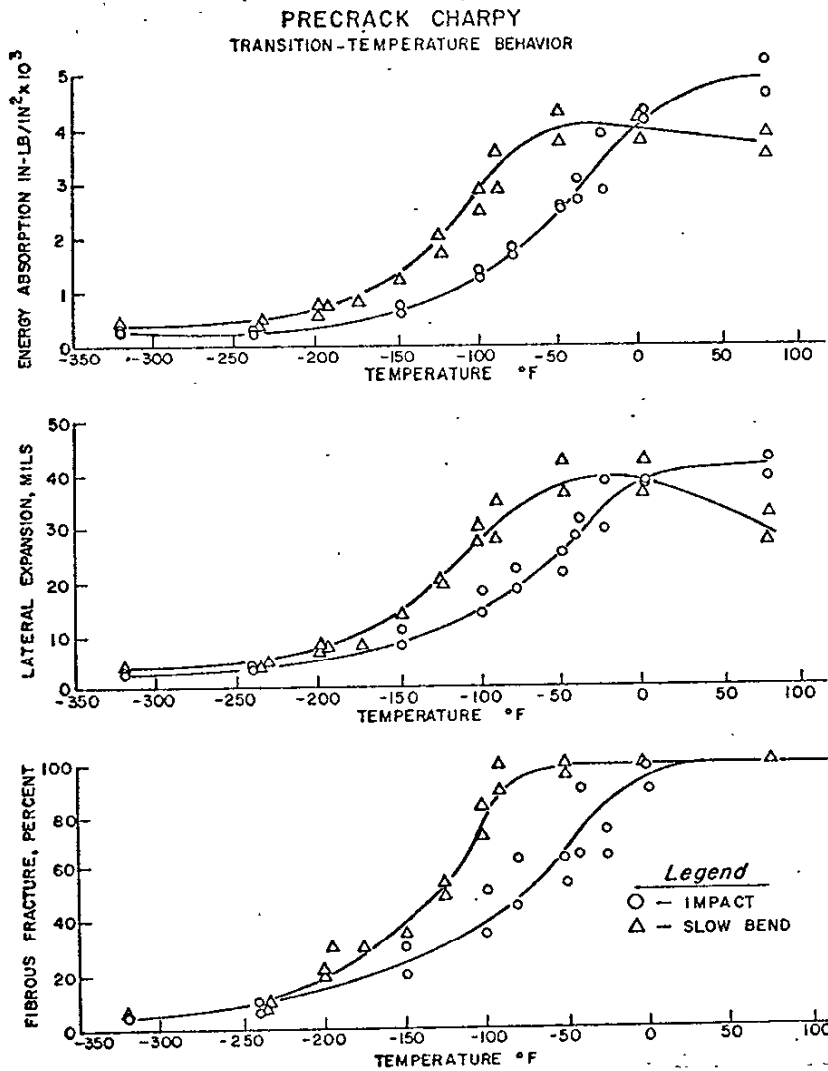


K_{IC} TEMPERATURE TRANSITION FOR A517-F STEEL
 (REFERENCE 32)
 FIGURE 4.33

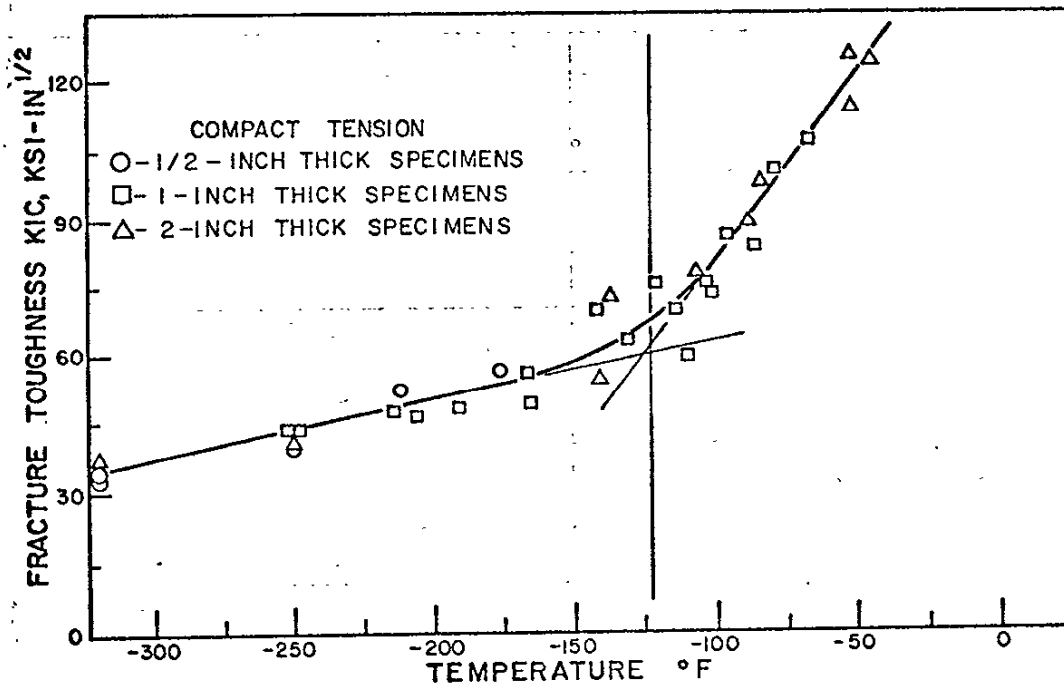
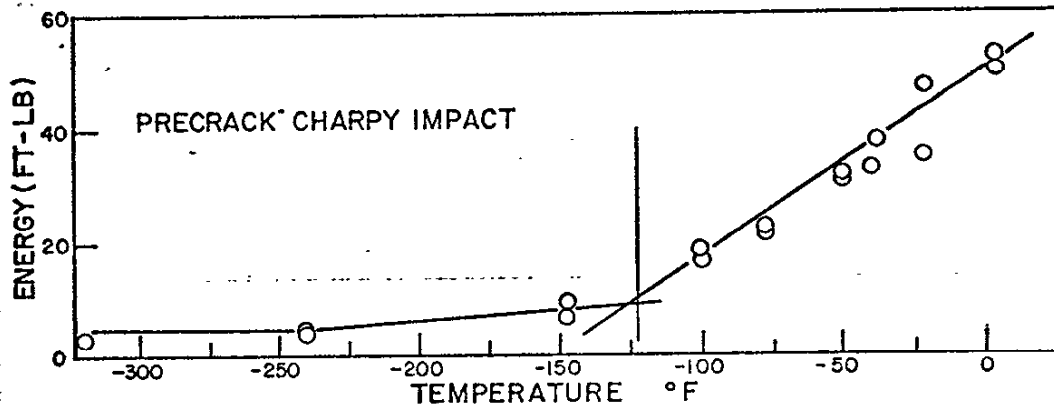


ENERGY, LATERAL-EXPANSION AND FRACTURE-APPEARANCE
TRANSITION CURVES FROM STANDARD CVN-IMPACT TESTS
OF A517-F HEAT 73B320 (REFERENCE 32)

FIGURE 4.34



**ENERGY, LATERAL-EXPANSION AND FRACTURE-APPEARANCE
TRANSITION CURVES FROM PCI TESTS OF A517-F HEAT 73B320
(REFERENCE 32)
FIGURE 4.35**



K_{IC} AND PCI TEMPERATURE
 TRANSITIONS BASED ON DATA FROM REFERENCE 32
 FIGURE 4.36

to higher temperature produced by impact loading when PCI and PCSB tests are compared is shown in Table 4.6. The results confirmed the general observation that low-strength steels are the most strain-rate sensitive. Dynamic K_{IC} data were obtained by impacting strain-gaged 3-point bend specimens with a falling weight. It was shown that the dynamic K_{IC} behavior of the various steels investigated could be predicted from static K_{IC} data by adjusting the latter along the temperature axis by the amount that fatigue-precracked Charpy slow-bend (PCSB) and impact (PCI) data were displaced from one another (Figure 4.37).

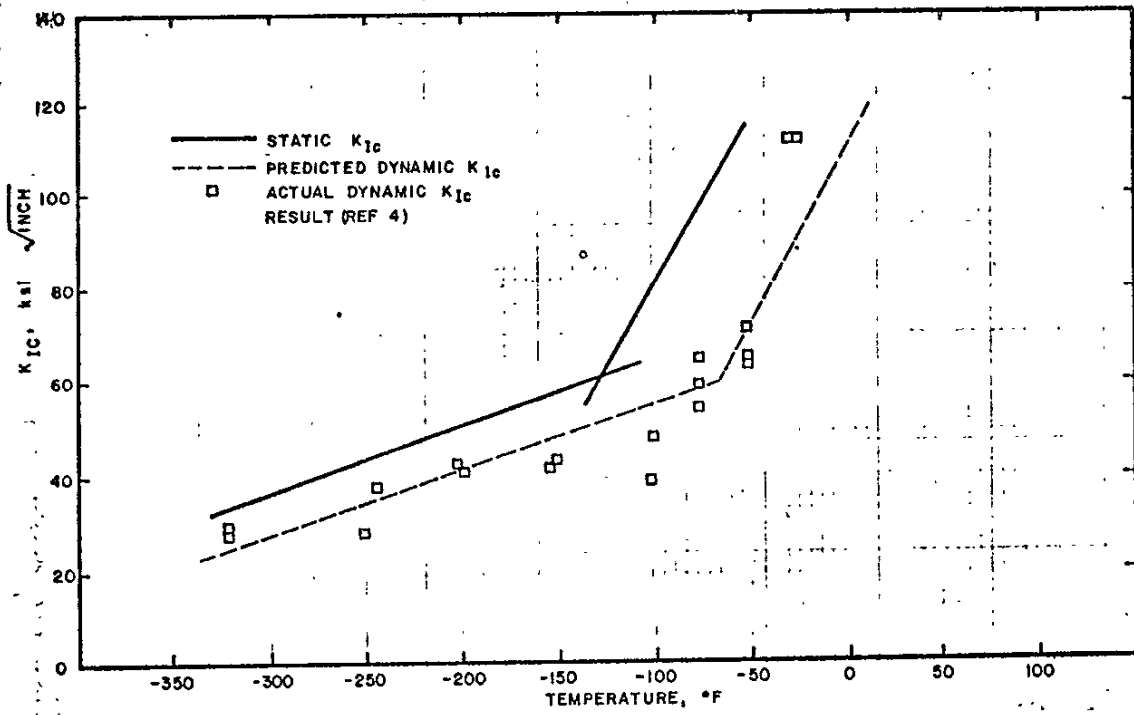
Barsom and Rolfe(4) later confirmed the observation that the onset of the temperature transition for static (slow-bend) and dynamic K_{IC} data occurs at about the same temperatures as the onset of the temperature transition for fatigue-cracked Charpy slow-bend and impact data, respectively. In discussing the observed correlations, Barsom and Rolfe pointed out that to attain such a correlation, the effects of both notch acuity and strain rate should be considered. Thus, the energy-absorption data obtained with slow bend fatigue-cracked Charpy (PCSB) specimens were compared with data obtained with slow-bend K_{IC} specimens, and the data obtained with dynamic (impacted) fatigue-cracked Charpy (PCI) specimens were compared with dynamic K_{IC} specimens. Figure 4.38 shows these comparisons; note that the empirical correlation between slow-bend K_{IC} and PCSB test results is the same as that between dynamic K_{IC} and PCI test results.

The U.S. Steel researchers(1,2,4,6) also investigated the possibility of empirical K_{IC} -CVN correlations. In this connection, they pointed out that the most widely used tests (in screening and specifications for toughness) are the static K_{IC} test and the standard Charpy V-notch (CVN) impact test. These two test specimens have different notch acuities and are tested at different loading rates. Nonetheless

TABLE 4.6

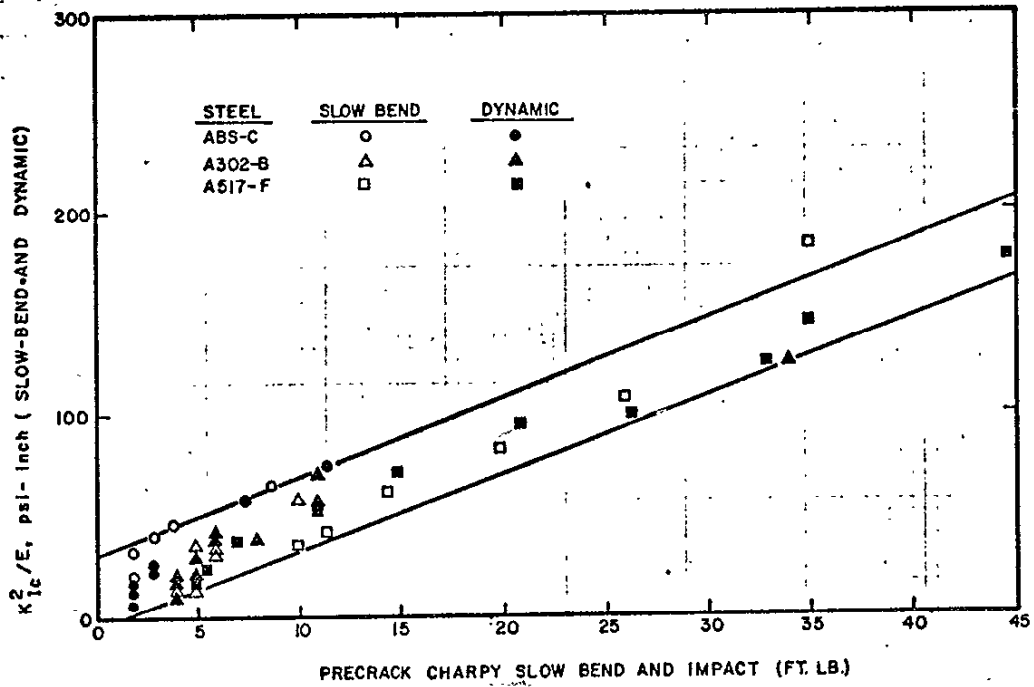
Increase in Transition Temperature as a
Result of Impact Loading(3)

<u>Steel</u>	<u>Yield Strength (ksi)</u>	<u>Shift Transition Temperature (°F)</u>
A36	37	160
ABS-C	39	140
A302B	56	130
HY-80	84	80
A517-F	118	60
HY-130	137	0
18Ni(180)	180	0



PREDICTION OF DYNAMIC K_{IC} BASED
ON PRECRACK CHARPY PCI AND PCSB TESTS
(REFERENCE 4)

FIGURE 4.37



STATIC AND DYNAMIC K_{Ic} PREDICTIONS
 BASED ON PCSB AND PCI TESTING (4)
 FIGURE 4.38

because even approximate correlations would be useful to the materials engineer, test results for these specimens were compared. The empirical correlation, based on tests at +80°F which corresponded to the upper shelf in the CVN impact testing of the U. S. Steel materials and dimpled rupture in the static K_{IC} specimens, is shown in Figure 4.39.

Gross(5) carried the correlation one step further. He combined the upper-shelf correlation

$$(K_{IC}/FTY)^2 = 5 (CVN - FTY/20)/FTY \quad (4.1)$$

with an expression from the work of Hahn and Rosenfield(33)

$$K_{IC} = FTY \cdot B^{1/2} \quad (4.2)$$

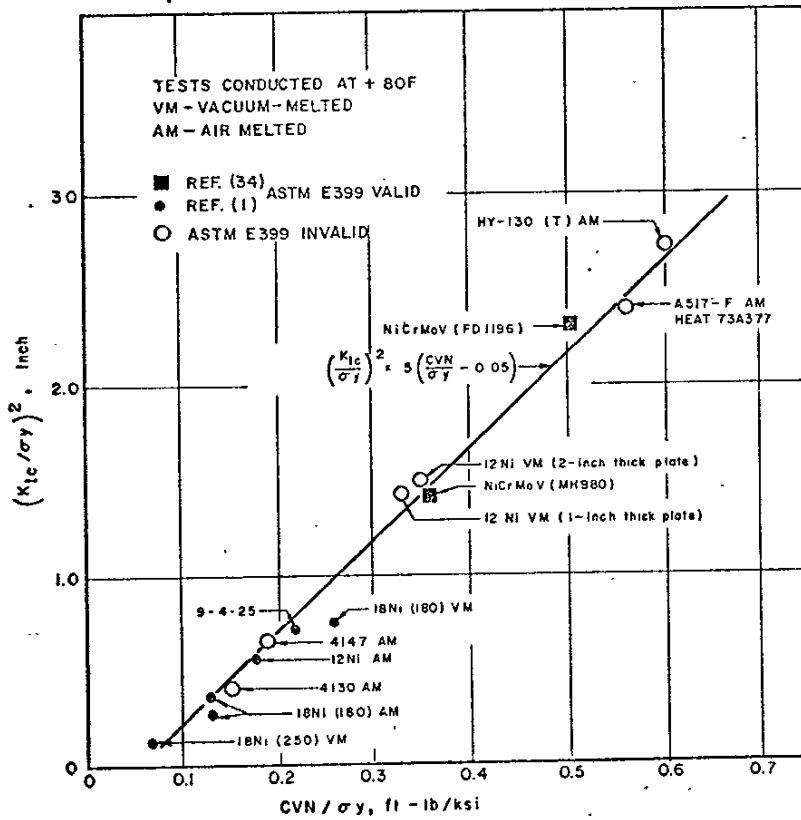
where K_{IC} is the plane-strain stress intensity for through-thickness yielding. The combination of these expressions resulted in the following simplified equation:

$$CVN = FTY (B + 0.25)/5 \quad (4.3)$$

This is the concept of through-thickness yielding as a basis for establishing a minimum Charpy V-notch impact energy level.

In terms of linear-elastic fracture mechanics, the concept of through-thickness yielding is the same as saying that the crack-tip plastic zone must be equal to the thickness of the plate. Under plane-stress conditions, the plastic zone is estimated to be

$$r_p = (K_c/FTY)^2/2\pi = B \quad (4.4)$$



UPPER-SHELF CVN-IMPACT K_{Ic} CORRELATION
 (REFERENCE 31)
 FIGURE 4.39

and in plane strain

$$r_p = (K_{Ic}/FTY)^2/6\pi = B \quad (4.5)$$

Wells(18) has shown that one can use the Charpy upper-shelf specific energy, W/A , as an indicator of ductility by proposing that if the plastic-zone size reaches the thickness of the plate containing the crack, the material should have enough ductility to tolerate through-thickness cracks enar general yielding. Wells' expression is

$$W/A = 4\pi FTY^2 B/E \quad (4.6)$$

This equation is under consideration in the United Kingdom for use in British Standards BS153 (Steel Girder Bridges), BS449 (Structural Steel Buildings) and BS2573 (Cranes). The criterion has been proposed for use in specifying the maximum allowable plate thickness for welded members in tension. Gross(5) rejected equation (4.6) because it required unrealistically high Charpy values, particularly at high values of yield strength and plate thickness. The derivation of Wells' equation assumes the relationship $G_c = 0.5(W/A)$. If, on the other hand, one substitutes W/A for G_c in the relationship $EG_c = K_c^2$ and then substitutes $E(W/A)$ for K_c^2 in equation (4.4), the equation becomes

$$W/A = 2\pi FTY^2 B/E \quad (4.7)$$

which is less conservative than equation (4.6) but more conservative than equation (4.3) proposed by U.S.Steel. With through-thickness yielding, a plane-stress condition will prevail, and therefore, the 2π coefficient (Wells' equation has 4π) of equation (4.7) appears to be realistic.

Rolfe and Novak(6), using four-point-bend test specimens, addressed themselves to the problem of measuring toughness in medium-strength steels. For purposes of studying the limitation of linear-elastic fracture mechanics, a series of slow-bend K_{Ic} tests were conducted on several steels. Because these materials were limited to a maximum of 2-in.-thickness, only five of the eleven steels investigated included tests which met the ASTM requirement that:

$$B \geq 2.5 (KQ/FTY)^2 \leq a$$

Furthermore, only six of the eleven steels met the ASTM bend requirement for specimen depth in bending, viz.,

$$W \geq 5 (KQ/FTY)^2$$

Thus, tests of five of the eleven steels, viz., A517-F(AM), 4147 (AM), HY-130T(AM), and 12Ni-5Cr-3MO(VM) in two heats, did not meet the ASTM Committee E24 size requirements. Nevertheless, the data from all eleven steels conformed to the relationship of equation (4.1) as shown in Figure 4.39.

Begley and Toolin(34) confirmed the upper-shelf relationship by adding two valid data points from intermediate-strength NiCrMoV rotor steels. The upper-shelf K_{Ic} values for the NiCrMoV steels were in excellent agreement with the Rolfe-Novak upper-shelf correlation as shown in Figure 4.39 (see the solid-squares. The Westinghouse investigators qualified the correlation as applying to materials not significantly strain-rate sensitive.

In addition to the upper-shelf relationship, Barsom and Rolfe(4) showed that an empirical correlation exists between standard CVN impact test data and static K_{IC} on the low side of the transition-temperature range. The relationship, based on data from five steels (ABS-C, A302-B, A517-F, HY-130 and 18Ni-250, is given by

$$K_{IC}^2/E = 2 (CVN)^{3/2} \quad (4.8)$$

The slow-bend K_{IC} tests for these steels were conducted in the transition region and satisfied the ASTM E24 requirements for K_{IC} testing. However, the data used to establish the relationship exhibited considerable scatter (as compared with Figure 4.39).

Corten and Salors(35) using pressure-vessel steels such as A533-B and A517-F established a different correlation, indicating the following empirical relation:

$$K_{IC} = 15.5 (CVN)^{1/2} \quad (4.9)$$

which is numerically equivalent to

$$K_{IC}^2/E = 8 (CVN) \quad (4.10)$$

They found the above expressions to provide a good empirical representation of the relation between static K_{IC} and CVN impact for thick-section steels in the range of 5 to 50 ft-lb as measured in the transition-temperature range. Corten and Sailors found the relation by Barsom and Rolfe to underestimate K_{IC} at low values of CVN and overestimate K_{IC} at higher values of CVN.

4.2.2 Charpy Test Results

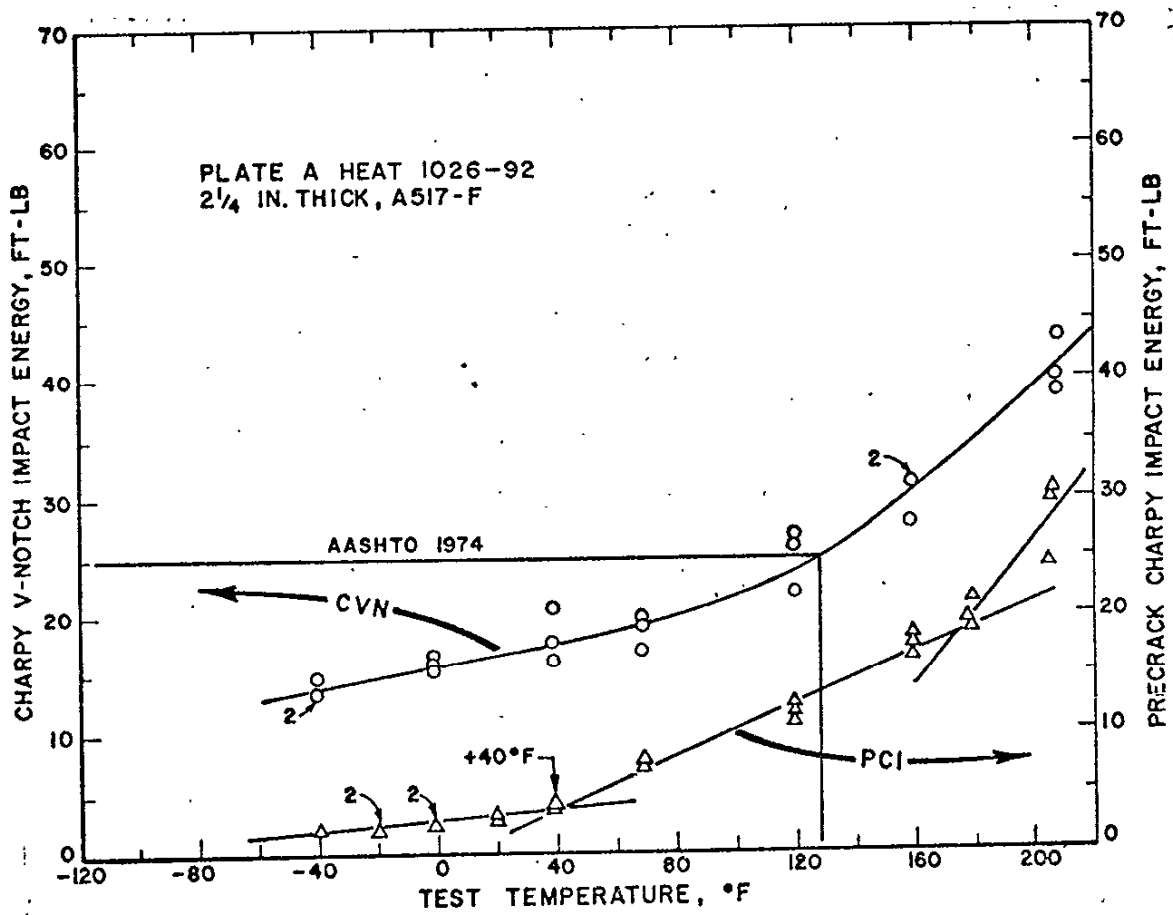
The plots of Charpy impact energy (ft-lb) versus test temperature ($^{\circ}\text{F}$) for seven steels tested using the ASTM E399 compact-tension K_{Ic} method are shown in Figures 4.40 through 4.46. Note that the PCI test had the characteristic of a well-defined inflection point (intersection of two straight lines) which has been shown previously to provide an approximation of the NDT temperature (36).

The well-defined change in the slope of the curve relating precrack Charpy energy and test temperature is substantiated by lateral expansion measurements. Figure 4.47 illustrates this in precrack Charpy impact (PCI) test results from A517-F plates A and B. A direct proportionality between energy and lateral expansion has been reported previously (37, 38, 39).

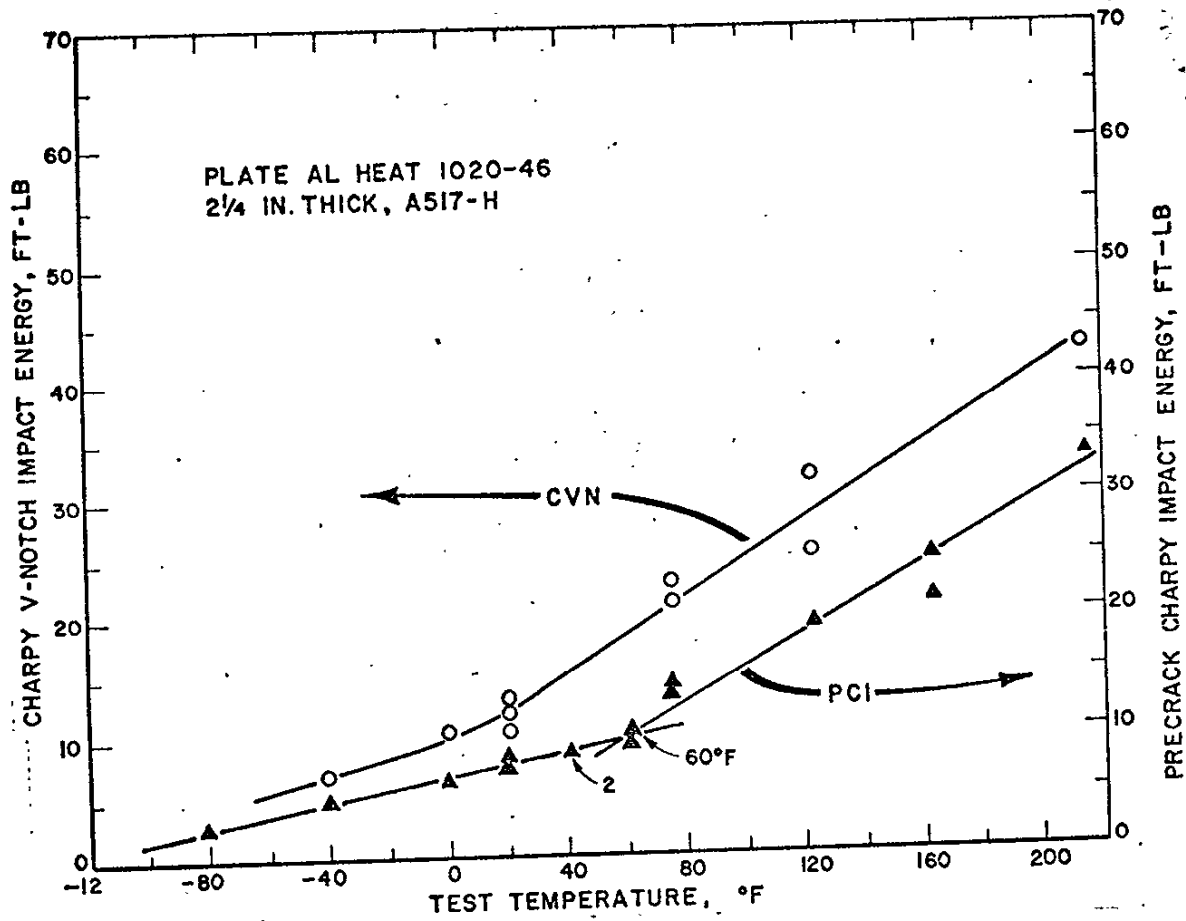
The temperatures corresponding to the inflection points in the PCI energy-versus-temperature plots are reported below. Note that the transition temperatures range from minus 90°F for plate M to over plus 200°F for plate CK. The double inflection found in the plate-A transition curve will be discussed in a later section of this report in connection with NDT testing.

Approximate Nil-Ductility Transition (NDT) Temperatures Based on Precrack Charpy Impact Tests

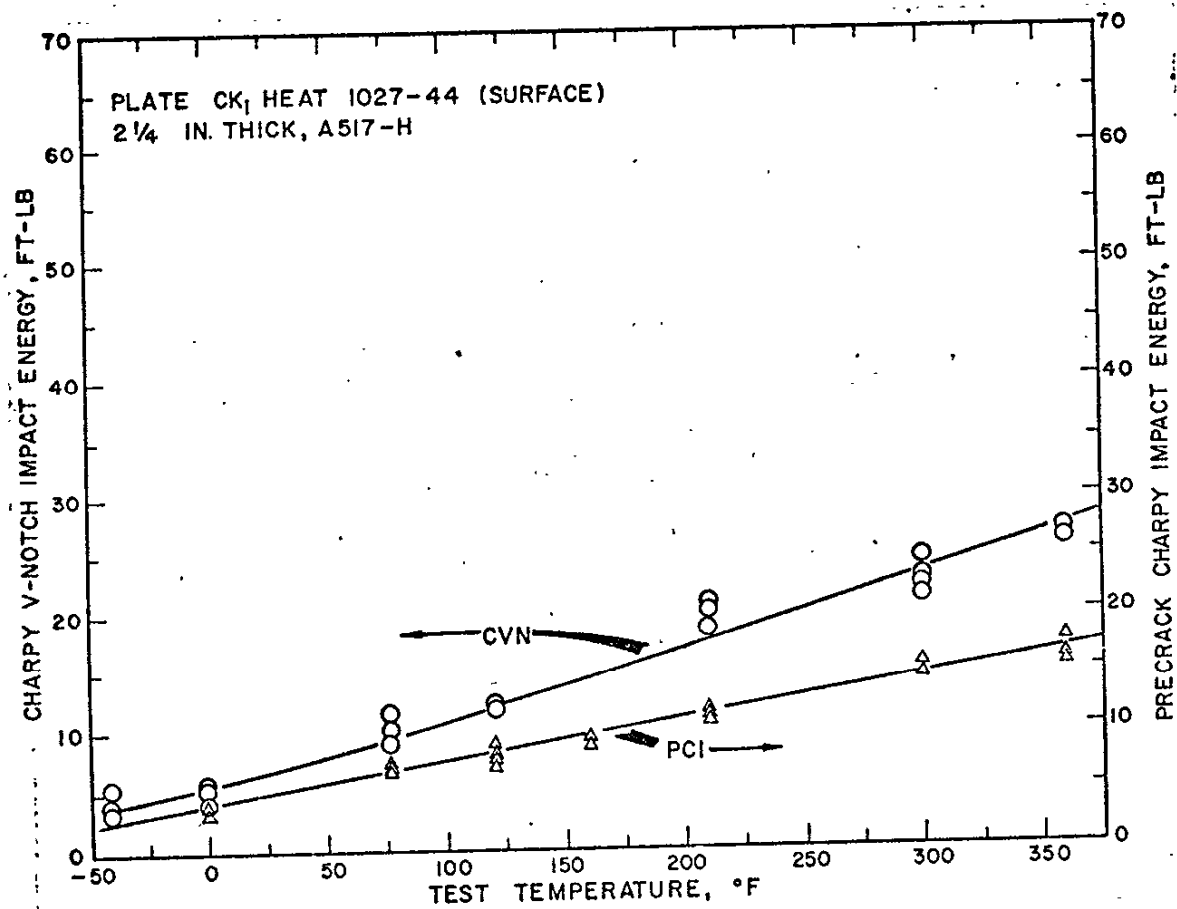
<u>Steel</u>	<u>NDT ($^{\circ}\text{F}$)</u>
M	-90
R	-40
L	-20
Z	-5
A	+40 (+180)
AL	+60
CK-1	> +200



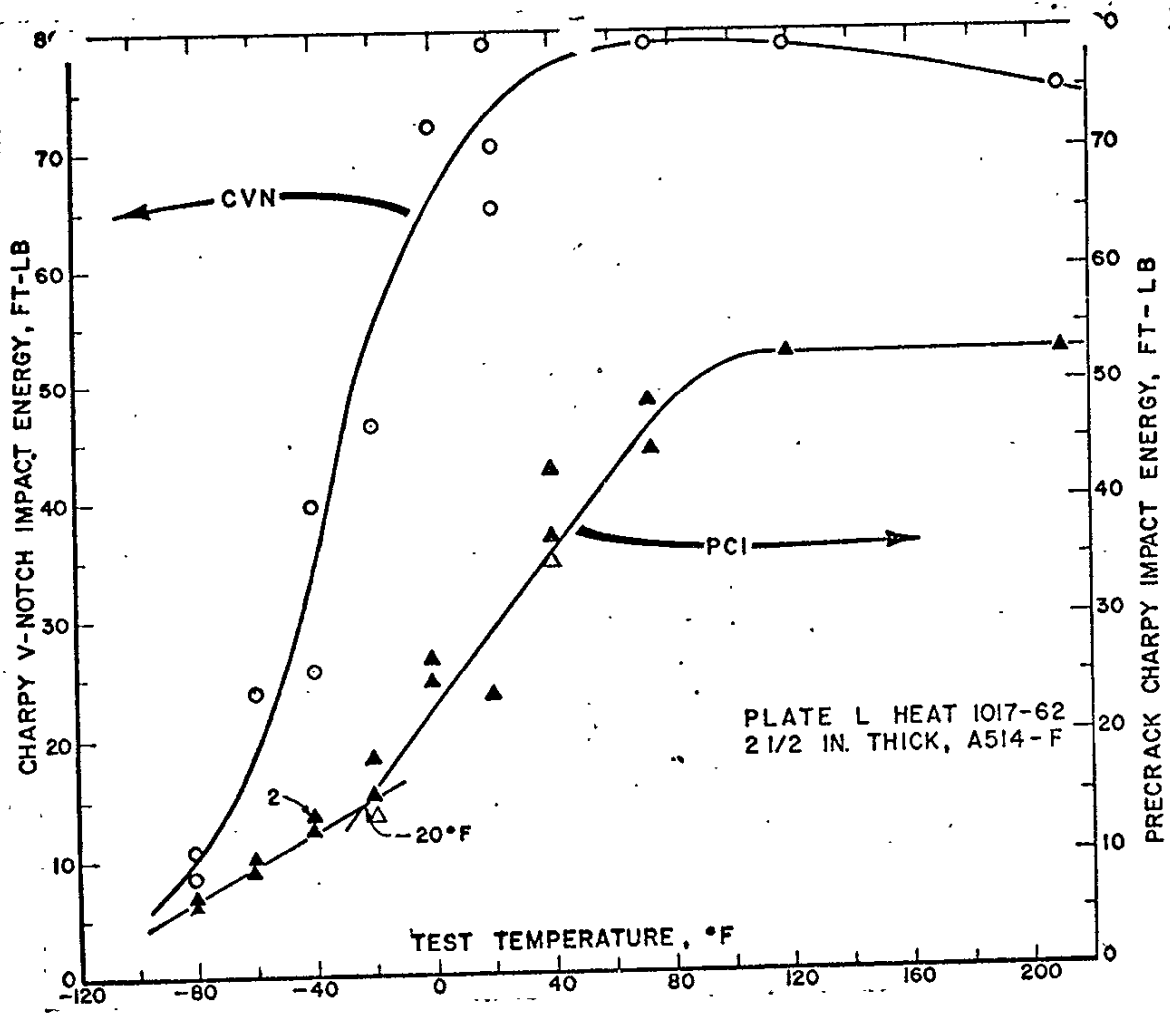
CVN-IMPACT AND PCI TRANSITION CURVES
FOR A517-F HEAT-SLAB 1026-92
FIGURE 4.40



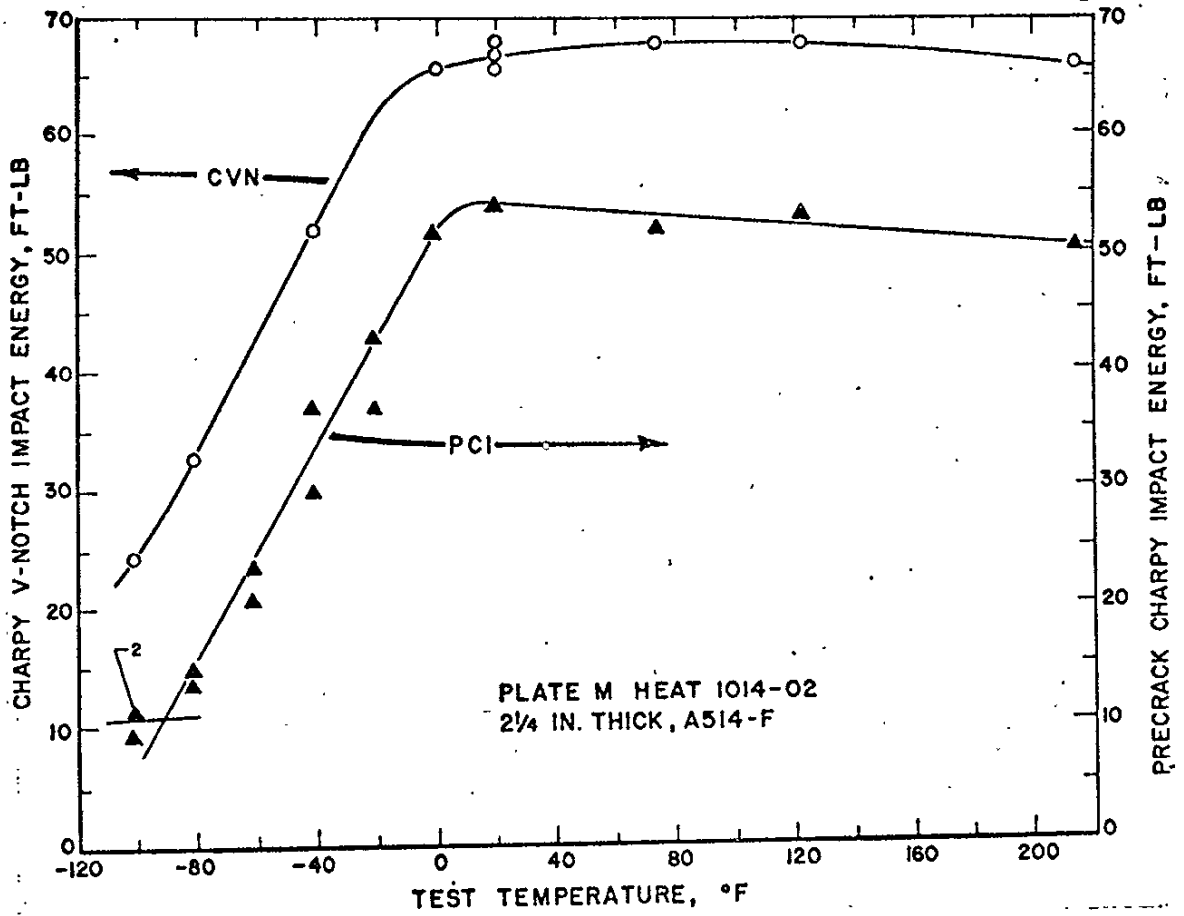
CVN-IMPACT AND PCI TRANSITION CURVES
FOR A517-H HEAT-SLAB 1020-46
FIGURE 4.41



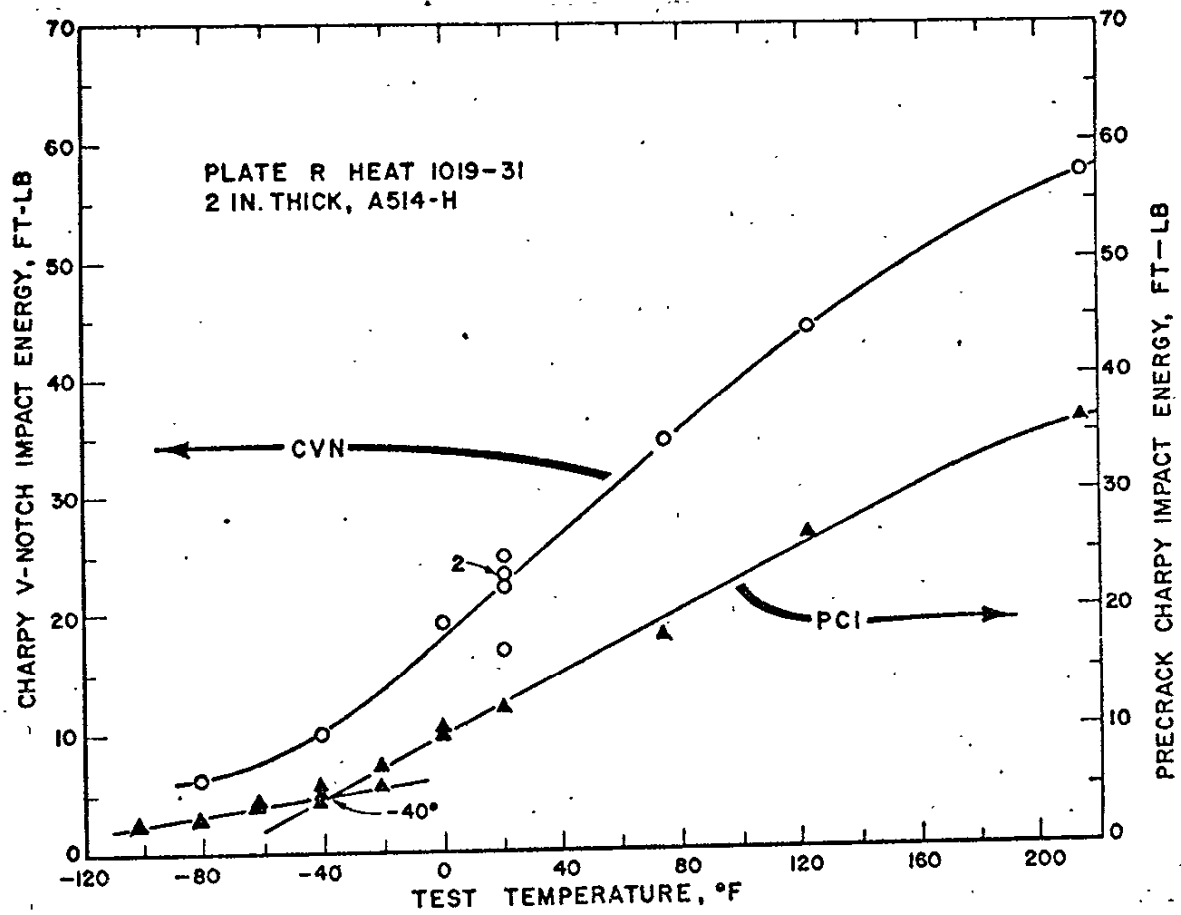
CVN-IMPACT AND PCI TRANSITION CURVES
FOR A517-H HEAT-SLAB 1027-44
FIGURE 4.42



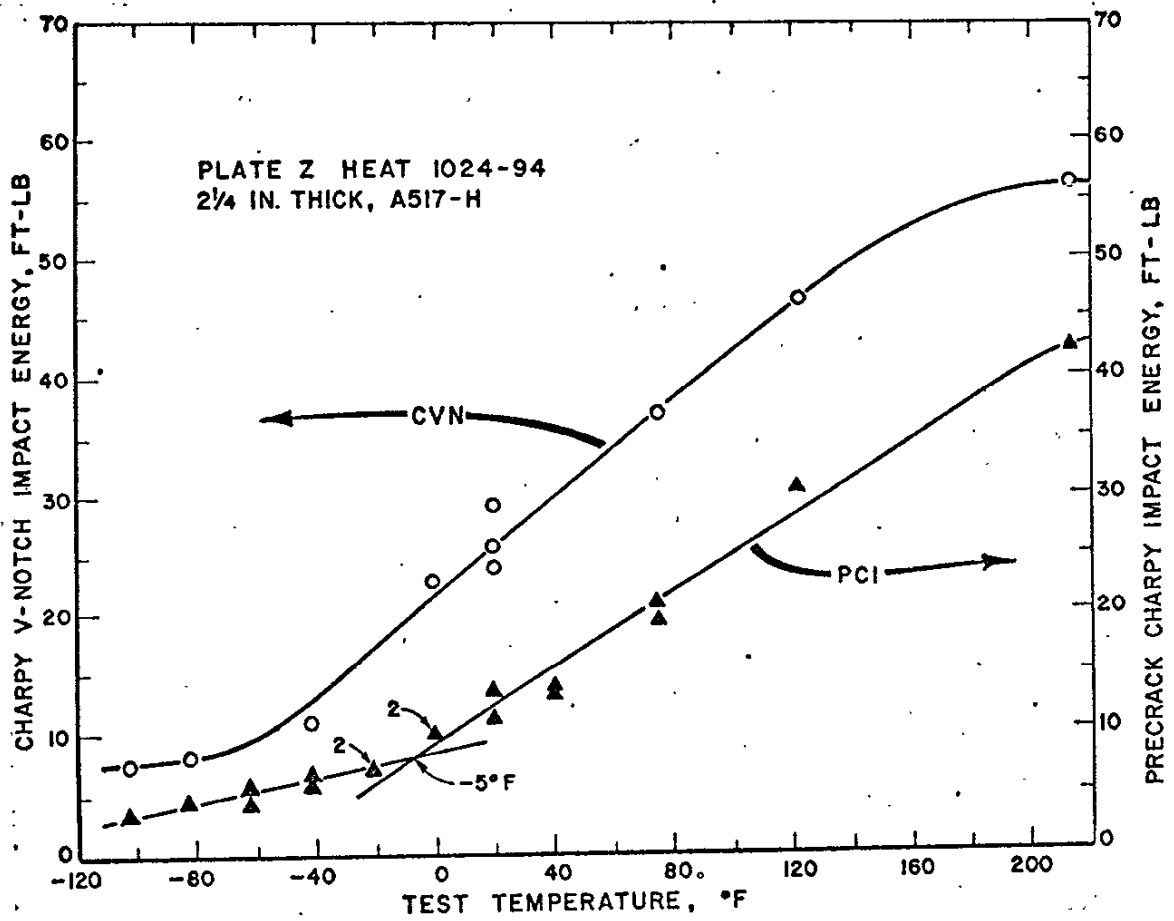
CVN-IMPACT AND PCI TRANSITION CURVES
FOR A514-F HEAT-SLAB 1017-62
FIGURE 4.43



CVN-IMPACT AND PCI TRANSITION CURVES
FOR A514-F HEAT-SLAB 1014-02
FIGURE 4.44

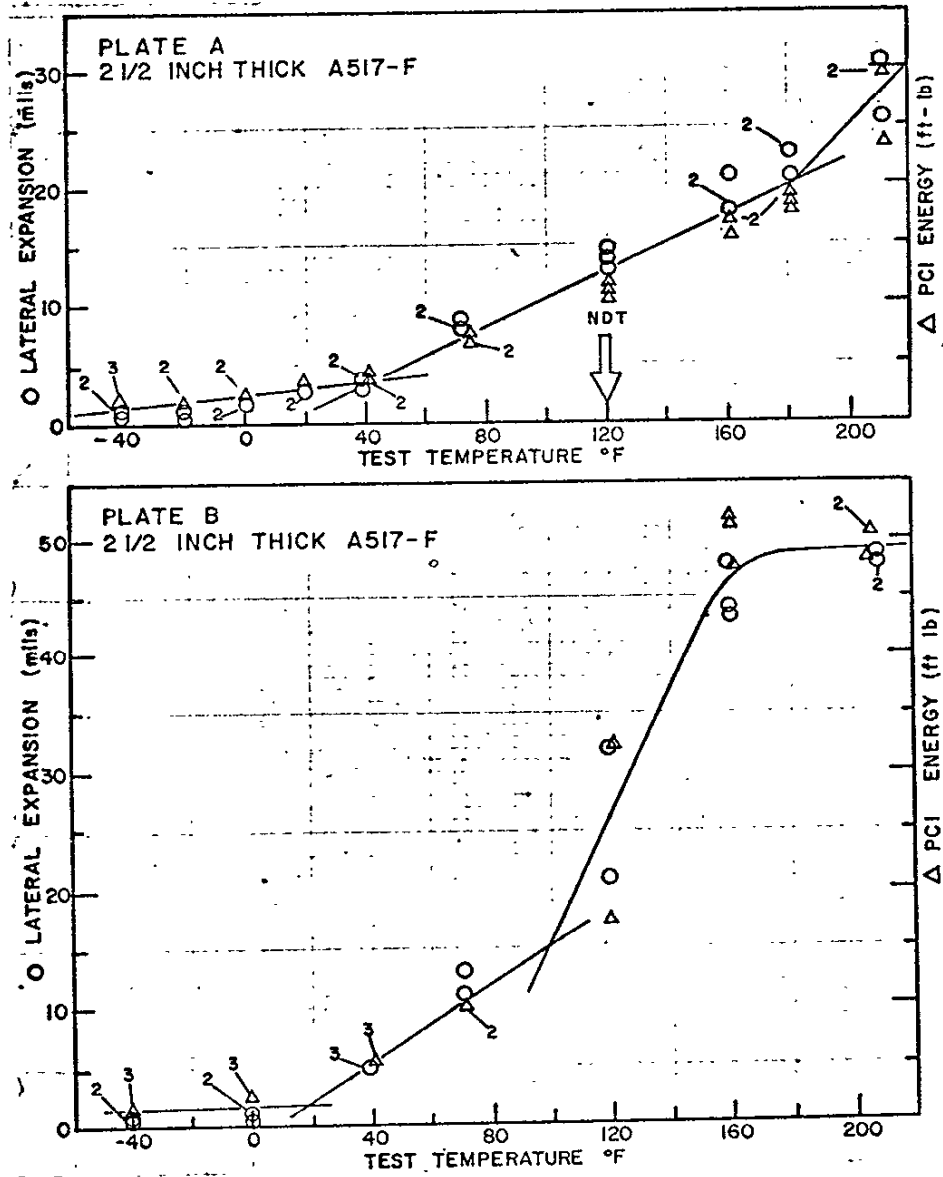


CVN-IMPACT AND PCI TRANSITION CURVES
FOR A514-H HEAT-SLAB 1019-31
FIGURE 4.45



CVN-IMPACT AND PCI TRANSITION CURVES
FOR A517-H HEAT - SLAB 1024-94

FIGURE 4.46



REINFORCEMENT OF THE ENERGY-TEMPERATURE PLOT WITH LATERAL EXPANSION IN A517-F PLATES A AND B
 FIGURE 4.47

4.2.3 Upper-Shelf K_{IC} -CVN Correlation

The U. S. Steel empirical correlation between standard Charpy V-notch (CVN) impact energy absorption values measured at the upper shelf and static K_{IC} values was based on several steels having room-temperature yield strengths ranging from 39 to 246 ksi, and room-temperature bend-test critical-stress-intensity values ranging from 87 to 246 ksi-in.^{1/2} (see equation 4.1 and Figure 4.39).

One of the steels used by the U. S. Steel investigators in establishing the correlation was A517-F heat 73A377; for this heat the upper-shelf CVN energy was 62 ft-lb at 80°F and the KQ value as determined by 2 x 6-in. cross-section bend specimens was 170 ksi-in.^{1/2}. All tests were conducted at 80°F; at this temperature the CVN impact values were reported to be "shelf" values on the basis that all specimens exhibited 100 percent fibrous fracture. The plane-strain fracture toughness test results for the A517-F heat investigated by U. S. Steel are shown in Table 4.7. From this tabulation, it will be seen that the three tests did not satisfy the ASTM specimen-size requirements. Nevertheless, the U. S. Steel A517-F data complied with the upper-shelf K_{IC} -CVN relationship of equation 4.1 (see Figure 4.39).

Of the A514/517 heats investigated from the Bryte Bend and Tuolumne River bridge steels, using the ASTM E399 compact-tension K_{IC} method, only A514-F plates L and M developed upper-shelf CVN energy values at 80°F or lower temperature. Therefore, for purposes of calculating K_{IC} values based on upper-shelf CVN impact test results, it was necessary to use CVN values obtained at temperatures higher than 80°F. Table 4.8 shows the calculated K_{IC} values at the upper-shelf test temperatures; note that the calculated values provided a reasonable approximation of the values obtained by an extrapolation of the compact-tension test results (see Figures 4.70 to 4.76) with the exception of the CK plate.

TABLE 4.7

U. S. STEEL PLANE-STRAIN FRACTURE-TOUGHNESS DATA FOR
A517-F HEAT 73A377*

THICKNESS			CRACK DEPTH		
B	$B/(KQ/FTY)^2$	$2.5(KQ/FTY)^2$	a	$a/(KQ/FTY)^2$	$2.5(KQ/FTY)^2$
1.84	0.71	6.48	2.60	1.01	6.44
1.85	0.87	5.32	2.55	1.20	5.31
1.85	0.69	6.70	1.78	0.67	6.64

BEAM DEPTH			KQ MEASUREMENT	
W	$W/(KQ/FTY)^2$	$5(KQ/FTY)^2$	10% Secant	Pop-In
6.0	2.32	12.93	177	177
6.0	2.83	10.60	160	-
6.0	2.24	13.39	175	180

*Under the provisions of ASTM E399, it is required that both the crack depth (a) and the specimen thickness (B) must be at least $2.5 (KQ/FTY)^2$, and the beam depth (W) must be twice the specimen thickness, i.e., $W > 5(KQ/FTY)^2$ (6).

TABLE 4.8

PLANE-STRAIN FRACTURE TOUGHNESS CALCULATED FROM CHARPY V-NOTCH
UPPER-SHELF ENERGY

Plate/Code	$(K_{IC}/FTY)^2 = 5(CVN-FTY/20)/FTY$					Calculated K_{IC} @ Shelf Temperature (ksi-in. ^{1/2})
	Charpy V-Notch (CVN) Shelf (ft-lb)	Shelf Temperature (°F)	At Shelf Yield (ksi)	Temperature CVN/FTY (ft-lb/ksi)	$(K_{IC}/FTY)^2$ (From Fig. 4.39) (in.)	
A/ZW	40	+200(a)	100	0.40	1.75	132
AL/ZY	42	+200(a)	98	0.43	1.90	135
L/ZV	79	+60	110	0.72	3.35	200
M/ZU	65	0	119	0.55	2.50	190
CK-1/ZZ	23	+300(a)	107	0.21	0.82	97
R/ZX	56	+200(a)	110	0.51	2.30	167
Z/ZT	55	+200	112	0.49	2.20	166

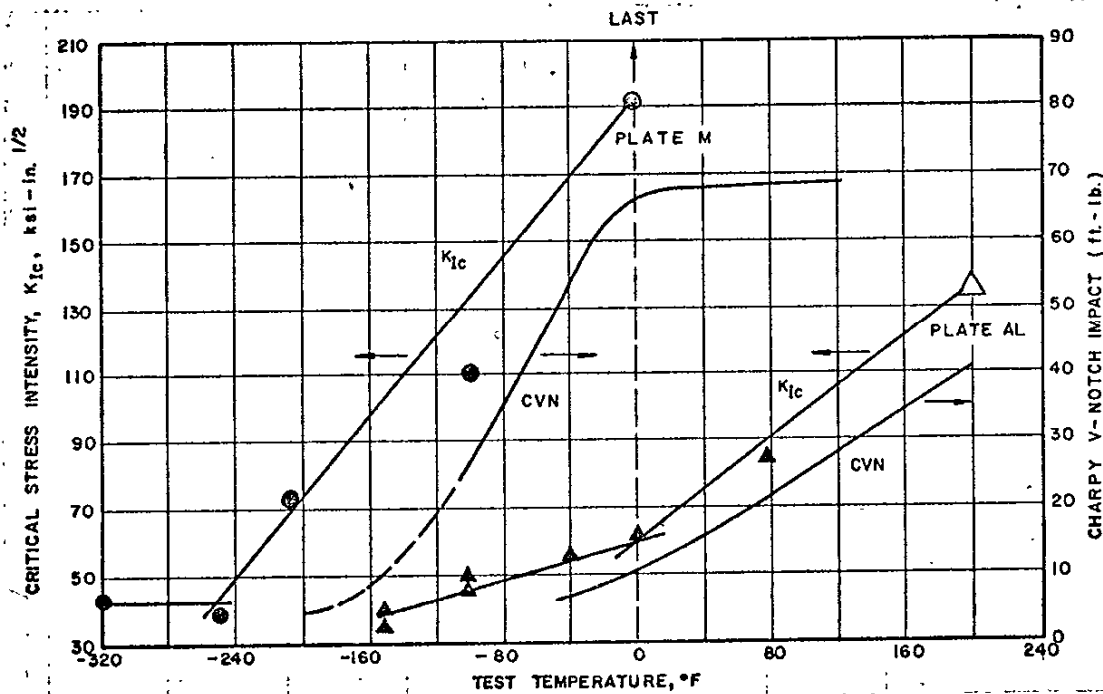
(a) Shelf may be at a higher temperature and, therefore, the shelf energy may be somewhat higher than the value indicated.

In the CK plate, the calculated value (97 ksi-in.^{1/2}) was too high based on the extrapolated value (70 ksi-in.^{1/2}) from Figure 4.74. However, the data from the CK plate as well as those from some of the other plates considered here should be used with caution in evaluating the K_{IC} -CVN upper-shelf correlation in that the Charpy tests at the highest temperatures tested were not on the upper-shelf.

If the Charpy upper-shelf occurs at a temperature higher than the lowest temperature anticipated in service, the calculated value of K_{IC} based on the CVN- K_{IC} upper-shelf correlation is meaningless in terms of the plane-strain fracture toughness at the lowest-anticipated-service temperature. Figure 4.48 illustrates this situation. For plate AL, based on the upper-shelf K_{IC} -CVN correlation, the calculated K_{IC} was 135 ksi-in.^{1/2} at plus 200°F; whereas, the measured K_{IC} at 0°F was only 60 ksi-in.^{1/2}. In the case of plate M, on the other hand, where the CVN upper-shelf occurred below the lowest anticipated service temperature (LAST), the calculated K_{IC} value of 190 ksi-in.^{1/2} was deemed to be meaningful in terms of service.

4.2.4 Lower-Shelf K_{IC} -PCI Correlation

Based on standard Charpy V-notch (CVN) impact values from the transition range and lower shelf of the Charpy transition curve, U. S. Steel investigators reported the correlation of equation (4.8). Charpy V-notch (CVN) impact and static K_{IC} data from the Bryte Bend and Tuolumne Bridge A517-F and A517-H steels were plotted to determine if they conformed to equation (4.8). The expression obtained by Corten and Sailors(35) also was examined (equation 4.10). From Figure 4.49, it will be seen that the U. S. Steel relationship appeared to fit the data but there was considerable scatter in the test results. Table 4.9 presents the data plotted in Figure 4.49, which includes tests by U. S. Steel and those of this investigation. Only valid K_{IC} values were plotted in Figure 4.49. From Figure 4.49 it can be seen that the U. S. Steel



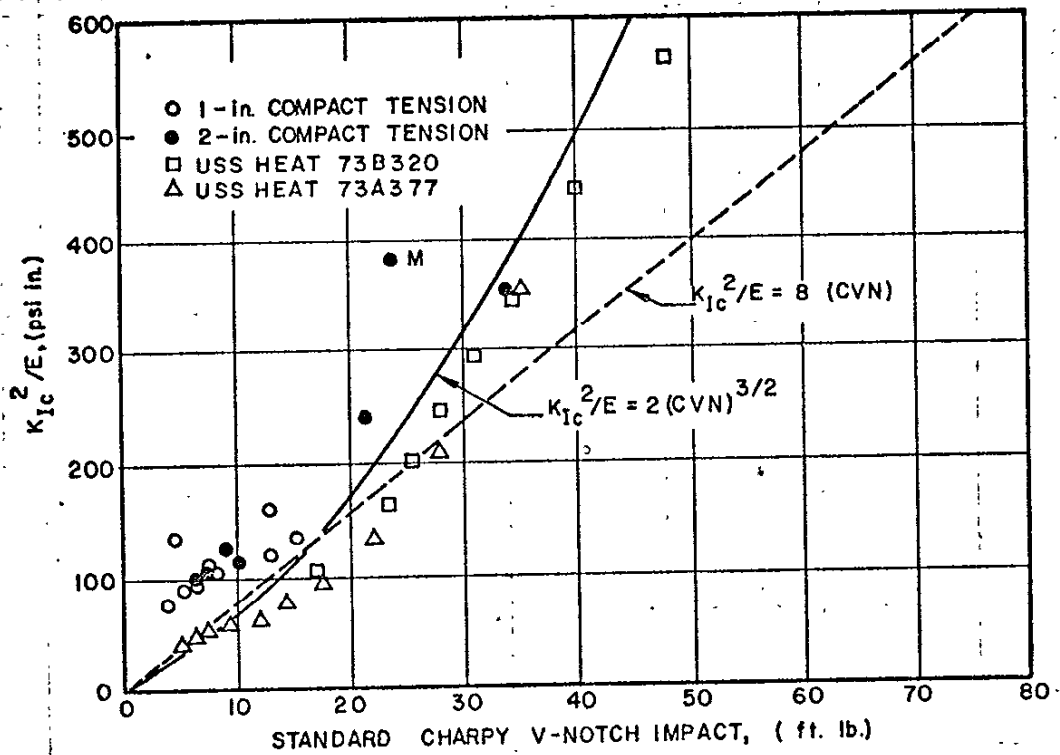
UPPER-SHELF CVN-IMPACT ESTIMATE OF K_{Ic}
 FRACTURE TOUGHNESS (SOLID SYMBOLS ARE ASTM
 E399 VALID K_{Ic} VALUES; OPEN SYMBOLS ARE
 CVN- K_{Ic} ESTIMATED VALUES)

FIGURE 4.48

TABLE 4.9
TRANSITION-RANGE CHARPY-K_{IC} CORRELATION DATA

Type	Specimen	PLANE-STRAIN FRACTURE TOUGHNESS TEST RESULT						CHARPY IMPACT (c)				
		Temp. (°F)	Size (in.)	2.5*(KQ/FTY) ² (in.)	KQ (ksi-in. ^{1/2})	KQ ² /E (psi-in.)	(KQ/FTY) ² (in.)	CVN (ft-lb)	PCI (ft-lb)	NDT (°F)		
A514F	M(ZU)	A	-100	2	1.890	108 (a)	388	0.756	24	10.5	-90	
		H	-103	1	1.645	101	340	0.658	23	10.5		
		D	-80	1	2.344	118	464	0.938	32	14		
		I	-40	1	1.790	102	347	0.716	51.5	32.5		
		B	+75	2	2.860	125	521	1.144	66.5(a)	52		
		L(ZV)	-100	2	1.012	74	182	0.405	-	4		-20
	D	-80	1	0.685	61	124	0.274	10	6.5			
	B	-55	2	2.464	114	433	0.986	28.5	10.5			
	F	-40	1	1.773	95 (a)	301	0.709	39.5	13			
	H	0	1	2.280	106	375	0.912	67	22.5			
	A	+75	2	3.270	126	529	1.308	79 (a)	47			
	A517F	A(ZW)	H	-39	1	2.201	104 (a)	361	0.880	14	2	+40
			D	-2	1	2.089	100	333	0.836	15	2.5	
			E	+39	1	1.863	93	288	0.745	18	4	
			F	+75	1	2.721	111	411	1.09	18.5	7.5	
	A514H	R(ZX)	E	-102	1	0.676	64	136	0.270	4.5	2.5	-40
			D	-80	1	0.482	53	94	0.193	6.5	3	
			C	-50	2	0.686	62	128	0.274	9	4.5	
G			0	1	1.150	79	208	0.460	17.5	10		
A			+75	2	1.995	102	356	0.798	34	19.5		
Z(ZT)		C	-100	2	0.507	56	104	0.203	7.5	3.5	-10	
		F	-79	1	0.533	57	108	0.213	8.5	4.5		
		H	-40	1	0.817	70	163	0.327	13	6.0		
		E	+20	1	1.466	92	282	0.486	25	12		
		B	+76	2	2.965	129	554	1.186	36.5	21		
A517H	AL(ZY)	D	-102	1	0.487	48	77	0.195	-	1.5	+60	
		F	-30	1	0.721	57	108	0.288	7	5		
		I	0	1	0.809	60	120	0.324	10.5	6.5		
		E	+40	1	1.293	75	187	0.517	15	8.5		
		B	+75	2	1.677	85	241	0.671	21.5	12		
		G	+120	1	2.071	93	288	0.828	28	19		
	CK-1(ZZ)	I	0	1	0.398	48	77	0.159	4	2.5	200	
		D	+40	1	0.520	52	90	0.208	5.5	4		
		CT2	+58	2	0.512(b)	55	101	0.205	6.5	4.5		
		H	+75	1	0.666	58	112	0.266	7.5	5.5		
A517F	73B320	CT9	75	2	0.630	56	104	0.252	7.5	5.5		
		CT7	+113	2	0.602(b)	59	116	0.241	10	6.5		
		F	+159	1	0.749	60	120	0.300	13	8.5		
		G	+200	1	0.859	64	137	0.344	15.5	10		
A517F	73B320		-148	(d)	0.648	56	104	0.259	17	6.0	-125	
			-112		1.012	70	163	0.405	23.5	9.5		
			-103		1.258	78	203	0.503	25.5	11.5		
			-93		1.528	86	246	0.611	28	13.8		
			-83		1.825	94	294	0.730	31	16.0		
			-72		2.190	102	347	0.876	34.5	18.3		
			-56		2.780	116	448	1.112	40	22.9		
			-39		3.492	130	563	1.397	48	27.5		

(a) On the upper shelf (with respect to transition temperature).
 (b) Average of three tests.
 (c) Estimated from PCI transition temperature.
 (d) See Ref. (2) Figures 3 & 9; bend tests 1/2, 1 and 2-in. thick, 4-in. deep.



TRANSITION-RANGE CVN-IMPACT CORRELATION
 WITH STATIC COMPACT TENSION K_{Ic} TEST RESULTS
 (VALID K_{Ic} DATA FROM TABLE 4.9)

FIGURE 4.49

transition-range CVN- K_{IC} correlation indicates that CVN-impact value of 25 ft-lb corresponds to a K_{IC}^2/E value of 250, whereas, in plate M, 25 ft-lb corresponded to a K_{IC}^2/E value of about 380; thus, the U.S. Steel CVN- K_{IC} correlation was conservative. The actual test results for plate M as seen in Table 4.9, were 24 ft-lb CVN-impact at -100°F and $108 \text{ ksi-in.}^{1/2} K_{IC}$. This was a valid compact-tension test in that the specimen size, 2 in., was greater than $2.5(KQ/FTY)^2$. Based on the U. S. Steel correlation the estimated K_{IC} value was $87 \text{ ksi-in.}^{1/2}$ ($K_{IC}^2/E = 250$).

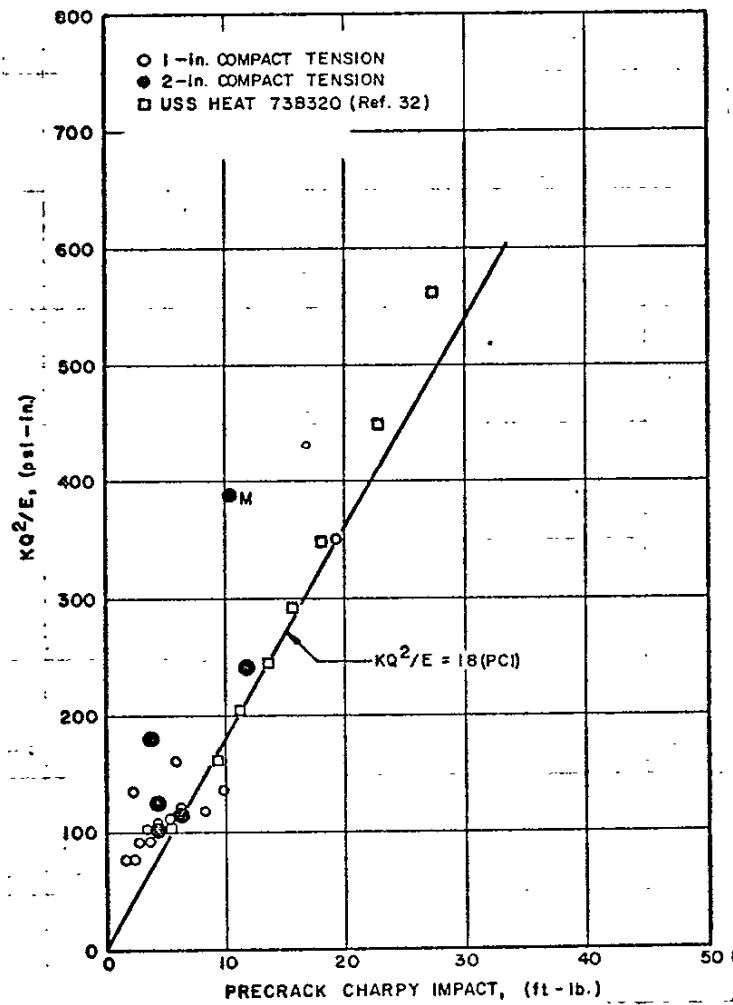
Figure 4.50 is a plot of precrack Charpy impact (PCI) data. Note that except for the plate-M test, the scatter was somewhat reduced as compared to Figure 4.49; again only valid K_{IC} data were plotted. From this plot it is concluded that the relationship

$$K_{IC}^2/E = 18 \text{ (PCI)} \quad (4.11)$$

gives a reasonably conservative estimate of the static K_{IC} value at any test temperature in or below the transition-temperature range.

4.2.5 Through-Thickness-Yielding Criteria

In practical applications of the through-thickness-yielding criterion, there is the tacit assumption that with the use of the Charpy V-notch (10-mil radius) upper-shelf-energy correlation, the start of the upper-shelf will be at or below the lowest anticipated service temperature (as in the case of plate M of Figure 4.48). In the U. S. Steel researches where through-thickness-yielding was proposed as a criterion of acceptable toughness for critical applications, the A517-F steel under consideration developed Charpy V-notch (10 mil radius) impact shelf-energy levels at room-temperature or lower. Four out of five of the U. S. Steel studies reviewed in connection with this



TRANSITION-RANGE PRECRACK CHARPY IMPACK CORRELATION WITH ASTM E399 VALID K_{IC} DATA (VALID K_{IC} DATA FROM TABLE 4.9)

FIGURE 4.50

study used a single heat of A517-F steel, viz., heat 73A377. Using the through-thickness-yielding criterion proposed by the U. S. Steel investigators, heat 73A377 with yield strength ranging from 110 to 121 ksi would have to develop 50 to 54 ft-lb of Charpy shelf energy at the lowest anticipated service temperature to meet the through-the-thickness yielding criterion for 2-in. thick plate. The reported CVN-impact shelf values for heat 73A377 at 80°F ranged from 47 to 62 ft-lb. From Figure 4.34 it will be seen that the CVN upper-shelf for this heat of A517-F steel extended below 0°F.

Of the seven A514/517 steels investigated using the ASTM E399 compact-tension K_{Ic} method, five of the seven had CVN upper-shelves starting at a temperature of 200°F or higher. From table 4.10 it will be seen that at the temperature corresponding to the CVN-impact-energy upper-shelf, only three of the seven A514/517 steels investigated in the correlation phase of this study (plates L, M, and R) developed the required energy levels to give through-thickness yielding in 2-1/4-in. plate based on the standard Charpy V-notch (10-mil radius) test. However, only in A514 grade-F plate M was the upper-shelf at or below 0°F. Plate L was borderline with the shelf starting at about 40°F; however, based on a shelf energy of 77 ft-lb, plate L more than met the through-thickness-yielding criterion at +40°F.

TABLE 4.10

CHARPY ENERGY REQUIREMENTS FOR THROUGH-THICKNESS YIELDING

<u>Steel Type</u>	<u>Plate No.</u>	<u>Yield Strength (ksi)</u>	<u>CVN Upper-Shelf Temp. (°F)</u>	<u>Energy (ft-lb)</u>	<u>CVN Energy(a) Required (ft-lb)</u>
A514F	M(ZU)	119	0	65	59
	L(ZV)	109	40	77	54
A517F	A(ZW)	100	200	40	50
A514H	R(ZX)	109	200	56	54
	Z(ZT)	115	200	55	58
A517H	AL(ZY)	100	200	42	50
	CK(ZZ)	109	200	16	54

(a) $CVN \geq FTY (B + 0.25)/5$ at the lowest anticipated service temperature.

A through-thickness-yielding criterion based on transition-temperature-range correlations was obtained by combining the Hahn and Rosenfield expression:

$$(K/FTY)^2/B = 1$$

and the CVN- K_{IC} correlation

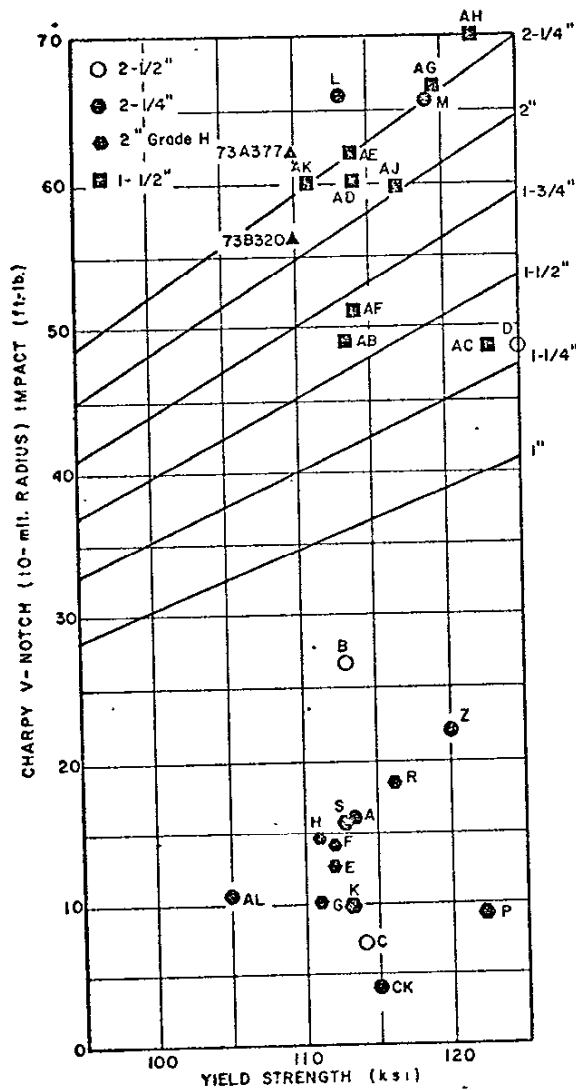
$$K_{IC}^2/E = 2 (CVN)^{3/2}$$

This provided the following relationship:

$$FTY^2 = 2(CVN)^{1.5} E/B \quad (4.12)$$

Of the seven Bryte Bend and Tuolumne bridge steels tested in compact tension (K_{IC}), only plates L and M met this criterion at 0°F. The two heats of A517-F used in the U. S. Steel researches also met this criterion at 0°F. A517 grade-F plate A, and A517 grade-H plates AL, CK, R, and Z all failed to meet the criterion even for 1-in. thickness.

Charpy data from the Tuolumne bridge and Tuolumne-bridge reinforcement steels were examined for compliance with the proposed criterion, including the seven heats tested using the compact-tension specimen. The plates were 1-1/2, 2, 2-1/4 and 2-1/2-in.-thick. The 1-1/2-in.-thick plates (AB thru AK) came from four heats of A517-F; data were available from nine slabs. The 2-in.-thick plates came from five heats of A514/517 grade-H steel; data for this thickness were available from eight slabs (plates E, F, G, H, K, P, R and S). The 2-1/2-in.-thick material was A514/517 grade-F plates A and L. The 2-1/2-in.-thick material was A514/517 grade-F plates D and M and grade-H plate C. Figure 4.51 is a plot of these data superimposed on the curves relating yield-strength, CVN-impact and plate thickness for through-thickness-yielding. From Figure 4.51, it will be seen that fourteen of the A514/517 plates tested would not meet the



CVN-IMPACT REQUIREMENT AT 0°F FOR THROUGH-THICKNESS
 YIELDING BASED ON THE U.S. STEEL TRANSITION TEMPERATURE
 CVN-K_{IC} CORRELATION (EQUATION 4.12)

FIGURE 4.51

through-thickness-yielding criterion for even 1-in. thickness. Eight of the nine 1-1/2-in.-thick A517 grade-F plates met the through-thickness-yielding criterion for 1-1/2-in.-thick plate; six of the 1-1/2-in. plates met the toughness requirement for 2-in. plate.

A comparison of criteria based on the upper-shelf and transition-temperature-range correlations is shown in Figure 4.52. Only the data for steels which developed upper-shelf energy at or below 0°F are plotted. Note that all the plates which developed upper-shelf at or below 0°F met the through-thickness-yielding criterion based on the upper-shelf correlation. The dash curves in Figure 4.52 are from Figure 4.51; thus, the dash curves represent the through-thickness-yielding criterion based on the U. S. Steel K_{IC} -CVN transition-temperature-range correlation. The super-position shows that the criterion based on the K_{IC} -CVN upper-shelf correlation is less stringent and, therefore, perhaps more practical, providing the steel industry can produce plate with the CVN-impact upper-shelf at or below the lowest anticipated service temperature for the particular bridge to be built.

Combining the Hahn and Resenfield expression

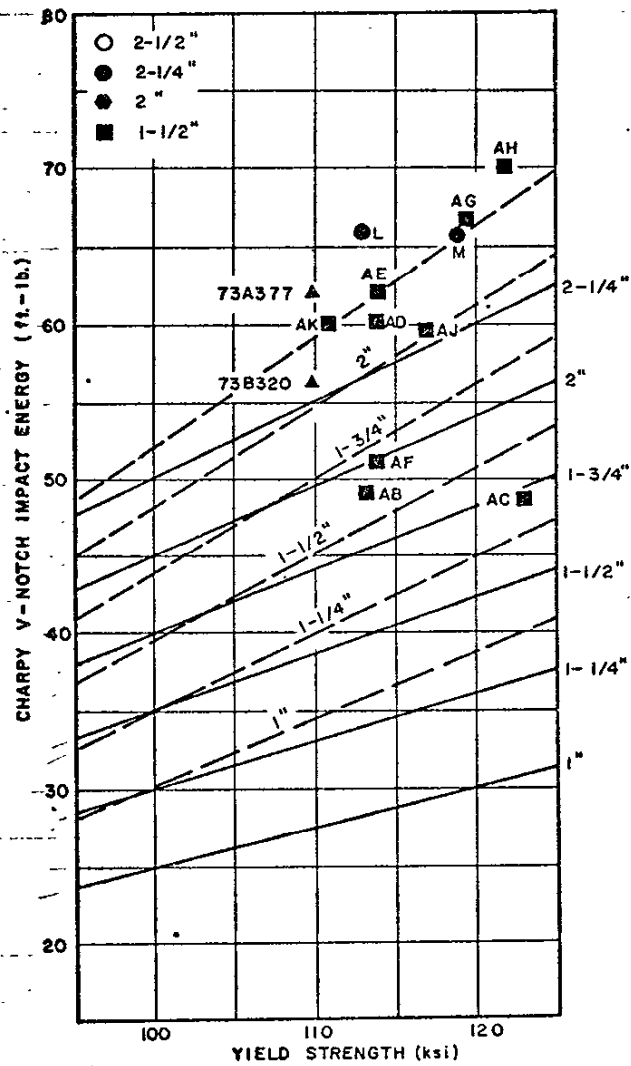
$$(K/FTY)^2/B = 1$$

and the PCI- K_{IC} correlation

$$K_{IC}^2/E = 18 \text{ (PCI)}$$

provides the following relationship for a through-thickness-yielding criterion based on the precrack Charpy impact transition-temperature-region test results:

$$PCI = FTY^2 \cdot B/18E \quad (4.13)$$



CVN-IMPACT REQUIREMENT AT 0°F FOR THROUGH-THICKNESS YIELDING BASED ON THE UPPER-SHELF CORRELATION (EQUATION 4.3) AND THE TRANSITION-RANGE CORRELATION (EQUATION 4.12 - DASHED LINES)

FIGURE 4.52

Of the seven Bryte Bend and Tuolumne bridge steels tested in compact tension (K_{IC}) only plate M came close to meeting this criterion at 0°F. U. S. Steel research heat 73B320 and plate L both failed to meet the criterion in their respective thicknesses. Figure 4.53 is a plot of these data superimposed on curves relating yield strength and PCI (ft-lb) for through-thickness-yielding; the data are from the same steels as in Figure 4.51. Note that all of the 1-1/2-in.-thick reinforcement-steel plates met the criterion except one. None of the A514/517 grade-H plates met the through-thickness-yielding criterion for even 1-in.-thickness. A517 grade-F plate L also failed to meet even the 1-in.-thickness criterion; the problem in this heat of steel was a considerable sensitivity to notch acuity. Note the excellent performance of 2-1/4-in.-thick plate L in Figure 4.51 where the standard (10-mil radius) CVN-impact test is involved.

Another approach providing a criterion for through-thickness-yielding is based on the plane-stress plastic-zone expression (equation 4.4).

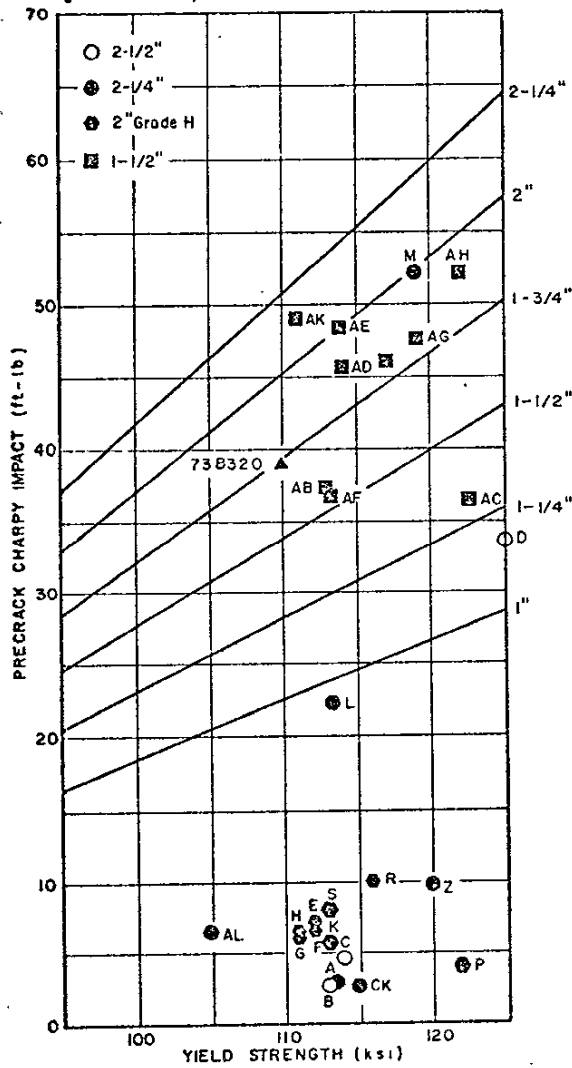
When this expression is equated to the plate thickness (i.e., a plastic zone equal to the plate thickness), and when $E(W/A)$ as determined from the precrack Charpy impact test is substituted for K^2 ,

$$W/A = 2 \pi FTY^2 B/E$$

with a nominal fatigue-precrack depth of 0.035 inch and \underline{W} is in ft-lb

$$W = 1.925 \times 10^{-9} B \cdot FTY^2 \quad (4.14)$$

where \underline{W} is precrack Charpy energy value and \underline{A} is the net-section area under the fatigue precrack. When this criterion was used as a basis for determining the precrack Charpy energy for through-thickness-yielding, the values were for all practical purposes the same as those calculated based on equation (4.13).



PCI REQUIREMENT AT 0°F FOR THROUGH-THICKNESS
 YIELDING BASED ON THE PRECRACK CHARPY IMPACT
 PCI-K_{IC} CORRELATION (EQUATION 4.13)

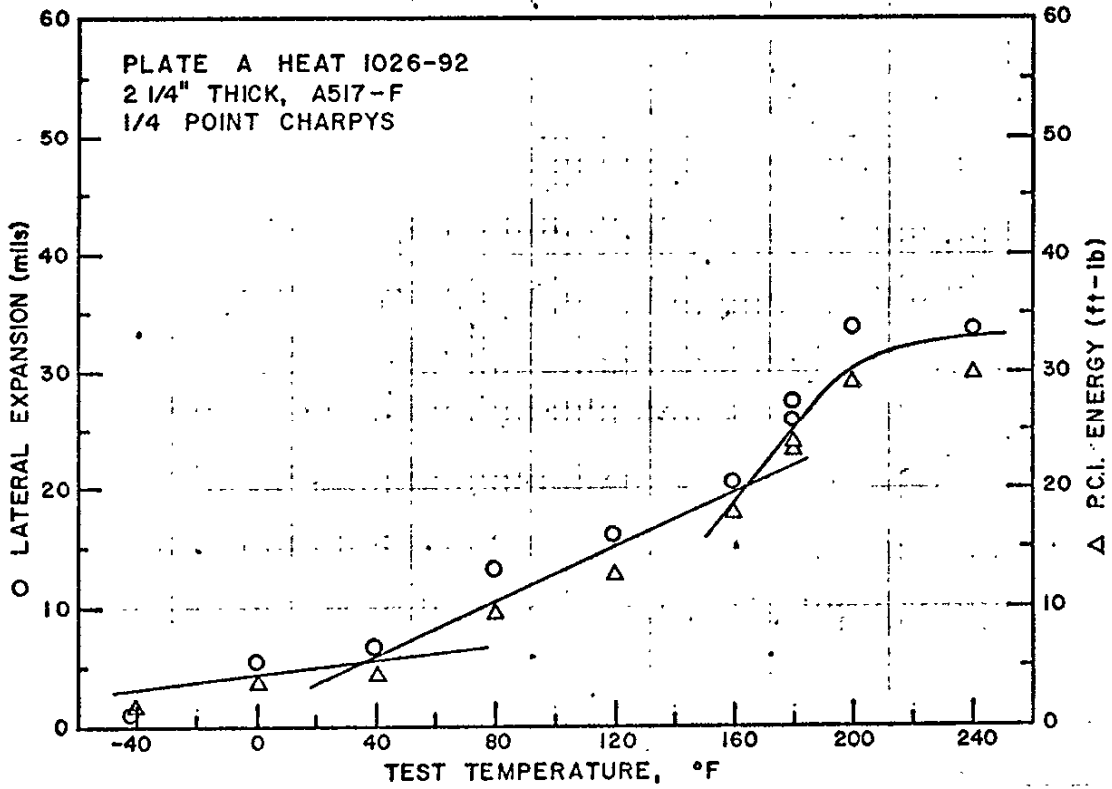
FIGURE 4.53

4.2.6 Inhomogeneity of Plate in the Thickness Direction

Microstructural gradients through the plate thickness can be a serious complication when correlations are sought between specimens of different size and/or location in the thickness. When A514/517 "T-1" type steels utilize boron as a hardening agent, surface-to-midthickness gradients of microstructure occur when the boron is not adequately protected by prior aluminum and titanium additions to the melt. This was the case in the Bryte Bend and Tuolumne River bridges.

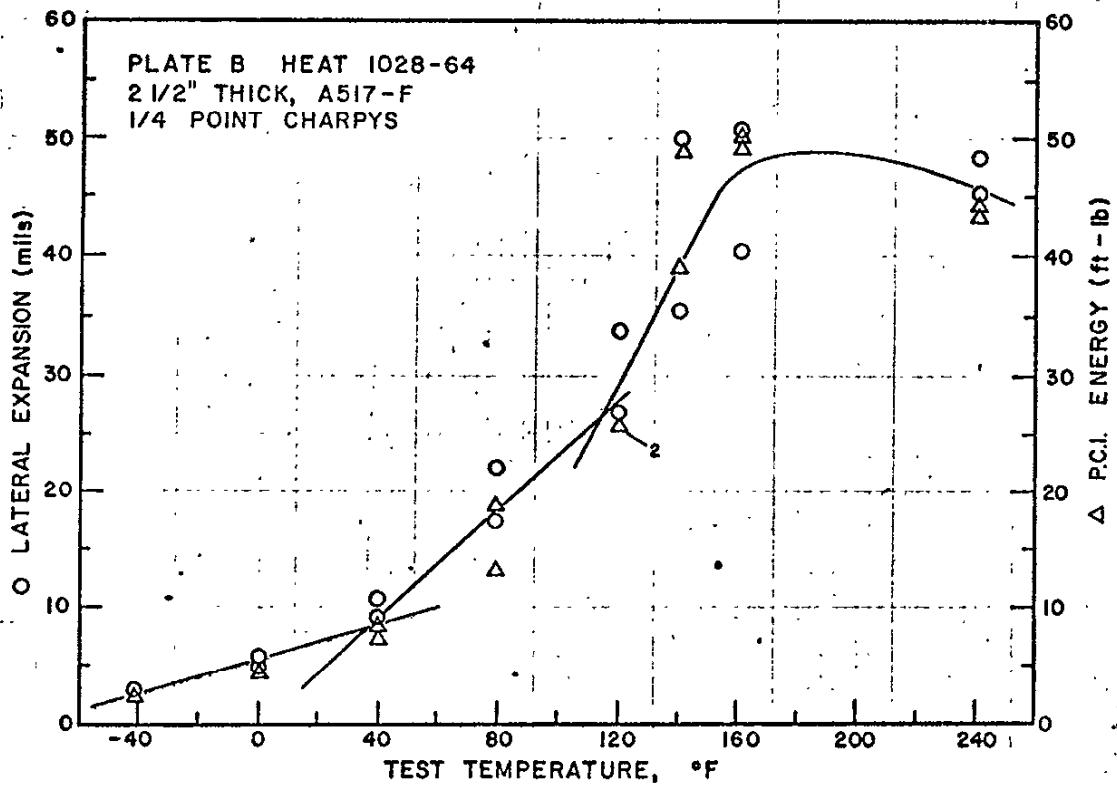
Both hardness surveys across the thickness and microstructure revealed the inhomogeneity. At midthickness and extending outward toward the surface, the microstructure was upper bainite rather than the desired tempered martensite. The upper bainite generally had lower hardness and was suspected to have lower toughness. A plot of hardness as a function of thickness position for plate A and is presented in connection with the dynamic-tear and NDT testing where the gradient proved to be a complication to correlation between specimen types (see Figure 4.90). Microstructure as a function of position in the thickness direction will be presented in a second report, METALLURGY OF A514/517 STEELS, showing the martensite at the surface and upper bainite at midthickness and mixed microstructure at intermediate positions.

To determine the effect of mixed microstructure at the intermediate positions, Charpys were machined from the quarter-point position (half way between midthickness and the as-rolled plate surface) in A517 grade-F plates A and B, and in A517 grade-H plates AL, Y and Z. The test results are plotted in Figures 4.54 thru 4.58. Note that the quarter-point was little different from the midthickness, in some cases even somewhat lower in toughness. The following tabulation compares the precrack Charpy impact transition behavior

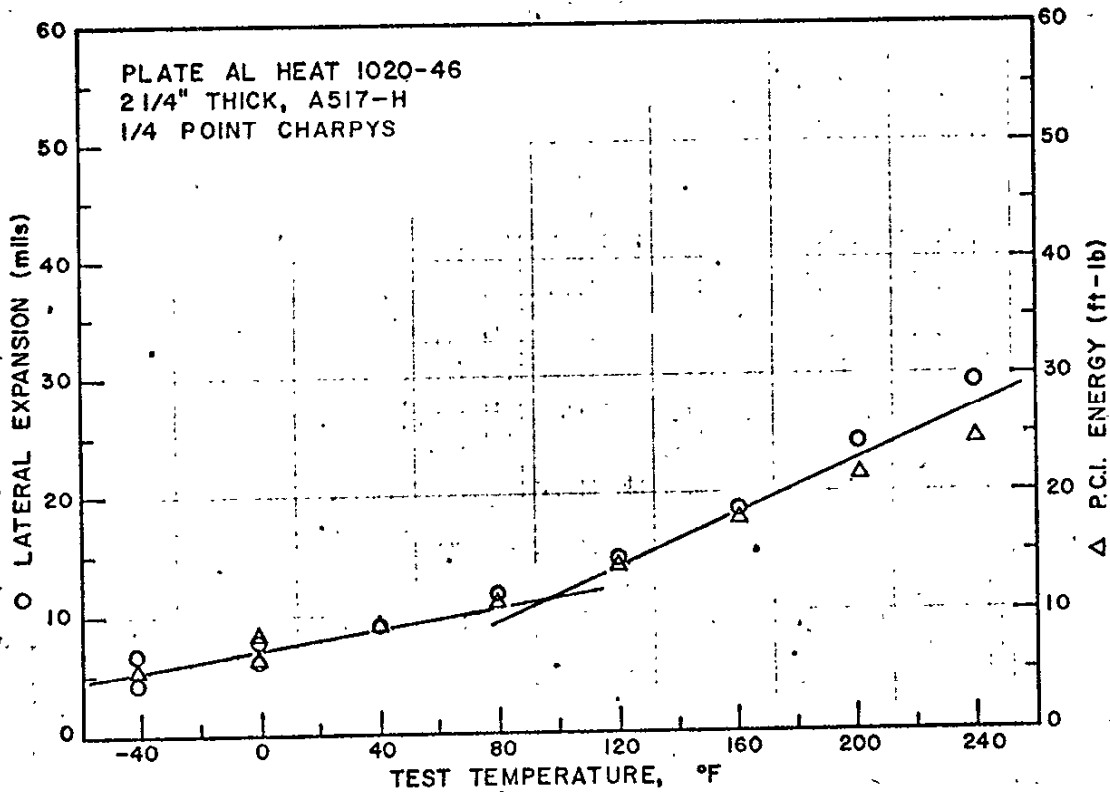


PCI TRANSITION CURVE FOR THE QUARTER-POINT
 POSITION IN A517-F PLATE A

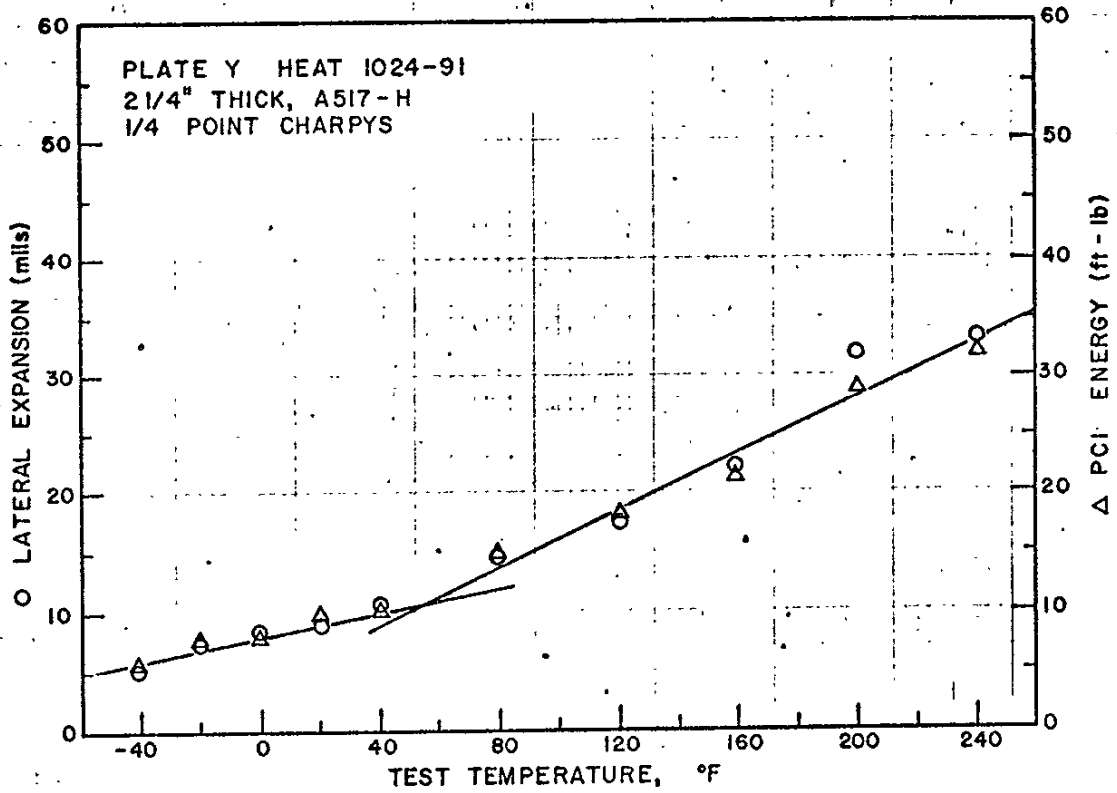
FIGURE 4.54



PCI TRANSITION CURVE FOR THE QUARTER-POINT
 POSITION IN A517-F PLATE B
 FIGURE 4.55

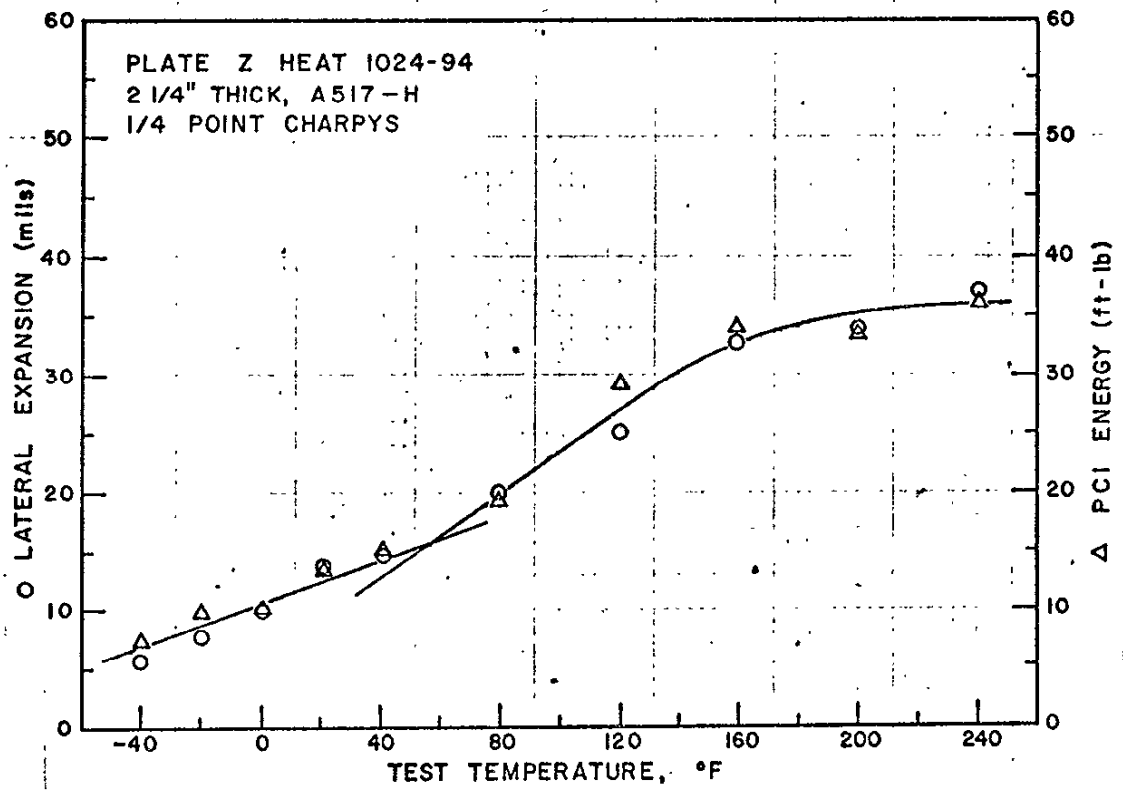


PCI TRANSITION CURVE FOR THE QUARTER-POINT
 POSITION IN A517-H PLATE AL
 FIGURE 4.56



PCI TRANSITION CURVE FOR THE QUARTER-POINT POSITION IN A517-H PLATE Y

FIGURE 4.57



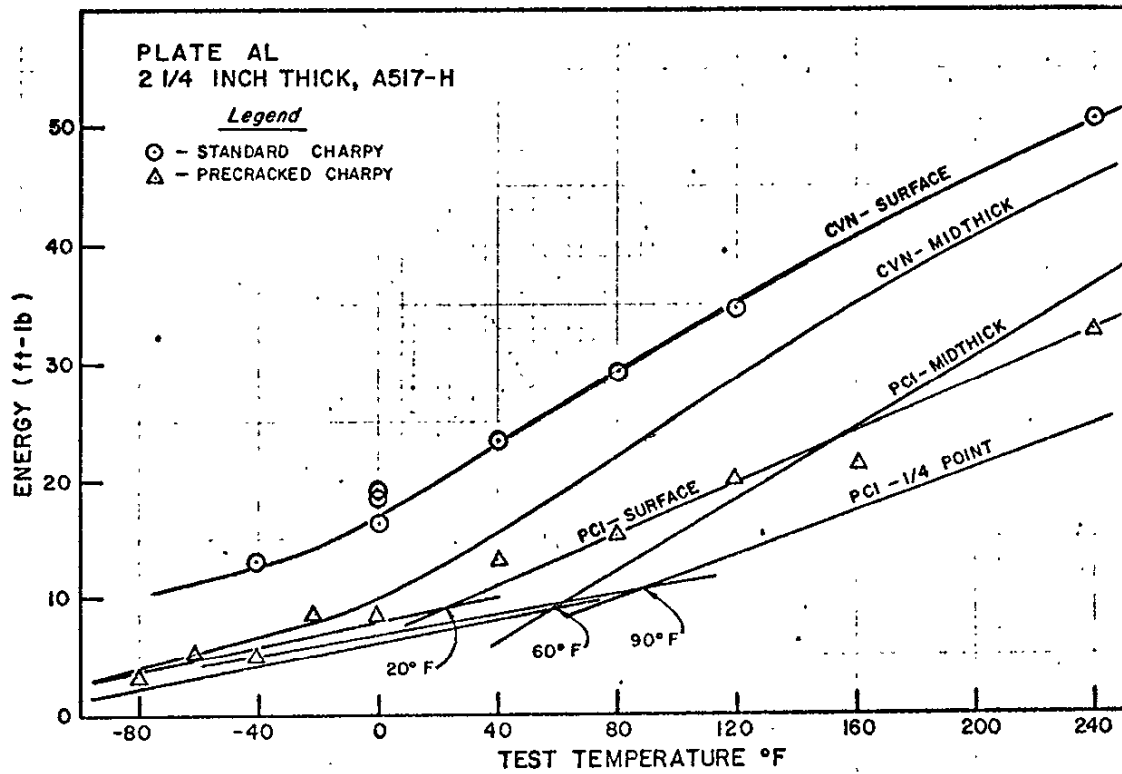
PCI TRANSITION CURVE FOR THE QUARTER-POINT
 POSITION IN A517-H PLATE Z
 FIGURE 4.58

(approximate NDT temperatures) at the two plate positions.

<u>Plate</u>	<u>Thickness position</u>	
	<u>mid</u>	<u>1/4 pt</u>
A	40/180 (a)	40/160 (a)
B	20/100 (a)	40/110 (a)
AL	60	100
Y	-20/100 (a)	60
Z	-5	50

(a) double inflection point in the transition curve.

As a further evaluation of the effect of microstructural gradients in the thickness direction, Charpy specimens were machined from the surface of plate AL; only enough steel was removed from the as-rolled surface to provide an acceptable finish on the Charpy specimen. Figure 4.59 shows somewhat of an improvement in the standard CVN-impact test result in the surface of the plate as compared with the midthickness position; however, the steel would still fail to meet the AASHTO-74 CVN-impact requirement of 25 ft-lb for either group-1 or group-2 service. At minus 30°F (test temperature for group-3 service), the steel gave less than 15 ft-lb at the surface. The precrack Charpy impact transition curve for the surface position was displaced from that of the quarter-point position, with an inflection point, although poorly defined, close to the lowest anticipated service temperature for the Bryte Bend bridge.



CVN-IMPACT AND PCI TRANSITION CURVES FOR THE SURFACE, MIDTHICKNESS AND 1/4 POINT POSITION IN A517-H PLATE AL

FIGURE 4.59

4.3 SUMMARY OF CVN-IMPACT TEST RESULTS

4.3.1 Procedure for Data Presentation

Two methods were utilized for purposes of summarizing the Charpy V-notch (CVN) impact test results:

(1) The data are presented in frequency tables which show the number of times (frequency) a specified energy or lateral expansion value appears in the data, and (2) the data are presented in the form of histograms, a form of bar graph, where the highest bar(s) shows the "most common" energy or lateral-expansion values found in each of the two grades of A514/517 steel tested. The frequency distributions are then compared with (1) the AASHTO-1974 CVN-impact energy requirements and (3) the ASTM A517-70a CVN-impact lateral expansion requirement.

The data used in determining the frequency distributions are listed in Tables 4.11 - 4.13 (p. 185). Table 4.11 presents the data from twenty-nine slabs of a single heat of A517 grade-F steel 1-3/8-in.-thick. Table 4.12 presents the data from sixteen heats of A514/517 grade-F steel in thicknesses ranging from 1-3/8 to 2-1/2 in. Table 4.13 presents the data from twelve heats of A514/517 grade-H steel in thicknesses ranging from 1-3/8 to 2-1/2 in.

Most slabs were tested at each of several temperatures, with triplicate tests at the lowest anticipated service temperature. A total of 74 slabs was tested.

4.3.2 Frequency Tables

In the frequency distribution table (Table 4.14), the energy and lateral-expansion values are grouped in intervals of ten:

0 to 9
10 to 19
20 to 29
30 to 39, etc.

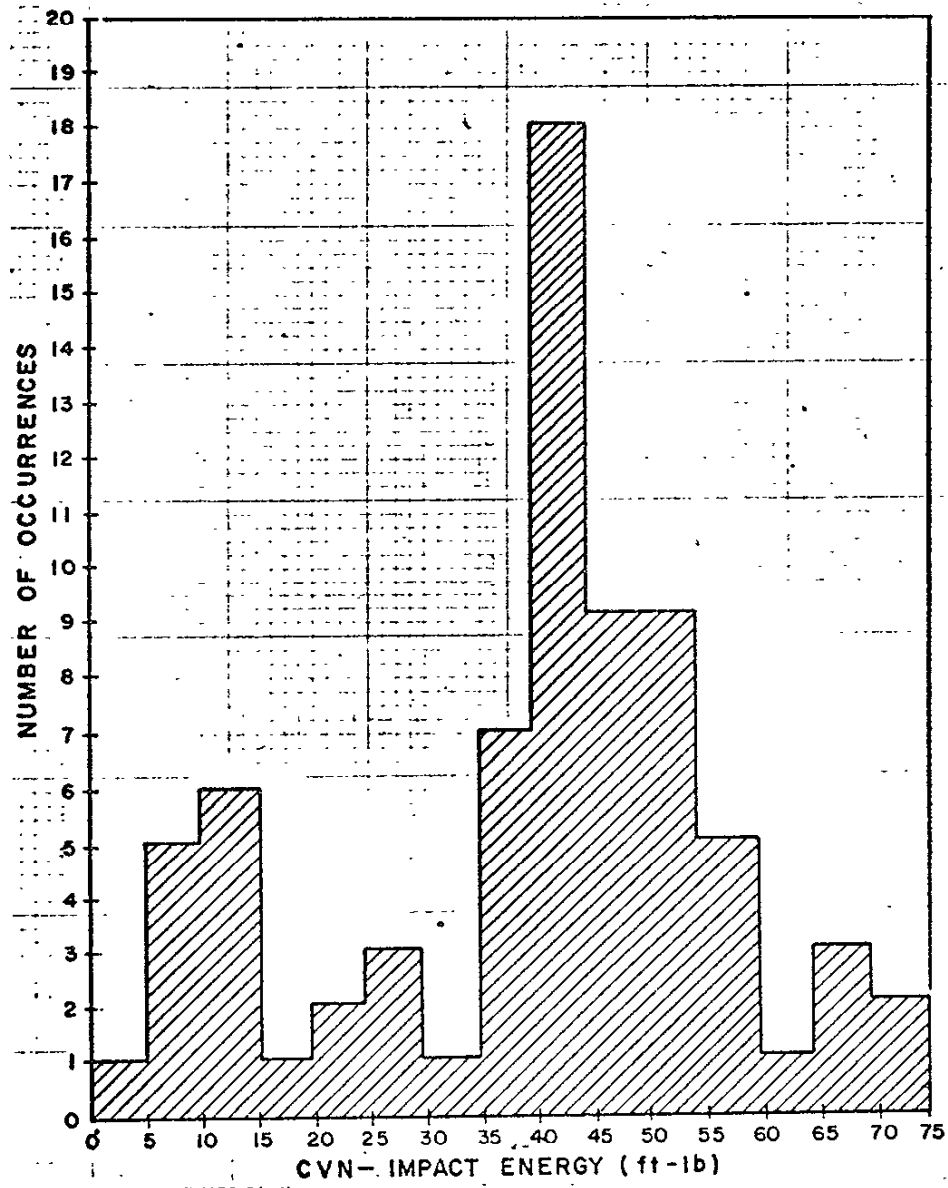
The table shows the number of times (the frequency) energy and lateral-expansion values occur in each interval. Note that for the grade-H slabs tested the mode of the distribution (the greatest frequency) occurred at 5 ft-lb and 5 mils for tests at both 0°F and -40°F. At +20°F the mode was again at 5-mils lateral expansion; the mode for CVN-impact energy in the grade-H slabs was 15 ft-lb at +20°F.

In the grade-F slabs tested, the mode of the distribution occurred at 45 ft-lb at +20°F, 0°F and -40°F; based on lateral expansion the mode was 35 mils, again irrespective of temperature (down to -40°F).

In addition to the mode, the arithmetic mean (average) values of energy and lateral expansion were determined for both grades at each of the three test temperatures. Table 4.15 presents the averages. Note that the average values for the grade-H slabs consistently fell below the current specification requirements (25 ft-lb AASHTO-74 and 15 mils ASTM A517-70a). The grade-F averages, without exception, exceeded the current specification requirements.

4.3.3 Frequency Distribution Histograms

Figure 4.60 is a histogram showing the distribution of CVN-impact energy values in +20°F tests without regard for steel grade. The vertical axis of the bar graph shows the number of tests producing energy values in each interval, and the horizontal axis is the interval used in counting. For purposes of counting, the CVN-impact energy was divided into the following intervals:



HISTOGRAM OF CVN-IMPACT ENERGY VALUES FROM 74 SLAB TESTED AT +20°F

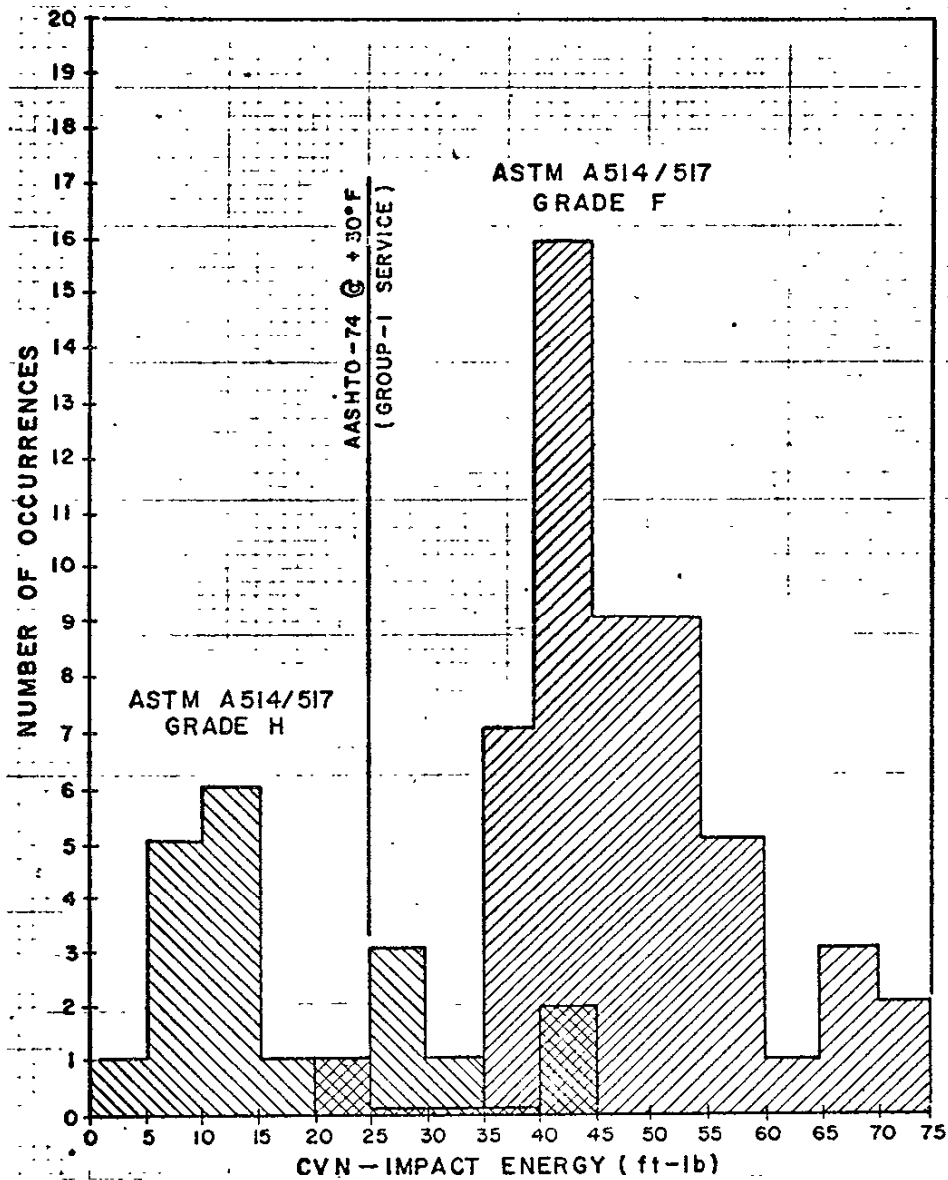
FIGURE 4.60

Ft-Lb

0 to 4
5 to 9
10 to 14
15 to 19
20 to 24
25 to 29, etc.

Thus, in Figure 4.60, only one of the 74 slabs tested at +20°F gave a CVN-impact energy value in the interval of 0-4 ft-lb; whereas, there were five slabs which gave energy values in the 5-9 ft-lb interval, etc. The two obvious peaks in the histogram at 10-14 ft-lb and at 40-44 ft-lb indicate a bimodal frequency distribution, as one might expect using data from two grades of steel. The significance of the two peaks will be examined by separating grades H and F.

Figure 4.61 is the same as Figure 4.60 except that the grade-H slabs are separated from the grade-F slabs. Note that fourteen of the twenty A514/517 grade H slabs tested did not meet the 1974 AASHTO CVN-impact energy requirement (25 ft-lb) at +20°F; whereas, only one of the grade F slabs did not meet the 25 ft-lb requirement. The temperature for these tests was +20°F, the lowest anticipated service temperature for the Bryte Bend bridge. For service down to 0°F, the AASHTO test temperature is +30°F (group 1); therefore, if the testing had been done at +30°F, the one grade-F slab that failed at +20°F might have passed (the interpolated value from the transition-curve plot was 27 ft-lb for A514-F heat 1013/32J). Likewise, A514 grade H heat 1019/31R might have met the 25 ft-lb requirement if tested at +30°F (the interpolated value from the transition-curve for this slab was 24 ft-lb at +30°F). Thus, at most, one grade F slab out of 53 would have been rejected by the current AASHTO specification, and 14 out of 20 grade H slabs would have been rejected. Note that for the grade-F steels tested at +20°F the mode of the distribution was at 40-44 ft-lb, AASHTO-74 requires 25 ft-lb.

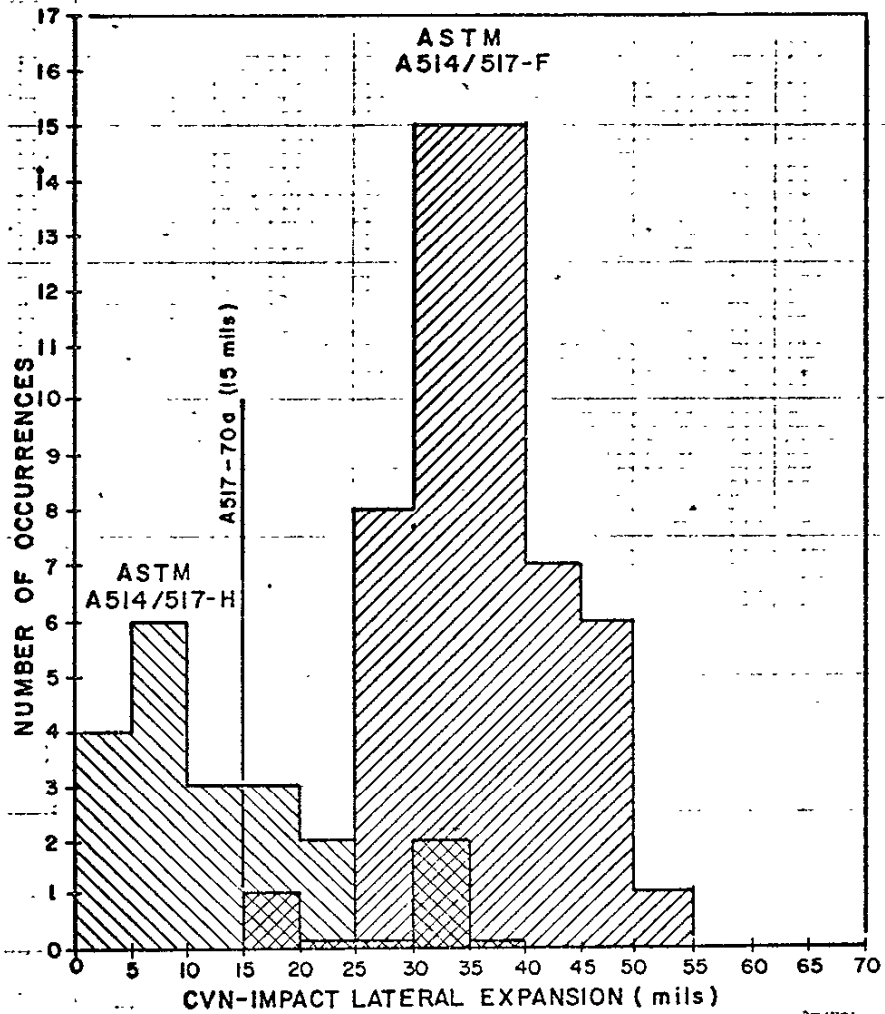


HISTOGRAM OF CVN-IMPACT ENERGY VALUES FROM 20 A514/517
 GRADE-H SLABS AND 53 A514/517 GRADE-F SLABS TESTED AT
 +20°F
 FIGURE 4.61

Lateral expansion in the CVN impact test piece is an independent measure of toughness which is directly proportional to the energy absorbed in fracturing the specimen. Figure 4.62 is a histogram showing the same trend as the energy histogram. ASTM A517-70a requires 15 mils of lateral expansion "...at the temperature specified on the order but no higher than 32°F (0°C)." Note that all 53 slabs of grade-F met the specification requirement; 13 of the 20 grade-H slabs tested failed. Note that for the grade-F steel tested at +20°F, the mode of the frequency distribution (the number that occurs most frequently in a set) was at 30-39 mils; ASTM A517-70 requires 15 mils.

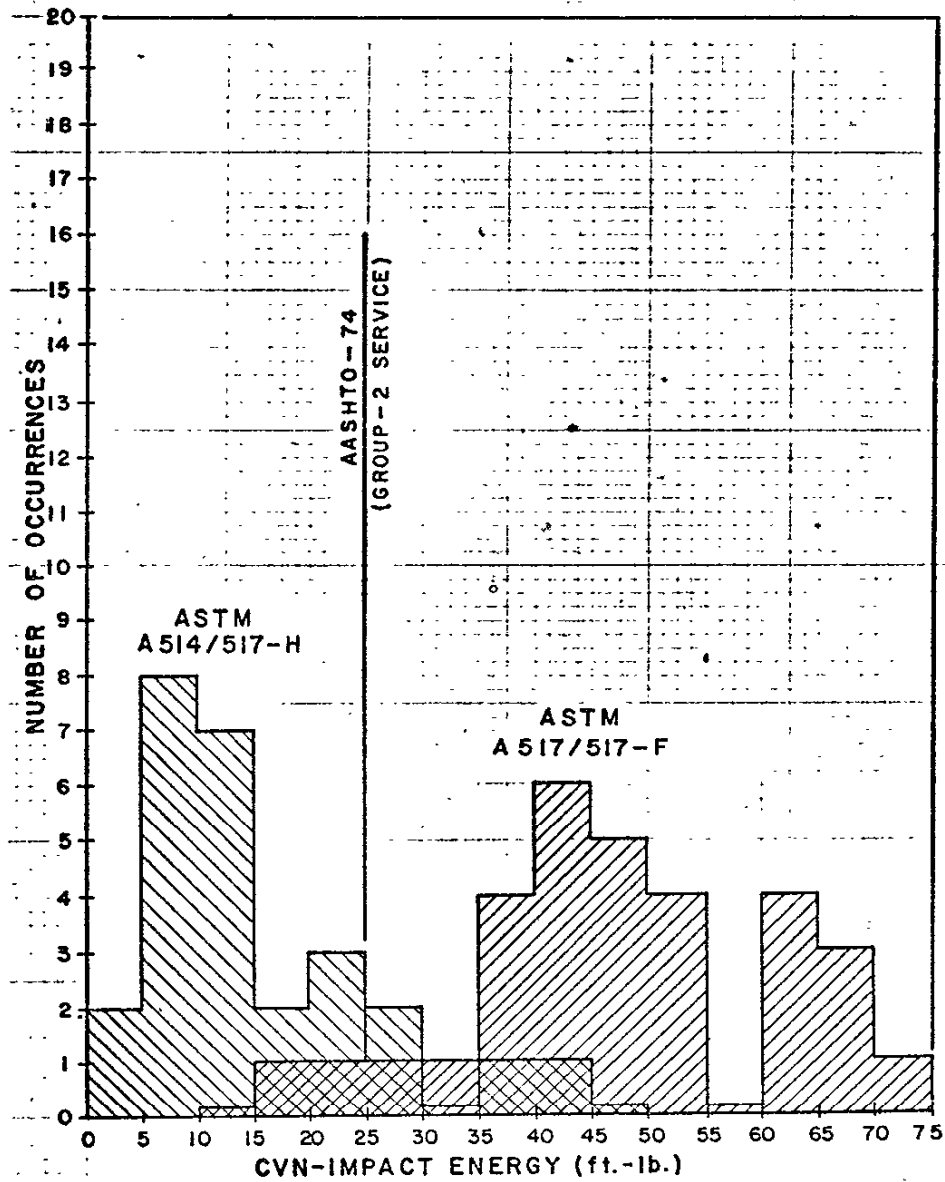
Figures 4.63 and 4.64 are the histograms for slabs tested at 0°F. From Figure 4.63 note that at this temperature (the AASHTO Group 2 test temperature) 22 of the 25 grade-H slabs failed; of the 32 grade-F slabs tested at 0°F, all but 2 passed the AASHTO 25 ft-lb requirement. This finding was largely confirmed by the ASTM A517-70a lateral expansion criterion (Figure 4.64), again with two slabs of grade-F steel failing, and 20 of the 31 grade-H slabs failing. Note that for the grade-F steel tested at 0°F, the mode of the distribution was at 40-44 ft-lb and at 30-44 mils.

Figures 4.65 and 4.66 are the histograms for slabs tested at -40°F. Note that at this temperature which is 10°F below the AASHTO group-3 test temperature, 24 of the 25 grade-H slabs failed, and of the 34 grade-F slabs tested at -40°F, all but 4 passed the AASHTO 25 ft-lb requirement. Again, this finding was largely confirmed by the ASTM A517-70a lateral expansion criterion. Note that the frequency-distribution mode shifted from the 5-9 interval to the 0-4 interval, indicating 17 of the grade-H slabs to be virtually devoid of toughness at -40°F. Also note that for the grade-F steel tested at -40°F, the mode of the distribution was at 40-44 ft-lb and 30-34 mils which are well above the AASHTO-74 and ASTM A517-70 CVN-impact requirements.



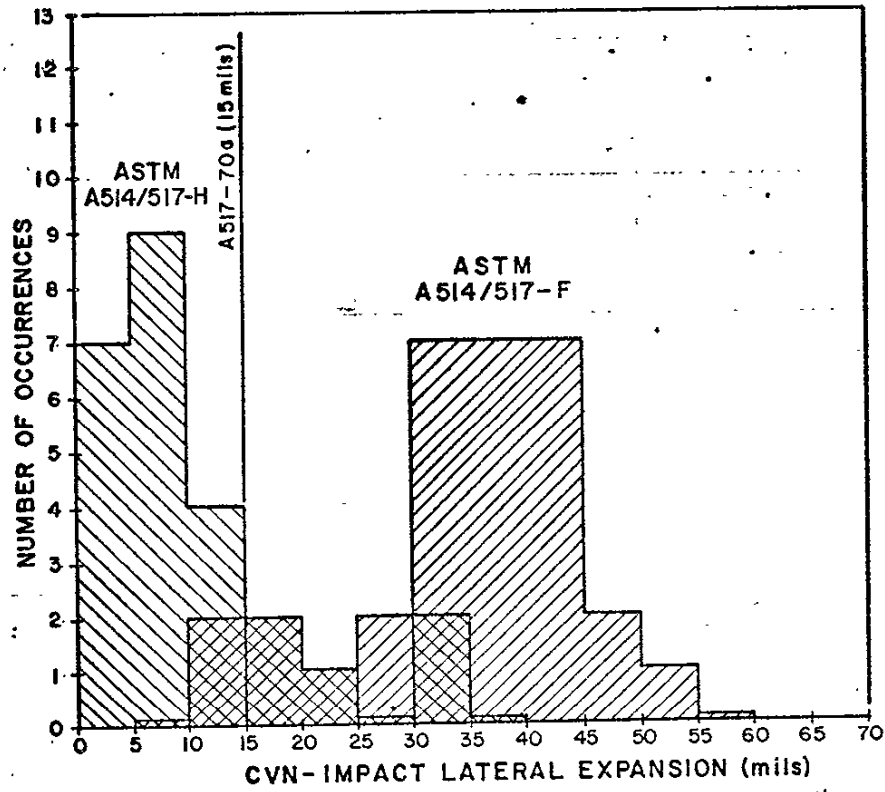
HISTOGRAM OF CVN-IMPACT LATERAL EXPANSION VALUES FROM 20 A514/517 GRADE-H SLABS AND 53 A514/517 GRADE-F SLABS TESTED AT +20°F

FIGURE 4.62



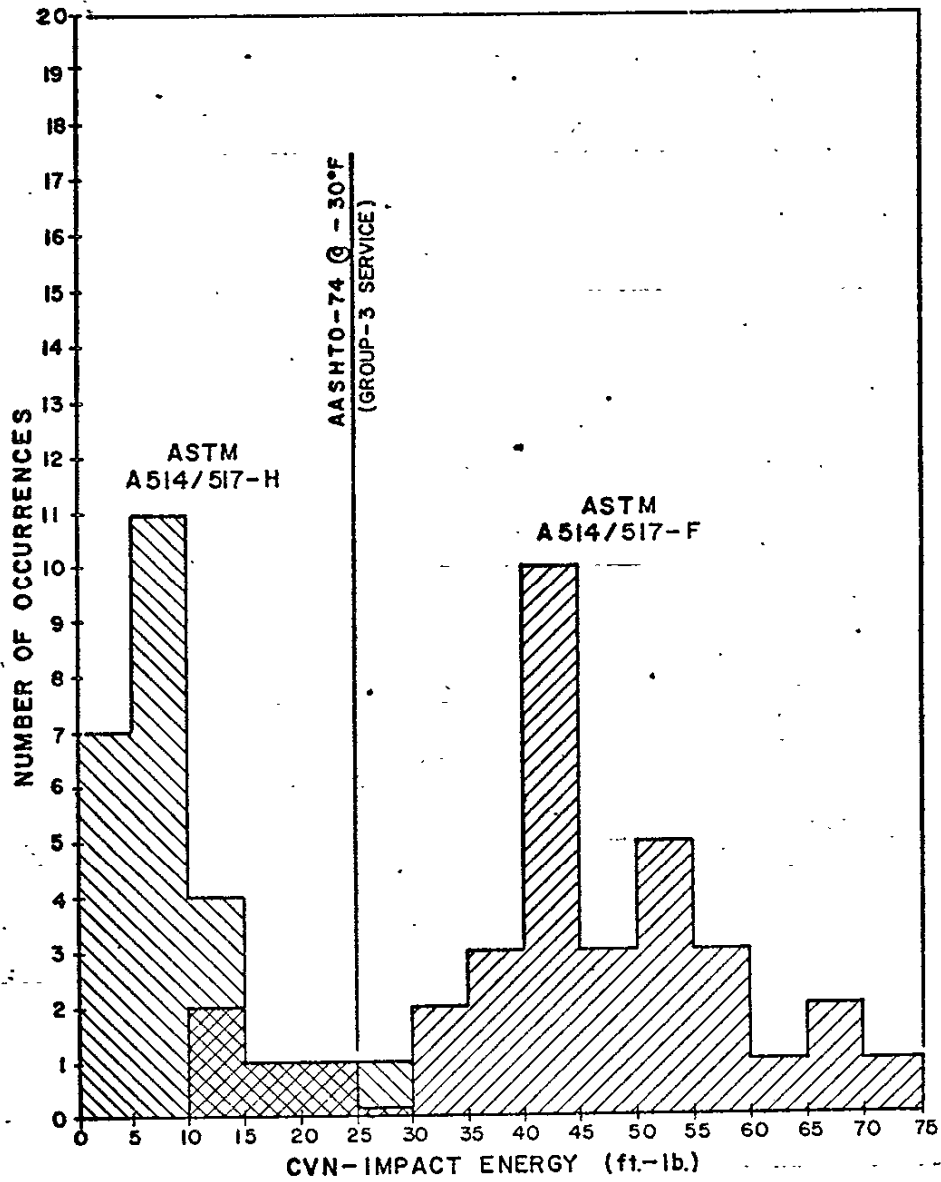
HISTOGRAM FOR CVN-IMPACT ENERGY VALUES FROM 25 A514/517 GRADE-H SLABS AND 32 A514/517 GRADE-F SLABS TESTED AT 0° F

FIGURE 4.63



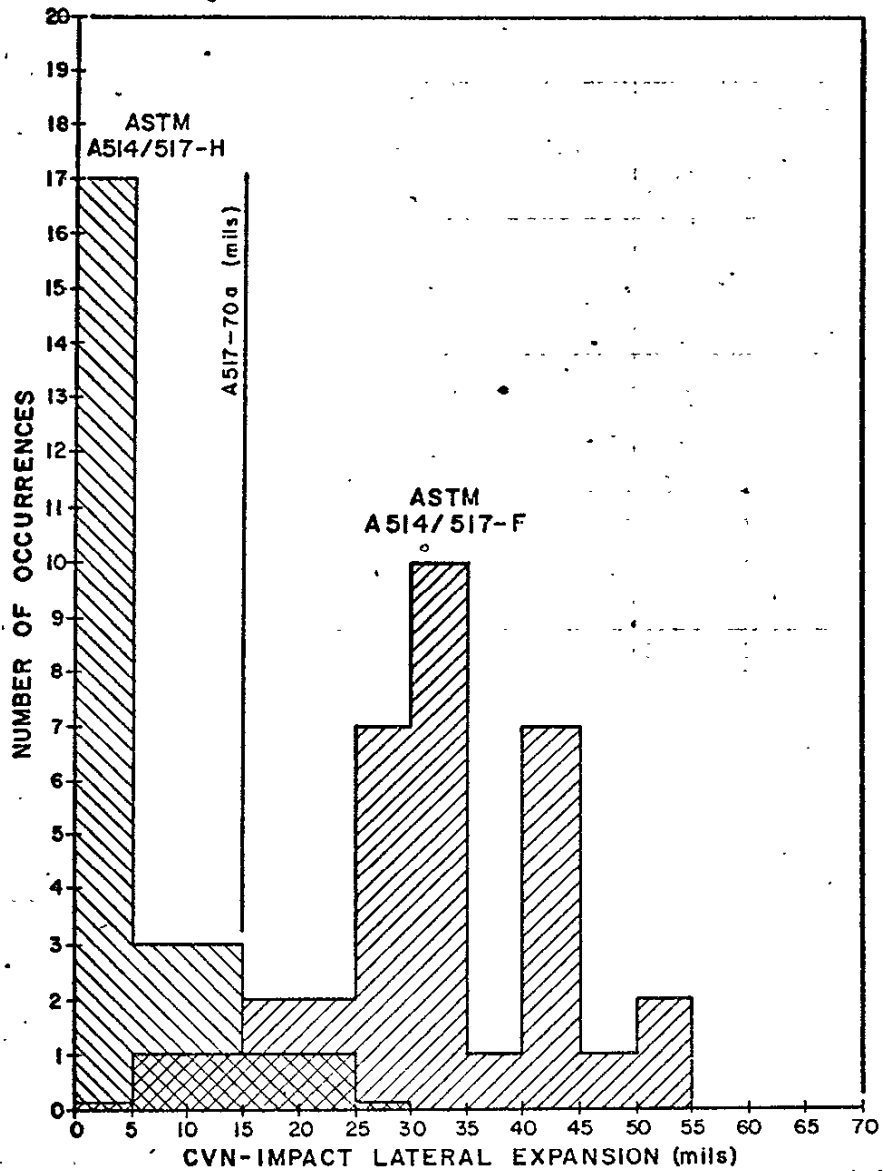
HISTOGRAM FOR CVN-IMPACT LATERAL EXPANSION VALUES FROM 25 A514/517 GRADE-H SLABS AND 32 A514/517 GRADE-F SLABS TESTED AT 0°F

FIGURE 4.64



HISTOGRAM FOR CVN-IMPACT ENERGY VALUES FROM 25 A514/517 GRADE-H SLABS AND 34 A514/517 GRADE-F SLABS TESTED AT -40°F

FIGURE 4.65



HISTOGRAM FOR CVN-IMPACT LATERAL EXPANSION VALUES FROM 25 A514/517 GRADE-H SLABS AND 34 A514/517 GRADE-F SLABS TESTED AT -40°F

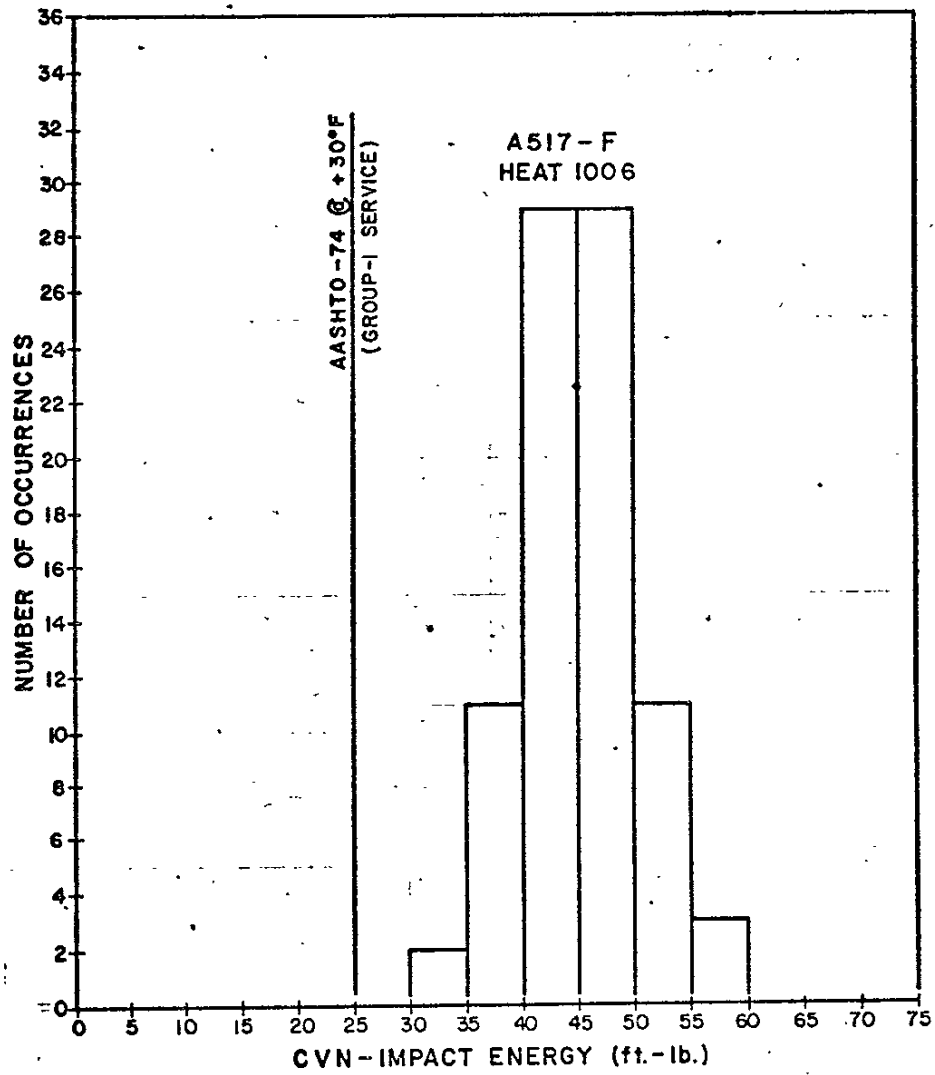
FIGURE 4.66

4.3.4 Frequency Distribution in 29 Slabs from a Single Heat

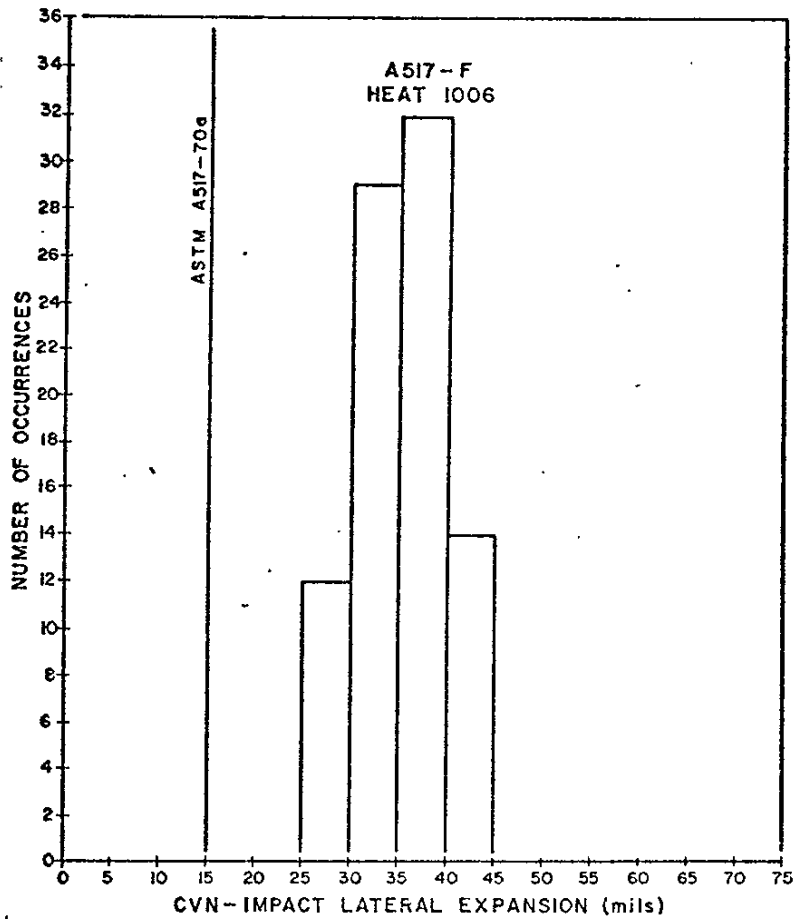
Figures 4.67 and 4.68 are histograms for the twenty-nine slabs of A517 grade-F heat 1006 tested in triplicate at +20°F. Note that the mode of distribution occurred at 45 ft-lb (58 out of 87 tests gave energy values in the 40-49 ft-lb interval. Only two tests gave values in the 30-34 ft-lb interval, and there were no values below 30 ft-lb at +20°F. Thus, the AASHTO-74 CVN-impact specification was easily met by this heat in all slabs. Likewise the ASTM A517-70a CVN-impact specification was met by all 29 slabs (87 tests) with comfortable margin to spare; there were no tests with lateral-expansion values below 25 mils at +20°F.

Figure 4.69 is a histogram based on mill-test-report data supplied by the steel producer. Twenty-seven of the 29 slabs were tested in triplicate at minus 50°F by the steel producer. The mode of the frequency distribution occurred in the 40-44 ft-lb interval, with no data below 30 ft-lb at -50°F. Thus, the AASHTO-74 group-3 requirement of 25 ft-lb CVN-impact energy at -30°F for service at temperatures between -31 and -60°F was easily met in this heat of A517-F steel. Lateral expansion values were not given in the mill test report.

Tables 4.16 and 4.17 summarize the CVN-impact findings from the point of view of (1) lowest anticipated service temperature (20°F at Bryte Bend and 0°F at Tuolumne River), (2) the AASHTO-74 group-3 service requirement and (3) the ASTM A517-70 lateral-expansion requirement. With a few exceptions, the ASTM A514/517 grade-F slabs more than met all existing toughness requirements; many of the A514/517 grade-H slabs, on the other hand, failed to meet either specification. Note that of the eight slabs of 2-in.-thick A514/517 grade-H steel tested, all failed to meet the 25 ft-lb AASHTO-74 CVN-impact energy requirement at +20°F and only one of the eight slabs met the ASTM A517-70 requirement of 15 mils

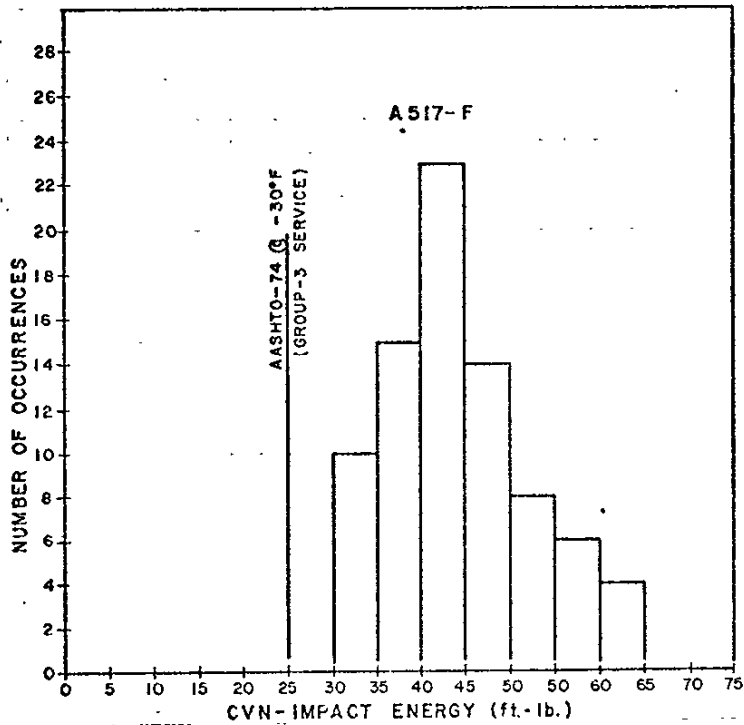


HISTOGRAM FOR CVN-IMPACT ENERGY VALUES
 FROM 29 A517 GRADE-F SLABS OF HEAT 1006 TESTED
 AT +20°F
 FIGURE 4.67



HISTOGRAM FOR CVN-IMPACT LATERAL EXPANSION VALUES
 FROM 29 A517 GRADE-F SLABS OF HEAT 1006 TESTED
 AT +20° F

FIGURE 4.68



HISTOGRAM FOR CVN-IMPACT ENERGY VALUES FROM 27 A517 GRADE-F SLABS OF HEAT 1006 TESTED BY THE STEEL PRODUCER AT MINUS 50° F

FIGURE 4.69

lateral expansion at the service temperature. The one slab that met the A517-70 requirement was tested at +20°F with five tests ranging from 12.4 to 16.9 mils, average 15.95 mils; i.e., it barely passed. It was an open-hearth heat (U.S.S. 07619-03W1).

Tables 4.18 and 4.18a summarize the slab-to-slab variability in the ASTM A514/517 grade-F and grade-H. The test temperatures selected as a basis of comparison are those corresponding to AASHTO-74 group 1, 2 and 3 service. The estimated plane-strain fracture toughness (K_{IC}) values at 0°F are based on equation (4.1) for the CVN- K_{IC} approximation and equation (4.11) for the PCI- K_{IC} approximation. The results indicate little variability from slab to slab in any given heat, with relatively good toughness in the grade-F plates and low toughness in the grade-H plates. The nil ductility transition (NDT) temperatures for the A514/517 grade-F slabs were all below minus 100°F based on the precrack Charpy impact test; whereas, the A514/517 grade-H slabs were indicated to have NDT temperatures ranging from a low of minus 20°F to a high of plus 60°F or higher. For reasonable assurance of crack arrest in the event of a pop-in, the NDT should be at least 30°F below the lowest anticipated service temperature (LAST). The LAST and AASHTO-74 group-1 service is 0°F and, therefore, the highest acceptable NDT temperature for the Bryte Bend and Tuolumne River bridges would be minus 30°F. All of the A514/517 grade-F heats listed in Table 4.18 met this requirement.

TABLE 4.1

STANDARD CHARPY V-NOTCH IMPACT PROPERTIES
A517 GRADE-F HEAT 1006 IN TWENTY-NINE SLABS

STEEL CODE	CVN-IMPACT +20°F		LATERAL EXPANSION +20°F		(MILS) AVG.		ENERGY (FT-LB) -50°F		AVG.
		AVG.		AVG.		AVG.		AVG.	
AR	48.7-48.2-49.2	(48.7)	40.0-38.5-38.0	(38.8)	35-43-39	(39)			
AS	37.7-39.1-39.2	(38.7)	30.5-28.0-27.5	(28.7)	34-31-33	(33)			
AT	49.7-50.2-48.1	(49.4)	41.0-40.0-38.5	(39.8)	34-34-34	(34)			
AU	41.6-40.8-40.6	(41.0)	30.0-29.5-29.5	(29.7)	58-55-60	(58)			
AV	41.6-41.0-43.5	(42.0)	34.0-35.0-34.5	(34.5)	38-39-40	(39)			
AW	44.3-43.0-42.7	(43.3)	32.0-31.0-32.0	(31.7)	38-39-40	(39)			
AX	39.6-42.5-41.5	(41.2)	31.0-32.5-30.0	(31.2)	41-42-40	(41)			
AY	36.0-36.1-35.5	(35.8)	28.0-28.0-28.0	(28.0)	35-41-39	(38)			
AZ	42.7-45.0-47.0	(44.9)	35.0-35.0-38.0	(36.0)	47-43-41	(44)			
BA	54.6-54.8-56.4	(55.3)	42.5-43.5-43.5	(43.2)	43-48-55	(49)			
BB	44.7-42.8-42.0	(43.2)	33.0-30.0-31.0	(31.3)	48-45-39	(44)			
BC	54.2-55.0-58.4	(55.9)	43.0-43.5-41.0	(42.5)	41-38-40	(40)			
BD	50.9-50.8-51.8	(51.2)	37.0-38.0-38.0	(37.7)	-----	-----			
BE	48.0-47.5-46.4	(47.3)	36.0-36.0-35.0	(35.7)	50-52-55	(52)			
BF	55.5-52.9-53.2	(53.9)	43.0-43.0-40.5	(42.2)	31-30-30	(30)			
BG	44.3-45.1-44.1	(44.5)	35.0-35.5-36.5	(35.7)	48-45-48	(47)			
BJ	45.9-45.2-44.8	(45.3)	33.5-34.5-36.5	(34.8)	38-39-40	(39)			
BK	38.9-39.7-37.5	(38.7)	30.0-29.0-28.5	(29.2)	33-35-35	(34)			
BL	46.8-47.4-46.4	(46.9)	36.0-36.5-37.0	(36.5)	52-54-50	(52)			
BM	40.4-43.7-38.6	(40.9)	33.5-36.0-32.0	(33.8)	41-42-42	(42)			
BN	41.6-42.7-44.8	(43.0)	33.0-33.5-34.0	(33.5)	44-41-40	(42)			
BP	41.0-42.8-41.3	(41.7)	34.0-32.0-31.0	(32.3)	40-38-40	(39)			
BR	46.9-48.4-49.0	(48.1)	35.5-36.5-36.5	(36.2)	50-53-48	(50)			
BS	48.2-50.6-52.8	(50.5)	38.5-39.0-42.0	(39.8)	63-60-63	(62)			
BT	49.8-46.8-48.4	(48.3)	40.0-35.0-36.5	(37.2)	48-48-48	(48)			
BU	47.9-46.2-49.4	(47.8)	35.0-32.5-35.0	(34.2)	48-49-48	(48)			
BV	44.7-43.1-44.8	(44.2)	34.0-31.5-31.5	(32.3)	58-50-48	(52)			
BW	45.2-46.9-47.1	(46.4)	34.5-37.0-35.5	(35.7)	45-42-41	(43)			
BZ	43.4-43.3-40.1	(42.3)	33.5-34.0-32.0	(33.2)	-----	-----			

TABLE 4.12

STANDARD CHARPY V-NOTCH IMPACT PROPERTIES
SIXTEEN HEATS, TWENTY-FOUR SLABS

ASTM A514/517 GRADE-F

STEEL CODE	CVN-IMPACT	ENERGY	(FT LB	LATERAL EXPANSION (MILS)		
	+20°F	0°F	-40°F	+20°F	0°F	-40°F
1005/22BX	35.1(a)	31	31	26.3	22	24
1009/40BH	65.2	--	67	48.7	--	50
1010/47AP	53.7	53	55	39.0	37	38
1011/92CA	50.0	--	13	38.8	--	22
1001/82AD	60	60.4	56	46	44.7	42
1001/83AE	57	63.6	60	42.0	44.2	42
1001/84AF	54	50.6	47	40.0	37.3	34
1002/82AB	50	49.1	50	36.0	35.8	40
1002/38AC	50	48.4	44	37.0	35.3	34
1004/44AG	66	65.8	68	46.0	45.8	48
1004/96AH	73	67.4	72	54.0	47.8	52
1004/98AJ	59	60.6	57	41.0	42.5	40
1012/99AK	59	61.3	56	45.0	44.2	42
1003/29CB	37.5	28	36	25.3	18	18
1013/32J	22.3	27	15	15.3	18	10
1014/02M	65.7	65	51	47.0	44	34
1017/62L	71.7	72	40	45.7	50	29
1008/76D	53.0	48.6	34.5	----	36.3	28.0
1028/64B	30.0	20.7	23.3	----	14.7	15.0
1026/92A	16.0	15.8	13.7	----	10.3	9.7
1006/48AS	38.7	38	49	28.7	30	28
1006/26BB	43.2	44	44	31.3	34	31
1006/71BF	53.9	53	52	42.2	42	40
1006/53BK	38.7	37	36	29.2	29	29
1006/56BM	40.9	44	42	33.8	36	34
1006/72BV	44.2	46	44	32.3	32	32
1006/73BZ	42.3	41	40	33.2	----	33

(a) Values reported to the first decimal place are averages of three or more tests; rounded-off values are interpolated from the transition-curve plots.

TABLE 4.13

STANDARD CHARPY V-NOTCH IMPACT PROPERTIES
TWELVE HEATS, TWENTY-FIVE SLABS

ASTM A514/517 GRADE-H

STEEL CODE	CVN-IMPACT			LATERAL EXPANSION (MILS)		
	+20°F	0°F	(FT-LB) -40°F	+20°F	0°F	-40°F
1007/11AM	29.1	27	19	23.7	22.0	14
1007/12AN	26.7	23	12	20.3	18.0	10
1015/32N	43.6	39	26	33.0	30.0	20
1016/41P	10.5	9	6	6.3	6.0	2
1016/11K	12.7	9	6	7.8	4.0	3
1018/81S	19.0	15	10	13.7	12.0	6
1019/31R	21.7	18	10	16.2	14.0	10
1023/51G	12	10.2	5.6	-----	5.0	1.7
1023/54E	16	12.6	7.8	-----	9.3	4.7
1022/54H	19	14.5	9.2	-----	10.5	5.2
1022/53F	16	14.2	8.7	-----	9.7	4.8
1022/51C	10	7.2	4.3	-----	5.0	2.0
1020/41AA	9.1	7	5	5.7	4	2
1020/43CF	12.2	9	5	10.3	8	2
1020/44CG	9.3	8	6	7.0	4	4
1020/46AL	11.8	10	7	7.7	7	2
1024/91Y	32.1	19	7	17.4	12	4
1024/94Z	25.1	21	11	18.2	16	6
1024/95CE	14.9	12	8	11.0	8	4
1025/91CC	7.4	6	4	3.2	3	2
1025/95CJ	11.4	9	4	9.0	6	2
1027/44CK	4.7	4	3	3.0	4	4
1027/45CK	5.2	5	4	1.8	1	1
1027/46CH	5.1	5	4	2.2	2	2
1029/99T	44.4	41	23	33.3	30	16

(a) Values reported to the first decimal place are average of three or more tests; rounded-off values are interpolated from the transition-curve plots.

TABLE 4.14

FREQUENCY DISTRIBUTION FOR CVN-IMPACT ENERGY AND LATERAL EXPANSION
 IN 74 SLABS OF A514/517 GRADE-F AND GRADE-H
 STEEL AT SELECTED TEMPERATURES
CVN-IMPACT ENERGY VALUES

FT-LB	INTERVAL	+20°F		0°F		-40°F	
		GRADE H	GRADE F	GRADE H	GRADE F	GRADE H	GRADE F
5	0-9	6	0	10	0	18	0
15	10-19	7	0	9	1	5	3
25*	20-29	4	1	4	3	2	1
35	30-39	1	7	1	5	0	5
45	40-49	2	25	1	11	0	13
55	50-59	0	14	0	4	0	8
65	60-69	0	4	0	7	0	3
75	70-79	<u>0</u>	<u>2</u>	<u>0</u>	<u>1</u>	<u>0</u>	<u>1</u>
Slab Total		20	53	25	32	25	34

CVN-IMPACT LATERAL-EXPANSION VALUES

MILS	INTERVAL	+20°F		0°F		-40°F	
		GRADE H	GRADE F	GRADE H	GRADE F	GRADE H	GRADE F
5	0-9	10	0	16	0	20	1
15*	10-19	6	1	6	4	4	3
25	20-29	2	8	1	3	1	9
35	30-39	2	30	2	14	0	11
45	40-49	0	13	0	9	0	8
55	50-59	<u>0</u>	<u>1</u>	<u>0</u>	<u>1</u>	<u>0</u>	<u>2</u>
Slab Total		20	53	25	31	25	34

* 25 ft-lb AASHTO-74 and 15 mils ASTM A517-70a

TABLE 4.15

ARITHMETIC MEAN VALUES OF CVN-IMPACT ENERGY AND LATERAL EXPANSION
IN A514/517 GRADE-H AND GRADE-F STEELS TESTED AT SELECTED TEMPERATURES

TEST TEMP.	GRADE H STEEL		GRADE F STEEL	
	RANGE	AVERAGE	RANGE	AVERAGE
+20°F	5 to 44 ft-lb	(20 slabs) <u>18 ft-lb</u>	16 to 73 ft-lb	(27 slabs) <u>49 ft-lb</u>
	2 to 33 mils	(20 slabs) <u>12 mils</u>	15 to 54 mils	(24 slabs) <u>38 mils</u>
0°F	4 to 41 ft-lb	(25 slabs) <u>14 ft-lb</u>	15 to 67 ft-lb	(25 slabs) <u>48 ft-lb</u>
	1 to 30 mils	(25 slabs) <u>10 mils</u>	10 to 48 mils	(24 slabs) <u>35 mils</u>
-40°F	4 to 26 ft-lb	(25 slabs) <u>9 ft-lb</u>	13 to 66 ft-lb	(27 slabs) <u>44 ft-lb</u>
	1 to 20 mils	(25 slabs) <u>5 mils</u>	10 to 52 mils	(27 slabs) <u>32 mils</u>

TABLE 4.16

SUMMARY OF A514/517 GRADE-F CVN-IMPACT TEST RESULTS

ASTM TYPE-GRADE	REPORT CODE HEAT/SLAB	THICK. (IN.)	CVN-IMPACT (FT-LB)			25 FT-LB TT (c)	LAT. EXPANS. at LAST (d)
			+20°F	0°F	-30°F		
			(a)	(b)	(b)		
A517-F	1005/22BX	1-3/8	35.1	34	32	> -60	26.3
A517-F	1009/40BH	1-3/8	65.2	66	66	> -60	48.7
A517-F	1010/AP	1-3/8	53.7	54	54	> -60	39.0
A517-F	1011/CA	1-3/8	50.0	43	31	-45	38.8
A517-F	1001/82AD	1-1/2	61	60.4	58	> -60	44.7
	1001/83AE	1-1/2	62	63.6	61	> -60	44.2
	1001/84AF	1-1/2	51	50.6	48	> -60	37.3
A517-F	1002/82AB	1-1/2	49	49.1	50	> -60	35.8
	1002/38AC	1-1/2	48	48.4	46	> -60	35.3
A517-F	1004/44AG	1-1/2	66	65.8	66	> -60	45.8
	1004/96AH	1-1/2	70	67.4	70	> -60	47.8
	1004/98AJ	1-1/2	60	60.6	60	> -60	42.5
A517-F	1012/99AK	1-1/2	60	61.3	59	> -60	44.2
A514-F	1003/29CB	2-1/4	37.5	28	14	-5	25.3
A514-F	1013/32J	2-1/4	22.3	19	15	+25	15.3
A514-F	1014/02M	2-1/4	65.7	65	56	> -60	47.0
A514-F	1017/62L	2-1/4	71.7	67	47	-60	45.7
A517-F	1026/92A	2-1/4	16	15.8	14	+130	10.0
A517-F	1008/76D	2-1/2	53	48.6	38	> -60	36.3
A517-F	1028/64B	2-1/2	31	20.7	20	-5	14.7
A517-F	1006/(e)	1-3/8	45.5	43	43	43.6(f)	33.0

(a) Data reported to one decimal place are averages of three tests by CALTRANS.

(b) Rounded-off ft-lb values are interpolated from the transition-curve plots.

(c) Temperature (°F) corresponding to 25 ft-lb CVN-impact energy.

(d) Lateral expansion values at the lowest anticipated service temperature (LAST) correspond to the ft-lb values reported to the 1st decimal place. Thus, the lateral expansion value for plate AM was the average of three tests at +20°F whereas the value for plate G was the average of three tests at 0°F.

(e) Twenty-nine slabs from heat 1006 were tested in triplicate; values reported for this heat to one decimal place were the average of 87 tests.

(f) Average CVN-impact value (ft-lb) of 81 tests made by the steel producers at -50°F.

TABLE 4.17

SUMMARY OF A514/517 GRADE-H CVN-IMPACT

ASTM TYPE-GRADE	REPORT CODE HEAT/SLAB	THICK. (IN.)	CVN-IMPACT (FT-LB)			25 FT-LB TT (c)	LAT. EXPANS. at LAST (d)
			+20°F (a)	0°F (b)	-30°F (b)		
A514-H	1007/11AM	1-1/2	29.1	27	21	-10	23.7
	1007/12AN	1-1/2	26.7	23	19	+10	20.3
A514-H	1015/32N	1-3/4	43.6	39	30	-45	33.0
A514-H	1016/41P	2	10.5	9	6	> 200	6.3
	1016/11K	2	12.7	9	7	+200	7.8
A514-H	1018/81S	2	19.0	15	11	+50	13.7
A514-H	1019/31R	2	21.7	18	12	+35	16.0
A517-H	1023/51G	2	12	10.2	7	+135	5.0
	1023/54E	2	16	12.6	9	+95	9.3
A517-H	1022/54H	2	19	14.5	10	+45	10.5
	1022/53F	2	16	14.2	11	+100	9.7
	1022/51C	2-1/2	10	7.2	5	+120	5.0
A517-H	1020/41AA	2-1/4	9.1	7	5	+70	5.7
	1020/43CF	2-1/4	12.2	9	6	+110	10.3
	1020/44CG	2-1/4	9.3	8	6	+130	7.0
	1020/46AL	2-1/4	11.8	10	8	+100	7.7
A517-H	1024/91Y	2-1/4	32.1	19	10	+20	17.4
	1024/94Z	2-1/4	25.9	21	15	+20	18.2
	1024/95CE	2-1/4	14.9	12	9	+90	11.0
A517-H	1025/91CC	2-1/4	7.4	6	5	+100	3.2
	1025/95CJ	2-1/4	11.4	9	6	+100	9.0
A517-H	1027/44CK	2-1/4	4.7	4	3	> 200	3.0
	1027/45CD	2-1/4	5.2	5	4	+100	1.8
	1027/46CH	2-1/4	5.1	5	4	> 200	2.2

(a) Data reported to one decimal place are averages of three tests or more by CALTRANS.

(b) Rounded-off ft-lb values are interpolated from the transition-curve plots.

(c) Temperature (°F) corresponding to 25 ft-lb CVN-impact energy.

(d) Lateral expansion values at the lowest anticipated service temperature (LAST) correspond to the ft-lb values reported to the 1st decimal place. Thus, the lateral expansion value for plate AM was the average of three tests at +20°F, whereas, the value for plate G was the average of three tests at 0°F.

TABLE 4.18

SLAB-TO-SLAB VARIABILITY IN A GIVEN HEAT - ASTM A517 GRADE F

HEAT CODE	INGOT (SLAB)	PLATE CODE	THICK. (IN.)	CVN-IMPACT (FT-LB)		PCI (FT LB)		EST. K _{IC} (CVN)	
				+30°F	0°F	+30°F	0°F	(PCI)	0°F
1001	82	AD	1-1/2	60	60	46	46	155	174
	83	AE	"	62	63	48	49	160	178
	84	AF	"	52	51	36	37	139	158
1002	82	AB	1-1/2	49	49	36	37	139	155
	38	AC	"	48	48	37	36	137	153
1004	44	AG	1-1/2	66	66	48	48	158	183
	96	AH	"	69	69	52	52	165	187
	98	AJ	"	60	60	46	47	157	174
1006	48	AS	1-3/8	39	38	38	28	121	133
	53	BK	"	39	38	28	28	121	133
	56	BM	"	42	42	31	32	129	141
	26	BB	"	44	44	33	33	131	145
	71	BF	"	54	53	38	38	141	164
72	BV	"	45	45	34	34	133	147	
73	BZ	"	42	42	30	30	125	141	

TABLE 4.18a

SLAB-TO-SLAB VARIABILITY IN A GIVEN HEAT - A514/517 GRADE H

HEAT CODE	INGOT (SLAB)	PLATE CODE	THICK. (IN.)	CVN-IMPACT (FT-LB)		PCI (FT LB)		NDT(PCI) (°F)	EST. K_{IC} (PCI) 0°F	
				+30°F	0°F	+30°F	0°F			
1007	11	AM	1-1/2	30	27	21	15	11	+20	88
	12	AN	1-1/2	28	23	18	9	7	+20	68
1016	41	P	2	12	8	6	5	4	---	51
	11	K	2	13	10	6	6	5	---	56
1020	41	AA	2-1/4	11	7	5	5	4	+30	51
	43	CF	"	12	9	7	5	4	+55	51
	44	CG	"	10	8	6	5	4	+20	51
	46	AL	"	14	10	8	6	5	+30	56
1022	51	C	2-1/2	12	8	5	4	3	---	46
	53	F	2	18	14	11	7	5	-15	60
	54	H	2	21	14	10	6	4	-20	56
1023	51	G	2	13	10	7	6	4	-20	56
	54	E	2	17	12	9	7	5	-20	60
1024	91	Y	2-1/4	28	19	10	5	3	-15	51
	94	Z	"	28	21	15	9	7	-10	68
	95	CE	"	16	12	9	6	5	+60	56
1025	91	CC	"	9	6	5	3	2	+60	40
	95	CJ	"	13	9	6	6	4	+75	56
1027	44	CK	2-1/4	5	3	3	2	---	---	32
	45	CD	"	6	5	4	3	2	+55	40
	46	CH	"	6	5	4	3	2	+60	40

4.4

ASTM E399 COMPACT TENSION TEST RESULTS

The following heats and plates of A514/517 steel were tested using the ASTM E399-70T Tentative Method of Test for Plane-Strain Fracture Toughness of Metallic Materials:

<u>ASTM Type-Grade</u>	<u>Report Code Heat/Slab</u>	<u>Plate ID</u>	<u>Specimen ID</u>
A514-F	1017/62	L	ZV
	1014/02	M	ZU
A517-F	1026/92	A	ZW
A514-H	1019/31	R	ZX
A517-H	1024/94	Z	ZT
	1020/46	AL	ZY
	1027/44	CK-1	ZZ
		CK-2	22CK

The data obtained from 1-in.-thick compact-tension tests are shown in Table 4.19. The data from the 2-in.-thick compact-tension tests are shown in Table 4.20. Note that there were test irregularities based on the ASTM E399 requirements for a valid fatigue precrack. Also at the higher test temperatures, the requirement that both thickness and crack depth be greater than

$$2.5 \text{ (KQ/FTY)}^2$$

was violated in a number of tests (see the last two columns of Tables 4.19 and 4.20).

The plots of KQ versus test temperature for the seven steels are shown in Figures 4.70 through 4.76 together with the precrack Charpy impact (PCI) curves (dashed) for each steel. Note that the static KQ curves were markedly displaced on the temperature scale as compared with the PCI curves. The displacement is

TABLE 4.19

SUMMARY OF ONE-INCH-THICK COMPACT TENSION TEST
RESULTS FOR SEVEN A514/517 STEELS

Plate Designation, Material Spec. Heat Number	Specimen No.	Test Temp. (°F)	Fatigue Final K (ksi-in. ^{1/2})	Crack Depth Avg.(in.)	Failure Secant PQ(kips)	Load Maximum (kips)	Ratio A/W	Critical Stress Intensity (ksi-in. ^{1/2})	Valid Min. Thick. (in.)	Test Irreg.
Plate L (2-1/4-in.) A514F Heat 1017/62	ZVE	-200	33.1	1.054	6.57	6.57	0.526	48.3	0.34	b,c,e
	ZVI	-150	29.6	0.980	8.69	8.69	0.490	57.2	0.55	-
	ZVG	-130	26.3	0.946	9.78	9.78	0.472	61.2	0.66	c,d
	ZVD	- 80	27.6	0.979	9.25	11.60	0.489	60.7	0.68	-
	ZVF	- 40	27.7	0.982	14.45	14.45	0.490	95.2	1.77	f,g
ZVH	0	28.7	1.006	15.60	18.00	0.502	106.5	2.28	f,g	
Plate M (2-1/4-in.) A514F Heat 1014/02	ZUE	-320	33.8	0.973	6.65	6.65	0.485	43.2	0.015	b
	ZUG	-210	28.3	0.949	11.45	11.45	0.474	72.0	0.70	c,d,e
	ZUF	-140	27.3	0.972	16.10	16.10	0.485	104.6	1.69	f,g
	ZUH	-103	27.6	0.980	15.30	18.30	0.489	100.6	1.65	f,g
	ZUD	- 80	27.6	0.981	18.00	24.00	0.490	118.4	2.34	f,g
ZUI	- 40	29.4	0.978	15.50	23.05	0.489	101.5	1.79	f,g	
Plate A (2-1/4-in.) A517F Heat 1026/92	ZWG	-200	30.8	1.051	7.40	7.40	0.525	54.3	0.46	b,e
	ZWI	-102	31.4	1.020	16.60	17.15	0.509	115.8	2.58	f,g
	ZWH	- 39	30.8	1.008	15.20	21.55	0.503	104.1	2.20	f,g
	ZWD	- 2	31.0	1.056	13.50	18.70	0.527	99.6	2.09	e,f,g
	ZWE	+ 39	36.4	1.023	13.25	20.15	0.511	92.9	1.86	f,g
ZWF	+ 75	29.5	1.024	15.75	20.10	0.511	110.6	2.72	f,g	
Plate R (2-in.) A514H Heat 1019/31	ZXH	-210	28.1	0.992	8.34	8.34	0.495	55.8	0.43	-
	ZXF	-151	28.7	0.959	6.55	6.55	0.479	41.8	0.27	b,c,d,e
	ZXE	-102	28.8	0.962	9.92	9.92	0.480	63.5	0.68	c,d
	ZXD	- 80	27.6	0.980	8.05	8.05	0.489	52.9	0.48	-
	ZXG	0	27.5	0.979	12.00	12.00	0.488	78.7	1.15	f,g
ZXI	+ 76	36.4	1.020	13.72	13.90	0.510	95.9	1.78	f,g	
Plate Z (2-1/4-in.) A517H Heat 1024/94	ZTG	-205	30.6	1.048	5.02	5.14	0.523	36.6	0.18	b
	ZTD	-144	33.4	1.131	5.60	5.60	0.564	48.8	0.33	a,b,e
	ZTF	- 79	31.1	1.058	7.70	7.70	0.528	57.0	0.53	e
	ZTH	- 40	30.0	1.035	9.75	9.75	0.517	69.7	0.82	-
	ZTE	+ 20	30.7	1.050	12.55	12.55	0.524	91.8	1.47	f,g
ZTI	+ 72	30.2	1.040	15.35	15.35	0.519	110.5	2.17	f,g	
Plate AL (2-1/4-in.) A517H Heat 1020/46	ZYD	-102	33.3	1.057	6.54	6.54	0.527	48.3	0.49	b,c,d,e
	ZYH	-101	33.6	1.063	6.85	6.85	0.531	51.1	0.54	b,e
	ZYF	- 39	33.8	1.065	7.64	7.64	0.532	57.4	0.72	b,e
	ZYI	0	33.9	1.069	7.96	7.96	0.534	60.0	0.81	e
	ZYE	+ 40	32.9	1.050	10.30	10.30	0.524	75.4	1.29	e,f,g
ZYG	+120	33.4	1.059	12.52	13.75	0.528	92.8	2.07	e,f,g	
Plate CK-1 (2-1/4-in.) A517H Heat 1027/44	ZZI	0	27.5	0.979	7.35	7.35	0.488	48.2	0.40	-
	ZZE	0	24.8	0.904	7.76	7.76	0.452	45.9	0.40	c
	ZZD	+ 40	28.0	1.023	7.35	7.93	0.511	51.5	0.52	-
	ZZH	+ 75	27.8	1.020	8.29	8.29	0.509	57.7	0.67	-
	ZZF	+159	27.6	0.980	9.12	9.85	0.489	59.9	0.75	-
ZZG	+200	26.0	0.973	9.82	10.30	0.485	63.8	0.86	-	

NOTE: for a valid K_{Ic} result, it was required under the provisions of ASTM 399-70 that:

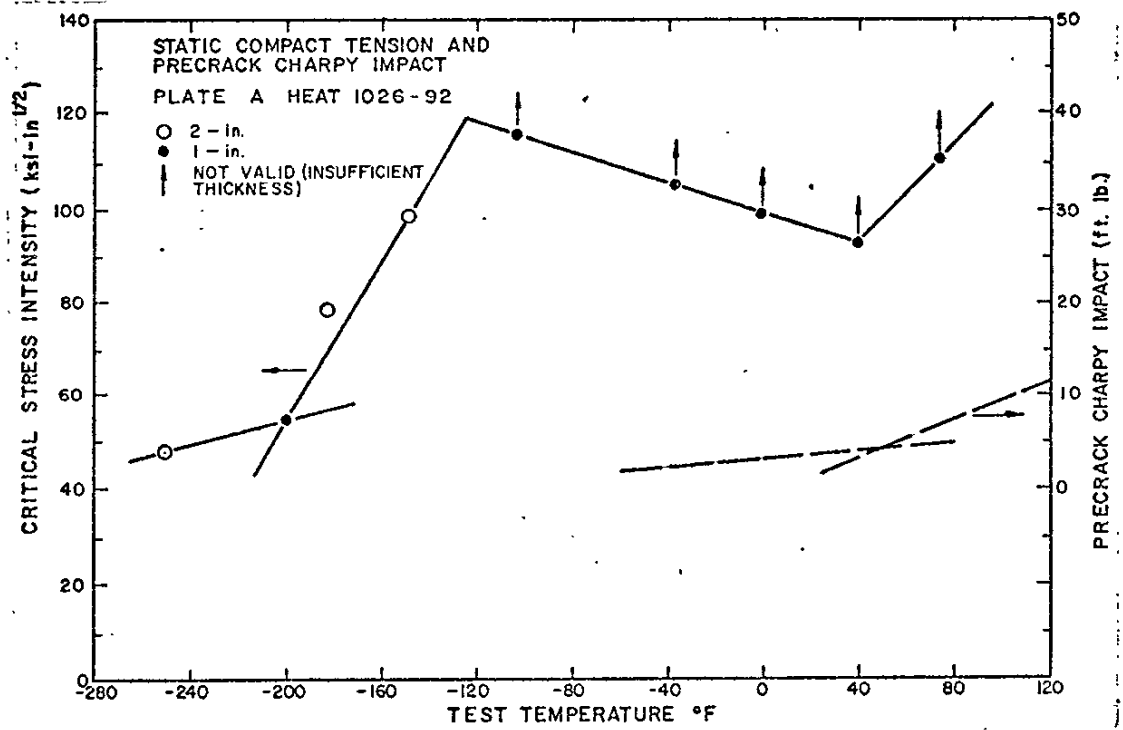
- (a) the crack length to specimen depth (A_{avg}/W) shall be 0.45 to 0.55;
- (b) in the final stage of fatigue precracking, the maximum stress intensity shall not exceed (1) $1.2 \times 10^{-3} \cdot E$ or (2) 60 percent of KQ;
- (c) the maximum irregularity in the crack envelope shall not exceed 5 percent of the average crack length;
- (d) the crack extension at the free surfaces shall be 5 percent of the average crack length, or 0.050-in., whichever is the greater measurement;
- (e) the crack extension at the free surfaces shall be at least 90 percent of the average crack length;
- (f) the crack length shall be at least $2.5 (KQ/FTY)^2$
- (g) the specimen thickness shall be at least $2.5 (KQ/FTY)^2$
- (h) the loading rate shall be within the range 30 to 150 ksi-in.^{1/2}/minute.

TABLE 4.20

SUMMARY OF TWO-INCH-THICK COMPACT TENSION TEST RESULTS FOR SEVEN A514/517 STEELS

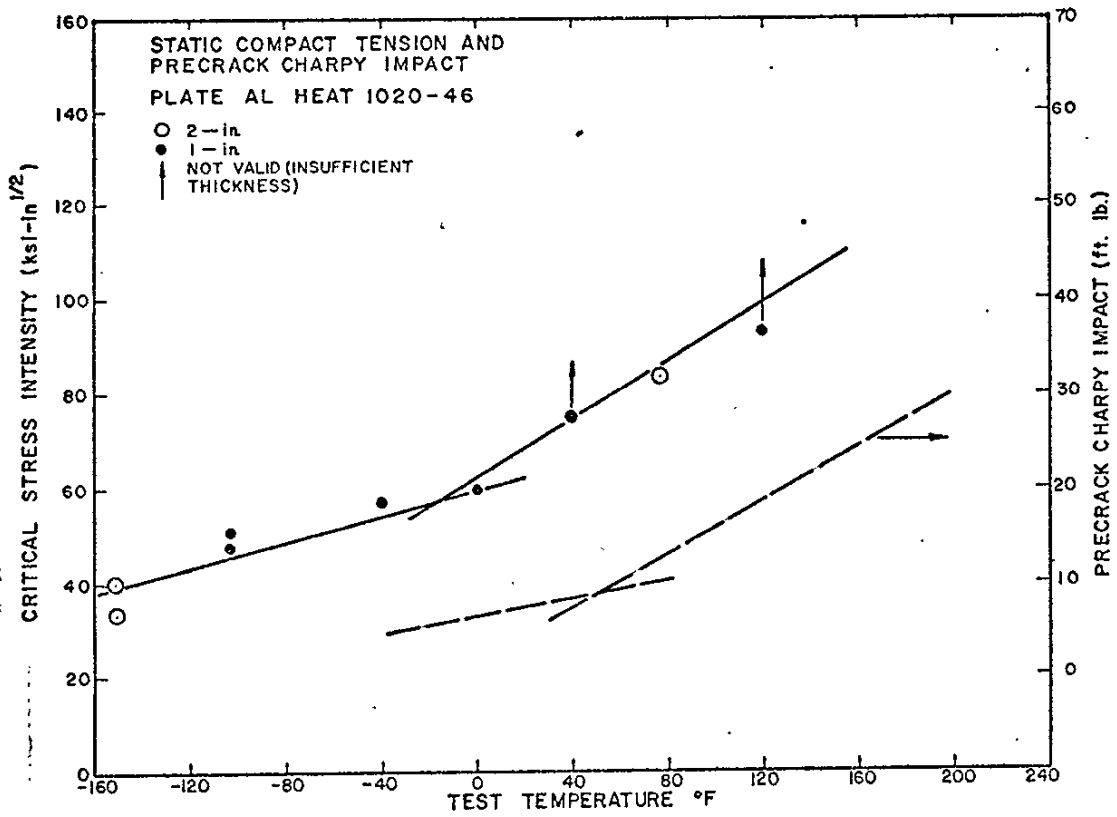
Plate Designation, Material Spec. Heat Number	Specimen No.	Test Temp. (°F)	Fatigue Final K (ksi-in. ^{1/2})	Crack Depth AVG. (in.)	Failure Secant PQ (kips)	Load Maximum (kips)	Ratio A/W	Critical Stress Intensity (ksi-in. ^{1/2})	Valid Min. Thick. (in.)	Test Irreg.
Plate 1, (2-1/4-in.) A514F Heat 1017/62	ZVC	-100	26.4	2.006	30.95	30.95	0.501	74.4	1.01	
	ZVB	-55	26.3	1.998	47.70	47.70	0.500	114.2	2.46	f,8
	ZVA	75	26.2	1.987	52.8	> 59.75	0.497	125.7	3.27	f,8
Plate M (2-1/4-in.) A514F Heat 1014/02	ZUC	-250	26.5	2.008	16.70	16.70	0.502	40.26	0.18	b
	ZUA	-100	26.4	2.002	44.95	44.95	0.500	107.84	1.89	
	ZUB	+75	26.7	2.018	51.50	59.80	0.504	125.16	2.86	f,8
Plate A (2-1/4-in.) A517F Heat 1026/92	ZWA	-250	30.8	2.196	17.05	17.05	0.549	47.74	0.32	b,e
	ZWC	-181	31.2	2.212	24.80	27.60	0.553	78.94	1.01	e
	ZWB	-150	31.0	2.205	35.00	35.00	0.551	98.70	1.69	e
Plate R (2-in.) A514H Heat 1019/31	ZXB	-200	27.7	2.064	14.88	14.88	0.516	37.46	0.19	b
	ZXC	-50	26.0	1.981	26.35	26.35	0.495	62.32	0.68	
	ZXA	+75	26.3	1.998	42.50	43.40	0.499	101.66	1.99	h
Plate Z (2-1/4-in.) A517H Heat 1029/94	ZTA	-155	29.3	2.134	16.90	16.90	0.533	44.98	0.30	b,e
	ZTC	-100	31.1	2.204	20.00	20.00	0.551	56.32	0.51	e
	ZTB	+76	30.6	2.188	46.40	48.10	0.547	129.06	2.96	e,f,8
Plate AL (2-1/4-in.) A517H Heat 1020/46	ZYC	-150	33.3	2.265	11.20	13.20	0.571	33.91	0.22	a,b,e
	ZYA	-150	34.2	2.313	12.95	12.95	0.578	40.24	0.32	a,b,c,d
	ZYB	+75	37.2	2.402	25.00	31.30	0.600	84.61	1.68	a,d,e
Plate (2-1/4-in.) A417H Heat 1027/44	CT1	+58	29.2	2.071	23.22	23.22	0.505	56.53	0.54	
	CT2	+58	29.3	2.025	21.95	23.30	0.506	53.66	0.49	
	CT3	+58	29.7	2.041	22.05	22.75	0.510	54.59	0.50	
CT9	CT9	+75	30.0	2.052	22.50	22.50	0.513	56.24	0.63	
	CT5	+113	29.7	2.039	23.65	23.90	0.510	58.45	0.60	
	CT7	+113	30.0	2.052	23.30	24.50	0.513	58.24	0.59	
CT8	+113	29.3	2.025	24.25	24.85	0.506	59.25	0.61		

*See Footnotes on Table 4.19



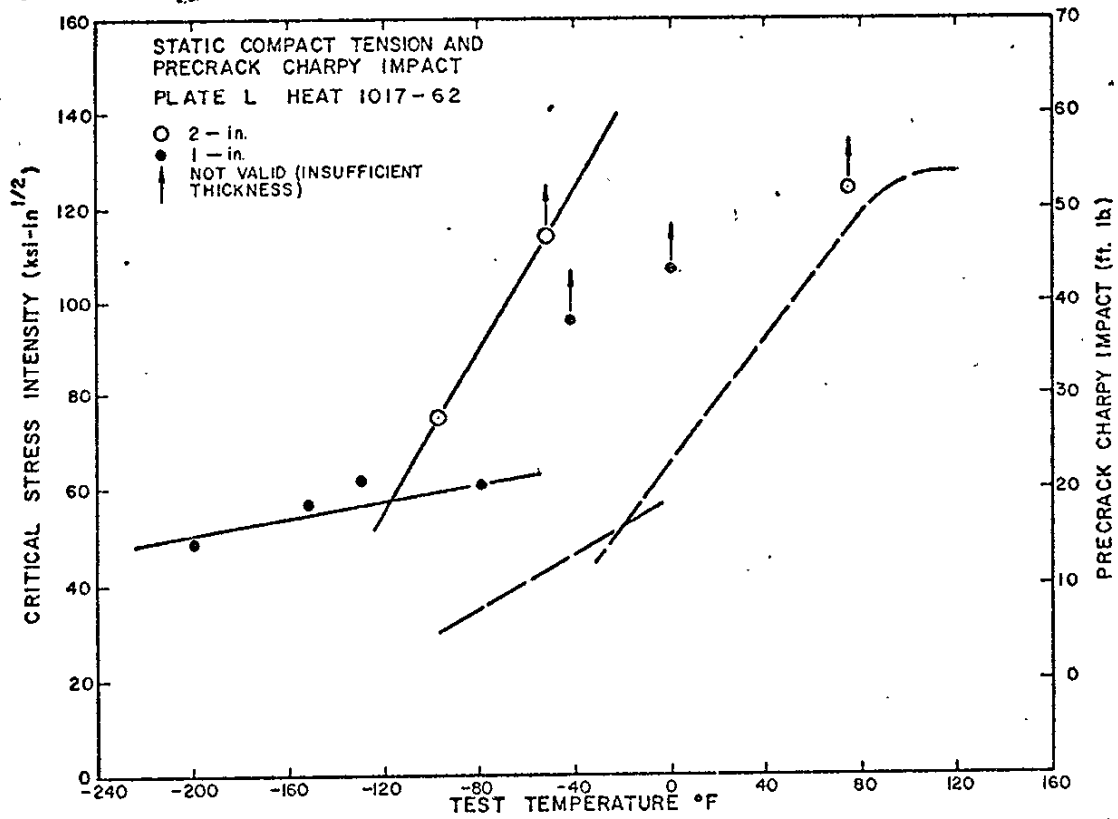
STATIC COMPACT-TENSION AND PRECRACK CHARPY IMPACT
TEST RESULTS FOR A517-F PLATE A

FIGURE 4.70



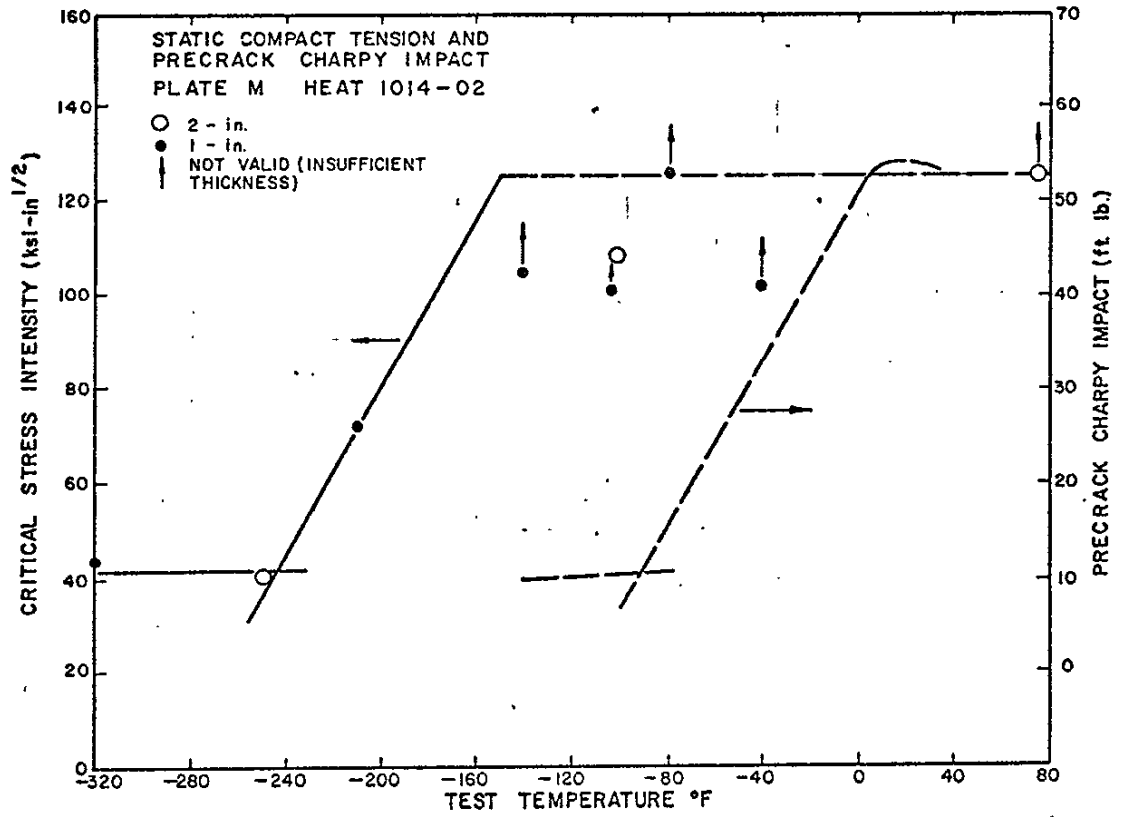
STATIC COMPACT-TENSION AND PRECRACK CHARPY IMPACT
TEST RESULTS FOR A517-H PLATE AL

FIGURE 4.71



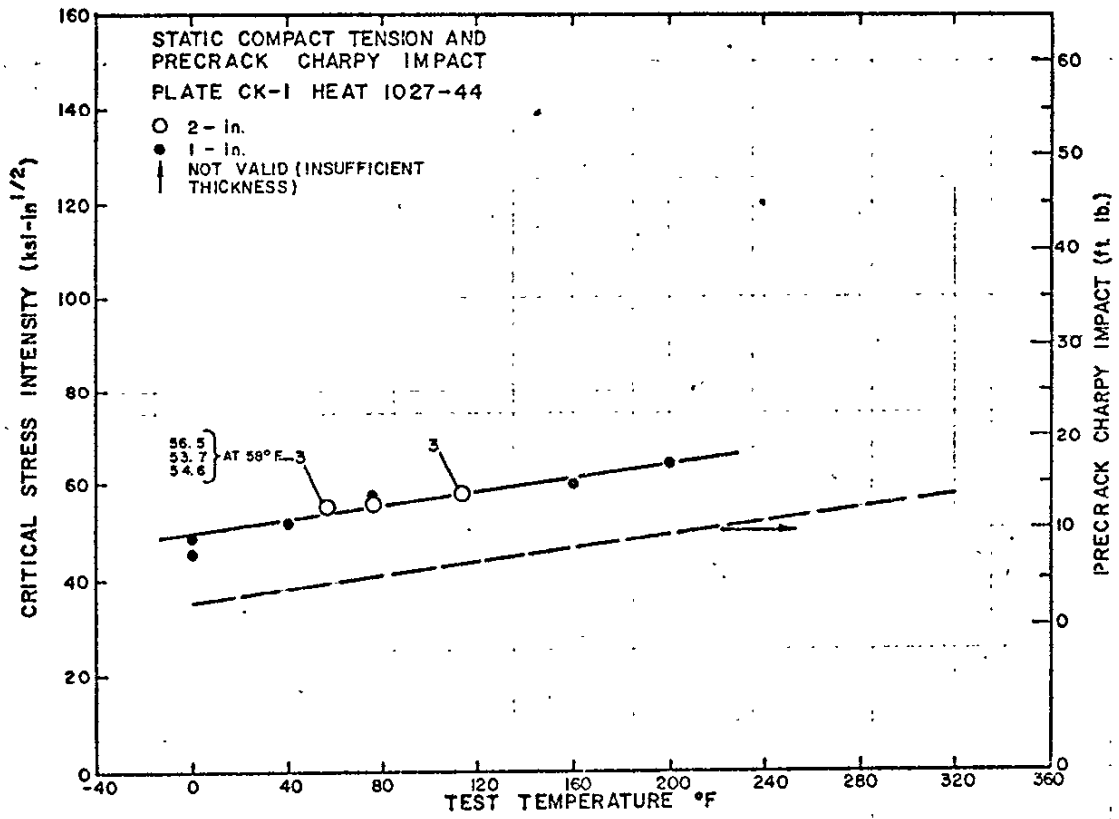
STATIC COMPACT-TENSION AND PRECRACK CHARPY IMPACT
 TEST RESULTS FOR A514-F PLATE L

FIGURE 4.72



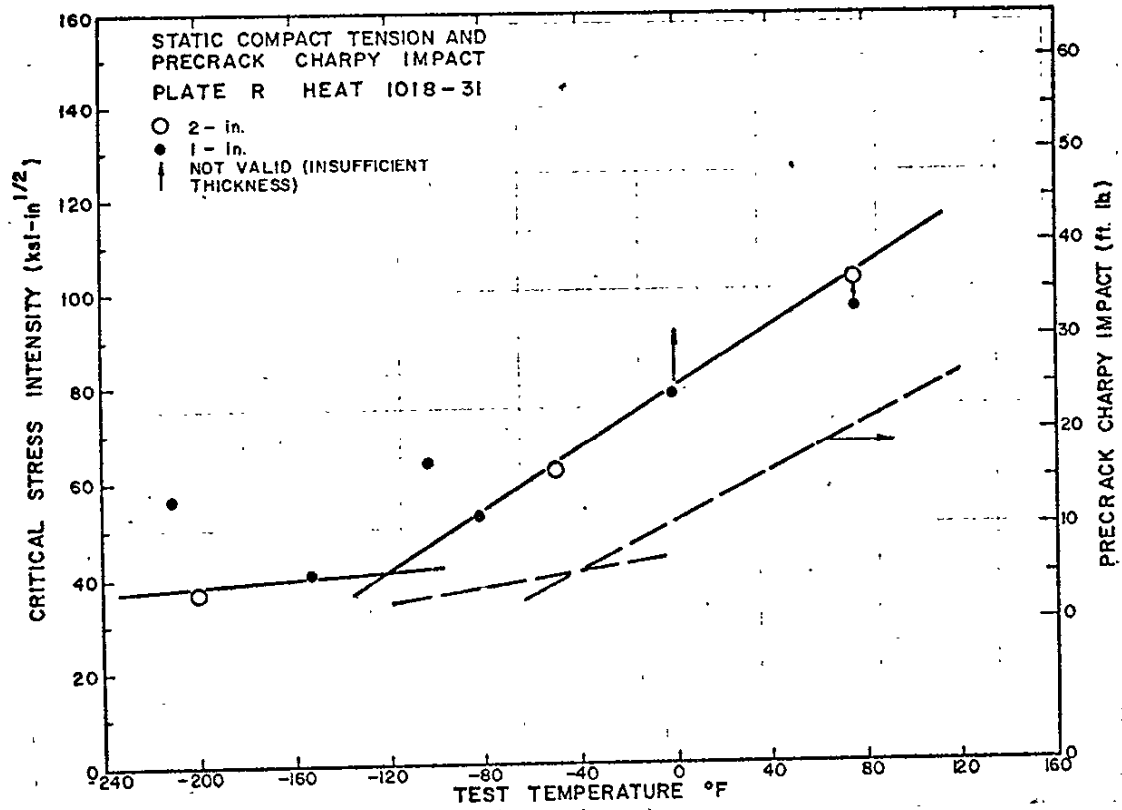
STATIC COMPACT-TENSION AND PRECRACK CHARPY IMPACT
TEST RESULTS FOR A514-F PLATE M

FIGURE 4.73



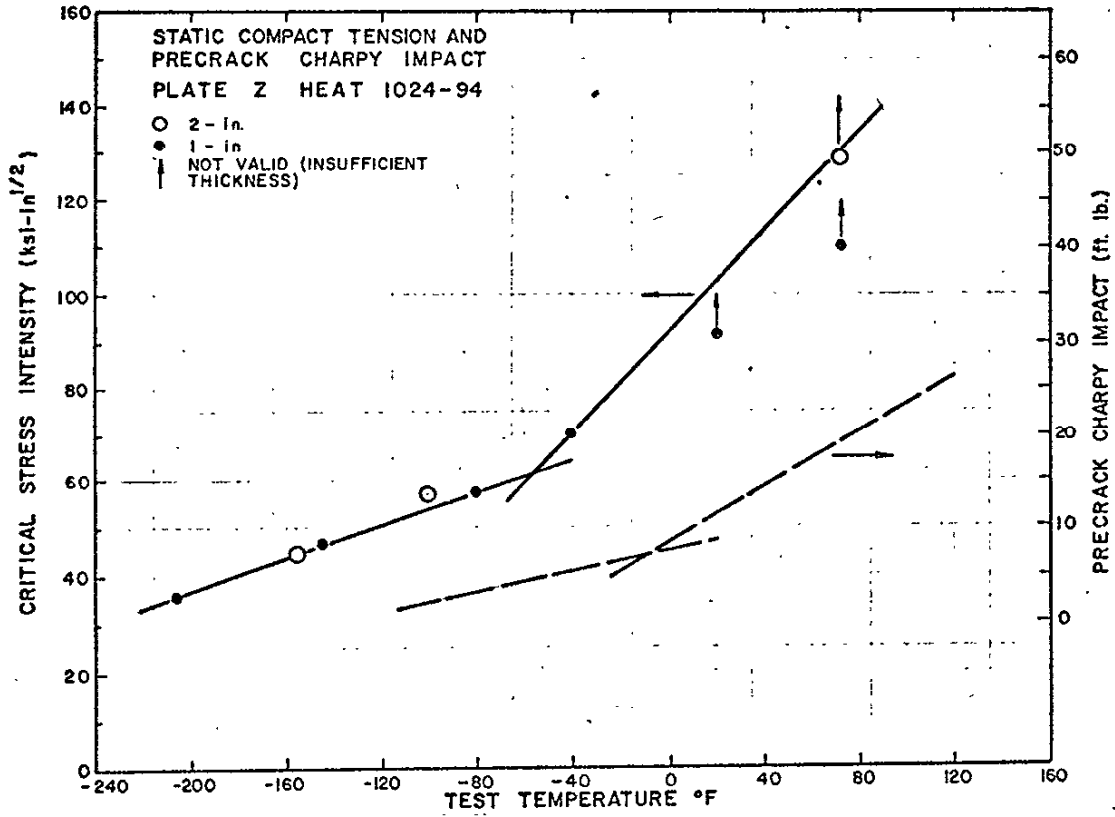
STATIC COMPACT - TENSION AND PRECRACK CHARPY IMPACT
TEST RESULTS FOR A517-H PLATE CK-1

FIGURE 4.74



STATIC COMPACT-TENSION AND PRECRACK CHARPY IMPACT
TEST RESULTS FOR A514-H PLATE R

FIGURE 4.75



STATIC COMPACT - TENSION AND PRECRACK CHARPY IMPACT
TEST RESULTS FOR A517-H PLATE Z

FIGURE 4.76

attributed to a rate-of-loading effect. Note that the steels varied in this displacement and that the extent of the displacement, as shown in Table 4.21, in some instances was much greater than the 60°F shift reported for A517-F steel by U. S. Steel investigators (3).

Behavior in Plate A was anomalous in that the static transition-temperature region (-120 to -200°F) was followed by decreasing KQ values in the upper shelf (between -120 and +40°F).

4.4.1 Effect of "Invalid" K_{IC} Tests

Of the 42 one-inch-thick compact-tension tests, only ten met all of the ASTM E399 requirements for a valid K_{IC} test. Fifteen of the "invalid" tests were the result of fatigue precracking irregularities; otherwise, these fifteen specimens conformed to ASTM E399. Fourteen of the remaining tests involved temperatures where the toughness was too great for the crack-length and specimen-thickness requirements, viz., $2.5 (KQ/FTY)^2$. Only three of the 1-in. specimens had both fatigue precrack irregularities and specimen-size violations.

Of the 25 two-inch-thick compact-tension tests, ten met all of the ASTM E399 requirements for a valid K_{IC} test. Only four of the tests involved temperatures where the toughness was too great for the crack-length and specimen-thickness requirements.

4.4.1.1 Effect of Fatigue-Precracking Discrepancies

At temperatures where the toughness permitted valid measurements with the 1-in. compact-tension specimens, it was possible to compare measured stress intensity values obtained from specimens with no discrepancies (valid tests) with values obtained from specimens involving one or more discrepancies. For example, in

Plate Z, there was remarkably little scatter introduced by the precracking discrepancies, inspite of the fact that three of the specimens involved excessive maximum stress intensity in the fatigue precracking operation.

TABLE 4.21

TRANSITION-TEMPERATURE SHIFT DUE TO
RATE OF LOADING (Static K_{Ic} vs PCI)

ASTM Type-Grade	Plate	Transition Temperature		Shift ΔT (°F)
		Precrack Charpy Impact (°F)	Compact Tension Static (°F)	
A514-F	M(ZU)	-90	-240	150
	L(ZV)	-20	-120	100
A517-F	A(ZW)	+40	-200	240
A514-H	R(ZX)	-40	-120	80
A517-H	Z(ZT)	-5	-60	55
	AL(ZY)	+60	0	60
	CK-1	undetermined	undetermined	undetermined

Table 4.22 summarizes the fatigue-precracking discrepancies for three of the plates investigated as obtained from the computer-program printout. The data from these three plates were selected for more detailed examination because each involved K_{Ic} -temperature plots with several data points below the transition temperature which fell in a more or less well defined band. In Table 4.22 the underscored values are the sources of discrepancy. A cursory examination of the underscored items shows that there were two principal sources of difficulty' viz., too little crack extension at the free surfaces, and stress intensity values in fatigue that exceeded the maximum allowable by ASTM. With regard to the latter, according to E399, when fatigue cracking is conducted at room temperature (T_1) and testing is done at a different temperature

TABLE 4.22
FATIGUE PRECRACKING DISCREPANCIES IN COMPACT-TENSION TESTS

Specimen Material	Specimen Size (in.)		Temperature (°F)	KFF ref-in. 1/2	Sources of Fatigue-Precrack Discrepancies (underlined)				
	Code	2			1	0.6 (FTV/FTVT)KQ (b)* (ksi-in. 1/2)	5% Avg Irregularity (c) (in.)	Maximum Extension (d) (in.)	Min. at Free Surface (e) (in.)
Plate A1 A517H	ZYC	2	-150	33.31	<u>18.60</u>	0.1142	0.0820	0.1240	<u>.818/.855</u>
	ZYA	2	-150	34.18	<u>22.07</u>	0.1157	0.1780	0.0000	<u>.894/.728</u>
	ZYD	1	-102	33.27	<u>27.37</u>	0.0528	0.0920	0.0010	<u>.804/.978</u>
	ZYH	1	-101	33.56	<u>28.92</u>	0.0532	0.0340	0.0860	<u>.878/.908</u>
	ZYF	1	-39	33.78	<u>33.28</u>	0.0532	0.0530	0.0570	<u>.849/.966</u>
	ZYI	1	0	33.93	<u>35.26</u>	0.0534	0.0380	0.0900	<u>.914/.877</u>
Plate L A514F	ZVE	1	-200	33.07	<u>24.46</u>	0.0527	<u>0.0810</u>	0.0850	<u>1.005/.887</u>
	ZVI	1	-150	29.62	30.89	0.0490	0.0190	0.0800	<u>.951/.982</u>
	ZVG	1	-130	26.28	33.87	0.0473	<u>0.1080</u>	0.0010	<u>1.050/.904</u>
	ZVC	2	-100	26.46	41.91	0.1003	0.0270	0.1570	<u>.952/.970</u>
	ZVD	1	-80	27.57	34.49	0.0489	0.0040	0.0780	<u>.952/.966</u>
	ZTG	1	-205	30.58	<u>18.97</u>	0.0524	0.0330	0.0770	<u>.934/.893</u>
Plate Z	ZTA	2	-155	29.28	<u>24.79</u>	0.1067	0.0600	0.1550	<u>.895/.920</u>
	ZTD	1	-144	33.41	<u>25.98</u>	0.0566	0.0380	0.1330	<u>.867/.916</u>
	ZTC	2	-100	31.08	32.02	0.1102	0.0870	0.1540	<u>.874/.863</u>
	ZTF	1	-79	31.11	32.83	0.0529	0.0450	0.0840	<u>.882/.948</u>
	ZTH	1	-40	30.04	40.64	0.0518	0.0300	0.0970	<u>.915/.925</u>

*See footnotes of Table 4.19

(T2), K_{FF} (maximum) must not exceed 60 percent of $(F_{TY}/F_{TYTT})K_Q$ where F_{TY} and F_{TYTT} are the yield strengths at the fatigue precracking temperature (T1) and the actual test temperature (T2), respectively. When the test plan was originally established, it was anticipated that the compact-tension testing would be done over approximately the same range of temperatures as the precrack Charpy impact tests, with no temperature more than 100°F below the PCI transition temperature. When it became necessary to test at lower temperatures because of the marked rate-of-loading effect in some of the plates, the higher yield strength at low temperature resulted in invalid tests $K_{FF} > 0.60 (F_{TY}/F_{TYTT})K_Q$.

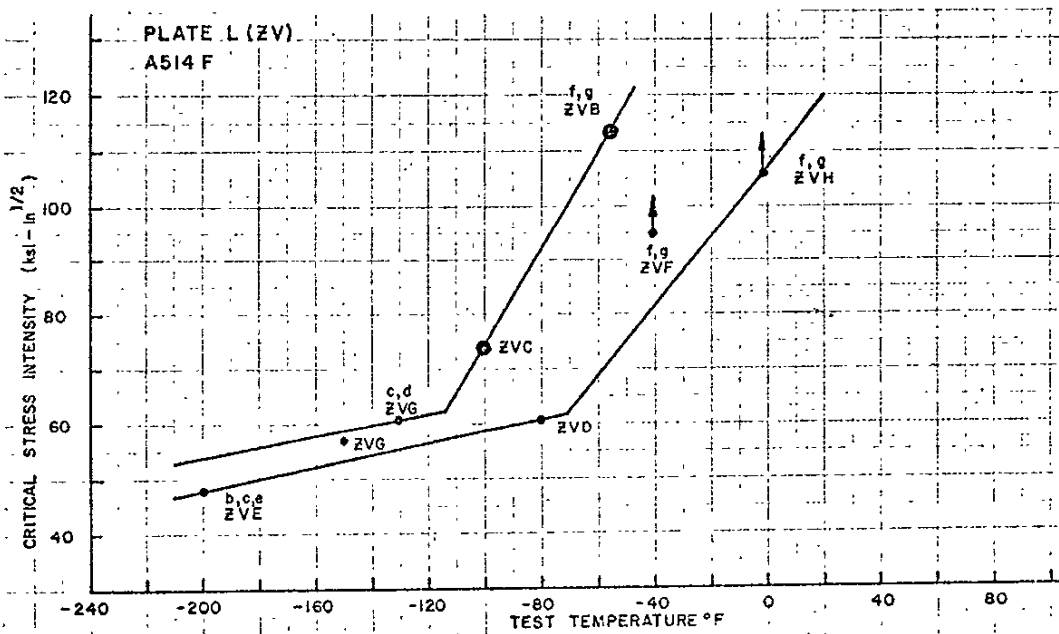
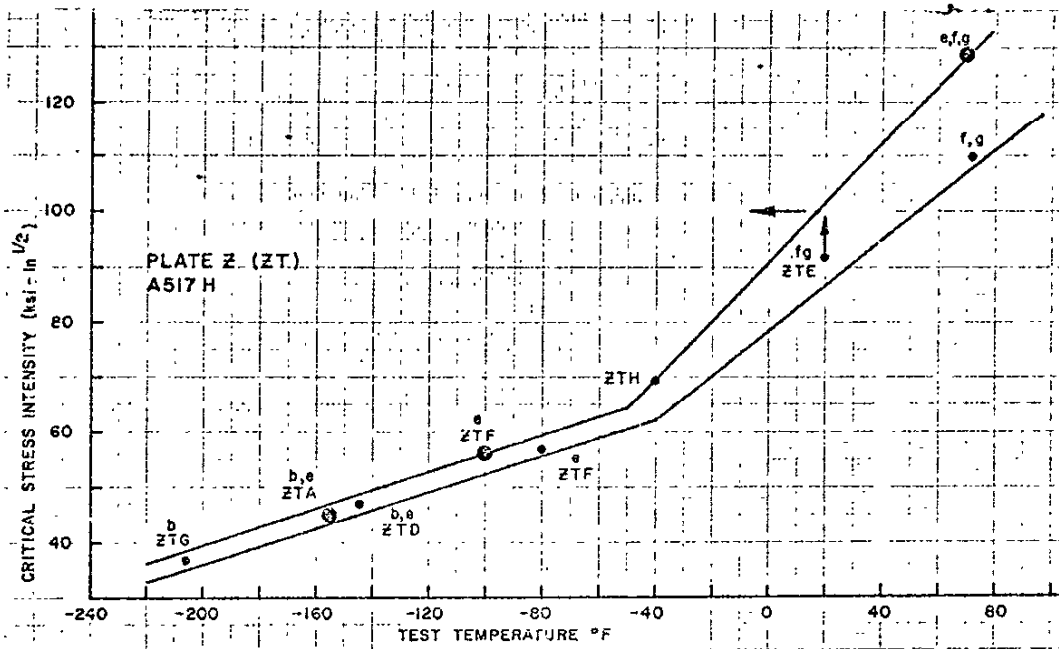
With $K_{FF} > 0.60 (F_{TY}/F_{TYTT})K_Q$ and the resulting large plastic zone at the crack tip, it would be expected that $K_Q > K_{IC}$; this observation is supported by Brown and Srawley(40). Kauffman(41) on the other hand, has observed the opposite behavior in some aluminum base alloys, i.e., $K_Q < K_{IC}$. In Kauffman's tests, with K_{FF} as high as 0.75 K_Q , the K_Q value varied from equal to K_{IC} to 10 percent less than K_{IC} . Based on the above observations, it seems reasonable to assume $K_Q = K_{IC}$ for $K_{FF} < .75K_Q$ and $K_Q > K_{IC}$ for $K_{FF} > .75 K_{IC}$.

The second most common discrepancy was an insufficient crack length as measured in the free surfaces. ASTM E399 specifies that the length of the surface trace of the crack in both surfaces shall be at least 90 percent of the average crack length. From Table 4.22 it will be seen that the shortest crack in the specimens tested was 72.8 percent of the average crack length; furthermore, that particular specimen (ZYA) showed no crack growth beyond the notch in one surface. Thus, that specimen was invalid in two counts. All the rest of the specimens violating this requirement had crack lengths in excess of 80 percent of the average crack length (a_0) in the free surface. With the exception of specimens taken from Plate AL, the crack lengths at the surface were greater than 0.85 a_0 and generally on the order of 0.88 a_0 . ASTM E399 makes

no distinction between specimens with a straight notch and with a chevron notch. It seems logical to assume that there would be little if any effect on KQ with a chevron notch as long as there is measurable crack extension in the free surfaces. For 1.0-inch and 2.0-inch thick specimens, the difference between 0.88 and 0.90 a_0 is approximately 0.02 inch and 0.04 inch, respectively.

A comparison of calculated fracture-toughness values obtained from valid and ASTM-"invalid" tests (Tables 4.19 and 4.20) provides some insight into the effect of these discrepancies. For example, in Plate L (Figure 4.76.1), specimens ZVE and ZVG with three and two discrepancies, respectively, were only slightly variant with respect to valid specimen ZVI. Specimen ZVD which was also valid, on the other hand, appeared to give a significantly lower value than would be expected. In Plate Z (Figure 4.76.1) there was remarkably little scatter introduced by the precracking discrepancies in spite of the fact that three of the specimens involved excessive maximum stress intensity values in fatigue precracking. Note also that specimens ZTC and ZTF, with crack lengths in the free surfaces of less than 90 percent of the average crack length also fell within a narrow scatter band. Specimen ZTC was a 2-in. thick specimen. In Plate AL (Figure 4.76.2), a comparison of specimens ZYC and ZYA, both 2-in. thick, indicated that the precracking discrepancies tended to produce slightly higher KQ values of 40.2 ksi-in.^{1/2} for ZYA with five discrepancies and 33.9 ksi-in.^{1/2} for ZYC with three discrepancies. When 1-in. specimens ZYD and ZYH, with four and two discrepancies respectively, are compared the opposite result is seen as ZYD gave the lower KQ value of 48.3 ksi-in.^{1/2}.

Plate R had wide scatter (Figure 4.76.2) with three specimens on the high side of the band, viz., two valid specimens ZXH and ZXC, and specimen ZXE with two discrepancies. On the low side of the band, there were two specimens, ZXB with one discrepancy and ZXF with four discrepancies. Specimen ZXD, a valid test, fell in the center of the scatter band.



**COMPACT TENSION TEST RESULTS SHOWING SCATTER
PRODUCED BY DEVIATING FROM ASTM E399 TEST
REQUIREMENT — PLATES Z AND L**

FIGURE 4.76.1

4.4.1.2 Effect of Specimen-Size Discrepancies

A common discrepancy in the specimens tested above the transition temperature was that the toughness was too great for the crack-length and specimen-thickness requirement; i.e., several of the test results were invalid because the thickness (B) and crack length (A) were less than $2.5 (KQ/FTY)^2$. There has been considerable controversy regarding this requirement; some feel that it may be too conservative(42) and others that it may be too liberal(43). It has been observed(42,43,44) that if specimens are machined in the same dimensional ratio as specified in ASTM E399-70, KQ will be less than K_{IC} when B is less than $2.5 (KQ/FTY)^2$. Consider, for example, the results when 1.0-in. and 2-in. thick specimens of a given material were tested at the same temperature.

<u>Specimen</u>	<u>Thick.</u>	<u>Temp.</u>	<u>KQ</u>	<u>$2.5 (KQ/FTY)^2$</u>
ZUH	1.0	-103	100.6	1.65
ZUA	2.0	-100	107.8	1.89 (valid)
ZXI	1.0	76	95.9	1.78
ZXA	2.0	75	101.7	1.99 (valid)
ZVF	1.0	-40	95.2	1.77
ZVB	2.0	-55	114.2	2.46
ZTI	1.0	72	110.5	2.17
ZTB	2.0	76	129.1	2.96

Note that in the case of the 2-in.-thick ZUA and ZXA specimens (both valid tests), the KQ (K_{IC}) values were slightly higher than the companion 1-in.-thick KQ values. Likewise in the case of 2-in.-thick specimens ZVB and ZTB with toughness too high for valid testing in 2-inches, the trend was the same.

Of the 21 specimens that were invalid because the thickness and/or crack length were less than $2.5(KQ/FTY)^2$, ten specimens had a PFAIL-to-PQ ratio at or close to unity (for two of the specimens, the ratio was 1.04). For these ten specimens, the assumption that

$K_Q = K_{Ic}$ should introduce only a minimal error. It has since been adopted (E399-74) that the ratio P_{max}/P_Q be limited to a value of 1.10 or less. The reason for this is to limit the amount of crack-tip plasticity contributing to P_Q . If the ratio P_{max}/P_Q does not exceed 1.10, it would be reasonable to assume that any deviation from linearity would be due to crack extension and not to plastic deformation.

4.4.2 Plate-to-Plate Variability in K_{Ic}

Among the many heats and plates examined, there was only one case where there were two flange plates tested from a single slab. This was in A517 grade-H heat/slab 1027/44. Two 30-in.-wide flange plates of this material were tested; one plate was the fractured flange in the Bryte Bend bridge (1027/44CK-1) and the second plate was cut from the bridge in another location (1027/44CK-2).

Eleven compact tension (CT) specimens were machined from plate CK-2 and tested at various temperatures. The purpose of these tests was to determine the plate-to-plate variability in plane-strain K_{Ic} fracture toughness.

The test results are presented in Table 4.23; the values of critical stress intensity are considered valid and quantitative based on the following observations: (1) the fatigue precracking stress intensity was less than $0.6 K_{Ic}$; (2) the difference between the three crack measurements in each specimen (at 1/4, 1/2, and 3/4 thickness) was less than 5 percent of the mean crack (a_o); (3) all measurements of fatigue crack depth were greater than $0.05 a_o$ or 0.050-in. whichever is greater; (4) the fatigue crack depth at the free surfaces was greater than $0.9 a_o$; (5) the plane of the fatigue crack deviated from the plane of the machined notch by less than 10 degrees; (6) the specimen thickness (B), and the crack length (a_o) both satisfied the requirement that B and $a_o \geq 2.5 (K_{Ic}/FTY)^{1/2}$; and (7) the load rate was about 70 ksi-in.^{1/2} per minute for all test specimens.

TABLE 4.23

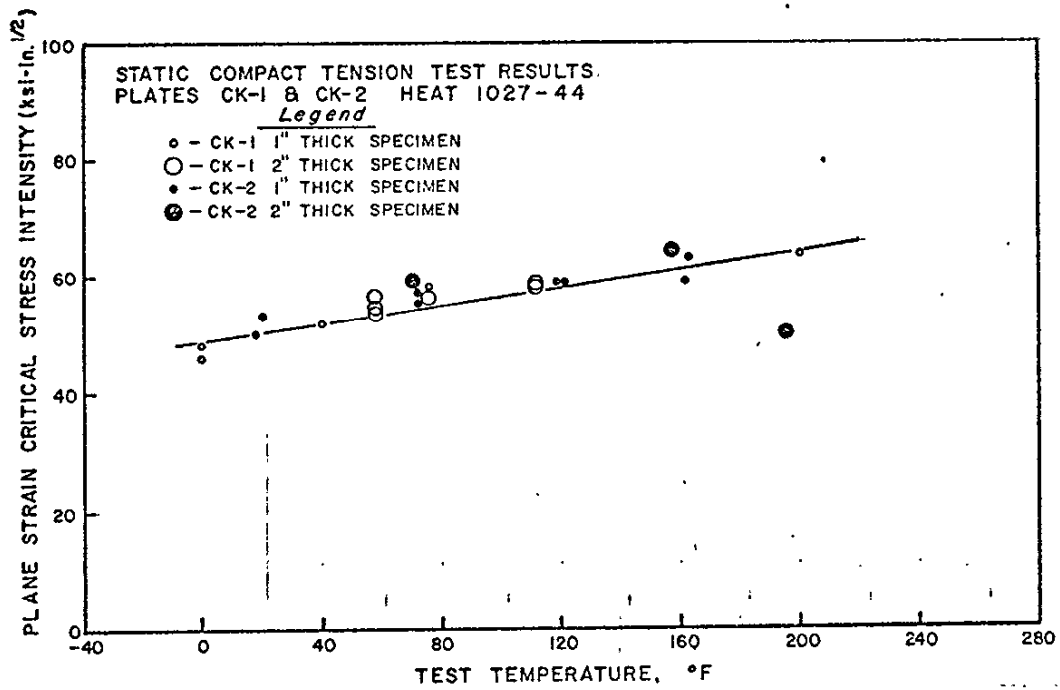
SUMMARY OF COMPACT-TENSION TEST RESULTS FROM A517 GRADE-H PLATE CK-2

Specimen No.	Test Temp. (°F)	Fatigue Final $1/2$ ksi-in.	Crack Depth (a)	Failure Secant PQ (kips)	Load Maximum (kips)	Ratio a/W	Critical Stress Intensity $1/2$ (ksi-in.)	Valid Min. Thick (in.)
22CK1B	18	27.8	0.951	7940	8290	0.475	50.2	0.44
22CK1T	20	28.0	0.954	8325	8325	0.477	53.0	0.48
22CK2B	73	27.8	0.951	8720	9030	0.475	55.0	0.52
22CK2T	73	28.4	0.965	8800	9060	0.482	56.8	0.56
22CK4B	119	27.5	0.941	9450	10325	0.470	58.9	0.60
22CK4T	122	28.2	0.960	9150	9800	0.480	58.7	0.60
22CK3B	163	28.2	0.958	9850	10400	0.479	63.0	0.69
22CK3T	162	28.2	0.961	9250	10600	0.480	59.3	0.61
TWO-INCH THICK								
22CK1T	70	27.2	1.925	25800	25800	0.481	58.6	0.60
22CK2T	158	27.6	1.941	28100	30150	0.485	64.6	0.72
22CK3T	195	27.2	1.925	22250	30450	0.481	50.5	0.44

The test results (Table 4.23) from the CK-2 test series were plotted in Figure 4.77 along with the results from the CK-1 test series (see Tables 4.19 and 4.20). Except for one data point, the data were remarkably consistent irrespective of the plate tested, and irrespective of whether one-inch or two-inch compact-tension specimens were used. The latter observation is consistent with the fact that with only one exception (specimen ZZE), all tests were valid according to the requirements of ASTM E399-70. The anomalous behavior of the 2-in.-thick specimen tested at +195°F is unexplained; this test met all E399 requirements. The low value was the result of a pop-in which determined the K_{IC} .

4.4.3 Discussion of the K_{IC} Test Results

Table 4.24 is a summary of the test results as plotted in Figures 4.70 to 4.76. Fractographic examination revealed increasing amounts of dimpled rupture (ductile fracture) above the lower inflection in the K_{IC} versus temperature plots. Thus, this point was taken as the onset of elastic-plastic behavior under static-load conditions. The corresponding inflection point under dynamic loading was 50°F to 240°F higher, except for plate CK (the heat which fractured in the Bryte Bend bridge). No inflection in the K_{IC} or precrack Charpy "transition" curves was found for plate CK. The K_{IC} values at the onset of plastic behavior are only of academic interest in plates L, M, A, and R because the temperatures are so low (minus 120°F and lower). However, the critical-stress-intensity values corresponding to the onset of elastic-plastic behavior in two of the three steels from the Bryte Bend bridge (AL and CK) are of concern, since they correspond to a dangerously small critical edge crack (approximately 0.6-in. or smaller) at temperatures that could occur in continental U.S. (Table 4.24).



STATIC COMPACT-TENSION TEST RESULTS FOR A517 GRADE-H
 PLATES CK-1 AND CK-2 FROM HEAT/SLAB 1027-44

FIGURE 4.77

TABLE 4.24

TEMPERATURE AT THE ONSET OF ELASTIC-PLASTIC BEHAVIOR UNDER PLANE-STRAIN STATIC LOADING AND CALCULATED CRITICAL CRACK SIZES AT THE LAST FOR AASHTO-74 GROUP-1 SERVICE

ASTM Type-Grade	Report Code Heat/Slab	Plate ID	Onset of Elastic- Plastic Behavior in Static Loading		K _{IC} (KSI-In. ^{1/2})	KQ (KSI-in. ^{1/2})	Critical Crack Size* (@0°F)	a _{cr} (in.)
			Temp (°F)	K _{IC} (KSI-In. ^{1/2})				
A514-F	1017/62	L	-120	60		>120	> 2.28	
	1014/02	M	-240	40		>120	> 2.28	
A517-F	1026/92	A	-200	55		100	1.58	
A514-H	1019/31	R	-120	45		80	1.02	
A517-H	1024/94	Z	-60	60		>90	> 1.28	
	1020/46	AL	-20	60		60	0.57	
	1027/44	CK	+200	65		45	0.32	

*Based on the measured critical stress intensity (KQ) at 0°F and assuming an edge crack in a 30-in.-wide flange with a working stress of 40 KSI.

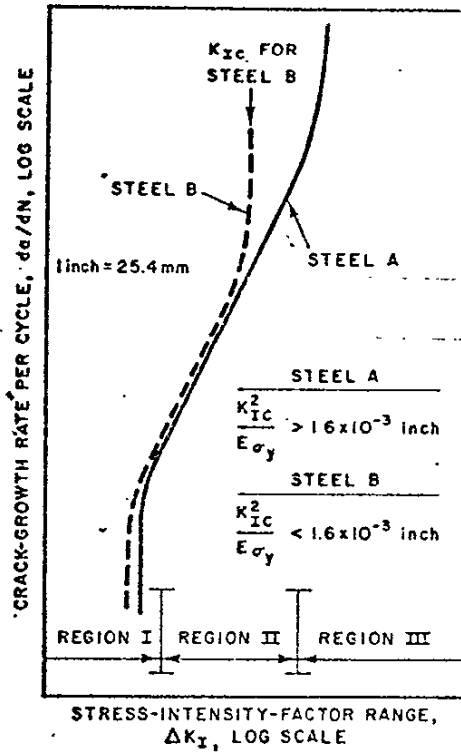
Edge cracks may occur in Q and T steels in flame cutting plates to flange width or as the result of welded attachments (cross bracing, stay-in-place forms, etc.). In the Bryte Bend bridge the crack which initiated the brittle fracture started as a welding hot crack in the flange edge. With a K_{IC} of only 45 ksi-in.^{1/2} at 0°F (55 ksi-in.^{1/2} at +60°F), there was danger not only of brittle fracture initiating from edge cracks, but also of an accelerated fatigue crack growth rate (see region III, Figure 4.78 from NCHRP 12-14)(46). In other words, if the crack in the Bryte Bend bridge flange had not reached critical crack size during construction, the combination of low toughness and hot-crack susceptibility in welding(47) might have resulted in accelerated fatigue crack growth and failure in a time less than the planned life of the bridge. NCHRP 12-14 final report, September 1974 points out that:

"the fatigue-crack-growth rate increases markedly ... when the value of the maximum stress-intensity factor becomes close to the K_{IC} of the material."

Likewise, Clark of Westinghouse Electric Corporation(48), in discussing the three regions of the log-log da/dN versus ΔK plot points out that:

"Region III represents unstable crack growth encountered just before the specimen fails. The ΔK level associated with the transition from Region II to Region III crack growth depends upon the inherent toughness of the material."

Thus both Barsom and Clark caution that low static plane-strain K_{IC} fracture toughness can have an effect on the fatigue life of our bridges. The following paragraphs deal with the question as to what level of toughness is required.



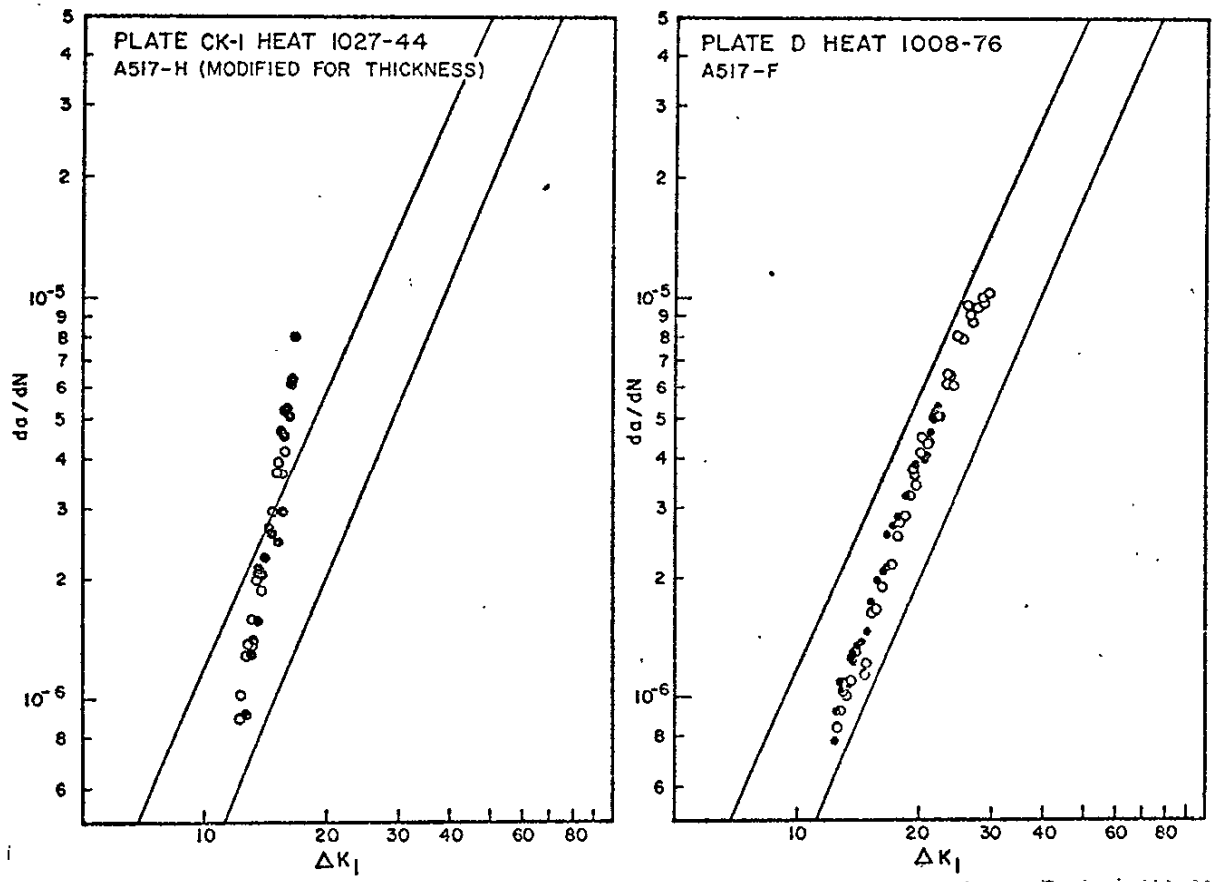
SCHEMATIC REPRESENTATION OF FATIGUE - CRACK GROWTH IN STEEL (46)

FIGURE 4.78

4.4.4 Subcritical Crack Growth in Plate CK

One-inch WOL (compact tension) specimens from plate CK (A517 grade-H heat 1027/44) and, for comparison, Plate D (A517 grade-F heat 1008/76) were tested in the Caltrans Laboratory. The procedure used was generally the same as that in the NCHRP 12-14 study(46). One notable difference in test procedure was the starting stress and the stress ratio. The NCHRP 12-14 fatigue-crack-growth-rate tests in air were conducted at a 10 percent stress ratio ($R = 0.10$); Caltrans used a stress ratio of $R = 0.73$ corresponding to a bridge working stress of 45,000 ksi and a dead-load stress of 33,000 psi. In NCHRP 12-14, $R = 0.10$ corresponded to a minimum stress of 1016 psi and a maximum stress of 16,250 psi at the start of the 1-in. WOL testing, which is unrealistic in terms of dead-load and dead-load plus live-load stresses in a bridge of 100-ksi yield-strength steel. The NCHRP 12-14 test procedure presumably was based on the premise that stress ratio (minimum/maximum stress has little or no effect on the crack-growth rate. The Caltrans testing did not make this assumption, and used stresses at the start of each test that were approximately the stresses that would be expected in a bridge designed with 100-ksi yield-strength steel.

Test results obtained with the CK- and D-plate samples plotted in Figure 4.79(49). Note that the initial stress-intensity range was approximately $12.5 \text{ ksi-in.}^{1/2}$ as compared with the NCHRP 12-14 initial stress-intensity range of $15 \text{ ksi-in.}^{1/2}$. The NCHRP 12-14 test results are represented by a scatter band showing the equation that is commonly used for martensitic (Q and T) steels. The data from plate D fell within the scatter band but with a somewhat steeper slope. Plate D had a CVN-impact value of 60 ft-lb at room temperature which corresponds to a K_{IC} of $176 \text{ ksi-in.}^{1/2}$. The CK plate, on the other hand, had a K_{IC} value of only $57 \text{ ksi-in.}^{1/2}$ at room temperature. The



LOG-LOG da/dN VS. ΔK PLOTS FOR TWO 1-INCH-WOL FATIGUE CRACK GROWTH RATE TESTS OF EACH OF TWO PLATES - A517-F PLATE D AND A517-H PLATE CK TESTED AT 45 KSI MAXIMUM STRESS AND A 0.73 STRESS RATIO

FIGURE 4.79

rapidly increasing crack-growth rate with increasing stress-intensity range in the CK plate and the attendant loss of fatigue life (100,000 cycles in CK versus 350,000 cycles in D) in the 1-in. WOL test was assumed to be primarily the result of low fracture toughness in the CK plate.

An equation is available which takes into account both stress-ratio and the accelerating effect of low fracture toughness when the stress-intensity factor approaches the K_{IC} value(50,51)

$$da/dN = C \Delta K^p / K_{IC} (1-R) - \Delta K \quad (4.15)$$

where C and p are the power-law constants and R is the stress ratio. The constants for both the Paris equation (Region II of Figure 4.78)

$$da/dN = A (\Delta K)^n \quad (4.16)$$

and the Forman equation (4.15) were determined by computer(52).

<u>Plate</u>	<u>Coefficient</u>	<u>Exponent</u>	<u>Equation</u>
D	0.251×10^{-9}	3.219	Paris
	0.550×10^{-7}	2.357	Forman
CK-1	0.265×10^{12}	6.03	Paris
	0.112×10^{-5}	0.385	Forman

Note that the plate-D constants for the Paris power-law equation are different from those commonly used for martensitic steels(46), viz.,

Coefficient	6.6×10^{-9}
Exponent	2.25

This difference may be the result of the larger stress ratio (0.73 as compared with 0.10) used in this study. The marked difference

in the CK-plate constants is attributed to Region III behavior, viz., accelerated crack growth as a result of low plane-strain K_{IC} fracture toughness.

4.4.5 Effect of Regions II and III on Fatigue Life

Numerical-integration procedures for estimating the fatigue life of a bridge or a building have been described in the published literature(53,54,55). The approach has evolved over the last decade, and is based on the assumptions (1) that there are preexisting flaws or cracks in a structural component, or that cracks are initiated early in the life of the component (perhaps by pop-in from a weld where there is high residual stress and/or metallurgical embrittlement), and (2) that the fatigue life of the component is determined by (a) the rate of growth of such cracks under cyclic loading and (b) the critical crack size (the fracture toughness) of the material. How fast the initial crack will grow can be determined by fatigue-crack-growth-rate testing; ASTM is presently attempting to standardize the test method(56). The critical crack size can be determined by ASTM E399 compact tension testing, or estimated by CVN- K_{IC} or PCI- K_{IC} correlations.

In connection with the Bryte Bend bridge failure, a computer was programmed to determine the fatigue life based on the published numerical-integration procedures and the following variables specific to the Bryte Bend bridge design:

- (1) flange width (30 inches)
- (2) type of cracking (edge)
- (3) crack growth rate constants (present program utilizes Barsom's constants from NCHRP 12-14, Figure A-3, p. 132)

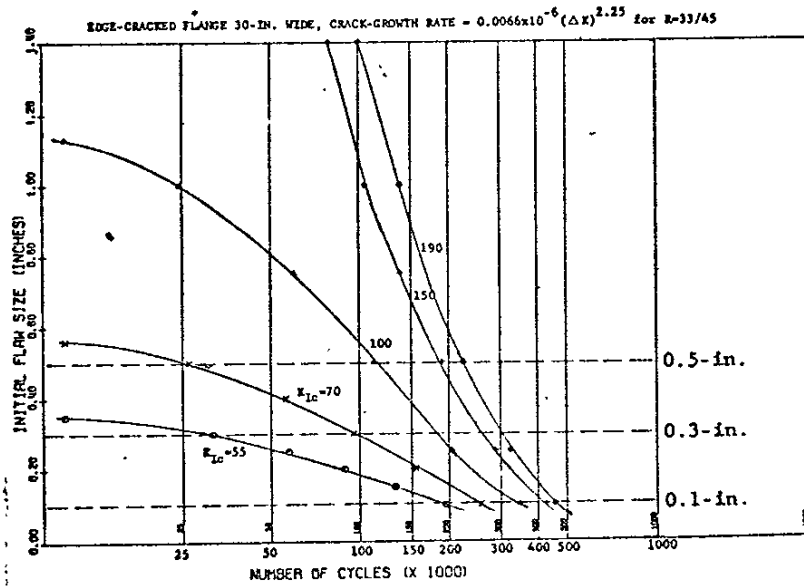
- (4) maximum stress (45 and 39 ksi)
- (5) fatigue-stress range (12 and 6 psi)
- (6) level of fracture toughness (55, 70, 100, 150, and 190 ksi-in.^{1/2} K_{IC}).

The program included plotting of the curves. Figures 4.79.1 - 4.79.3 show the computer-plotted curves based on equation 4.16 and the crack-growth-rate power-law constants determined in NCHRP 12-14 for martensitic steel.

In connection with these plots, it should be noted first of all that with very small edge cracks of the order of 0.10 in. or shallower, the fatigue crack growth may be in Region I (Figure 4.78) where the crack growth rate is exceedingly small. Thus, with initial crack sizes of the order of 0.10 in., the curves should be turning parallel to the X-axis, indicating longer life than shown in Figures 4.79.1 - 4.79.3. However, with edge cracks greater than say 1/4 in. deep, the life of a 30 in. wide flange is predicted to be alarmingly short for low-toughness steel using the numerical integration procedure as proposed by Professor Rolfe (53,54) and Wei (55). Table 4.25 is a summary of the calculated life (cycles to failure) based on fatigue crack growth rate and critical crack size. Again, in this table, it should be noted that with small initial crack sizes of the order of 0.10 in., the Region I phenomenon will result in even greater life than indicated by the calculated values. With fabrication and inspection such that the largest initial crack is 0.10 inch or smaller, the toughness of the steel is of little consequence; even brittle 55 ksi-in.^{1/2} steel is indicated to have a life expectancy of the order of 250,000 cycles with a 12-ksi stress range. However, in bridges, larger cracks can and do escape detection in heavy sections, with incomplete penetration welds and/or with an

INITIAL FLAW SIZE VS. CYCLES TO FAILURE

- $R = 33$
- $R = 45$
- $R = 100$
- $R = 200$
- ◇ $R = 300$
- △ $R = 400$

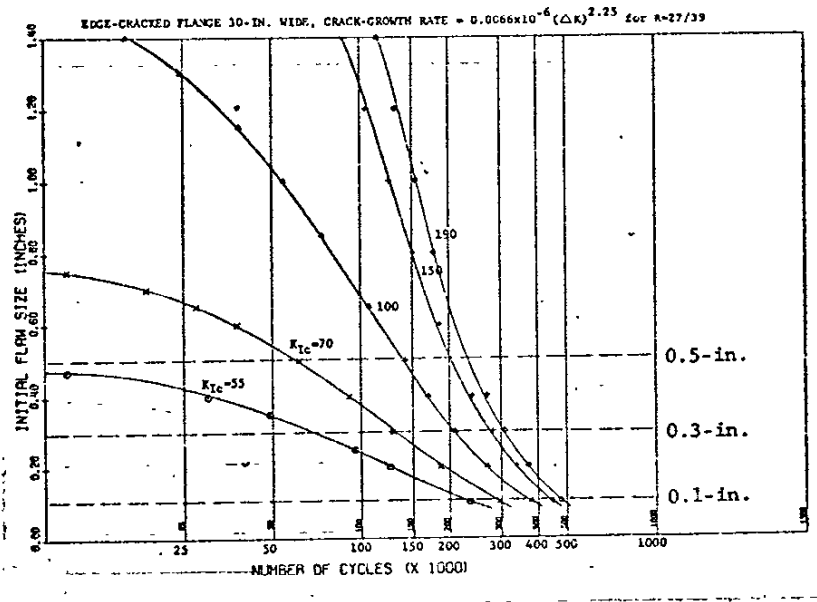


COMPUTER PLOTTED CURVES SHOWING FATIGUE LIFE OF AN EDGE CRACKED 30" WIDE FLANGE WITH $R=33 \text{ ksi} / 45 \text{ ksi}$

FIGURE 4.79.1

INITIAL FLAW SIZE VS. CYCLES TO FAILURE

- K_{IC} = 155 K
- K_{IC} = 150 K
- K_{IC} = 110 K
- K_{IC} = 70 K
- K_{IC} = 55 K

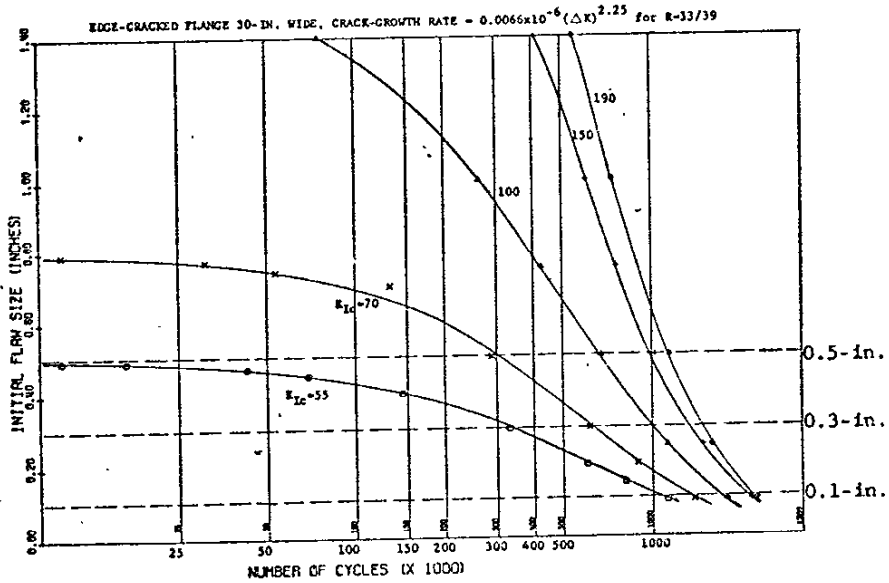


COMPUTER PLOTTED CURVES SHOWING FATIGUE LIFE OF AN EDGE CRACKED 30" WIDE FLANGE WITH R=27 ksi/39Ksi

FIGURE 4.79.2

INITIAL FLAW SIZE VS. CYCLES TO FAILURE

- $R_c = 30$
- △ $R_c = 35$
- × $R_c = 40$
- $R_c = 45$
- $R_c = 50$



COMPUTER PLOTTED CURVES SHOWING FATIGUE LIFE OF AN EDGE CRACKED 30" WIDE FLANGE WITH R=33ksi/39ksi

FIGURE 4.79.3

insufficient number of trained welding inspectors. In the Bryte Bend bridge, there were 3/4-in.-deep cracks in the flange edges, found after the failure at the junction of cross bracings and flange plates of A517-H heat 1027 ($K_{IC} = 55 \text{ ksi-in.}^{1/2}$ at 60°F). These either occurred after inspection (delayed cracking) or were not detected during inspection.

Figures 4.79.1 - 4.79.3 and Table 4.25 show that with cracks of the order that can and do sometimes escape detection, the plane-strain fracture toughness of the steel can have a very significant effect on the life of a flange plate.

Among fracture-mechanics experts, it is generally accepted that if fatigue-crack growth occurs and the crack-growth rate conforms to the Paris power law (equation 4.16) then the life of a structural member can be estimated by the numerical integration procedure proposed by Professors Rolfe and Wei. Professor Fisher(57) acknowledges the usefulness of the fracture mechanics approach to crack propagation

"The fracture mechanics approach to crack propagation appears to be the most rational method currently available for predicting the fatigue life".

Professor Fisher(57) uses the numerical integration procedure, but he integrates to an arbitrary "final size (a_f)" rather than the critical crack size as determined from fracture-toughness and maximum-stress considerations. Moreover, Professor Fisher has placed very little if any emphasis on maximum stress, stress ratio and/or fracture toughness as factors determining the life of a bridge member.

Figures 4.79.1 - 4.79.3, based on a single crack configuration - the edge crack, indicate that with cracks of about 0.3 inch and deeper, the life of a 30-in/-wide flange will be less than 100,000

TABLE 4.25

PREDICTED LIFE IN A 30-INCH-WIDE FLANGE AS A FUNCTION OF
EDGE CRACK DEPTH, FRACTURE TOUGHNESS AND STRESS RANGE

Initial Flaw Size	Fracture Toughness	MAXIMUM STRESS 39 KSI					
		Critical Crack	Cycles to Failure	Critical Crack	Cycles to Failure	Critical Crack	Cycles to Failure
0.10	55	0.503	1,117,404	0.503	0.503	234,905	
0.30	55	0.503	333,554	0.503	0.503	70,121	
0.50	55	0.503	3,881	0.503	0.503	816	
0.10	70	0.812	1,406,941	0.812	0.812	295,776	
0.30	70	0.812	623,109	0.812	0.812	130,992	
0.50	70	0.812	293,436	0.812	0.812	61,687	
0.10	100	1.617	1,789,429	1.617	1.617	376,190	
0.30	100	1.617	1,005,633	1.617	1.617	211,406	
0.50	100	1.617	675,960	1.617	1.617	142,101	

cycles when (1) A514/517 steel is used with K_{IC} values of 70 ksi-in.^{1/2} or lower, (2) the design allowable is 45 ksi and (3) the stress range 12 ksi. Two of the three A514/517 grade-H steels from the Bryte Bend bridge tested by the ASTM E399 compact tension method had K_{IC} values of less than 70 ksi-in.^{1/2}; the CK plate had K_{IC} values of less than 55 ksi-in.^{1/2} at temperatures anticipated in service (Figure 4.77).

The use of 100,000-psi steel has generally been utilized in bridges with large dead loads in combination with lane loading for live load and, was governed by the 100,000-cycle fatigue criterion. In the 1974 AASHTO Interim Specification, the 100,000-cycle criterion was changed to 500,000 and 100,000 cycles. The toughness required to meet the 100,000-cycle criterion appears reasonable from the standpoint of both the maximum stress allowable and the maximum size of crack that may escape detection. From Figure 4.79.2 note that with working stresses such as those in the Bryte Bend bridge, an edge crack up to 0.7-inch deep would have allowed 100,000 cycles of life in the flange before the crack would grow to critical size if the fracture toughness of the steel had been at least 100 ksi-in.^{1/2} at the lowest anticipated service temperature. Based on the U.S. Steel upper-shelf correlation, the AASHTO-74 CVN-impact energy requirement of 25 ft-lb corresponds to a K_{IC} value of approximately 100 ksi-in.^{1/2}. However, based on the transition-range correlation of the University of Illinois, 25 ft-lb CVN-impact energy corresponds to about 80 ksi-in.^{1/2} (equation 4.10). ASTM A514/517 "T-1" type steels are widely advertised as being typically tough, with plane-strain K_{IC} values of 120 ksi-in.^{1/2} or higher shown in published reports at temperatures above -60°F (see Figure 4.33).

In repair of the Bryte Bend and Tuolumne River bridges, the 1-3/8 in. to 1-1/2 in. thick A517 grade-F cover-plate steel had

CVN-impact values ranging from 35 to 65 ft-lb which, from the CVN- K_{IC} upper-shelf correlation, correspond to plane-strain fracture toughness values of

$$K_{IC} = 127 \text{ to } 182 \text{ ksi in.}^{1/2}$$

(see Table 4). These data are from nine (9) heats providing 43 slabs.

From Figure 4.79.3 note that with a reduced stress range (6 ksi) and a maximum stress of 39 ksi, a fracture toughness as low as 55 ksi-in.^{1/2} would give a life of 100,000 cycles with edge cracks up to 0.4 inch. However, to get 500,000 cycles of life with a maximum stress of 39 ksi, a stress range of 6 ksi and edge cracks up to 0.4-inch deep, a fracture toughness of about 80 ksi-in.^{1/2} is required (AASHTO-74 CVN-impact 25 ft-lb values). With 3/4 inch deep edge cracks such as existed in the Bryte Bend Bridge at the time of failure, a toughness of about 120 ksi-in.^{1/2} would have been required to get 500,000 cycles with a maximum stress of 39 ksi and a stress range of 6 ksi.

With a maximum stress of 39 ksi and a stress range of 12 ksi, numerical integration indicates that with the practical limitations that presently exist on both bridge-steel toughness and weld inspection, there is no way we can be assured of 500,000 cycles of fracture-safe service.

4.5 Drop-Weight NDT and Dynamic Tear Test Results

The DT test was developed at the Naval Research Laboratory (NRL) starting in 1960. For this investigation the specimens were tested at NRL using the NRL double-pendulum machine (see Figure 3.11). A standard procedure was used (MIL-STD-1601 (SHIPS) 8 May 1973) with a type-M (machined) notch, sharpened by pressing a sharp tip on the machined notch.

Specimens (5.8-in. thick) were machined from both the plate-surface and midthickness positions of one heat (1027/44CK). In four other heats the specimens were taken only from the mid-thickness position. All specimens were oriented in the plate so that the fracture would propagate transverse to the principal rolling direction of the plate, i.e., in the direction one would expect fracture in a bridge flange.

4.5.1 A517 Grade-H Heat 1027/44 CK

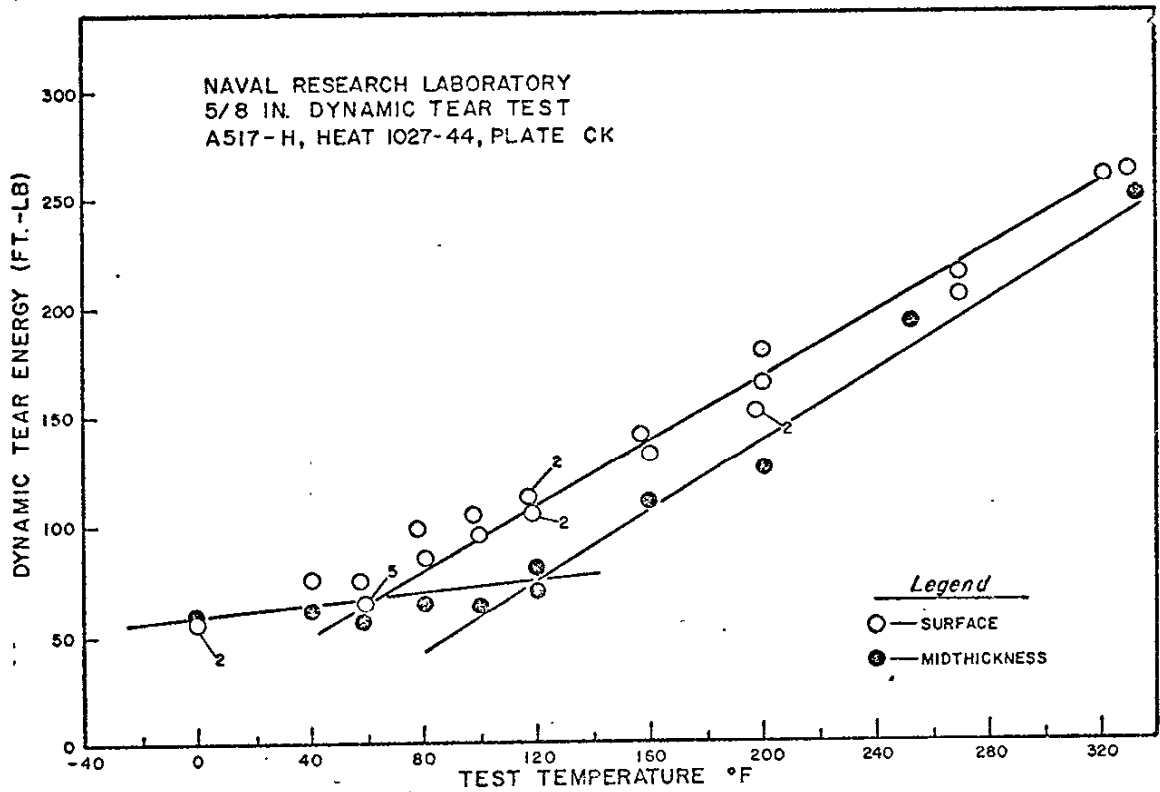
Table 4.26 gives the results obtained at three positions with respect to the 2-1/4-in. plate thickness. Note that the steel was indicated to have very low toughness over a wide range of temperature, with the lowest toughness at the midthickness position. Figure 4.80 confirms these observations, showing generally low toughness over and above the range of temperatures

TABLE 4.26

DYNAMIC TEAR TEST RESULTS FROM GRADE-H HEAT 1027/44CK
AS A FUNCTION OF THICKNESS POSITION

Steel Code	Test Temp (°F)	Thickness Position		
		Top (ft-lb)	Center (ft-lb)	Bottom (ft-lb)
1027/44CK	0	59	58	55
	40	--	61	76
	60	76-68-70	57-51-53	70-66-69
	80	99	65	84
	100	105	65	97
	120	105-112	71-79	104-109
	160	143	111	131
	200	157-150	128-126	180-165
	270	214	194(a)	205
	330	263	251	261(b)

(a) tested at 254°F
(b) tested at 325°F



DYNAMIC TEAR TEST RESULTS FROM A517 GRADE-H HEAT 1027/44 CK FOR SURFACE AND MIDTHICKNESS POSITIONS

FIGURE 4.80

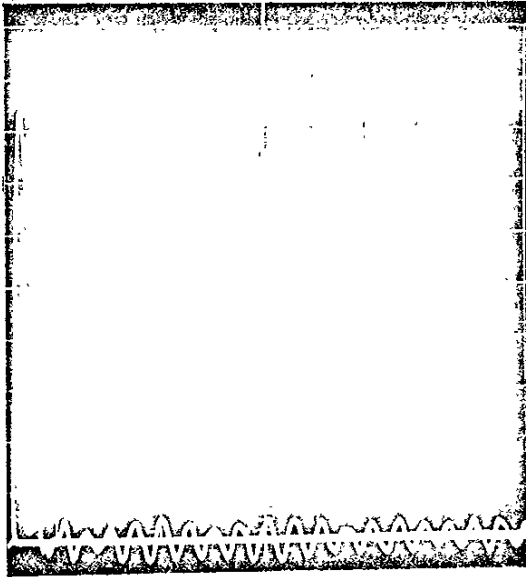
expected in service. Also there was a consistent but small difference with respect to thickness position, with midthickness less tough than the surface of the plate. The brittle nature of the midthickness position at temperatures below 120°F is confirmed in Figure 4.81, which shows representative Polaroid prints of the force-time traces for test temperatures of +60, +100, +200 and +330°F. A single spike in the force-time trace can be expected to occur at and below the nil-ductility-transition (NDT) temperature; whereas, at higher temperatures there are multiple spikes.

NRL investigators have reported that the beginning of the energy rise in the DT energy-temperature plot

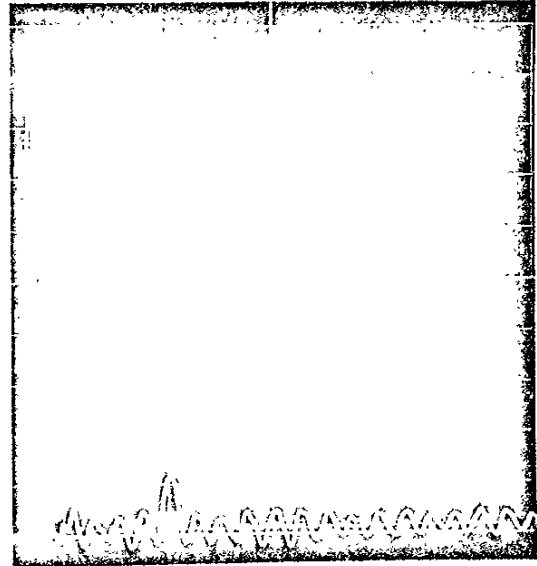
"...is invariably indexed to the drop-weight-test NDT temperature, because this temperature indicates the beginning of a rapid increase in microfracture ductility for the case of dynamic loading".

Thus, based on the energy-temperature plot and the force-time traces, the NDT temperature for the midthickness position is approximately +120°F, and +60°F for the surface-position plate material.

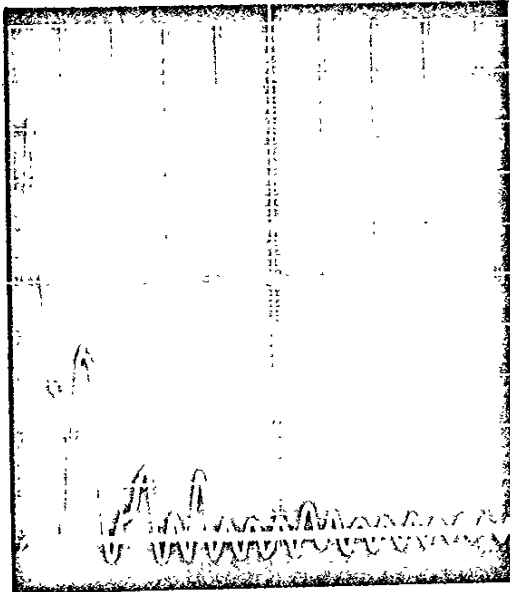
The atypical nature of heat 1027/44CK is further evidenced by the lack of an abrupt increase in DT energy with increasing temperature above the NDT. Many steels have been investigated at NRL using the DT test. NRL experience has shown that the DT energy curve can be divided into three toughness regimes. Regime 1 is associated with temperatures near NDT where small flaws can result in catastrophic failure under dynamic LEFM conditions. Regime 3 is associated with a high degree of plastic deformation where unstable fracture is impossible except by overload or buckling-type conditions.



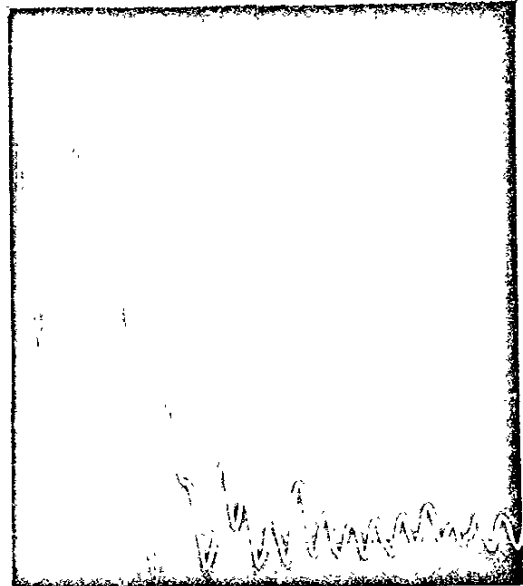
+60° F 57 FT-LB



+100° F 65 FT-LB



+200° F 126 FT-LB



+330° F 251 FT-LB

FORCE-TIME TRACES CORRESPONDING TO SELECTED
TEMPERATURES IN FIGURE 4.80 MIDTHICKNESS POSITION

FIGURE 4.81

Regime 2 corresponds to the transition between the two extremes in which nominal stresses approaching yield-strength magnitude are necessary to propagate fracture. The midpoint energy in regime 2 corresponds to the fracture-transition elastic (FTE) for steels of the A514/517 toughness level.

In heat 1027/44CK, there was no abrupt increase in DT energy with increasing temperature. Like the standard CVN-impact and precrack Charpy impact tests, the dynamic tear test energy-temperature plot showed a gradually increasing energy to fracture out to about 300°F.

The drop-weight NDT temperature testing, in accord with ASTM E208 Standard procedure was done at NRL using specimens from the surface of the CK plate. The NDT temperature from such testing was +80°F, which is in good agreement with the DT-NDT corresponding to regime 1 at +60°F.

4.5.2 Heats 1008/76D, 1020/46AL, 1024/91Y and 1026/92A.

Table 4.27 gives the results obtained in the midthickness position of two heats of A517 grade F and two heats of A517 grade H steel. Only one of these heats approached the quality level that is

TABLE 4.27
DYNAMIC TEAR TEST DATA

Test Temp	A517-F 1008/76D	A517-F 1026/92A	A517-F 1020/46AL	A517-H 1024/91Y
-100	92	- - -	- - -	- - -
-80	101	- - -	- - -	- - -
-60	147	- - -	- - -	- - -
-40	246	- - -	- - -	- - -
-20	- - -	- - -	80*	72*
0	515	59*	67*	68*
+20	- - -	88	96	108
+40	569	67*	126	141
+60	- - -	99	168	- - -
+80	- - -	121	207	204
100	- - -	- - -	- - -	- - -
120	- - -	123-124	265	301
140	- - -	- - -	- - -	- - -
160	- - -	271	349	399
180	- - -	- - -	- - -	- - -
200	- - -	224-234	303-386	448
220	- - -	- - -	- - -	- - -
240	- - -	- - -	- - -	479

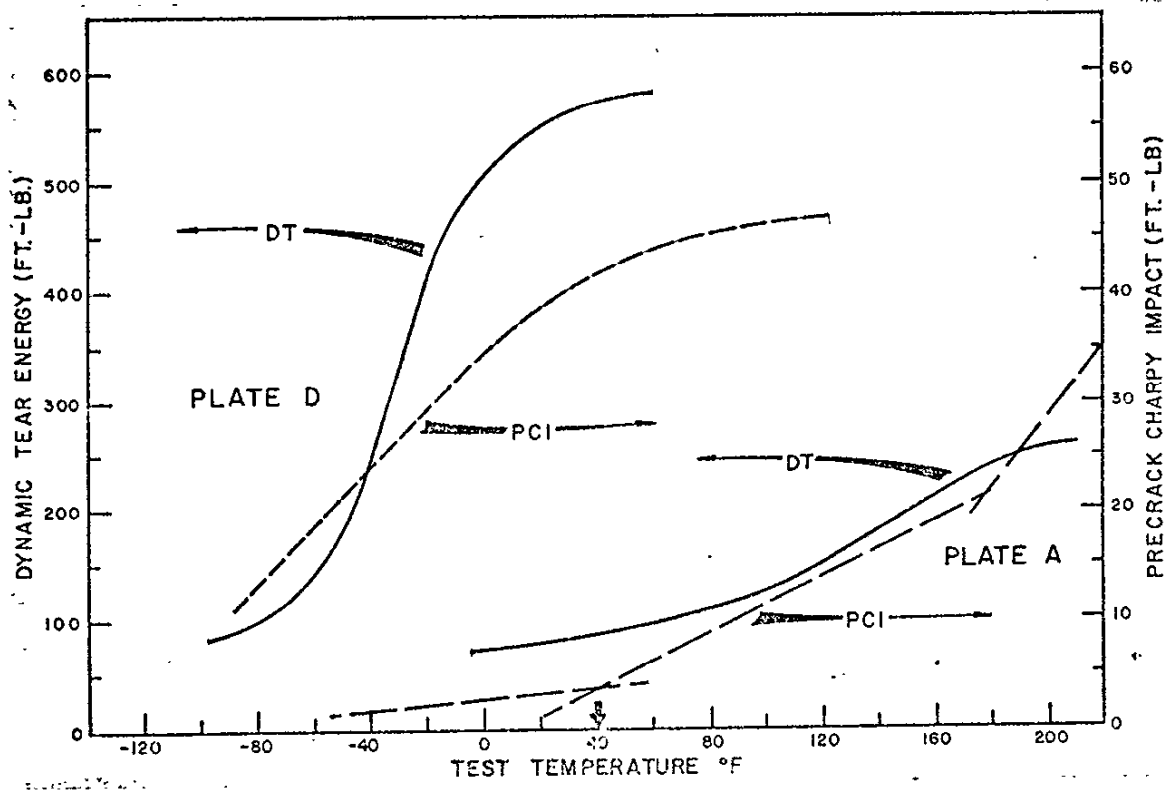
*Single Spike = Est. of NDT 235

generally considered to be typical of conventional pressure-vessel-grade steels at the 100-ksi yield-strength level. At this strength level (Q&T steel) one can expect regime 1 in the DT test to occur between -80 and -40°F , and regime 3 to correspond to a maximum energy of between 700 and 900 ft-lb in the 5/8-in. standard DT test(22).

Figure 4.82 shows the widely divergent test results obtained in two heats of A517 grade-F steel melted by different practices. Plate D was open-hearth steel with the boron protected by a prior addition of aluminum, vanadium and titanium. Plate A was D-H process electric-furnace steel with boron added to the ladle prior to the addition of aluminum and vanadium - no titanium was used in the melting practice. Plate A was indicated to have an NDT temperature of $+40^{\circ}\text{F}$ based on force-time traces (see Figure 4.83). The precrack Charpy impact test also indicated the NDT temperature to be at $+40^{\circ}\text{F}$; however, as will be shown in subsequent paragraphs, the NDT temperature for the midthickness-position was $+120^{\circ}\text{F}$.

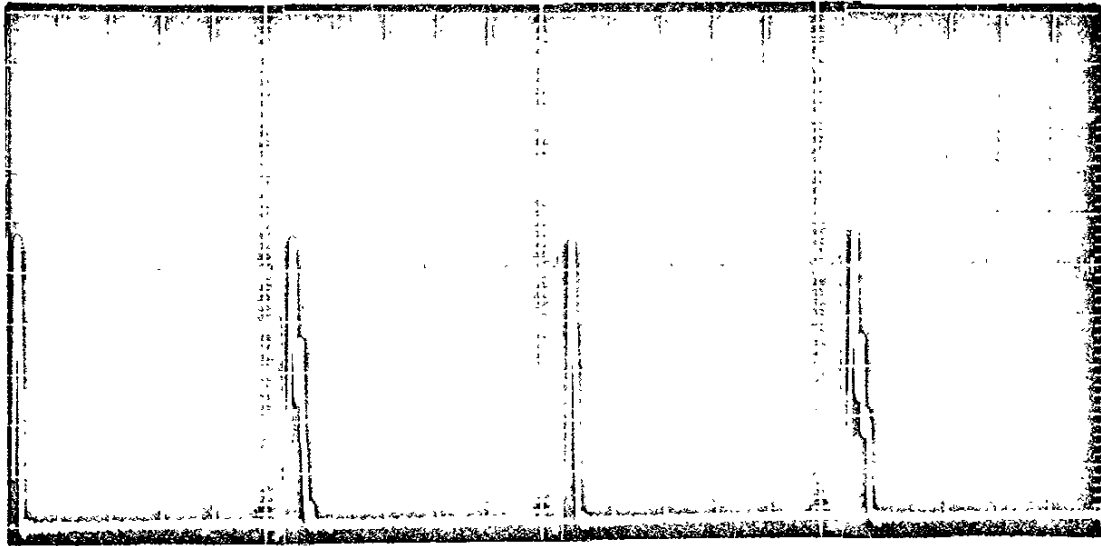
Figures 4.84-4.86 provide additional comparisons between the DT energy-temperature plots and the precrack Charpy impact transition curves. In Figure 4.84 note that the precrack Charpy impact "transition" curve showed no inflection; whereas, the DT test showed a small but reproducible change in slope at the DT-NDT temperature (regime 1). Figures 4.85 and 4.86 present the test results from two additional A517 grade-H heats. Note that the precrack Charpy impact test transition curves were somewhat more conservative than the DT energy-temperature curves.

Figure 4.87 is a summary plot comparing the DT test results from the two heats of grade-F steel (made with different melting practices) and three heats of grade-H steel (of the same melting practice as grade-F plate A). Note that grade-F Plate D was markedly superior to the other four heats of steel, with the Bryte Bend bridge casualty plate (CK) the poorest heat of all. The NDT temperatures indicated on this plot are discussed in the following section.

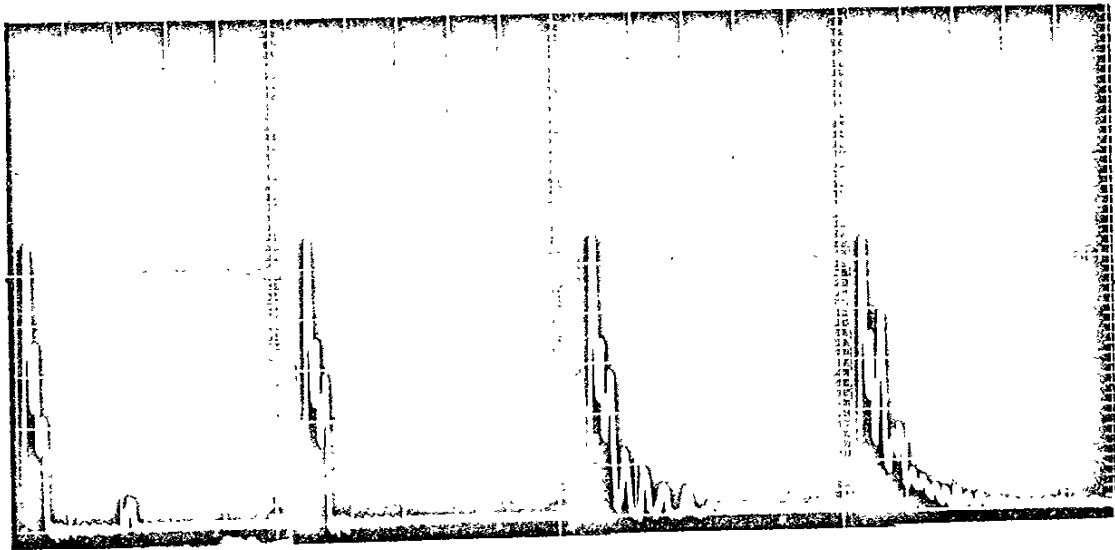


DYNAMIC TEAR AND PRECRACK CHARPY IMPACT TEST RESULTS FROM TWO HEATS OF A517 GRADE-F STEEL BY DIFFERENT MELTING PRACTICES

FIGURE 4.82



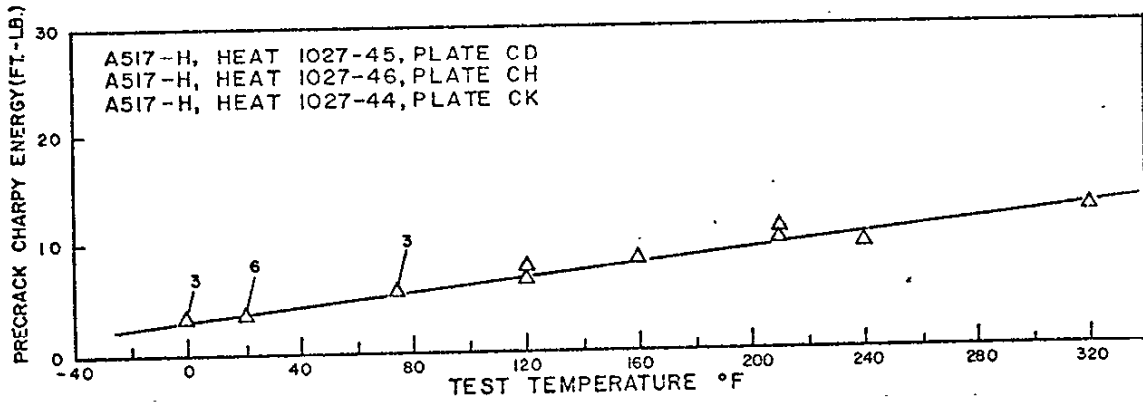
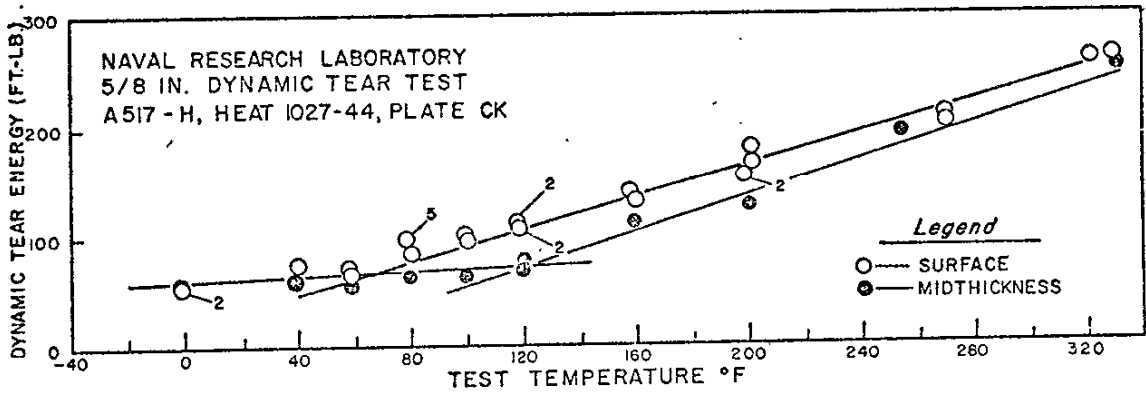
+0°F 59 FT-LB +20°F 88 FT-LB +40°F 67 FT-LB +60°F 99 FT-LB



+80°F 121 FT-LB +120°F 124 FT-LB +160°F 271 FT-LB +200°F 224 FT-LB

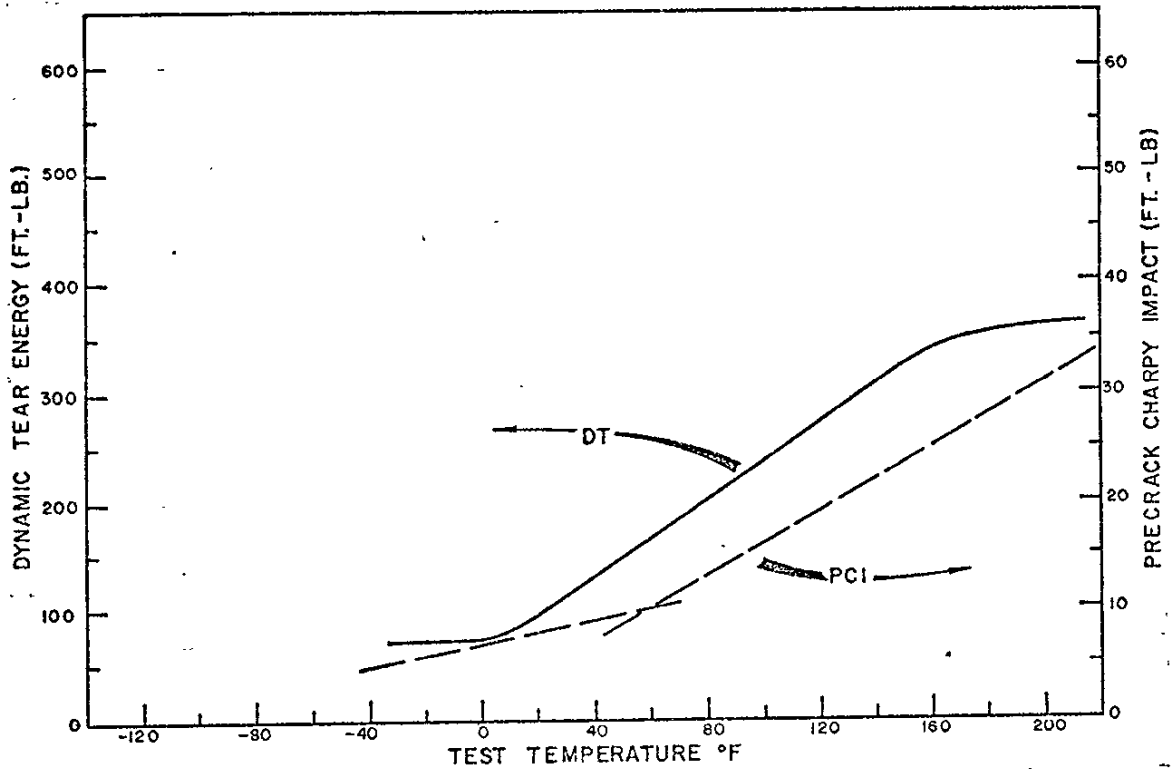
DYNAMIC-TEAR-TEST FORCE-TIME
TRACES OF A517 GRADE-F PLATE A

FIGURE 4.83



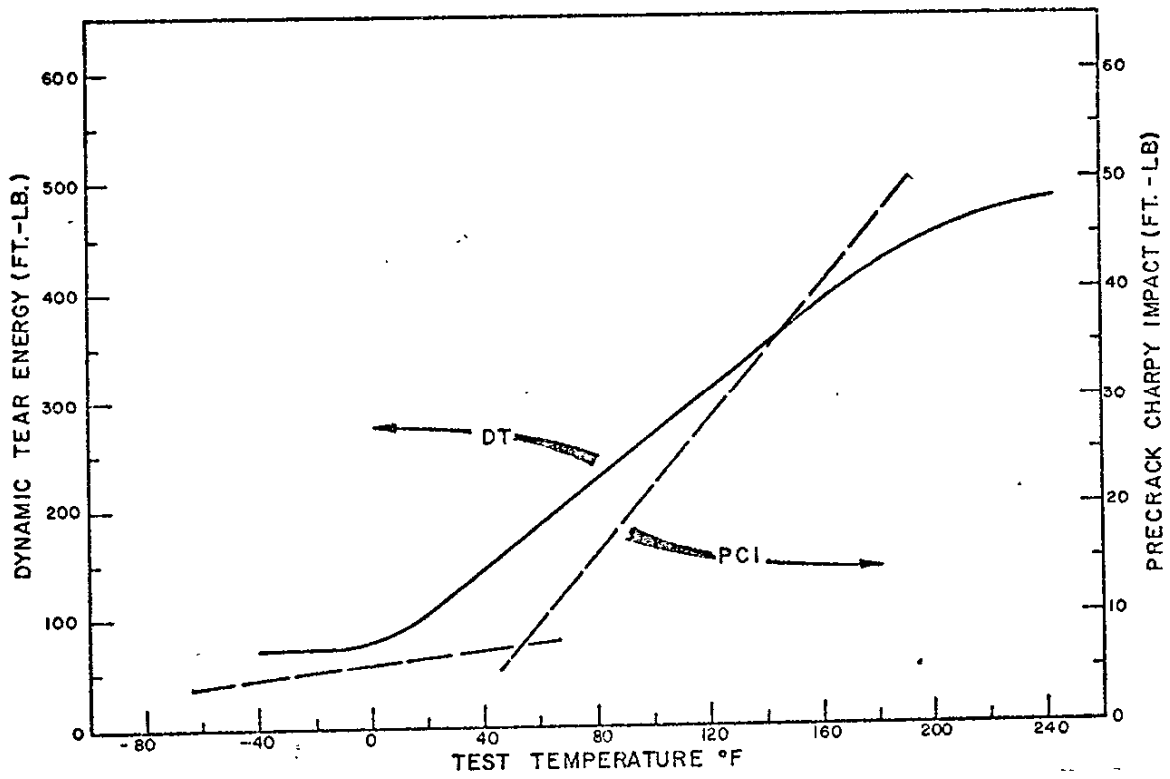
DYNAMIC TEAR AND PRECRACK CHARPY IMPACT TEST RESULTS
FROM A517 GRADE - H HEAT 1024/44 CK

FIGURE 4.84



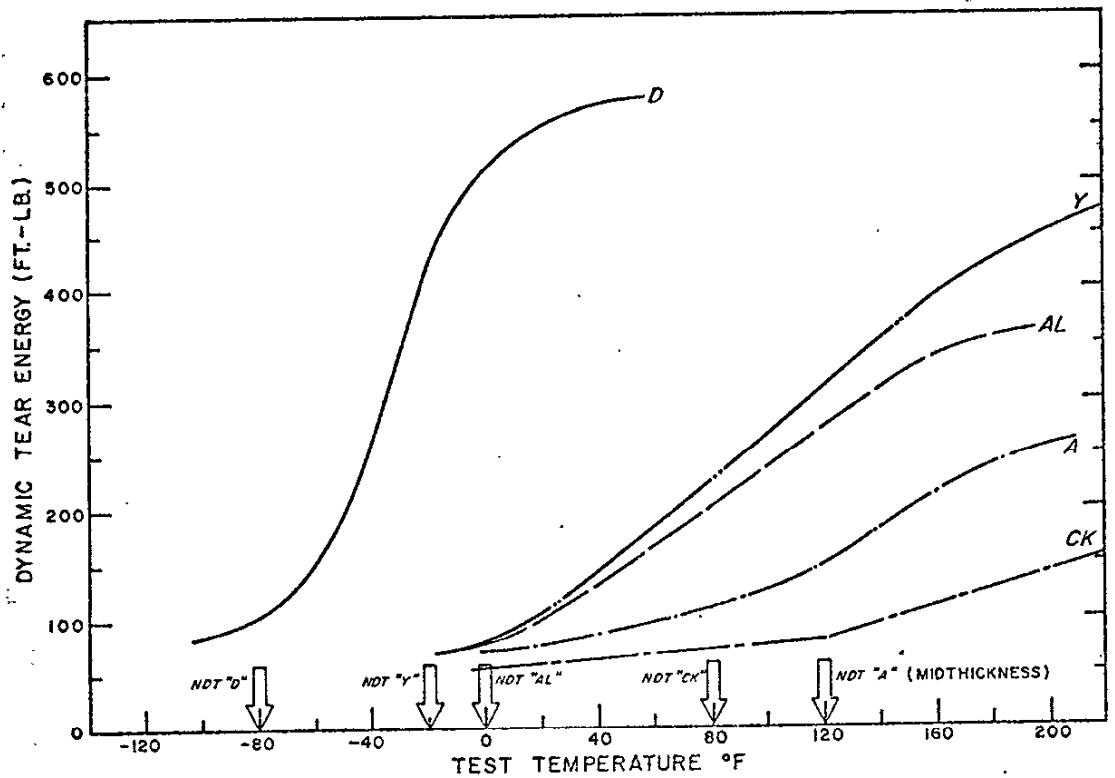
DYNAMIC TEAR AND PRECRACK CHARPY IMPACT TEST RESULTS FROM A517 GRADE-H HEAT 1020/46 AL

FIGURE 4.85



DYNAMIC TEAR AND PRECRACK CHARPY IMPACT TEST RESULTS
FROM A517 GRADE-H HEAT 1024/91Y

FIGURE 4.86



SUMMARY OF DYNAMIC TEAR TEST RESULTS ON SELECTED HEATS OF A514/517 STEEL WITH ASTM E208 NDT TEMPERATURES INDICATED

FIGURE 4.87

4.5.3 ASTM E208-69 Drop-Weight NDT Temperature.

The drop-weight NDT test method was developed at the Naval Research Laboratory (NRL) in 1952 and has been used extensively to investigate the temperature at which brittle fracture will occur in structural steels. The method is used for specification purposes by industrial organizations and is referenced in several ASTM Specifications and in the ASME Boiler and Pressure Vessel Code.

The nil-ductility transition (NDT) temperature is defined as the maximum temperature at which a standard drop-weight specimen breaks when tested according to the provisions of ASTM standard method E208. The test specimen usually used involves a notched bead-on-plate crack-starter weld made with a hard-surfacing electrode to assure easy crack initiation. The ASTM E208 Standard cautions that:

"Anomalous behavior may be expected for materials where the heat-affected zone created by deposition of the crack-starter weld is made more fracture resistant than the unaffected plate. This condition is developed for quenched-and-tempered steels of high hardness ... the heat-affected zone problem is not encountered with conventional structural-grade steel of a pearlitic microstructure or quenched-and-tempered steels tempered at high temperatures to develop maximum fracture toughness."

The question naturally arises here as to whether the Bryte Bend and Tuolumne River Bridge A514/517 steels were subject to anomalous behavior because of weld heat-affected-zone (HAZ) effects. When the HAZ constitutes a crack arrestor, the NDT temperature will tend to be fictitiously low.

4.5.4 A517 Grade-H heat 1027/44CK. NDT Temperature

Table 4.28 gives the DW-NDT test results obtained for the top and bottom surfaces of the 2-1/2-in.-thick flange plate. ASTM E208-69 specifies that:

"Products thicker than the standard specimen thickness shall be machine-cut to standard thickness from one side, preserving an as-fabricated surface unless otherwise specified, or agreed to in advance by the purchaser. The as-fabricated surface so preserved shall be the welded (tension) surface of the specimen during testing."

It should be recalled that the dynamic-tear test showed the surface of the CK plate to be somewhat tougher than the midthickness material. According to the E208 Standard Method, the NDT temperature has not been reached until the specimen is fractured to one or both edges of the tension surface. If the microstructure in the plate surface (the tension side of the test specimen) is relatively tough, the specimen may nearly completely fracture and yet be "unbroken" because the corners of the tension surface are not fractured.

The correlation between the DT test and the DW-NDT test result is good with the surface DT test indicating the NDT at +60°F as compared with the drop-weight-measured value of +80°F. The precrack Charpy impact (PCI) test indicated little or no difference between surface and center of the CK plate, with the steel consistently of low toughness irrespective of thickness position. The PCI data plotted as a straight line out to +320°F with no evidence of an inflection in the transition curves and, therefore, provided no indication of NDT temperature.

TABLE 4.28

DROP-WEIGHT NIL-DUCTILITY TRANSITION (NDT DATA)
E208 STD-TYPE P1 100 LB FROM 12 FT

Steel Code	Top-Surface Position		Bottom-Surface Position	
	Temp.	Break	Temp.	Break
1027/44CK A517-H	+60°F	X	+60°F	X
	+80	X (NDT)	+70	0
	+90	0	+80	0
	100	0	+90	0
	120	0	100	0
	200	0	120	0

4.5.5 Heats 1008/76D, 1020/46AL, 1024/91Y and 1026/92A.

Table 4.29 gives the results obtained in the midthickness and the surface positions of two heats of A517 grade-F and two heats of A517 grade-H steel. These are the same heats and plates tested with the DT test. Note that the tests indicated a marked difference between surface and midthickness. Except for plate D, the midthickness position had the higher NDT temperature. A517 grade-F plate A was a flagrant example of this, with a 120°F shift between the NDT temperatures for surface and midthickness. In testing a steel like plate A, the present ASTM E208 Standard Method is seriously unconservative when the specimen is cut from the plate-surface position.

Figures 4.88 and 4.89 show graphically the differences in plate-thickness position and the differences from heat to heat. Note that plate Y was indicated to be the best of the three heats of A517 grade-H steel investigated.

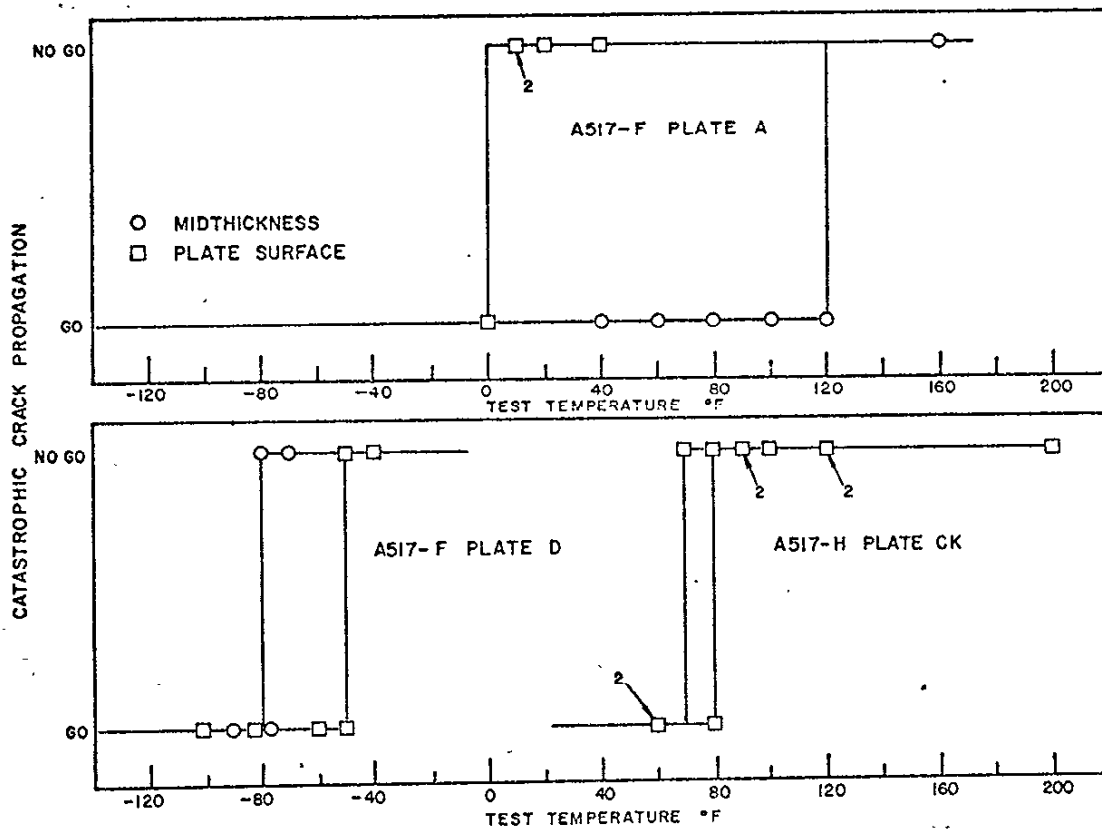
Table 4.30 is a summary of the ASTM E208 NDT temperatures, and the estimated NDT temperatures based on DT and PCI tests which are devoid of possible weld heat-affected zone complications.

Because of differences between the surface and midthickness positions in these plates, comparisons between test methods can be made only at a given position with respect to thickness. For the midthickness positions note that the DT-NDT and the ASTM E208 NDT temperatures were in good agreement except in Plate A. In Plate A, the dynamic-tear and the precrack Charpy tests were in agreement, indicating the NDT temperature to be 80°F lower than the ASTM E208 NDT temperature. This anomalous result cannot be explained as a crack-starter-weld heat-affected-zone (HAZ) complication in the ASTM E208 NDT testing; when the HAZ has an effect on the test results, it usually causes the E208 NDT temperature

TABLE 4.29

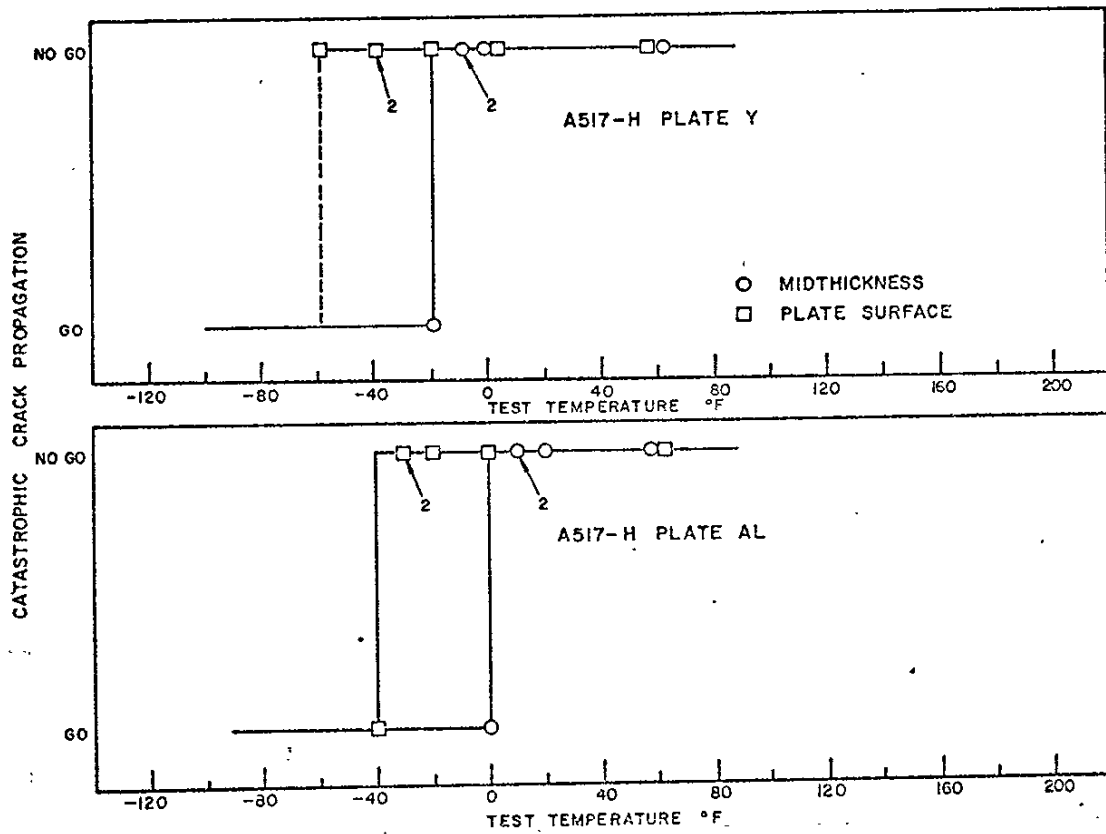
DROP-WEIGHT NIL-DUCTILITY-TRANSITION (NDT DATA)
E208 STD-TYPE P2 60 LB from 6 FT

Steel Code	Midthickness Position		Plate-Surface Position	
	Temp. °F	Break / No-Break	Temp. °F	Break / No-Break
1026/92A A517-F	+40	X	+10	X
	+60	X	+10	0
	+80	X	+20	0
	100	X	+40	0
	120	X (NDT)		
	160	0		
1020/46AL A517-H	0	X (NDT)	-40	X (NDT)
	+10	0	-30	0
	+10	0	-30	0
	+20	0	-20	0
	+60	0	0	0
	+60	0	+60	0
1008/76D A517-F	-90	X	-100	X
	-80	1/2 X (NDT)	-80	X
	-80	0	-60	X
	-70	0	-50	1/2 X (NDT)
			-50	0
			-40	0
1024/91Y A517-H	-20	X (NDT)	-60	0
	-10	0	-40	0
	-10	0	-40	0
	0	0	-20	0
	+60	0	0	0
	+60	0	+60	0



ASTM E208 DROP-WEIGHT NDT TEMPERATURE TEST RESULTS
 FOR A517 GRADE-F PLATES OF TWO MELTING PRACTICES AND
 BRYTE BEND BRIDGE CASUALTY PLATE A517 GRADE-H HEAT
 1027/44 CK

FIGURE 4.88



ASTM E208 DROP-WEIGHT NDT TEMPERATURE TEST RESULTS FOR A517 GRADE-H PLATES Y AND AL

FIGURE 4.89

TABLE 4.30

NIL DUCTILITY TRANSITION (NDT) TEMPERATURES

<u>Steel Grade</u>	<u>Heat Code</u>	<u>E208-69 Midthick</u>	<u>Dynamic Tear Midthick (a)</u>	<u>Precrack Charpy Midthick</u>
A517-F	1026/92A	+120	+40	+40
	1008/76D	-80	-100	-100
A517-H	1020/46AL	0	0	+60
	1024/91Y	-20	0	-20

<u>Steel Grade</u>	<u>Heat Code</u>	<u>E208-69 Surface</u>	<u>Precrack Charpy Quarter Point</u>
A517-F	1026/92A	0	+40
	1008/76D	-50	---
A517-H	1020/46AL	-40	+90
	1024/91Y	-60	+60

(a) based on single-spike force-time traces

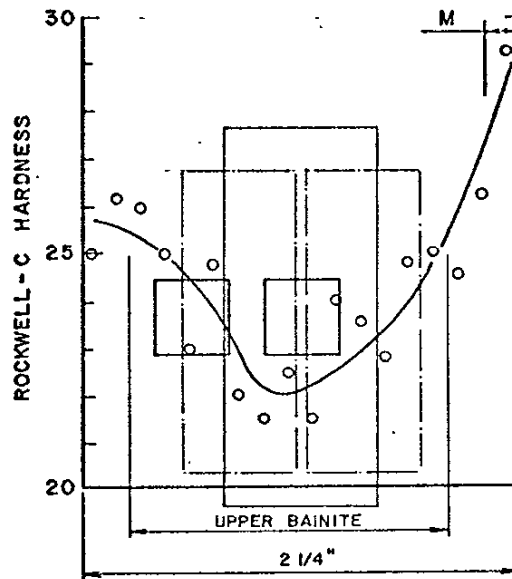
to be fictitiously low. Also in plate D, the dynamic-tear and the precrack Charpy tests were in agreement and, again, the indicated NDT temperature was lower than the ASTM E208 NDT temperature. However, in this plate the difference between the estimated NDT temperature and the ASTM E208 NDT temperature was only about 20°F.

In plate D, the microstructure throughout the thickness was found (58) to consist of a uniform, dense, dispersion of fine carbide particles in a tempered martensite matrix. The steel was almost entirely (95%) tempered martensite. This fine-scale, uniform microstructure is known to possess excellent fracture toughness. In plate A, on the other hand, at a depth of only 1/4-in. below the plate surface, the microstructure was found(58) to consist of 50 percent intermediate-temperature transformation product (a ferrite-carbide aggregate resembling upper bainite). Moreover, at a distance of 1-1/8-in. below the plate surface (midthickness) the microstructure contained islands of ferrite in combination with pools of martensite of higher-than-average carbon content. At midthickness, there was less than 5 percent tempered martensite. Thus, in A517 grade-F plates A and D, the quantitative agreement between the dynamic-tear and precrack Charpy NDT temperatures was consistent with the relatively uniform microstructures that existed throughout the center section of each plate. In plate A, the center section was uniformly poor (low-toughness upper bainite) and in plate D, it was uniformly good (tempered-martensite). The fact that in plate A, the PCI-NDT temperature was the same at the quarter-point and the midthickness positions was consistent with the fact that upper bainite extended from midthickness to within about 1/4-in. of the plate surface.

In this connection, Figure 4.90 shows the relative position of each specimen type with respect to thickness and microstructure in plate A(59). Note that with the 3/4-in.-thick ASTM E208 type P-2 NDT specimen at midthickness, the tension surface (which determines break or no-break performance) was approaching the quarter-point position in 2-1/4-in.-thick plate.

PLATE A HEAT 1026-92
2 1/4 IN. THICK, A517-F

M = MARTENSITE
— DT TEST
— NDT TEST
— CVN TEST



SPECIMEN POSITIONS RELATIVE TO HARDNESS
AND MICROSTRUCTURE IN PLATE-A THICKNESS

FIGURE 4.90

In A514/517 grade-H plates AL and Y, the microstructural and attendant hardness gradients precluded correlation between specimen types. When surface Charpy specimens were machined from plate AL, the precrack Charpy impact NDT temperature was +20°F (see Figure 4.59). When the tension surface of the E208 NDT test specimen contained tough, tempered martensite, one would expect a low NDT temperature (e.g. -40°F in plate AL and -60°F in plate Y); whereas, the Charpy specimen which integrates the resistance to crack propagation over a 0.4-in.-thick surface layer, encompasses both the shallow martensitic surface and the less-tough intermediate transformation products below the surface. Apparently the mixed structures (martensite plus a ferrite-carbide aggregate resembling upper bainite) at the quarter-point position were even more brittle than the mid-thickness microstructure.

Because of the obvious complication introduced by a gradient of microstructure (toughness) from surface to midthickness, the DW-NDT specimens which were classified by E208 as "no break" were placed in a furnace at 900°F, heat tinted, and then broken apart at low temperature to determine the extent of the original fracture inside the test piece. At 900°F the original fracture surfaces were tinted dark blue, and the new fracture produced in breaking the specimen apart (for purposes of viewing the fracture surfaces) was bright and readily distinguished from the heat-tinted, original fracture. The findings confirmed the earlier observations that the present ASTM E208 NDT test method is unconservative in steels with a surface-to-midthickness gradient of toughness.

Figure 4.91 is a photograph of the fracture surface in AL-plate midthickness specimens. Note that at temperatures above the E208 NDT temperature there was extensive interior fracturing. In fact, at +20°F there was only a tiny corner of unfractured metal which disqualified the specimen as a "break". It should

be recalled (Figure 4.90) that the tension surface of the "midthickness" NDT specimen is approximately at the quarter-point position with respect to thickness.

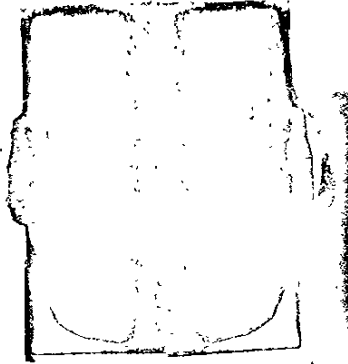
Likewise, in the plate-AL surface specimens, there was extensive interior fracturing at temperatures up to 20°F above the E208 NDT temperature. Also it was discovered that one of the -30°F test specimens (AL-6) was in fact a "break" by E208 definition. Unmistakeable bluing of the original crack-propagation fracture surface revealed complete separation on one side of the crack-starter weld and only a tiny unfractured corner on the other side. Thus, visual inspection of the test pieces failed to reveal what must have been a hair-line crack extending across one corner of the specimen.

Plate Y also developed extensive interior fracturing at temperatures up to 40°F above the E208 NDT temperature in the surface testing and up to 20°F above the NDT temperature in the midthickness testing.

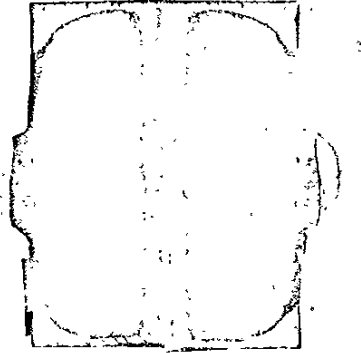
Another anomaly was discovered in the heat-tinting experiments; specimens were found with the crack-starter weld deposit fractures but 100% arrest of the crack at the fusion line. In other words, the weld heat-affected zone prevented the brittle weld-metal crack from entering the parent metal.

Figure 4.92 is an example of this behavior in one of the "surface" specimens from plate A. In connection with this figure, it should be recalled that the "midthickness" NDT test specimens fractured at temperatures up to +120°F. Thus, it appears that the crack-starter-weld heat-affected-zone formed in the microstructure at the plate surface arrested the brittle weld crack and was responsible for the anomalously great difference between the two specimen positions.

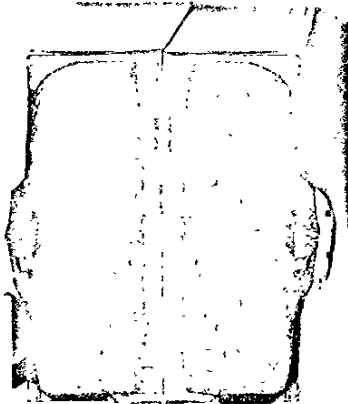
AL-23
+20°F



AL-24
+10°F

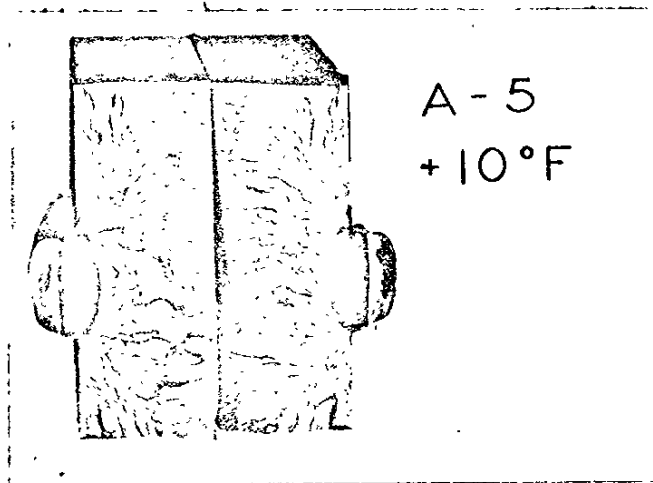


AL-25
+10°F



E208 NDT SPECIMENS HEAT TINTED AND BROKEN APART TO
SHOW THE EXTENT OF FRACTURE IN THE NDT TESTING
(THE E208 NDT TEMPERATURE WAS 0°F)

FIGURE 4.91

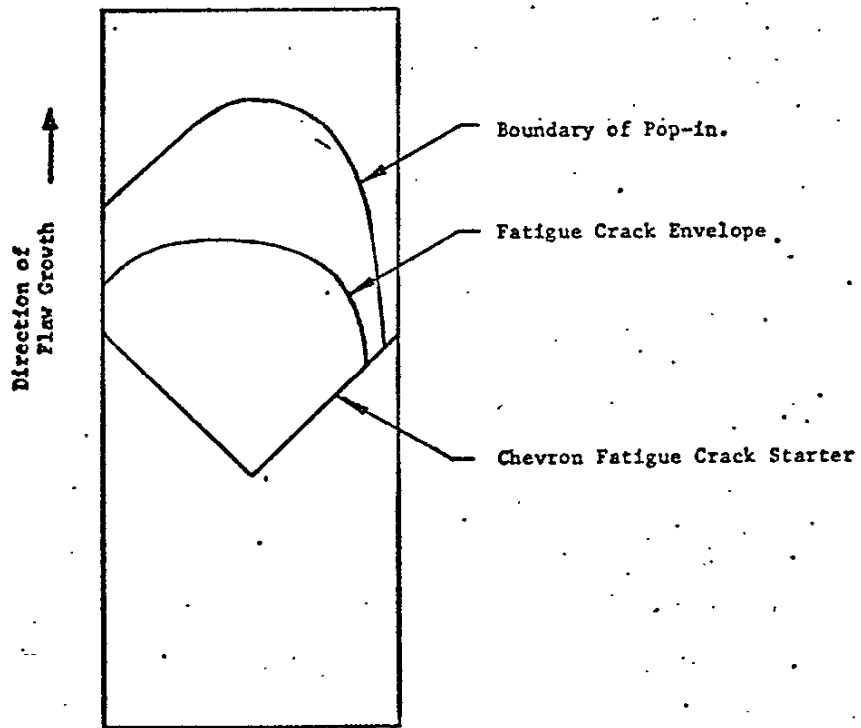


CRACK ARREST IN THE WELD
HEAT-AFFECTED ZONE OF PLATE-A ASTM E208 NDT
TEST OF SPECIMEN A-5

FIGURE 4.92

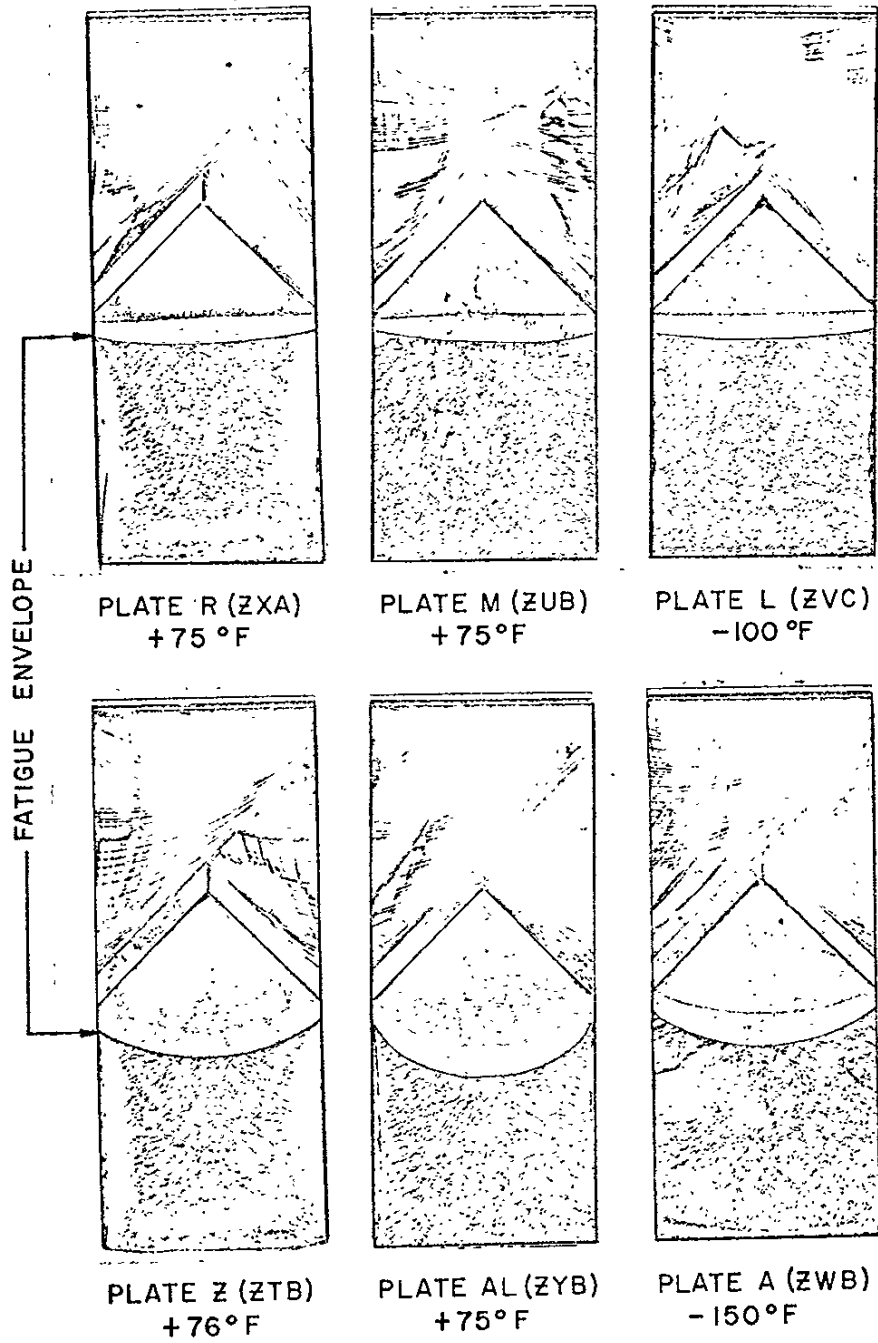
4.6 Effect of Microstructure on Fatigue

Table 4.20 on page 196 shows that there was a problem in compact-tension testing plates A, AL and Z. All of the 2-in. compact-tension tests of these plates were "invalid" according to ASTM K399 because of tunneling of the fatigue cracks (see footnotes c, d and e on Table 4.19). Plates A, AL and Z were melted by electric-furnace DH - practice with an improper sequence in adding the boron and, consequently, were deficient in hardenability. The 2-in.-thick compact tension specimens encompassed all or nearly all of the plate thickness and, consequently, in plates A, AL and Z had crack-resistant tempered martensite (or at least lower bainite) at the surfaces of the test specimens and low-toughness upper bainite generally from 1/4-point to 1/4-point. Plates L, M and R from a different steel producer presented no difficulty with fatigue-crack tunneling. Figure 4.93 shows an extreme case; this shows the fracture surface in a 2-in.-thick Cr specimen from plate AL. Not only was there fatigue crack tunneling but also the envelope of the arrested pop-in was more or less parallel to the fatigue precrack. Figure 4.94 provides a comparison between typical specimens from two steel producers (different melting practices). Note that the fatigue cracks in plates L, M and R were essentially flat and those in plates A, AL and Z were tunneling in the low-toughness upper bainite. This appears to confirm the Region-III accelerating effect of low toughness on fatigue crack growth rate.



FRACTURE SURFACES IN 2 INCH COMPACT TENSION
SPECIMEN FROM PLATE AL

FIGURE 4.93



FRACTURE SURFACES IN 2 INCH COMPACT TENSION SPECIMENS FROM PLATES R, M, L, Z, AL, AND A

FIGURE 4.94

5.0 REFERENCES

1. Rolfe, S. T.; "The Use of Fracture Mechanics in Designing to Prevent Fracture in Bridges", Civil Engineering, ASCE, August, 1972.
2. Barsom, J. M., and Rolfe, S. T.; " K_{IC} Transition-Temperature Behavior of A517F Steel", ENGINEERING FRACTURE MECHANICS, Volume 2, pp. 341357, 1971.
3. Shoemaker, A. K., and Rolfe, S. T.; "The static and Dynamic Low-Temperature Crack Toughness Performance of Seven Structural Steels", ENGINEERING FRACTURE MECHANICS, Volume 2, pp. 319339, 1971.
4. Barsom, J. M., and Rolfe, S. T. "Correlations Between K_{IC} and Charpy V-Notch Test Results in the Transition-Temperature Range", IMPACT TESTING OF METALS, ASTM STP 466, pp. 281-302, 1970.
5. Gross, J. H.; "Effect of Strength and Thickness on Notch Ductility", IMPACT TESTING OF METALS, ASTM STP-466, pp. 21-52, 1970.
6. Rolfe, S. T., and Novak, S. R.; "Slow Bend K_{IC} Testing of Medium-Strength High-Toughness Steels", ASTM STP 463, American Society for Testing and Materials, pp. 124-159, 1970.
7. C. E. Hartbower, "Crack Initiation and Propagation in V-Notch Charpy Impact", ASTM PROCEEDINGS, Vol. 56 (1956), p. 521; also WELDING JOURNAL, Vol. 36(11), p. 494-s, Nov. 1957.
8. G. M. Orner and C. E. Hartbower, "Effect of Specimen Geometry on Charpy Low-Blow Transition Temperature", WELDING JOURNAL, Vol. 36(12), p. 521-s, Dec. 1957.

REFERENCES (Continued)

15. Brown, W. F., Jr. and J. E. Srawley, "Plane Strain Crack Toughness Testing of High Strength Metallic Materials", ASTM STP-410, 1966.
16. Ronald, T. M. F., J. A. Hall and C. M. Pierce, "Usefulness of Precracked Charpy Specimens for Fracture Toughness Screening Tests of Titanium Alloys", Met. Trans, 3(4)813 (April 1972).
17. Witt, F. J., "Equivalent Energy Procedures for Predicting Gross Plastic Fracture", USAEC Report ORNL-TM-3172, Oak Ridge National Laboratory.
18. Wells, A. A. "Notch Ductility, Design and the Specification of Permissible Defect Sizes in Welded Metal Structures" Practical Fracture Mechanics for Structural Steel, Risley, 1969.
19. Pellini, Puzak and Eschbacher, "Procedures for NRL Drop Weight Tests", NRL Memo Report 316, June 1954.
20. Puzak, Schuster and Pellini, "Crack Starter Tests of Ship Fracture and Project Steels", Welding Journal Vol 33, p. 481-s (October 1954) and Vol 34, p. 196-s (April 1955).
21. Puzak and Babecki, "Normalization Procedures for NRL Drop-weight Test", Ibid, Vol 38, p. 209-s (May 1959).
22. Lange, Puzak and Cooley, "Standard Method for the 5/8-Inch Dynamic Tear Test", NRL Report 7159, August 27, 1970.
23. A Review of Engineering Approaches to Design Against Fracture, ASME, United Engineering Center, New York, N.Y. 10017, November 1964.

REFERENCES (Continued)

31. Rolfe, S. T. and Gensamer, M., "Fracture-Toughness Requirements for Steels", AD 835 923L, September 20, 1968.
32. Barsom, J. M. and Rolfe, S. T., " K_{IC} Transition-Temperature Behavior of A517-F Steel" AD846 124L, November 29, 1968, and ENGINEERING FRACTURE MECHANICS, 1971, Vol. 2, pp. 341-357.
33. Hahn, G. T. and Rosenfield, S. R., "Plastic Flow in the Locale of Notches and Cracks in Fe-3Si Steel under Conditions Approaching Plane Strain", Final Report SSC-191 on Ship Structure Committee Project SR-164, "Local Strain Movement", November 1968.
34. Begley, J. A. and Toolin, P. R., "Fracture Toughness and Fatigue Crack Growth Rate Properties of a NiCrMoV Steel Sensitive to Temper Embrittlement", presented at the Fourth National Symposium on Fracture Mechanics, Carnegie Mellon University, Pittsburgh, PA, August 1970.
35. Corten, H. T. and Sailors, R. H., "Relationship Between Material Toughness Using Fracture Mechanics and Transition-Temperature Tests", University of Illinois Department of Theoretical and Applied Mechanics, Report No. 346, August 1971 (UCCND Sub-Contract 3398 for Oak Ridge National Laboratory).
36. WELDING HANDBOOK, Section 1, 5th Edition, Table 6.3, American Welding Society, New York.
37. Hartbower, C. E. and Pellini, W. S., "Mechanical and Material Variables Affecting Correlation", THE WELDING JOURNAL, Vol. 29(7), p. 347-s, Figure 15, July 1950.

REFERENCES (Continued)

38. Hartbower, C. E., "The Posson Effect in the Charpy Test", ASTM PROCEEDINGS, Vol. 54 (1954), p. 929.
39. Gross, J. H. and Stout, R. D., "Ductility and Energy Relations in Charpy Tests of Structural Steels", THE WELDING JOURNAL, Vol. 37(4), p. 151-s, April 1958.
40. Brown, W. F., Jr., and Srawley, J. E., "Commentary on Present Practice", ASTM STP 463, American Society of Testing Metals, 1970.
41. Kaufman, J. G., Minutes of ASTM Committee E-24 Subcommittee III, September 23 and 24, 1969.
42. Reuter, W. G and Flens, F. J., "Effect of Thickness on 7039-T63 Aluminum Alloy Plane-Strain Fracture Toughness", unpublished data from the NERVA program.
43. May, M. J., presented in "Revisions to E399-70T", by W. F. Brown, Jr., E24.01 Minutes, Attachment 3, September 29, 1971.
44. Nelson, W. G., Schilling, P. E., and Kaufman, J. G., "The Effect of Specimen Size on the Results of Plane-Strain Fracture-Toughness Tests", presented at National Symposium on Fracture Mechanics, August 18, 1970.
45. Reuter, Walter G., private communication, June 21, 1973.

REFERENCES (Continued)

46. Barsom, J. M. and Noval, S. R., "Subcritical Crack Growth in Steel Bridge Members", Final Report NCHRP 12-14, September 1974.
47. Warren Savage, Private Communication.
48. Clark, W. G., "How Fatigue Crack Initiation and Growth Properties Affect Material Selection and Design Criteria", Metals Engineering Quarterly, August 1974, pp. 16-22.
49. Crozier, William and Kendrick, Charles, Private Communication.
50. Forman, R. G., et al, "Numerical Analysis of Crack Propagation in Cyclic Loaded Structures:", Journal of Basic Engineering, Paper No. 66-WA/Met-4, Trans. ASME, Vol. 89, Series D., September 1967, p. 459.
51. "Fatigue Crack Growth Rate Laws Accounting for Stress-Ratio Effects" ASTM Task Force E24.04.04 Report No. 1.
52. Charles Kendrick, Private Communication.
53. Rolfe, S. T., "Fracture Mechanics in Bridge Design", Civil Engineering - ASCE, August 1972, pp. 37-41.
54. Rolfe, S. T. and Egan, G. R., "Designing to Prevent Fracture in Tall Buildings", State-of-Art Report 6, Technical Committee 18, ASCE-IABSE, International Conference on Tall Buildings, August 1972.
55. Wei, R. P., "Fracture Mechanics Approach to Fatigue Analysis in Design", ASME Preprint 73-DE-22.

REFERENCES (Continued)

56. Clark, W. G. Jr, and Hudak, S. J. Jr., "Variability in Fatigue Crack Growth Rate Testing", ASTM E24.04.01 Task Group Report, September 18, 1974.
57. Fisher, John W., et al, "Fatigue Strength of Steel Beams with Welded Stiffeners and Attachments", NCHRP Report 147, pp 34-35, 1974.
58. Pellissier, George E., Private Communication, March 10, 1975.
59. Russell, John, Private Communication.
60. Carter, C. S. and Caton, R. G., "Stress-Corrosion Susceptibility of Highway Bridge Construction Steels-Phase II A" Final Report DOT-FH-11-7836 April 1973.
61. Irwin, G. R., Robert, R., Fracture Toughness of Bridge Steels - Phase I Report" FHWA-RD-74-599 July 1972.

6.0

APPENDICES

- A. Tensile Properties of 76 Slabs from 30 Heats of A514/517 Steel as Recorded in the Mill Test Report and as Determined by Caltrans Lab.
- B. Chemistry of 30 Heats of A514/517 Steel as Recorded in the Mill Test Reports and as Determined by Caltrans Lab.
- C. Charpy V-Notch and Precrack Charpy Impact Test Results of 76 Slabs from 30 Heats of A514/517 Steel.
- D. Effects Technology, Inc. Charpy Impact Test Results on Seven Heats of A514/517 Steel.
- E. National Bureau of Standards Charpy Impact Test Results of Selected Heats of A514/517 Steel.

Appendix A

Tensile Properties of 76 Slabs from 30 Heats
of A514/517 Steel as Recorded in the Mill Test
Reports and as Determined by Caltrans Laboratory.

TENSILE PROPERTIES A514/A517

ASTM SPEC	YIELD STRENGTH KSI		TENSILE STRENGTH KSI		% ELONGATION		% REDUCTION OF AREA	
	100 MIN.		115 to 135		16 MIN.		45 MIN.	
Heat/Slab ID	MILL	CALTRANS	MILL	CALTRANS	MILL	CALTRANS	MILL	CALTRANS
1004/44 AG	114.9 124.0 (119.5)	113.5 114.0 (113.8)	124.6 131.4 (128.0)	125.2 126.0 (125.6)	20.0 19.0 (19.5)	17.5 17.5 (17.5)	59.0 54.1 (56.6)	51.0 55.0 (53.0)
1004/96 AH	120.3 123.3 (121.8)	115.0 113.0 (114.0)	131.5 134.8 (133.2)	126.5 124.5 (125.5)	19.0 19.0 (19.0)	17.5 18.5 (18.0)	54.8 53.5 (54.2)	57.0 58.0 (57.5)
1004/98 AJ	117.4 114.9 (116.2)	116.5 117.5 (117.0)	127.3 125.3 (126.3)	128.2 128.7 (128.5)	19.0 20.0 (19.5)	18.0 17.5 (17.8)	55.0 55.0 (55.0)	51.0 51.0 (51.0)
1005/22 BX	107.0 103.2 (105.1)	121.0 121.0 (121.0)	120.9 119.9 (120.4)	133.5 132.5 (133.0)	16.0 16.0 (16.0)	16.0 15.0 (15.5)	54.0 54.0 (54.0)	42.8 44.5 (43.0)
1006/47 AR	111.9 105.9 (108.9)	-- -- --	123.1 118.3 (120.7)	-- -- --	19.0 18.5 (19.3)	-- -- --	53.6 54.8 (54.2)	-- -- --
106/48 AS	118.8 114.8 (116.8)	117.0 115.5 (116.3)	128.8 124.8 (126.8)	126.7 125.7 (126.2)	18.0 18.5 (18.3)	17.0 17.0 (17.0)	51.9 53.1 (52.5)	51.3 52.7 (52.0)
1006/49 BJ	109.8 111.8 (110.8)	-- -- --	119.8 123.3 (121.6)	-- -- --	20.0 19.0 (19.5)	-- -- --	53.1 53.3 (53.2)	-- -- --

TENSILE PROPERTIES A514/A517

ASTM SPEC	YIELD STRENGTH KSI			TENSILE STRENGTH KSI			% ELONGATION			% REDUCTION OF AREA		
	100 MIN.			115 to 135			16 MIN.			45 MIN.		
	MILL	CALTRANS		MILL	CALTRANS		MILL	CALTRANS		MILL	CALTRANS	
1006/50 AT	111.9	--		122.8	--		19.0	--		52.1	--	
	112.8	--		123.3	--		19.5	--		53.3	--	
	(114.4)	--		(123.0)	--		(19.3)	--		(52.7)	--	
1006/51 AU	119.2	--		131.4	--		16.0	--		53.0	--	
	106.6	--		120.8	--		18.0	--		53.0	--	
	(112.9)	--		(126.1)	--		(17.0)	--		(53.0)	--	
1006/52 AV	109.8	--		121.3	--		19.0	--		51.9	--	
	104.8	--		117.3	--		21.5	--		53.3	--	
	(107.3)	--		(119.3)	--		(20.3)	--		(52.6)	--	
1006/53 BK	117.8	116.5		127.3	126.5		16.0	16.5		53.0	46.4	
	109.5	117.5		120.9	127.2		17.0	15.5		53.0	42.5	
	(113.6)	(117.0)		(124.1)	(126.9)		(16.5)	(16.0)		(53.0)	(44.5)	
1006/54 BL	108.2	--		120.1	--		17.0	--		54.0	--	
	106.0	--		117.8	--		16.0	--		49.0	--	
	(107.1)	--		(119.0)	--		(16.5)	--		(51.5)	--	
1006/56 BN	104.3	105.0		118.3	117.0		17.0	18.5		52.0	45.1	
	123.3	104.5		133.6	116.7		16.0	17.5		52.0	48.1	
	(113.8)	(104.8)		(126.0)	(116.9)		(16.5)	(18.0)		(52.0)	(46.6)	

TENSILE PROPERTIES A514/A517

ASTM SPEC	YIELD STRENGTH KSI			TENSILE STRENGTH KSI			% ELONGATION			% REDUCTION OF AREA		
	100 MIN.			115 to 135			16 MIN.			45 MIN.		
	MILL	CALTRANS		MILL	CALTRANS		MILL	CALTRANS		MILL	CALTRANS	
Heat/Slab ID												
1006/57	AW	109.8 110.3 (110.0)	--	120.8 121.8 (121.3)	--	--	20.0 20.5 (20.3)	--	51.7 53.1 (52.4)	--	--	
1006/58	AX	113.9 108.9 (111.4)	--	124.3 122.1 (123.2)	--	--	18.0 18.0 (18.0)	--	52.2 53.5 (52.9)	--	--	
1006/59	BN	113.9 116.0 (115.0)	--	123.3 121.4 (122.4)	--	--	17.0 18.0 (17.5)	--	54.0 54.0 (54.0)	--	--	
1006/60	BP	120.3 106.8 (113.5)	--	126.0 118.5 (122.3)	--	--	18.0 20.0 (19.0)	--	53.0 54.0 (53.5)	--	--	
1006/61	AY	111.4 121.3 (116.4)	--	123.8 130.8 (127.3)	--	--	19.5 17.5 (18.5)	--	55.2 51.9 (53.6)	--	--	
1006/62	AZ	108.2 108.0 (108.1)	--	120.8 120.1 (120.5)	--	--	18.0 17.0 (17.5)	--	53.0 53.7 (53.4)	--	--	
1006/25	BA	113.4 120.8 117.1	--	120.8 129.5 (125.2)	--	--	18.0 16.0 (17.0)	--	55.0 51.0 (53.0)	--	--	

TENSILE PROPERTIES A514/A517

ASTM SPEC	YIELD STRENGTH KSI			TENSILE STRENGTH KSI			% ELONGATION			% REDUCTION OF AREA		
	100 MIN.			115 to 135			16 MIN.			45 MIN.		
Heat/Slab ID	MILL	CALTRANS	MILL	CALTRANS	MILL	CALTRANS	MILL	CALTRANS	MILL	CALTRANS	MILL	CALTRANS
1006/26 BB	107.5 122.3 (114.9)	118.0 116.5 (117.3)	117.4 130.3 (123.9)	130.0 126.5 (128.3)	17.0 17.0 (17.0)	15.0 15.0 (15.0)	55.0 52.0 (53.5)	45.1 46.2 (45.7)				
1006/64 BC	105.3 126.8 (116.0)	--	119.3 134.3 (126.8)	--	19.0 17.0 (18.0)	--	57.0 51.0 (54.0)	--				
1006/65 BR	104.4 107.3 (105.8)	--	115.9 119.2 (117.5)	--	20.0 16.0 (18.0)	--	54.0 51.0 (53.0)	--				
1006/66 BS	104.3 105.2 (104.8)	--	117.2 117.8 (117.5)	--	18.0 18.0 (18.0)	--	57.0 52.0 (54.5)	--				
1006/67 BT	102.5 112.4 (107.5)	--	115.7 123.3 (119.5)	--	17.0 16.0 (16.5)	--	51.0 51.0 (51.0)	--				
1006/68 BD	117.8 119.3 (118.5)	--	128.8 133.3 (131.0)	--	17.0 16.0 (16.5)	--	52.0 50.0 (51.0)	--				
1006/69 BE	107.3 116.8 (112.0)	--	119.3 127.3 (123.3)	--	21.0 20.5 (20.8)	--	56.0 53.3 (54.7)	--				

TENSILE PROPERTIES A514/A517

ASTM SPEC	YIELD STRENGTH KSI		TENSILE STRENGTH KSI		% ELONGATION		% REDUCTION OF AREA	
	100 MIN.		115 to 135		16 MIN.		45 MIN.	
	MILL	CALTRANS	MILL	CALTRANS	MILL	CALTRANS	MILL	CALTRANS
1006/70 BU	119.9	--	129.8	--	19.0	--	53.0	--
	116.9 (118.4)	--	126.8 (128.3)	--	19.0 (19.0)	--	54.0 (53.5)	--
1006/71 BF	109.8	105.0	120.3	116.7	23.0	17.0	64.5	51.0
	108.8 (109.3)	106.5 (105.8)	120.3 (120.3)	117.5 (117.1)	20.0 (21.5)	17.5 (17.3)	56.0 (60.3)	51.5 (51.3)
1006/72 BV	111.2	122.5	123.8	130.5	17.0	16.0	51.0	48.4
	124.8 (118.0)	121.0 (121.8)	134.7 (129.3)	129.0 (129.8)	16.0 (16.5)	15.0 (15.5)	50.0 (50.5)	44.0 (46.2)
1006/73 BZ	115.0	117.2	123.8	127.0	19.0	14.5	55.0	39.1
	120.9 (118.0)	118.5 (117.8)	129.7 (126.8)	127.5 (127.3)	18.0 (18.5)	16.0 (15.3)	50.0 (52.5)	44.1 (41.6)
1006/74 BG	110.0	--	120.9	--	18.0	--	53.6	--
	108.0 (109.0)	--	119.4 (120.2)	--	20.5 (19.3)	--	49.5 (51.6)	--
1006/75 BW	117.4	--	126.3	--	19.0	--	51.1	--
	111.9 (114.6)	--	128.3 (127.3)	--	19.0 (19.0)	--	53.6 (52.4)	--

TENSILE PROPERTIES A514/A517

ASTM SPEC	YIELD STRENGTH KSI				TENSILE STRENGTH KSI				% ELONGATION				% REDUCTION OF AREA	
	100 MIN.				115 to 135				16 MIN.				45 MIN.	
	MILL	CALTRANS	MILL	CALTRANS	MILL	CALTRANS	MILL	CALTRANS	MILL	CALTRANS	MILL	CALTRANS	MILL	CALTRANS
1007/11 AM	117.8	107.0 103.0 (105.0)	124.8	118.0 119.0 (118.5)	18.0	17.5 17.5 (17.5)	59.5	50.5 50.8 (50.7)						
1007/12 AN	112.8	119.0 119.0 (119.0)	124.6	128.0 127.5 (127.8)	18.0	16.0 16.0 (16.0)	59.3	47.1 47.7 (47.4)						
1008/76 D	123.3 126.3 (124.8)	110.0 108.5 (109.3)	131.6 134.8 (133.2)	120.7 118.7 (119.7)	19.0 19.0 (19.0)	18.5 19.0 (18.8)	61.3 59.8 (60.5)	55.4 57.5 (56.5)						
1009/40 BH	110.3 107.2 (108.8)	108.5 108.0 (108.3)	122.3 121.3 (121.7)	120.7 120.5 (120.6)	20.0 19.0 (19.5)	19.0 20.5 (19.8)	67.0 64.9 (66.0)	56.0 56.2 (56.1)						
1010/47 AP	107.9 103.3 (105.6)	111.0 114.0 (112.5)	120.8 117.8 (119.3)	122.2 124.0 (123.1)	18.0 17.0 (17.5)	17.0 17.0 (17.0)	55.0 55.0 (55.0)	54.9 54.9 (54.9)						
1011/92 CA	105.1 108.3 (106.7)	112.0 117.5 (114.8)	115.9 119.8 (117.4)	124.3 121.7 (123.0)	18.0 19.0 (18.5)	16.0 15.0 (15.5)	57.0 57.0 (57.0)	46.6 45.2 (45.9)						
1012/99 AK	109.6 112.5 (111.0)	110.5 109.0 (109.8)	119.4 121.9 (120.7)	120.5 119.2 (119.9)	23.0 22.0 (22.5)	17.0 17.5 (17.3)	65.3 64.1 (64.7)	55.0 55.0 (55.0)						

TENSILE PROPERTIES A514/A517

ASTM SPEC	YIELD STRENGTH KSI			TENSILE STRENGTH KSI			% ELONGATION			% REDUCTION OF AREA		
	100 MIN.			115 to 135			16 MIN.			45 MIN.		
Heat/Slab ID	MILL	CALTRANS	MILL	CALTRANS	MILL	CALTRANS	MILL	CALTRANS	MILL	CALTRANS	MILL	CALTRANS
1013/32 J	105.5	91.5 101.5 (96.5)	117.9	106.2 116.0 (111.1)	20.0	18.0 15.0 (16.5)	59.9	48.0 44.0 (46.0)				
1014/02 M	123.3	118.0 115.5 (116.8)	131.3	126.5 124.0 (125.8)	20.0	16.0 15.0 (15.5)	65.7	47.0 44.5 (45.8)				
1015/32 N	114.7	118.0 119.0 (118.5)	124.3	126.8 127.7 (127.3)	20	16.5 16.0 (16.3)	61.8	51.0 49.0 (50.0)				
1016/41 P	113.8	122.5 121.5 (122.0)	125.1	132.5 132.0 (132.3)	18.5	15.5 14.5 (15.0)	50.9	46.0 43.0 (44.5)				
1016/11 K	--	114.5 111.5 (113.0)	--	124.5 121.8 (123.2)	--	17.0 17.0 (17.0)	--	52.2 48.5 (50.4)				
1017/62 L	112.8	110.0 109.0 (109.5)	122.6	120.5 120.0 (120.3)	20	16.0 16.5 (16.3)	67.5	46.0 48.0 (47.0)				
1018/81 S	112.8	112.3 114.0 (113.2)	122.8	123.0 124.5 (123.8)	20	16.5 16.5 (16.5)	60.3	53.0 48.5 (50.8)				

TENSILE PROPERTIES A514/A517

ASTM SPEC	YIELD STRENGTH KSI		TENSILE STRENGTH KSI		% ELONGATION		% REDUCTION OF AREA	
	100 MIN.		115 to 135		16 MIN.		45 MIN.	
Heat/Slab ID	MILL	CALTRANS	MILL	CALTRANS	MILL	CALTRANS	MILL	CALTRANS
1019/31 R	112.8	109.5 113.0 (111.3)	121.8	120.5 123.8 (122.2)	20.0	16.5 16.5 (16.5)	63.0	49.3 48.7 (49.0)
1020/41 AA	104.0 101.0 (102.5)	92.5 89.0 (90.8)	116.3 115.9 (116.1)	106.5 103.0 (104.8)	22.0 22.0 (22.0)	18.0 19.5 (18.8)	63.7 64.7 (64.2)	56.0 56.0 (56.0)
1020/43 CF	102.0 103.0 (102.5)	99.5 99.5 (99.5)	116.7 117.5 (117.1)	115.3 115.0 (115.2)	20.0 20.0 (20.0)	17.5 17.5 (17.5)	54.8 60.5 (57.2)	45.2 50.0 (47.6)
1020/44 CG	105.0 102.5 (103.8)	102.5 102.0 (102.3)	118.5 118.0 (118.3)	117.5 116.7 (117.1)	18.0 18.0 (18.0)	17.5 17.5 (17.5)	50.5 49.0 (49.8)	51.4 49.2 (50.3)
1020/46 AL	110.5 108.5 (109.5)	106.5 102.3 (104.4)	119.0 117.5 (118.3)	121.5 118.0 (119.8)	24.0 24.0 (24.0)	16.0 17.0 (16.5)	55.0 55.0 (55.0)	51.0 51.0 (51.0)
1021/42 CM	128.5 122.0 (125.3)	126.0 127.5 (126.8)	134.5 129.0 (131.8)	133.6 132.0 (132.8)	18.0 20.0 (19.0)	16.0 16.0 (16.0)	52.0 52.0 (52.0)	49.5 51.1 (50.3)

TENSILE PROPERTIES A514/A517

ASTM SPEC	YIELD STRENGTH KSI				TENSILE STRENGTH KSI				% ELONGATION				% REDUCTION OF AREA	
	100 MIN.				115 to 135				16 MIN.				45 MIN.	
	MILL	CALTRANS	MILL	CALTRANS	MILL	CALTRANS	MILL	CALTRANS	MILL	CALTRANS	MILL	CALTRANS	MILL	CALTRANS
1022/51 C	112.8	103.0	123.2	121.0	20.0	17.0	57.7	50.0						
	115.0 (113.9)	105.0 (104.0)	126.1 (124.7)	117.3 (119.1)	20.0 (20.0)	17.0 (17.0)	56.7 (57.2)	49.7 (49.9)						
1022/53 F	115.3	107.0	124.4	120.0	19.0	18	54.8	52.5						
	107.7 (111.5)	109.0 (108.0)	118.7 (121.6)	121.0 (120.5)	26.0 (22.5)	17.5 (17.8)	56.7 (55.8)	52.0 (52.3)						
1022/54 H	116.0	99	125.1	112.0	20.0	18.0	57.7	56.5						
	105.6 (110.8)	99 (99)	117.2 (121.2)	112.0 (112.0)	20.0 (20.0)	19.0 (18.5)	57.7 (57.7)	56.0 (56.3)						
1023/51 G	115.5	106.5	124.6	119.0	18.0	18.5	55.2	51.8						
	105.9 (110.7)	108.5 (107.5)	116.7 (120.7)	120.0 (119.5)	18.0 (18.0)	16.0 (17.3)	57.7 (56.5)	51.5 (51.7)						
1023/54 E	113.8	105.0	124.1	117.0	18.0	17.5	53.3	53.0						
	110.3 (112.0)	104.0 (103.0)	119.7 (121.9)	117.0 (117.0)	22.0 (20.0)	17.5 (17.5)	69.5 (61.4)	53.5 (53.3)						
1024/91 Y	121.0	106.5	129.5	118.0	18.0	18.0	54.5	56.0						
	120.6 (120.8)	106.5 (106.5)	130.2 (130.0)	118.2 (118.1)	18.0 (18.0)	18.0 (18.0)	51.8 (53.2)	56.0 (56.0)						
1024/94 Z	124.4	113.0	132.8	129.0	20.0	15.0	60.2	47.0						
	127.0 (125.7)	118.5 (115.8)	134.5 (133.7)	129.0 (129.0)	20.0 (20.0)	16.0 (15.5)	60.0 (60.1)	48.5 (47.8)						

TENSILE PROPERTIES A514/A517

ASTM SPEC	YIELD STRENGTH KSI			TENSILE STRENGTH KSI			% ELONGATION			% REDUCTION OF AREA		
	100 MIN.			115 to 135			16 MIN.			45 MIN.		
	MILL	CALTRANS	ID	MILL	CALTRANS	ID	MILL	CALTRANS	ID	MILL	CALTRANS	ID
1024/95	125.0	123.0	CE	134.0	134.5		18.0	16.0		52.0	49.2	
	124.6 (124.8)	121.0 (122.0)		134.5 (134.3)	133.0 (133.8)		20.0 (19.0)	16.0 (16.0)		49.8 (50.9)	49.2 (49.2)	
1025/91	124.4	112.5	CC	133.3	127.0		18.0	16.5		54.8	50.6	
	124.0 (124.2)	114.0 (113.3)		134.5 (133.9)	127.0 (127.0)		17.0 (17.5)	17.5 (17.0)		49.0 (51.9)	52.8 (51.7)	
1025/95	115.4	111.0	CJ	126.4	124.0		20.0	16.0		64.7	49.8	
	122.8 (119.1)	112.5 (111.8)		130.2 (128.3)	125.5 (124.8)		16.0 (18.0)	16.5 (16.3)		49.1 (56.9)	50.6 (50.2)	
1026/92	109.5	92.5	A	127.6	120.7		21.0	19.0		57.7	52.5	
	117.4 (113.5)	89.0 (90.8)		126.6 (127.1)	120.0 (120.4)		19.0 (20.0)	19.5 (19.8)		57.7 (57.7)	55.0 (53.8)	
1027/44	120.8	117.0	CK	130.7	131.0		18.0	15.0		46.5	42.6	
	121.9 (121.4)	117.5 (117.3)		131.8 (131.3)	131.0 (131.0)		17.0 (17.5)	14.8 (14.9)		46.3 (46.4)	43.1 (42.9)	
1027/45	124.9	115.5	CD	133.3	129.0		16.0	15.5		45.3	44.8	
	122.9 (123.9)	122.0 (118.8)		132.3 (132.8)	134.5 (131.8)		17.0 (16.5)	15.5 (15.5)		52.2 (48.8)	44.3 (44.6)	
1027/46	124.6	119.0	CH	133.0	131.0		16.0	14.0		47.4	43.5	
	125.0 (124.8)	119.0 (119.0)		133.0 (133.0)	131.0 (131.0)		18.0 (17.0)	15.0 (14.5)		49.0 (48.2)	44.6 (44.0)	

TENSILE PROPERTIES A514/A517

ASTM SPEC	YIELD STRENGTH KSI		TENSILE STRENGTH KSI		% ELONGATION		% REDUCTION OF AREA	
	100 MIN.		115 to 135		16 MIN.		45 MIN.	
Heat/Slab ID	MILL	CALTRANS	MILL	CALTRANS	MILL	CALTRANS	MILL	CALTRANS
1028/64 B	109.5	102.5	124.4	117.0	20.0	18.0	57.3	52.5
	117.4 (113.5)	103.0 (102.8)	125.1 (124.8)	116.5 (116.8)	19.0 (19.5)	19.0 (18.5)	56.7 (57.0)	53.7 (53.1)
1029/99 T	--	109.0	--	120.0	--	17.0	--	51.0
		108.5 (108.8)		119.2 (119.6)		17.5 (17.3)		51.0 (51.0)

Appendix B

Chemistry of 30 Heats of A514/517 Steel as
Recorded in the Mill Test Reports and as
Determined by Caltrans Laboratory.

B-1 thru B-6

CHEMISTRY A514/A517

CHEMISTRY		C	Mn	P	S	Si	Cu	Ni	Cr	Mo	V	B	Ti	Al	Zr
Ht/Slab	Gr ID	Test	By												
		.08 to .022	.55 to 1.05	.035 Max	.040 Max	.13 to 0.37	.12 to 0.53	.67 to 1.03	.36 to 0.79	.36 to 0.64	.02 to 0.09	.002 to .006	---	---	---
		.10 to 0.23	.90 to 1.35	.035 Max	.040 Max	.18 to 0.37	.17 to 0.73	.27 to 0.69	.36 to 0.69	.17 to 0.33	.02 to 0.09	.0005 Min	---	---	---
1000/39	B BY	0.17	0.85	.007	.027	.023	---	---	0.56	0.17	0.04	.003	.02	---	---
	CT	0.20	0.82	0.01	0.03	0.30	---	---	0.59	0.18	0.04	---	---	---	---
1001/82	F AD	0.17	0.89	.012	.015	0.25	0.24	0.81	0.58	0.45	0.04	.003	.01	.005	.005
	" CT	0.18	0.90	0.02	0.01	0.26	0.22	0.86	0.56	0.41	0.03	---	.01	.005	.005
	AE "	0.19	0.85	0.02	0.01	0.28	0.22	0.86	0.52	0.41	0.03	---	.01	.005	.005
	AF "	0.18	0.88	0.02	0.01	0.24	0.25	0.83	0.57	0.41	0.03	---	.01	.005	.005
1002/82	F AB	0.17	0.85	0.01	0.02	0.26	0.25	0.83	0.53	0.45	0.04	.003	.01	.005	.005
	" CT	0.16	0.88	0.02	0.01	0.24	0.25	0.83	0.53	0.41	0.03	---	.01	.005	.005
	AC "	0.18	0.87	0.02	0.01	0.25	0.25	0.83	0.52	0.41	0.03	---	.01	.005	.005
1003/29	F CB	0.17	0.86	.012	.016	0.23	0.24	0.81	0.52	0.44	0.04	.003	---	---	---
	" CT	0.21	0.83	0.02	0.02	0.26	0.24	0.83	0.58	0.43	0.04	---	---	---	---
1004/44	F AG	0.19	0.84	.015	.016	0.24	0.25	0.80	0.56	0.45	0.04	.004	.002	.005	.005
	" CT	0.20	0.85	0.02	0.01	0.24	0.23	0.86	0.53	0.42	0.03	---	.005	.005	.005
	AH "	0.20	0.82	0.02	0.01	0.24	0.23	0.84	0.54	0.42	0.03	---	.005	.005	.005
	AJ "	0.22	0.86	0.02	0.01	0.24	0.23	0.84	0.54	0.42	0.03	---	.002	.005	.005
1005/22	F BX	0.18	0.79	.020	.019	0.22	0.23	0.77	0.55	0.46	0.04	.003	---	---	---
	" CT	0.18	0.72	.032	0.02	0.22	0.24	0.78	0.60	0.43	0.03	---	---	---	---

*CT - Calltrans Laboratory

CHEMISTRY A514/A517

Ht/Slab	Gr	ID	Test By	CHEMISTRY													
				C	Mn	P	S	Si	Cu	Ni	Cr	Mo	V	B	Ti	Al	Zr
1006/	F	AR	Mill	0.16	0.87	0.014	0.023	0.25	0.24	0.99	0.53	0.46	0.04				
"	47	"	CT	NO CHEMICAL ANALYSIS													
"	48	AS	"	0.20	0.83	0.02	0.02	0.22	0.25	1.02	0.54	0.39	0.03				
"	49	BJ	"	NO CHEMICAL ANALYSIS													
"	50	AT	"	NO CHEMICAL ANALYSIS													
"	51	AU	"	"	"	"	"										
"	52	AV	"	"	"	"	"										
"	53	BK	"	0.18	0.87	0.02	0.02	0.22	0.24	1.02	0.53	0.37	0.03				
"	54	BL	"	NO CHEMICAL ANALYSIS													
"	56	BM	"	0.22	0.86	0.02	0.02	0.24	0.24	1.03	0.53	0.40	0.03				
"	57	AW	"	NO CHEMICAL ANALYSIS													
"	58	AX	"	"	"	"	"										
"	59	BN	"	"	"	"	"										
"	60	BP	"	"	"	"	"										
"	61	AY	"	"	"	"	"										
"	62	AZ	"	"	"	"	"										
"	25	BA	"	0.19	0.83	0.02	0.02	0.24	0.25	1.03	0.53	0.39	0.04				
"	26	BB	"	NO CHEMICAL ANALYSIS													
"	64	BC	"	"	"	"	"										
"	65	BR	"	"	"	"	"										
"	66	BS	"	"	"	"	"										
"	67	BT	"	"	"	"	"										
"	68	BD	"	"	"	"	"										
"	69	BE	"	"	"	"	"										

CHEMISTRY A514/A517

CHEMISTRY	Ht/Slab	Gr ID	Test By	C	Mn	P	S	Si	Cu	Ni	Cr	Mo	V	B	Ti	Al	Zr
ASTM - Grade F				.08 to .022	.55 to 1.05	.035 Max	.040 Max	.13 to 0.37	.12 to 0.53	.67 to 1.03	.36 to 0.79	.36 to 0.64	.02 to 0.09	.002 to .006			
ASTM - Grade H				.10 to 0.23	.90 to 1.35	.035 Max	.040 Max	.18 to 0.37		.27 to 0.73	.36 to 0.69	.17 to 0.33	.02 to 0.09	.0005 Min			
1006/70	F	BU	CT	NO CHEMICAL ANALYSIS													
71		BF	"	0.17	0.83	0.02	0.02	0.23	0.24	1.02	0.54	0.40	0.04				
72		BV	"	0.18	0.84	0.02	0.02	0.23	0.24	1.00	0.51	0.39	.022				
73		BZ	"	0.18	"				0.24	1.03		0.41					
74		BG	"	NO CHEMICAL ANALYSIS													
75		BW	"	"	"												
1007/	H	AM	Mill	0.19	1.17	0.01	0.02	0.26	0.03	0.57	0.47	0.23	0.06	.004			
11		"	CT	0.16	1.23	0.01	0.02	0.24	---	0.45	0.42	0.21	0.05				
12		AN	"	*0.17	1.24	0.01	0.02	0.23	---	0.45	0.40	0.21	0.05				
				*By Aerojet													
1008/76	F	D	Mill	0.17	0.89	0.01	.016	0.24	0.23	0.80	0.49	0.45	0.04	.002			
"		"	CT	0.14	0.91	0.017	.019	0.24	0.21	0.83	0.44	0.45	0.03				
1009/40	F	BH	Mill	0.17	0.93	0.011	0.017	0.26	0.25	0.77	0.49	0.45	0.04	.004			
"		"	CT	0.18	0.97	0.02	0.01	0.27	0.27	0.85	0.52	0.43	0.04				
1010/47	F	AP	Mill	0.17	0.84	0.01	0.02	0.23	0.22	0.80	0.54	0.44	0.04	.003			
"		"	CT	0.19	0.78	0.02	0.02	0.22	0.22	0.82	0.57	0.40	0.03				
.1011/92	F	CA	Mill	0.16	0.75	0.01	0.015	0.20	0.26	0.79	0.49	0.45	0.04	.003			
"		"	CT	0.17					0.25	0.81		0.43					

CHEMISTRY A514/A517

CHEMISTRY		C	Mn	P	S	Si	Cu	Ni	Cr	Mo	V	B	Ti	Al	Zr
Ht/Slab	Gr ID	Test By													
			0.08 to 0.22	0.55 to 1.05	0.035 Max	0.040 Max	0.13 to 0.37	0.12 to 0.53	0.67 to 1.03	0.36 to 0.79	0.02 to 0.09	0.002 to 0.006			
ASTM - Grade F			0.10 to 0.23	0.90 to 1.35	0.035 Max	0.040 Max	0.18 to 0.37		0.27 to 0.73	0.17 to 0.33	0.02 to 0.09	0.0005 Min			
ASTM - Grade H															
1012/99	F AK	Mill CT	0.16	0.82	0.014	0.017	0.20	0.26	0.86	0.46	0.05	0.002	0.01		.005
"	"	"	0.16	0.84	0.02	0.01	0.23	0.23	0.87	0.43	0.03				
1013/32	F J	Mill CT	0.17	0.90	0.01	0.025	0.23	0.24	0.73	0.45	0.05	0.003	0.01		
"	"	"	0.17	0.91	0.01	0.01	0.22	0.23	0.75	0.39	0.04				
1014/02	F M	Mill CT	0.16	0.94	0.011	0.023	0.21	0.26	0.81	0.49	0.05	0.003			
"	"	"	0.16	0.96	0.02	0.01	0.18	0.25	0.81	0.42	0.04				
1015/32	H N	Mill CT	0.18	1.22	0.01	0.024	0.28	0.26	0.53	0.24	0.06	0.003	0.01		
"	"	"	0.17	1.24	0.01	0.01	0.30	0.26	0.52	0.21	0.04				
1016/41	H P	Mill CT	0.17	1.10	0.014	0.02	0.27	0.02	0.51	0.25	0.06	0.004			
11	"	"	0.17	1.17	0.01	0.01	0.28	0.04	0.52	0.23	0.04				
"	"	"	0.16	1.13	0.01	0.02	0.26	0.04	0.43	0.23	0.05				
1017/62	F L	Mill CT	0.16	0.82	0.01	0.016	0.18	0.25	0.82	0.47	0.05	0.004	0.01		
"	"	"	0.15	0.86	0.01	0.01	0.15	0.25	0.81	0.41	0.04				
1018/81	H S	Mill CT	0.18	1.14	0.01	0.02	0.24	0.03	0.46	0.25	0.05	0.004	0.01		
"	"	"	0.18	1.13	0.01	0.01	0.25	0.03	0.47	0.23	0.04				
1019/31	H R	Mill CT	0.18	1.16	0.014	0.02	0.27	0.02	0.46	0.25	0.05	0.004	0.01		
"	"	"	0.16	1.14	0.01	0.01	0.23	0.02	0.42	0.20	0.04				

CHEMISTRY A514/A517

CHEMISTRY		C	Mn	P	S	Si	Cu	Ni	Cr	Mo	V	B	Ti	Al	Zr
Ht/Slab	Gr ID	Test By	Mn	P	S	Si	Cu	Ni	Cr	Mo	V	B	Ti	Al	Zr
1020/41	H AA	Mill	1.08	.008	.040	0.27	0.22	0.32	0.53	0.24	0.06	.003	.03		.005
43	"	CT	1.09	.01	Max	0.23	0.22	0.35	0.48	0.25	0.06				
44	CF	"	1.12	.01	Max	0.25		0.29	0.51	0.26	0.06				
46	CG	"	1.15	.01	Max	0.32		0.29	0.53	0.26	0.06				
	AL	"	1.14	.01	Max	0.32	0.25	0.34	0.51	0.26	0.06		.04		.005
1021/42	B CM	Mill	0.80	.012	.040	0.22	0.24	0.24	0.54	0.20	0.06	.0037	.018		.005
"	"	CT	0.81	.013	Max	0.21		.020	0.44	0.21	0.06		.02		
1022/51	H C	Mill	1.01	.011	.020	0.27	0.26	0.42	0.53	0.25	0.05	.0038	.02	Tr	.01
53	"	CT	1.07	.014	.029	0.29	0.25	0.41	0.47	0.26	0.056		.03	.03	
54	F H	"	1.08	.01	.02	0.24	0.25	0.42	0.44	0.25	0.05		.03	.03	
	"	"	1.02	.01	.01	0.24	0.25	0.42	0.44	0.25	0.05		.03	.03	.01
1023/51	H G	Mill	1.00	.011	.020	0.25	0.26	0.33	0.51	0.25	0.05	.003	.03	.02	.005
54	"	CT	1.10	.01	.01	0.24	0.26	0.36	0.44	0.28	0.05	0.05	.03	.04	
	E	"	1.06	.01	.02	0.23	0.26	0.35	0.44	0.30	0.05		.03	.04	.005
1024/91	H Y	Mill	1.07	.015	.020	0.34	0.26	0.36	0.54	0.26	0.06	.0032	.03		.005
94	"	CT	1.13	.01	.01	0.32	0.26	0.38	0.48	0.26	0.06		.03		.005
95	Z	"	1.18	.01	.01	0.33	0.26	0.39	0.50	0.26	0.06		.03		.005
	CE	"	1.16	.02	.02	0.32	0.27	0.40	0.54	0.29	0.06		.03		.005

CHEMISTRY A514/A517

CHEMISTRY	Ht/Slab	Gr	ID	Test By	C	Mn	P	S	Si	Cu	Ni	Cr	Mo	V	B	Ti	Al	Zr
					.08 to .022	.55 to 1.05	.035 Max	.040 Max	.13 to 0.37	.12 to 0.53	.67 to 1.03	.36 to 0.79	.36 to 0.64	.02 to 0.09	.002 to .006	---	---	---
					.10 to 0.23	.90 to 1.35	.035 Max	.040 Max	.18 to 0.37		.27 to 0.73	.36 to 0.69	.17 to 0.33	.02 to 0.09	.0005 Min	---	---	---
1025/91	H	CC		Mill	0.19	1.03	.009	.021	0.30	0.21	0.33	0.53	0.26	0.06	.0025			
1025/95	"	"		CT	0.21	1.04	.01	.01	0.34		0.33	0.53	0.27	0.06				
				"	0.20	1.04	.01	.01	0.29		0.29	0.55	0.25	0.06				
1026/92	F	A		Mill	0.15	0.78	.015	.015	0.24	0.29	0.80	0.52	0.45	0.06	.0030			
"	"	"		CT	0.11	0.79	.015	.013	0.25	0.29	0.80	0.42	0.48	0.064				Tr
1027/44	H	CK		Mill	0.19	1.03	.008	.023	0.29	0.22	0.35	0.54	0.27	0.06	.0052			
1027/45	"	"		CT	0.22	1.11	.015	.02	0.30	0.23	0.34	0.47	0.30	0.065	.005	.001		
1027/46	"	"		"	0.21	1.06	.02	.01	0.30	0.23	0.36	0.52	0.29	0.06				
				"	0.20	1.11	.02	.02	0.29	0.23	0.32	0.54	0.27	0.06				
1028/64	F	B		Mill	0.14	0.79	.014	.017	0.18	0.25	0.75	0.55	0.43	0.05	.004			
"	"	"		CT	0.10	0.88	.015	.022	0.20	0.25	0.75	0.45	0.46	0.05				Tr .005
1029/99	H	T		CT	0.18	1.03	.01	.01	0.21	0.20	0.52	0.48	0.24	0.04	.006			.005

Appendix C

Charpy V-Notch and Precrack Charpy Impact Test
Results from 76 Slabs from 30 Heats of A514/517
Steel.

APPENDIX C

FIGURES CORRESPONDING TO HEAT NUMBERS

STEEL COMPANY HEAT/SLAB	REPORT CODE HEAT/SLAB	ID	ASTM TYPE-GRADE	PLATE THICK.	FIG. NO.
69D478-198339A	1000/39	BY	A517-B	7/8	-
70E729-261282	1001/82	AD	A517-F	1-1/2	C-1
261283	1001/83	AE	A517-F	1-1/2	C-2
261284	1001/84	AF	A517-F	1-1/2	C-3
71D653-258582	1002/82	AB	A517-F	1-1/2	C-4
258638	1002/38	AC	A517-F	1-1/2	C-5
72A033-033429	1003/29	CB	A514-F	2-1/4	C-6
72A166-073144	1004/44	AG	A517-F	1-1/2	C-7
072196	1004/96	AH	A517-F	1-1/2	C-8
073198	1004/98	AJ	A517-F	1-1/2	C-9
72A618-209722	1005/22	BX	A517-F	1-3/8	C-10
72A625-212147	1006/47	AR	A517-F	1-3/8	-
212148	1006/48	AS	A517-F	1-3/8	C-11
212149	1006/49	BJ	A517-F	1-3/8	-
212150	1006/50	AT	A517-F	1-3/8	-
212151	1006/51	AU	A517-F	1-3/8	-
212152	1006/52	AV	A517-F	1-3/8	-
212153	1006/53	BK	A517-F	1-3/8	-
212154	1006/54	BL	A517-F	1-3/8	-
212156	1006/56	BM	A517-F	1-3/8	C-12
212157	1006/57	AW	A517-F	1-3/8	-
212158	1006/58	AX	A517-F	1-3/8	-
212159	1006/59	BN	A517-F	1-3/8	-
212160	1006/60	BP	A517-F	1-3/8	-
212161	1006/61	AY	A517-F	1-3/8	-
212162	1006/62	AZ	A517-F	1-3/8	-
212225	1006/25	BA	A517-F	1-3/8	-
212226	1006/26	BB	A517-F	1-3/8	C-13
212564	1006/64	BC	A517-F	1-3/8	-
212565	1006/65	BR	A517-F	1-3/8	-
212566	1006/66	BS	A517-F	1-3/8	-

Continued

APPENDIX C

FIGURES CORRESPONDING TO HEAT NUMBERS

<u>STEEL COMPANY HEAT/SLAB</u>	<u>REPORT CODE HEAT/SLAB</u>	<u>ID</u>	<u>ASTM TYPE-GRADE</u>	<u>PLATE THICK.</u>	<u>FIG. NO.</u>
72A625-212567	1006/67	BT	A517-F	1-3/8	-
212568	1006/68	BD	A517-F	1-3/8	-
212569	1006/69	BE	A517-F	1-3/8	-
212570	1006/70	BU	A517-F	1-3/8	-
212571	1006/71	BF	A517-F	1-3/8	C-14
212572	1006/72	BV	A517-F	1-3/8	C-15
212573	1006/73	BZ	A517-F	1-3/8	C-16
212574	1006/74	BG	A517-F	1-3/8	-
212575B	1006/75	BW	A517-F	1-3/8	-
73A434-145011	1007/11	AM	A514-H	1-1/2	C-17
145012	1007/12	AN	A514-H	1-1/2	C-18
74E002-001876	1008/76	D	A517-F	2-1/2	C-19
74E397-135040	1009/40	BH ₁	A517-F	1-3/4	C-20
75A179-063447	1010/47	AP	A517-F	1-3/8	C-21
75A703-217592	1011/92	CA	A517-F	1-3/8	C-22
75B082-030699	1012/99	AK	A517-F	1-1/2	C-23
78L-15-03W2	1013/32	J	A514-F	2-1/4	C-24
92L088-10W2	1014/02	M	A514-F	2-1/4	C-25
96L114-03W2	1015/32	N	A514-H	1-3/4	C-26
97L151-04W1	1016/41	P	A514-H	2	C-27
01W1	1016/11	K	A514-H	2	C-28
97L168-06W2	1017/62	L	A514-F	2-1/4	C-29
97L170-08W1	1018/81	S	A514-H	2	C-30
E07619-03W1	1019/31	R	A514-H	2	C-31
A4071-1	1020/41	AA	A517-H	2-1/4	C-32
3	1020/43	CF	A517-H	2-1/4	C-33
4	1020/44	CG	A517-H	2-1/4	C-34
6	1020/46	AL	A517-H	2-1/4	C-35
A4099-2B	1021/42	CM	A517-B	7/8	C-36
A5491-1B	1022/51	C	A517-H	2-1/2	C-37
3B	1022/53	F	A517-H	2	C-38
4A	1022/54	H	A517-H	2	C-39

APPENDIX C

FIGURES CORRESPONDING TO HEAT NUMBERS

<u>STEEL COMPANY HEAT/SLAB</u>	<u>REPORT CODE HEAT/SLAB</u>	<u>ID</u>	<u>ASTM TYPE-GRADE</u>	<u>PLATE THICK.</u>	<u>FIG. NO.</u>
A5550-1A	1023/51	G	A517-H	2	C-40
4A	1023/54	E	A517-H	2	C-41
B9093-1	1023/91	Y	A517-H	2-1/4	C-42
4B	1024/94	Z	A517-H	2-1/4	C-43
5B	1024/95	CE	A517-H	2-1/4	C-44
B9131-1	1025/91	CC	A517-H	2-1/4	C-45
5	1025/95	CJ	A517-H	2-1/4	C-46
B9863-2C	1026/92	A	A517-F	2-1/4	C-47
C4913-4	1027/44	CK	A517-H	2-1/4	C-48
5	1027/45	CD	A5-17-H	2-1/4	C-49
6	1027/46	CH	A517-H	2-1/4	C-50
C6369-4	1028/64	B	A517-H	2-1/2	C-51
Unknown-Unknown	1029/99	T	A514-H	1-3/8	C-52

APPENDIX C

FIGURES CORRESPONDING TO PLATE ID

<u>ID</u>	<u>ASTM TYPE-GRADE</u>	<u>REPORT CODE HEAT/SLAB</u>	<u>STEEL COMPANY HEAT/SLAB</u>	<u>PLATE THICK</u>	<u>FIG. NO.</u>
A	A517-F	1026/92	B9863-2C	2-1/4	C-47
B	A517-F	1028/64	C6369-4	2-1/2	C-51
C	A517-H	1022/51	A5491-1B	2-1/2	C-37
D	A517-F	1008/76	74E002-001876	2-1/2	C-19
E	A517-H	1023/54	A5550-4A	2	C-41
F	A517-H	1022/53	A5491-3B	2	C-38
G	A517-H	1023/51	A5550-1A	2	C-40
H	A517-H	1022/54	A5491-4A	2	C-39
J	A514-F	1013/32	78L015-03W2	2-1/4	C-24
K	A514-H	1016/11	97L151-G1W1	2	C-28
L	A514-F	1017/62	97L168-06W2	2-1/4	C-29
M	A514-F	1014/02	92L088-10W2	2-1/4	C-25
N	A514-H	1015/32	96L114-03W2	1-3/4	C-26
P	A514-H	1016/41	97L151-04W1	2	C-27
R	A514-H	1019/31	E07619-03W1	2	C-31
S	A514-H	1018/81	97L170-08W1	2	C-30
T	A514-H	1029/99	Unknown	1-3/8	C-52
Y	A517-H	1024/91	B9093-1	2-1/4	C-42
Z	A517-H	1024/94	B9093-4B	2-1/4	C-43
AA	A517-H	1020/41	A4071-1	2-1/4	C-32
AB	A517-F	1002/82	71D653-258582	1-1/2	C-4
AC	A517-F	1002/38	71D653-258638	1-1/2	C-5
AD	A517-F	1002/38	70E729-261282	1-1/2	C-1
AE	A517-F	1001/83	70E729-261283	1-1/2	C-2
AF	A517-F	1001/84	70E729-261284	1-1/2	C-3
AG	A517-F	1004/44	72A166-73144	1-1/2	C-7
AH	A517-F	1004/96	72A166-73196	1-1/2	C-8
AJ	A517-F	1004/98	72A166-73198	1-1/2	C-9
AK	A517-F	1012/99	75B082-30699	1-1/2	C-23
AL	A517-H	1020/46	A4071-6	2-1/4	C-35
AM	A514-H	1007/11	73A434-145011	1-1/2	C-17

APPENDIX C

FIGURES CORRESPONDING TO PLATE ID

<u>ID</u>	<u>ASTM TYPE-GRADE</u>	<u>REPORT CODE HEAT/SLAB</u>	<u>STEEL COMPANY HEAT/SLAB</u>	<u>PLATE THICK</u>	<u>FIG. NO.</u>
AN	A514-H	1007/12	73A434-145012	1-1/2	C-18
AP	A517-F	1010/47	75A179-63447	1-3/8	C-21
AR	A517-F	1006/47	72A625-212147	1-3/8	-
AS	A517-F	1006/48	72A625-212148	1-3/8	C-11
AT	A517-F	1006/50	72A625-212150	1-3/8	-
AU	A517-F	1006/51	72A625-212151	1-3/8	-
AV	A517-F	1006/52	72A625-212152	1-3/8	-
AW	A517-F	1006/57	72A625-212157	1-3/8	-
AX	A517-F	1006/58	72A625-212158	1-3/8	-
AY	A517-F	1006/61	72A625-212161	1-3/8	-
AZ	A517-F	1006/62	72A625-212162	1-3/8	-
BA	A517-F	1006/25	72A625-212225	1-3/8	-
BB	A517-F	1006/26	72A625-212226	1-3/8	C-13
BC	A517-F	1006/64	72A625-212564	1-3/8	-
BD	A517-F	1006/68	72A625-212568	1-3/8	-
BE	A517-F	1006/69	72A625-212569	1-3/8	-
BF	A517-F	1006/71	72A625-212571	1-3/8	C-14
BG	A517-F	1006/74	72A625-212574	1-3/8	-
BH	A517-F	1009/40	74E397-135040	1-3/4	C-20
BJ	A517-F	1006/49	72A625-212149	1-3/8	-
BK	A517-F	1006/53	72A625-212153	1-3/8	-
BL	A517-F	1006/54	72A625-212154	1-3/8	-
BM	A517-F	1006/56	72A625-212156	1-3/8	C-12
BN	A517-F	1006/59	72A625-212159	1-3/8	-
BP	A517-F	1006/60	72A625-212160	1-3/8	-
BR	A517-F	1006/65	72A625-212565	1-3/8	-
BS	A517-F	1006/66	72A625-212566	1-3/8	-
BT	A517-F	1006/67	72A625-212567	1-3/8	-
BU	A517-F	1006/70	72A625-212570	1-3/8	-
BV	A517-F	1006/72	72A625-212572	1-3/8	C-15
BW	A517-F	1006/75	72A625-212575B	1-3/8	-

APPENDIX C

FIGURES CORRESPONDING TO PLATE ID

<u>ID</u>	<u>ASTM TYPE-GRADE</u>	<u>REPORT CODE HEAT/SLAB</u>	<u>STEEL COMPANY HEAT/SLAB</u>	<u>PLATE THICK</u>	<u>FIG. NO.</u>
BX	A517-F	1005/22	72A618-209722	1-3/8	C-10
BY	A517-B	1000/39	69D478-198339A	7/8	-
BZ	A517-F	1006/73	72A625-212573	1-3/8	C-16
CA	A517-F	1011/92	75A703-217592	1-3/8	C-22
CB	A514-F	1003/29	72A033-033429	2-1/4	C-6
CC	A517-H	1025/91	B9131-1	2-1/4	C-45
CD	A517-H	1027/45	C4913-5	2-1/4	C-49
CE	A517-H	1024/95	B9093-5B	2-1/4	C-44
CF	A517-H	1020/43	A4071-3	2-1/4	C-33
CG	A517-H	1020/44	A4071-4	2-1/4	C-34
CH	A517-H	1027/46	C4913-6	2-1/4	C-50
CJ	A517-H	1025/95	B9131-5	2-1/4	C-46
CK	A517-H	1027/44	C4913-4	2-1/4	C-48
CM	A517-B	1021/42	A4099-2B	7/8	C-36

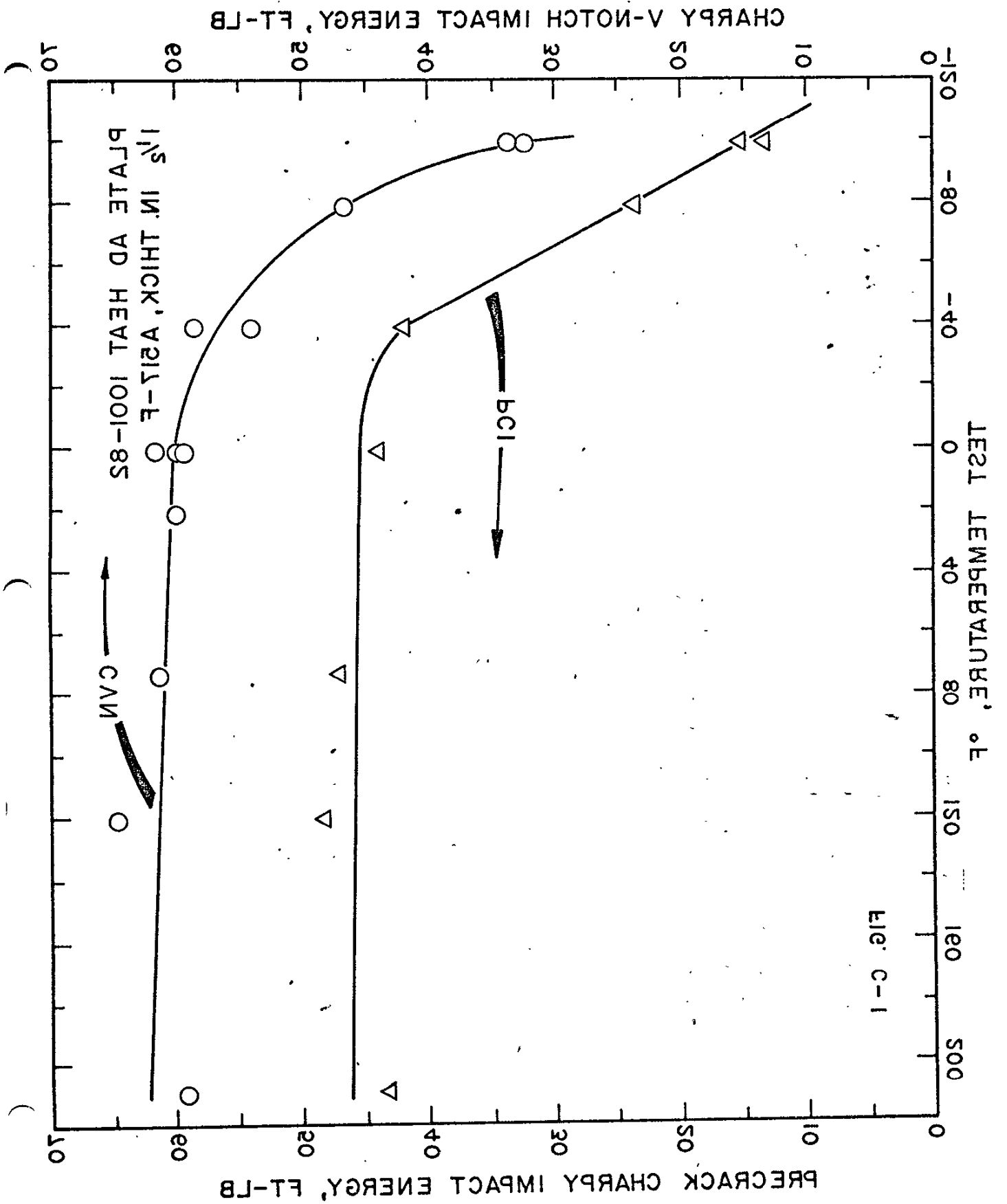
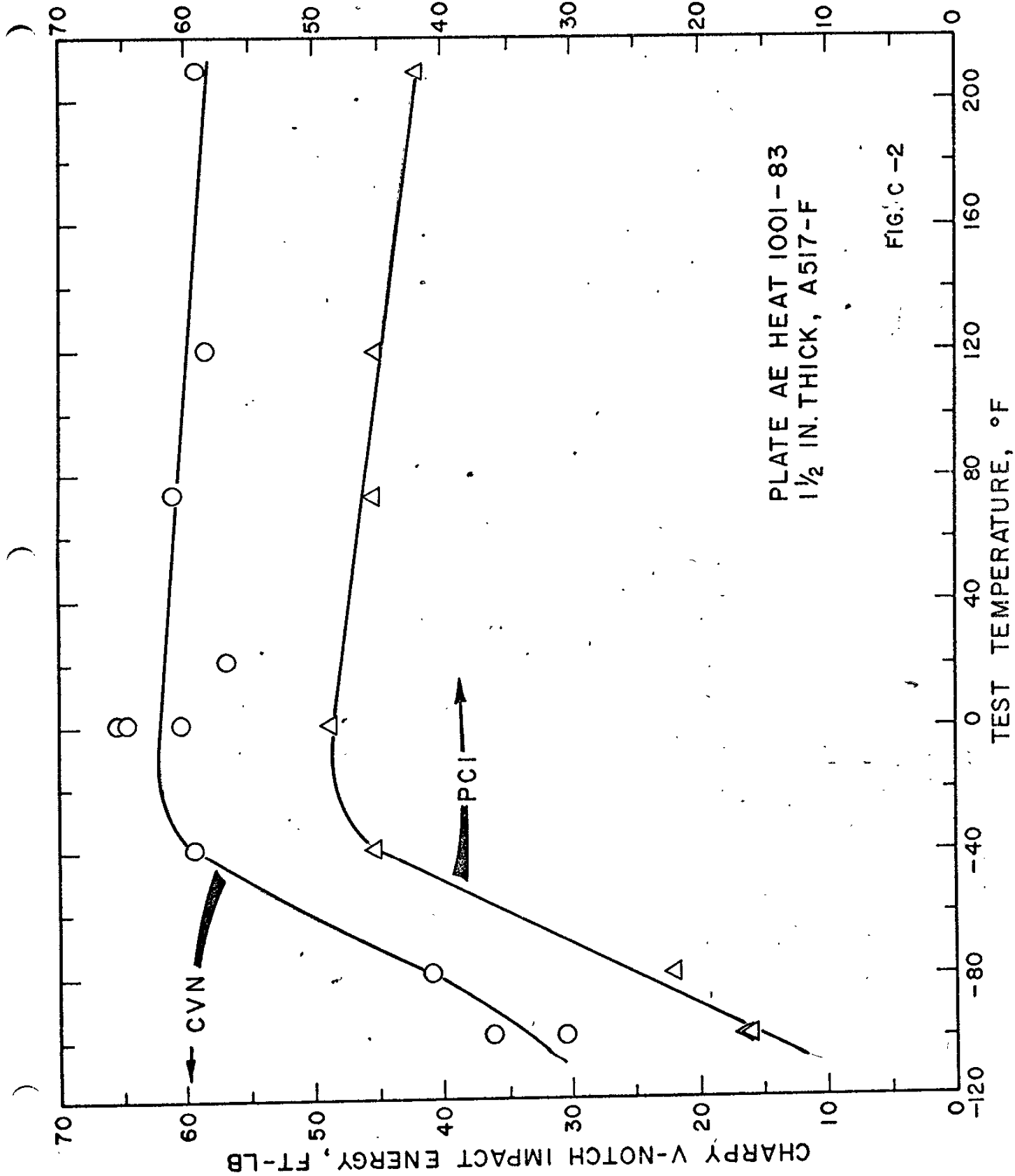


FIG. C-1

PRECRACK CHARPY IMPACT ENERGY, FT-LB



CHARPY V-NOTCH IMPACT ENERGY, FT-LB

8-C

PRECRACK CHARPY IMPACT ENERGY, FT-LB

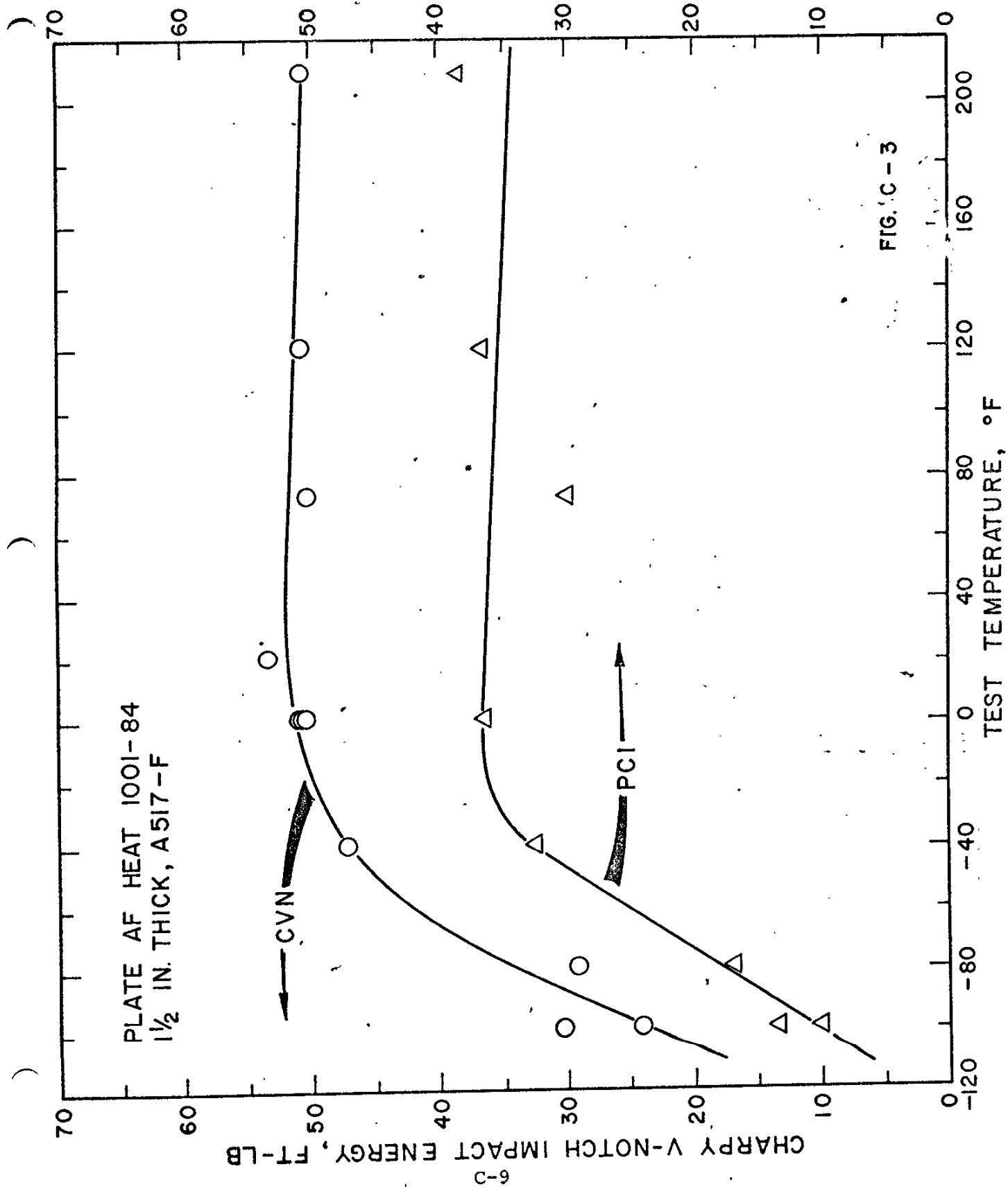


FIG. C-3

PLATE AB HEAT 1002-82
1 1/2 IN. THICK, A517-F

PRECRACK CHARPY IMPACT ENERGY, FT-LB

CHARPY V-NOTCH IMPACT ENERGY, FT-LB

TEST TEMPERATURE, °F

FIG. C-4

CVN

PCI

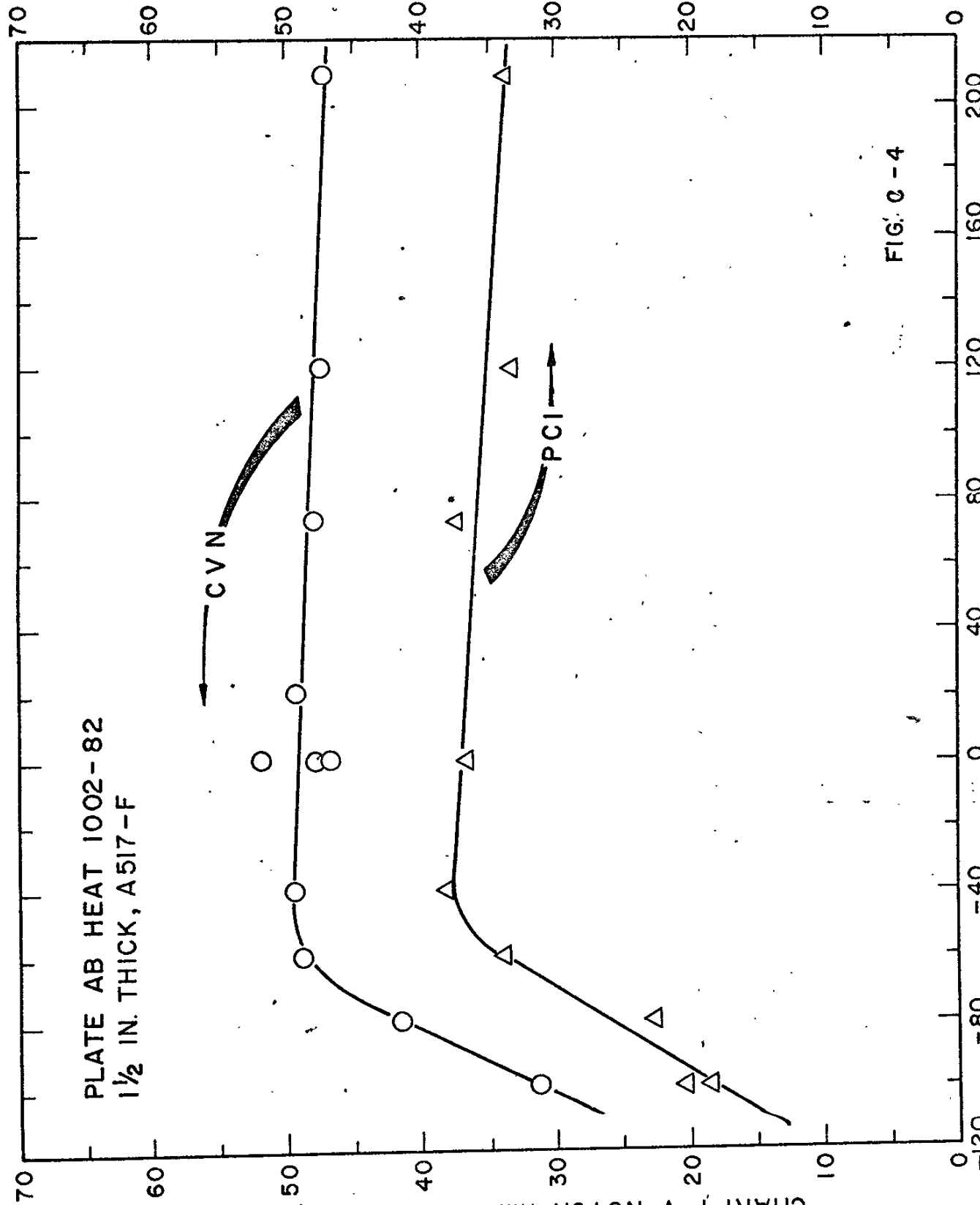


PLATE AC HEAT 1002-38
1 1/2 IN. THICK, A517-F

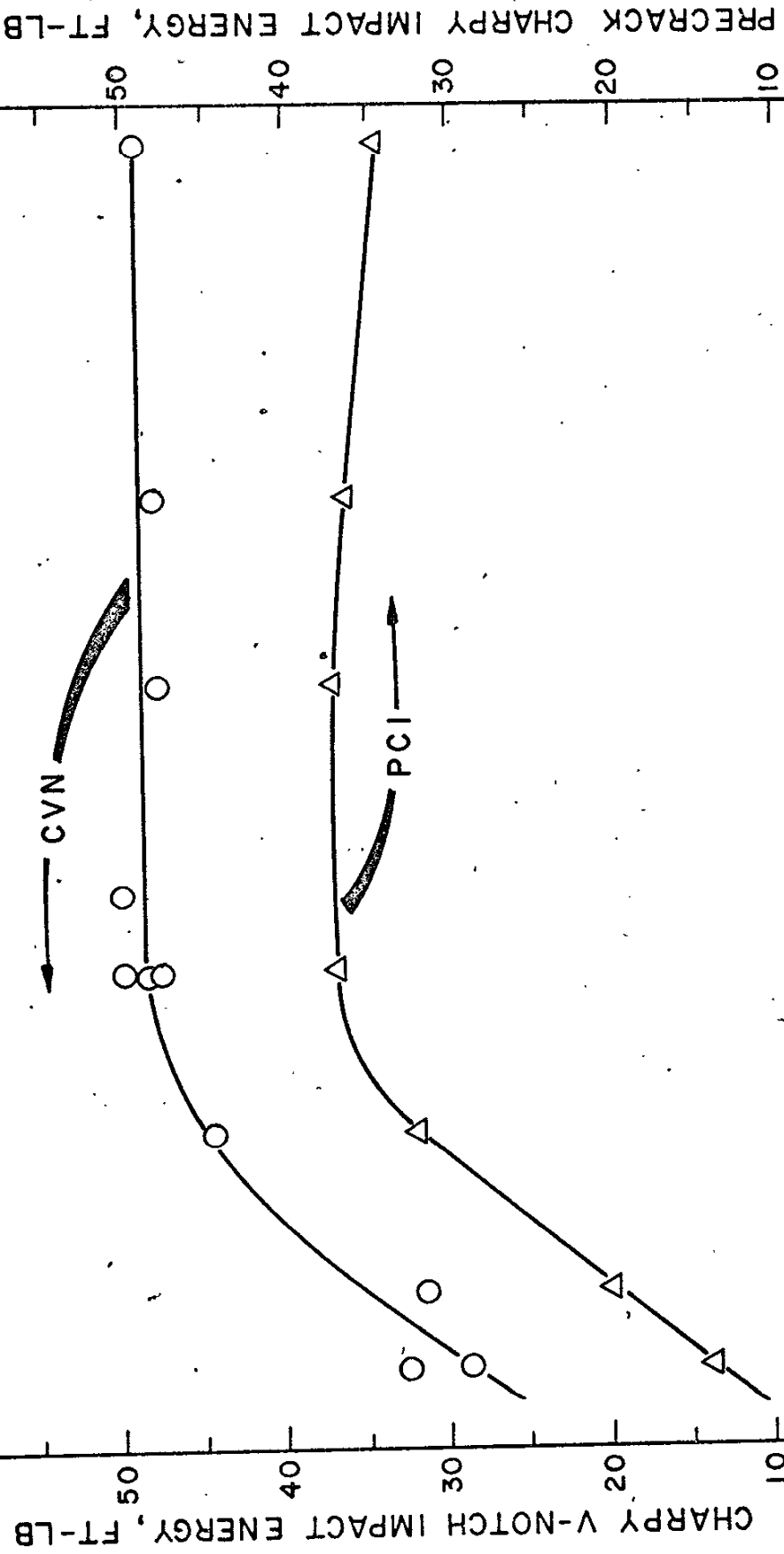


FIG. C - 5

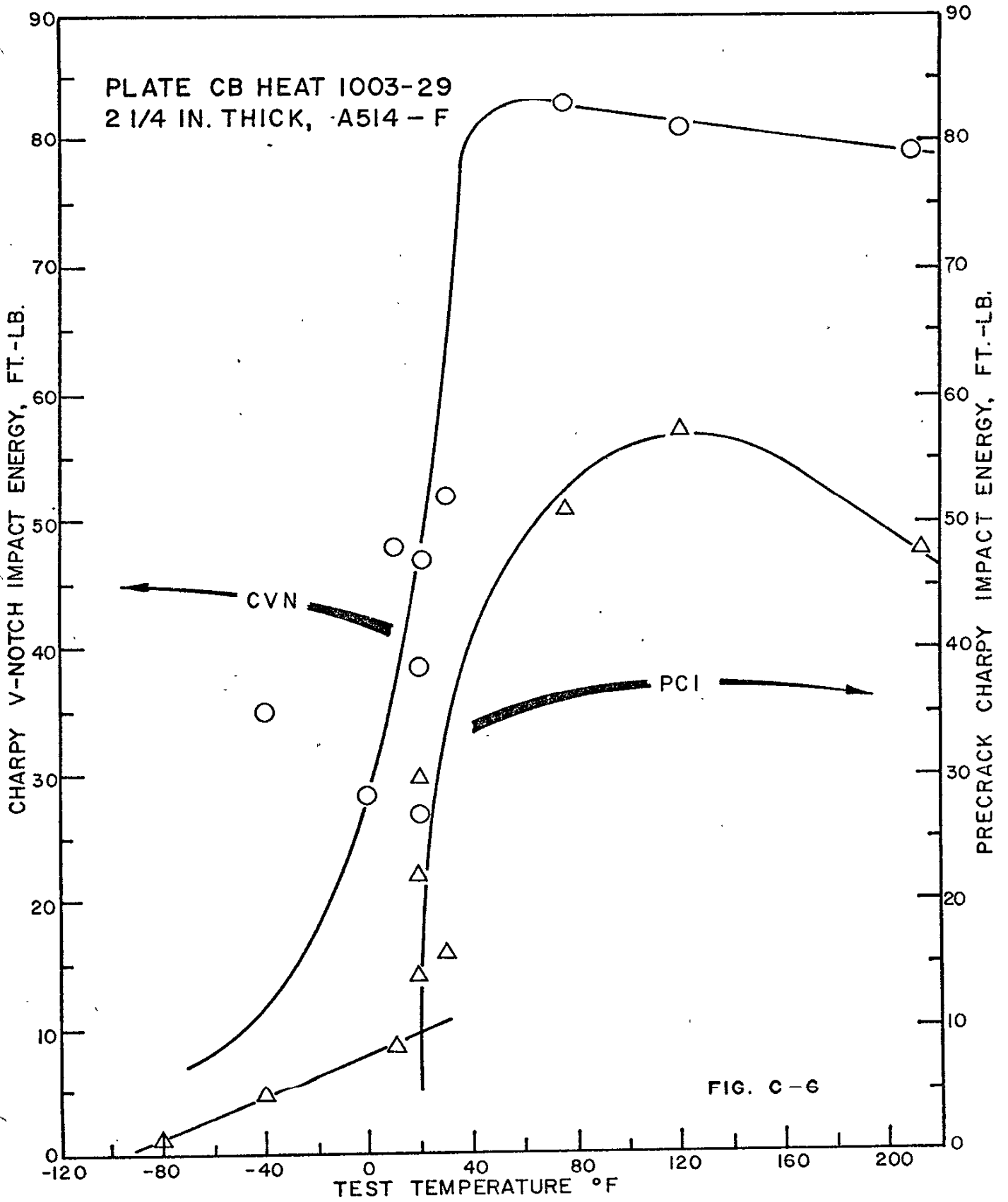


FIG. C-6

PRECRACK CHARPY IMPACT ENERGY, FT-LB

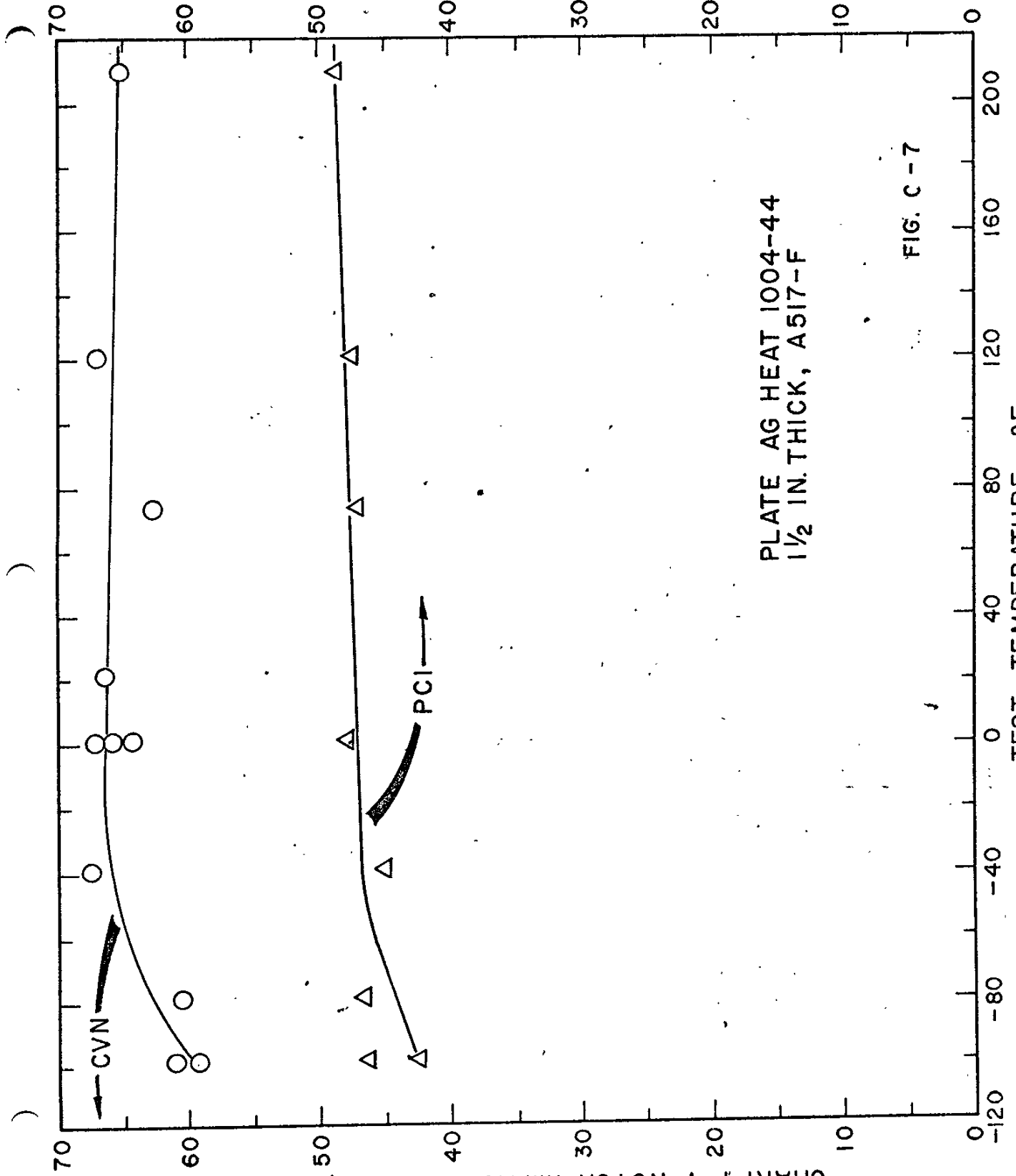


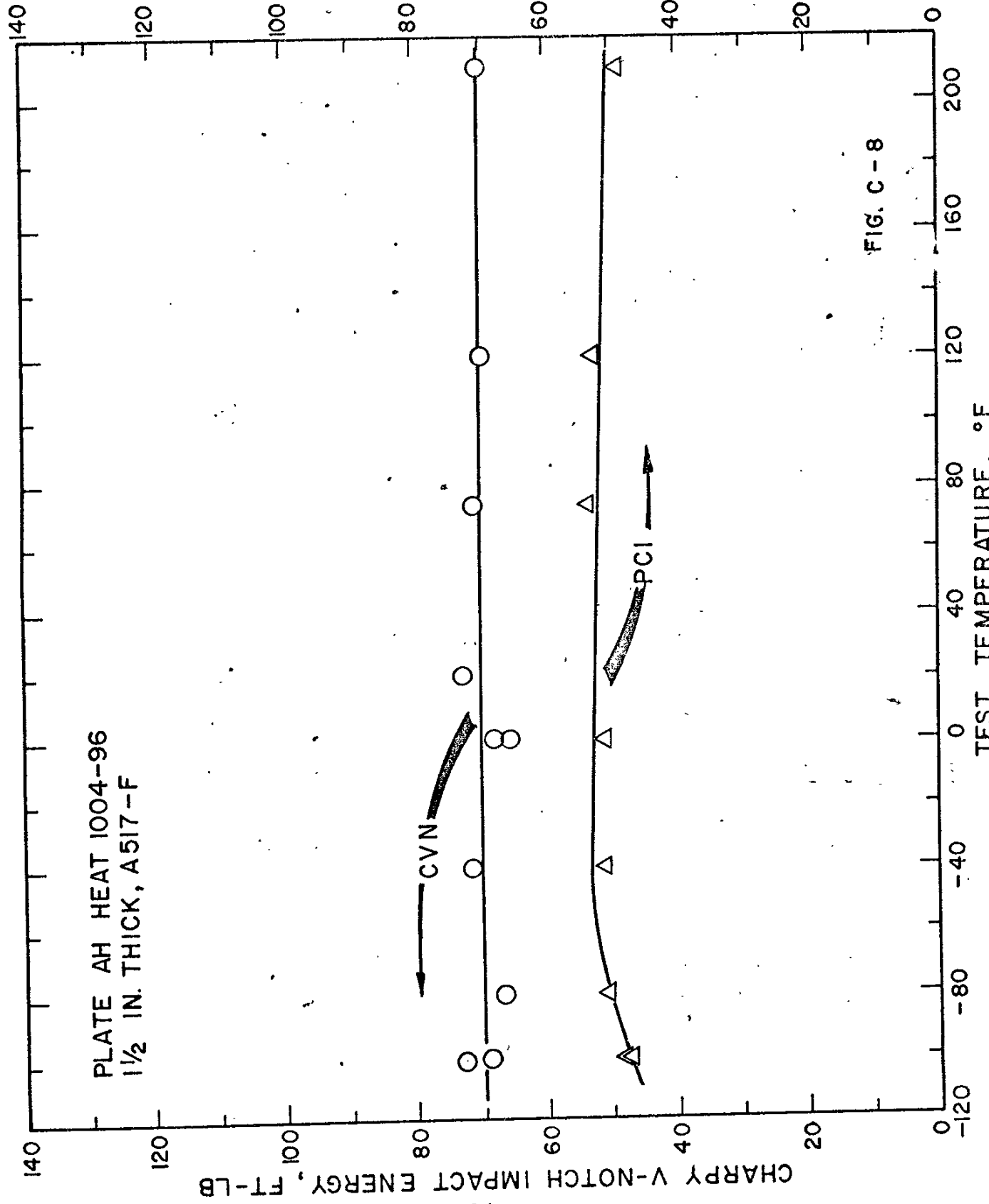
PLATE AG HEAT 1004-44
1 1/2 IN. THICK, A517-F

FIG. C-7

CHARPY V-NOTCH IMPACT ENERGY, FT-LB

PLATE AH HEAT 1004-96
1 1/2 IN. THICK, A517-F

PRECRACK CHARPY IMPACT ENERGY, FT-LB



CHARPY V-NOTCH IMPACT ENERGY, FT-LB

C-14

FIG. C-8

TEST TEMPERATURE, °F

PRECRACK CHARPY IMPACT ENERGY, FT-LB

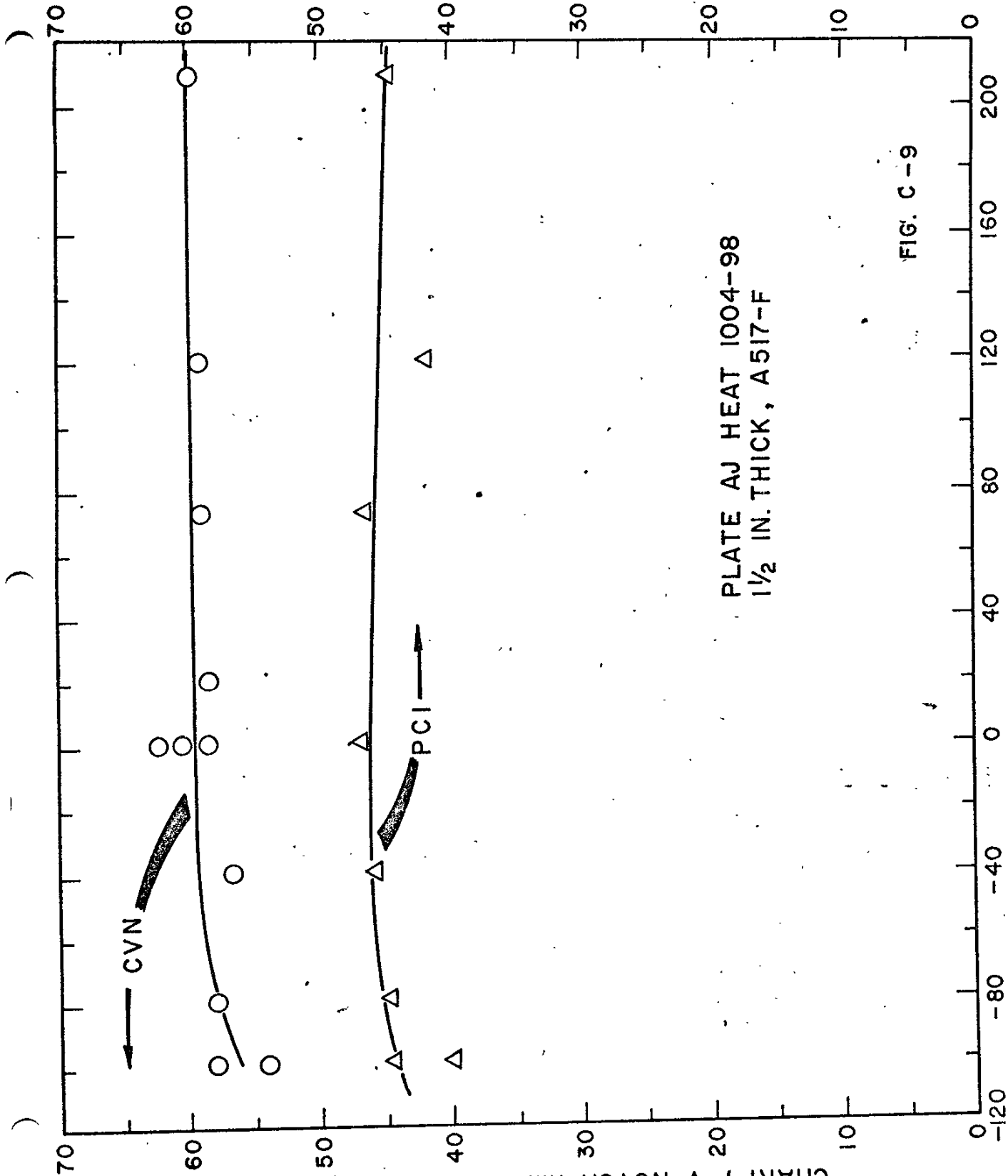


FIG. C-9

CHARPY V-NOTCH IMPACT ENERGY, FT-LB

51-C

PLATE BX HEAT 1005-22
3/8 IN. THICK, A517-F

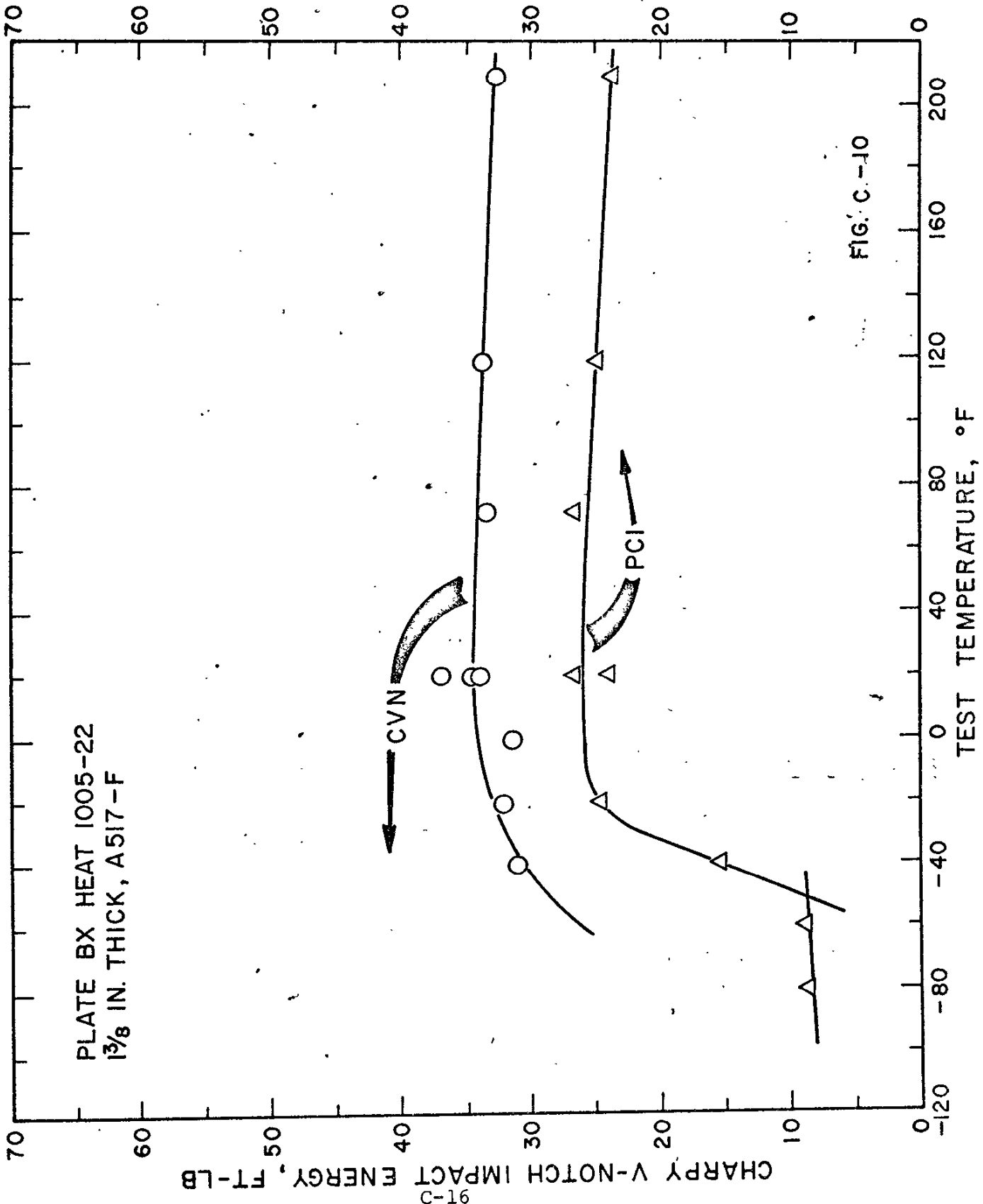


FIG. C-10

PRECRACK CHARPY IMPACT ENERGY, FT-LB

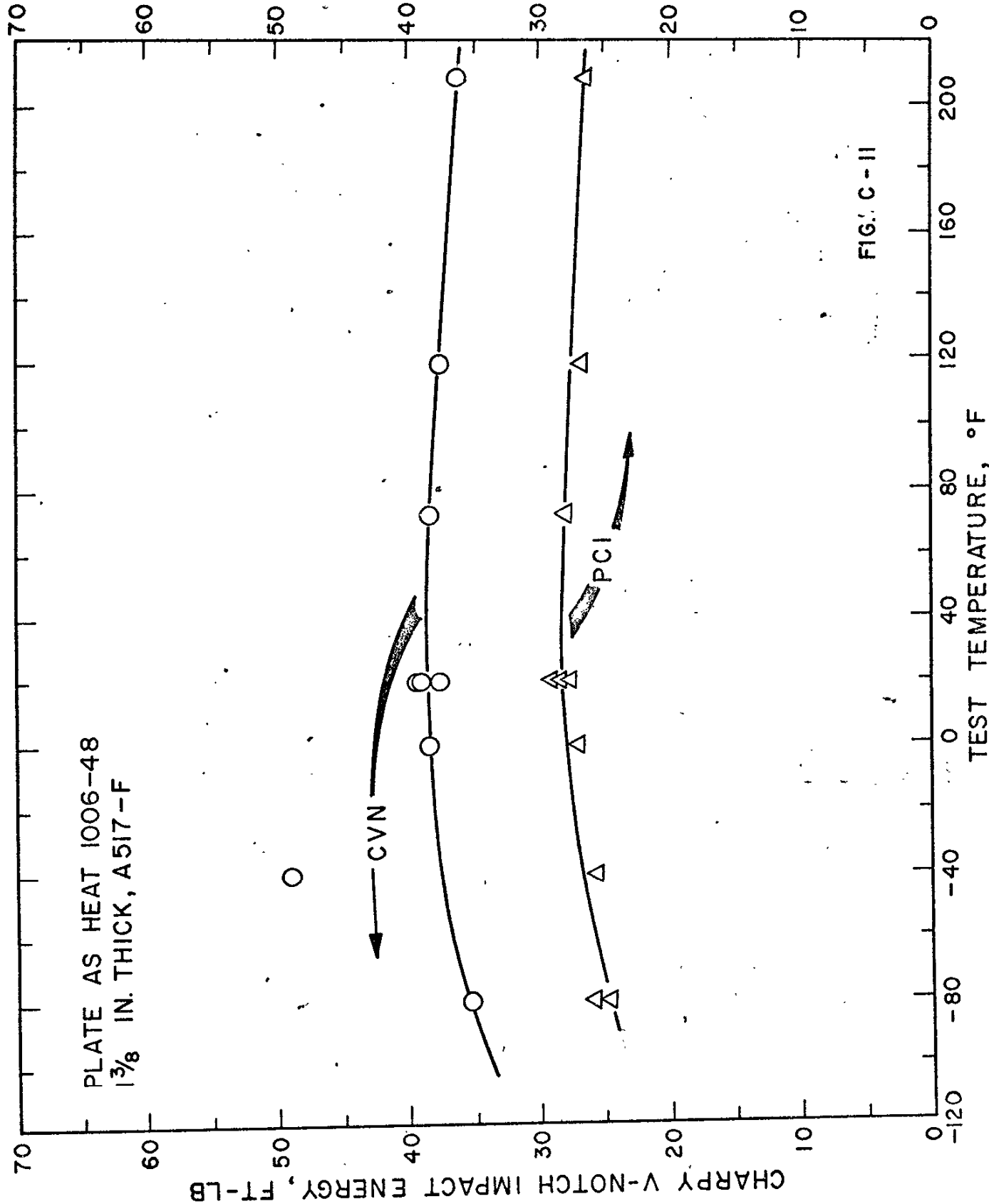
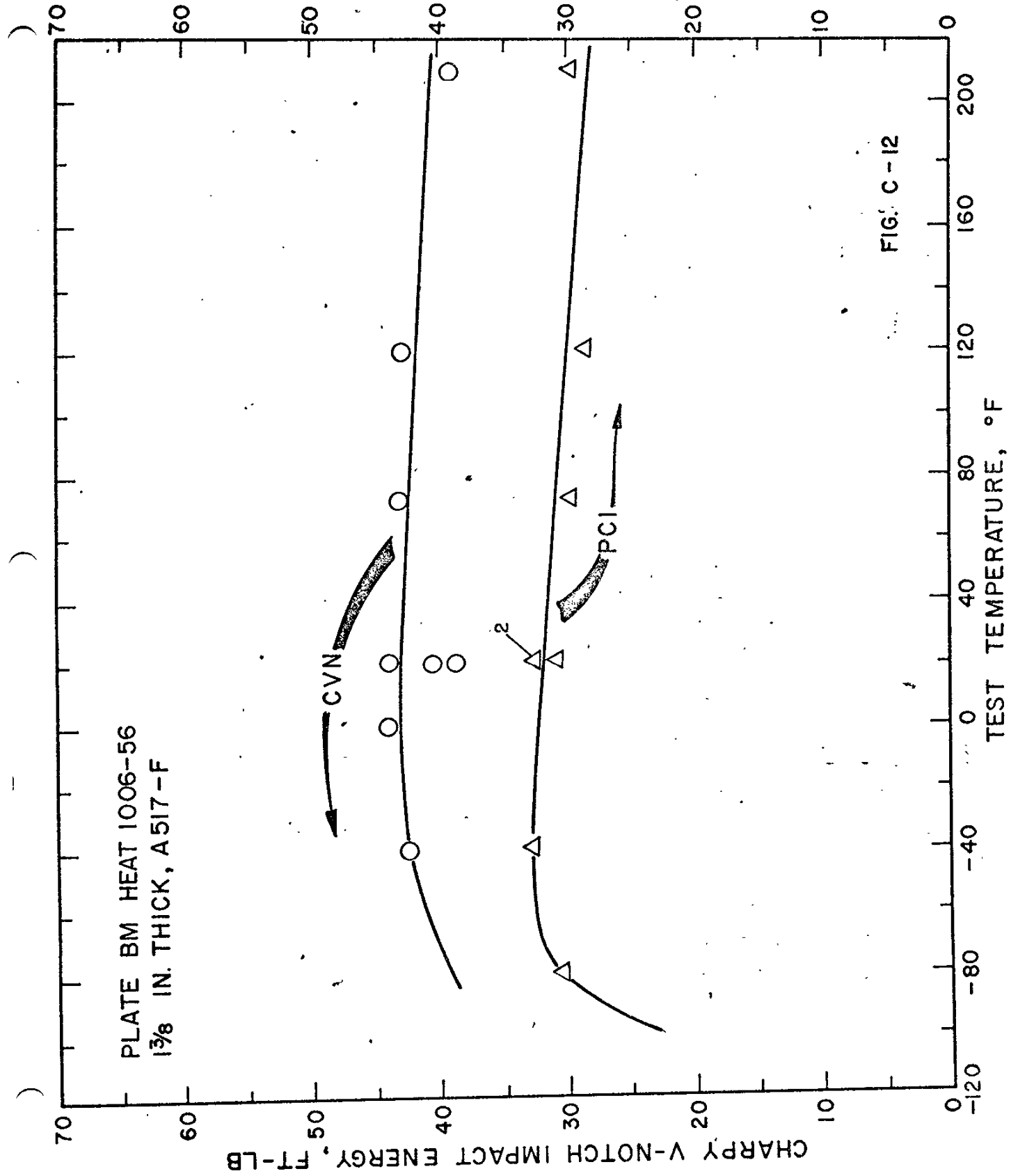


FIG. C-II

PRECRACK CHARPY IMPACT ENERGY, FT-LB



CHARPY V-NOTCH IMPACT ENERGY, FT-LB

FIG. C-12

PRECRACK CHARPY IMPACT ENERGY, FT-LB

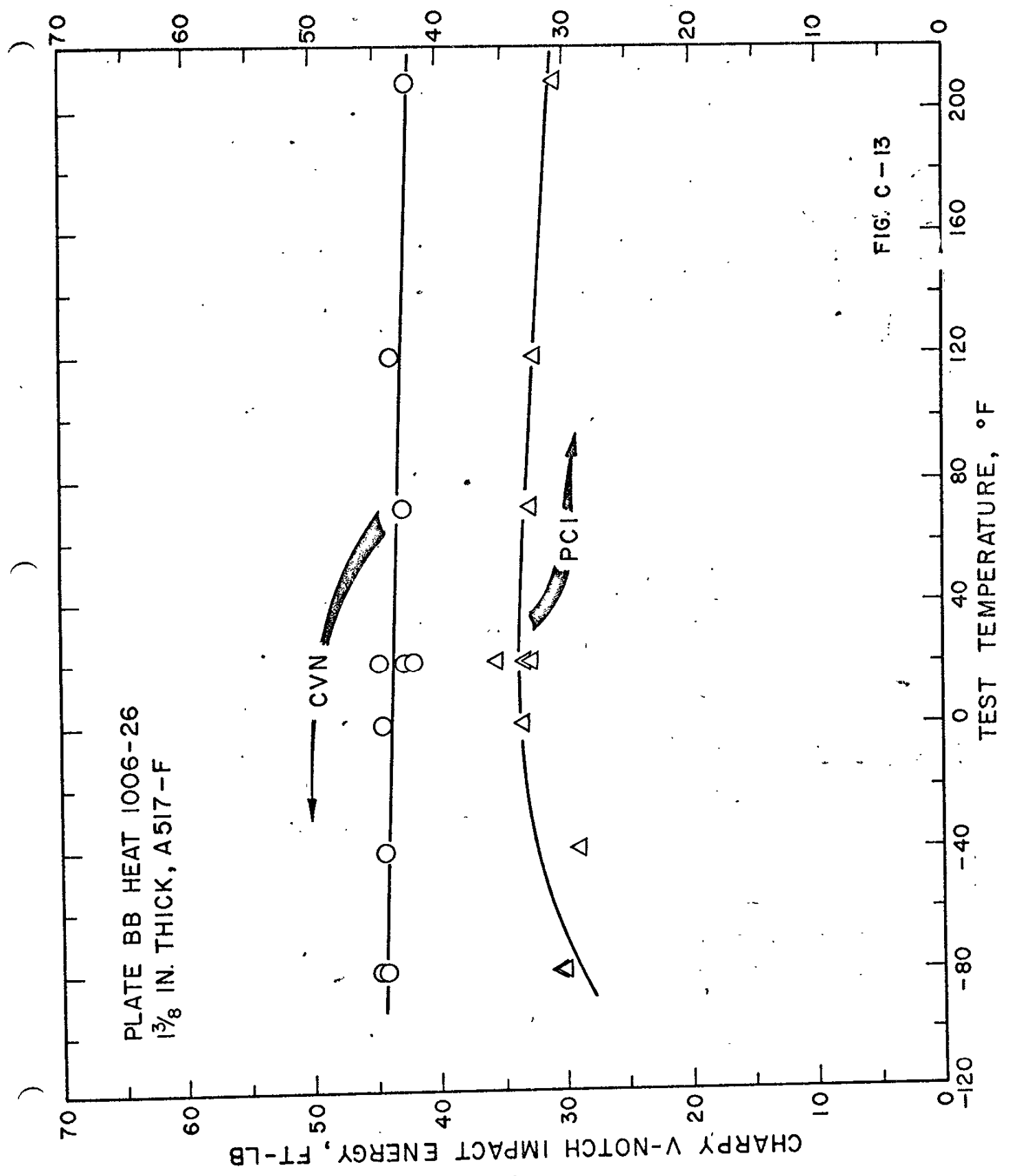


FIG. C-13

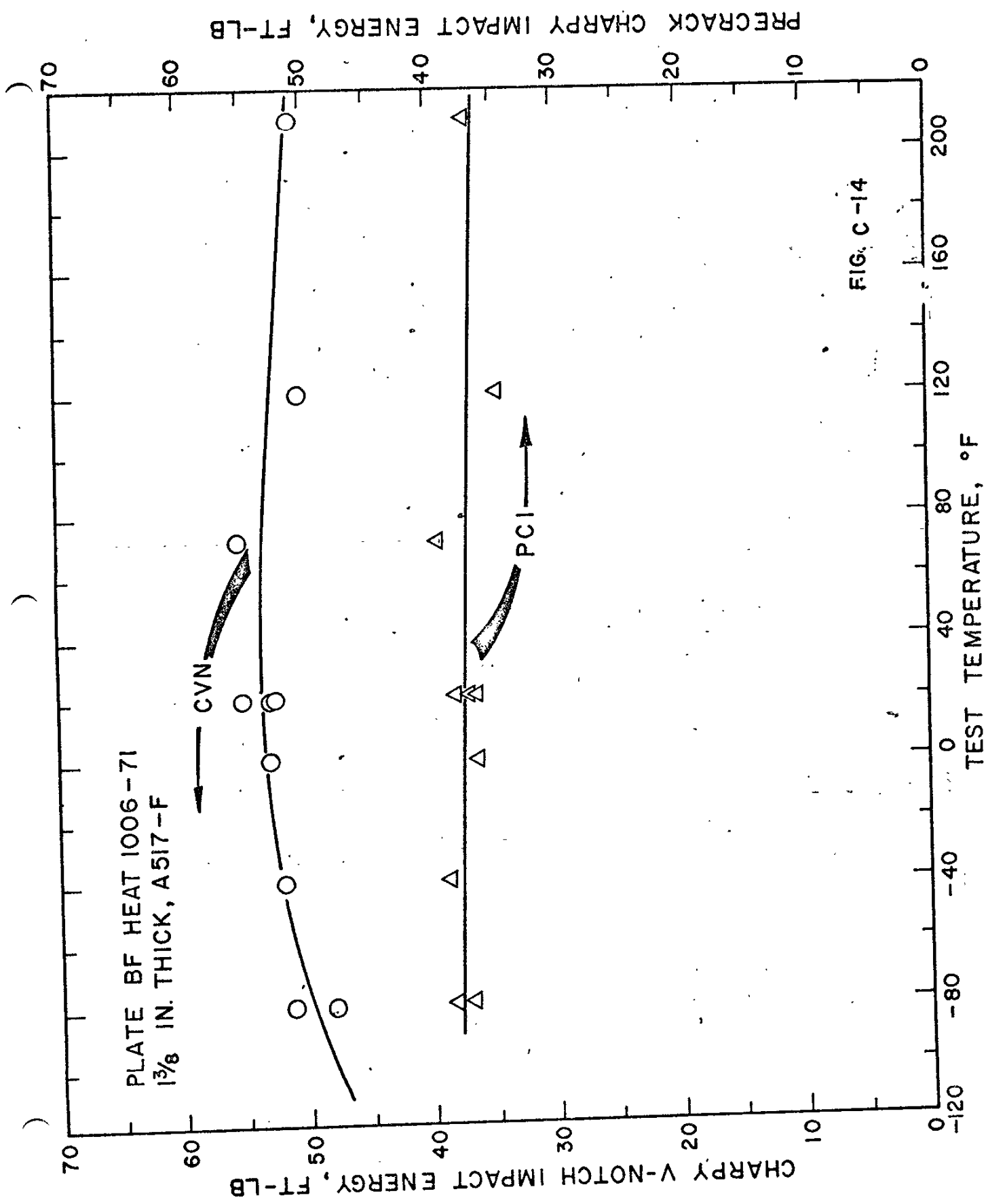


FIG. C-14

PRECRACK CHARPY IMPACT ENERGY, FT-LB

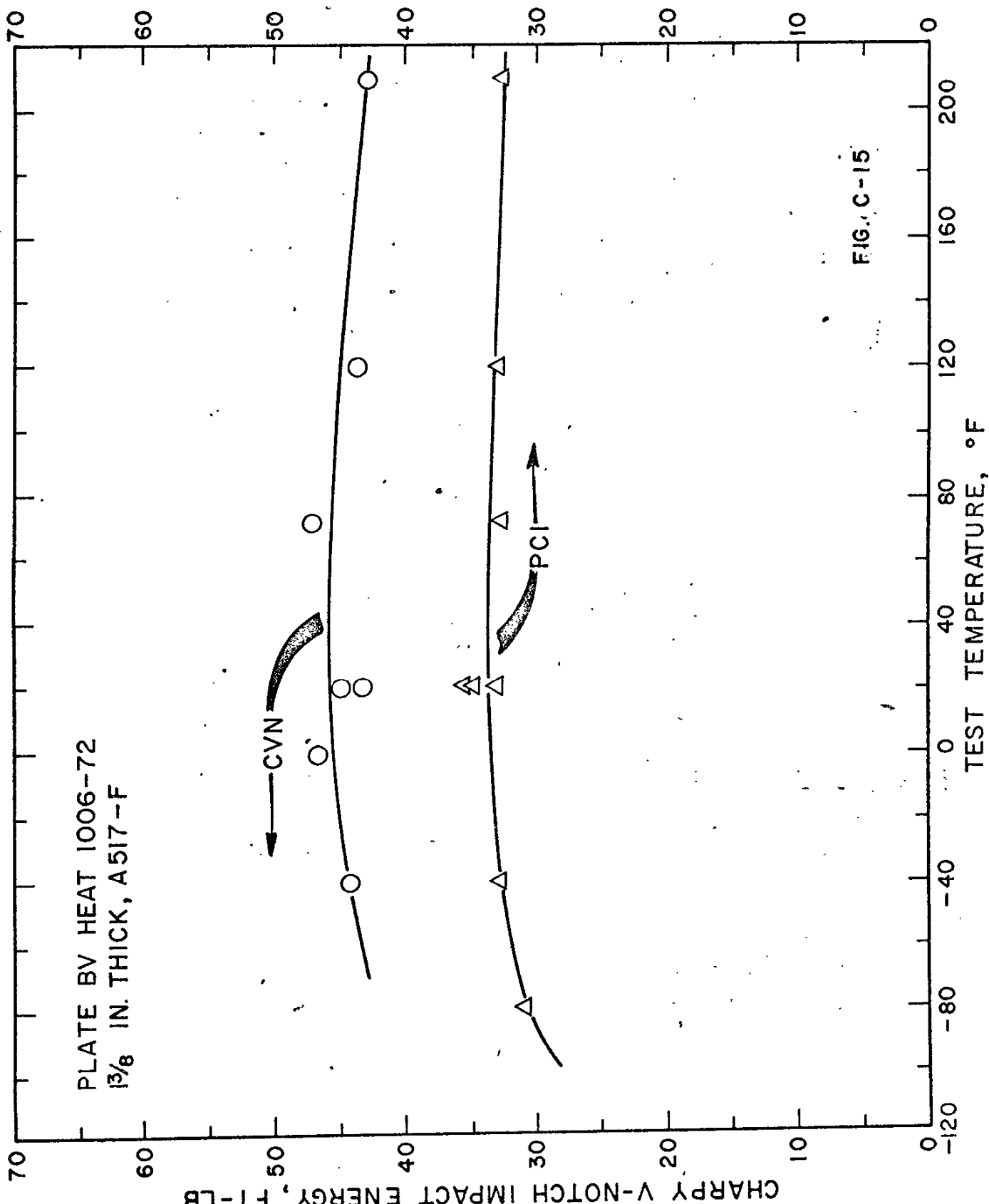
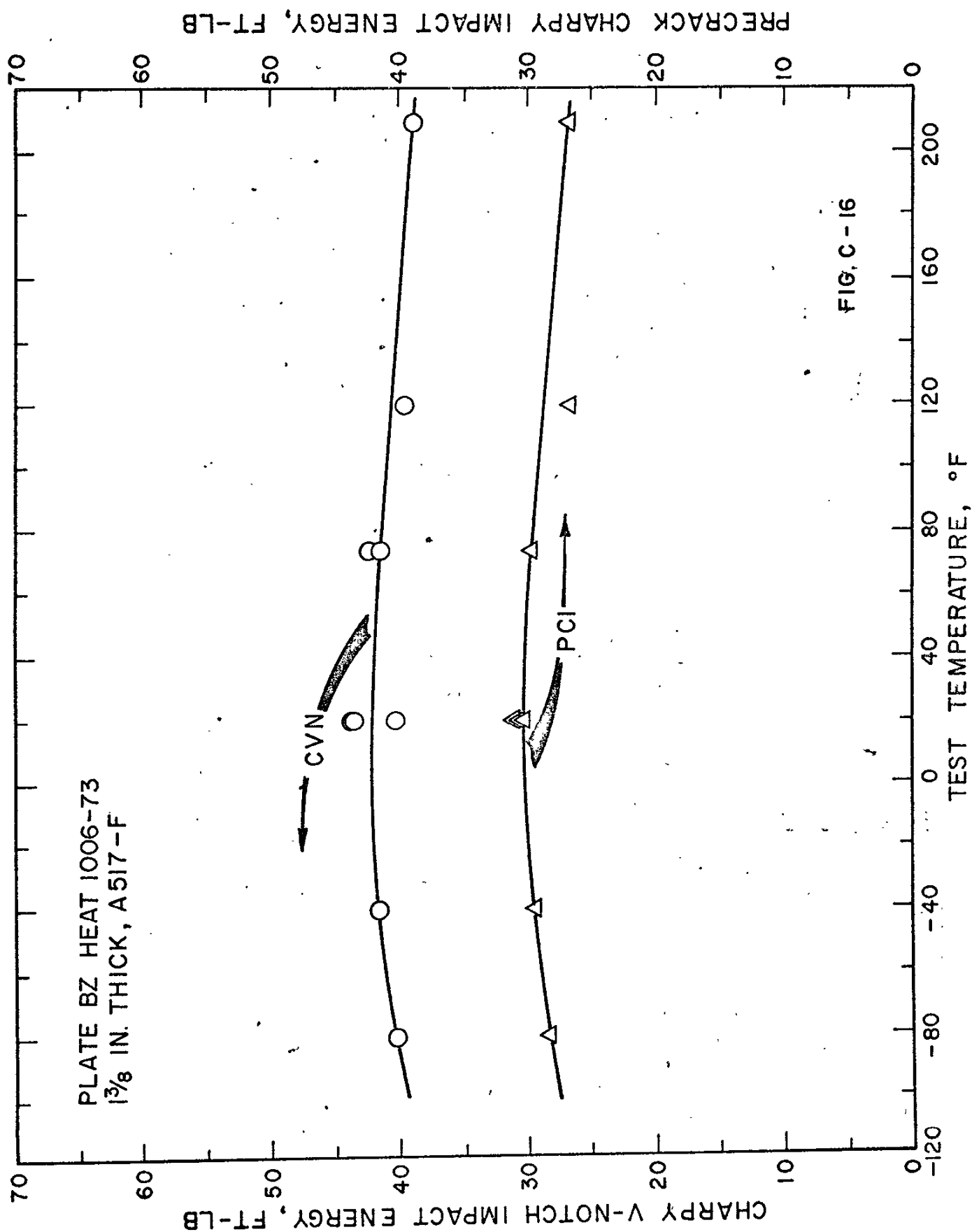


PLATE BV HEAT 1006-72
3/8 IN. THICK, A517-F

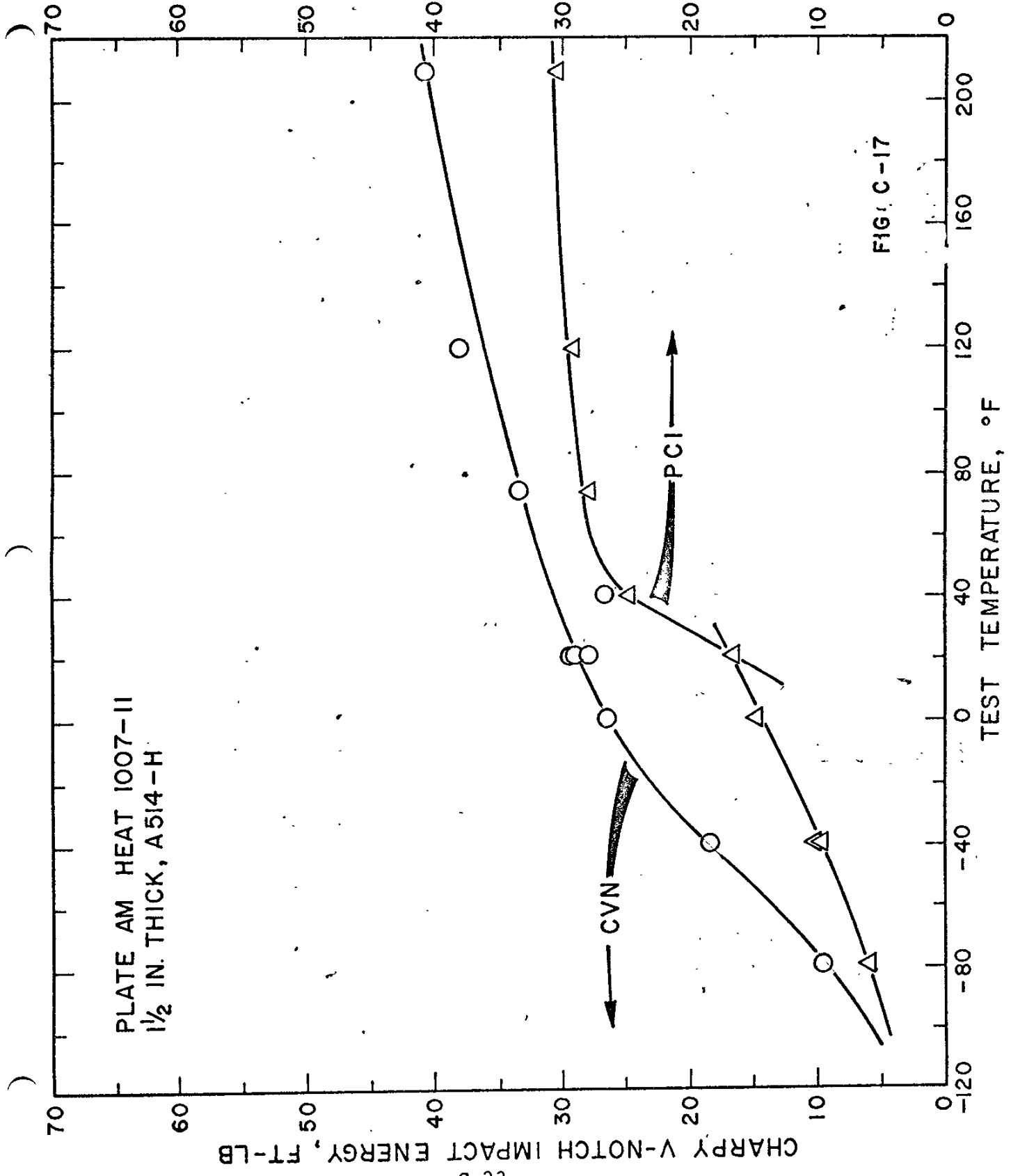
FIG. C-15

CHARPY V-NOTCH IMPACT ENERGY, FT-LB

TEST TEMPERATURE, °F

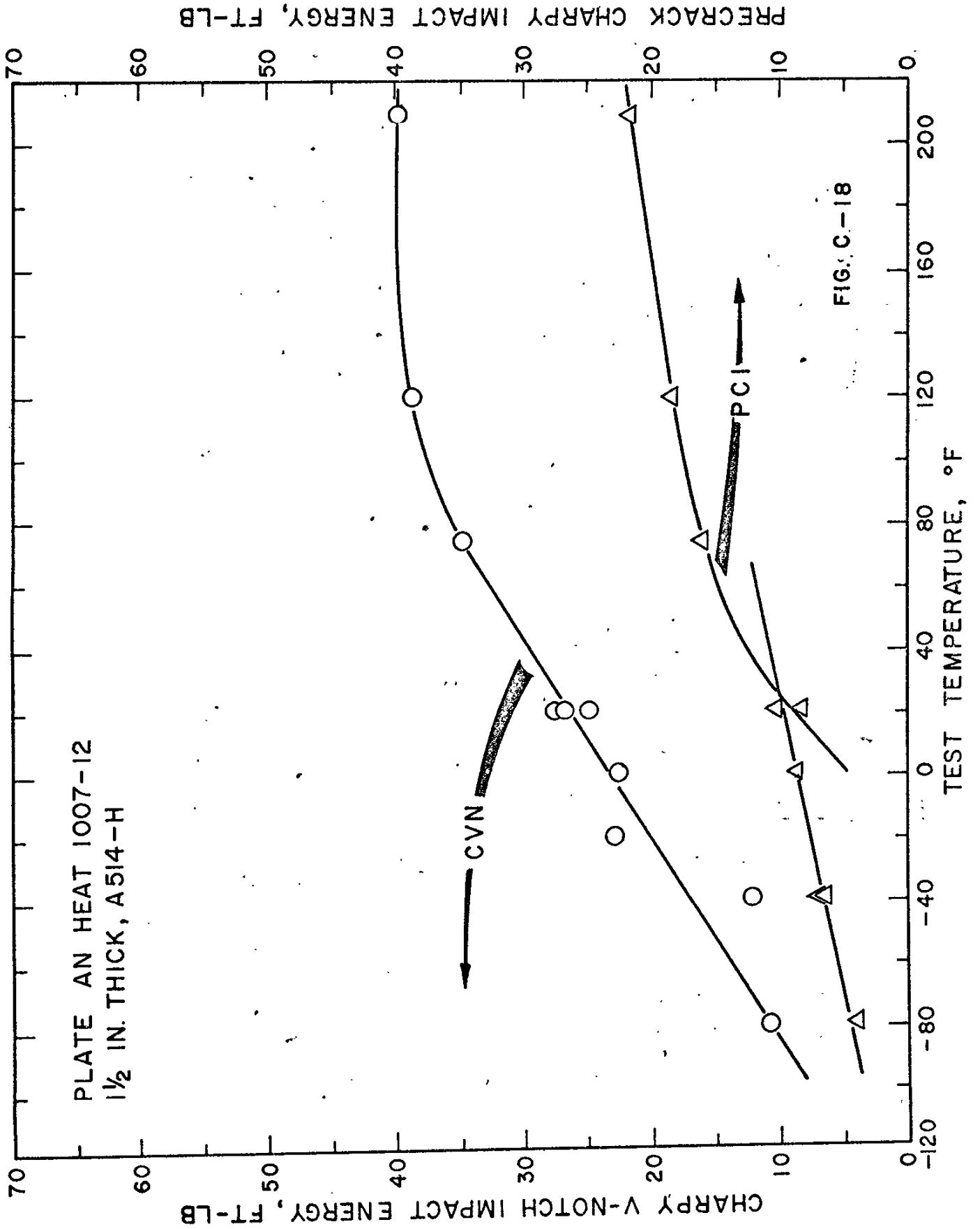


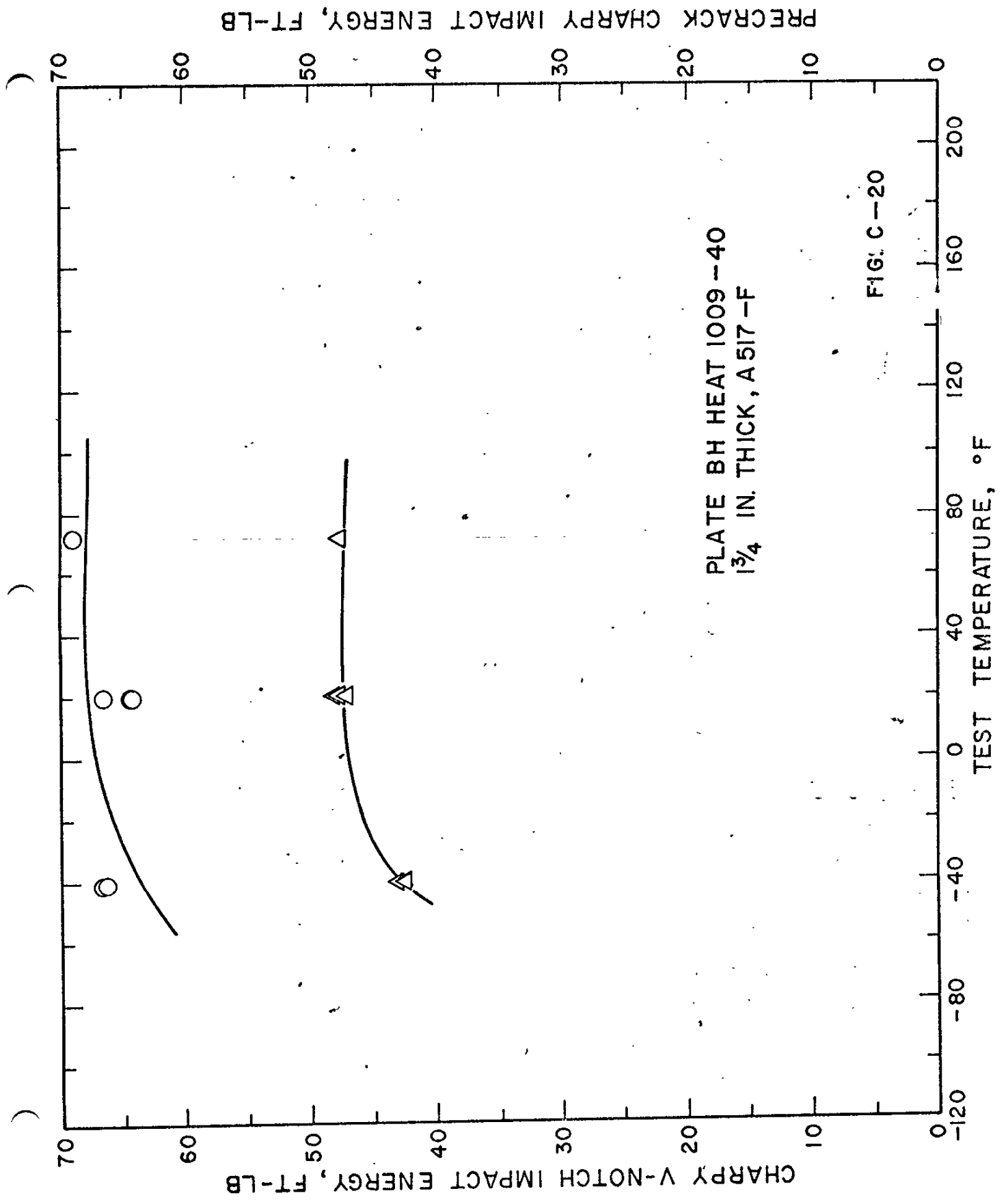
PRECRACK CHARPY IMPACT ENERGY, FT-LB



CHARTY V-NOTCH IMPACT ENERGY, FT-LB

32-C





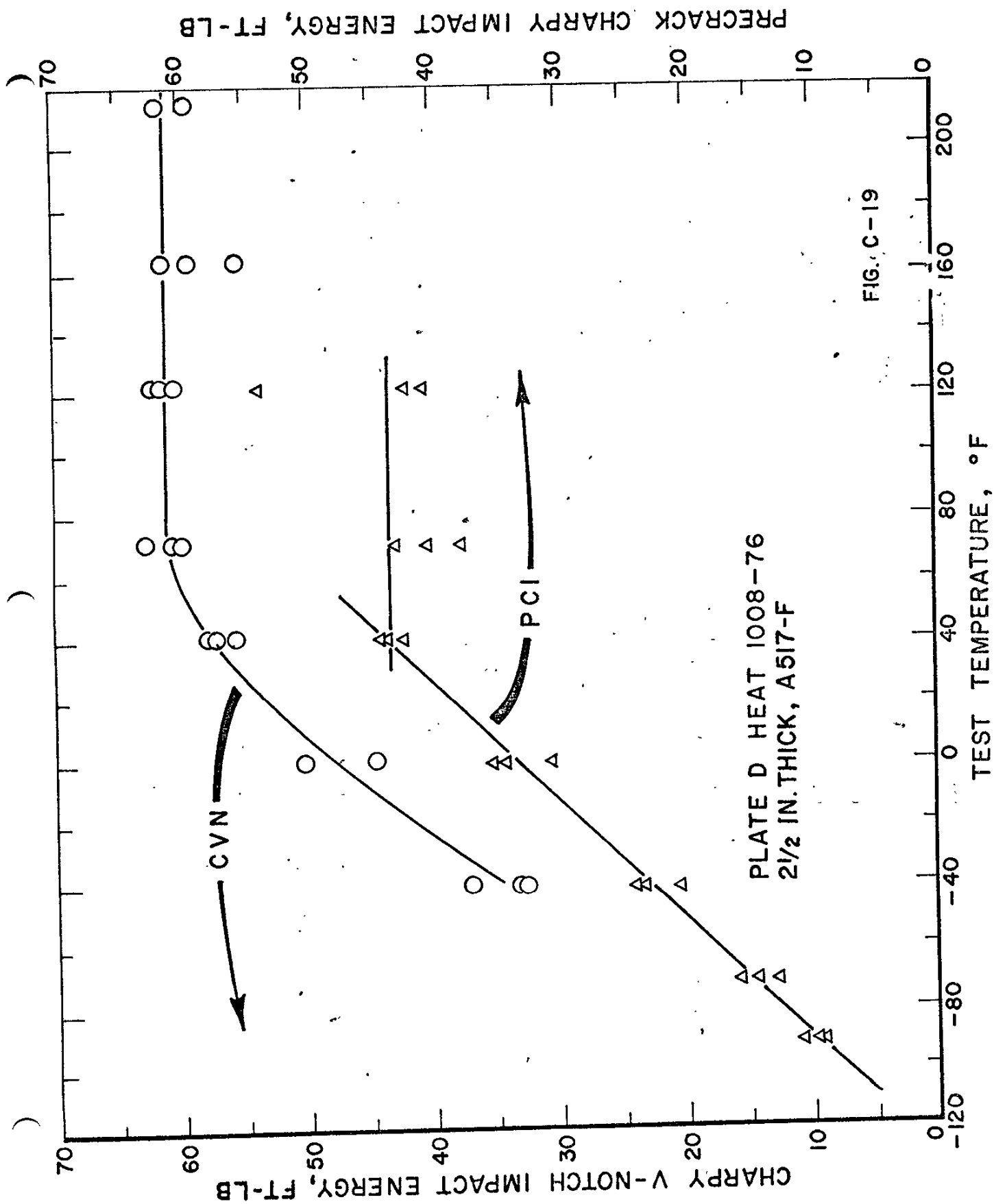
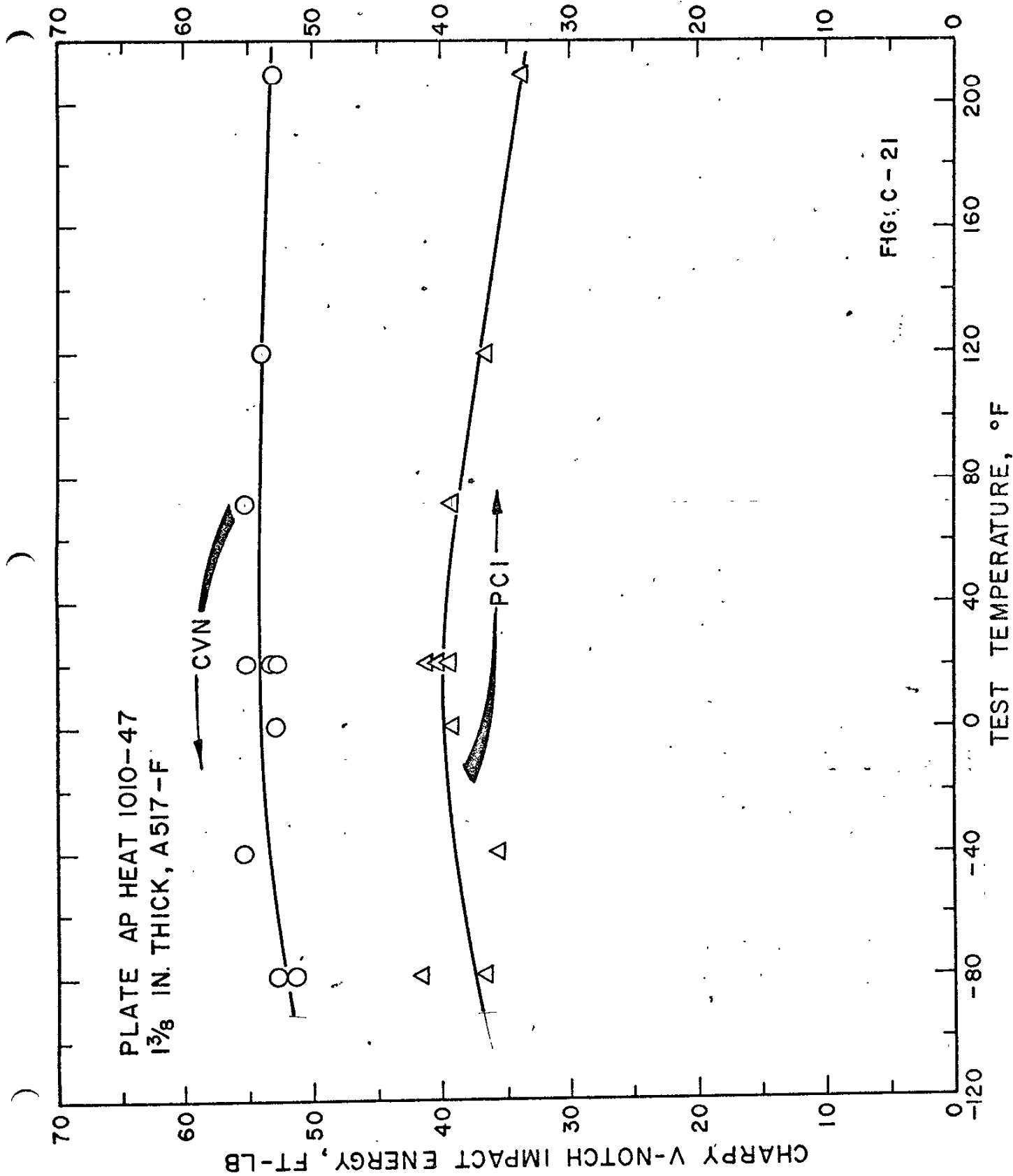


FIG. C-19

PRECRACK CHARPY IMPACT ENERGY, FT-LB



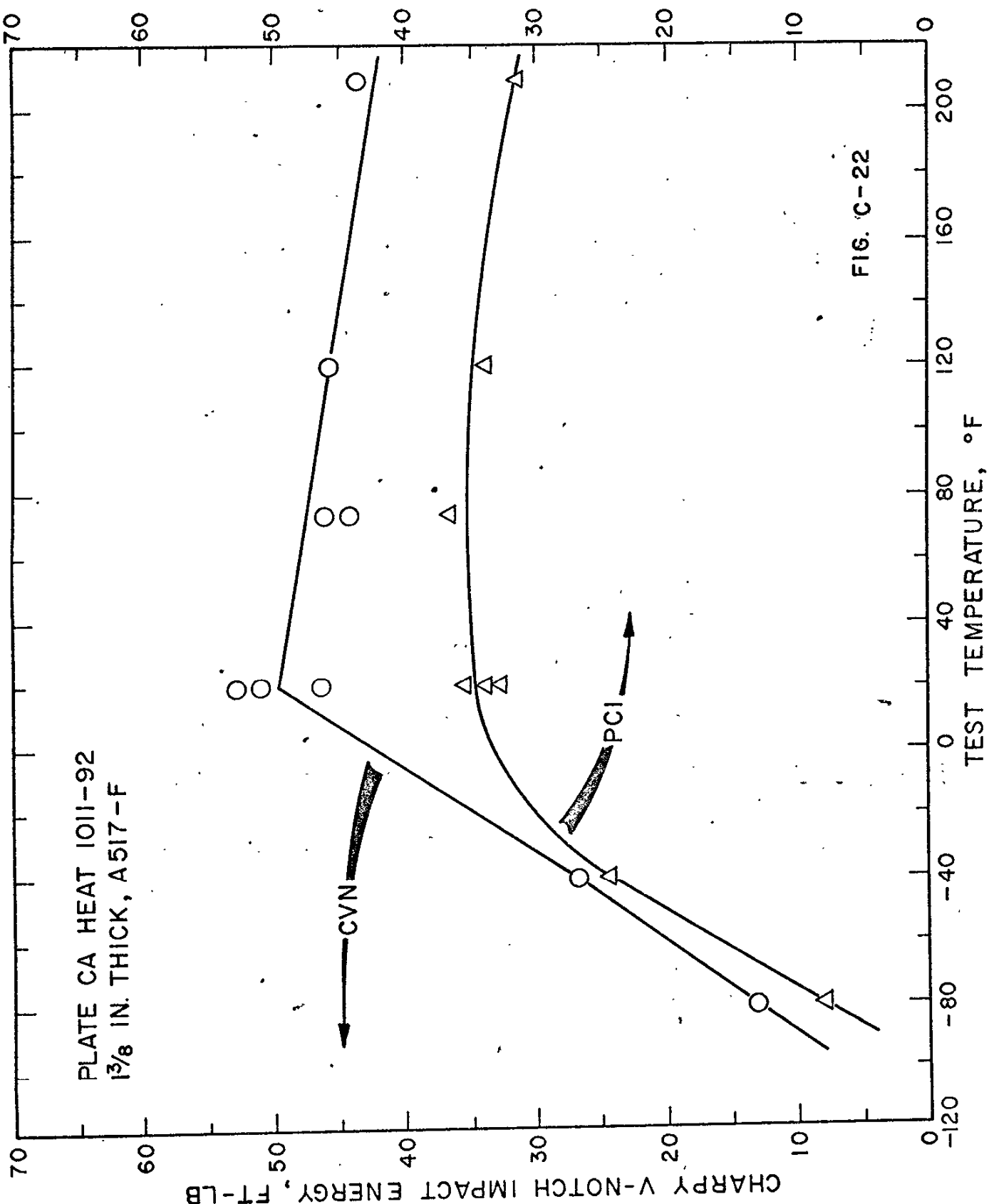


FIG. C-22

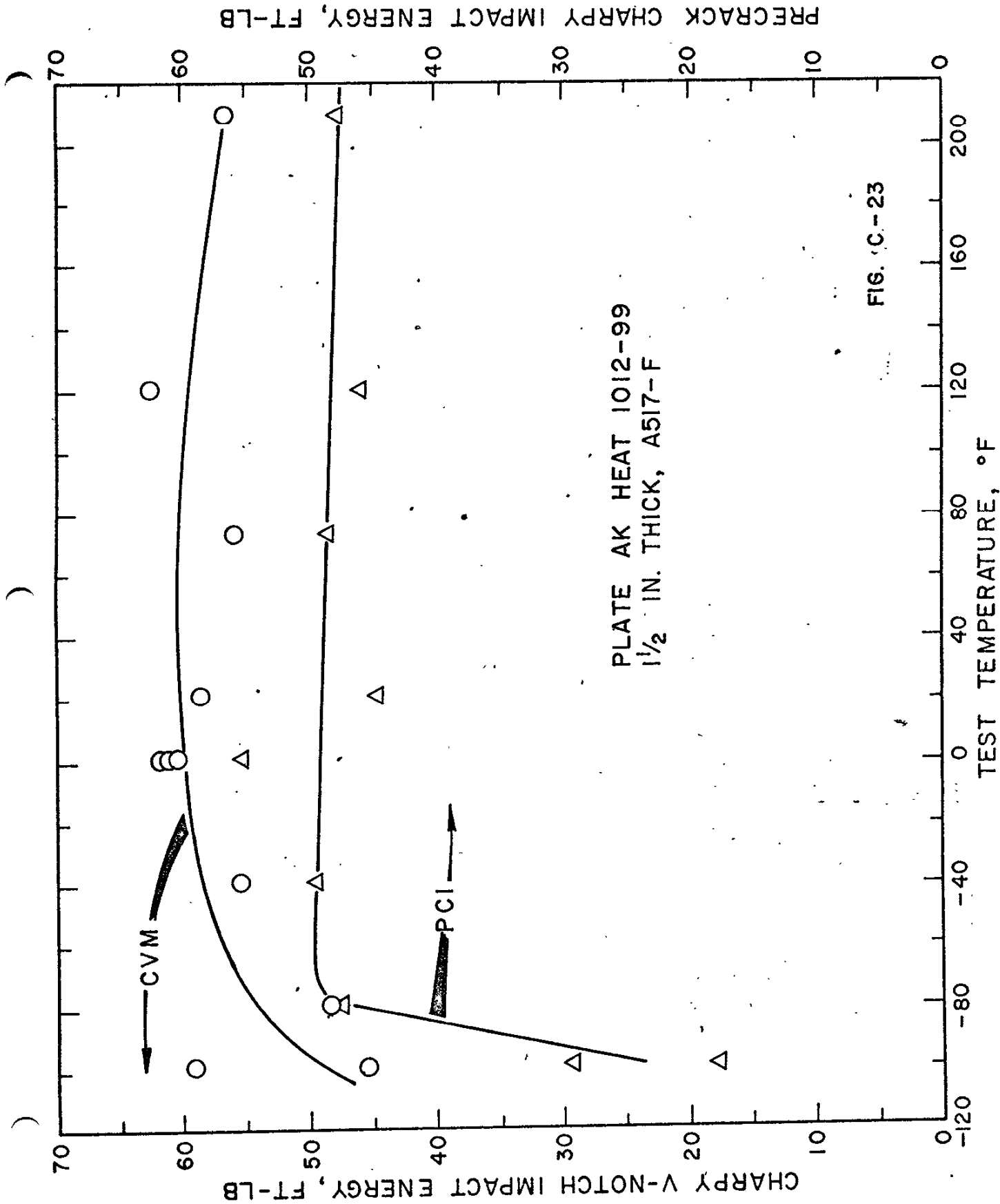


FIG. C-23

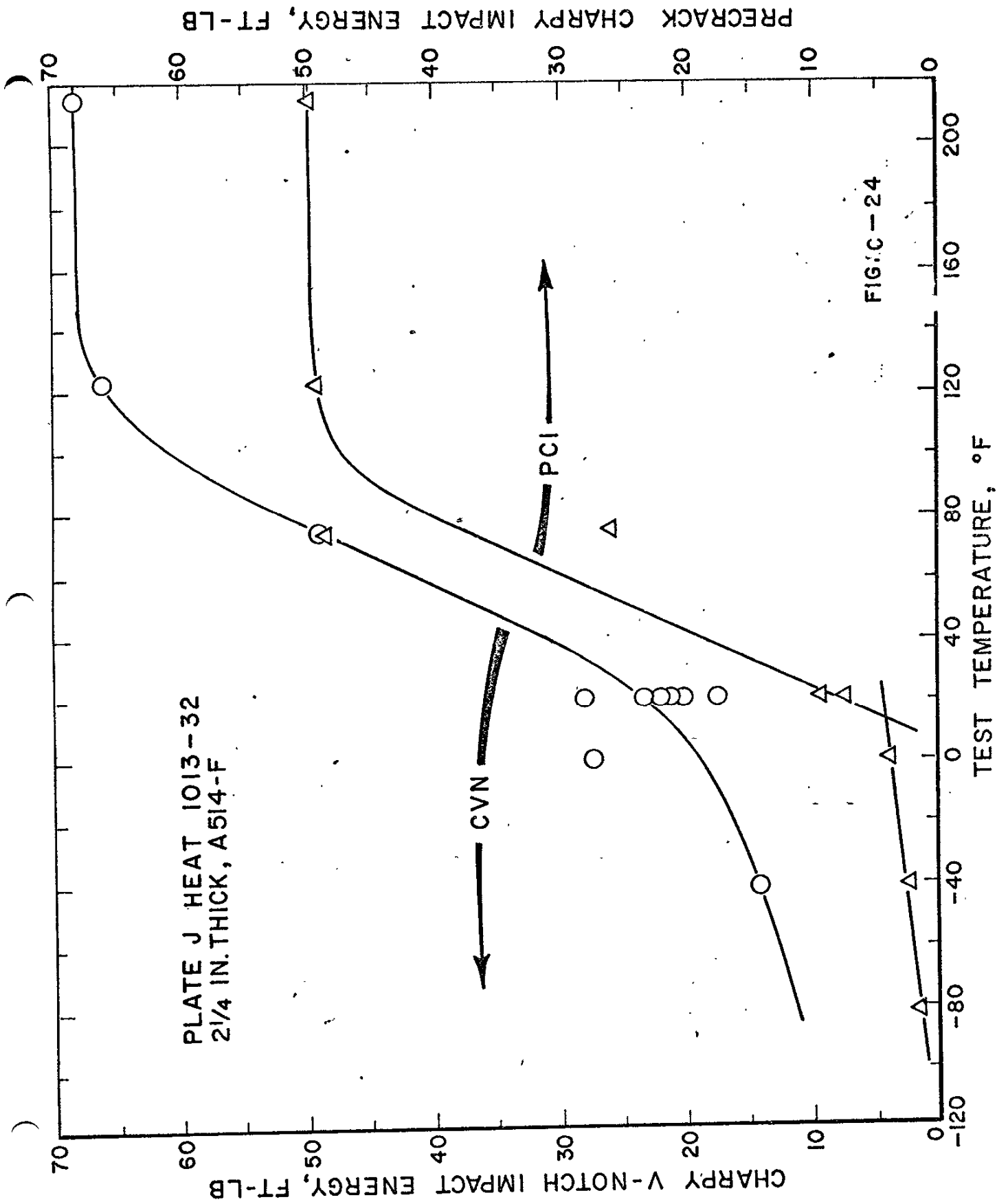


FIG. C-24

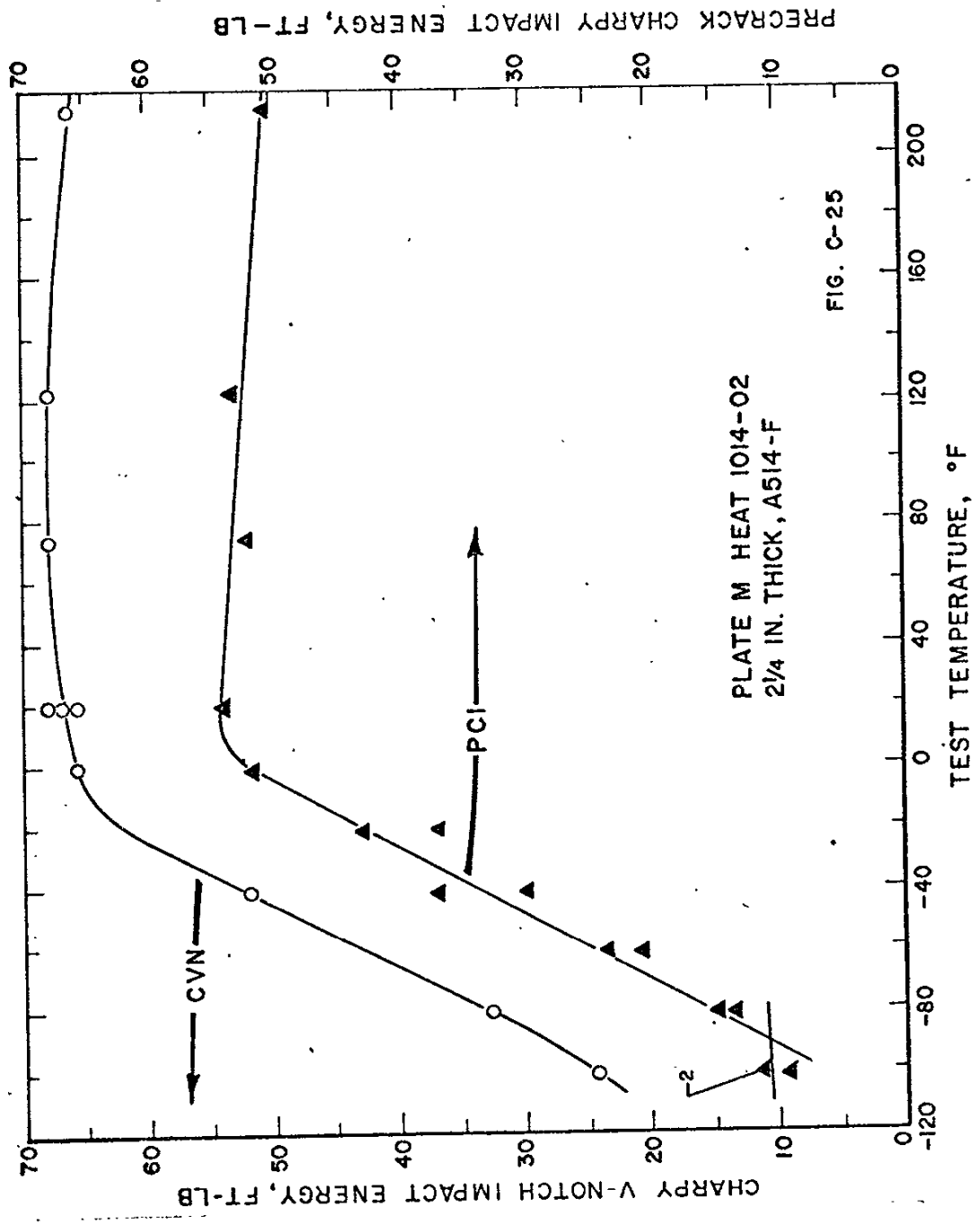


PLATE N HEAT 1015-32
1 3/4 IN. THICK, A514-H

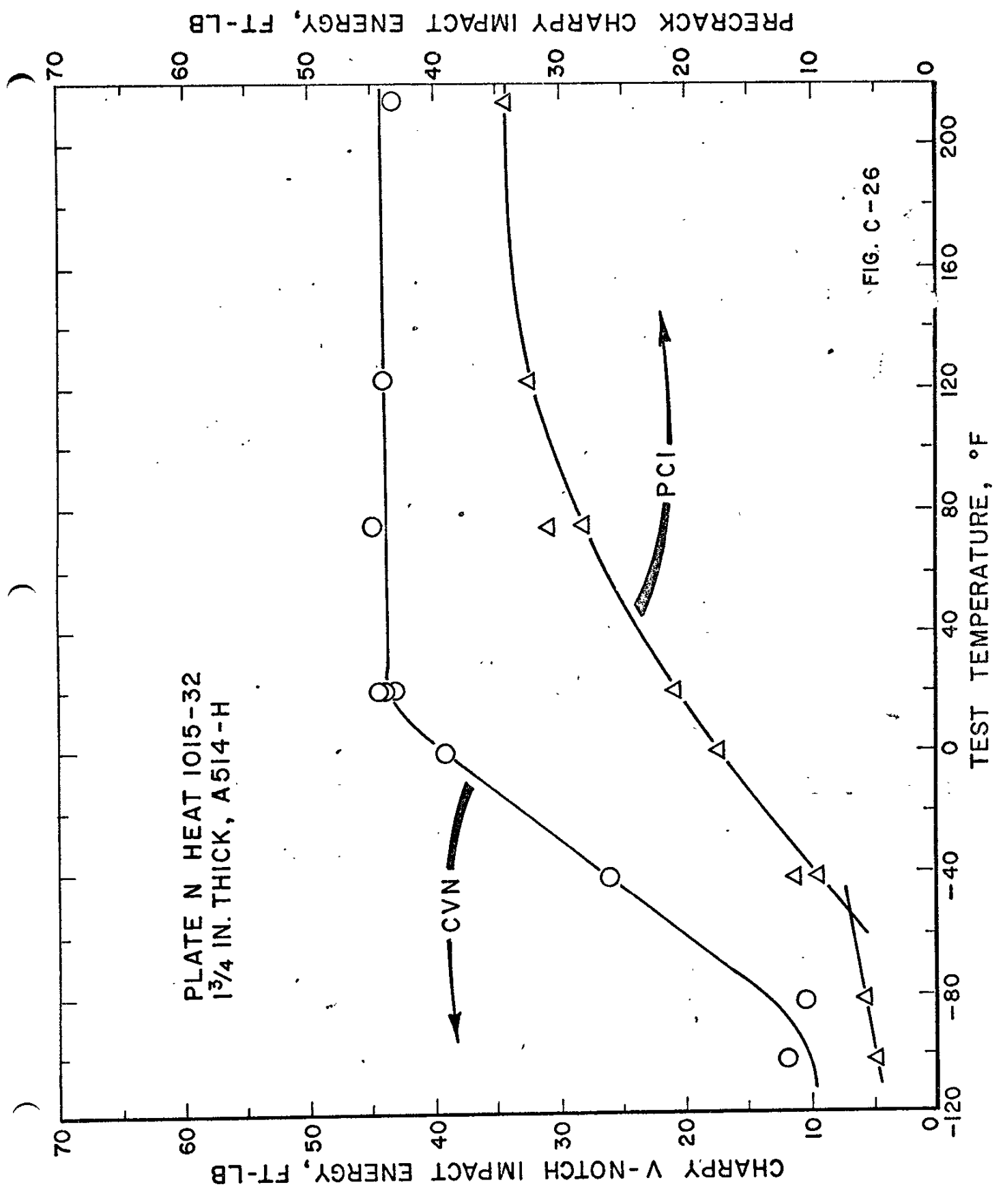


FIG. C-26

PRECRACK CHARPY IMPACT ENERGY, FT-LB

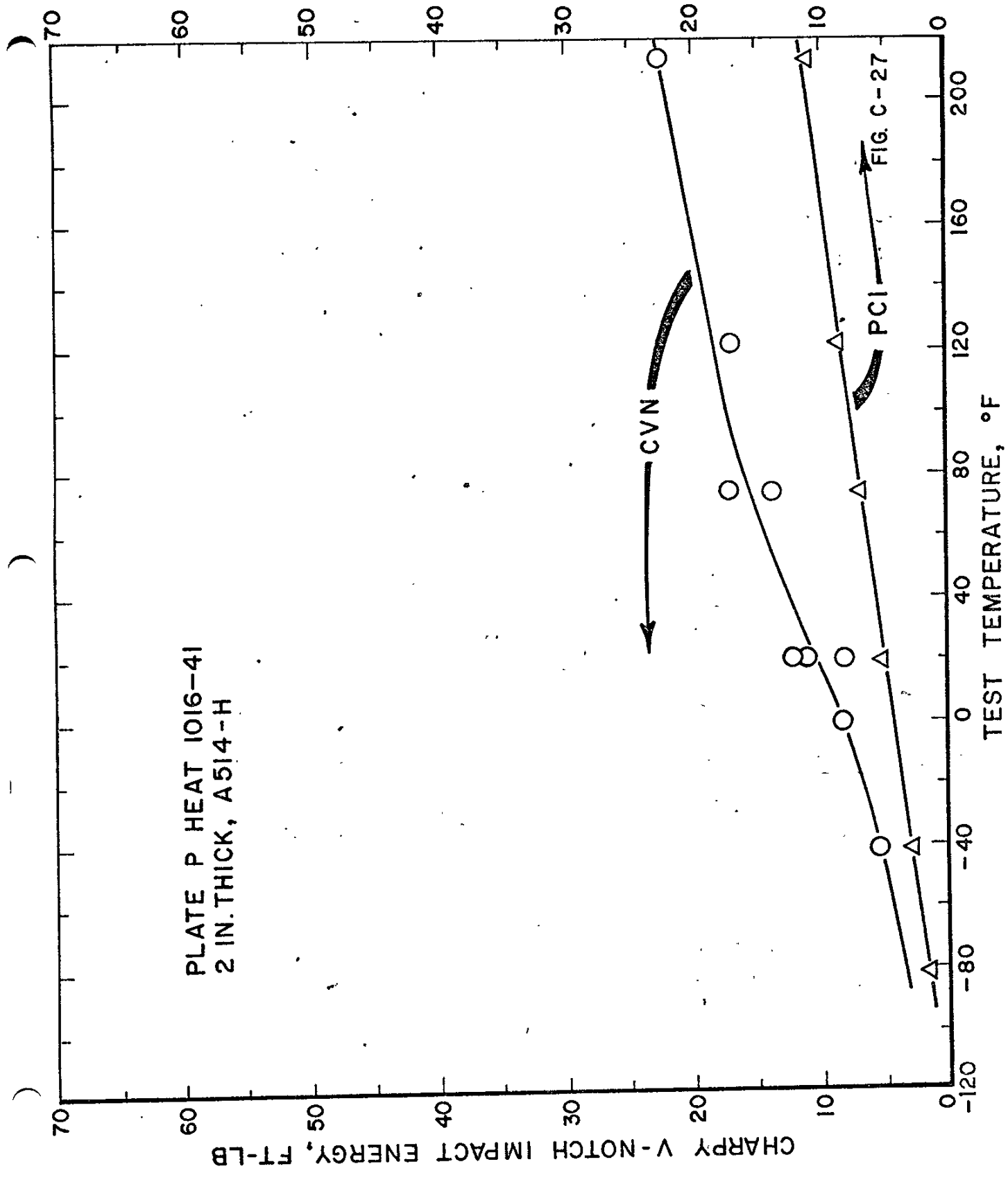


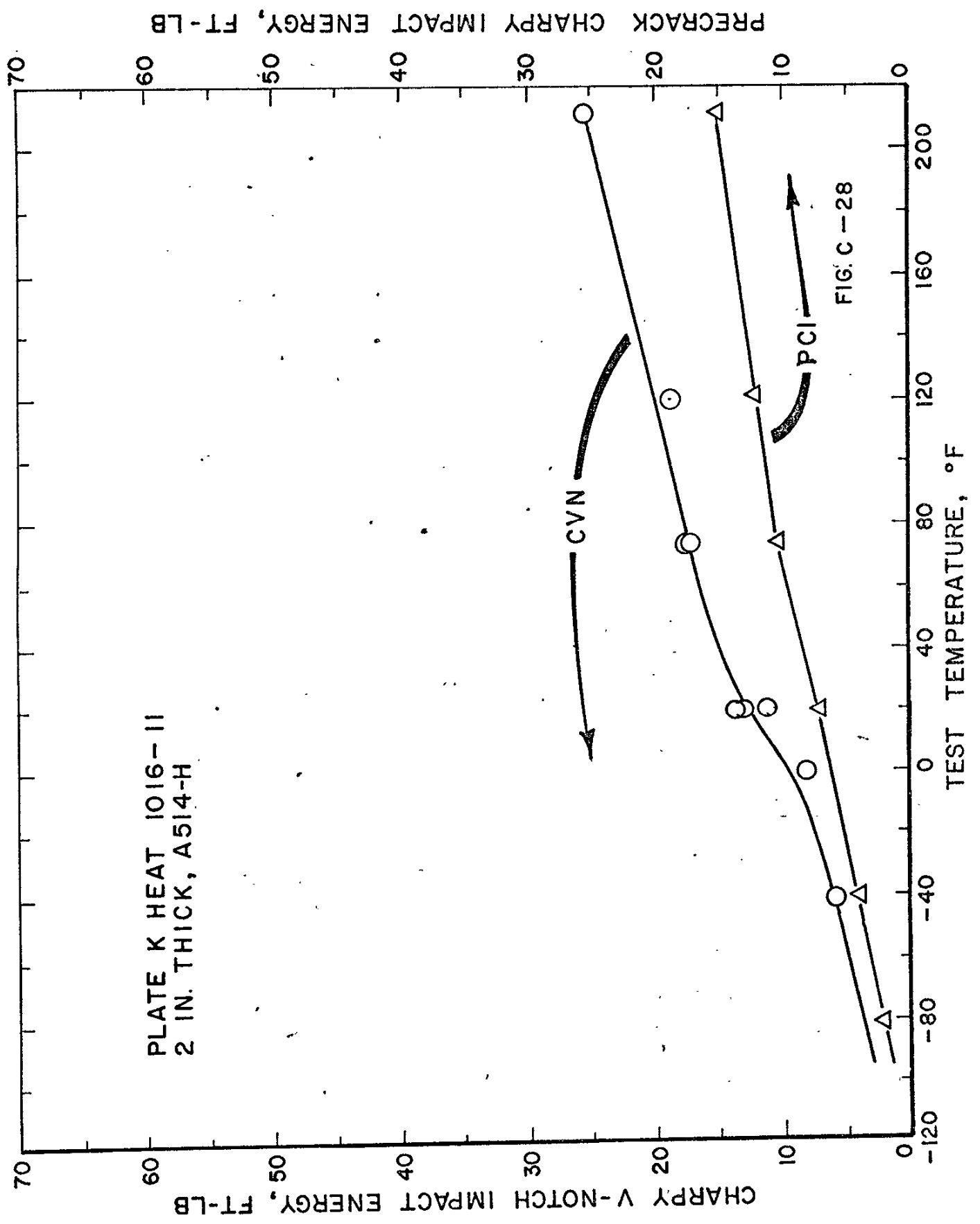
PLATE P HEAT 1016-41
2 IN. THICK, A514-H

CHARPY V-NOTCH IMPACT ENERGY, FT-LB

TEST TEMPERATURE, °F

FIG. C-27

PLATE K HEAT 1016-II
2 IN. THICK, A514-H



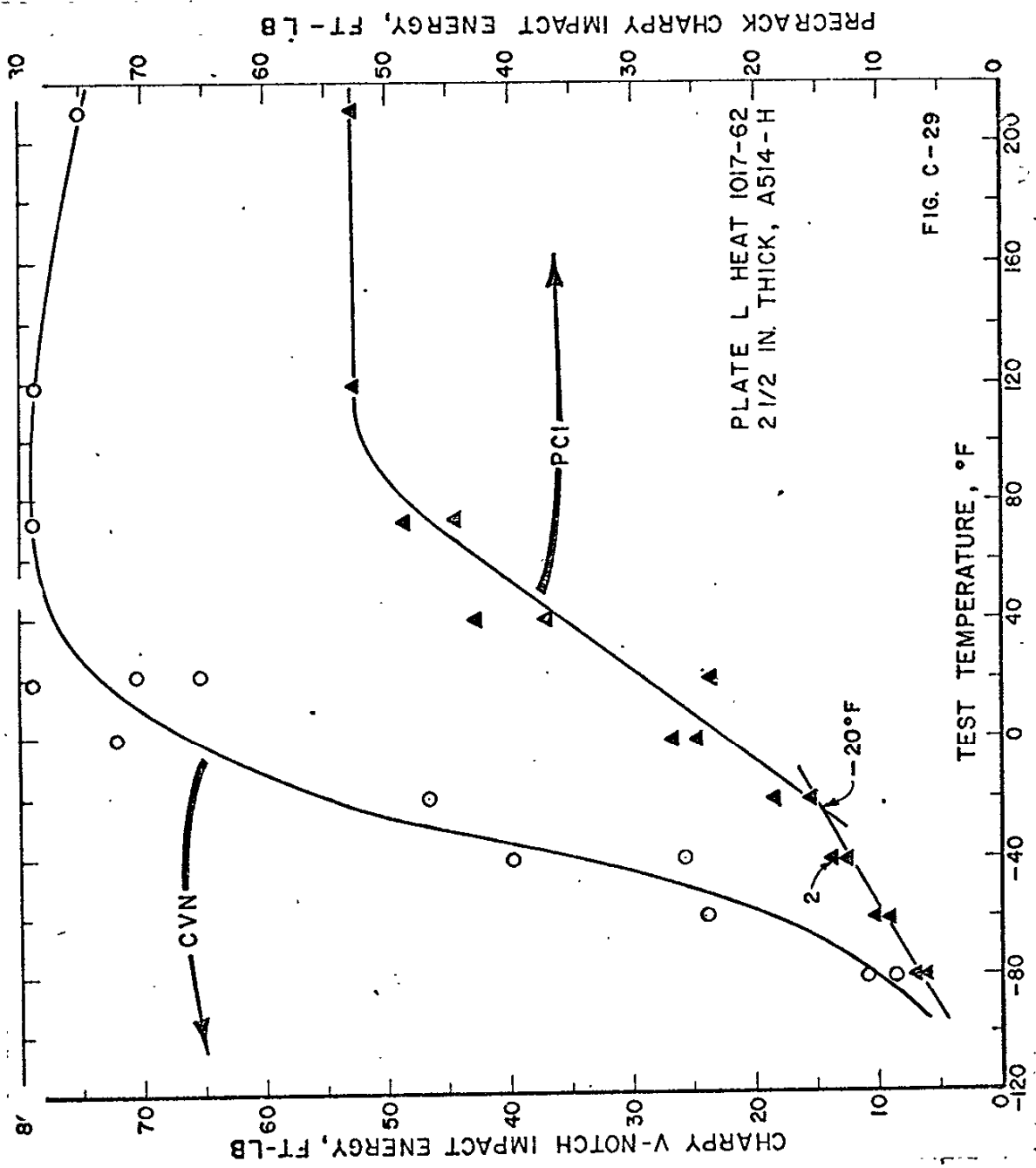


FIG. C-29

PLATE S HEAT 1018-81
2 IN. THICK, A514-H

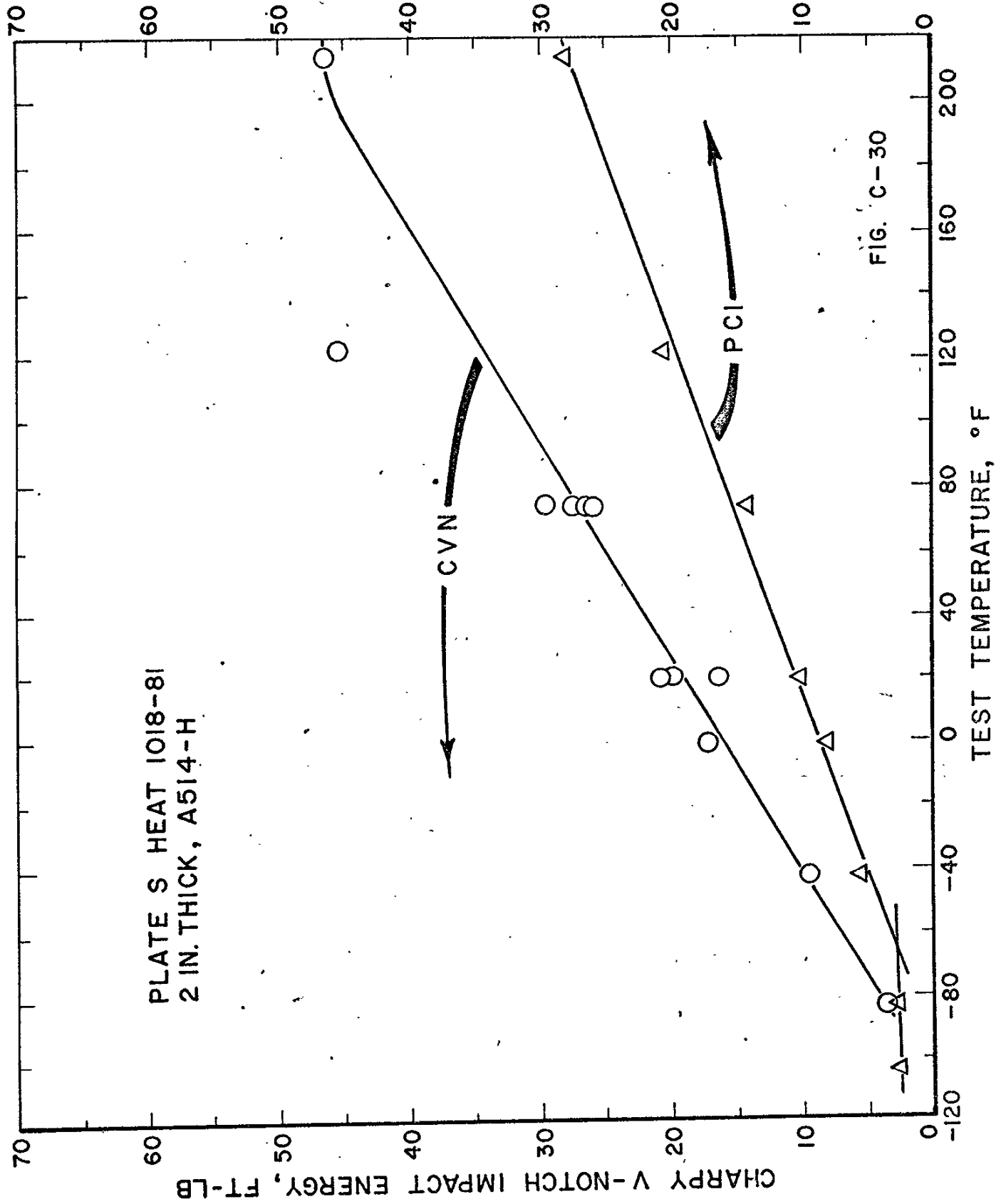


FIG. C-30

PRECRACK CHARPY IMPACT ENERGY, FT-LB

CHARPY V-NOTCH IMPACT ENERGY, FT-LB

PLATE R HEAT 1019-31
2 IN. THICK, A514-H

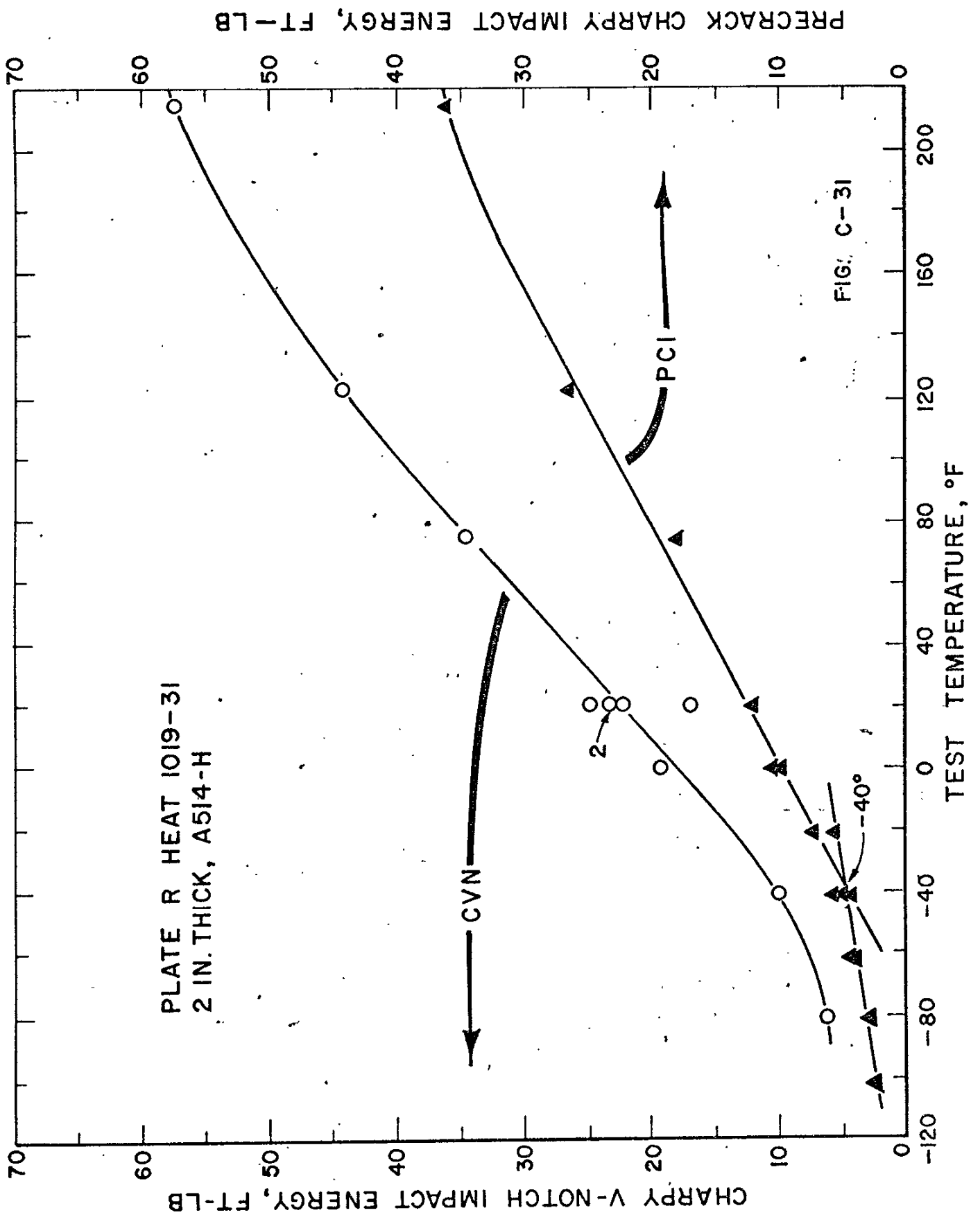


PLATE AA HEAT 1020-41
2 1/4 IN. THICK, A517-H

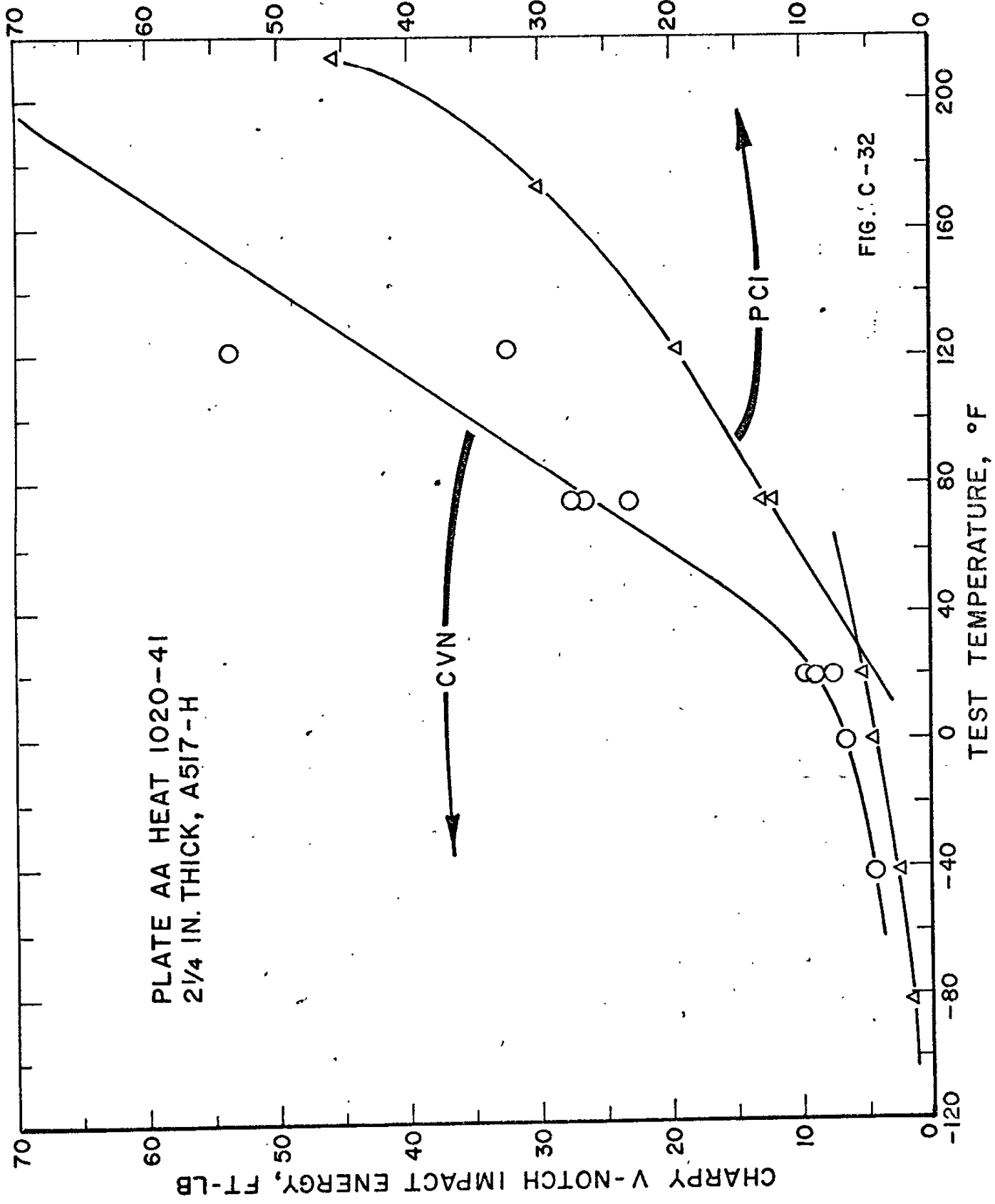


FIG. C-32

PRECRACK CHARPY IMPACT ENERGY, FT-LB

CHARPY V-NOTCH IMPACT ENERGY, FT-LB

PLATE CF HEAT 1020-43
2/4 IN. THICK, A517-H

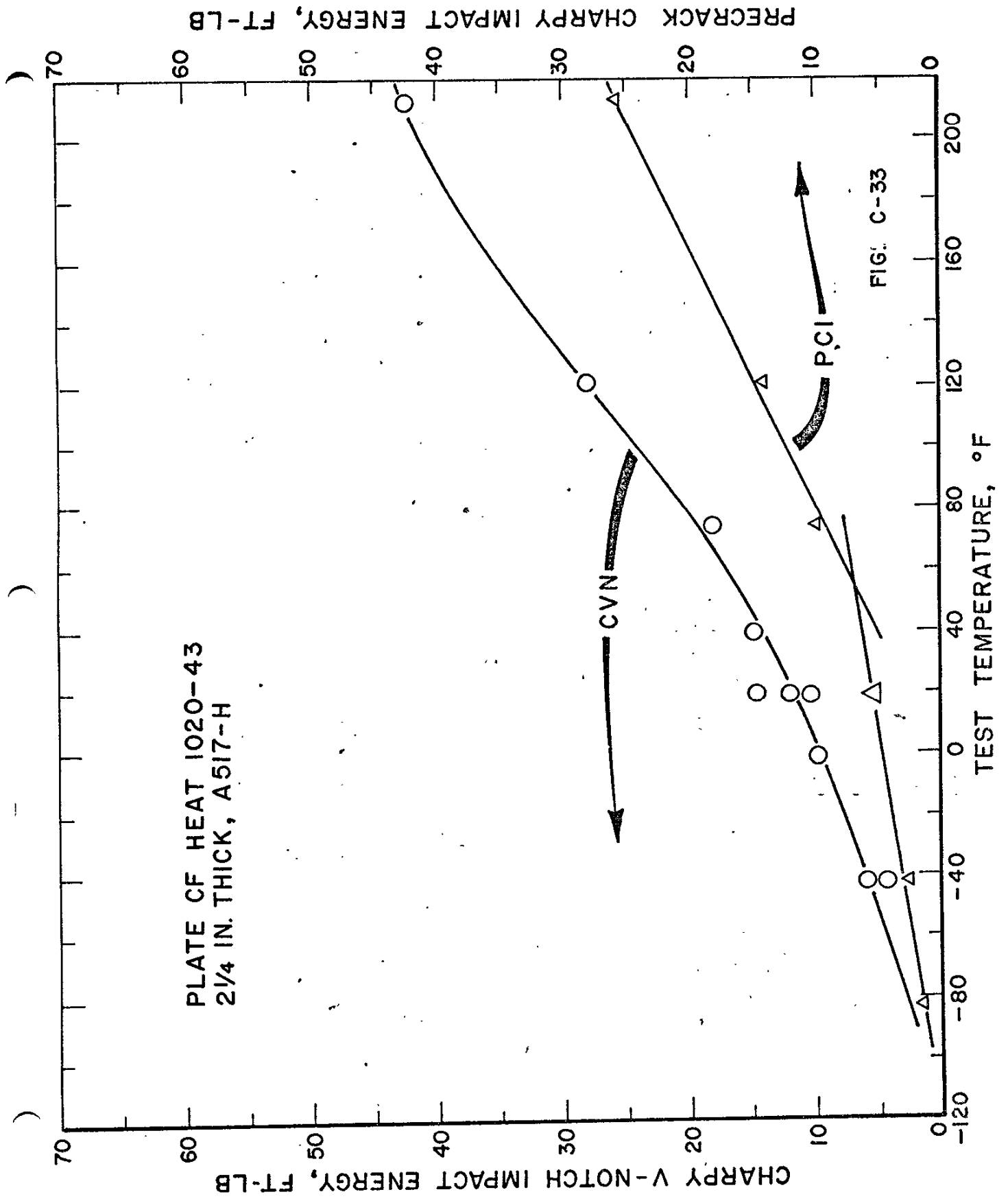


FIG. C-33

PRECRACK CHARPY IMPACT ENERGY, FT-LB

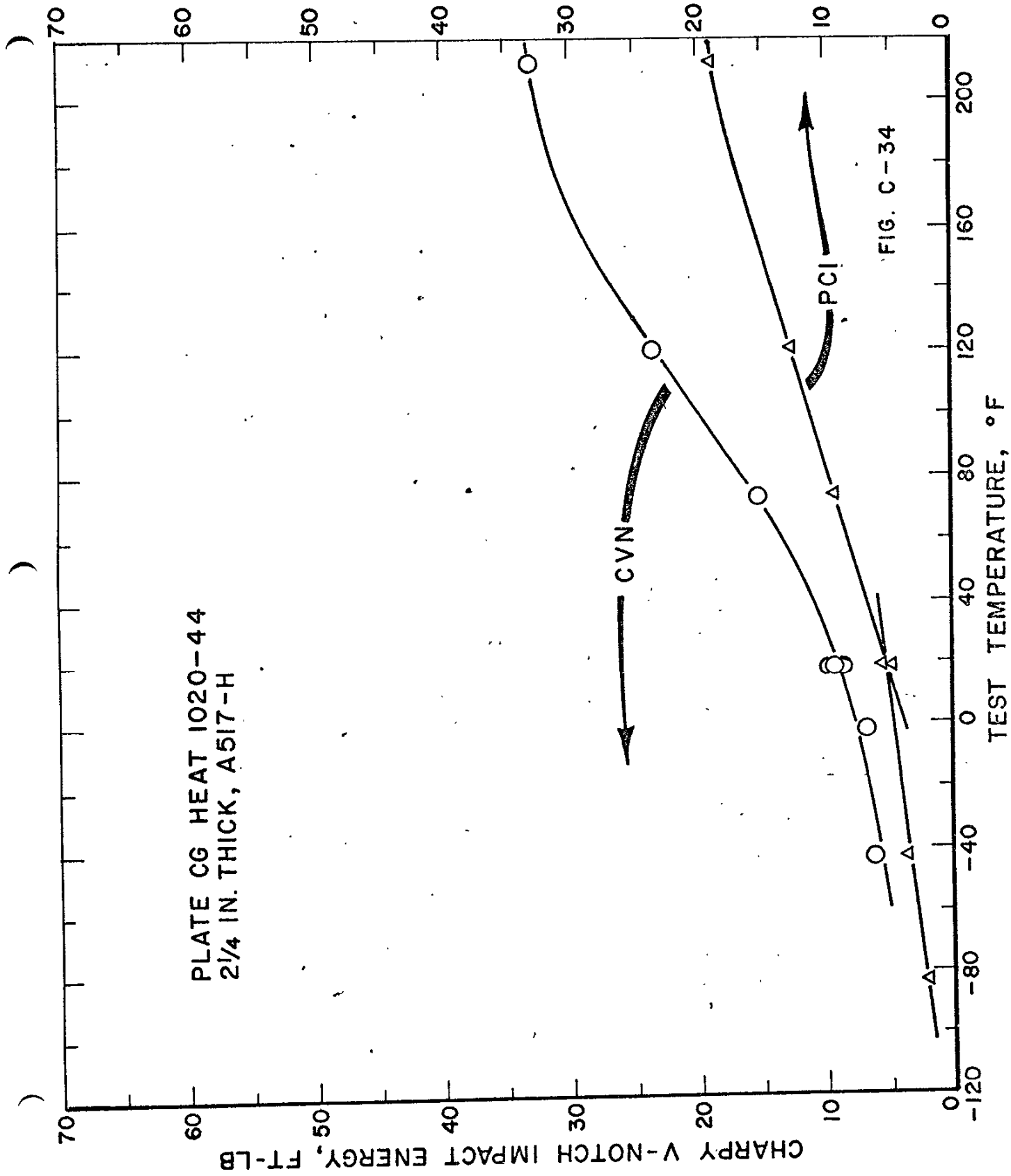


FIG. C-34

CHARPY V-NOTCH IMPACT ENERGY, FT-LB

PLATE AL HEAT 1020-46
2 1/4 IN. THICK, A517-H

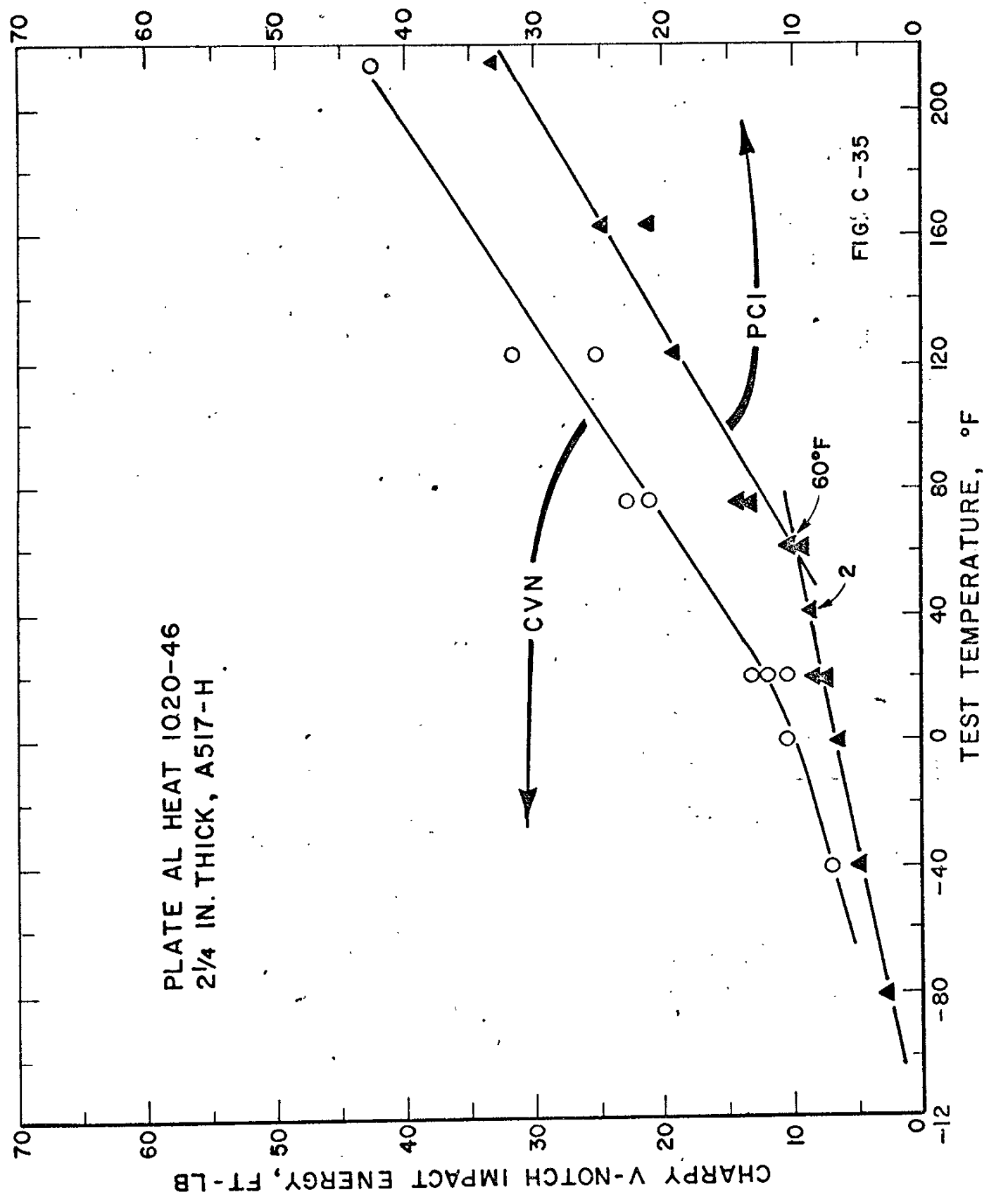
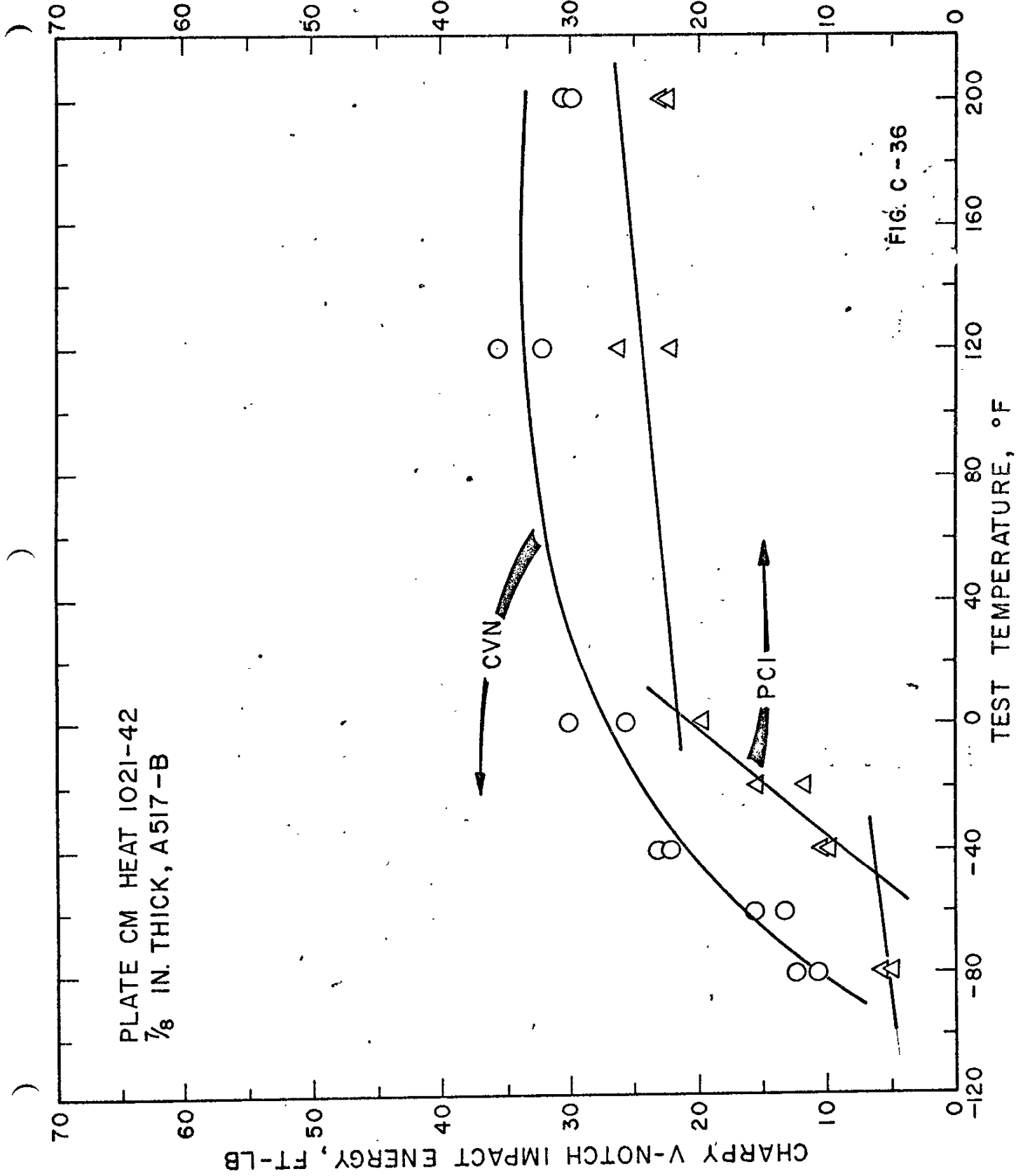


FIG. C-35

PRECRACK CHARPY IMPACT ENERGY, FT-LB



PRECRACK CHARPY IMPACT ENERGY, FT-LB

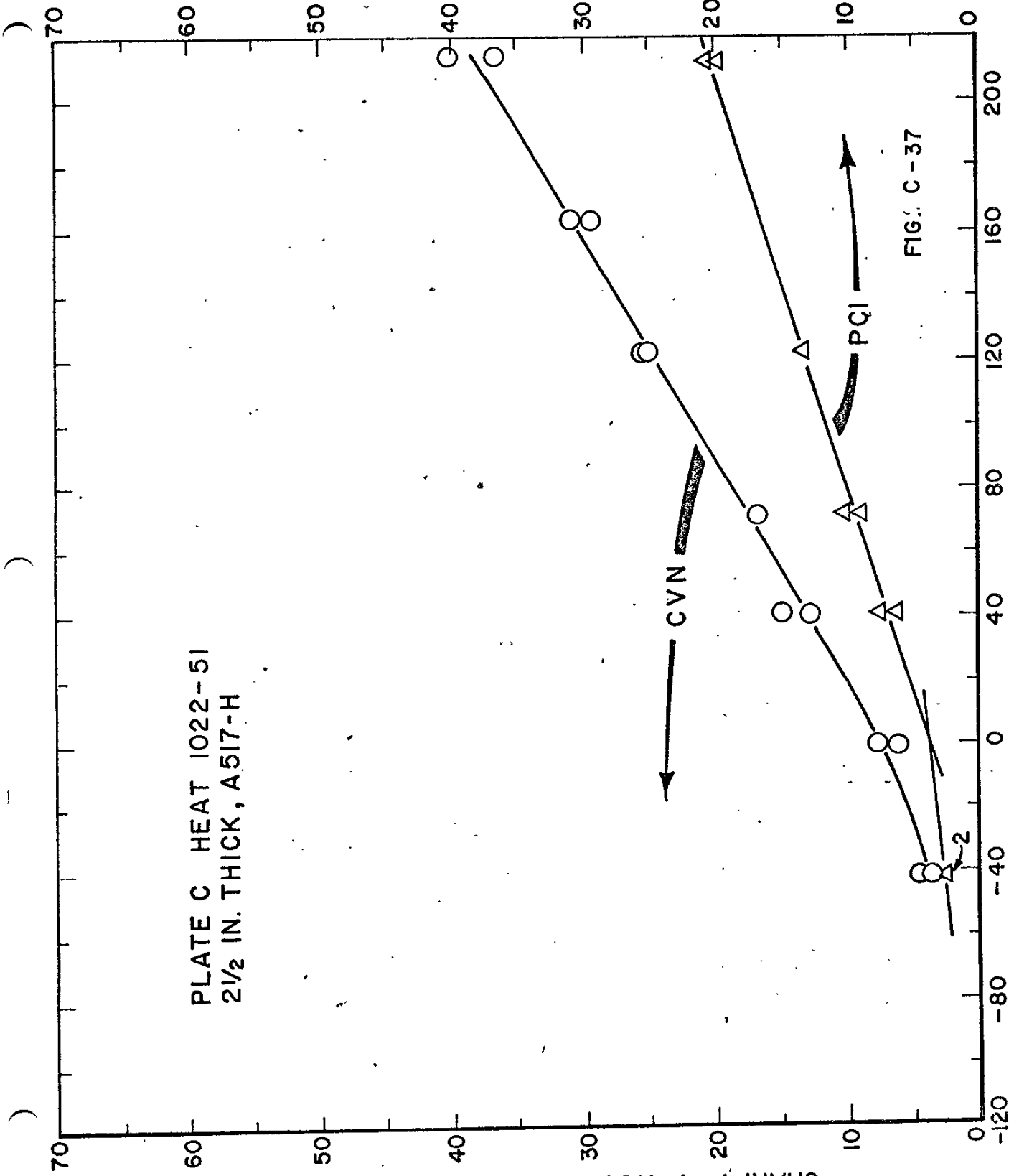


PLATE C HEAT 1022-51
2 1/2 IN. THICK, A517-H

CHARPY V-NOTCH IMPACT ENERGY, FT-LB

TEST TEMPERATURE, °F

FIG. C-37

PRECRACK CHARPY IMPACT ENERGY, FT-LB

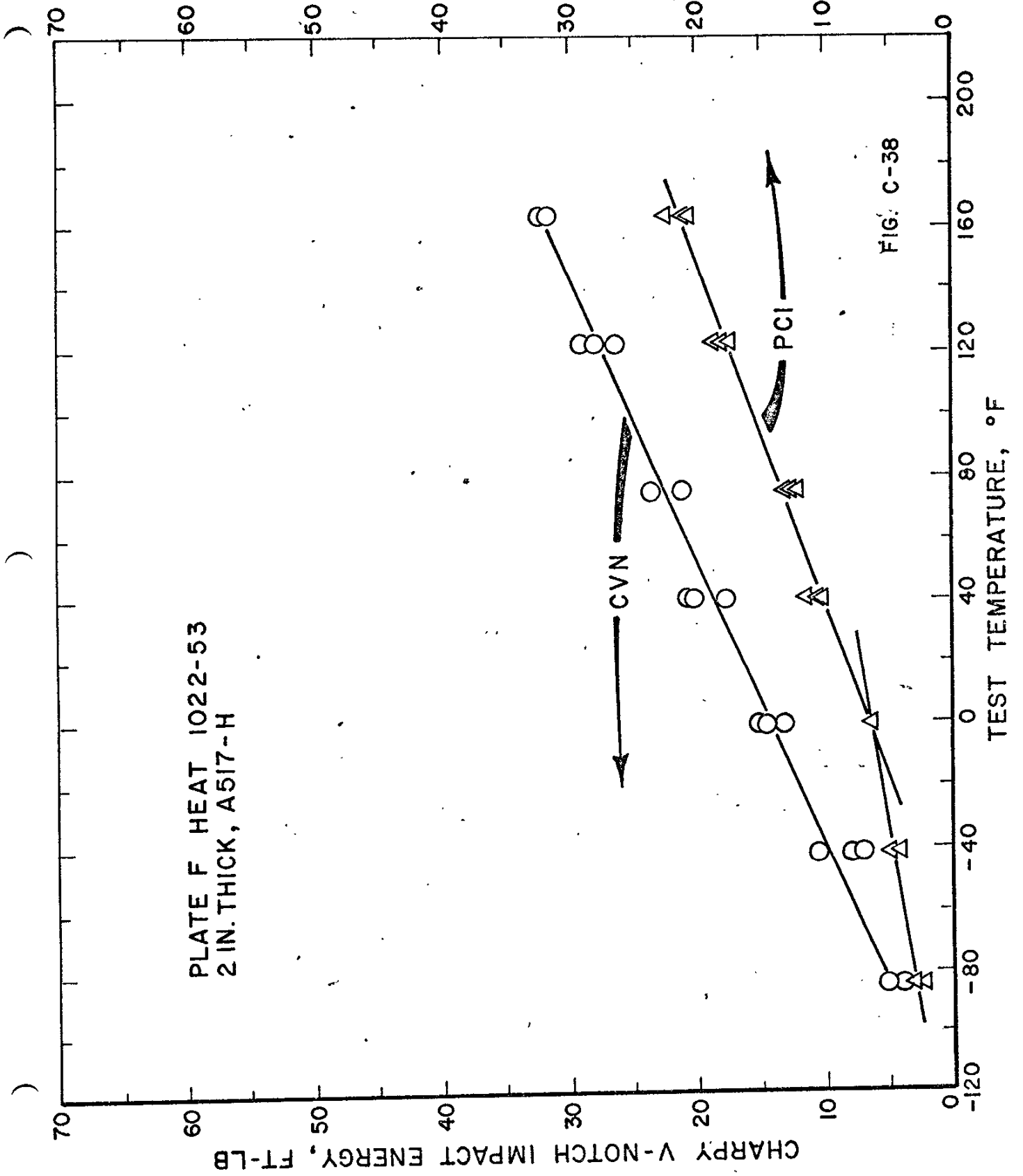


FIG. C-38

PLATE H HEAT 1022-54
2 IN. THICK, A517-H

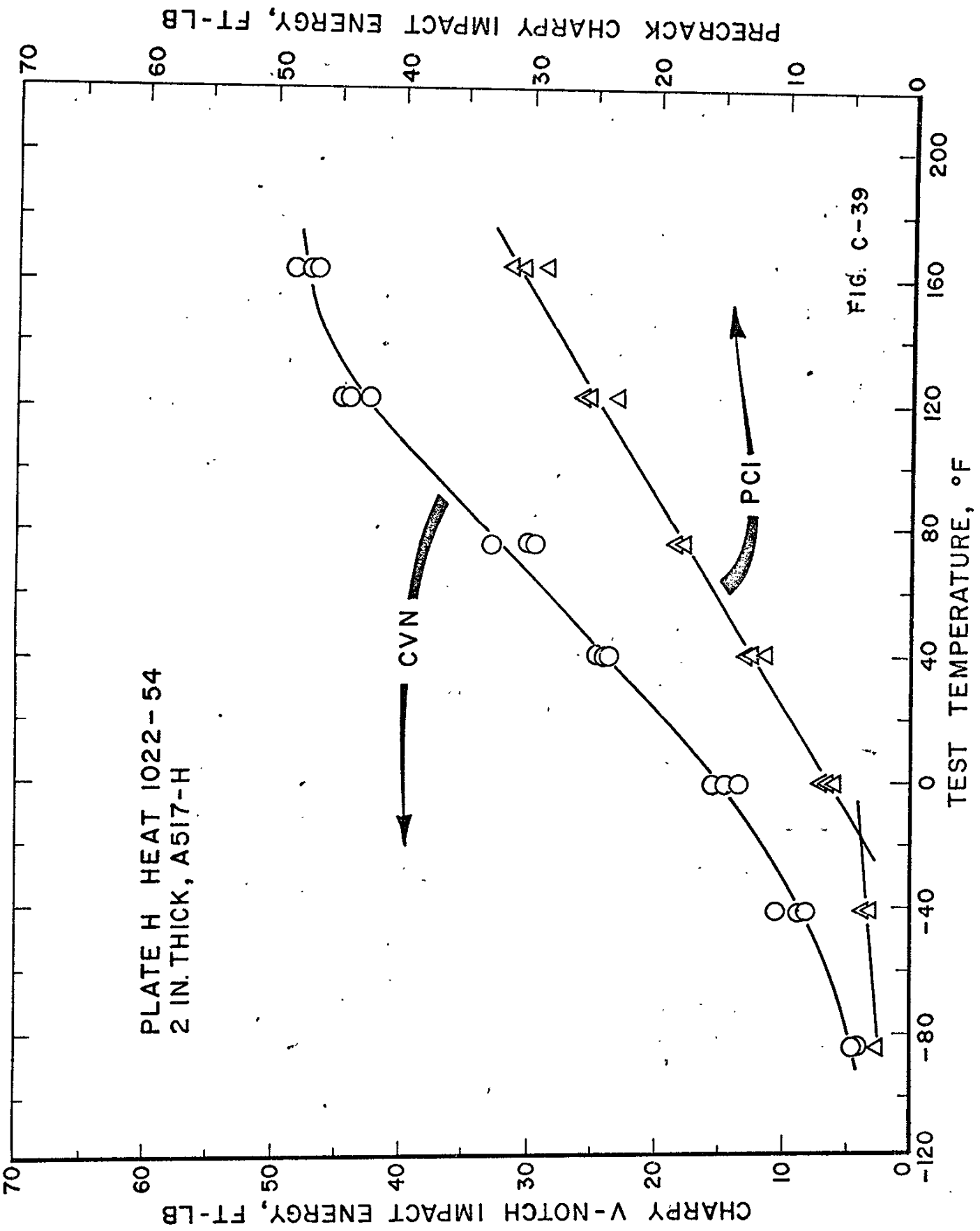


FIG. C-39

PRECRACK CHARPY IMPACT ENERGY, FT-LB

CHARPY V-NOTCH IMPACT ENERGY, FT-LB

PLATE G HEAT 1023-51
2 IN. THICK, A517-H

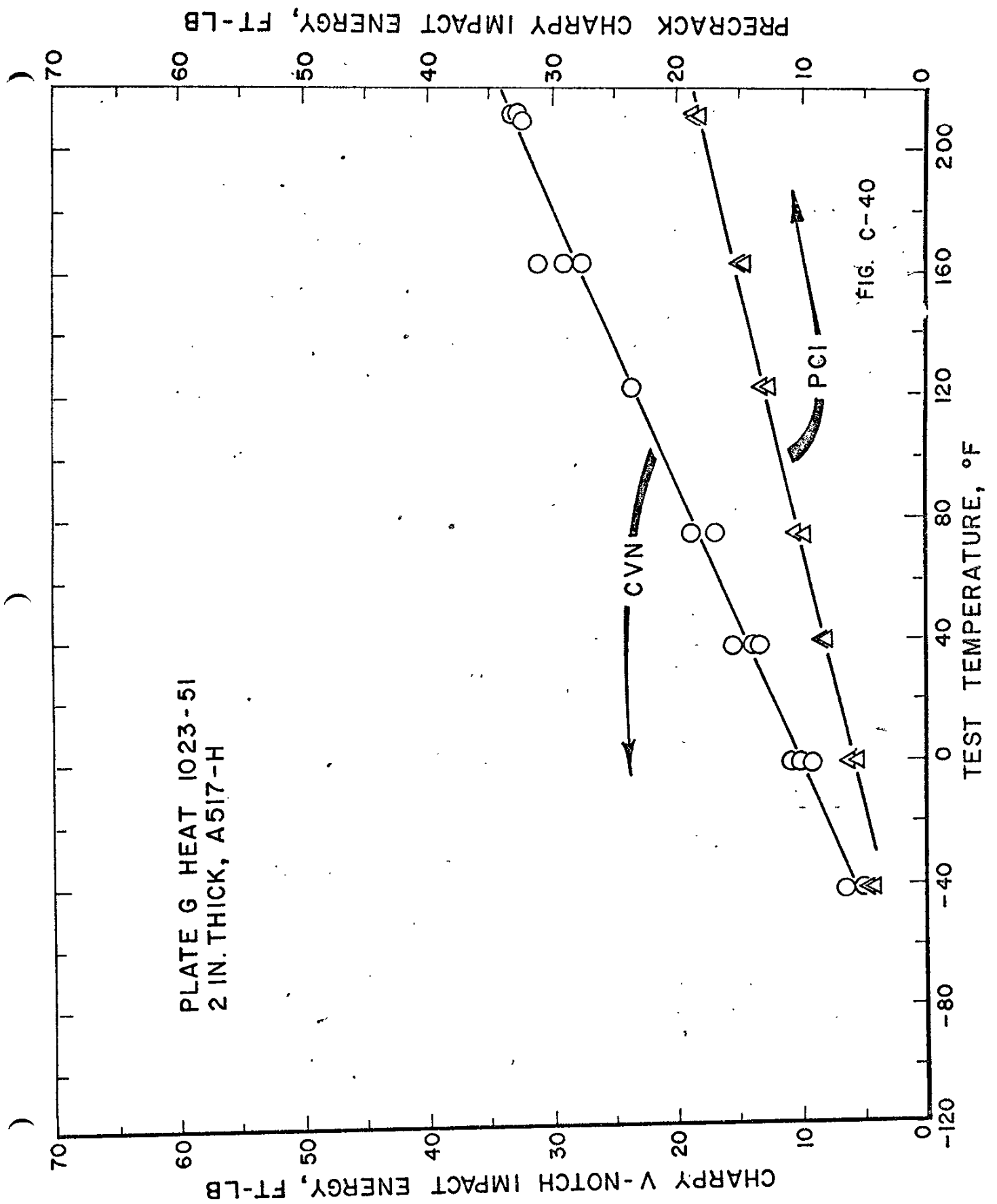


FIG. C-40

PLATE E HEAT 1023-54
2 IN. THICK, A517-H

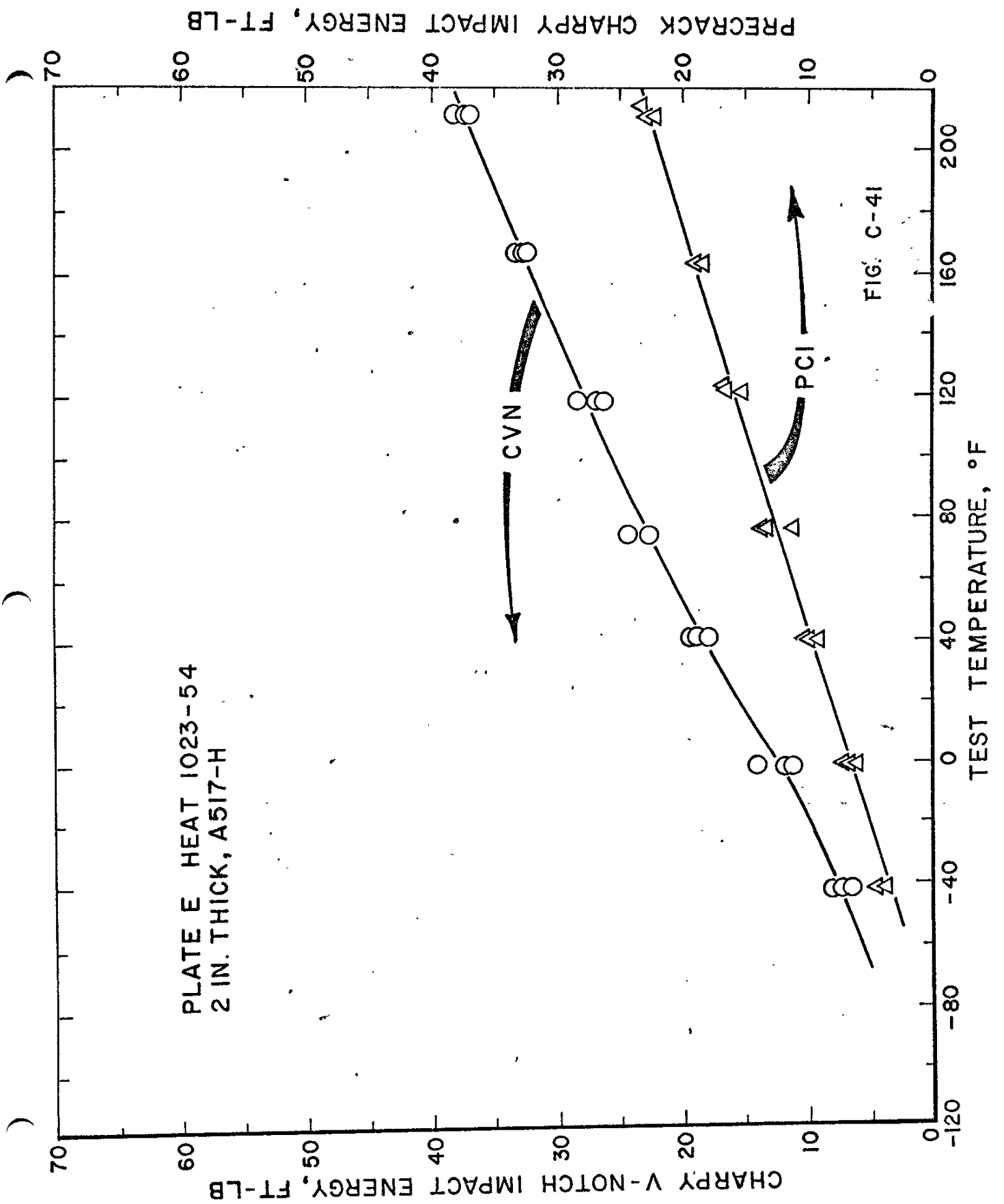


FIG. C-41

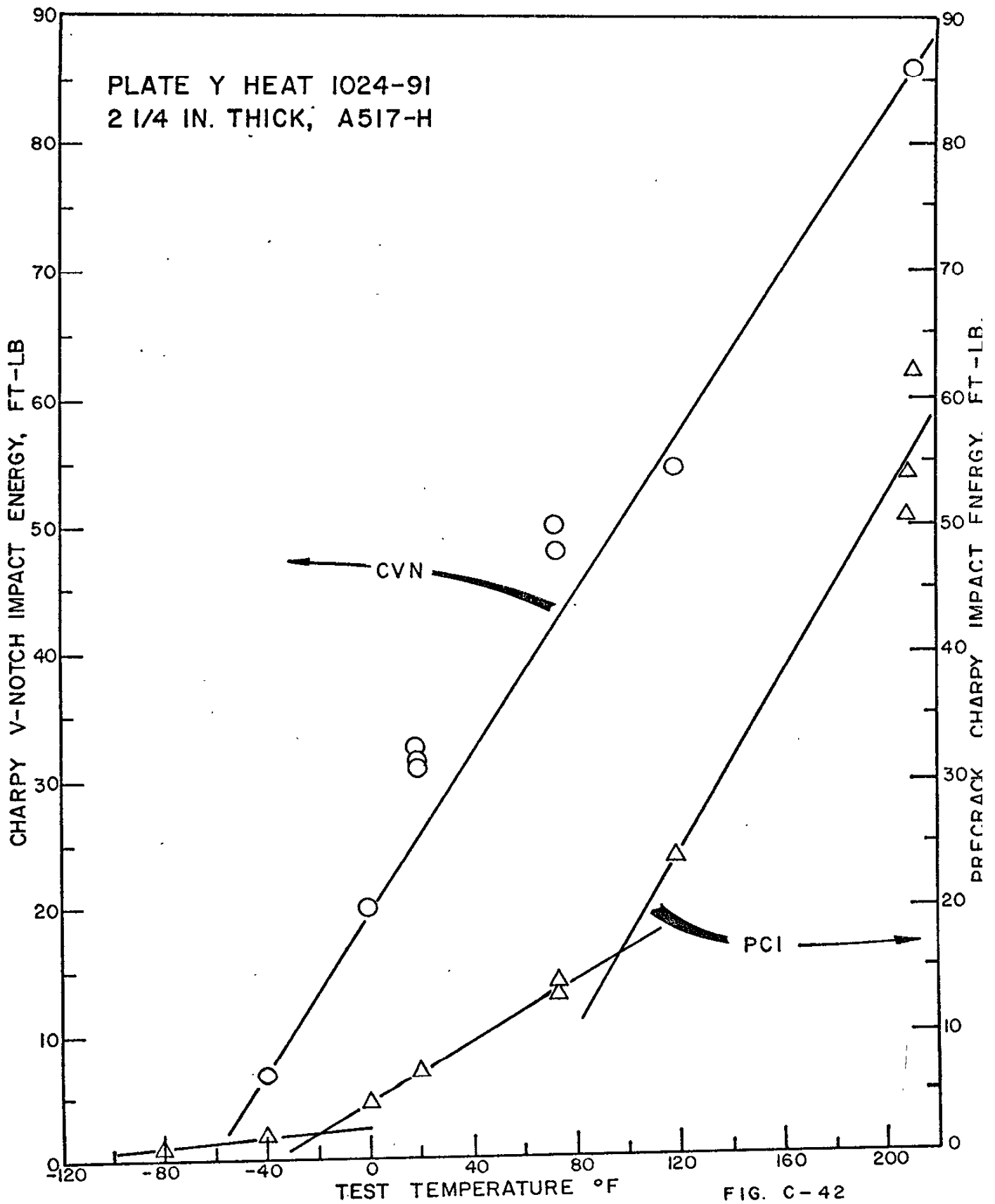


FIG. C-42

PLATE Z HEAT 1024-94
2 1/4 IN. THICK, A517-H

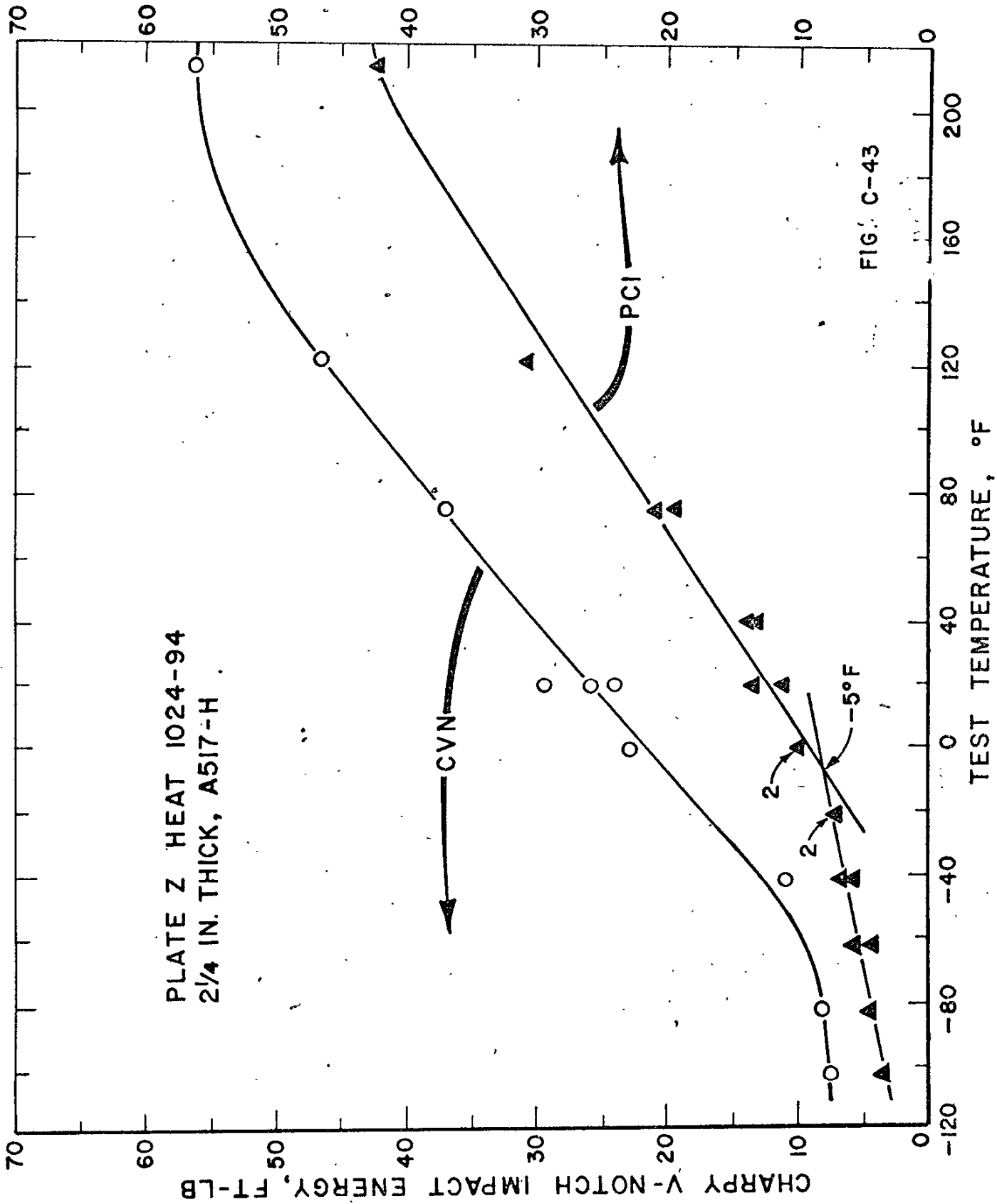


FIG. C-43

PLATE CE HEAT 1024-95
2 1/4 IN. THICK, A517-H

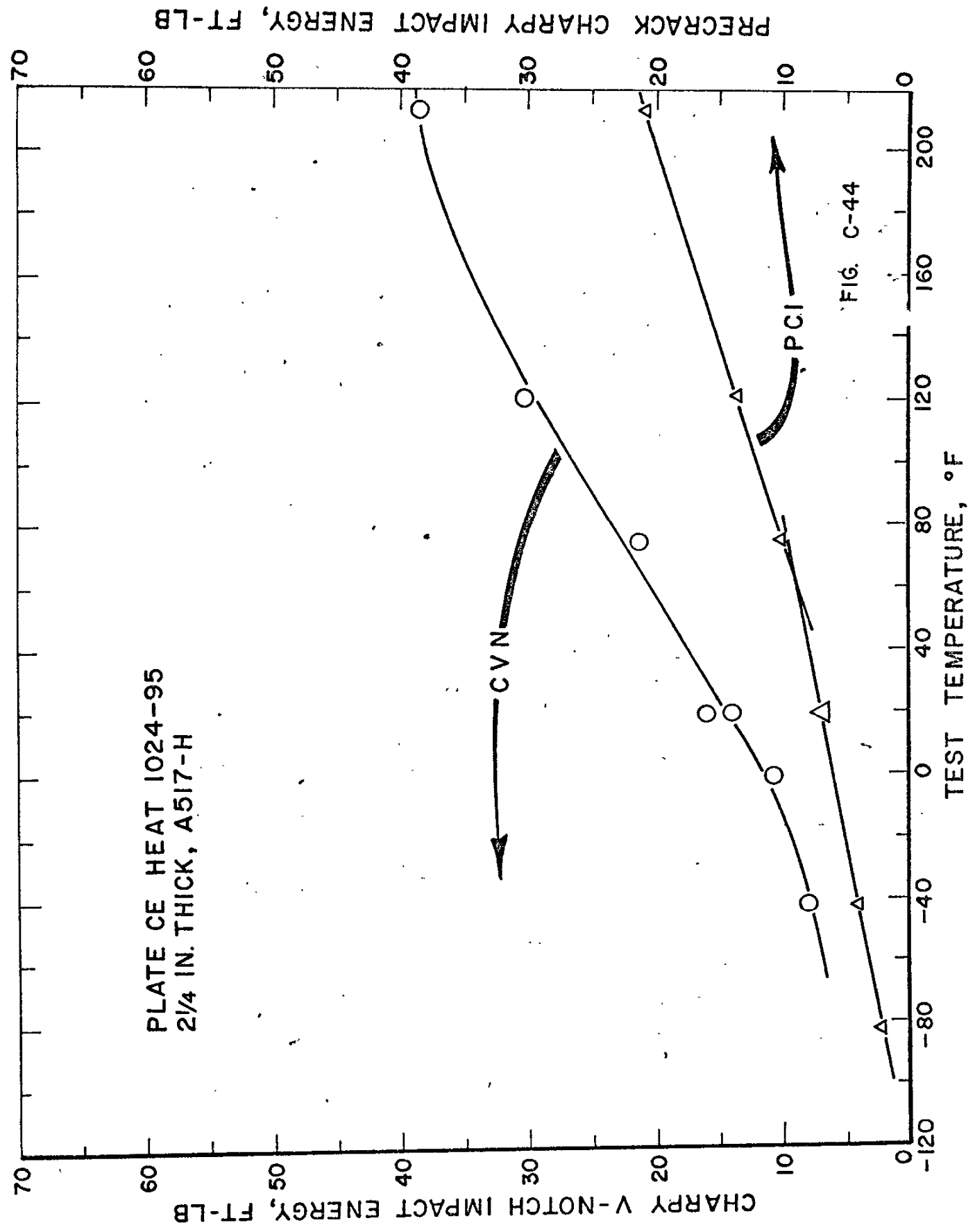


FIG. C-44

PLATE CC HEAT 1025-91
2 1/4 IN. THICK, A517-H

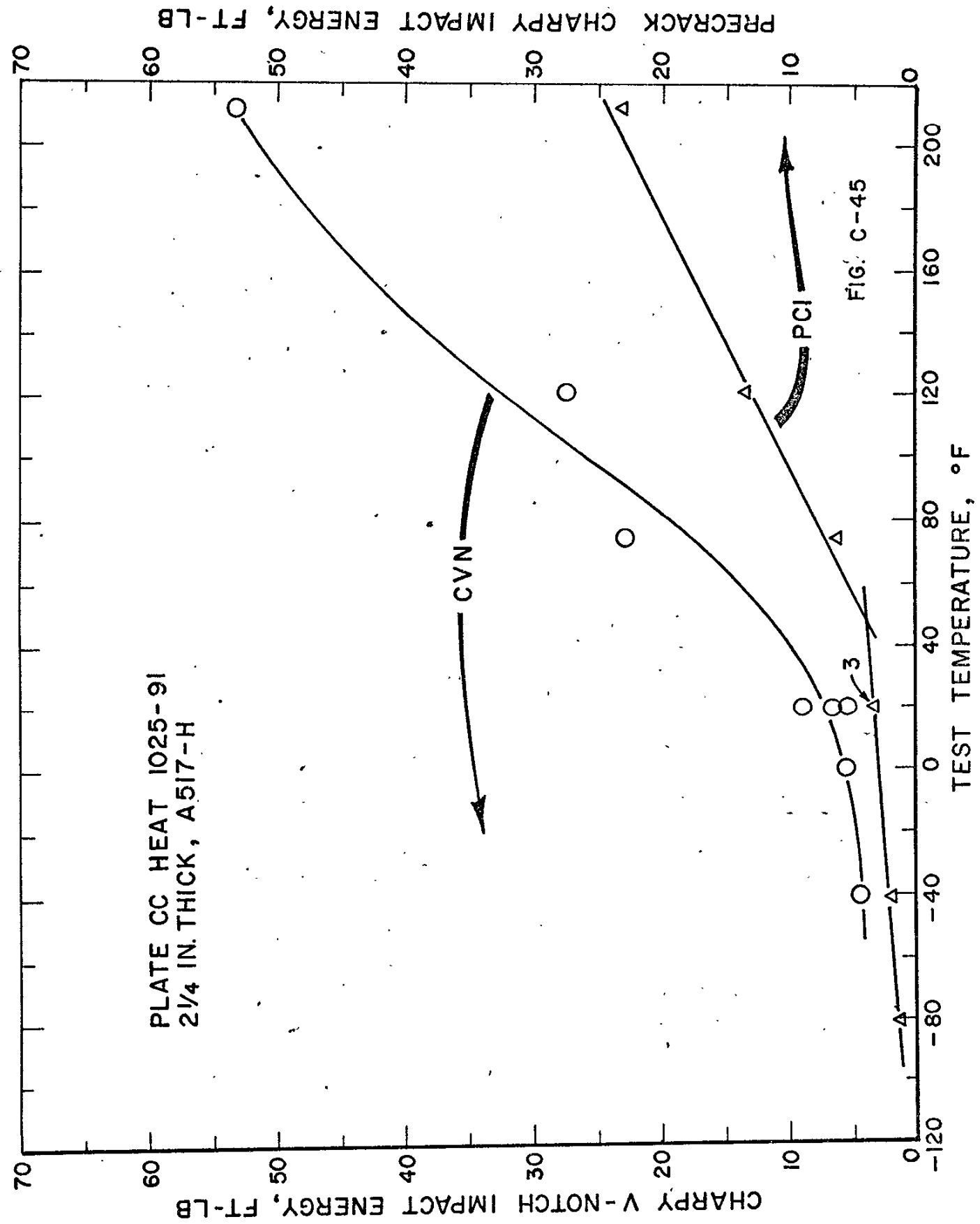


FIG. C-45

PRECRACK CHARPY IMPACT ENERGY, FT-LB

CHARPY V-NOTCH IMPACT ENERGY, FT-LB

PRECRACK CHARPY IMPACT ENERGY, FT-LB

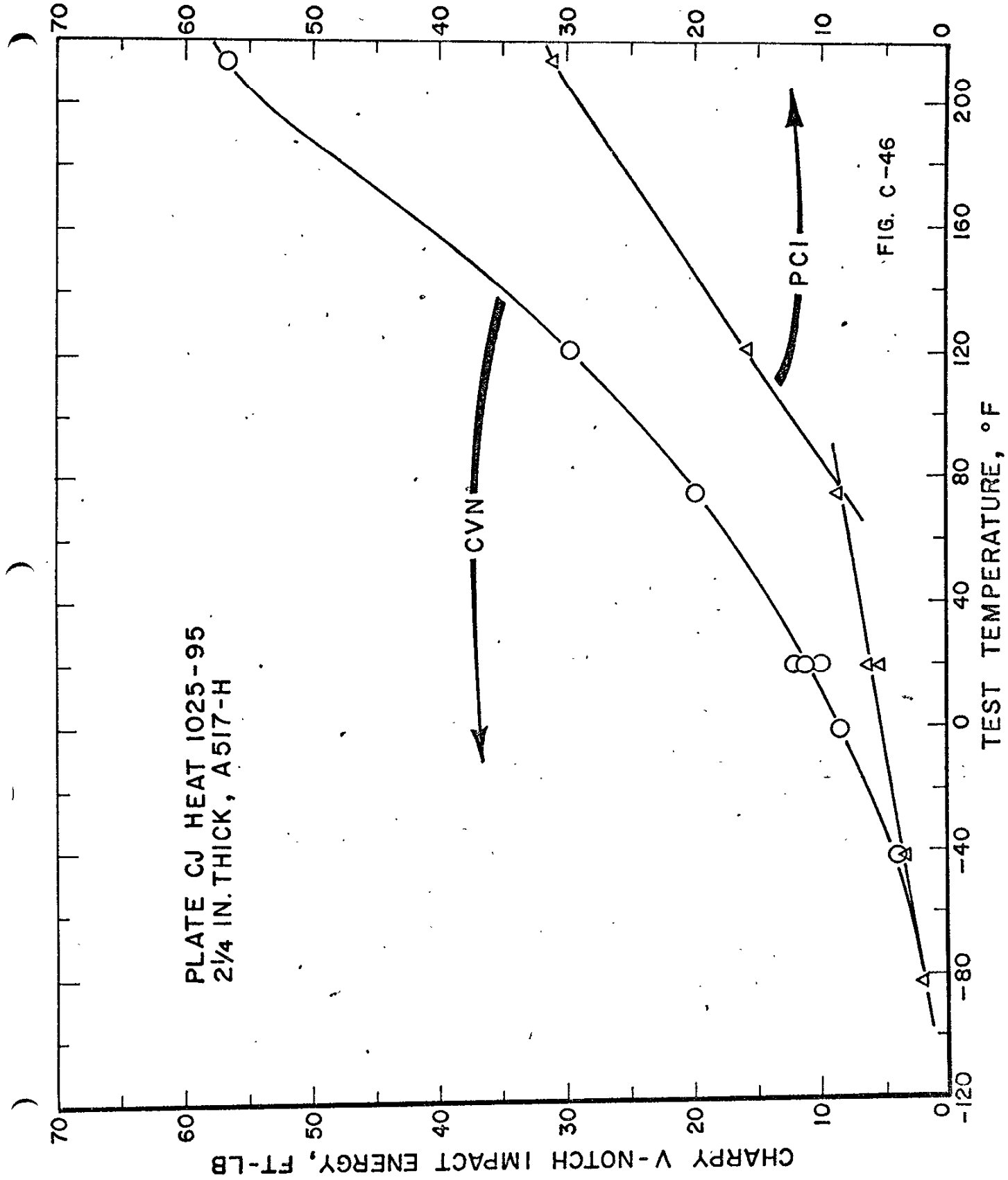


PLATE CJ HEAT 1025-95
2 1/4 IN. THICK, A517-H

FIG. C-46

CHARPY V-NOTCH IMPACT ENERGY, FT-LB

PRECRACK CHARPY IMPACT ENERGY, FT-LB

CHARPY V-NOTCH IMPACT ENERGY, FT-LB

PLATE A HEAT 1026-92
2 1/4 IN. THICK, A517-F

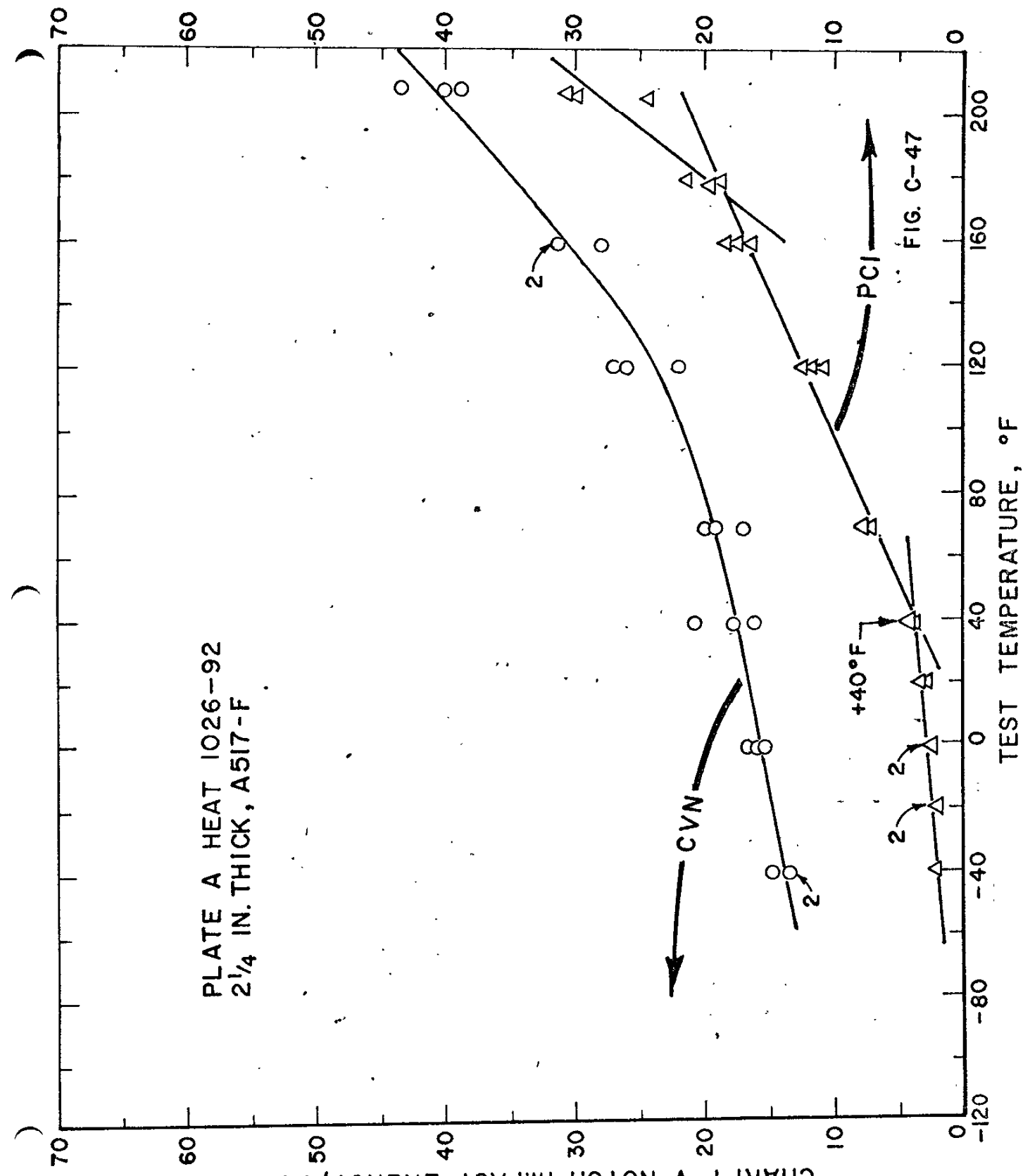


FIG. C-47

PRECRACK CHARPY IMPACT ENERGY, FT-LB

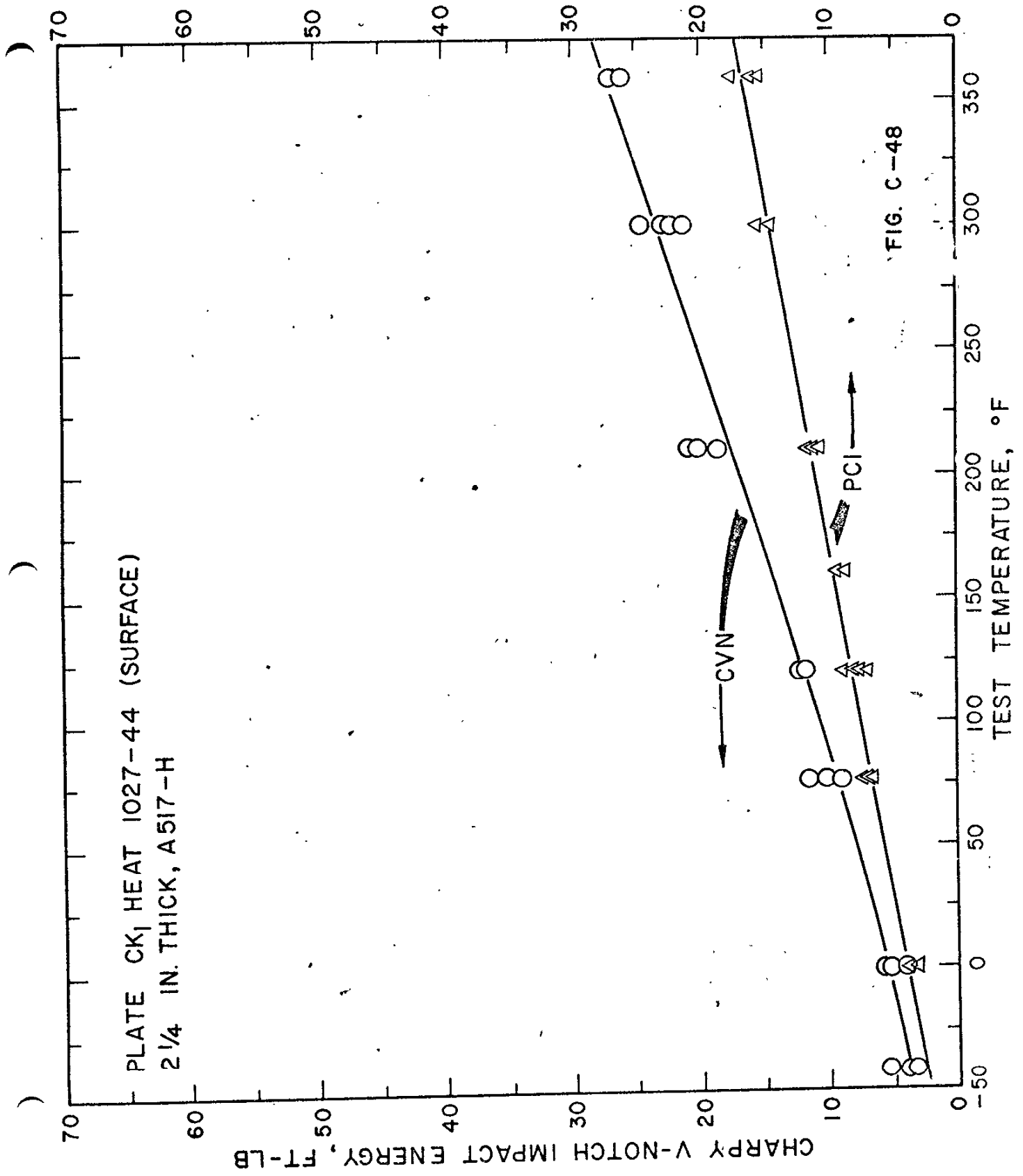


FIG. C-48

PRECRACK CHARPY IMPACT ENERGY, FT-LB

PLATE CK₁ HEAT 1027-44 (CENTER)
2 1/4 IN. THICK, A517-H

CHARPY V-NOTCH IMPACT ENERGY, FT-LB

TEST TEMPERATURE, °F

FIG. C-48.1

CVN

PCI

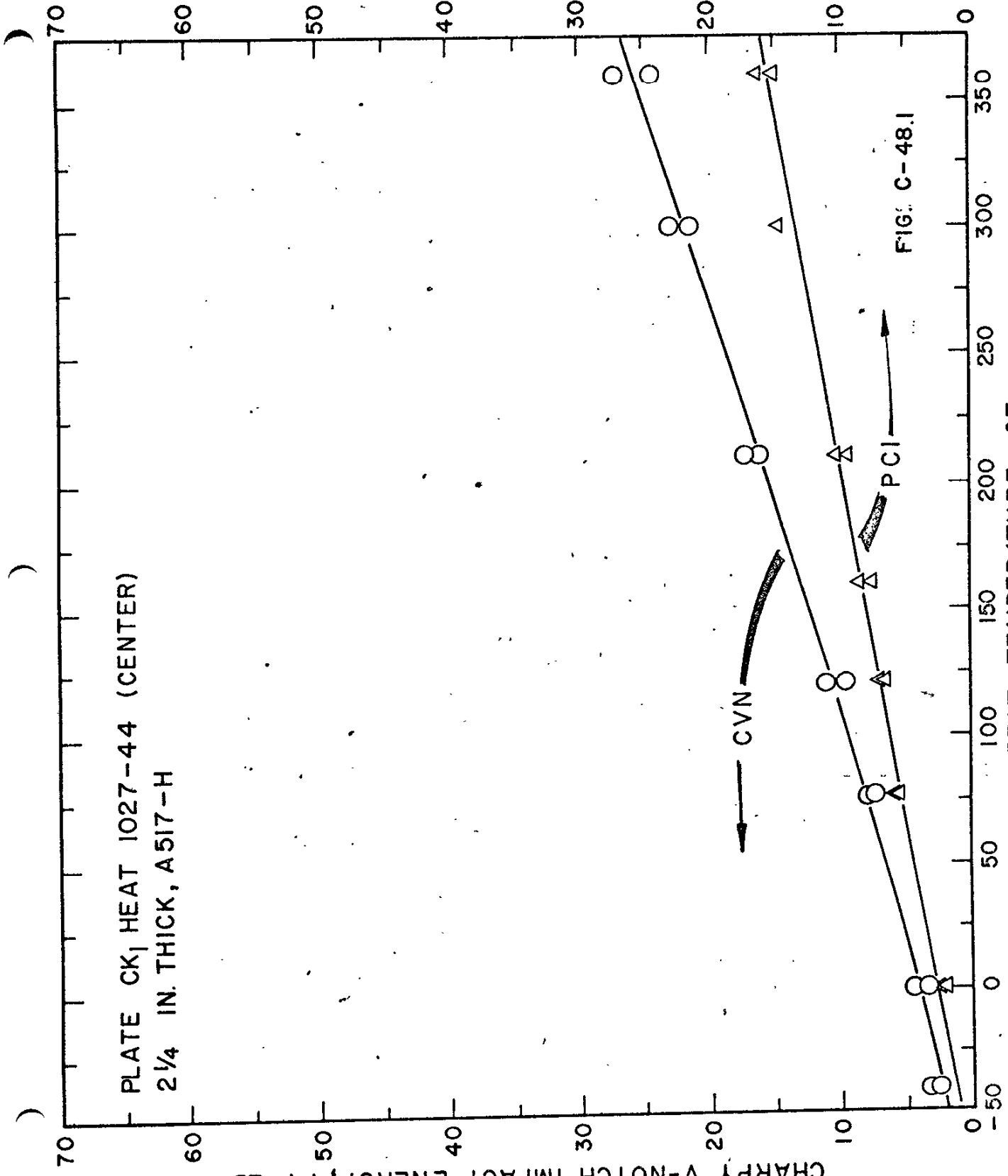


PLATE CK₂ HEAT 1027-44 (LONGITUDINAL-SURFACES)
2 1/4 IN. THICK, A517-H

PRECRACK CHARPY IMPACT ENERGY, FT-LB

CHARPY V-NOTCH IMPACT ENERGY, FT-LB

TEST TEMPERATURE, °F

FIG. C-48.2

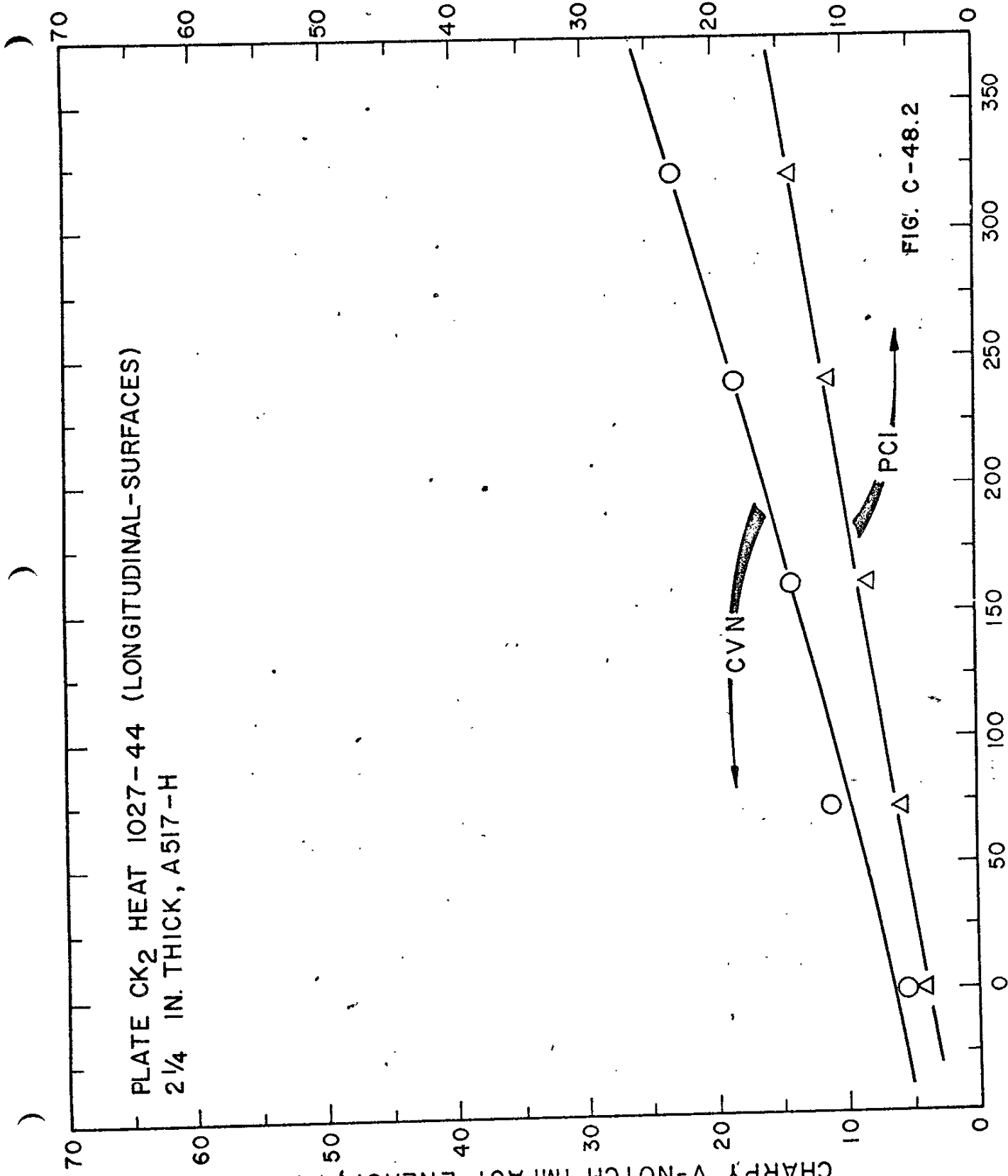


PLATE CK₂ HEAT 1027-44 (LONGITUDINAL-CENTER)
2 1/4 IN. THICK, A517-H

PRECRACK CHARPY IMPACT ENERGY, FT-LB

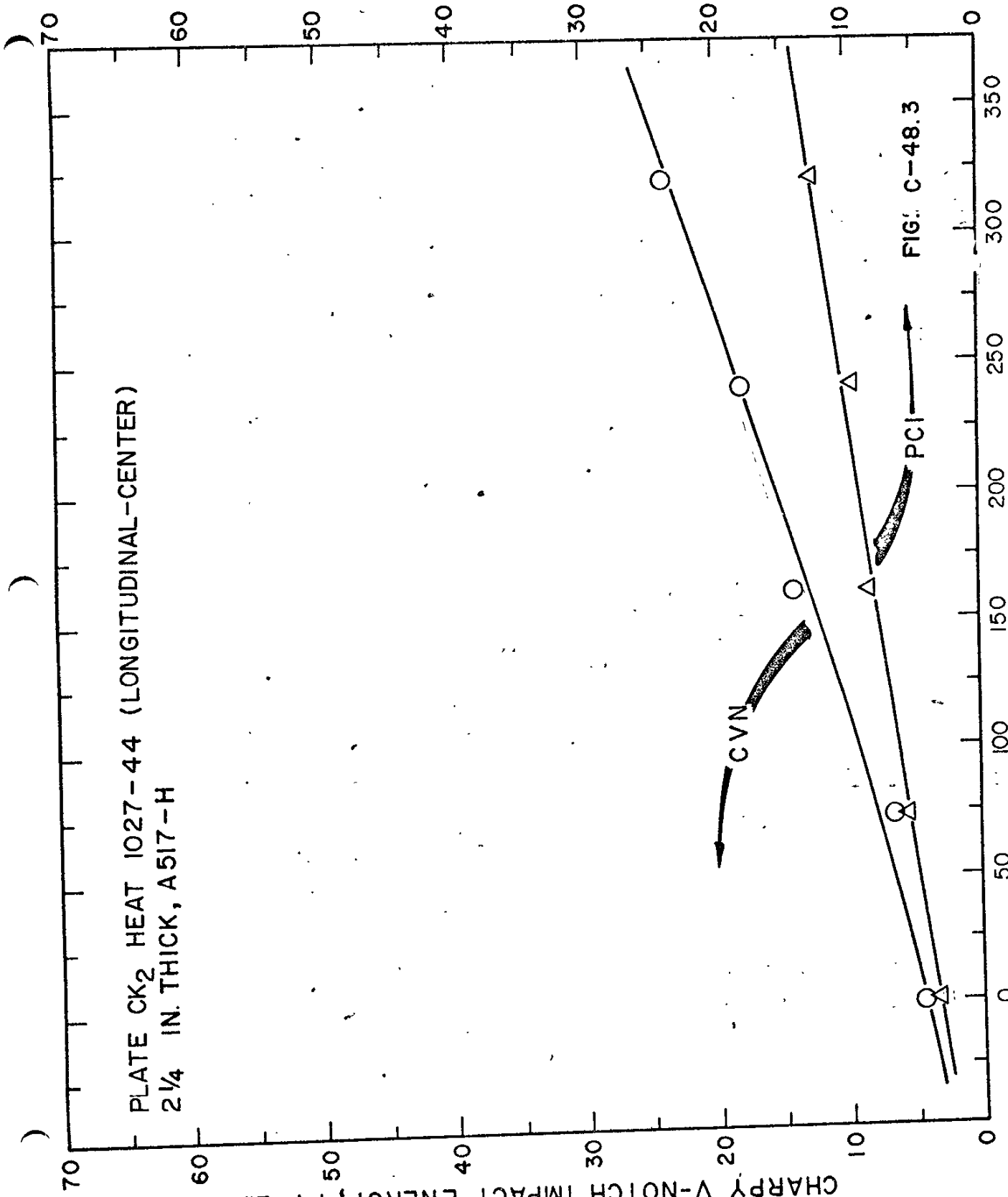
CHARPY V-NOTCH IMPACT ENERGY, FT-LB

FIG. C-48.3

CVN

PCI

TEST TEMPERATURE, °F



PRECRACK CHARPY IMPACT ENERGY, FT-LB

PLATE CK₂ HEAT 1027-44 (TRANSVERSE-SURFACES)
2 1/4 IN. THICK, A517-H

CHARPY V-NOTCH IMPACT ENERGY, FT-LB

TEST TEMPERATURE, °F

FIG. C-48.4

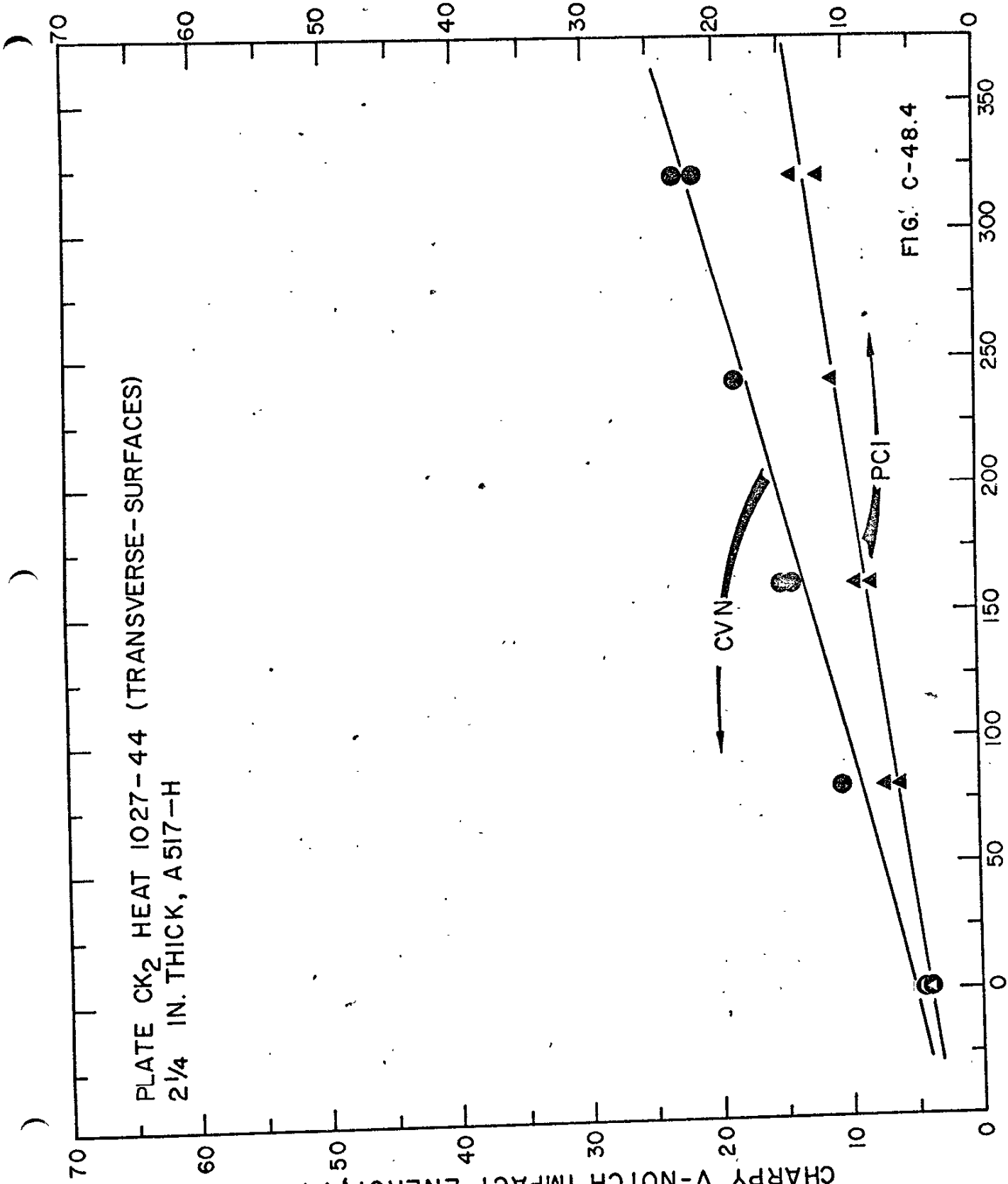


PLATE CK₂ HEAT 1027-44 (TRANSVERSE-CENTER)
2 1/4 IN. THICK, A517-H

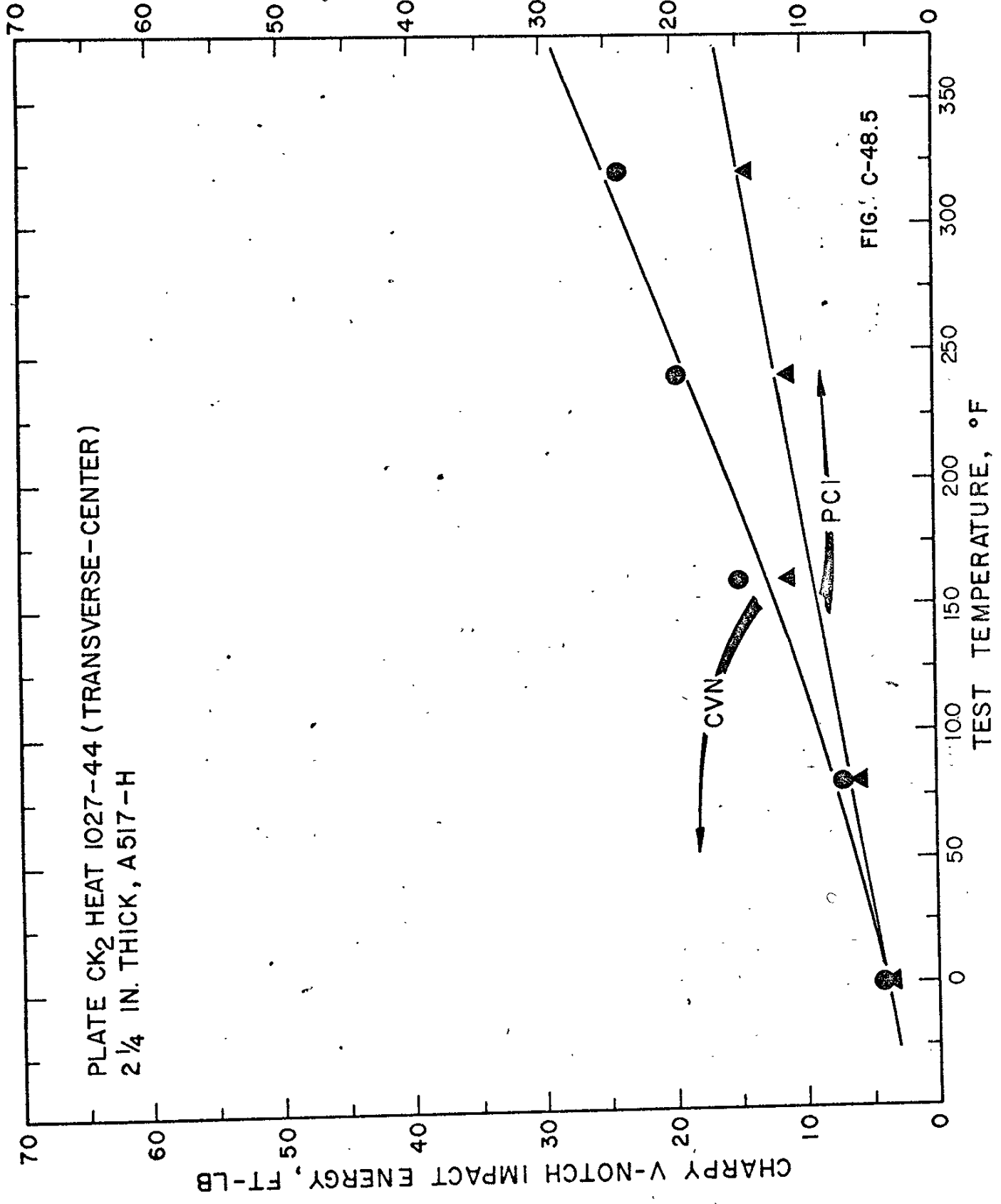


FIG. C-48.5

PRECRACK CHARPY IMPACT ENERGY, FT-LB

CHARPY V-NOTCH IMPACT ENERGY, FT-LB

PLATE CH HEAT 1027-46
2 1/4 IN. THICK, A517-H

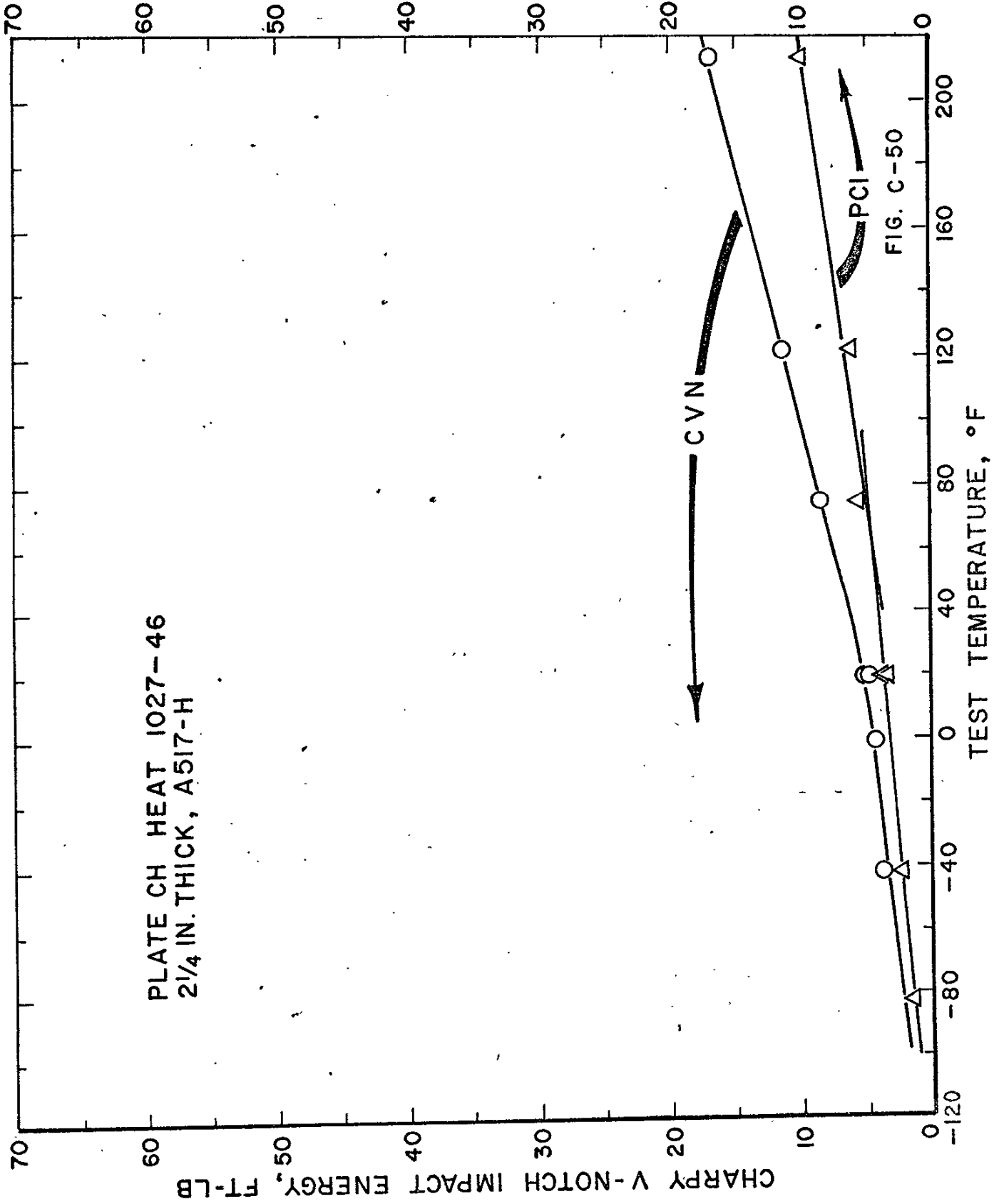


FIG. C-50

PRECRACK CHARPY IMPACT ENERGY, FT-LB

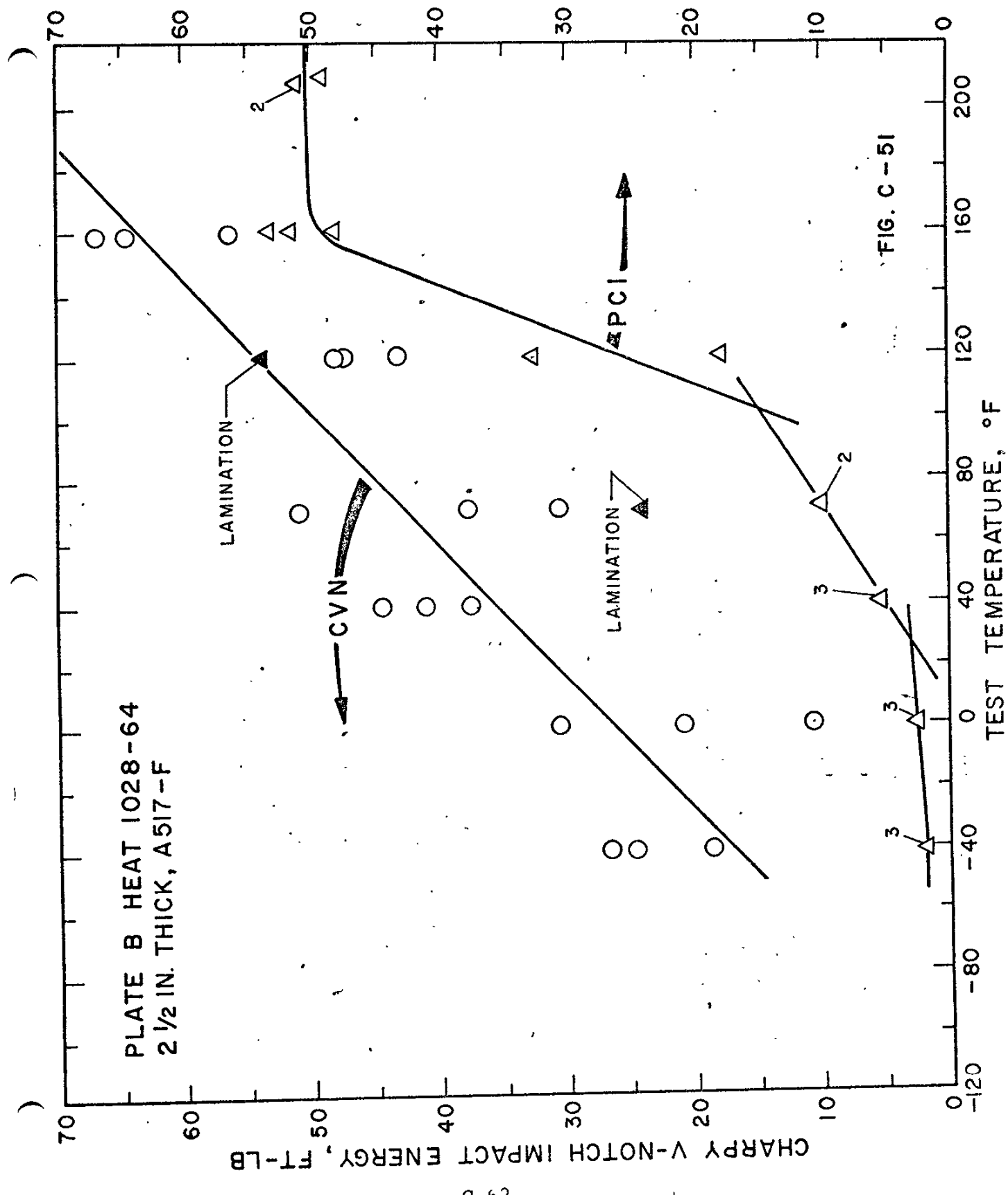


PLATE B HEAT 1028-64
2 1/2 IN. THICK, A517-F

CHARPY V-NOTCH IMPACT ENERGY, FT-LB

TEST TEMPERATURE, °F

FIG. C-51

PRECRACK CHARPY IMPACT ENERGY, FT-LB

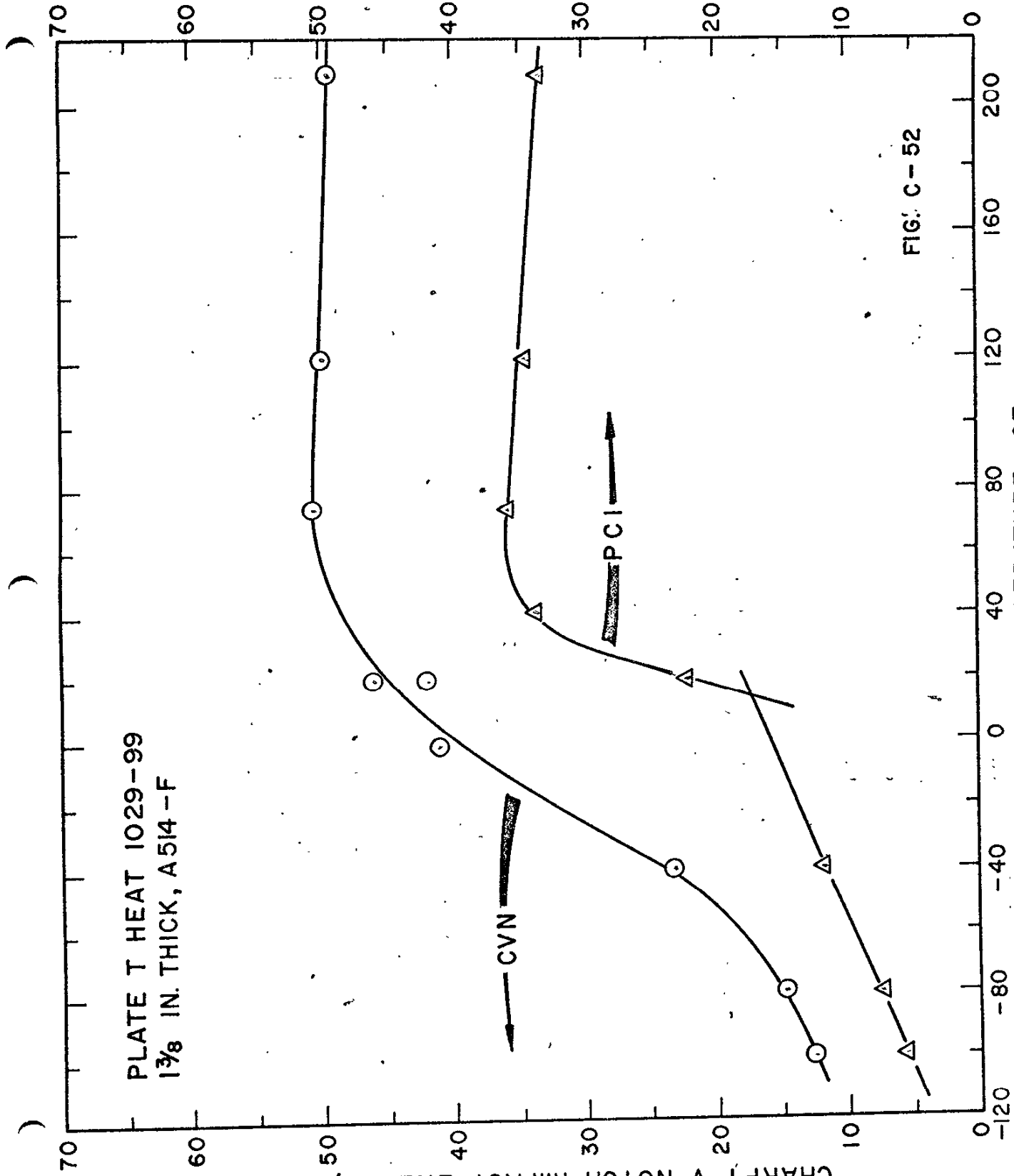


FIG: C-52

Appendix D

Effects Technology, Inc. Charpy Impact Test Results
on Seven Heats of A514/517 Steel.

Fig. D-1	W/A as a Function of Temperature for Plate A								
"	D-2	"	"	"	"	"	"	"	AL
"	D-3	"	"	"	"	"	"	"	L
"	D-4	"	"	"	"	"	"	"	M
"	D-5	"	"	"	"	"	"	"	CK
"	D-6	"	"	"	"	"	"	"	R
"	D-7	"	"	"	"	"	"	"	Z
"	D-8	K_{Id}	"	"	"	"	"	"	A
"	D-9	"	"	"	"	"	"	"	AL
"	D-10	"	"	"	"	"	"	"	L
"	D-11	"	"	"	"	"	"	"	M
"	D-12	"	"	"	"	"	"	"	CK
"	D-13	"	"	"	"	"	"	"	R
"	D-14	"	"	"	"	"	"	"	Z
"	D-15	Components of Charpy V-Notch Energy for Plate L							
"	D-16	"	"	"	"	"	"	"	M
"	D-17	"	"	"	"	"	"	"	CK

D-1 thru D-17

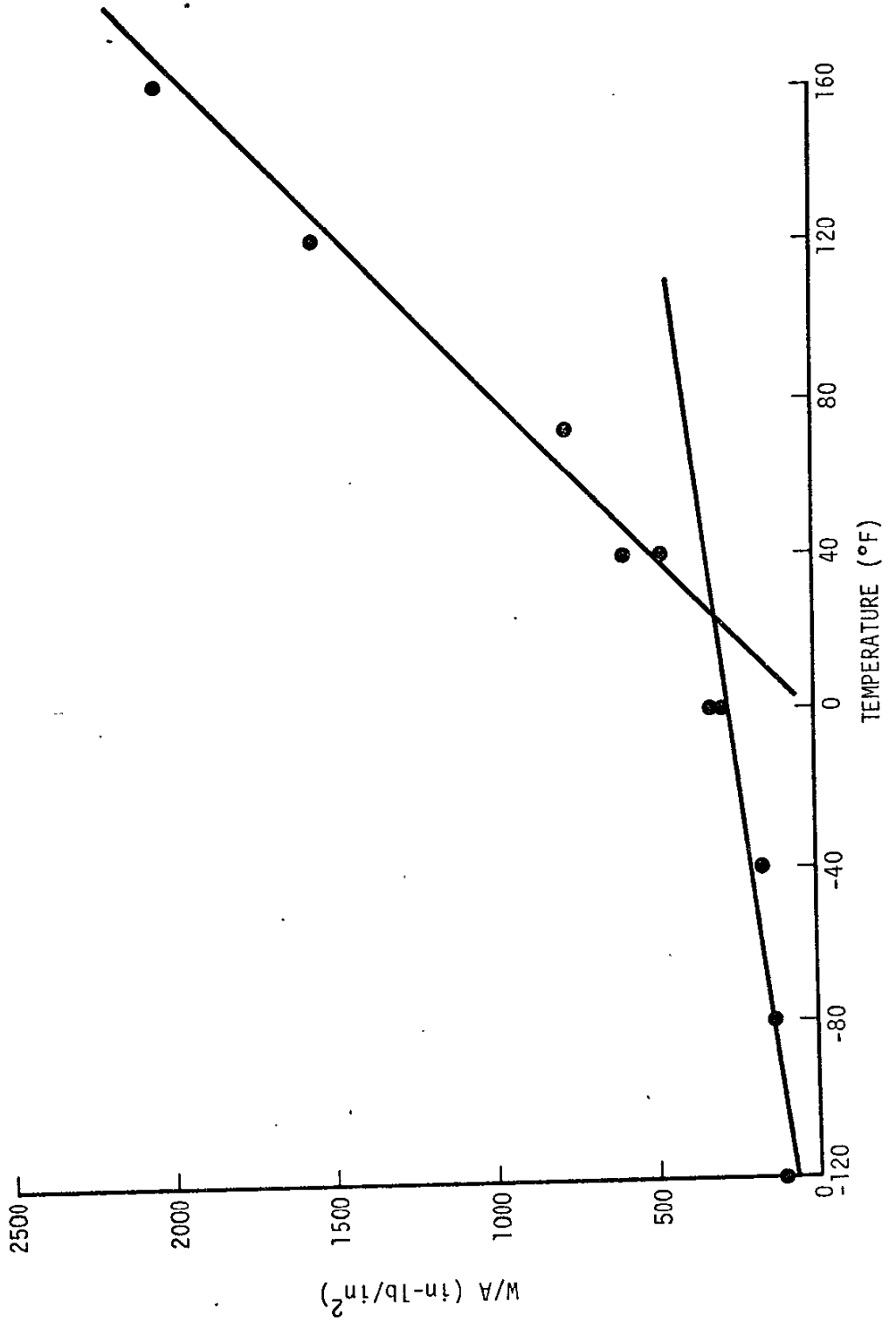


Figure D-1 W/A as a Function of Temperature for Plate A

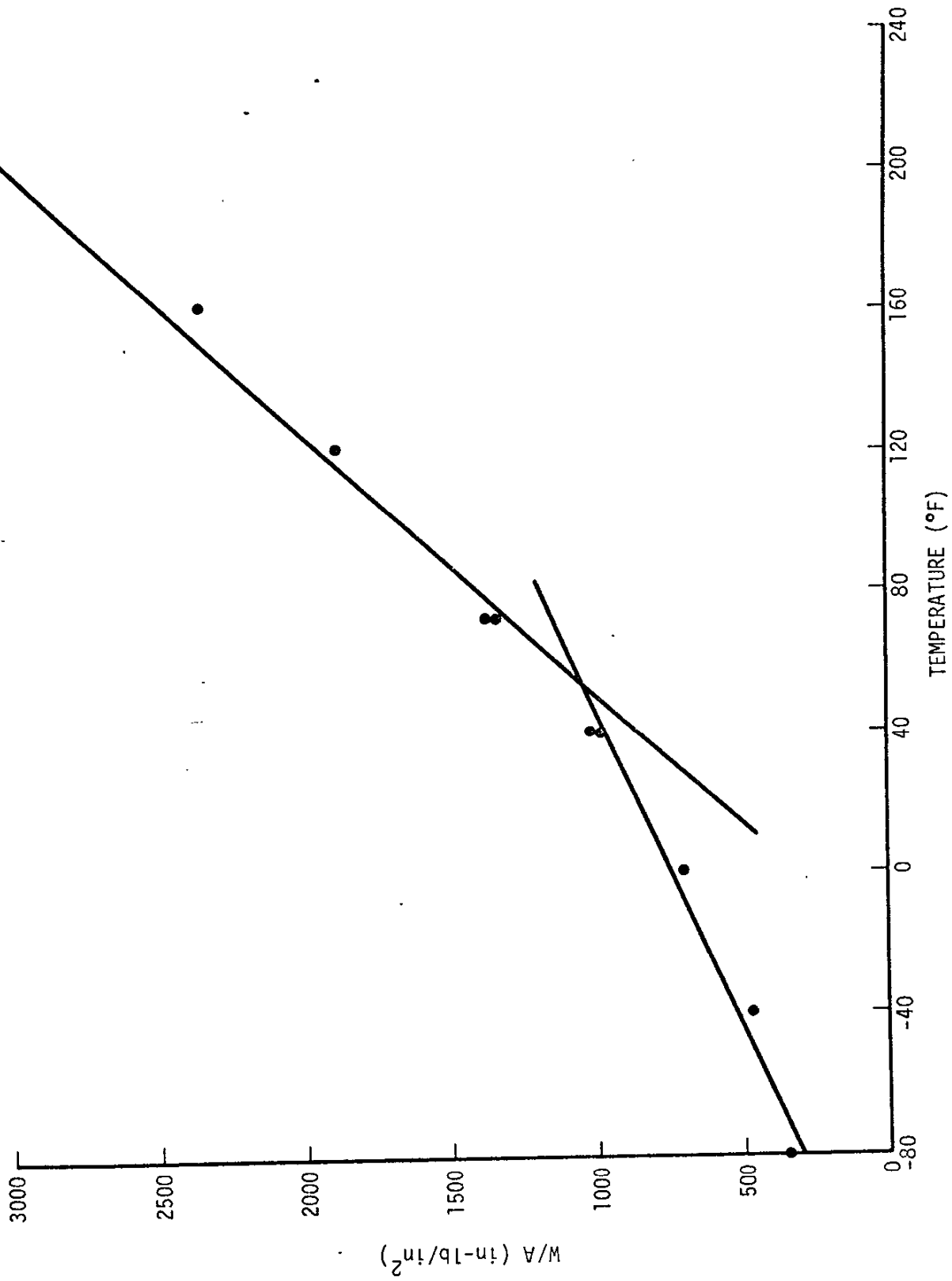


Figure D-2 W/A as a Function of Temperature for Plate AL

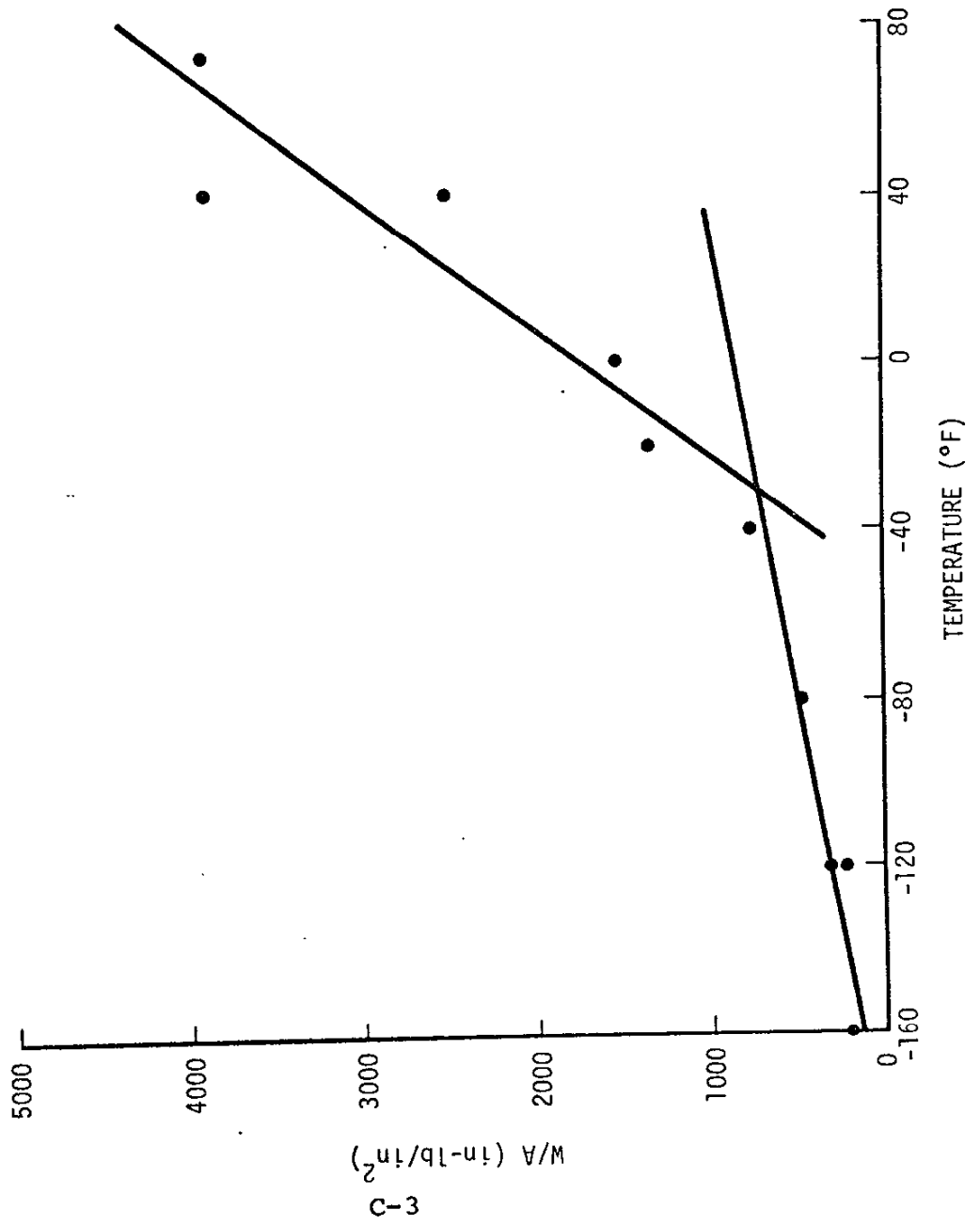


Figure D-3 W/A as a Function of Temperature for Plate L

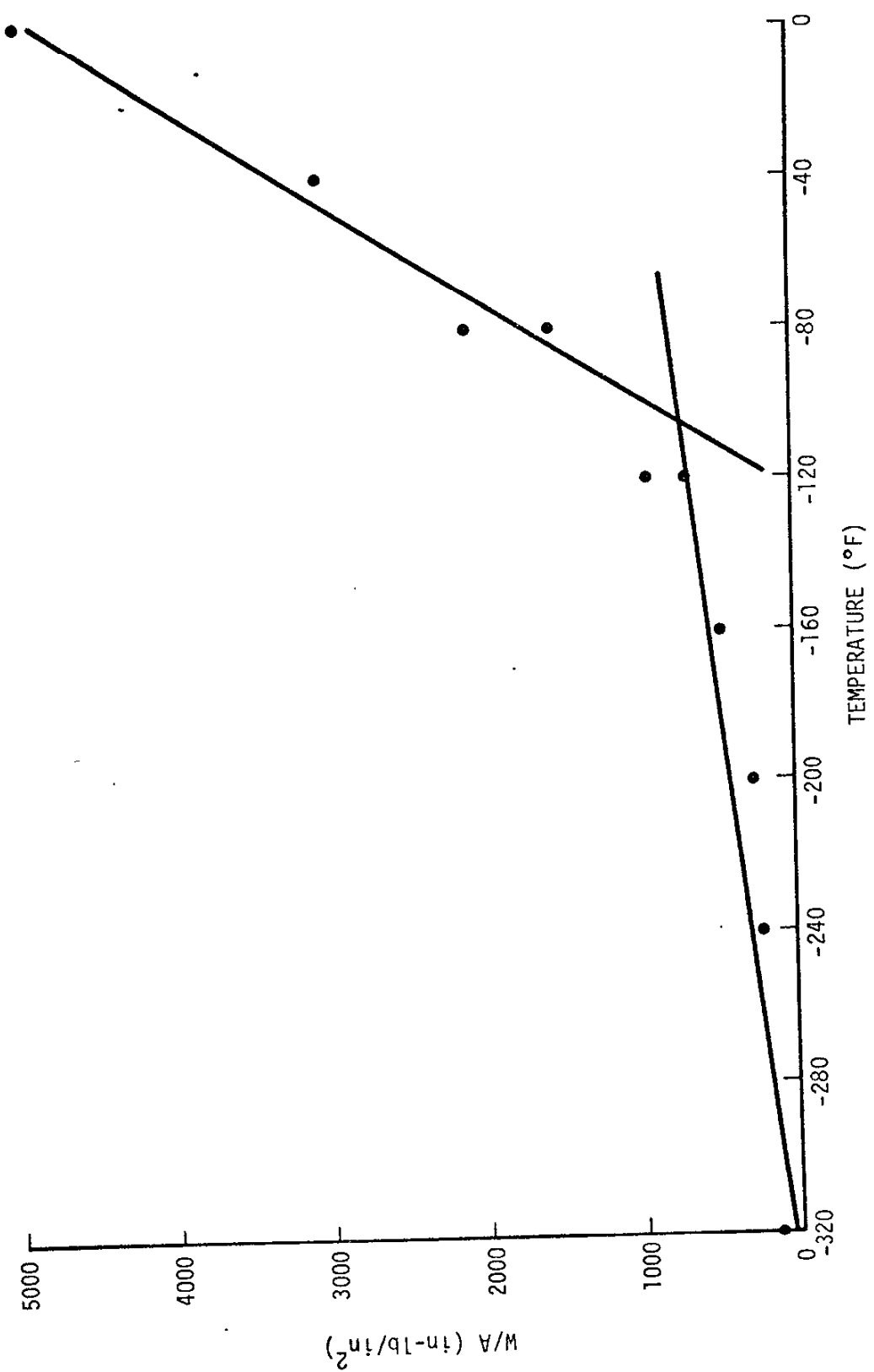


Figure D-4 W/A as a Function of Temperature for Plate M

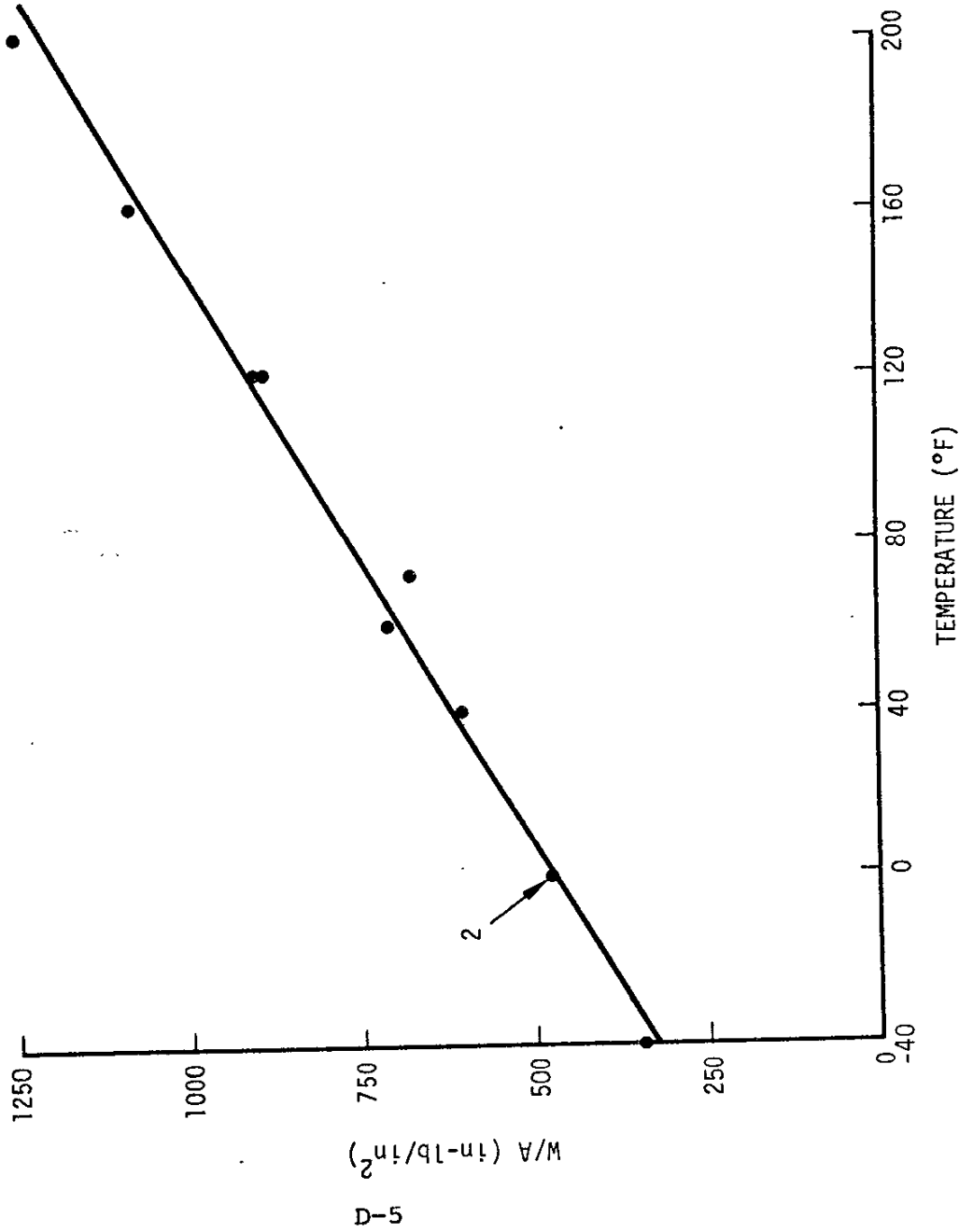


Figure D-5 W/A as a Function of Temperature for Plate CK

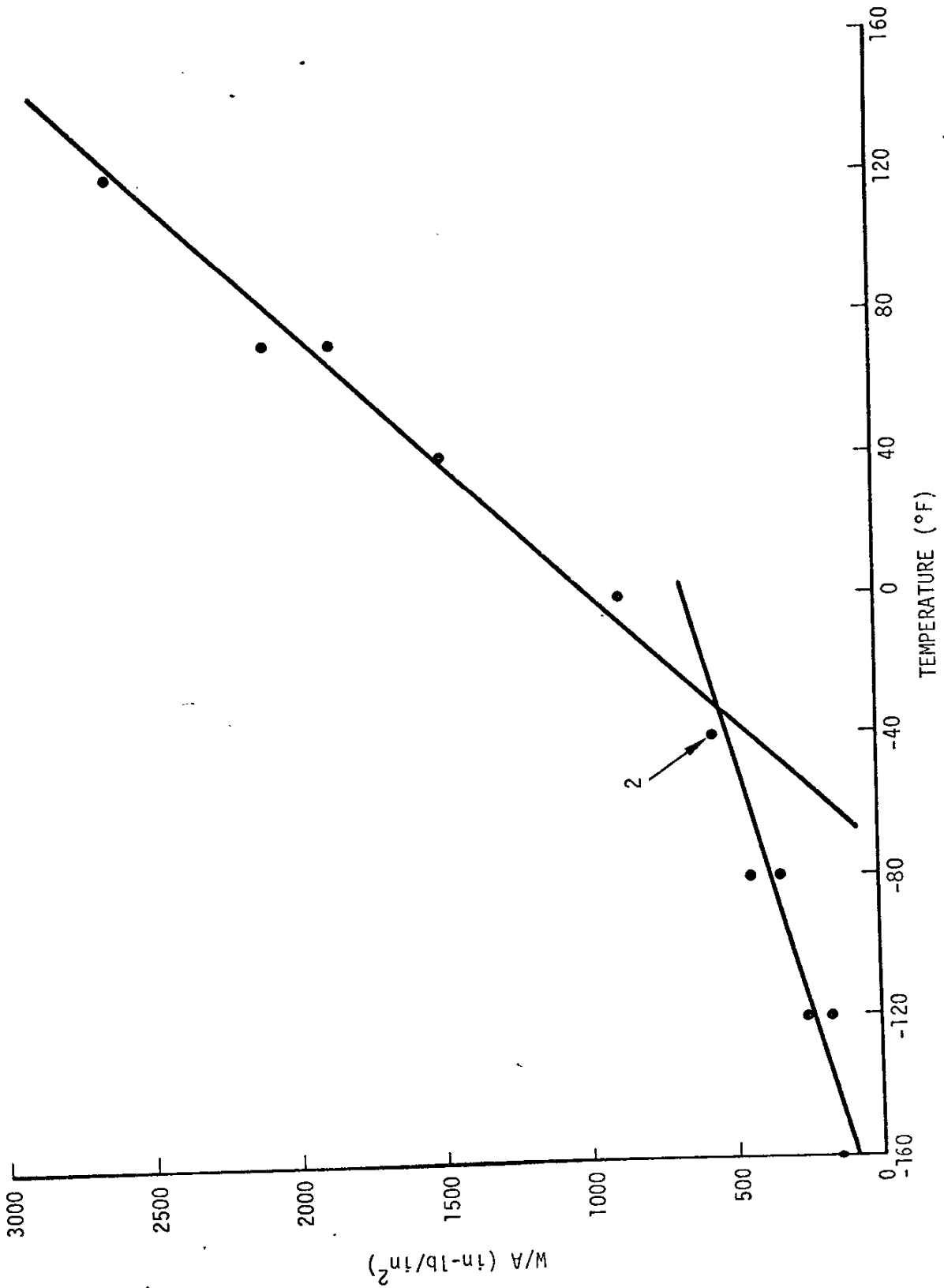


Figure D-6 W/A as a Function of Temperature for Plate No. 6

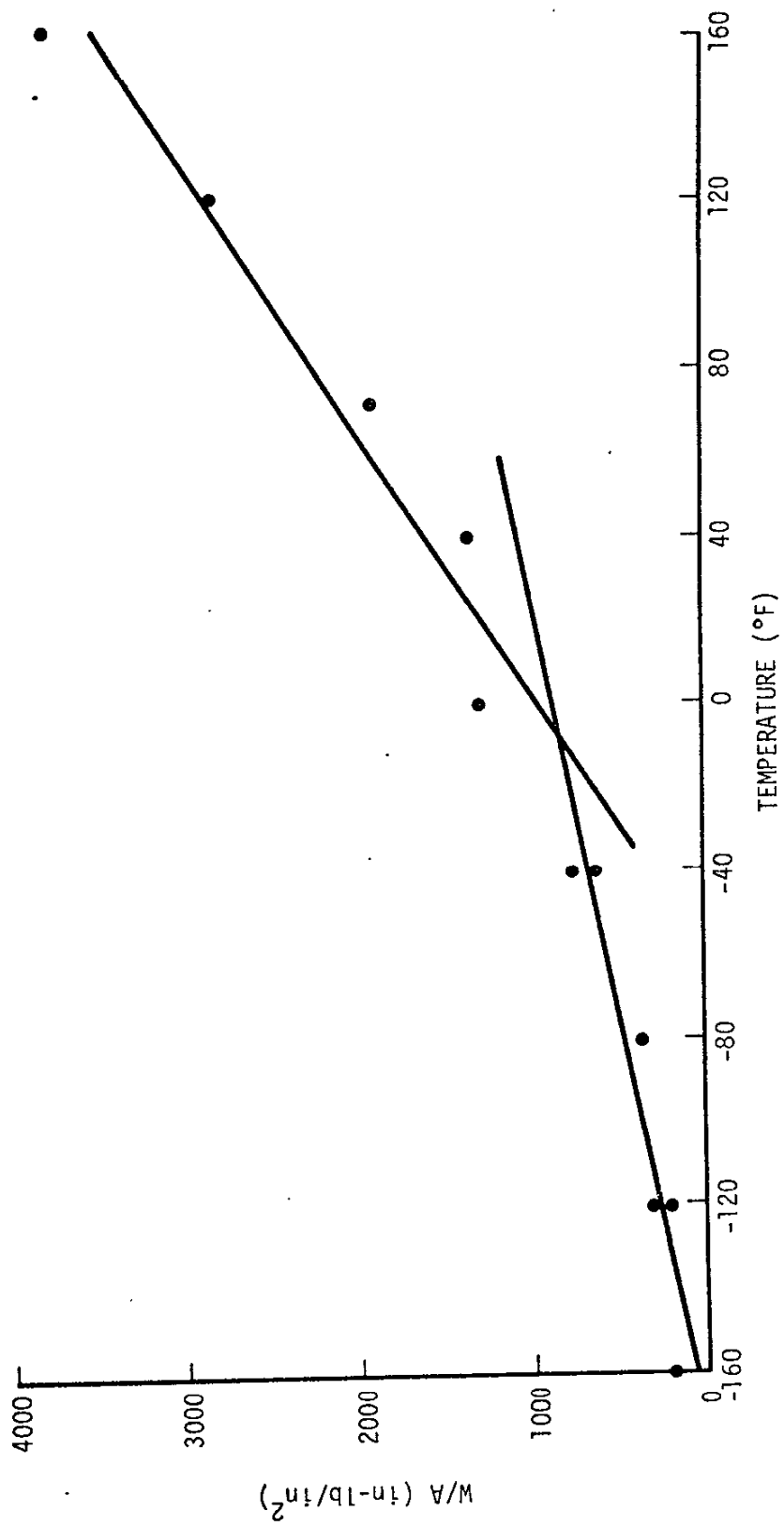


Figure D-7 W/A as a Function of Temperature for Plate Z

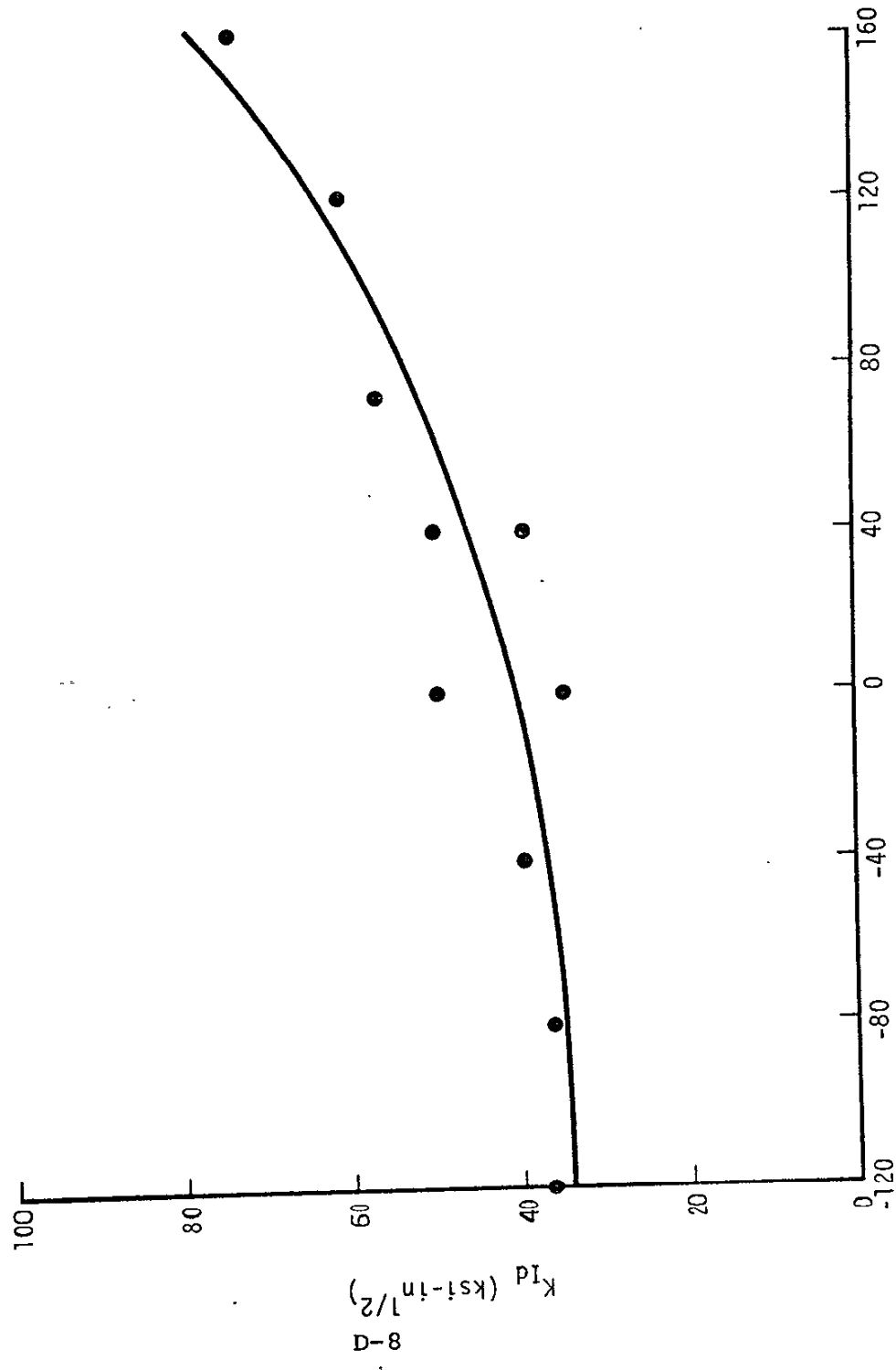


Figure D-8 K_{ID} as a Function of Temperature for Plate A

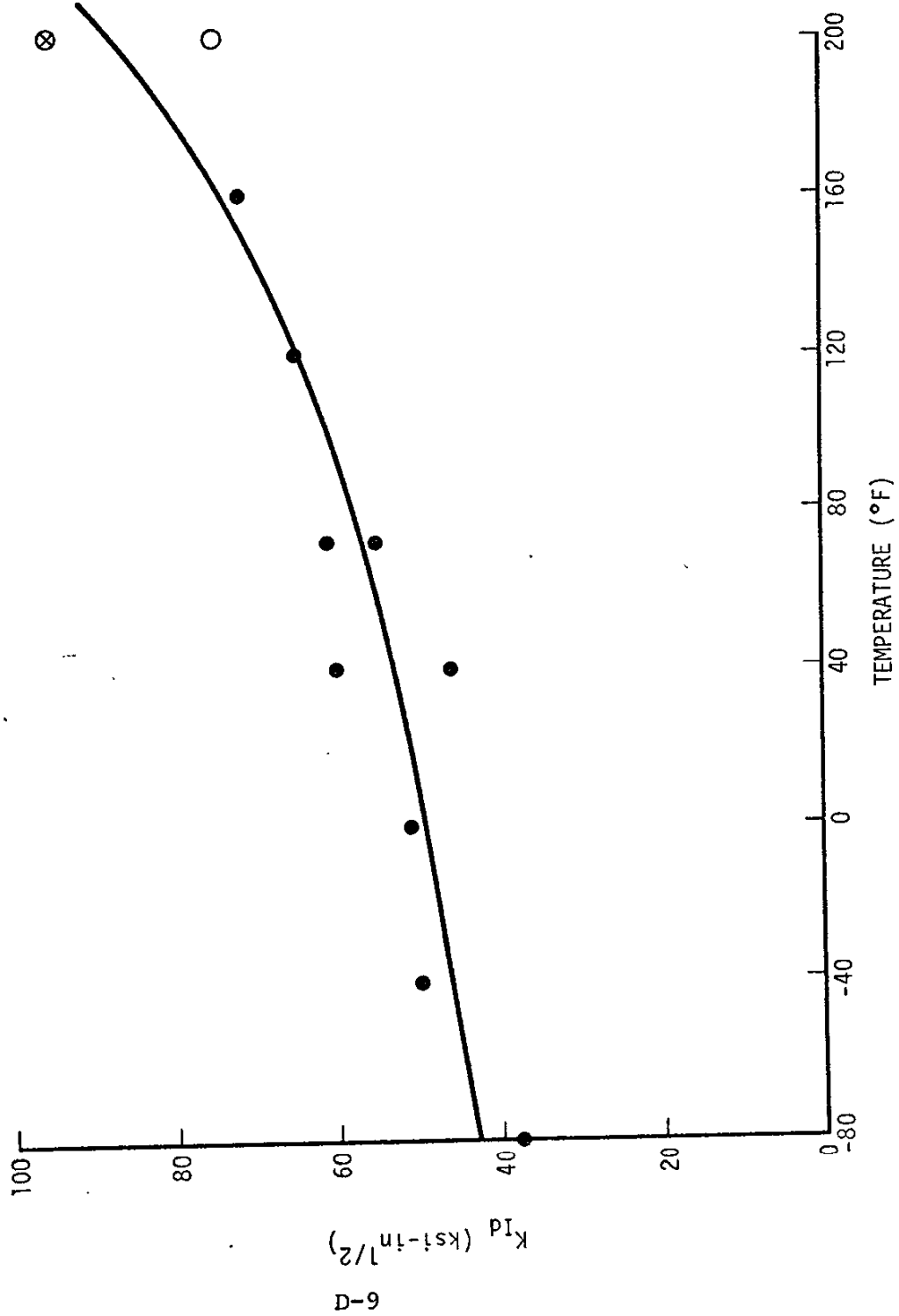


Figure D-9 K_{ID} as a Function of Temperature for Plate AL

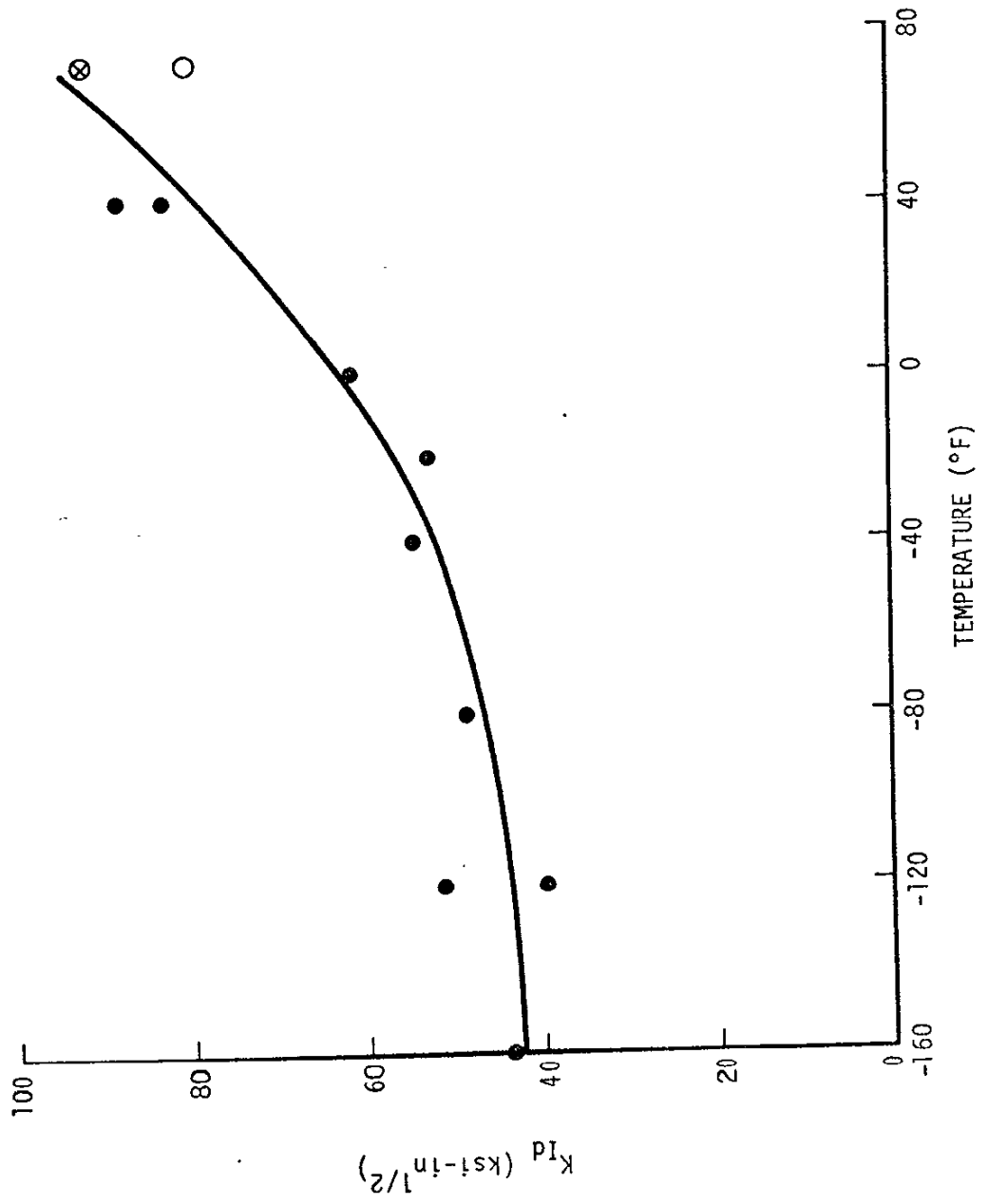


Figure D-10 K_{Id} as a Function of Temperature for Plate L

D-10

D-11

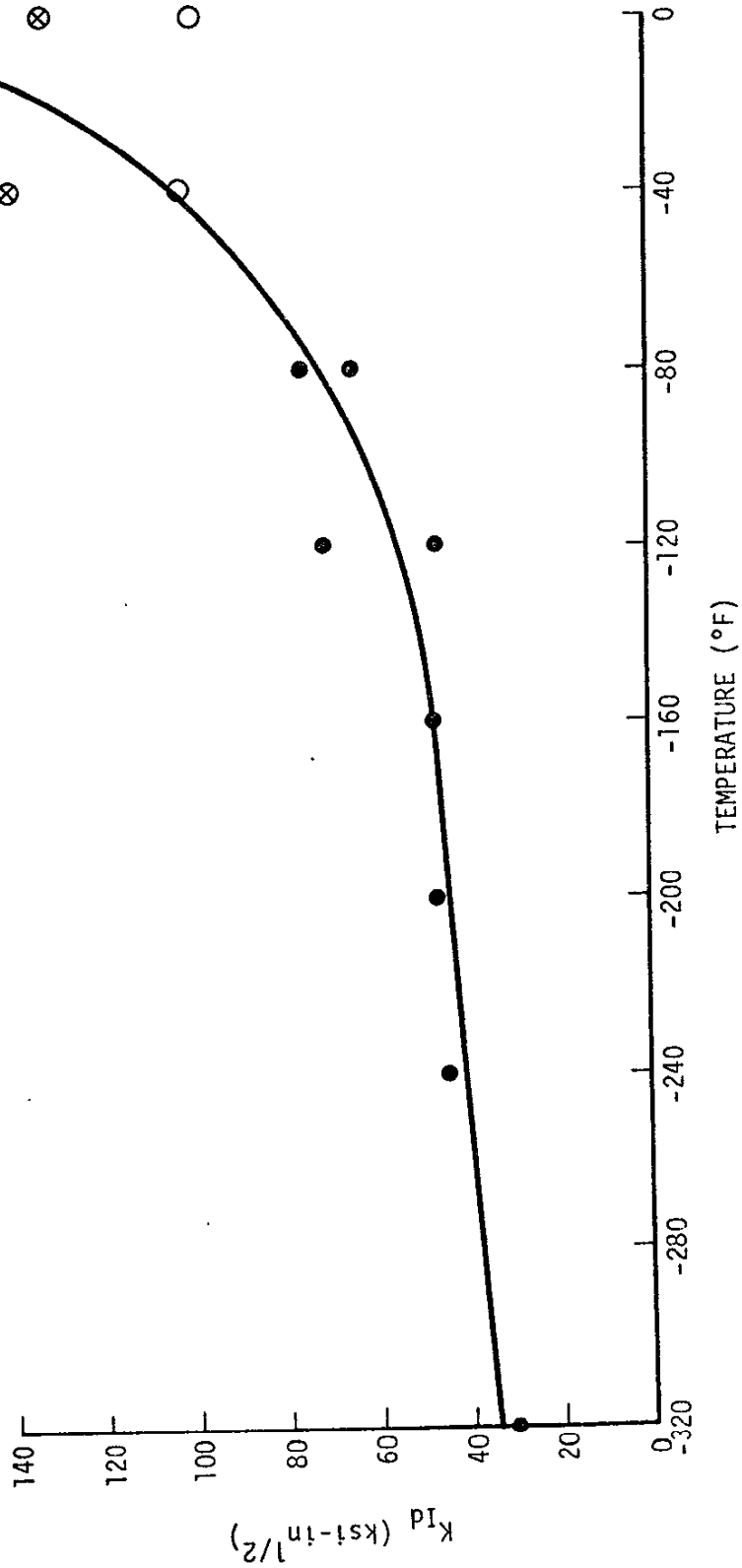


Figure D-11 K_{ID} as a Function of Temperature for Plate M

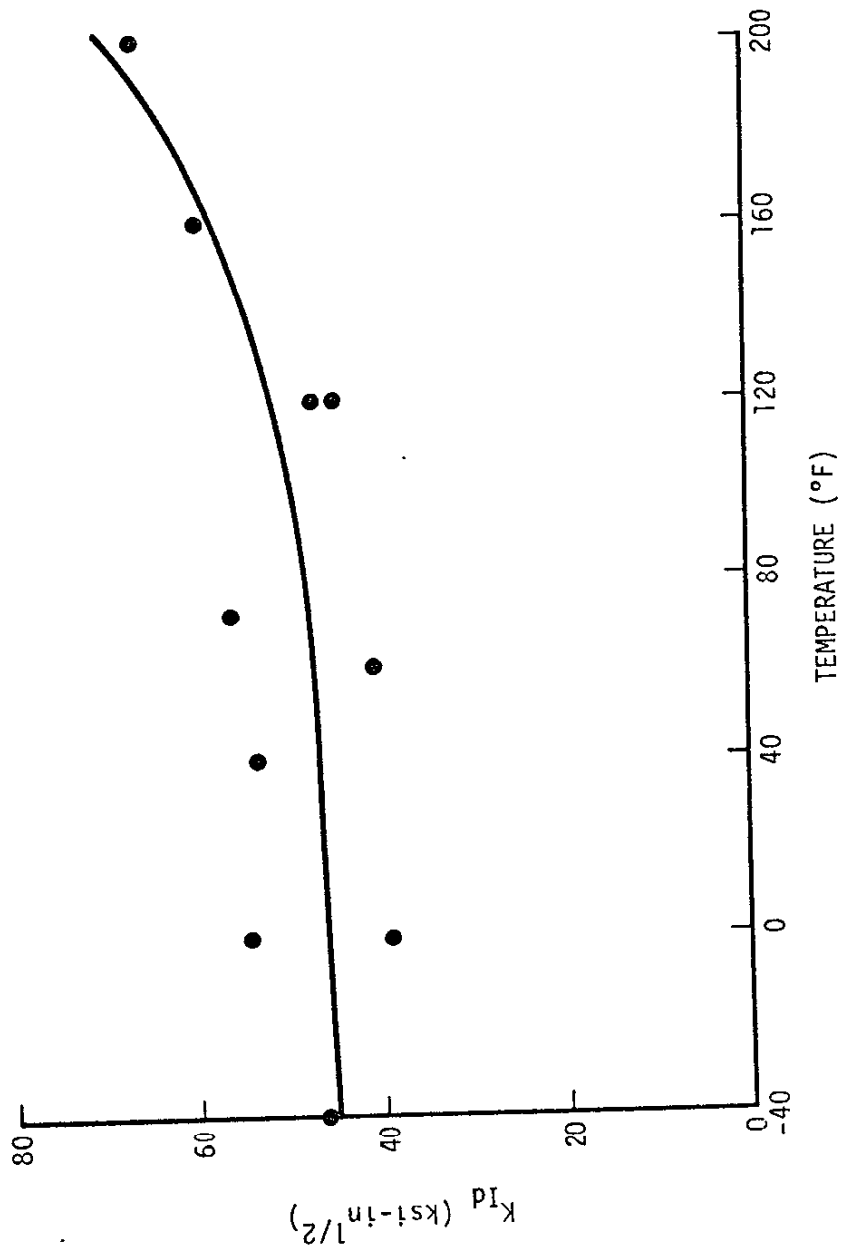


Figure D-12 K_{ID} as a Function of Temperature for Plate CK

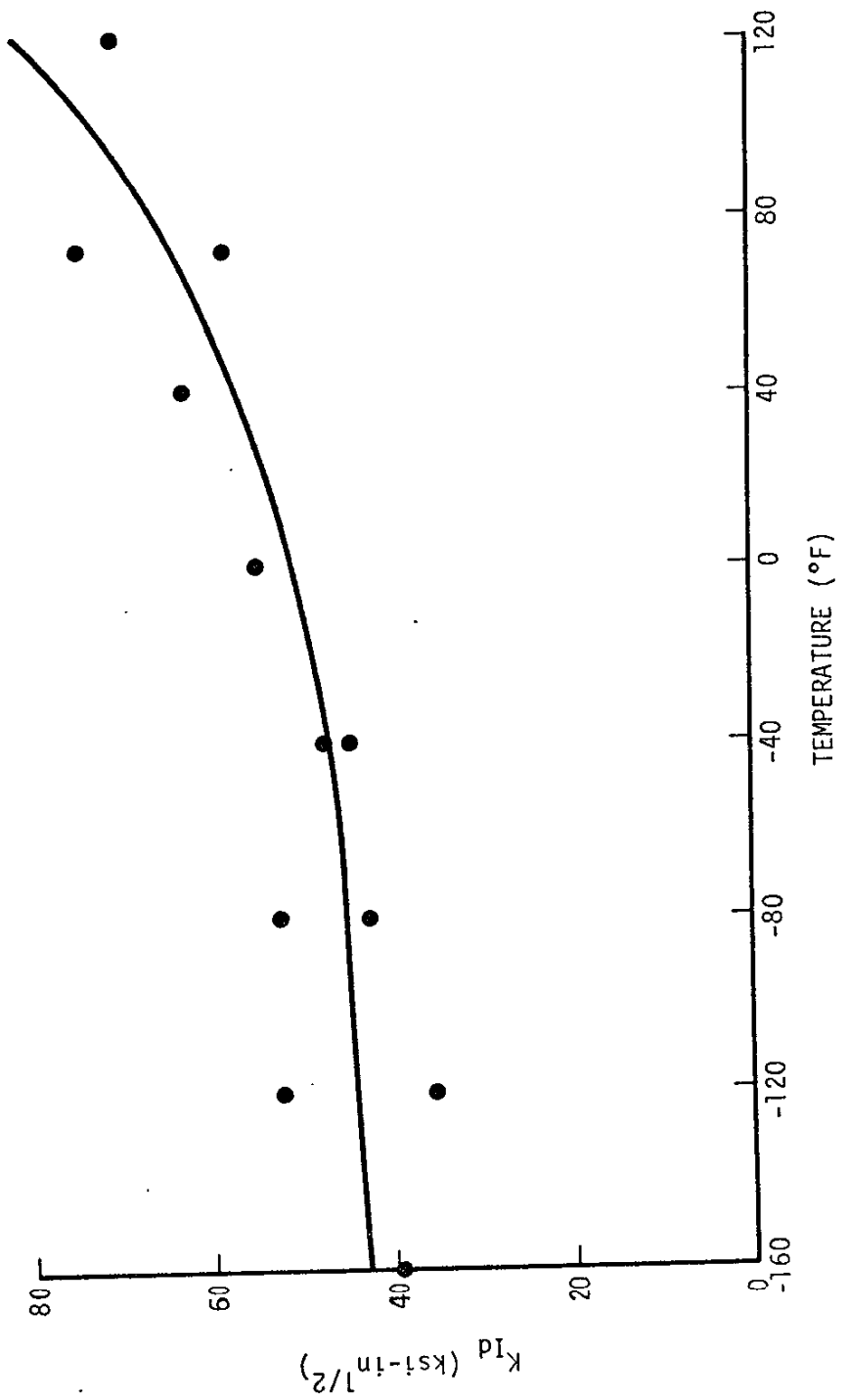


Figure D-13 K_{Id} as a Function of Temperature for Plate R

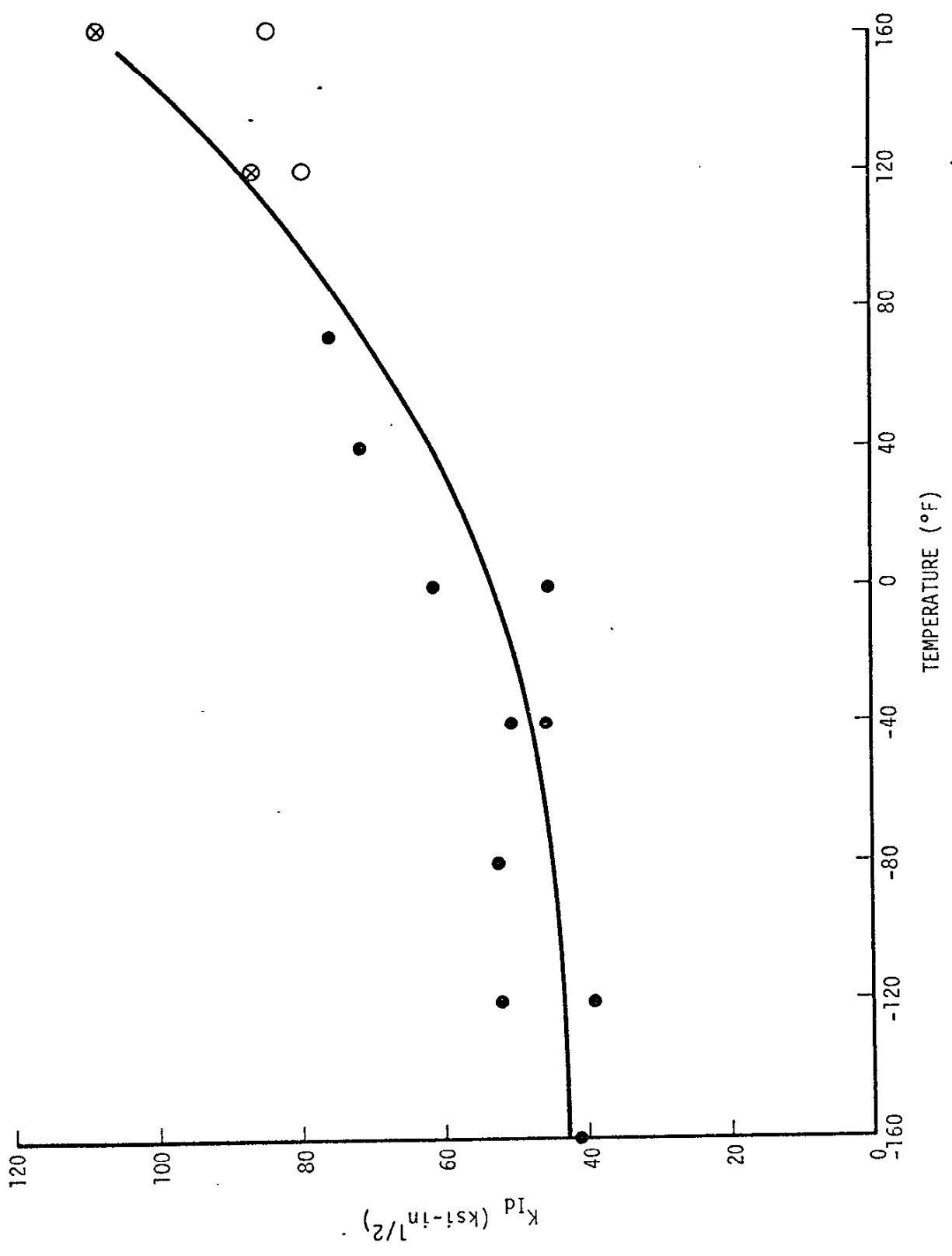


Figure D-14 K_{ID} as a Function of Temperature for Plate 7

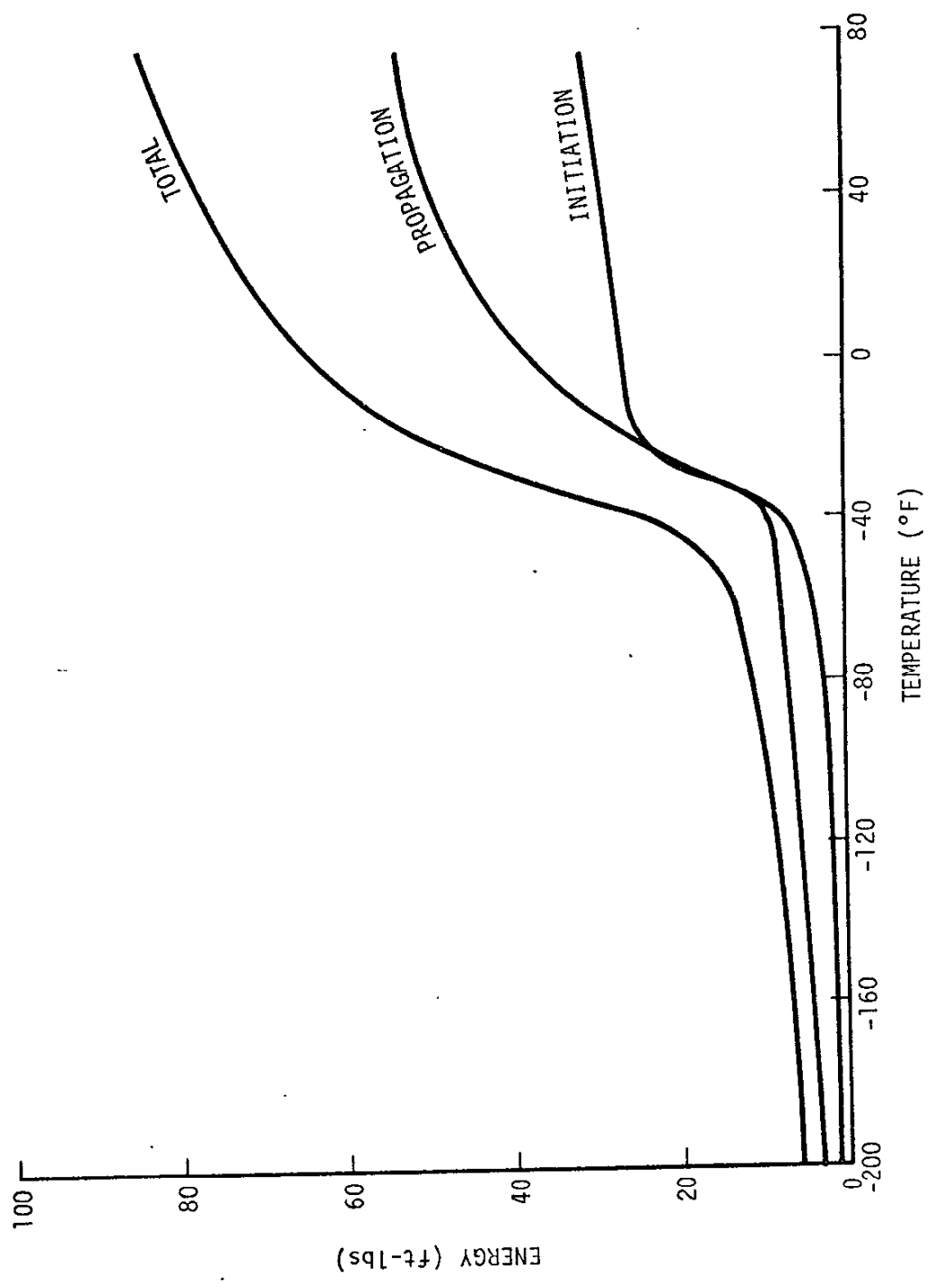


Figure D-15 Components of Charpy V-Notch Energy for Plate L

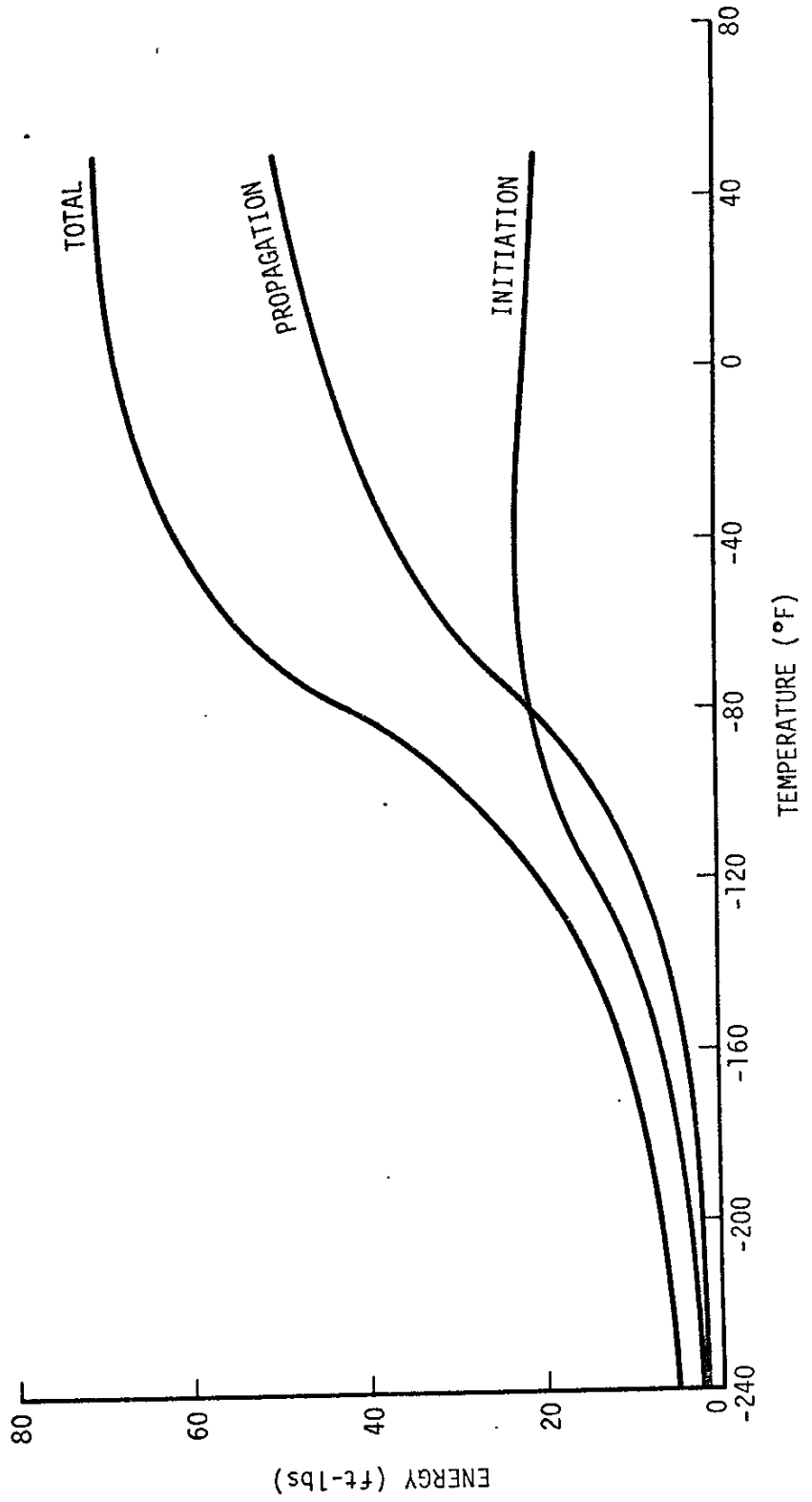


Figure D-16 Components of Charpy V-Notch Energy for Plate M

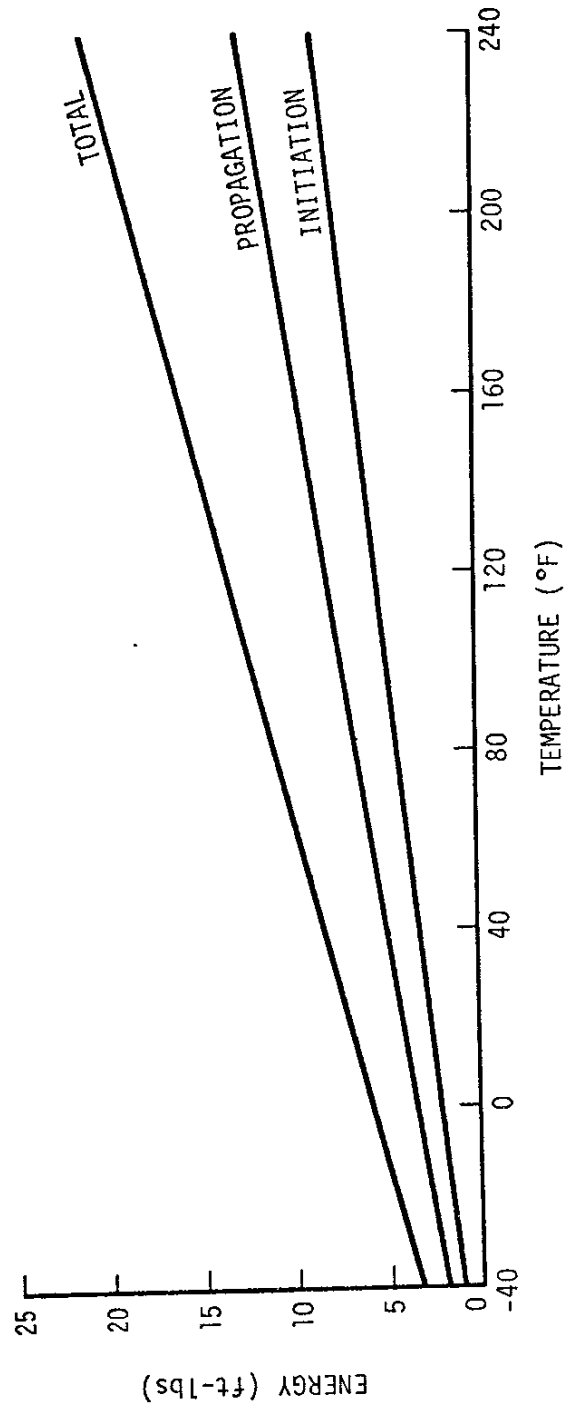


Figure D-17 Components of Charpy V-Notch Energy for Plate CK

Appendix E

National Bureau of Standards Charpy Impact Test
Results on Selected Heats of A514/517 Steel.

Plate CK - Longitudinal CVN Specimens

Fig. E-1a Energy Absorption

Fig. E-1b Energy/Area

Fig. E-1c Lateral Expansion

Plate CK - Transverse CVN Specimens

Fig. E-2a Energy Absorption

Fig. E-2b Energy/Area

Fig. E-2c Lateral Expansion

Plate CK - Longitudinal Precracked Specimens

Fig. E-3a Energy Absorption

Fig. E-3b Energy/Area

Fig. E-3c Lateral Expansion

Plates CK & Q - Longitudinal Precracked Specimens

Fig. E-4a Energy Absorption

Fig. E-4b Energy/Area

Fig. E-4c Lateral Expansion

Plates CK & Q - Longitudinal and Transverse
CVN Specimens

Fig. E-5a Energy Absorption

Fig. E-5b Energy/Area

Fig. E-5c Lateral Expansion

Plate CK - Longitudinal Precracked Specimens

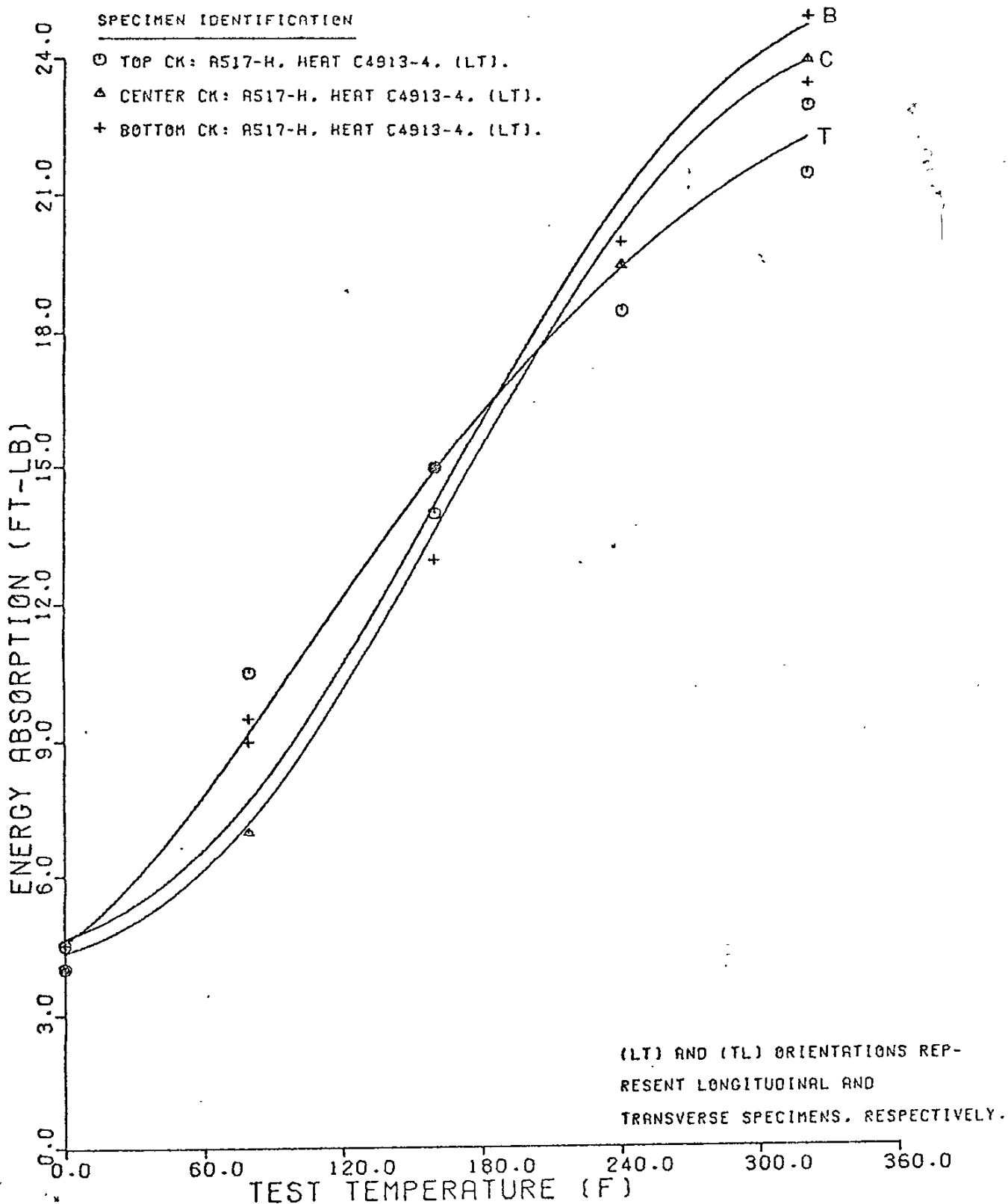
Calculations for:

Fig. E-6a Energy Absorption

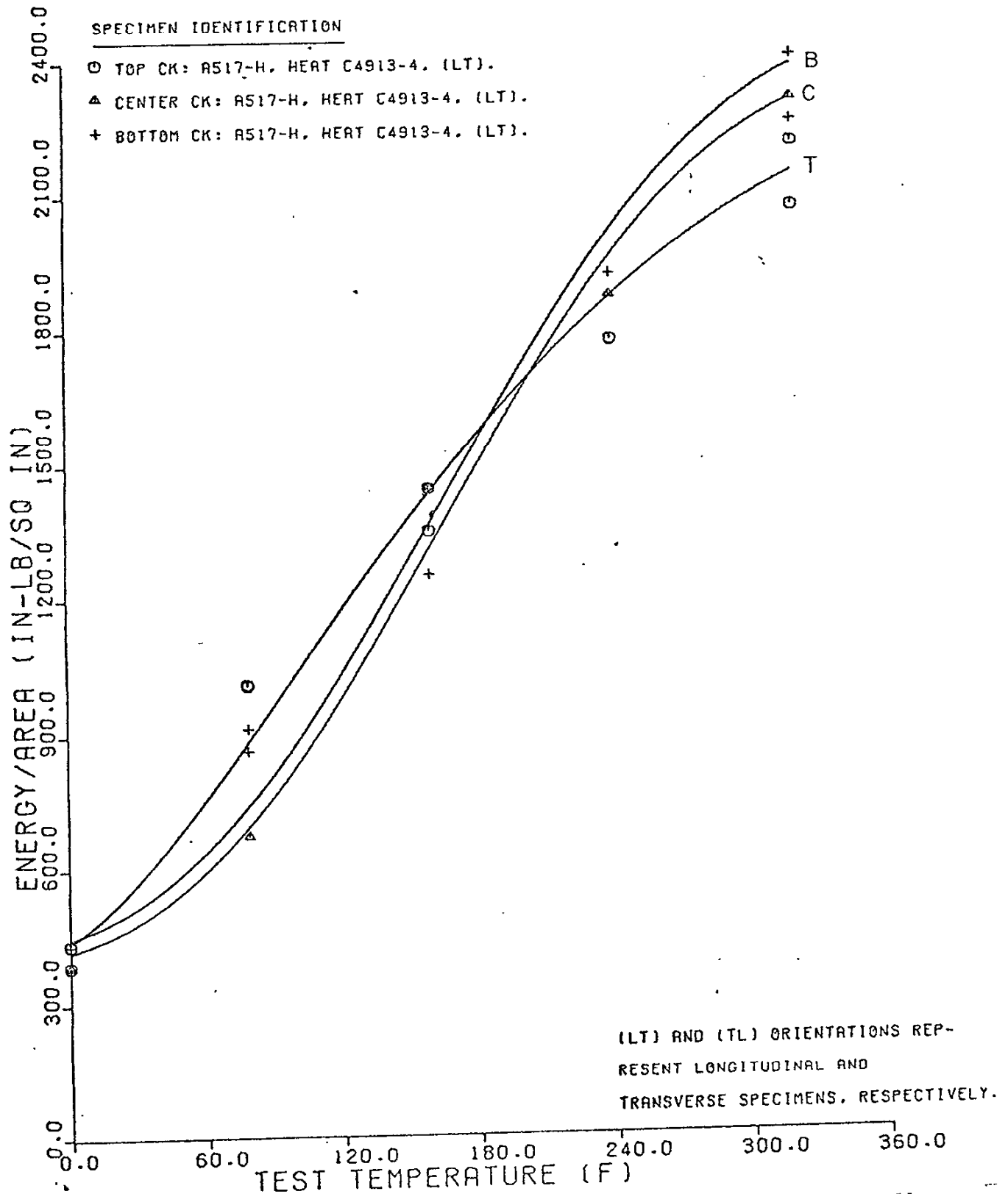
Fig. E-6b Energy/Area

Fig. E-6c Lateral Expansion

RESULTS OF NBS TESTS OF LONGITUDINAL CHARPY V-NOTCH IMPACT SPECIMENS OF PLATE CK. HEAT C4913-4 OF A517-H STEEL.



RESULTS OF NBS TESTS OF LONGITUDINAL CHARPY V-NOTCH IMPACT SPECIMENS OF PLATE CK. HEAT C4913-4 OF A517-H STEEL.



RESULTS OF NBS TESTS OF LONGITUDINAL CHARPY V-NOTCH IMPACT SPECIMENS OF PLATE CK, HEAT C4913-4 OF A517-H STEEL.

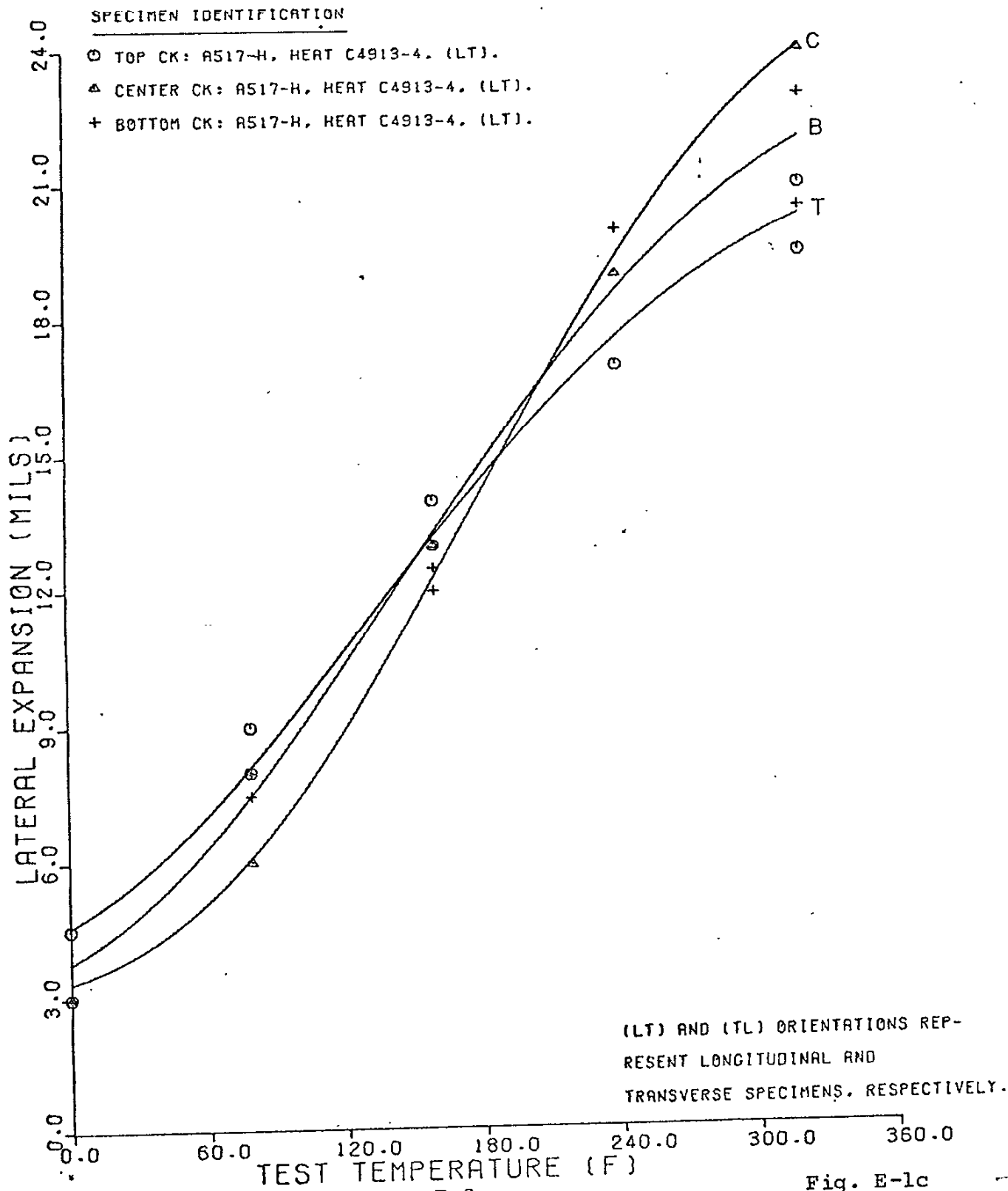
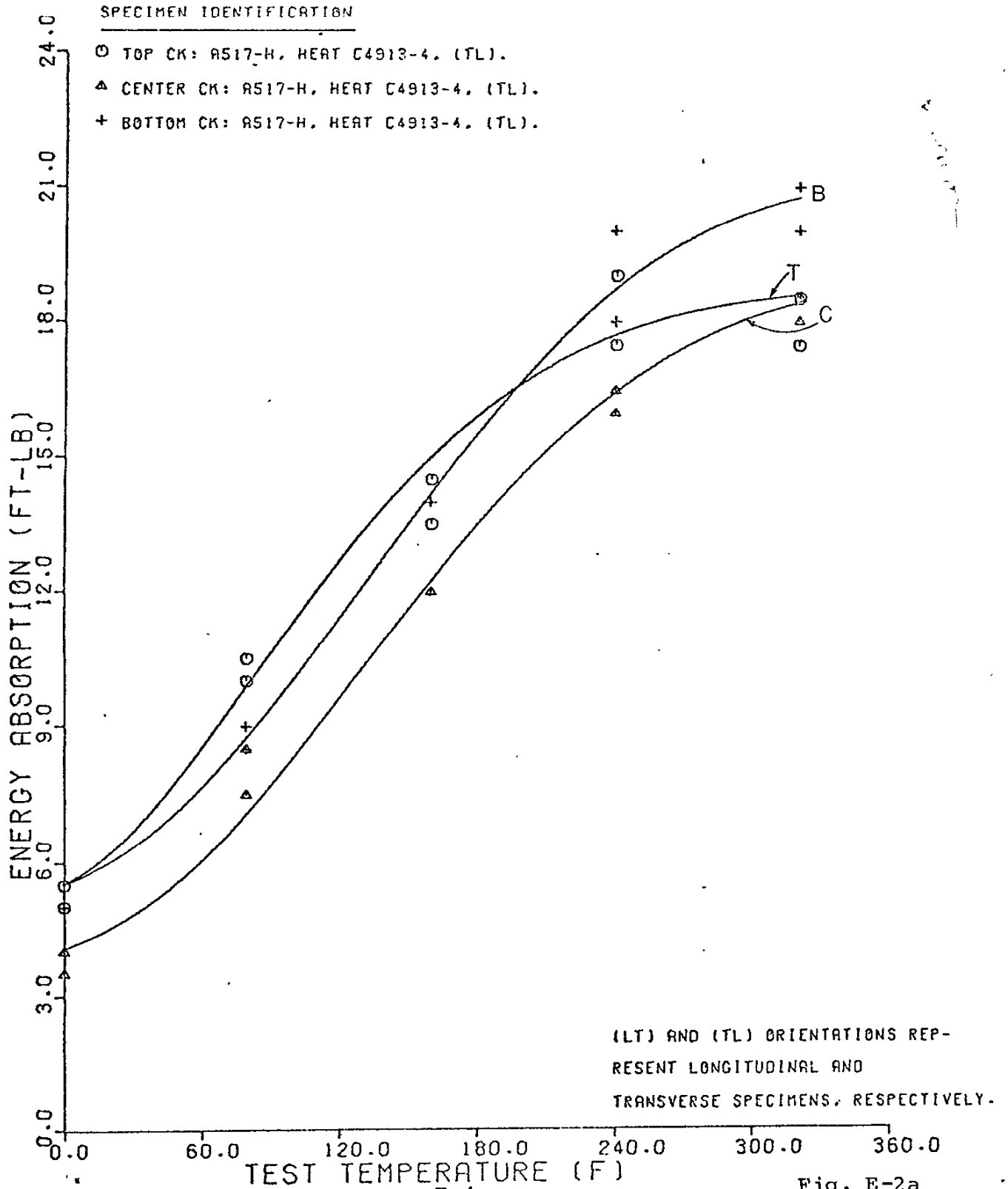


Fig. E-1c

RESULTS OF NBS TESTS OF TRANSVERSE CHARPY V-NOTCH IMPACT SPECIMENS OF PLATE CK. HEAT C4913-4 OF A517-H STEEL.



RESULTS OF NBS TESTS OF TRANSVERSE CHARPY V-NOTCH IMPACT SPECIMENS OF PLATE CK. HEAT C4913-4 OF A517-H STEEL.

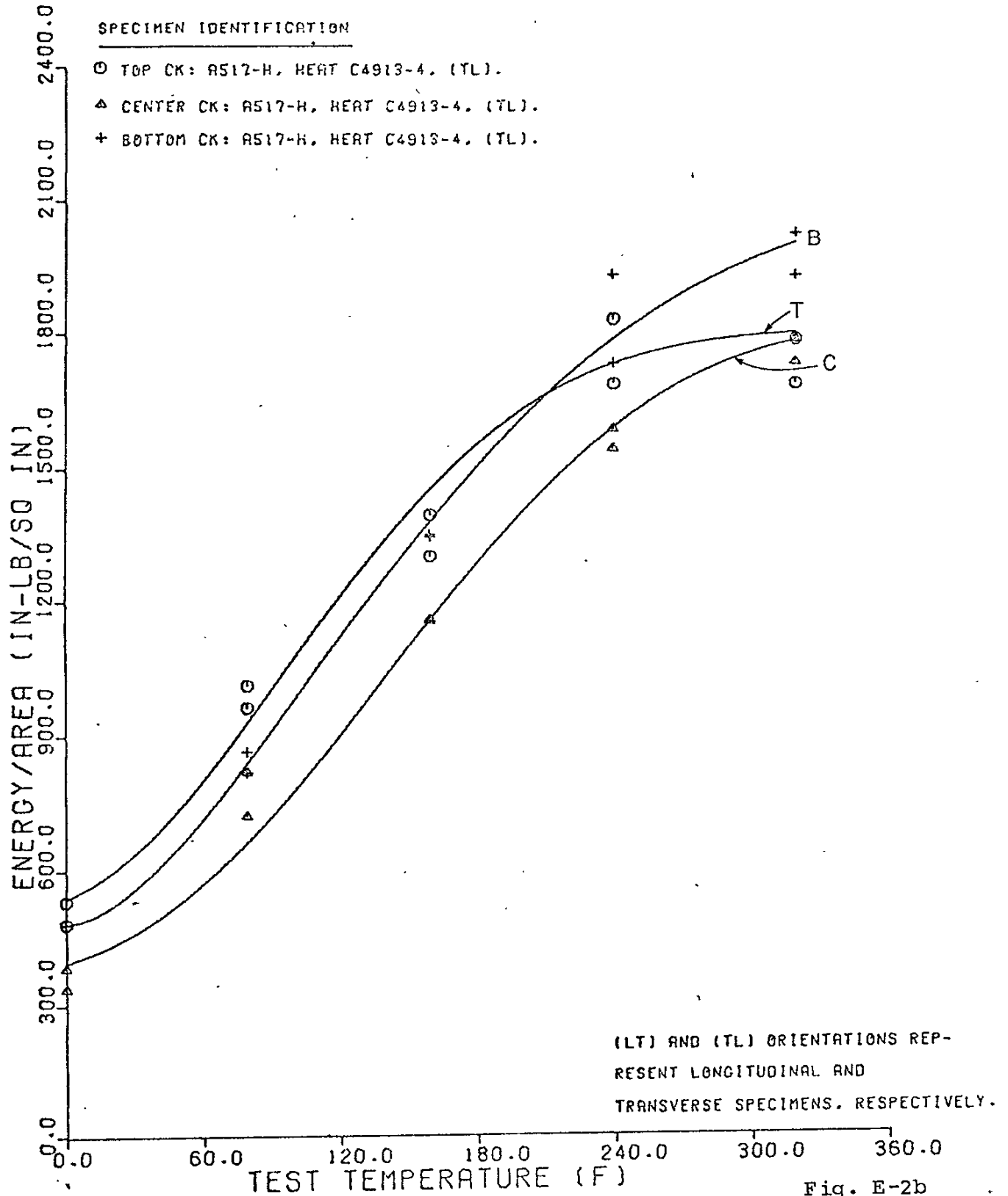
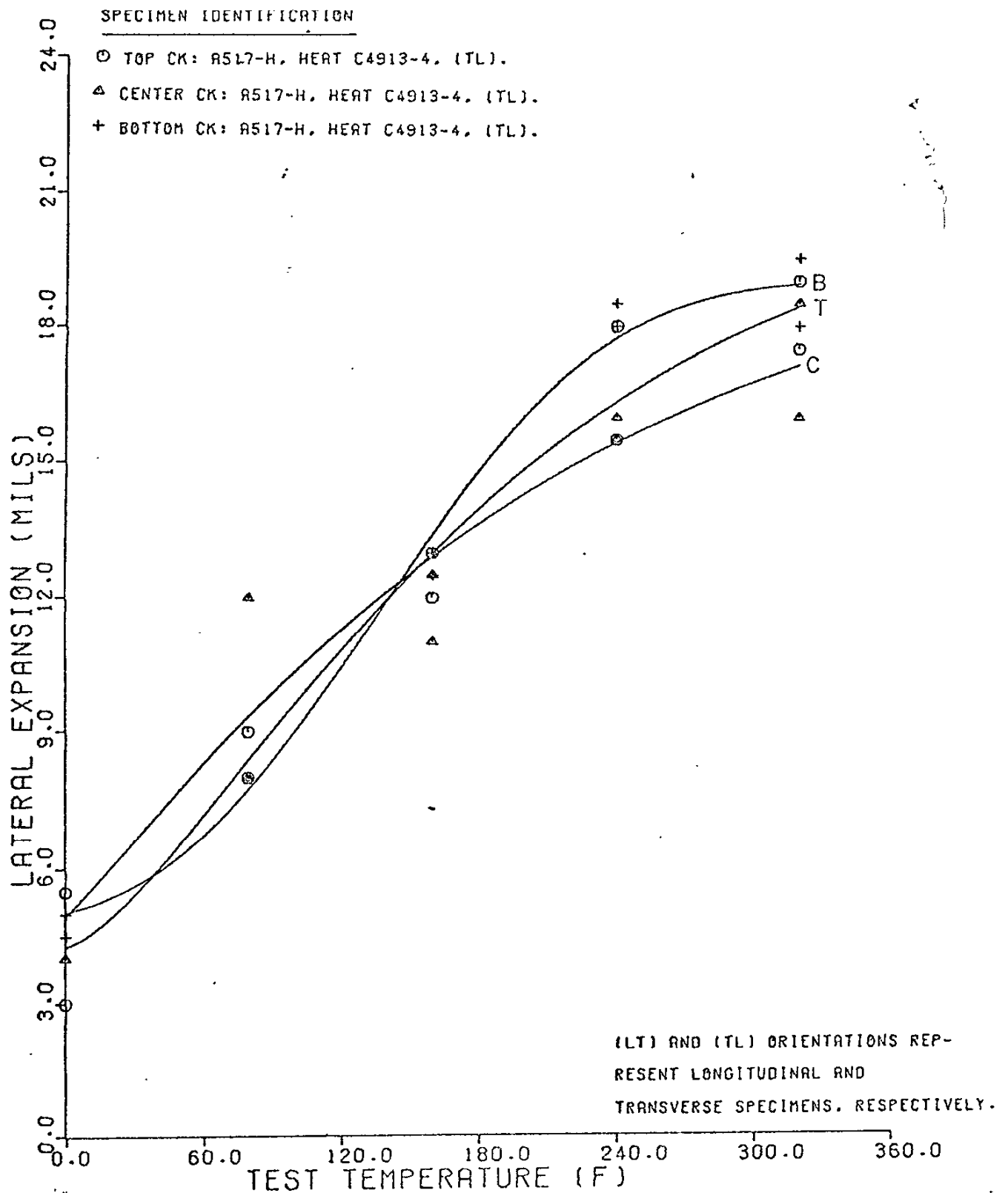
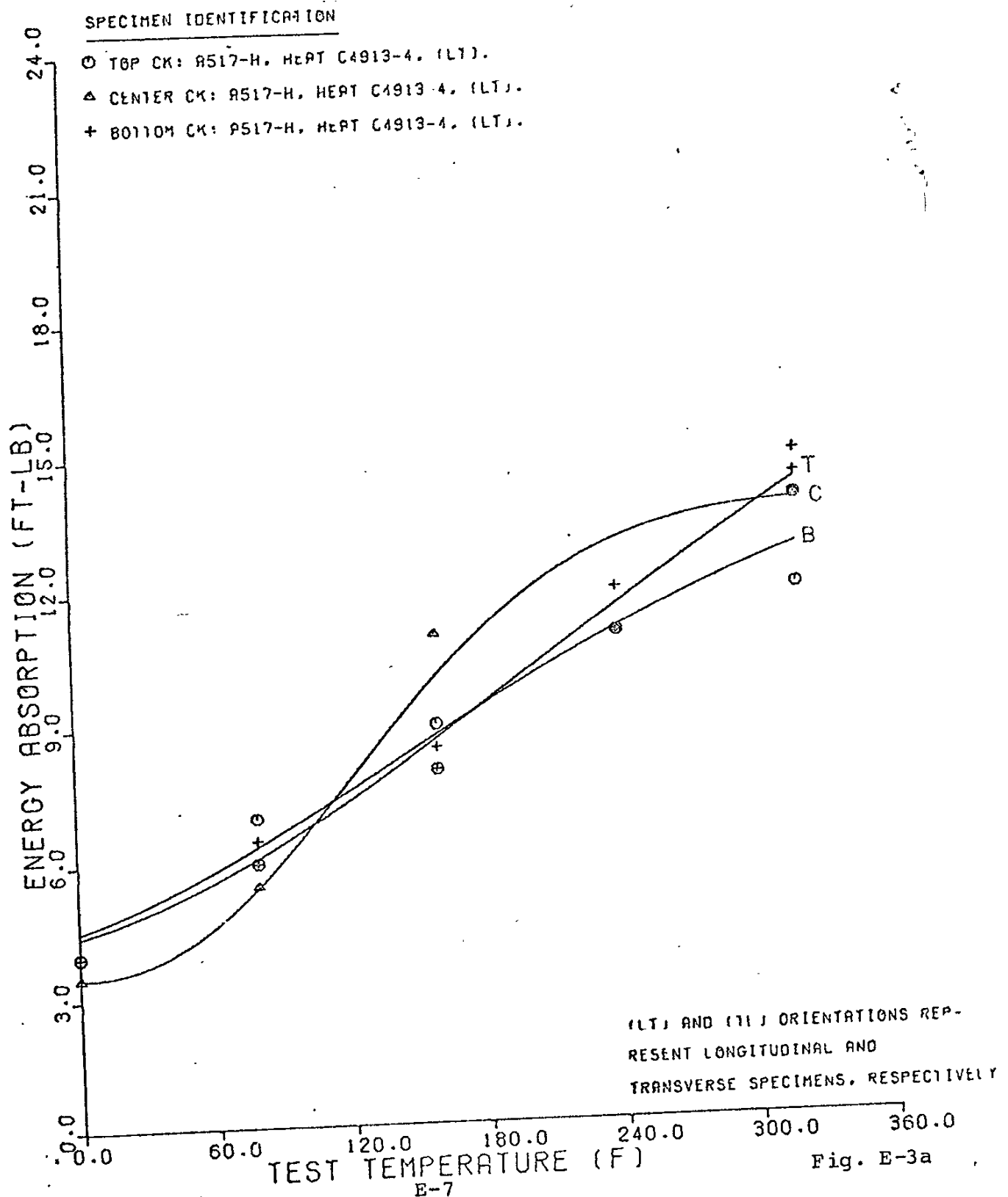


Fig. E-2b

RESULTS OF NBS TESTS OF TRANSVERSE CHARPY V-NOTCH IMPACT SPECIMENS OF PLATE CK, HEAT C4913-4 OF A517-H STEEL.



RESULTS OF NBS TESTS OF LONGITUDINAL PRECRACKED CHARPY IMPACT SPECIMENS OF PLATE CK. HEAT C4913-4 OF A517-H STEEL.



RESULTS OF NBS TESTS OF LONGITUDINAL PRECRACKED CHARPY IMPACT SPECIMENS OF PLATE CK, HEAT C4913-4 OF A517-H STEEL.

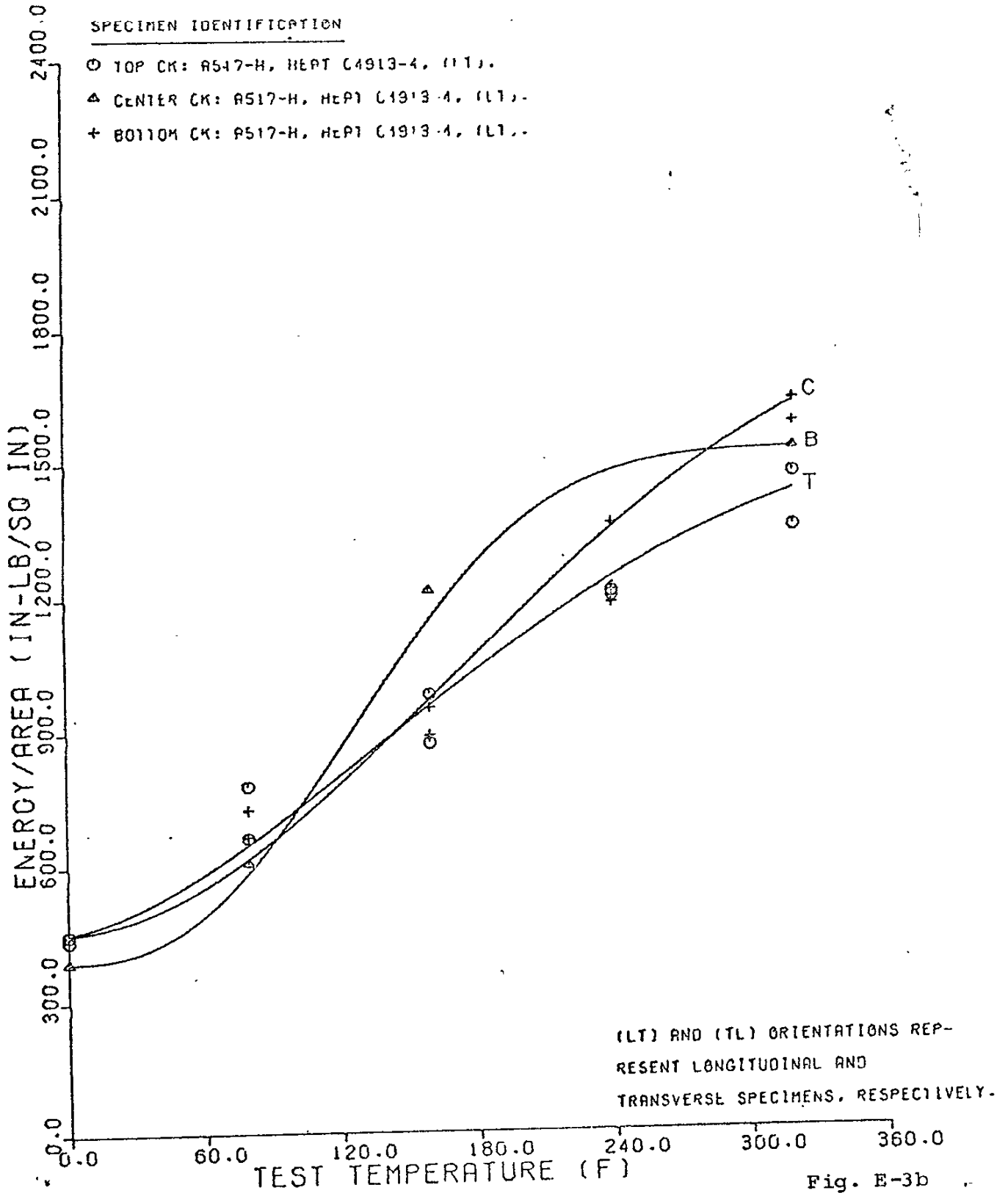
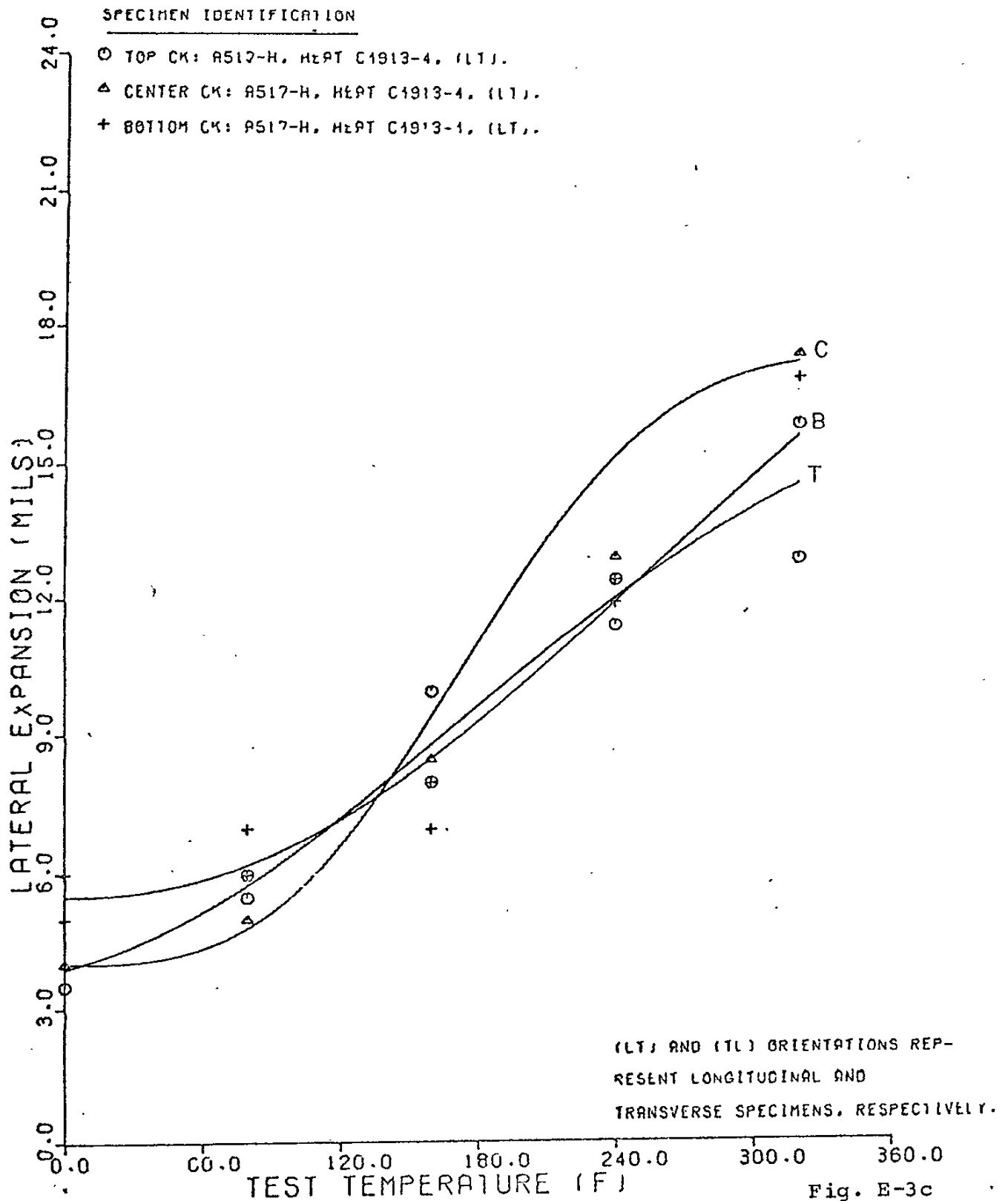
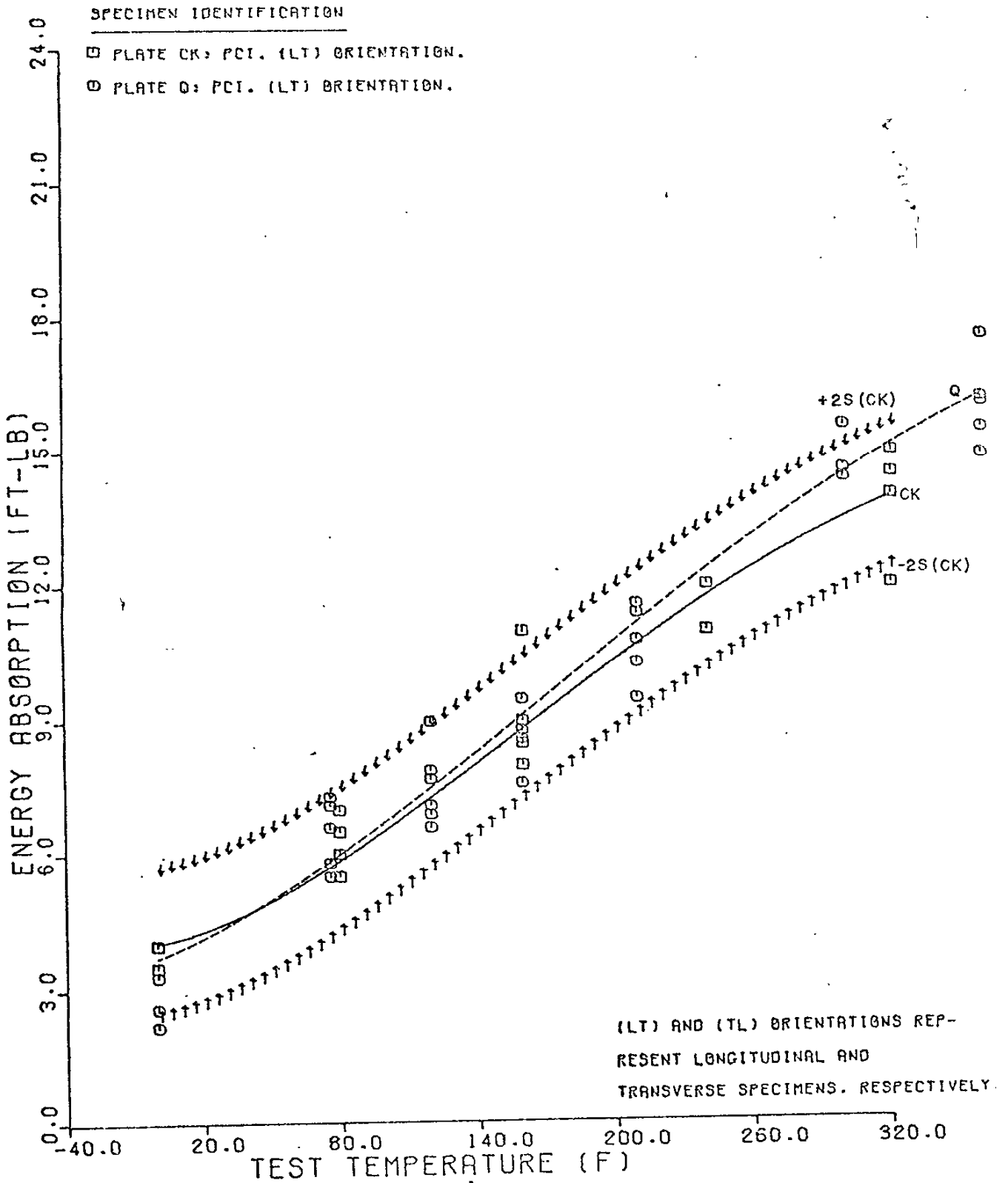


Fig. E-3b

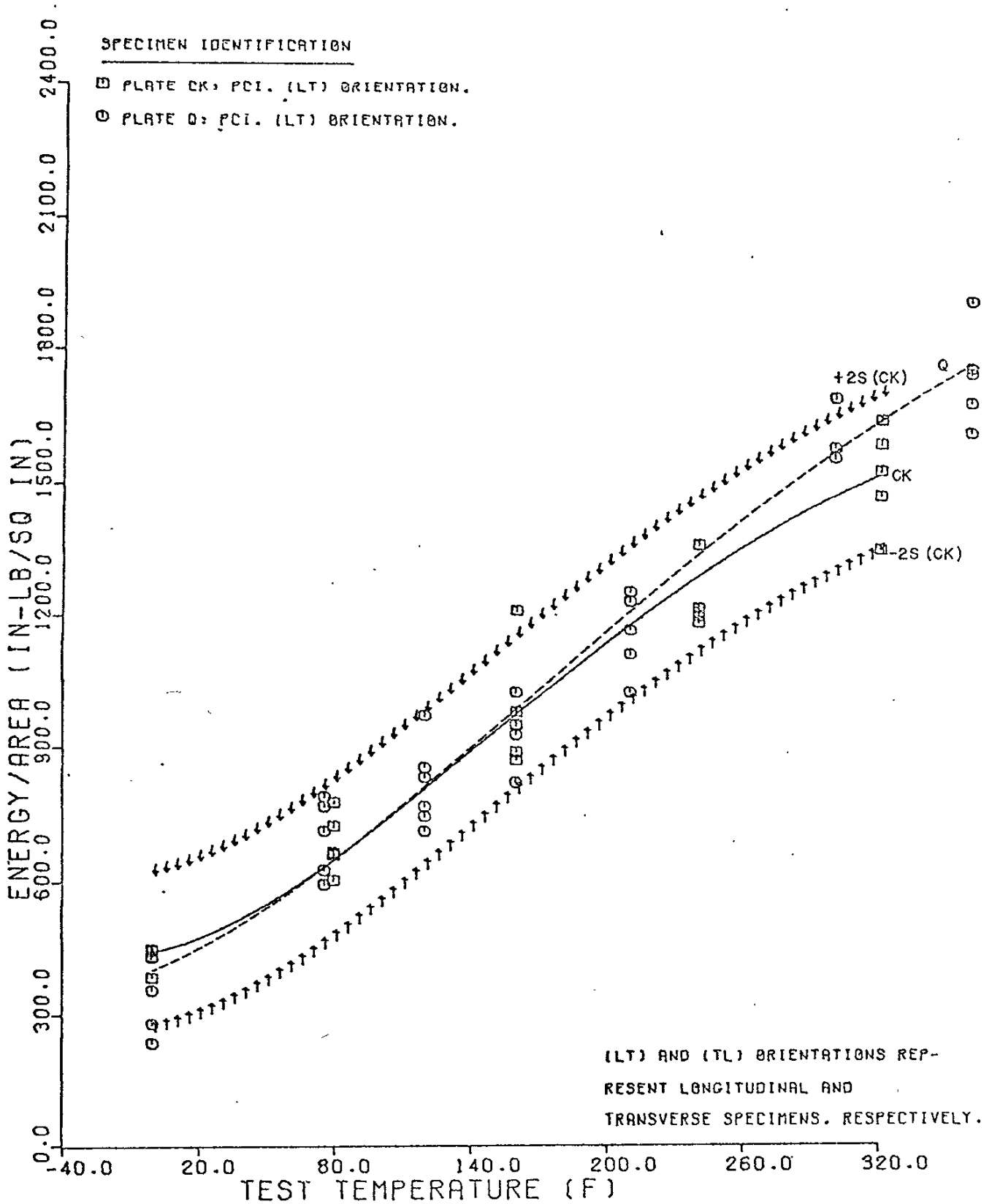
RESULTS OF NBS TESTS OF LONGITUDINAL PRECRACKED CHARPY IMPACT SPECIMENS OF PLATE CK. HEAT C4913 4 OF A517-H STEEL.



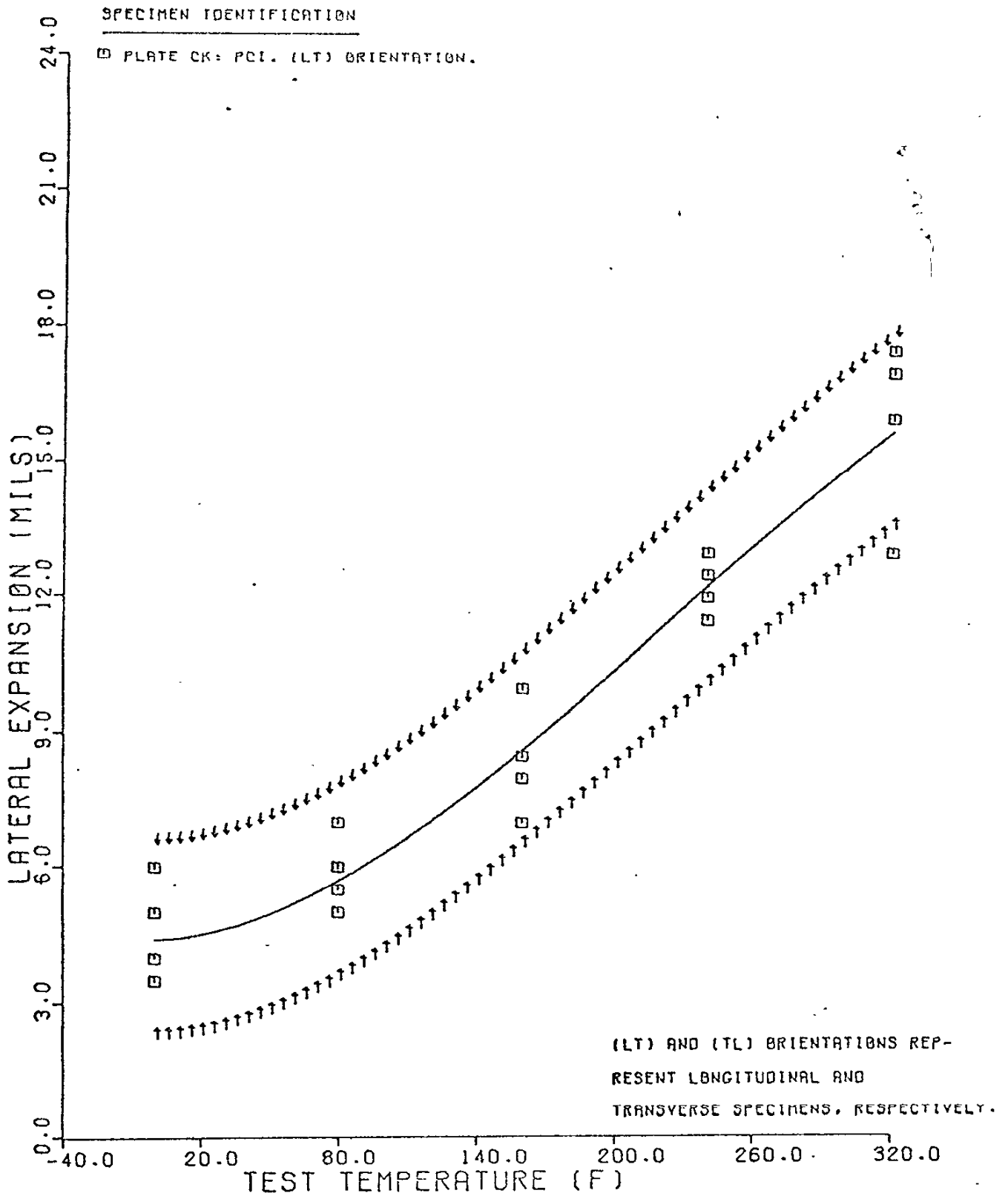
RESULTS OF TESTS OF PCI
SPECIMENS OF PLATES CK AND Q. HEAT C4913-4 OF A517-H STEEL.



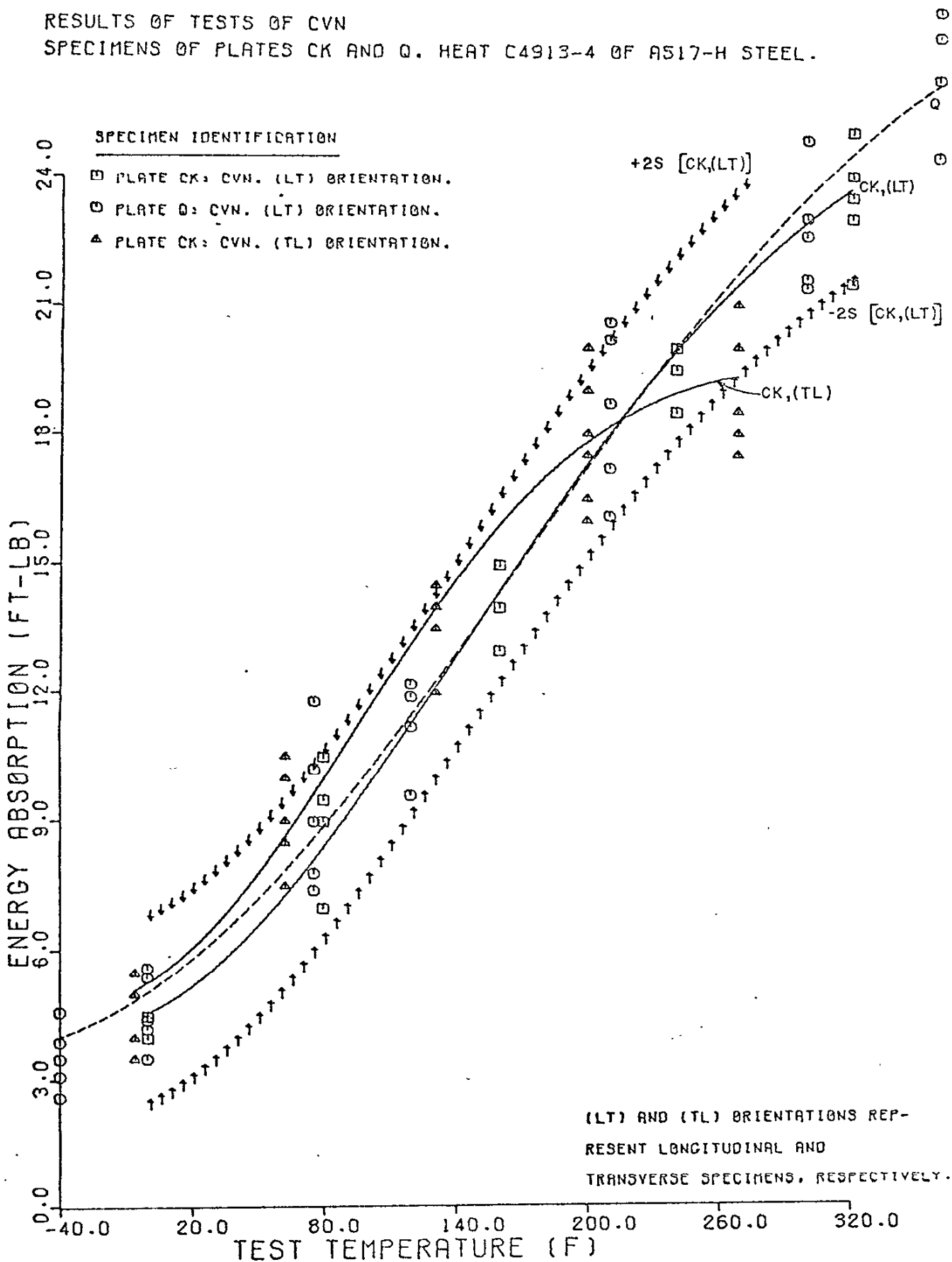
RESULTS OF TESTS OF PCI
SPECIMENS OF PLATES CK AND Q. HEAT C4913-4 OF A517-H STEEL.



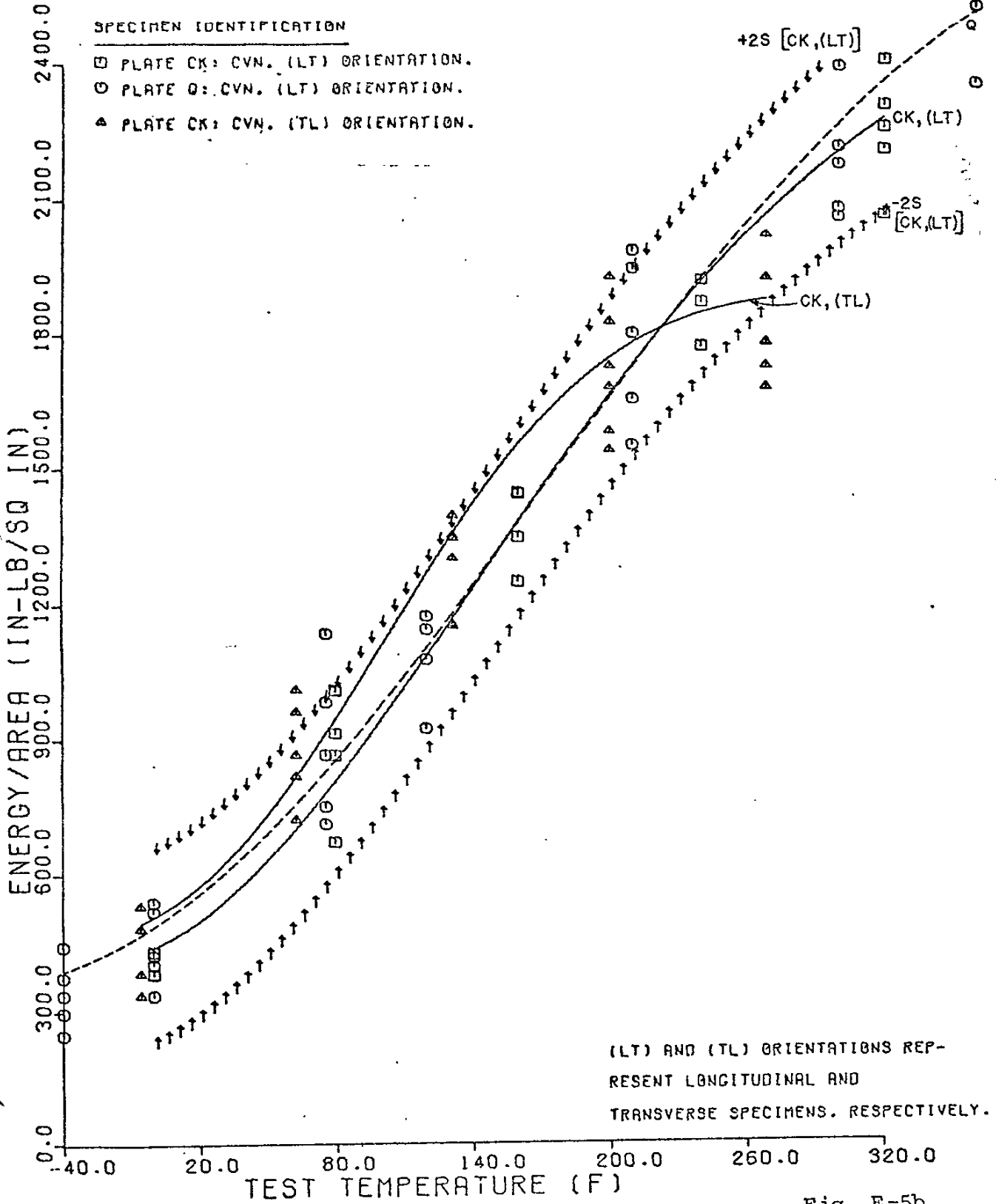
RESULTS OF TESTS OF PCI
SPECIMENS OF PLATES CK AND Q. HEAT C4913-4 OF A517-H STEEL.



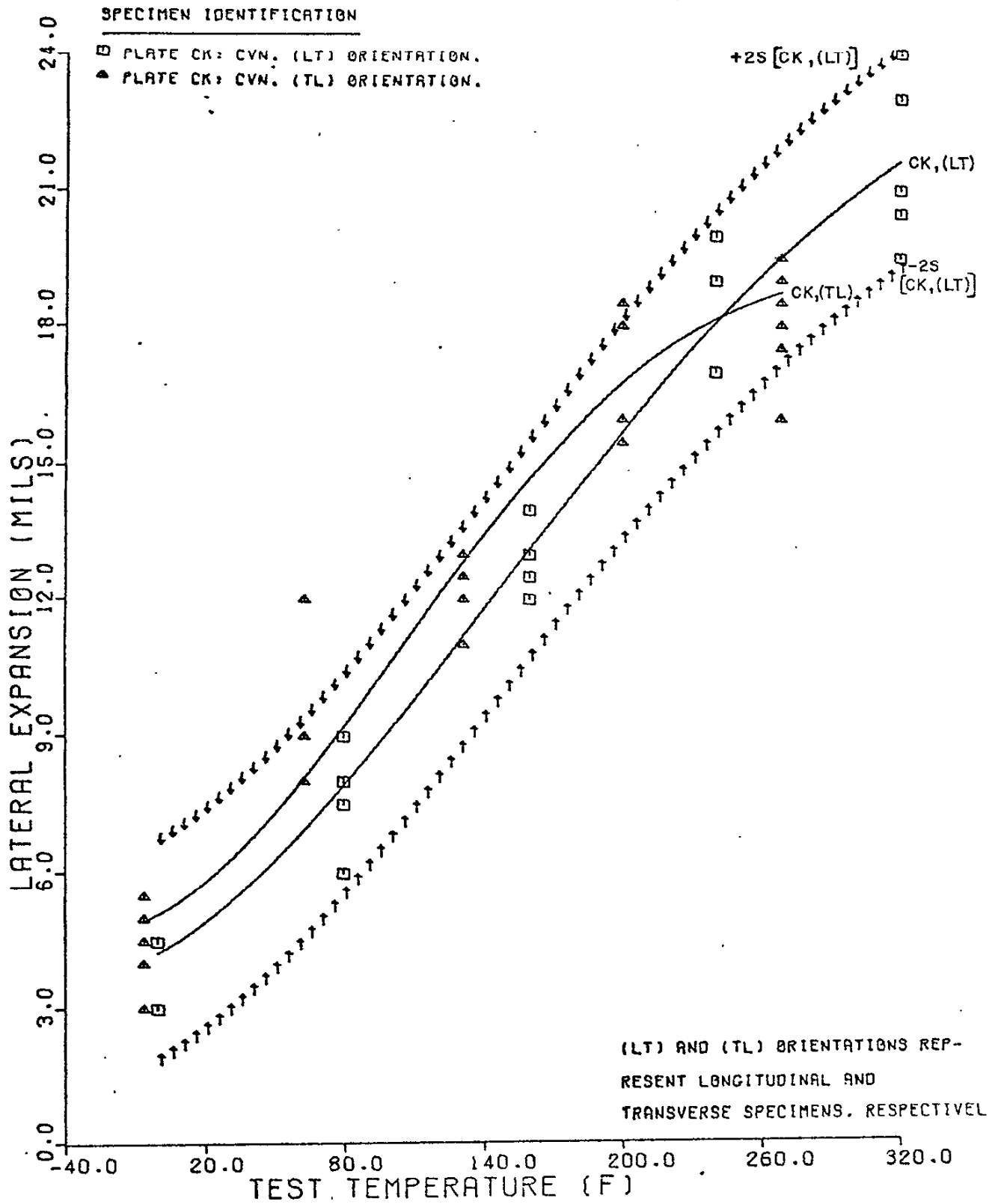
RESULTS OF TESTS OF CVN
 SPECIMENS OF PLATES CK AND Q. HEAT C4913-4 OF A517-H STEEL.



RESULTS OF TESTS OF CVN
SPECIMENS OF PLATES CK AND Q. HEAT C4913-4 OF A517-H STEEL.



RESULTS OF TESTS OF CVN
SPECIMENS OF PLATES CK AND Q. HEAT C4913-4 OF A517-H STEEL.



RESULTS OF NBS TESTS OF LONGITUDINAL PRECRACKED CHARPY IMPACT
 SPECIMENS OF PLATE CK, HEAT C4913-4 OF A517-H STEEL.
 CALCULATIONS FOR ENERGY ABSORPTION DATA OF
 TOP CK: A517-H, HEAT C4913-4, (LT).
 (LT) AND (TL) ORIENTATIONS REPRESENT LONGITUDINAL AND
 TRANSVERSE SPECIMENS, RESPECTIVELY.

SPECIMEN	TEMPERATURE (F)	OBSERVED ENERGY ABSORPTION (FT-LB)	CALCULATED ENERGY ABSORPTION (FT-LB)
17CK6T	.0	4.00	4.5
18CK6T	.0	4.00	4.5
17CK7T	80.0	7.00	6.4
18CK7T	80.0	6.00	6.4
17CK8T	160.0	8.00	8.8
18CK8T	160.0	9.00	8.8
17CK9T	240.0	11.00	11.1
18CK9T	240.0	11.00	11.1
17CK10T	320.0	14.00	12.9
18CK10T	320.0	12.00	12.9

TRANSITION REGION, CALCULATED VALUES

ENERGY ABSORPTION	CALCULATED TEMPERATURE (F)	TEMPERATURE (F)	CALCULATED ENERGY ABSORPTION (FT-LB)
5.0	25.2	30.0	5.1
10.0	200.9	35.0	5.2
		40.0	5.3
		45.0	5.4
		50.0	5.6
		55.0	5.7
		60.0	5.8
		65.0	5.9
		70.0	6.1
		75.0	6.2
		80.0	6.4
		85.0	6.5
		90.0	6.6
		95.0	6.8
		100.0	6.9
		105.0	7.1
		110.0	7.2
		115.0	7.4
		120.0	7.5
		125.0	7.7

RESULTS OF NBS TESTS OF LONGITUDINAL PRECRACKED CHARPY IMPACT

SPECIMENS OF PLATE CK, HEAT C4913-4 OF A517-H STEEL.

CALCULATIONS FOR ENERGY / AREA DATA OF

TOP CK: A517-H, HEAT C4913-4, (LT).

(LT) AND (TL) ORIENTATIONS REPRESENT

LONGITUDINAL AND

TRANSVERSE SPECIMENS, RESPECTIVELY.

SPECIMEN	TEMPERATURE (F)	OBSERVED ENERGY AREA (IN-LB/SQ IN)	CALCULATED ENERGY /AREA (IN-LB/SQ IN)
17CK6T	.0	450.19	451.7
18CK6T	.0	437.11	451.7
17CK7T	80.0	781.56	650.3
18CK7T	80.0	664.90	650.3
17CK8T	160.0	876.79	962.8
18CK8T	160.0	987.11	962.8
17CK9T	240.0	1215.23	1246.3
18CK9T	240.0	1206.16	1246.3
17CK10T	320.0	1479.97	1438.2
18CK10T	320.0	1357.43	1438.2

TRANSITION REGION, CALCULATED VALUES

ENERGY/AREA (IN LB/SQ IN)	CALCULATED TEMPERATURE (F)	/	TEMPERATURE (F)	CALCULATED ENERGY /AREA (IN-LB/SQ IN)
455.0	3.2	/	10.0	463.8
495.0	27.2	/	25.0	490.3
535.0	43.7	/	40.0	525.3
570.0	55.8	/	55.0	567.5
610.0	68.3	/	70.0	615.5
650.0	79.9	/	85.0	668.3
690.0	90.9	/	100.0	724.5
730.0	101.4	/	115.0	783.0
770.0	111.7	/	130.0	842.9
810.0	121.8	/	145.0	903.1
850.0	131.8	/	160.0	962.8
890.0	141.7	/	175.0	1021.2
930.0	151.7	/	190.0	1077.7
970.0	161.8	/	205.0	1131.8
1010.0	172.1	/	220.0	1183.0
1050.0	182.6	/	235.0	1231.0
1090.0	193.4	/	250.0	1275.7
1130.0	204.5	/	265.0	1316.9
1170.0	216.1	/	280.0	1354.6
1210.0	228.3	/	295.0	1388.8
1250.0	241.2	/		
1290.0	255.1	/		
1330.0	270.0	/		
1370.0	286.6	/		
1410.0	305.2	/		

Fig. E-6b

RESULTS OF NBS TESTS OF LONGITUDINAL PRECRACKED CHARPY IMPACT
 SPECIMENS OF PLATE CK, HEAT C4913-4 OF A517-H STEEL.
 CALCULATIONS FOR LATERAL EXPANSION DATA OF
 TOP CK: A517-H, HEAT C4913-4, (LT).
 (LT) AND (TL) ORIENTATIONS REPRESENT LONGITUDINAL AND
 TRANSVERSE SPECIMENS, RESPECTIVELY.

SPECIMEN	TEMPERATURE (F)	OBSERVED LATERAL EXPANSION (MILS)	CALCULATED LATERAL EXPANSION (MILS)
17CK6T	.0	3.50	3.9
18CK6T	.0	3.50	3.9
17CK7T	80.0	5.50	5.8
18CK7T	80.0	6.00	5.8
17CK8T	160.0	8.00	8.8
18CK8T	160.0	10.00	8.8
17CK9T	240.0	11.50	12.1
18CK9T	240.0	12.50	12.1
17CK10T	320.0	16.00	14.7
18CK10T	320.0	13.00	14.7

TRANSITION REGION, CALCULATED VALUES

LATERAL EXPANSION (MILS)	CALCULATED TEMPERATURE (F)	TEMPERATURE (F)	CALCULATED LATERAL EXPANSION (MILS)
5.0	54.6	60.0	5.1
10.0	187.9	65.0	5.3
		70.0	5.4
		75.0	5.6
		80.0	5.8
		85.0	5.9
		90.0	6.1
		95.0	6.3
		100.0	6.4
		105.0	6.6
		110.0	6.8
		115.0	7.0
		120.0	7.2
		125.0	7.4
		130.0	7.6
		135.0	7.8
		140.0	8.0
		145.0	8.2
		150.0	8.4
		155.0	8.6